THE UNIVERSITY OF ADELAIDE

The Formation of Hardpans within Tailings as Possible Inhibitors of Acid Mine Drainage, Contaminant Release and Dusting

Mandy K. Agnew
B.Sc. Hons

Dept. of Geology and Geophysics, The University of Adelaide

Submitted in fulfillment of the requirement for Degree of Doctor of Philosophy

August, 1998

CSIRO
AUSTRALIA
CSIRO Minesite Rehabilitation Research Program

Table of Contents

CHAPTER 1 : INTRODUCTION **1**

1.1 AMD AND CONTAMINANT TRANSPORT 1
1.1.1 AMD - Generating reactions *1*
1.2 CONTAMINANT RELEASE 2
1.3 PRESENT DAY TECHNIQUES OF AMD AND CONTAMINANT AMELIORATION 3
1.3.1 Collection and Treatment *4*
1.3.2 Infiltration Controls *4*
1.3.3 Sulfide - Oxidation Controls *4*
1.3.4 Prevention of Sulfide Oxidation *4*
1.4 HARDPAN HYPOTHESIS 5
1.4.1 Potential Benefits of Hardpans *5*
1.4.1.1 AMD and Contaminant Suppression 5
1.4.1.2 Depletion of Contaminant Transport 6
1.4.1.3 Trafficability and Dust Suppression 6
1.4.2 Review of Previous Hardpan Studies *6*
1.4.2.1 Review of Hardpan Mineralogy & Geochemical Observations 6
1.4.2.2 Review of Hardpan Genesis 9
1.4.2.3 Review of Permeability and Diffusion Results and Environmental Implications 12
1.4.2.4 Review of Previous Laboratory Experiments to Develop Hardpans 15
1.4.2.5 Review of Field Experiments to Develop Cements 17
1.5 RESEARCH OBJECTIVES 18
1.5.1 Aim *18*
1.5.2 Research Methods Employed *18*

CHAPTER 2 : SITE INVESTIGATIONS **19**

2.1 SITE SELECTION 19
2.2 GEOLOGY, TOPOGRAPHY, CLIMATE, DRAINAGE, VEGETATION AND LAND USAGE 20
2.2.1 Kanmantoo Trough, S.A *20*
2.2.1.1 Brukunga Pyrite Mine 20
2.2.1.2 Kanmantoo Cu Mine 20
2.2.2 Willyama Block, N.S.W. *21*
2.2.2.1 Broken Hill, Pb-Zn-Ag Mine. 21
2.2.3 Lachlan Fold Belt, N.S.W *21*
2.2.3.1 Elura Zn-Pb-Ag Mine 22
2.2.3.2 CSA Cu-Pb-Zn Mine 22
2.2.3.3 Peak Au Mine 23
2.2.3.4 Disused Chesney Au-Cu Mine 23
2.2.3.5 Woodlawn Cu-Pb-Zn Mine 23
2.2.4 Pine Creek Inlier, N.T *24*
2.2.4.1 Ranger U Mine 24
2.2.4.2 Woodcutters Pb-Zn Mine 24
2.2.4.3 Pine Creek Au Mine 24
2.2.5 Dundas Trough, Tas. *25*
2.2.5.1 Renison Bell Sn Mine 25

CHAPTER 3 : METHODS **26**

3.1 OVERVIEW 26
3.2 FIELD AND LABORATORY SAMPLING 26
3.3 TAILINGS AND HARDPAN COLOUR AND TEXTURE DESCRIPTIONS 27
3.4 PHYSICAL CHEMISTRY 27
3.5 MINERALOGY 27
3.6 CHEMISTRY 27
3.7 GEOTECHNICAL TESTING 28
3.8 GAS ANALYSIS 28

CHAPTER 4 : NATURALLY OCCURRING HARDPANS AND CEMENTED LAYERS DEVELOPED IN TAILINGS IMPOUNDMENTS 29

4.1 INTRODUCTION 29
4.2 KANMANTOO TROUGH, S.A 30
4.2.1 Brukunga Pyrite Mine *30*
4.2.1.1 Tailings Dam History 31
4.2.1.2 Sampling Description 31
4.2.1.3 Tailings Mineralogical Description 31
4.2.1.4 Secondary Mineralogy and Morphology 32
4.2.1.5 Cemented Layers 32
4.2.2 Disused Kanmantoo Cu Mine *34*
4.2.2.1 Tailings Dam History 35
4.2.2.2 Sampling Description 36
4.2.2.3 Gangue and Sulfide Mineralogy 36
4.2.2.4 Secondary Mineralogy and Morphology 36
4.2.2.5 Discussion 36
4.3 WILLYAMA BLOCK, N.S.W 37
4.3.1 Broken Hill, Pb, Zn, Ag Mine *37*
4.3.1.1 Tailings Dam History 39
4.3.1.2 Sampling Description 40
4.3.1.3 Gangue & Sulfide Mineralogy 40
4.3.1.4 Secondary Mineralogy and Morphology 41
4.3.1.5 Discussion 44
4.4 LACHLAN FOLD BELT, N.S.W 45
4.4.1 Elura Zn-Pb-Ag Mine *45*
4.4.1.1 Tailings Dam History 46
4.4.1.2 Sampling Description 46
4.4.1.3. Gangue and Sulfide Mineralogy 47
4.4.1.4 Secondary Mineralogy and Morphology 47
4.4.1.5 Discussion 51
4.4.2 CSA Cu-Pb-Zn Mine *53*
4.4.2.1 Tailings Dam History 54
4.4.2.2 Seepage Dam Investigations 55
4.4.2.3 Tailings Dam Investigations 56
4.2.2.4 Discussion 60
4.4.3 Peak Au Mine *61*
4.4.3.1 Tailings History 61
4.4.3.2 Sampling Description 62
4.4.3.3 Gangue and Sulfide Mineralogy 62
4.4.3.4 Secondary Mineralogy and Morphology 62
4.4.3.5 Discussion 63
4.4.4 Disused Chesney Au-Cu Mine *64*
4.4.4.1 Tailings History 65
4.4.4.2 Sampling Description 66
4.4.4.3 Gangue and Sulfide Mineralogy 67
4.4.4.4 Secondary Mineralogy and Morphology 67
4.4.4.5 Discussion 68
4.4.5 Woodlawn Cu-Pb-Zn Mine *69*
4.4.5.1 Tailings Dam History 70
4.4.5.2. Sampling Description 70
4.4.5.3 Gangue and Sulfide Mineralogy 71
4.4.5.4 Secondary Mineralogy and Morphology 71
4.4.5.5 Water Investigations 72
4.4.5.6 Discussion 72
4.5 PINE CREEK INLIER, N.T 73
4.5.1 Ranger U Mine *73*
4.5.1.1 Tailings History 73
4.5.1.2 Sampling Description 74
4.5.1.3 Gangue and Sulfide Mineralogy 74
4.5.1.4 Secondary Mineralogy and Morphology 74
4.5.1.5 Discussion 75
4.5.2 Woodcutters Pb-Zn Mine *76*
4.5.2.1 Tailings Dam History 76
4.5.2.2 Sampling Description 76

4.5.2.3 Gangue and Sulfide Mineralogy 77
4.5.2.4 Secondary Mineralisation and Morphologies, and associated Water Investigations 77
4.5.2.5 Discussion 80
4.5.3 Pine Creek Au Mine *81*
4.5.3.1 Tailings History 82
4.5.3.2 Sampling Description 82
4.5.3.3 Gangue and Sulfide Mineralogy 83
4.5.3.4 Secondary Mineralogy and Morphology 84
4.5.3.5 Discussion 84
4.6 DUNDAS TROUGH, TAS. 85
4.6.1 Renison Bell Sn Mine *85*
4.6.1.1 Tailings Dam History 86
4.6.1.2 Sampling Description 87
4.6.1.3 Gangue and Sulfide Mineralogy 87
4.6.1.4 Secondary Mineralogy and Morphology. 87
4.6.1.5 Discussion 94
4.8 CONCLUSIONS 96

CHAPTER 5 : TAILINGS DAM GEOCHEMISTRY 97

5.1 INTRODUCTION 97
5.2 GEOCHEMICAL REACTIONS OF HARDPAN/CEMENT FORMATION 97
5.2.1 Sulfide Oxidation, Acid Generation/Neutralisation and Selected Secondary Mineral Precipitation Reactions *98*
5.2.2 CONDITIONS OF SECONDARY MINERAL PRECIPITATION 102
5.3 OVERVIEW OF THE PROCESSES INFLUENCING THE GEOCHEMICAL EVOLUTION AND FINAL MORPHOLOGY OF TAILINGS AND CEMENTS 104
5.3.1 Deposition Style *104*
5.3.2 Palaeo-surfaces *105*
5.3.3 Final Surface Morphology *105*
5.3.4 Implications and Complications *106*
5.4 GEOCHEMISTRY OF SOLUTES FROM TAILINGS PROFILES 106
5.4.1 Willyama Block, N.S.W *107*
5.4.1.1 Broken Hill 107
5.4.2 Lachlan Fold Belt, N.S.W *125*
5.4.2.1 Elura Zn-Pb-Ag Mine 125
5.4.2.2 CSA Cu-Pb-Zn Mine 132
5.4.2.3 Disused Chesney Au-Cu Mine 146
5.4.3 Pine Creek Inlier, N.T *151*
5.4.3.1 Woodcutters Pb-Zn Mine 151
5.4.4 Dundas Trough, Tas. *156*
5.4.4.1 Renison Bell Sn Mine 156
5.4.5 Geochemical Overview of Site Investigations *161*

CHAPTER 6 : LABORATORY SIMULATIONS OF HARDPAN FORMATION AND IMPLICATIONS.. 163

6.1 OVERVIEW 163
6.2 PRELIMINARY HARDPAN ENHANCEMENT AND LEACHING EXPERIMENTS 164
6.2.1 Selection and Design of Experimental Parameters *164*
6.2.1.1 Column Design 164
6.2.1.2 Column Packing 164
6.2.1.3 Determination of Liquid Additive Regime 165
6.2.2 Experimental Conditions *165*
6.2.2.1 Experiment 1 - Natural Enhancement of Hardpans 165
6.2.2.2 Experiments 2 - Biological and Chemical Enhancement of Hardpans 165
6.2.2.3 Experiment 3 - Leaching Characterisation 165
6.3 RESULTS AND COMPARISONS OF NATURAL ENHANCEMENT VS. BIOLOGICAL AND CHEMICAL ENHANCEMENT OF HARDPANS 166
6.3.1 Discussion *168*
6.4 EXPERIMENT 3 - LEACHING CHARACTERISATION 169
6.4.1 General mineralogical reactions and by-products *181*
6.4.2 Solute Release *182*

6.4.3 Leachate Trends *185*
6.4.4 Leachate Overview *187*
6.5 USE OF ADDITIVES FOR THE ENHANCEMENT OF HARDPAN FORMATION AND INTEGRITY 188
6.5.1 Experimental Design *189*
6.5.1.1 Selection of Tailings 188
6.5.1.2 Selection of Experimental Parameters 189
6.5.1.3 Selection of Additive Types 190
6.5.1.4 Selection from Potential Additives 193
6.5.2 Review of Investigations *194*
6.5.3 Results *195*
6.5.3.1 Permeability 195
6.5.3.2 Porosity Investigations 204
6.5.3.3 Cementation, Eh, pH, Solute Chemistry, Degree of Saturation 209
6.5.3.4 CO_2 Analysis 233
6.5.4 Overview of Results and Conclusions *240*

CHAPTER 7 : EFFECTIVENESS OF HARDPAN IN THE REDUCTION OF AMD AND CONTAMINANT TRANSPORT 242

7.1 OVERVIEW OF INVESTIGATIONS 242
7.2 PERMEABILITY INVESTIGATIONS 244
7.2.1 Discussion on Permeability *245*
7.3 Porosity Investigations *245*
7.3.1 Total Porosity *246*
7.3.2 Moisture Retention Characteristics and Pore Size Distribution *247*
7.3.2.1 Pore Size Distribution Results 251
7.3.2.2 Relationship of Pore Size Distribution, Mineralogy and Grain size 252
7.4 RELATIVE HYDRAULIC CONDUCTIVITY MODELLING 255
7.5 EXTENT OF EVAPORATION 257
7.6 GAS DIFFUSION 259
7.6.1 Gas Diffusion Modelling *259*
7.6.2 Variations in CO_2 Concentrations *264*
7.6.3 Gas Diffusion Measurements *268*
7.7 THE EFFECTIVENESS OF HARDPAN IN THE REDUCTION OF AMD AND CONTAMINANT TRANSPORT - AN OVERVIEW 270

CHAPTER 8 : HARDPANS - EFFECTIVENESS IN ENVIRONMENTAL MANAGEMENT 273

8.1 REVIEW OF AIMS 273
8.2 NATURAL DEVELOPMENT OF HARDPANS AND CEMENTED LAYERS IN TAILINGS DAMS 274
8.2.1 Development and classification of secondary mineral accumulations *274*
8.2.2 Parameters Effecting Hardpan and Cemented Layer Development *274*
8.2.3 The Morphology and Cycling of Hardpans and Cemented Layers *277*
8.3 ABILITY OF NATURALLY DEVELOPED HARDPANS AND CEMENTED LAYERS TO INHIBIT AMD, CONTAMINANT GENERATION AND TRANSPORT AND DUSTING 282
8.4 DEVELOPMENT OF ARTIFICIALLY ENHANCED HARDPANS AND THEIR ABILITY TO INHIBIT AMD, CONTAMINANT GENERATION AND TRANSPORT AND DUSTING. 284
8.6 RESEARCH RECOMMENDATIONS 286

APPENDIX 1A : METHODS 287

1A.1 PHYSICAL CHEMISTRY 287
1A.1.1 pH *287*
1A.1.2 Electrical Conductivity (EC) *284*
1A.1.3 Redox Potential *287*
1A.2 MINERALOGY 287
1A.2.1 X-ray Powder Diffraction *287*
1A.2.2 Microscopic examinations *287*
1A.2.3 Sulfate/Sulfide Determination by HCl - HNO_3 Extraction *288*
1A.3 CHEMISTRY 289

1A.3.1 Solute concentration determination - Inductively Coupled Plasma Atomic Emisson Spectrometry 289
1A.3.2 X-Ray Fluorescence Major and Trace Elemental Analysis 289
1A.3.3 Acid - Base Accounting 290
1A.3.3.1 Net Acid Generation - Performed by CRA-ATD 290
1A.3.3.2 H_2O_2 Modified "Acid Neutralising Capacity" - Performed by CRA-ATD 291
1A.3.4 Direct Extraction for Chloride Analysis 293
1A.3.5 Isotope Analysis Extraction 293
1A.4 GEOTECHICAL TESTING 294
1A.4.1 Particle Size Distribution 294
1A.4.2 Gravimetric water content 295
1A.4.3 Particle Density 296
1A.4.4 Bulk Density Determinations 297
1A.4.5 Void Ratio and Porosity Determinations 297
1A.4.6 Moisture Characteristics - Pore Size Distribution 297
1A.4.7 Permeability Tests 299
1A.4.7.1 Falling Head Infiltration Tests 299
1A.4.7.2 Field Permeameter Tests 299
1A.4.7.3 Laboratory Oedometer Tests 300
1A.4.7.4 Laboratory Constant Head Infiltration Tests 301
1A.5 GAS ANALYSIS 302
1A.5.1 Gas Sampling 302
1A.5.2 CO_2 Concentration Determination 303
1A.5.3 Diffusion Measurements (performed by ANSTO) 303

APPENDIX 2A TAILINGS DAM GEOCHEMISTRY 306

2A.1 KANMANTOO TROUGH, S.A 306
2A.1.1 Brukunga Pyrite Mine 306
2A.1.2 Kanmantoo Cu Mine 309
2A.2 LACHLAN FOLD BELT, N.S.W 312
2A.2.1 Peak Au Mine 312
2A.2.2 Woodlawn Cu-Pb-Zn Mine 317
2A.2.2.1 Discussion 321
2A.3 PINE CREEK INLIER, N.T 322
2A.3.1 Ranger U Mine 322
2A.3.2 Pine Creek Au Mine 325
2A.3.2.1 Discussion 325

APPENDIX 3A : LABORATORY SIMULATION INDIVIDUAL RESULTS 326

3A.1 REVIEW OF PRELIMINARY EXPERIMENTS - BRUKUNGA TAILINGS 326
3A.1.1 Natural Hardpan Enhancement (E1) vs Biological and Chemical Hardpan Enhancement (E2) - Brukunga Trials 326
3A.1.2 Leaching Characteristics of the Brukunga Tailings 328
3A.2 REVIEW OF PRELIMINARY EXPERIMENTS - BROKEN HILL TAILINGS 331
3A.2.1 Natural Hardpan Enhancement (E1) vs Biological and Chemical Hardpan Enhancement (E2) - Broken Hill Trials 331
3A.2.2 Leaching Characteristics of the Broken Hill Tailings 332
3A.3 REVIEW OF PRELIMINARY EXPERIMENTS - ELURA TAILINGS 334
3A.3.1 Natural Hardpan Enhancement (E1) vs Biological and Chemical Hardpan Enhancement (E2) - Elura Trials 334
3A.3.2 Leaching Characteristics of the Elura Tailings 335
3A.4 REVIEW OF PRELIMINARY EXPERIMENTS - CSA TAILINGS 337
3A.4.1 Natural Hardpan Enhancement (E1) vs Biological and Chemical Hardpan Enhancement (E2) - CSA Trials 337
3A.4.2 Leaching Characteristics of the CSA Tailings 338
3A.5 REVIEW OF PRELIMINARY EXPERIMENTS - PEAK TAILINGS 340
3A.5.1 Natural Hardpan Enhancement (E1) vs Biological and Chemical Hardpan Enhancement (E2) - Peak Trials 340
3A.5.2 Leaching Characteristics of the Peak Tailings 341

TABLE 5.8 RENISON BELL SOLUTE CONCENTRATIONS (1:5 BATCH LEACHING) 160
TABLE 6.1 SUMMARY OF PRELIMINARY COLUMN EXPERIMENTS 167
TABLE 6.2 CHARACTERISATION OF CEMENT TYPE AND LOCATION WITHIN PRELIMINARY EXPERIMENTS E1 AND E2 168
TABLE 6.3 AVAILABILITY, RELEASE AND RATE OF RELEASE FOR SELECTED ELEMENTS - EXPT 3 : LEACHING CHARACTERISATION 183
TABLE 6.4 DESCRIPTION OF LIMESTONE SAMPLES 193
TABLE 6.5 CONTROL TAILINGS OEDOMETER TEST RESULTS 196
TABLE 6.6 TYPICAL RESULTS FOR OEDOMETER TEST - EXAMPLE OF FLYASH & CSA TAILINGS MIX 197
TABLE 6.7 ORIGINAL AND FINAL BULK DENSITIES, PERMEABILITIES AND POROSITIES FOR THE MAIN COLUMN EXPT 198
TABLE 6.8 AVERAGE RESULTS OF PORE CONNECTIVITY TESTS 208
TABLE 6.9 MAIN EXPERIMENT CEMENT CLASSIFICATION 213
TABLE 7.1 SUMMARY OF FIELD AND LABORATORY PERMEABILITY TESTING 243
TABLE 7.2 POROSITY MEASUREMENTS FOR SELECTED HARDPANS AND FRESH TAILINGS 246
TABLE 7.3 MOISTURE CONTENT, DEUTERIUM ($\delta D‰$) AND CL RESULTS FOR CSA AND ELURA PROFILES 259
TABLE 7.4 POROSITY AND ASSOCIATED MEASUREMENTS FOR CSA AND ELURA TAILINGS PROFILES 261
TABLE 7.5 OXYGEN DIFFUSION COEFFICIENTS, SULFIDE OXIDATION DEPTHS AND TOTAL TIMES FOR OXIDATION OF VADOSE ZONES FOR ELURA AND CSA TAILINGS IMPOUNDMENTS 262
TABLE 7.6 CO_2 CONCENTRATIONS (VOL %) IN CSA AND ELURA PROFILES 264
TABLE 7.7 : TYPICAL EH, PH, AND EC IN ELURA AND CSA TAILINGS PROFILE (SAMPLED JULY 1997) 266
TABLE 7.8 EFFECTIVE DIFFUSION COEFFICIENTS FOR SELECTED CSA AND ELURA HARDPANS 269
TABLE 7.9 COMPARISON OF OXYGEN DIFFUSION COEFFICIENTS, SULFIDE OXIDATION DEPTHS AND TOTAL TIMES FOR OXIDATION OF VADOSE ZONES, FOR ELURA AND CSA HARDPANS 270
TABLE 8.1 SECONDARY MINERALS ASSOCIATED WITH HARDPAN AND CEMENTED LAYERS DEVELOPED WITHIN TAILINGS. 281
TABLE 2A.1 BRUKUNGA SOLUTE CONCENTRATIONS (1:5 BATCH LEACHING) 308
TABLE 2A.2 KANMANTOO SOLUTE CONCENTRATIONS (1:5 BATCH LEACHING) 311
TABLE 2A.3 PEAK SOLUTE CONCENTRATIONS (1:5 BATCH LEACHING) 316
TABLE 2A.4 WOODLAWN SOLUTE CONCENTRATIONS (1:5 BATCH LEACHING) 321
TABLE 2A.5 RANGER SOLUTE CONCENTRATIONS (1:5 BATCH LEACHING) 324
TABLE 2A.6 PINE CREEK SOLUTE CONCENTRATIONS (1:5 BATCH LEACHING) 325
TABLE 3A.1 PH AND EC RESULTS FOR BRUKUNGA (B1) - A AND BRUKUNGA (B2) - B 327
NATURAL (E1) AND CHEMICAL AND BIOLOGICAL (E2) HARDPAN ENHANCED TRIALS 327
TABLE 3A.2 ICP-AES RESULTS FOR BRUKUNGA (B1) NATURAL (E1) AND CHEMICAL AND BIOLOGICAL (E2) HARDPAN ENHANCED TRIALS 327
TABLE 3A.3 ICP-AES RESULTS FOR BRUKUNGA (B2) NATURAL (E1) AND CHEMICAL AND BIOLOGICAL (E2) HARDPAN ENHANCED TRIALS 328
TABLE 3A.4 PH AND EC RESULTS FOR BRUKUNGA (B1) LEACHING CHARACTERISATION EXPERIMENT 329
TABLE 3A.5 SOLUTE LEACHING RESULTS FOR BRUKUNGA (B1) - LEACHING CHARACTERISATION EXPERIMENT 329
TABLE 3A.6 PH AND EC RESULTS FOR BRUKUNGA (B2) - LEACHING CHARACTERISATION EXPERIMENT 330
TABLE 3A.7 SOLUTE LEACHING RESULTS FOR BRUKUNGA (B2) - LEACHING CHARACTERISATION EXPERIMENT 330
TABLE 3A.8 PH AND EC RESULTS FOR BROKEN HILL NATURAL (E1) AND CHEMICAL AND BIOLOGICAL (E2) HARDPAN ENHANCED TRIALS 332
TABLE 3A.9 ICP-AES RESULTS FOR BROKEN HILL NATURAL (E1) AND CHEMICAL AND BIOLOGICAL (E2) HARDPAN ENHANCED TRIALS 332
TABLE 3A.10 SOLUTE LEACHING RESULTS FOR BROKEN HILL - LEACHING CHARACTERISATION EXPERIMENT .. 333
TABLE 3A.11 PH AND EC RESULTS FOR BROKEN HILL - LEACHING CHARACTERISATION EXPERIMENT 334
TABLE 3A.12 PH AND EC RESULTS FOR ELURA NATURAL (E1) AND CHEMICAL AND BIOLOGICAL (E2) HARDPAN 335
TABLE 3A.13 ICP-AES RESULTS FOR ELURA NATURAL (E1) AND CHEMICAL AND BIOLOGICAL (E2) HARDPAN ENHANCED TRIALS 335
TABLE 3A.14 SOLUTE LEACHING RESULTS FOR ELURA - LEACHING CHARACTERISATION EXPERIMENT 336
TABLE 3A.15 PH AND EC RESULTS FOR ELURA - LEACHING CHARACTERISATION EXPERIMENT 337
TABLE 3A.16 PH AND EC RESULTS FOR CSA NATURAL (E1) AND CHEMICAL AND BIOLOGICAL (E2) HARDPAN 338
TABLE 3A.17 ICP-AES RESULTS FOR CSA NATURAL (E1) AND CHEMICAL AND BIOLOGICAL (E2) HARDPAN ENHANCED TRIALS 338
TABLE 3A.18 SOLUTE LEACHING RESULTS FOR CSA - LEACHING CHARACTERISATION EXPERIMENT 339
TABLE 3A.19 PH AND EC RESULTS FOR CSA - LEACHING CHARACTERISATION EXPERIMENT 340
TABLE 3A.20 PH AND EC RESULTS FOR PEAK NATURAL (E1) AND CHEMICAL AND BIOLOGICAL (E2) HARDPAN 340
TABLE 3A.21 ICP-AES RESULTS FOR PEAK NATURAL (E1) AND CHEMICAL AND BIOLOGICAL (E2) HARDPAN ENHANCED TRIALS 341
TABLE 3A.22 PH AND EC RESULTS FOR PEAK - LEACHING CHARACTERISATION EXPERIMENT 342
TABLE 3A.23 SOLUTE LEACHING RESULTS FOR PEAK - LEACHING CHARACTERISATION EXPERIMENT 342

TABLE 3A.24 PH AND EC RESULTS FOR WOODLAWN NATURAL (E1) AND CHEMICAL AND BIOLOGICAL (E2) HARDPAN....343
TABLE 3A.25 ICP-AES RESULTS FOR WOODLAWN NATURAL (E1) AND CHEMICAL AND BIOLOGICAL (E2) HARDPAN ENHANCED TRIALS....344
TABLE 3A.26 PH AND EC RESULTS FOR WOODLAWN - LEACHING CHARACTERISATION EXPERIMENT....346
TABLE 3A.27 SOLUTE LEACHING RESULTS FOR WOODLAWN - LEACHING CHARACTERISATION EXPERIMENT....346
TABLE 3A.28 PH AND EC RESULTS FOR RANGER NATURAL (E1) AND CHEMICAL AND BIOLOGICAL (E2) HARDPAN347
TABLE 3A.29 ICP-AES RESULTS FOR RANGER NATURAL (E1) AND CHEMICAL AND BIOLOGICAL (E2) HARDPAN ENHANCED TRIALS....347
TABLE 3A.30 PH AND EC RESULTS FOR RANGER - LEACHING CHARACTERISATION EXPERIMENT....348
TABLE 3A.31 SOLUTE LEACHING RESULTS FOR RANGER - LEACHING CHARACTERISATION EXPERIMENT....349
TABLE 3A.32 PH AND EC RESULTS FOR WOODCUTTERS NATURAL (E1) AND CHEMICAL AND BIOLOGICAL (E2) HARDPAN....350
TABLE 3A.33 ICP-AES RESULTS FOR WOODCUTTERS NATURAL (E1) AND CHEMICAL AND BIOLOGICAL (E2) HARDPAN ENHANCED TRIALS....350
TABLE 3A.34 PH AND EC RESULTS FOR WOODCUTTERS - LEACHING CHARACTERISATION EXPERIMENT....352
TABLE 3A.35 SOLUTE LEACHING RESULTS FOR WOODCUTTERS - LEACHING CHARACTERISATION EXPERIMENT352
TABLE 3A.36 PH AND EC RESULTS FOR PINE CREEK NATURAL (E1) AND CHEMICAL AND BIOLOGICAL (E2) HARDPAN....353
TABLE 3A.37 ICP-AES RESULTS FOR PINE CREEK NATURAL (E1) AND CHEMICAL AND BIOLOGICAL (E2) HARDPAN ENHANCED TRIALS....354
TABLE 3A.38 PH AND EC RESULTS FOR PINE CREEK - LEACHING CHARACTERISATION EXPERIMENT....355
TABLE 3A.39 SOLUTE LEACHING RESULTS FOR PINE CREEK - LEACHING CHARACTERISATION EXPERIMENT....355
TABLE 3A.40 ELEMENT AVAILABILITY, RELEASE AND RATE OF RELEASE (mg/day) - EXPT 3 : LEACHING CHARACTERISATION....356
TABLE 3A.40 CONT ELEMENT AVAILABILITY, RELEASE AND RATE OF RELEASE (mg/day)- EXPT 3 : LEACHING CHARACTERISATION....357
TABLE 3A.41 LIMESTONE XRF DATA FOR SOLID ADDITIVE HARDPAN ENHANCEMENT....358
TABLE 3A.42 PHOSPHATE XRF DATA FOR SOLID ADDITIVE HARDPAN ENHANCEMENT....358
TABLE 3A.43 SOLUTE RESULTS FOR VARIOUS PH WATER 1:5 EXTRACTIONS FOR SELECTED PHOSPHATE SAMPLES359
TABLE 3A.44 FLYASH XRF DATA FOR SOLID ADDITIVE HARDPAN ENHANCEMENT....359
TABLE 3A.45 SOLUTE RESULTS FOR VARIOUS PH WATER 1:5 EXTRACTIONS FOR SELECTED FLYASH SAMPLES.360
TABLE 3A.46 BULK DENSITY, PERMEABILITY AND POROSITY RESULTS FROM OEDOMETER TESTING OF PURE TAILINGS AND ADDITIVES....361
TABLE 3A.47 BULK DENSITY, PERMEABILITY AND POROSITY RESULTS FROM OEDOMETER TESTING OF TAILINGS AND ADDITIVE MIXTURES....362
TABLE 3A.48 ICP-AES RESULTS OF 1:5 EXTRACTS FROM THE SOLID ADDITIVE HARDPAN ENHANCEMENT EXPERIMENT - CONTROL TRIALS....363
TABLE 3A.49 ICP-AES RESULTS OF 1:5 EXTRACTS FROM THE SOLID ADDITIVE HARDPAN ENHANCEMENT EXPERIMENT - FLYASH AND LIME LAYER TRIALS....363
TABLE 3A.50 ICP-AES RESULTS OF 1:5 EXTRACTS FROM THE SOLID ADDITIVE HARDPAN ENHANCEMENT EXPERIMENT - FLYASH AND LIME MIX TRIALS....364
TABLE 3A.51 ICP-AES RESULTS OF 1:5 EXTRACTS FROM THE SOLID ADDITIVE HARDPAN ENHANCEMENT EXPERIMENT - LIME MIX TRIALS....364
TABLE 3A.52 ICP-AES RESULTS OF 1:5 EXTRACTS FROM THE SOLID ADDITIVE HARDPAN ENHANCEMENT EXPERIMENT - PHOSPHATE AND LIME MIX TRIALS....365
TABLE 3A.53 ICP-AES RESULTS OF 1:5 EXTRACTS FROM THE SOLID ADDITIVE HARDPAN ENHANCEMENT EXPERIMENT - PHOSPHATE MIX TRIALS....365
TABLE 3A.54 PH AND EH RESULTS FROM THE SOLID ADDITIVE HARDPAN ENHANCEMENT EXPERIMENT....366
TABLE 3A.54 CONT. PH AND EH RESULTS FROM THE SOLID ADDITIVE HARDPAN ENHANCEMENT EXPERIMENT 367

Abstract

The effectiveness of hardpans in the inhibition of acid drainage generation is dependent on reducing oxygen diffusion and water infiltration into the underlying tailings, while maintaining long term stability. A reduction in water infiltration can also diminish the transport of contaminants developed during sulfide oxidation and subsequent reactions. Hardpans developing in base metal, tin and gold mine tailings in Australia have been investigated to determine the factors controlling their formation, mineralogical and geochemical characteristics and their ability to inhibit acid drainage. Three basic types of hardpans have been identified and examined: laterally extensive surface hardpans, laterally extensive cemented layers; and laterally discontinuous hardpans developing in locations of seepage. Their mineralogy, morphology, lateral extent, depth and rate of formation is dictated by sulfide and gangue mineralogy and content, milling and depositional techniques of the tailings and the climate.

Water and gas movement through the hardpans at the CSA (Cu, Zn, Pb) and the Elura (Pb, Zn, Ag) mines has been investigated. Permeability tests indicate the hardpans can reduce infiltration rates by 10 to 100 times that of the fresh tailings. Oxygen diffusion rates were calculated and were shown to be up to 1000 times lower in hardpans than in fresh tailings. Such decreases are explained by persistent elevated 'degrees of saturation' within the hardpans. These conditions were verified using a conceptual model of sulfide oxidation reactions, which allowed comparisons of diffusion coefficients with modelled and observed depths of oxidation within the tailings impoundments.

Concerns regarding the long-term integrity and sealing capacity of the hardpans have been expressed by Canadian researchers. Present field observations indicated that the natural hardpans formed by cementing with secondary minerals from sulfide oxidation are very dynamic due to their susceptibility to chemical and physical erosion. Laboratory tests using a wide range of additives have been undertaken to develop hardpans more akin to naturally occurring duricrusts. Some additives have developed cements which have the low permeability and porosity characteristics required, while maintaining a high level of resistance to both chemical and physical break down.

Declaration

This work contains no material which has been accepted for the award of any other degree or diploma in any university or other tertiary institution and, to the best of my knowledge and belief, contains no material previously published or written by another person, except where due reference has been made in the text.

I give consent to this copy of my thesis, when deposited in the University Library, being available for loan and photocopying.

Mandy Agnew

Acknowledgements

This research has promoted a journey of both scientific and personal discovery. I have many people to thank for this wonderful experience, who have helped me through support and via intellectual enlightenment on many levels.

Firstly to the companies that have supported this work, Pasminco, Rio Tinto, Cobar Mines and Denehurst. Thank you for the sponsorship and support, this assistance has been invaluable. Additional thanks to the mine site staff who provided access and information on the tailings dams and mining procedures.

To my supervisor Graham Taylor, I thank you for the time and energy you have invested in helping me to develop my research and the friendship we have shared over the years. Thanks also to Professor Ypma and Dr Both for their assistance with thesis editing.

Similarly I want to express my deepest gratitude to all of the people at the CSIRO, ANSTO and University of Adelaide that have given their time and expertise to advance my knowledge about many of the scientific approaches and skills that I have learnt over the years. Special thanks must go to the staff of the CSIRO Minesite Rehabilitation Research Group whom I have hounded over the years. I have been continuously overwhelmed and delighted by the many people who have been willing to spend time helping me to uncover new directions. These times have given me unexpected enjoyment during a period that otherwise may have been daunting. I feel I have made some life long friends during this experience and am grateful to have been given this opportunity.

This time has been challenging on many levels and I thank my friends and family for their undying love and support through out this adventure. To my husband Richard, you have been a tower of strength on which I have lent so many times. I hope that you realised how much your friendship and love have helped me achieve many of the goals I have set in my life.

To the other people not mentioned directly, thank you all.

Chapter 1 : Introduction

Base metal, gold, uranium, iron ore and coal have been mined in Australia for many decades and contribute significantly to Australia's export income. The recent awareness of the impact of mining on the environment has led to extensive environmental research in the past two decades. Chapter 1 presents an introduction to investigations on Acid Mine Drainage (AMD), pollutant generation and release, and the present techniques of amelioration.

Hardpans, similar to ferricretes and silcretes, form naturally in tailings dams and waste rock dumps. The aims of this research has been to determine the processes of hardpan development within tailings dams and the affect hardpans have on reducing environmental impacts. This chapter reviews previous research on hardpans in both tailings dams and waste rock dumps. Additionally an overview of the aims of this study is outlined.

1.1 AMD and Contaminant Transport

Tailings and waste rock produced during the mining and milling process, have, if sulfidic, the potential to produce Acid Mine Drainage (AMD). AMD generation is one of the major issues faced by the mining industry.

The interactions between water flow and the mineralogy and geochemistry of the mine wastes can produce highly acidic solutions laden with sulfate and heavy metals. The solutions may then seep from the site contaminating the surrounding environment. As a result of research on the effects of AMD and pollutant generation, abatement issues are now being addressed from the mine development through to the close-out stages. Mechanisms for the inhibition of these processes have been investigated for some time, however many amelioration techniques are very expensive and seldom completely effective.

Waste rock dumps and tailings dams contain the non-economic residue of mining and milling processes and commonly represent more than 90% of the mined material in base and precious metal deposits. Thus large volumes of waste material are generated (Robertson, 1994). In Australia most tailings impoundments are constructed using retaining dams, which are elevated above the surrounding topography. The design parameters vary from site to site. Similarly, waste rock dumps most commonly occur as landforms of greater relief than the surroundings.

1.1.1 AMD - Generating reactions

The chemical reactions which play a major role in controlling the physio-chemical conditions in waste dumps and tailings dams include sulfide oxidation, processes of metallic and gangue element dissolution and secondary mineral precipitation.

Acid mine drainage (AMD) forms when sulfide is oxidised. There are two important oxidising agents - dissolved oxygen and ferric iron (Fe^{3+}). An example of oxidation of pyrite by dissolved oxygen can be expressed as:

$$FeS_2 + {}^7/_2O_2 + H_2O \Leftrightarrow Fe^{2+} + 2SO_4^{2-} + 2H^+ \quad (1.1)$$

in which only the sulfur atoms of the pyrite are oxidised, from S^{2-} to SO_4^{2-}, and iron remains in the ferrous state. Two moles of H^+ are produced for each mole of FeS_2.

Oxidation by ferric iron can be written

$$FeS_2 + 14Fe^{3+} + 8H_2O \Leftrightarrow 15Fe^{2+} + 2(SO_4)^{2-} + 16H^+ \quad (1.2)$$

Again only the sulfur of the pyrite is oxidised and Fe^{2+} is released. In this case, 16 moles of H^+ are produced for each mole of FeS_2. Oxidation by Fe^{3+} is rapid compared with that by dissolved oxygen. Reaction (1.2) can only proceed at a significant rate if sufficient Fe^{3+} is present. The amount of Fe^{3+} is dependent on the rate of oxidation of Fe^{2+} produced in reaction (1.1) and (1.2), and also on the pH of the system, which governs the solubility of ferric oxy-hydroxides. Ferrous iron is oxidised according to the following equation:

$$2Fe^{2+} + {}^1/_2O_2 + 2H^+ \Leftrightarrow Fe^{3+} + H_2O \quad (1.3)$$

Reaction (1.3) can occur abiotically, but is strongly catalysed (by factors of 10 to 10^5, according to various authors) by acidophilic, aerobic bacteria, mainly thiobacilli. If the reaction occurs in acidic conditions, then the Fe^{3+} produced remains in solution and is available to degrade pyrite as in eq (1.2). However, if the pH is greater than about 3 (Thornber & Taylor, 1992), then most of the Fe^{3+} is precipitated as, for example

$$Fe^{3+} + 3H_2O \Leftrightarrow Fe(OH)_3 + 3H^+ \quad (1.4)$$

In a lower pH environment (Bigham et al. 1992) and in the presence of high concentrations of sulfate, jarosite-type compounds can be formed, eg.

$$Fe^{3+} + K^+ + SO_4^{2-} + 6H_2O \Leftrightarrow KFe_3(SO_4)_2 + 6H^+ \quad (1.5)$$

Combining equations (1.1), (1.3) and (1.4), that is the stage of sulfide oxidation, of ferrous iron oxidation, and of ferric iron precipitation, gives the equation generally written to describe the generation of AMD:

$$2FeS_2 + {}^{15}/_2O_2 + 7H_2O \Leftrightarrow 2Fe(OH)_3 + 4SO_4^{2-} + 8H^+ \quad (1.6)$$

1.2 Contaminant Release

The impact of mining on the surrounding environment is strongly controlled by rainfall and the general hydrology. Rainfall quantity dictates the transport of soluble salts down through the tailings profile, while the hydrology of the dam and the surrounds dictates the movement of these contaminants off-site.

The degree to which particular elements are transported or precipitated significantly influences the chemistry of pore water within the system. The extent of elemental mobilisation depends on the solubility controls dictated by the influence of other dissolved species in solution (cations, anions and organic acids) and the interactions between these solutions and the surface of primary and secondary minerals. Various elements may be held in mineral lattices; loosely bound within a layer of the changing potential field at the interface; or mobile in solution, either solvated by the water molecules or complexed with one or more other soluble ions. The solubilities of cations, hydroxide precipitates and anions of elements are affected by changes in pH, where cations are generally more mobile at low pH and anions more often mobile at higher pH (Thornber and Taylor, 1992).

The extent to which elements are adsorbed at the mineral/solution interface is also pH dependent. In general, with increasing OH^- concentrations, surfaces become increasingly negatively charged and thus more cations become adsorbed from solution. Correspondingly on decreasing the pH, the surface is usually more positively charged, decreasing the adsorption of cations but increasing the adsorption of anions. Similarly the degree to which co-precipitation can occur is pH controlled. Co-precipitation describes the precipitation of elements from solutions in which they would normally be soluble, as a result of precipitation of some other, more abundant elements. Cation co-precipitation occurs readily when cation concentrations and pH are high, and are co-precipitated with Fe oxides or with carbonates. Co-precipitation of anions is similarly influenced, with low solubility and low pH favoring greater anion co-precipitation (Thornber and Taylor, 1992).

1.3 Present Day Techniques of AMD and Contaminant Amelioration

Since recognition of the AMD and contaminant problems associated with mining, the techniques of abatement have been continuously reviewed and improved. Research into prediction, remediation and prevention are being undertaken to achieve a better understanding of the interaction between the hydrogeological, geochemical, mineralogical and microbiological characteristics of both waste rock dumps and tailings dams.

Robertson (1987) reviewed many abatement techniques and prepared a cost benefit comparison for the various approaches for tailings dams. The techniques were grouped into 3 categories

I. collection and treatment of tailings-derived discharge
II. infiltration controls
III. sulfide oxidation controls

Blowes et al. (1994b) discussed the techniques involved with each of these processes and considered a fourth technique; prevention of sulfide oxidation.

1.3.1 Collection and Treatment

Collection and treatment techniques have been employed throughout sites in both North America and Australia. These facilities collect all polluted seepage from tailings, waste rock dumps and benches, which is then neutralised using, in many cases lime. Problems include continuous operating costs, along with the disposal of the resultant low density sludge residue, suggesting strongly that this is not a viable long-term solution.

Alternative passive treatment systems which have been examined include downstream polishing, via metal scavenging using natural or constructed wetlands, wood-waste or peat, or limestone-lined trenches. Additionally Blowes and Ptacek (1992, 1994) proposed intercepting Fe^{2+} and SO_4^{2-} laden groundwater through the use of porous reactive walls containing labile organic carbon.

1.3.2 Infiltration Controls

Numerous techniques have been used for the control of tailings pore water, however the most effect management technique is to reduce infiltration of surface water, groundwater and meteoric waters, thus reducing the amount flowing through the waste (Robertson, 1987). Blowes et al. (1994b) explain that suitable site selection can avoid much ground and surface infiltration, while synthetic liners and impermeable barriers, cut-off walls and diversion trenches can be used if suitable locations are not available.

1.3.3 Sulfide - Oxidation Controls

Abatement techniques for the reduction of sulfide oxidation considered by Robertson (1987) included bactericidal controls, precipitates that coat sulfide grains and oxygen barriers. As mentioned previously, sulfide oxidising bacteria play a large role in catalysing sulfide oxidation reactions, particularly in tropical and sub-tropical regions. Bactericidal controls can be used to inhibit these microbiological processes.

Armoring of the sulfide minerals within the waste via insoluble, non-reactive precipitates has also been considered. These effectively isolate the sulfide minerals from water and oxygen, thus reducing oxidation and elemental dissolution. The third type of sulfide oxidation control is the use of diffusion barriers between the atmosphere and the reactive sulfide. These covers consist of fine-grained material such as clay with high moisture holding potentials, synthetic material and/or barriers of oxygen-consuming materials (eg wood waste, sewage sludge and industrial by-products).

1.3.4 Prevention of Sulfide Oxidation

The prevention of oxidation discussed by Blowes et al. (1994b) basically covers alternative methods of tailings deposition e.g. deposition in deep lakes, separation of sulfide minerals for separate disposal,

disposal of tailings as a thickened slurry with improved moisture retaining capabilities and enhanced sulfate reduction within tailings impoundments through the addition of solid phase organics.

1.4 Hardpan Hypothesis

Hardpans, not unlike the naturally occurring ferricretes, calcretes and silcretes found throughout Australia, can develop within tailings dams at different depths within the profile under varying conditions of climate, mineralogy and grain size. These hardpans have the potential to inhibit oxidation of the underlying sulfide tailings through the reduction of oxygen and water penetration (Boorman and Watson, 1976; Kennedy and Hawthorne, 1987; McSweeny and Madison, 1988; Blowes et al. 1987 & 1991; and Whitney et al. 1995). The benefits of hardpan development are not only in the reduction of AMD and contaminant development, but also amelioration of dust problems and improved trafficability. The development of hardpans also have the potential to reduce the cost of close out.

If sulfide oxidation is reduced, acid generation is attenuated accordingly, resulting in the abatement of pollutant generation and thus reducing the impact on the surrounding environment. By gaining a better understanding of the mineralogy, chemistry, physical properties and climatic conditions under which hardpans form in tailings dams, their potential use as a close-out technique can be fully explored.

1.4.1 Potential Benefits of Hardpans

1.4.1.1 AMD and Contaminant Suppression

Sulfide oxidation reactions occur in the vadose zone of the tailings impoundment profile where oxygen diffusion through the partly saturated tailings is rapid. These reactions release H^+, SO_4^{2-}, Fe^{2+} and other metals to the infiltrating water. Simulations conducted using the model of Davis and Ritchie (1986) indicate that, under conditions typical of tailing impoundments in central and eastern Canada, sulfide oxidation reactions will continue for a period of decades to centuries (Blowes et al. 1991). The concentrations of dissolved solutes in the vadose zone, however, will vary depending on the sulfide content of tailings, the rate of oxygen transport into the tailings, the rate of sulfide oxidation and metal release, the velocity of groundwater moving through the tailings and the extent of attenuation of dissolved species in the tailings.

Oxidation rates are rapid shortly after deposition is completed and reduce over time as the length of the oxygen gas diffusion path increases. Additionally, diffusion decreases as water content increases deeper in the impoundment (Blowes and Jambor, 1990). Presently utilised abatement techniques are designed to reduce influx of oxygen and water, but are seldom fully effective.

If oxygen diffusion can be further inhibited with the development of hardpans at the surface of the tailings dam, oxidation rates can be reduced. The cements which make-up hardpans have a three way action to reduce AMD and subsequent contaminant development. Firstly, they may bind the skeletal

gangue minerals grains together, reducing porosity and permeability and thus oxygen and water infiltration. Secondly, the secondary minerals have the potential to act as a natural amour around residual sulfide grains, further reducing oxidation reactions and thus contaminant development. Thirdly, the cements themselves incorporate many of the potential contaminants into their structures. Secondary sulfates scavenge numerous elements, with jarosite ($KFe_3(SO_4)_2(OH)_6$) for example able to incorporate Pb, Al, Zn, Ba, Hg, As, Sb etc. in the structure (Scott, 1987). Iron oxides also have the ability to combine some elements into their structures, or absorb them on their large surface area (Thornber & Wildman, 1984).

1.4.1.2 Depletion of Contaminant Transport

Tailings dam hardpans are suggested to have lower permeability than fresh tailings and thus cause a decrease of water infiltration into the fresh tailings beneath. Thus contaminated seepage may to some extent be attenuated.

1.4.1.3 Trafficability and Dust Suppression

Mines located in close proximity to surrounding towns, such as Kalgoorlie (W.A) and Broken Hill (N.S.W), have an on-going problem during the life of the mine due to production of dust from the exposed tailings facilities. Once the tailings dams are filled, expensive techniques of soil/rock cover are often implemented to reduce the impact of dust. The development of natural or geo-engineered hardpans has the ability to bind both sulfide and gangue mineral grains together producing a potentially wind resistant surface.

Furthermore, the benefit of improved trafficability widens the range of close-out techniques, if hardpans are not considered as a long-term close-out option. In many cases, the time for tailings dams to de-water and stabilise is extensive, allowing oxidation reactions to begin at the surface prior to treatment. If the conditions are not suitable for natural hardpan development, additives may allow in-situ geo-engineering of cements and thus more rapid access to the dam surface for covering with rock or soil and possible revegetation.

1.4.2 Review of Previous Hardpan Studies

1.4.2.1 Review of Hardpan Mineralogy & Geochemical Observations

This project was initiated after an investigation of the Brukunga tailings dam in South Australia during 1994. Between 1952 and 1972, this pyrite deposit were mined by Nairne Pyrites Ltd. to manufacture sulfuric acid for superphosphate production (SADME, 1989). Since abandonment, contaminated, acidic drainage from the mine has been polluting the local and down-stream water and soil systems. The tailings consist of 2-3% sulfide, predominantly pyrite, with minor sphalerite, pyrrhotite, galena and chalcopyrite. The gangue mineralogy includes muscovite, feldspar, quartz, clinochlore, calcite, tremolite and biotite with minor rutile, pyrophyllite, anatase and apatite. A series of cemented layers were

observed in the tailings dam at the base of the active zone of oxidation producing a boundary between oxidised and unoxidised sulfidic tailings at 1-1.4m below the surface. They consist of jarosite, ferrihydrite ($Fe_{4-5}(OH,O)_{12}$), gypsum and siliceous material occurring as 0.5-1cm thick layers (Agnew, 1994).

The existence of hardpans in tailings dams has been widely observed over the last 20 years. Kennedy and Hawthorne (1987) observed layers in the inactive tailings impoundments at the Sherridon and Farley mine-sites in Northern Manitoba. Hardpans, characterised by the incomplete oxidation of sulfide minerals, consist of goethite and jarosite cements. Gypsum is common, and some hardpans contained analcite ($Na(AlSi_2)O_6.H_2O$). The tailings in which sulfide had been completely oxidised were poorly cemented, lacked gypsum and featured lepidocrocite as the principal authigenic mineral. Kennedy and Hawthorne explained that the cementation was due to acid attack, resulting in the replacement of phlogopite and biotite by jarosite and Mg chlorites, quartz and clay, whereas muscovite reacted to form jarosite and illite or kaolinite.

McSweeny and Madison (1988) examined similar profiles at the 70 year old sulfide roaster waste pile at Mineral Point, Wisconsin. The ores consisted mainly of galena, sphalerite and smithsonite ($ZnCO_3$). Iron bearing minerals were converted to the magnetic state for separation; metallic oxides were recovered leaving wastes consisting of about 30% Fe and 15%S as sulfides, plus minor constituents of Al/Fe oxy-hydroxides, along with quartz, siderite, barite and dolomite. The 6m high waste pile has undergone oxidation reactions producing pH conditions of <2.5. Precipitation reactions have produced a hardpan at 0.5-1m depth, consisting of jarosite ($KFe_3(SO_4)_2(OH)_6$), natrojarosite ($NaFe_3(SO_4)_2(OH)_6$), ferrihydrite, kalinite ($KAl(SO_4)_2.11H_2O$), alumino-copiapite ($(Al,Mg)Fe_4(SO_4)_6(OH,O)_2.20H_2O$) and on exposure precipitated rozenite ($FeSO_4.4H_2O$) and melanterite ($FeSO_4.7H_2O$).

It is however the Heath Steele tailings dams in New Brunswick and the Waite Amulet dam near Noranda, Quebec, that have been examined extensively for both mineralogical and hydrological attributes, environmental effects and remediation (Boorman and Watson, 1976; Blowes et al. 1987; Blowes et al. 1988; Blowes and Jambor, 1990; Jambor and Blowes, 1990; Blowes et al. 1991; Yanful and St-Arnaud, 1991; Blowes et al. 1992; St-Arnaud et al. 1989). It is through these studies that hardpans were identified and characterised fully.

Boorman and Watson (1976) where the first to observe and identify hardpans in tailings at Heath Steele. These tailings were first deposited at the Heath Steele site in 1957 and contain 85wt% sulfide minerals, 1-3wt% carbonate and 12-14wt% aluminosilicates. The older 40ha impoundment is 0.5-8m deep and was used during 1957-1965. A second impoundment 200ha in area was commissioned in 1965 and has been used until present, excluding 1982-1989 when the mine was shut down. The principal sulfide mineral is pyrite with much lesser amounts of sphalerite, chalcopyrite, pyrrhotite and galena and traces of magnetite, arsenopyrite, cassiterite and tetrahedrite (Boorman & Watson, 1976). The principal gangue minerals are quartz, chlorite, siderite, calcite and dolomite (Chen and Petruk, 1980). Boorman

and Watson examined the old tailings dams and observed 4-10cm thick hardpan at 40-60cm depth, consisting of brown stained cemented tailings which separated a zone of leached tailings from fresh tailings below. The cements were tentatively identified as iron oxides (hydroxides) and gypsum. Attempts to identify the cements by X-ray diffraction were unsuccessful, suggesting they are amorphous iron hydroxides. Boorman and Watson also observed large increases in Cu and Zn levels within the hardpan and discussed the cementation of copper as covellite on pyrrhotite, galena, chalcopyrite and sphalerite in that order.

Blowes et al. (1987) re-examined the profile in the Heath Steele tailings dam and observed little or no change in the profile structure, suggesting the hardpan was limiting the movement of the oxidation front down the profile. The main cements were believed to be melanterite ($FeSO_4.7H_2O$) and ferrosic hydroxide ($Fe_3(OH)_8$), on the basis of equilibrium calculations. The upper oxide zone was also investigated using equilibrium calculations which indicated pore waters exceeded saturation levels with respect to $Fe(OH)_3$ and jarosite.

Further reviews of the Heath Steele tailings impoundment by Blowes et al. (1988), Blowes and Jambor (1990), Jambor and Blowes (1990), Blowes et al. (1991), Yanful and St-Arnaud (1991), and Blowes et al. (1992), indicated that the position of the hardpan remained essentially unchanged and mineral analysis indicated the main secondary mineral cementing the hardpan was a combination of gypsum and melanterite, with little influence by Fe^{3+} minerals. These cements precipitated 20-30cm below the active oxidation zone in a continuous layer.

During the same period, examination of the Waite Amulet tailings dams in Quebec showed what was described as the preliminary stages of hardpan formation (Blowes et al. 1991), . The operations at this site started in 1929 with final closure in 1962 , after mining 10 separate ore deposits. The tailings, rich in sulfide minerals (from 30-90% depending on the ore body), were deposited in a 41ha tailings dam, 2-15m deep. Tailings mineralogy was principally pyrite and pyrrhotite with magnetite, quartz, chlorite, muscovite, K-feldspar, plagioclase, pyroxene and talc. Unlike the hardpans observed at Heath Steele the mineralogy of the Waite Amulet hardpan consists of Fe^{3+} minerals including lepidocrocite (γ-FeO.OH), ferrihydrite and goethite (α-FeO.OH), with lesser jarosite and gypsum. These cements were not localised at a certain depth, but rather occurred between 10 and 100cm depth within the oxidised zone, as thin (1-2cm thick) laterally discontinuous layers (Blowes et al. 1991).

More recent examinations of the mine/mill waste dump from the Topeka Mine, near Central City, Colorado, also revealed the presence of cements (Whitney et al. 1995). The waste pile contains both mine (tens of centimetres) and mill (submicrometres) waste and is very heterogeneous. The gold and silver ore was hosted in rocks composed of quartz, plagioclase, hornblende and biotite, along with a sulfide mineralogy of pyrite, sphalerite, galena, chalcopyrite and bornite. The Topeka mine effectively ended production of gold ore in 1913 and at the time of the study the waste dump had a minimum age of 81 years. The examination revealed 4 alteration zones: a predominantly unaltered surface zone, a

leached zone 1-3m depth, below which a 1-2m thick cemented zone caps the unaltered waste. The cements consist of copiapite ($Fe^{2+}Fe^{3+}_4(SO_4)_6(OH)_2.20H_2O$) and coquimbite ($Fe^{3+}_2(SO_4)_3.9H_2O$). Copiapite and coquimbite are highly soluble and normally precipitate from fluids with pH = 0.8-1.5 (Nordstrom et al. 1979). The cemented zone varies in thickness and in some places appears to occur in discontinuous pods or lenses. Adjacent to the cemented zone, jarosite and gypsum have precipitated on and around grains of primary waste rock, indicating less extensive alteration and higher pH than in the cemented zone. SEM investigations showed that the Fe sulfates have precipitated after the gypsum, while leaching studies indicated that the cements are enriched in Fe, Al, Cu, Zn and Mn.

A review has also been undertaken to assess the occurrence and importance of impermeable layers in tailings heaps in the United Kingdom (Merrington and Alloway, 1993). Two heaps were selected, the tailings at the West Chiverton Pb-Zn-Cu mine in Cornwall and the Frongoch Pb-Zn mine in Mid Wales. The mines were reworked in the 1920s after the cessation of their main periods of economic production in 1885 and 1908 respectively. The local rocks at West Chiverton consist of soft, shaly slates that alternate with hard sandstone, grit and fine conglomerate, while at Frongoch grey or greensih shales, flags and mudstones persist. The gangue mineral at both mines is quartz.

Examination of the tailings heaps revealed significant accumulations of Pb, Zn, Cd and Cu relative to the bulk tailings. Concentrations were due to the accumulation of fine sulfide particles (galena and sphalerite) in fine grained, impermeable and reduced layers. The base and top of these layers are characterised by Fe oxide cements.

Hardpans have also been observed in the Canadian Malartic impoundment, in Northwestern Quebec (Tasse et al. 1997). The base of the impoundment contains mildly reactive tailings associated with Au extraction (Malartic tailings), the top is covered by strongly reactive, sulfurous tailings produced from Cu-Ni extraction (Marbridge tailings). Malartic hardpans were recognised below 50-60cm depth and were continuous throughout. Where the Marbridge tailings were exposed, hardpans had formed at approximately 70cm depth. The hardpans formed of Fe oxyhydroxides are limited laterally, while sulfate (gypsum) hardpans are more continuous.

1.4.2.2 Review of Hardpan Genesis

Of the examples discussed in detail in the previous section, there is general agreement that hardpans are related to pH/Eh changes in the tailings profile. All of the reviewed studies recognised the oxidation reactions, acid generation and subsequent neutralisation reactions that commonly take place within the tailings environment. Additionally, leaching of by-products from the surface oxidation zone down the profile and their subsequent concentration as cements were also identified.

The observations at the Sherridon and Farley tailings impoundments led the authors to suggest that the extent of hardpan formation was dependent on sulfide content and availability of K- and Fe-bearing gangue minerals. The Sherridon tailings contained 20-25% sulfide minerals and abundant phlogopite

and biotite, resulting in an extensive hardpan. Farley tailings have comparatively less sulfides (10%) resulting in a thinner hardpan (Kennedy and Hawthorne, 1987).

McSweeny and Madison (1988) suggested precipitation of secondary minerals at Mineral Pt, Wisconsin, was due to pH variations, degree of oxidation, moisture content and solution composition. They also suggested that irregularities in inter-aggregate pores due to random packing were probably the initial site for precipitation. The occurrence within the hardpans of secondary minerals of different solubility was explained by variations in moisture content and a distinct bimodal pore pattern within the waste. Inter-aggregate cements of Fe oxy-hydroxides and hydroxides were suggested to form from redistribution of overlying weathering products produced under saturated conditions. Intra-aggregate cements of jarosite developed through similar processes but under slightly more acidic conditions due to their close proximity to sulfide grains.

Blowes et al. (1991) made an extensive review of the Waite Amulet and Heath Steele hardpans, and compared them with similar studies by Kennedy and Hawthorne (1987) in Manitoba and McSweeny and Madison (1988) in Wisconsin, and suggested that there are at least two types of hardpan. The first type encompassed hardpans which develop at the depth of oxidation and contain Fe^{3+} minerals eg. jarosite, goethite and $Fe(OH)_3$. Within this group they included the Waite Amulet, Sherridon, Farley, and Mineral Pt hardpans. The second type of hardpan is that found at the Heath Steele site, where the hardpan developed 20 to 30 cm below the active zone of oxidation and cements consist of Fe^{2+} minerals, principally melanterite, along with gypsum.

They attributed the difference between the hardpan types to sulfide content, where the Heath Steele's high sulfide content developed low pH and near-surface reducing conditions. Because of the high sulfide content of the tailings atmospheric oxygen is rapidly consumed at the tailings surface. The presence of the high pyrite content also limits Fe^{3+} concentrations by rapid reduction to Fe^{2+} (as per equation 1.2) The degree of saturation with respect to Fe^{3+} oxy-hydroxide and hydroxide minerals is limited by their high solubility at low pH. These effects limit the formation of Fe^{3+} sulfate and oxy-hydroxide minerals, as a result Fe^{2+} and SO_4 concentrations increase and approach saturation with respect to melanterite as the water moves down the profile and the pH increases. At both Waite Amulet and Heath Steele hardpans developed at depths where pH increased. This increase in pH enhances the precipitation of Fe^{3+} hydroxide minerals when there is an abundance of Fe^{3+}, and also enhances melanterite precipitation when Fe^{3+} is reduced to Fe^{2+}.

These explanations are not dissimilar to Boorman and Watson's (1976) suggestions for hardpan formation at Heath Steele, although they encompassed the precipitation of ferric hydroxide rather than Fe^{2+} minerals within the cements. They considered the depth at which the hardpan developed was dictated by the availability of oxygen for bacterial activity. Rather than oxygen concentration being low and dictated purely by sulfide oxidation consumption, they attributed the low permeability of the tailings as a limiting factor. They suggested that oxygen was consumed within the first few centimetres of

tailings with initial concentrations not sufficient to support the regeneration of Fe^{3+}. Under these conditions, the solubility of Fe^{2+} is less than that of Fe^{3+} and precipitation of Fe occurs from the Fe-saturated solution to form a hardpan of Fe^{3+} oxides and hydroxides.

Whitney et al. (1995) discussed a scenario for the formation of the cemented layers at the Topeka Mine dump which are composed of highly soluble Fe sulfate minerals. The authors proposed a number of steps for hardpan formation:

1) water enters the surface during summer thunderstorms or snow melt, only moistening the upper waste. At the surface, drying is rapid and oxidation of surface material cannot be achieved, thus a predominantly unaltered sulfidic layer is preserved.

2) a below surface zone becomes periodically saturated with oxygenated fluids, allowing oxidation of the sulfides

3) descending fluids transport soluble by-products down the profile

4) at a certain depth determined by fluid volume, oxygen content and rates of evaporative concentration, the fluids become super-saturated and precipitate secondary minerals

5) this layer of secondary minerals becomes a retardant to subsequent fluid flow, grows thicker and prevents fluid flow to deeper levels.

When cemented layers were first observed in the Brukunga Pyrite Mine in 1994, their formation was suggested to have occurred in response to varying conditions occurring during the chemical evolution of the tailings (Agnew, 1994). The initial development of minor cemented layers may have formed in response to capillary rise associated with a shallow water table, during the final stages of deposition of tailings, and the fluctuations of water associated with this. During the first few years after mine closure, seepage from the dam toe was pumped to the surface of the dam, providing additional solute loads for cement development through capillary rise from a shallow water table.

Another option suggested for Brukunga was that minor cements originally developed at the plane of "zero flux", once the water table had dropped after the deposition of tailings was completed. Hillel (1971) explains that in the field, the process of evaporation hardly ever occurs independently of other processes. In general, the beginning of evaporation follows wetting, at the end of which the typical moisture profile (in the absence of a high water table condition) consists of a wet layer overlying relatively dry soil beneath. Under such conditions, two processes may be occurring simultaneously: (1) evaporation at the surface, which induces upward flow, and (2) redistribution, or internal drainage, by which water moves downward in response to gravitational and suction gradients within the deeper part of the profile. The balance between the processes occurring at the plane of zero flux would induce the precipitation of relatively soluble salts and then eventually insoluble sulfates and oxy-hydroxides.

The initial cemented layer may also have developed in response to textural changes. Whatever the origin, the development of a perched water table would enhance the formation of cemented layers over

time. This process may be still occurring today, resulting in the development of a more impervious layer to both water and oxygen, thus reducing movement of the oxidation front.

Various origins were postulated for the cemented layers observed in the West Chiverton and Frongoch tailings (Merrington and Alloway, 1993). Variations in depositional conditions have resulted in fine silt and clay size tailings deposited between coarse tailings. The fine-grained layers are suggested to be more impermeable, resulting in reducing conditions due to persistent water logging. Thin Fe oxide crusts have formed at the top and base of these layers at the interface between the fine-grained reducing conditions and the oxidising conditions of the coarse-grained tailings. These crusts may further seal the silt layers, promoting the development of a perched water table. Absorption and coprecipitation of metals in these Fe oxides would explain the increased concentrations of Cd, Zn, Pb and Cu in the upper Fe rich layers.

The Malartic hardpans are thought to have formed early after impoundment closure, when alteration was very active. Tasse et al. 1997, explained that along water flow paths, centimetre scale variations in Eh, pH, P_{CO2} and ion concentration redefine the ion speciation and the equilibrium condition of the mineral phases. Precipitation of secondary minerals can be so extensive, as to cement the tailings, resulting in hardpan formation.

1.4.2.3 Review of Permeability and Diffusion Results and Environmental Implications

All recent studies which have reported the presence of discrete, geochemically precipitated layers, propose a decrease in the movement of oxygen and dissolved metals through the tailings and a consequent moderation of the severity of the environmental effects. Boorman and Watson's (1976) initial review of the Heath Steeles tailings impoundment reported vertical hydraulic conductivities of $1.1\text{-}3.14\times10^{-4}$ and $<4.72\times10^{-5}$ cm/s horizontal conductivity for the surface of the tailings but failed to review the actual hardpan permeability. They discussed the benefits of the hardpan with reference to decreases in the level of the more toxic heavy metals (Cu and Zn in particular), by incorporation into the cements thus reducing their release into the surrounding environment. However, they also indicated that metal concentrations remained unacceptably high in seepage from the underlying tailings.

When discussing the permeability of the hardpans observed at Sherridon and Farley tailings impoundments, Kennedy and Hawthorne (1987) noted that, although the hardpan was an order of magnitude more impermeable than other tailings, it was doubtful that it could completely seal the underlying tailings to groundwater percolation. A subsequent laboratory study of hardpan samples from the Sherridon mine was undertaken by McGreger and Kamineni (1992). Falling head permeameter tests indicated saturated horizontal hydraulic conductivity ranged from 5.7×10^{-6} to 5.6×10^{-5} m/s and vertical hydraulic conductivity ranged from 3.4×10^{-7} to 5.2×10^{-5} m/s. In general, for each sample tested, horizontal hydraulic conductivity was slightly greater than the vertical hydraulic conductivity due to

horizontal layering of the hardpans. It was noted that the hydraulic conductivity values determined in this study were within the range of values calculated in previous tailings permeability studies ($1.1x10^{-6}$ and $7.9x10^{-7}$ m/s). It is uncertain whether these results are for cemented or non-cemented tailings. They indicated the permeability results were within the range calculated for a sandstone or unconsolidated material ranging from glacial tills to clean sand. No permeability measurements of the original tailings were presented.

McSweeny and Madison's (1988) study of the Mineral Pt. Wisconsin roaster pile, discussed the benefits of hardpans but did not report oxygen or permeability measurements of the site. They did, however, discuss the importance of hardpans for developing reclamation strategies because they may form effective barriers to significant transport of pollutants to groundwater.

Blowes et al. (1988) review of the Heath Steele tailings impoundment compared permeability of the old and new tailings surfaces, using a rising head response test. This method is biased towards horizontal hydraulic conductivity. The vertical conductivity was expected to be somewhat slower. The old tailings surface produced hydraulic conductivity's between $2x10^{-6}$ to $2x10^{-5}$ cm/s, with an average of $3.7x10^{-5}$ cm/s. The new tailings hydraulic conductivity was between $5x10^{-7}$ to $1x10^{-4}$ cm/s an average of $4.5x10^{-5}$ cm/s, indicating that the conductivities of the old and new tailings are similar. No direct measurement was conducted on the hardpan at 35-50cm depth.

During the Blowes et al. (1988) study, the emphasis again concerned the benefits of metal incorporation but also, extrapolated CO_2 profile measurements suggested the hardpan layer restricted the movement of gases and pore water in the vadose zone. A comparison with Boorman and Watson (1976) study indicated that the pore water chemistry, including pH, EC and distribution of dissolved constituents had remained relatively unchanged for the period 1976-1986. They concluded that the hardpan layers would remain in place as long as sulfide oxidation continued to generate high concentrations of Fe^{2+} and SO_4. They proposed that the hardpan layer was an important factor in controlling the rate of geochemical evolution of the tailings. However they anticipated that the tailings would ultimately oxidise to a depth at or near the water position over a prolonged period of time.

In the comparative study between hardpans found at the Waite Amulet and Heath Steele tailings dams, Blowes et al. (1991) reported that the data from the Heath Steele impoundment supported the speculations of Boorman and Watson (1976) on Heath Steele, Kennedy and Hawthorne (1987) on Sherridon and Farley, and McSweeny and Madison (1988) on Mineral Pt. that hardpans had the potential to restrict both the transport of dissolved metals and the diffusion of gaseous oxygen into the tailings. Oxygen concentration profiles in the Heath Steele impoundment indicated that oxygen decreased abruptly from atmospheric concentrations of 20.9% at the surface to less than 0.1% within the upper 20cm of the tailings, indicating the present depth of oxidation. Thus, at that stage the hardpan at 35-50cm depth was not acting as an oxygen barrier. The effectiveness of the layer as a gas diffusion barrier was investigated further, utilising pore gas CO_2 concentrations present through dissolution reactions of

carbonate minerals. Below the hardpan, CO_2 levels were 60% of the total gas phase, while above the hardpan CO_2 levels were reduced to 15% of the total gas phase. This suggested that CO_2 diffuses very slowly through the hardpan and into the overlying tailings, suggesting the hardpan is reducing the upward movement of CO_2.

The gas diffusion coefficient of the upper 30cm of uncemented tailings was estimated using the empirical relationship of Reardon and Moddle (1985), which indicated diffusion coefficients of between $6.5x10^{-8}$ and $3.8x10^{-6}$ m^2/s, while the hardpan was $1.3x10^{-8}$ m^2/s. Thus the hardpan was estimated to have diffusion coefficient approximately two orders of magnitude lower than the uncemented tailings. The study further considered the influence of varying diffusion coefficients on the time to completely oxidise the tailings, using the model of oxidation in pyritic wastes (Davis and Ritchie, 1986). Using the diffusion coefficient and porosity of the uncemented surface tailings, the time to oxidise the upper 1m of tailings was calculated to be 150 years. However using the hardpan parameters and modelling a hardpan existing at 25-40cm depth, the estimated time to oxidise the upper 40cm was increased to 300 years. The authors concluded that the lack of change in mineralogy and geochemistry over a 10 year period, the CO_2 profile and calculated diffusion coefficients and reduced levels of SO_4 production over time are a result of hardpan formation which is an effective barrier to oxygen and water.

Oxygen and CO_2 concentrations were also determined at the Malartic tailings impoundment (Tasse et al. 1997). Oxygen profiles showed a rapid decrease in concentrations, with the O_2 concentration terminating at the depth of the observed hardpan, while CO_2 generated at depth has accumulated beneath these hardpans suggesting the hardpan is acting as a CO_2 diffusion barrier. Additionally trace metals derived from leaching and alteration diminished in concentration along flow paths toward the saturated zone, due to adsorption, precipitation and/or coprecipiation. Gas evidence (CO_2 and O_2) combined with geochemical analysis suggests that oxidation rates are considerably reduced by the presence of hardpans composed of sulfate.

As part of a field evaluation of sulfide oxidation rates by Elberling et al. (1993), hardpans at Falconbridge East Mine, Ontario were investigated to determine their impact on the overall rate of oxygen flux into the tailings. They discussed the low permeability of the hardpans observed by Blowes et al. (1991), and explained that this could lead to a storage of infiltrating water above the hardpan in periods of high infiltration. If the base of active oxidation coincided with the top of this saturated zone, the overall oxidation rate would also be impeded. Elberling et al. (1993), combined these observations with those made previously by Boorman and Watson (1976) and Blowes et al. (1991) and suggested that the formation of hardpans may be as important as a fine-grained top layer in the control of the overall oxidation rate when the active oxidation front is close to the hardpans.

Whitney et al. (1995) reported that the cements produced at the Topeka Mine were highly water soluble metal-bearing sulfate minerals. The main concern at this site was the remediation strategies, which included moving the dump. Whitney et al. (1995), reported that after 81 years of exposure the by-

products of oxidation had not been flushed from the dump, but had been concentrated at a depth of 1-2m. Suggestions regarding the excavation and movement of the dump were not supported, as the soluble Fe sulfates could be exposed directly to rainfall and snow melt, resulting in the release of heavy metals. Thus again the cements were considered valuable in reducing the impact on the surrounding environment.

It has been suggested that the cements at the Brukunga Pyrite Mine may reduce the environmental impact by several mechanisms (Agnew, 1994). Modelling of the tailings evolution using the Davis and Ritchie (1986) method, indicated that over the 22 years of exposure the cemented layers may have reduced the movement of the oxidation front down the profile. Modelling suggests the oxidation front position after 22 years would be at 5.9m, while in the coarse-grained section of the dam the oxidation front is only at 1.5-2m depth. It was further noted that the cement coating on residual sulfides in the cemented zone had reduced acid generation and element liberation. Additionally, the ability of the secondary minerals to scavenge the liberated elements reducing elemental loadings in water and soils was noted.

Similarly the enrichment zones observed in the West Chiverton and Frongoch tailings were regarded as acting as temporary sinks for heavy metals. Merrington and Alloway (1993) explained that if the impermeable layers were broken up for some reason, metal release would occur. Sulfide oxidation would be enhanced and leaching of soluble metal species into the local drainage system would occur.

1.4.2.4 Review of Previous Laboratory Experiments to Develop Hardpans

Since hardpans were observed developing naturally in tailings dams, several authors have proposed mechanisms to enhance and accelerate their formation. Blowes et al. (1991) proposed enhancing the formation of these layers through the selective layering of tailings during the late stages of deposition. They observed the coincidence of the hardpan layer development with the depth of the first appearance of solid phase carbonate content and increased pH levels at the Heath Steele and Waite Amulet tailings dams and suggested a buffering link. They proposed addition of carbonate buffering material during the late stages of tailings deposition to moderate the pH of the near-surface tailings water and stimulate the formation of hardpan layers. It was also suggested that mixing of carbonate minerals with tailings generated near the end of the mine life may be economically feasible as a method of arresting the generation of low pH waters and the attendant deleterious environmental effects.

Blowes et al. (1994b) further discussed the idea in the general context of hardpan development, but no laboratory or field experiments appear to have been undertaken by them. Chermak and Runnells (1995), however, have undertaken laboratory column experiments using acid generating overburden material with an added surface amendment of limestone and/or lime. Eight columns were used in the experiment combining different quantities of lime, limestone, oxide waste, waste rock and sodium hydroxide. After construction, one inch of simulated rainfall was added periodically and allowed to drain.

Water was added 26 times at irregular intervals between August 1994 to July 1995. Upon completion, 2 columns were dismantled for mineralogical analysis, while the remainder were utilised during permeability testing. Results indicated that the limestone and/or lime reacted with the acid rock, initiating the precipitation of a hardpan layer of gypsum and amorphous iron oxy-hydroxide at the surface. Permeability was measured using the falling head permeameter technique. Results indicated that it was critical that the sulfide overburden and limestone (and/or lime) to be in direct contact to allow reactions to occur and cause hardpans to develop. These hardpans significantly reduced the effective permeability from $1.3x10^{-4}$ to $1.4x10^{-3}$ cm/s in controls columns to $2.8x10^{-7}$ to $7.8x10^{-7}$ cm/s in the hardpan induced columns.

Prior to this laboratory work, Ahmed (1991, 1994, 1995) had studied the development of hardpans through electrochemical and chemical additives. Ahmed (1991) reported an electrochemical control method to prevent AMD, in which tailings can remain unoxidised by coating with secondary minerals. The concept of growing an adherent and protective asphalt film on the sulfide mineral surface was also described.

Ahmed's later work (1994, 1995) concentrated on the development of hardpans in pyrrhotite tailings. Attempts were made to grow hardpans in columns, and to determine the effects of sulfide oxidation in air, Fe^{2+} treatment, humidity, pH and water coverage, on hardening and acid formation. He concluded that pyrrhotite hardpans can be prepared on a small scale by surface chemical treatments with Fe^{2+} under controlled pH, moisture and oxygen supply. The hardpans can also be made by cathodic treatment. Ahmed also surmised that the hardpans formed as a result of oxidation of absorbed Fe^{2+} to Fe^{3+} on FeS surfaces and the precipitation of oxyhydrates in the intergranular spaces. Ferric oxyhydrates then appeared to consolidate into a hardpan on aging. As a result of the study, it was suggested that under field conditions, existing tailings could be treated with minimal Fe^{2+} to prevent air oxidation and the tailings could then be topped with hardpan. The Fe oxide in the hardpan would require further stabilisation by converting to a less soluble state. For new tailings, Fe^{3+} could be added in low concentrations followed by hydrolysis to produce enhanced hardpans.

Ahmed (1995) reported on the stability of chemical and electrochemically developed hardpans produced from pyrrhotite tailings. Two types of hardpan were identified. A grey variety represented the fully reduced form containing Fe^{2+} in solid phase, developed by treatment of Fe^{2+}, but not oxidised during the experiment. A reddish brown variety represented full surface oxidation of FeS, to Fe oxide with a goethite structure, fully covering the FeS grains. Several intermediate types were also observed depending on the degree of oxidation and goethite coverage. The fully oxidised and fully reduced forms were found to be chemically stable in air, while intermediate forms tended to react with moist air producing surficial jarosite. With the exception of the densely formed hardpan produced by electrochemical methods, all hardpans underwent hydrolysis reactions on contact with water, forming loose Fe oxyhydrate precipitates. As a result of this study, Ahmed (1995) suggested hardpan stability could be greatly improved by making dense hardpans with well-developed goethite structures. Again

reference was made to further converting Fe oxide surfaces into less soluble compounds such as silicates.

The most recently published work on enhanced hardpan development is the Self-Sealing/Self Healing Barrier (SS/SH) technology based on microscale properties of diffusion and chemical reactions (McGregor, et al. 1997). This process occurs through precipitation reactions at the boundary between two materials. The precipitation reactions produce a concentration gradient which leads to the diffusion of additional reagents until the pore spaces between the materials are completely filled. If the barrier is damaged the parent material will react again, sealing/healing the barrier.

1.4.2.5 Review of Field Experiments to Develop Cements

The Self Sealing/Self Healing (SS/SH) barrier concept has been tested at the Falconbridge East Mine tailings impoundment located in Falconbridge, Ontario (McGregor, et al. 1997). A 100m^2 field plot was constructed to determine the effectiveness of the barrier in reducing gas diffusion and water infiltration. Pore gas measurements showed a marked decrease in oxygen concentration below the barrier and an increase of up to 17% CO_2 in this same region. Calculated diffusivities of the pore gas oxygen suggest the barrier is less than 1/1000 that of the overlying tailings due to the water saturated conditions produced. The average vertical hydraulic conductivity was determine for the barrier as 3.6×10^{-8} cm/s while the surrounding tailings were 3.9×10^{-4} cm/s. These preliminary results indicate that SS/SH barrier is retarding pore gas diffusion and groundwater flow into the tailings (McGregor et al. 1997).

Only one other reference could be found on the development of hardpans in the field. Blight et al. (1981) discussed measures (including cement formation) being undertaken to prevent air and water pollution from the abandoned tailings dams in the Witwatersrand, South Africa. In the area investigated, the gold mines have largely been worked out and abandoned and the area now consists of urban and industrial developments. The methods being used to minimise environmental impacts are essentially geotechnical and include construction of catchment walls and dams, terracing of slopes to minimise erosion and stabilisation of surface using cement and lime to prevent wind and water erosion.

Blight et al. (1981) suggested that much of the difficulty with revegetation on the top surface of the dam had arisen because of the unstable nature of the tailings which enabled wind action to undermine root systems. For this reason it was decided that stabilisation trials would be set up using Portland cement and slaked lime. A series of large test panels 30 x 5m, stabilised to a depth of 150mm were laid out using 2%, 3% and 4% by mass of both lime and cement. The panels were subsequently moisture-cured for 6 days using water sprays. The erosion resistance was assessed using a portable erosion test that directed a 0.8mm diameter jet of water at the surface from a distance of 25mm. The pressure was increased until the surface was broken. Portland cement appeared more effective than lime in the early stages, with the optimal addition of 3%. Four tailings dams have been cemented using this technique and show natural revegetation by wind blown seeds.

1.5 Research Objectives

1.5.1 Aim

The aim of this research project is to firstly obtain an understanding of the physical and chemical characteristics of tailings residues which support the in-situ formation of cemented layers and hardpans in typical Australian climatic conditions, and secondly to investigate the promotion of hardpan formation to inhibit Acid Mine Drainage (AMD) and pollutant generation. In achieving this overall aim there are two main strategies:

-Through laboratory and field studies gain and understanding of the conditions for formation of cemented layers/hardpans.

- Ascertain parameters to hasten their formation in tailings dams and to increase impermeability so as to inhibit AMD and contaminant generation.

1.5.2 Research Methods Employed

These strategies were accomplished through observing in nature the development of secondary minerals in tailings as by-products of AMD, and the subsequent production of surface hardpans and cemented layers within tailings. Questions addressed included:

a) How do hardpans form? Does the position of formation correspond to textural variations, present or previous water levels and/or oxygen/water penetration, and

b) What conditions promote hardpan formation, eg geology, climate, groundwater salinity?

c) Can the formation of hardpans and cemented layers be promoted so as to decrease oxygen/water penetration and thus AMD generation?

Laboratory experimentation was undertaken to determine the necessary conditions. During these experiments it was possible to determine the mineralogical and geochemical properties of the secondary products in relation to the effects of weathering and AMD generation.

The program was divided into:

- Stage 1 : Review of relevant literature on both hardpan formation and AMD generation in mine waste.
- Stage 2 : Review of mine sites and operations and selection of relevant sites.
- Stage 3 : Field Studies.
- Stage 4 : Laboratory Studies.
- Stage 5 : Collation, interpretation and presentation of results.

Chapter 2 : Site Investigations

2.1 Site Selection

Twelve sites throughout Australia were selected for investigation on the basis of commodity, sulfide and gangue mineralogy, sulfide content and climate, all of which determine the nature and extent of hardpan formation (Fig 2.1). Comparisons between sites have been made to investigate the effects these characteristics have on hardpan development, and at some sites, profiles have been compared annually to determine their rate of evolution.

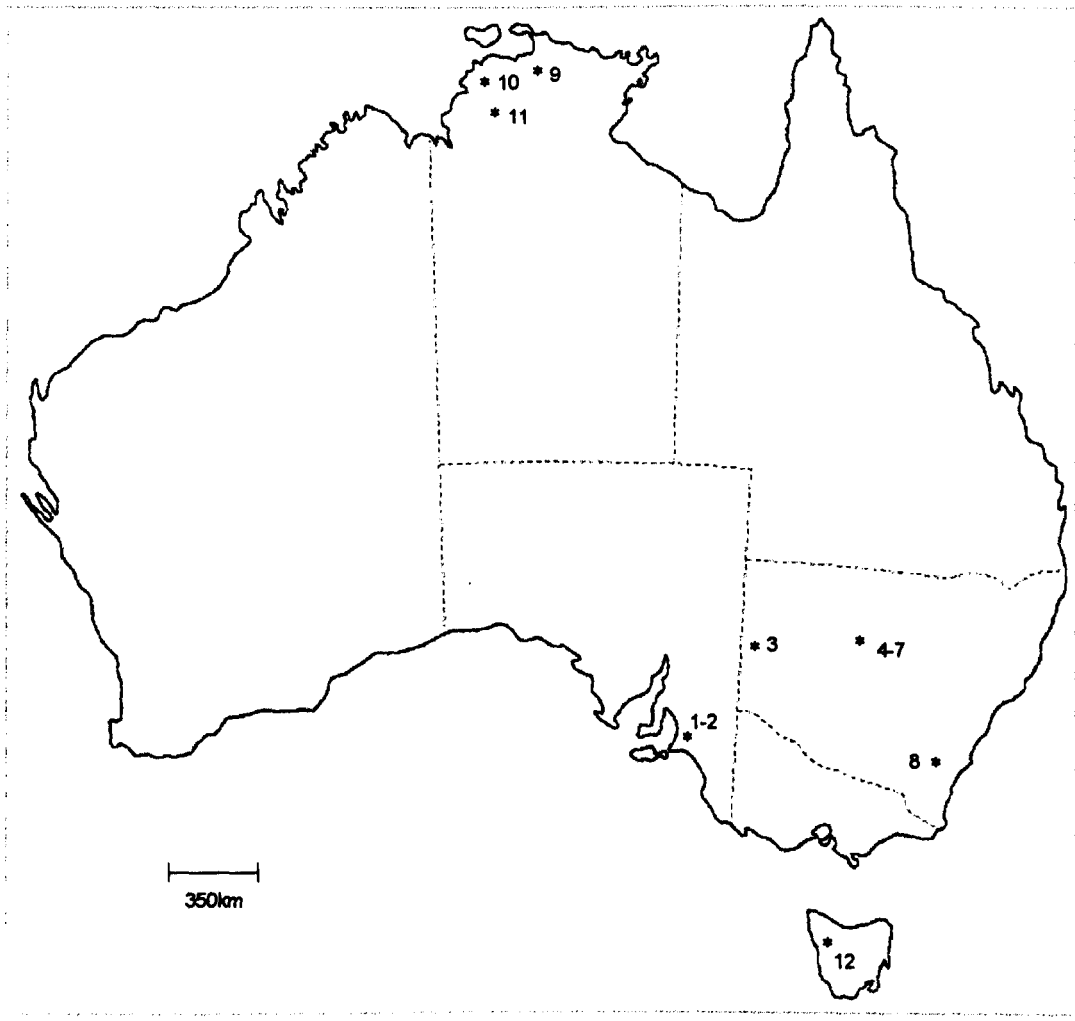

FIG 2.1 MAP OF AUSTRALIA SHOWING LOCATIONS WHERE MINE TAILINGS WERE INVESTIGATED.

Location 1-2 - Brukunga pyrite and Kanmantoo Cu Mines
3 - Broken Hill Mine
4-7 - Cobar : Elura Zn-Pb-Ag, CSA Cu-Pb-Zn, Peak Au and Chesney Au-Cu Mines
8 - Woodlawn Cu-Pb-Zn Mine
9 - Ranger U Mine
10 - Woodcutters Pb-Zn Mine
11 - Pine Creek Au Mine
12 - Renison Bell Sn Mine

2.2 Geology, Topography, Climate, Drainage, Vegetation and Land Usage

2.2.1 Kanmantoo Trough, S.A

Tailings dams at the abandoned Brukunga Pyrite Mine and Kanmantoo Copper Mine were investigated as part of this study. The deposits are situated in the Kanmantoo Trough, a fault controlled basin that developed in the early Cambrian along the eastern and southern Mount Lofty Ranges, S.A. The clastic flyschoid sediments of the Kanmantoo Group underwent deformation, metamorphism and granite intrusion during the Delamerian Orogeny (Sprigg and Campana, 1953).

This region is one of moderate relief, with dissected plateaus and ranges and is under the influence of a warm to temperate Mediterranean climate. Typical conditions consist of long hot dry summers and mild wet winters (Mabutt, 1980). Annual temperatures range from a mean minimum of 7°C to a mean maximum of 27°C. The average annual rainfall is 730 mm/yr (Bureau of Meteorology, 1998). The ranges have direct, co-ordinated drainage within the Bremer Catchment, which eventually drains to Lake Alexandrina (Mabbutt, 1980). They support natural woodlands, rain-fed crops and sclerophyll forests (Learmonth & Learmonth, 1971). This area has a high rural population density of between 10-200 people per square kilometer (Plumb, 1980).

2.2.1.1 Brukunga Pyrite Mine

At the Brukunga Pyrite Mine, pyritic beds were mined as a source of sulfur for the manufacture of sulfuric acid. The major sulfide minerals were pyrite and pyrrhotite occurring as stratiform layers in metamorphosed pelitic sedimentary host rocks. The ore contained 12 vol% pyrite and 6 vol% pyrrhotite, while the waste contained 0-2 vol% pyrite and 10 vol% pyrrhotite (George, 1969). Minor amounts of sphalerite, chalcopyrite, galena and arsenopyrite were also present.

2.2.1.2 Kanmantoo Cu Mine

The Kanmantoo Copper deposit is the largest base metal deposit known in the Kanmantoo Group. The deposit was discovered in 1962, and development of the open cut began in 1970, closing in 1976 because of low Cu prices. Mine production was 4.05Mt of ore averaging approximately 1% Cu, and at least 8 Mt of mineralisation still exists below the abandoned mine (Seccombe et al. 1985). The deposit occurs in a garnet-andalusite-biotite schist, with mineralisation largely as veinlets, layers and disseminations. The dominant ore minerals are chalcopyrite, pyrrhotite and magnetite in approximately equal proportions with lesser pyrite (Both, 1990).

2.2.2 Willyama Block, N.S.W

2.2.2.1 Broken Hill, Pb-Zn-Ag Mine.

The Broken Hill Pb-Zn-Ag deposit is situated in the far west of New South Wales (Fig 2.1). This is an area of low relief with pedimented regions and aeolian landforms. It is arid and hot and has erratic rainfall which drains unco-ordinately, radiating from uplands to separate terminals or to aligned playa lakes (Mabbutt, 1980). Annual temperatures range from a mean minimum of 6°C to a mean maximum of 32°C. The average annual rainfall is 250 mm/yr (Bureau of Meteorology, 1998). The prevailing vegetation is mulga, bluebush, saltbush (chenopods) and other arid shrubs (Learmonth & Learmonth, 1971). The area has a low population density of between 0.03-0.3 people per square kilometre (Plumb, 1980).

Open cut mining was first employed between 1891-1901 in the BHP Mine, and over time both open pit and underground mining have been utilised, with underground mining still taking place today. The complex history of ownership, mining and production is not within the scope of this review, however readers are directed to Van der Heyden & Edgecombe, 1990, and Mackenzie & Davis, 1990.

The main tailings study was undertaken on dams from the southern end of the lode, originally owned by the Zinc Corporation, but currently owned by Pasminco Ltd. The main ore lenses at the ZC mine are hosted by mineralogically variable, clastic and chemical metasediments of the early to middle Proterozoic Willyama Supergroup. This unit ranges from 60-400m thick, and has undergone granulite facies metamorphism. The mine has distinct Pb and Zn lodes, each having a discrete gangue mineralogy, bulk grades of Pb, Ag, Zn and trace metal associations (Mackenzie and Davis, 1990). The sulfide mineralogy includes sphalerite, galena, chalcopyrite, pyrrhotite, arsenopyrite. The gangue mineralogy includes quartz, garnet, rhodonite, manganoan hedenbergite, sillimanite, muscovite, staurolite, gahnite, loellingite, apatite, gypsum, fluorite, feldspars, calcite, almandine, spessartine, tremolite, bustamite, manganoan wollastonite, siderite and trace cubanite, ilvaite, vesuvianite, johannesenite, sulphosalts, chloritoids and pyrosmalite (Plimer, 1984).

2.2.3 Lachlan Fold Belt, N.S.W

The Elura Pb-Zn, CSA Cu-Zn, Peak Au, abandoned Chesney Au-Cu and Woodlawn Cu-Pb-Zn mines, occur within the Lachlan Fold Belt (LFB). The LFB is a major structural unit which forms the south eastern part of the Tasman Fold Belt system, extending from Tasmania to Queensland. The LBF is a complex orogenic belt developed from the Cambrian to Middle Devonian Pre-Cratonic Province and the Early Devonian to Early Carboniferous Cambrian Transitional Tectonic Province. It consists of Carboniferous post-kinematic granites and minor felsic volcanics along with turbiditic sediment, chert, and ophiolite sequences (Suppel & Scheibner, 1990).

The fold belt is extensive and traverses numerous climate regions of varied natural vegetation and human contact. The currently producing Elura, CSA and Peak mines, along with the abandoned Chesney mine are located in central NSW (Fig 2.1). This area has low relief with pediment regions and aeolian landforms. It is semi-arid, generally warm and has uniform light rainfall which drains uncoordinately from uplands to separate terminals (Mabbutt, 1980). Annual temperatures range from a mean minimum of 5°C to a mean maximum of 34°C. The average annual rainfall is 420 mm/yr (Bureau of Meteorology, 1998). The natural vegetation is mulga and other arid shrubs (Learmonth & Learmonth, 1971). The rural population density is low, 0.03-0.3 person per square kilometer (Plumb, 1980)

The mines are within the Cobar Supergroup which was deposited in a series of troughs and basins and on adjacent shelves during early Devonian extension along reactivated basement faults. It consists of a sequence of marine sediments deposited in a trough to the west of a Cambro-Ordivician land mass. This mass consists of metamorphosed turbidites and minor basic volcanics of the Girlambone Group, and is intruded in places by Silurian granitoids. In the Cobar region the Cobar Supergroup is divided into the Nurri Group, which contains the Peak and Chesney deposits, and the overlying Amphitheatre Group which contains the CSA and Elura deposits (Suppel & Scheibner, 1990).

2.2.3.1 Elura Zn-Pb-Ag Mine

The Pasminco owned Elura Zn-Pb-Ag mine commenced production in 1983, and is the northern-most deposit of the Cobar mineral field (43km NNW of Cobar). The host rocks comprise a moderately deformed, turbiditic sequence of mudstone and siltstone with minor (<5%) thin, fine-grained sandstone. The sequence is lithologically equivalent to the CSA Siltstone. Unaltered CSA Siltstone typically contains 35-40% of both quartz and muscovite, 10-15% chlorite, 5% albite, 1-5% calcite and minor pyrite, kerogen, various detrital heavy minerals and biotite (Schmidt, 1990). The ore can be divided into 3 types; siliceous, massive and pyrrhotitic, representing epigenetic replacement (Robertson, 1974, Glen & Pogson, 1985, Glen, 1987, de Roo, 1987) or deformed syngenetic deposits (Gilligan & Suppel, 1978, Sangster, 1979, Marshall & Sangamesthwar, 1982).

2.2.3.2 CSA Cu-Pb-Zn Mine

The CSA mine is an underground Cu-Pb-Zn operation, 11km NNW of Cobar. Although a small amount of ore was mined before 1920, significant production did not commence until 1965. Mineralisation occurs in vein complexes and submassive to massive bodies of pyrite, pyrrhotite, chalcopyrite, sphalerite, and galena, with varying banding and composition. The rocks are thin bedded and rhythmically banded CSA Siltstones and contain fine to medium grained greywackes at irregular intervals. The siltstones consist chiefly of quartz and chlorite with minor muscovite and calcite. They grade from fine-grained quartzite or greywackes at the base to slate, often carbonaceous at the top (Scott & Phillips, 1990).

2.2.3.3 Peak Au Mine

The recently opened Peak Gold mine is situated 8km SE of Cobar. The deposit occurs within the Nurri Group, deposited as a series of fans extending westward from the eastern margin of the subsiding basin. It consists of lithic sandstone and minor conglomerate and siltstone of the Chesney Formation, and is overlain by mudstone and siltstone of the Great Cobar Slate. The deposit occurs in a narrow belt of strong deformation on the eastern margin of the Cobar Basin (Hinman & Scott, 1990).

2.2.3.4 Disused Chesney Au-Cu Mine

The disused Chesney mine occurs within the same sequence, only 2km north of the Peak. The Chesney mine was first discovered in 1887 and first worked for gold (Andrews, 1911). The orebody is a siliceous Cu-Ag deposit, with gossaniferous Au at the surface and chalcopyrite at depth (Mele, 1995). The sulfide minerals include chalcopyrite, pyrite, pyrrhotite, magnetite, sphalerite, galena and arsenopyrite, the gangue includes quartz, calcite and stilpnomelane and the host is chloritic and in part silicified to chert (Rayner, 1969).

2.2.3.5 Woodlawn Cu-Pb-Zn Mine

The Woodlawn mine, also present within the Lachlan Fold Belt, is located within the north trending fault system where the Captains Flat-Goulburn and Hill End synclinal zones merge, in southern NSW. The area has moderate to high relief with dissected plateaus and ranges. It has a warm to temperate, humid climate, with cool winters, and long warm summers (Mabutt, 1980). Annual temperatures range from a mean minimum of 0°C to a mean maximum of 28°C. The average annual rainfall is 630 mm/yr (Bureau of Meteorology, 1998). The uniform rainfall drains directly into Lake George or the Sydney metropolitan water catchment. The natural vegetation includes woodlands and sclerophyll forests, along with rain-fed crops (Learmonth & Learmonth, 1971). The area has a medium population density of 1.2-5 people per square kilometer (Plumb, 1980)

The deposit was discovered in the 1960's, with mining commencing in 1978. The mineralisation is a stratabound sulfide deposit. The primary ore is complex, the dominant sulfide being pyrite, with sphalerite, galena, chalcopyrite common, and minor tennantite, tetrahedrite and arsenopyrite. Much rarer are gold, electrum, pyrrhotite, marcasite, bismuthinite, cassiterite, magnetite and stannite. Gangue mineralogy includes Fe and Mg chlorite, mica and quartz, while barite, calcite, dolomite, siderite and other Fe-Mg bearing carbonates commonly occur (Davis, 1990).

2.2.4 Pine Creek Inlier, N.T

Woodcutters (Pb-Zn), Pine Creek (Au) and the Ranger (U) deposits exist within the Pine Creek Inlier, N.T (Fig 2.1). The inlier encompasses moderate to high relief plateaus and ranges, flanked by low relief pedimented regions. The climate is hot, humid and monsoonal, with warm dry winters and hot wet summers (Mabutt, 1980). Annual temperatures range from a mean minimum of 19°C to a mean maximum of 38°C. The average annual rainfall is 1480 mm/yr (Bureau of Meteorology, 1998). The region has co-ordinated drainage resulting in drainage terminating externally (Mabbutt, 1980). The natural land cover is woodlands (Learmonth & Learmonth, 1971). The rural population density is low with 0-0.03 people per square kilometer with occasional small towns (Plumb, 1980).

The main geological components of the Pine Creek Inlier are the Late Archaean granite basement rocks known as the Namambu Complex, exposed as small domes, an extensive but poorly exposed Early Proterozoic sedimentary sequence of low-medium metamorphic grade deposited in a shallow cratonic geosyncline, late Early Proterozoic rift related felsic volcanics and subhorizontal platform sandstones of Middle Proterozoic age (Needham et al. 1980).

2.2.4.1 Ranger U Mine

The Ranger deposits are located in the NE part of the Pine Creek Geosyncline, 250km east of Darwin. The deposits are hosted by the Early Proterozoic Cahill Formation which overlies the Namambu complex. The lower units of the Cahill Formation host the uranium mineralisation and consist of quartz schists, mica schist, para-amphibolite, calc-silicate and carbonates. Pitchblende is the most common of the primary uranium minerals and is associated with chlorite alteration. Secondary uranium minerals including saleeite, sklodowskite, metatorbernite and gummite are common in the oxidised zone (Kendall, 1990). Drainage from this site flows directly into the Kakadu wetlands.

2.2.4.2 Woodcutters Pb-Zn Mine

The Woodcutters deposit is stratabound and is a transgressive dolomite-silica lode cutting dolomite and dolomitic shales. Mineralisation is thought to have been formed by low temperature hydrothermal remobilisation of metals from syngenetic stratiform pre concentrations (Needham and de Ross, 1990). The main sulfide minerals include pyrite, galena and sphalerite, while gangue mineralogy consists of quartz, muscovite, dolomite, dravite and cerussite.

2.2.4.3 Pine Creek Au Mine

The Pine Creek-Enterprise Au deposit is a large complex saddle reef within the Early Proterozoic metasediments, along a southerly shallow plunging anticline, and is over-printed by a stockwork of inter-reef and fault related quartz veins (Needham & de Ross, 1990). The unoxidised veins are composed of

quartz, ankerite, carbonate, pyrite, alkali feldspar, muscovite, chalcopyrite, galena, sphalerite, pyrrhotite, antimony, bismuth, tetrahedrite, tennantite and arsenopyrite with inclusions of gold, in decreasing order of magnitude (Nicholson & Eupene, 1990). The mine is on the banks of the Pine Creek which runs adjacent to the town of the same name.

2.2.5 Dundas Trough, Tas.

2.2.5.1 Renison Bell Sn Mine

The Renison Bell tin operation is located on the west coast of Tasmania, 10km west of the mining town of Rosebery and 16km east of the town of Zeehan (Fig 2.1). The Dundas Trough landscape is characterised by dissected plateaus and ranges. The area has a warm to temperate climate with cold winters, short mild summers and uniform rainfall (Mabbutt, 1980) which supports temperate rainforest and alpine vegetation (Learmonth & Learmonth, 1971). Annual temperatures range from a mean minimum of 3°C to a mean maximum of 20°C. The average annual rainfall is 2450 mm/yr (Bureau of Meteorogy, 1998). The drainage is co-ordinated and flows to external locations (Mabbutt, 1980). The population density ranges between 0.3-1.2 people per square kilometer (Plumb, 1980).

The Renison Bell orebodies are located within a thick lower Palaeozoic sedimentary and volcanic sequence deposited in the Dundas Trough between 2 blocks of Proterozoic metasediments. The tin mineralisation is associated with Late Devonian granite emplacement (Morland, 1990) and resulted from magmatic hydrothermal fluid migrating from the granite along major faults. Replacement of dolomitic units resulted in the precipitation of cassiterite and sulfides and the formation of talc and actinolite. Mineralisation occurs as massive pyrrhotite with talc, fluorite, siderite, pyrite, galena and sphalerite, or as shears of siliceous ores containing increased arsenopyrite, pyrrhotite and quartz, and lesser tourmaline, stannite, chalcopyrite, pyrite, ilmenite, bismuth, fluorite and apatite (Morland, 1990).

Chapter 3 : Methods

3.1 Overview

This chapter presents a brief overview of the methods utilised during this study and outlines the reasons for their use. The full descriptions of the methods are presented in Appendix 1A.

3.2 Field and Laboratory Sampling

Surface specimens of fresh tailings, hardpans, seepage waters and salts were selected as representative for each site and sampled in air/water-tight containers for transportation.

Field and laboratory sub-surface tailings samples were removed using a soft sediment piston core sampler and rig. Cores were obtained with a jacking device, which forced the sampling tube into the sediment, thereby minimizing sample disturbance. The rig was fastened to the tailings dam surface with screw anchors, or onto columns by means of a bolting system. When appropriately anchored, the jacking device was attached and activated. Core removal through this method allowed cores to be removed from desired depths without needing to remove sediments located above. A combination of thin walled UPVC plastic core tubes and stainless steel core tubes were used. In locations where the soft sediment sampler could not be used because of cemented and hard surfaces, a solid head sampler and stainless steel cores were forced into the tailings using a sledge hammer.

Immediately after sampling, the cores were sealed with putty and rubber bungs for transportation to the laboratory. The seals and bungs held the cores firmly in place reducing sample disturbance and inhibiting reactions with air.

Sediment stratigraphy, bulk density, pH, Electrical Conductivity (EC) and porewater chemistry were determined after extrusion of the cored samples. UPVC cores used for Fe^{2+}/Fe^{3+} determination and Eh measurements were pre-cut and sub-sampled while confined in a glove box filled with argon. Cores in stainless steel tubes were extruded and placed directly into the glove box with minimal atmospheric oxidation.

Gas samples, for determination of CO_2 concentration, were removed from tailings in the field and within laboratory column experiments using a specifically designed gas sampling rod. The rod was forced into the tailings to the desired depth using a sledge hammer. A gas sample was then removed using a syringe and placed immediately into air tight gas vials. The gases were analysed within 2 days of sampling to maintain sample integrity.

3.3 Tailings and Hardpan Colour and Texture Descriptions

Samples were assessed for texture and wet colour (McDonald et al. 1984). Colour was recorded as hue, value and chroma using Munsell colour charts to

- estimate the degree of oxidation and secondary mineralisation
- determine locations of preferential cementation
- outline textural variations, palaeo-surfaces and palaeo-hardpans which may affect the geochemical evolution of the tailings.

3.4 Physical Chemistry

Measurement of pH, Electrical Conductivity (EC) and redox potential (Eh) were carried out in both the laboratory and field to achieve an understanding of the geochemical reactions taking place and the extent to which they were occurring. pH gives an indication of sulfide oxidation, acid generation and neutralisation reactions taking place. Electrical conductivity indicates the concentrations of soluble salts that have been produced by these reactions. Eh gives an indication of the activity of electrons in the tailings porewaters, which gives an insight into the direction the chemical reactions may proceed, i.e. a measure of the oxidation/reduction potential.

3.5 Mineralogy

The mineralogy of the tailings and hardpans was investigated to determine the geochemical reactions taking place at each site. Sulfide oxidation, acid generation, neutralisation and gangue mineral degradation processes could then be determined and their effect on hardpan development and AMD generation concluded.

Mineralogy was investigated by:

X-ray powder diffraction (XRD)

Optical microscope examination and scanning electron microscope (SEM)

HCl - HNO_3 extractions (to quantify sulfate and sulfide concentrations)

3.6 Chemistry

Chemical analyses were carried out to quantify the element concentrations of fresh and oxidised tailings and hardpans. The analyses gave information on the changes in mineralogy and element content. X-ray fluorescence (XRF) was used to determine major and trace element concentrations of the solids (both soluble and insoluble), while Inductively Coupled Plasma Atomic Emisson Spectrometry (ICP-AES) of 1:5 extracts and leachates was used to determine solute concentrations.

Additionally, acid-base accounting was carried out to establish links between acid producing potentials, acid neutralising potentials, hardpan development and solute release. Net Acid Generation determination and H_2O_2 Modified "Acid neutralising capacity" determination were employed for this task.

Investigations of the role evaporation plays in the development of hardpans was investigated through chloride analysis and deuterium isotope analysis.

3.7 Geotechnical Testing

Basic geotechnical investigations were undertaken in order to study the movement of water and gases through fresh tailings, hardpans and laboratory column tests. Tests included:

- Particle Size Distribution
- Gravimetric water content
- Particle Density
- Bulk Density
- Void Ratio and Porosity
- Drainage Suctions Tests to determine pore size ranges
- Permeability Tests
  - Field Falling Head Infiltrometer Tests
  - Disk Permeameter Tests
  - Laboratory Oedometer Tests
  - Laboratory Constant Head Infiltration Tests

3.8 Gas Analysis

Tailings profile CO_2 concentrations were investigated in both the field and laboratory to determine the effect of hardpans on gas diffusivity. Variations in concentrations within the profiles gave an indication of the movement and build up of gases through diffusion processes.

Chapter 4 : Naturally occurring Hardpans and Cemented layers developed in tailings impoundments

4.1 Introduction

This chapter contains observations and descriptions of each of the twelve sites investigated, which have been grouped into metallogenic provinces. The number of visits to each site was dictated by access to the mines and funding restrictions. Thus in many cases only a single site visit was possible, resulting in brief overviews of mineralogy, geochemistry and cementing potentials. However, extensive investigations including 5 site visits or more were possible at Brukunga, Broken Hill, Elura, CSA, Peak and Chesney mines. At these locations a large number of profiles were examined and comparisons on a yearly basis were made.

A summary table is presented at the beginning of each site overview. The discussions which follow, outline the nature and extent of any hardpans or cemented layers developed at each site. This information, along with geochemical analysis (Chapter 5) and laboratory trials (Chapter 6), have been compiled to obtain an understanding of physical and chemical characteristics which effect the development of hardpans or cements in tailings (Chapter 8). Table 4.1 lists selected data for the secondary minerals discussed in this chapter and Chapter 5.

TABLE 4.1 SELECTED CHARACTERISTICS OF SECONDARY MINERALS DISCUSSED IN CHAPTER 4 AND 5.

Mineral	Formula	Crystal system	Appearance
alunite	$KAl_3(SO_4)_2(OH)_6$	rhombohedral	vitreous white, greyish, yellowish, reddish
anglesite	$PbSO_4$	orthorhombic	adamantine/sub-metallic blackish-brown
basaluminite	$Al_4SO_4(OH)_{10}.4H_2O$	monoclinic	translucent white
beudantite	$PbFe_3(AsO_4,SO_4)_2(OH)_6$	rhombohedral	vitreous/resinous black, dark green, brown
bianchite	$(Fe,Zn)SO_4.6H_2O$	monoclinic	vitreous white, yellowish
blodite	$Na_2Mg(SO_4)_2.4H_2O$	monoclinic	vitreous colourless, bluish-green, reddish
boussingaulitite	$(NH_4)_2Mg(SO_4)_2.6H_2O$	monoclinic	transparent colorless, yellowish-pink
boyleite	$(Zn,Mg)SO_4.4H_2O$	monoclinic	earthy white
ferrihydrite	$Fe_{4-5}(OH,O)_{12}$	hexagonal	yellow-brown, dark brown
goethite	α-FeO(OH)	orthorhombic	admantine-metallic/earthy brown, yellow
gypsum	$CaSO_4.2H_2O$	monoclinic	sub-vitrous colourless, white,grey, yellowish, brownish
halite	NaCl	cubic	vitreous colorless, white, yellow, red,blue, purple
halotrichite	$FeAl_2(SO_4)_4.22H_2O$	monoclinic	vitreous colorless, white, yellowish,, greenish
hematite	α-Fe_2O_3	rhombohedral	metallic/earthy grey
hemimorphite	$Zn_4Si_2O_7(OH)_2.H_2O$	orthorhombic	vitreous/pearly white, bluish, greenish, yellowish, brown
hexahydrite	$MgSO_4.6H_2O$	monoclinic	pearly/vitreous colourless, white, pale green
hydrobasaluminite	$Al_4SO_4(OH)_{10}.15H_2O$	monoclinic	white
jarosite	$KFe_3(SO_4)_2(OH)_6$	rhombohedral	sub-adamantine/vitreous yellow, brown
kalinite	$KAl(SO_4)_2.11H_2O$	monoclinic	light blue
lepidocrocite	γ-FeO(OH)	orthorhombic	sub-metallic red, reddish-brown
loweite	$Na_{12}Mg_7(SO_4)_{13}.15H_2O$	rhombohedral	vitreous colourless, reddish-yellow

TABLE 4.1 CONT. SELECTED CHARACTERISTICS OF SECONDARY MINERALS DISCUSSED IN CHAPTER 4 AND 5.

Mineral	Formula	Crystal system	Appearance
melanterite	$FeSO_4.7H_2O$	monoclinic	vitreous green, greenish-blue, blue
mirabilite	$Na_2SO_4.10H_2O$	monoclinic	vitreous colourless, white
natrojarosite	$NaFe_3(SO_4)_2(OH)_6$	rhombohedral	vitreous yellow, brown
pickeringite	$MgAl_2(SO_4)_4.22H_2O$	monoclinic	vitreous colourless, white, yellowish, reddish
rozenite	$FeSO_4.4H_2O$	monoclinic	vitrous white, greenish white
schwertmannite	$Fe_8O_8(OH)_6SO_4$	Tetrogonal	yellow brown
sulfur	α-S	orthorhombic	translucent resinous yellow
sylvite	$K_{0.8}Na_{0.2}Cl$	cubic	white
szomolnokite	$FeSO_4.H_2O$	monoclinic	vitreous yellow, reddish-brown, blue, colourless
thenardite	α-$NaSO_4$	orthorhombic	vitreous/pearly colourless, white
wattevilleite	$Na_2Ca(SO_4)_2.4H_2O$	unknown	white
zinc blodite	$Na_2Zn(SO_4)_2.4H_2O$	monoclinic	colourless

4.2 Kanmantoo Trough, S.A

4.2.1 Brukunga Pyrite Mine

Dam	Only one dam present - valley fill, rock wall, covered with waste rock, soil, sewage sludge, neutralisation sludge and native vegetation.
Original tailings mineralogy	pyrite, pyrrhotite, (sphalerite) quartz, muscovite, phlogopite, albite, anorthite, clinochlore, tremolite, vermiculite, chloroapatite, strengite
Tailings grain size distribution	coarse sand 7-41% silt 7-20% fine sand 46-64% clay 1-4%

Typical XRF analysis of original tailings:

SiO2 %	Al2O3 %	Fe2O3 %	Fe %	MnO %	MgO %	CaO %	K2O %	TiO2 %	P2O5 %	SO3 %
59.2	17.7	6.33	4.33	0.10	3.10	2.48	3.27	0.72	0.13	3.50
S %	Ba ppm	Ce ppm	Co ppm	Cr ppm	Cu ppm	Ga ppm	La ppm	Ni ppm	Pb ppm	Rb ppm
1	2860	105	17	120	55	30	65	40	155	165
Sr ppm	Th ppm	U ppm	V ppm	Y ppm	Zn ppm	Zr ppm				
165	55	20	125	40	530	170				

Hardpan/Cemented Layers/No cements	Cemented layers
Period of exposure	25 years
Hardpan/cement depth in profile	discontinous layers throughout oxidised zone, esp 1-1.4m
Lateral extent of hardpan/cemented layers	Over entire dam depending on water level
Thickness of hardpan / cemented layers	5mm-20cm
Cement mineralogy	gypsum, ferrihydrite, jarosite, alunite, opaline siliceous material
Surface Salt mineralogy	N/A soil/rock/vegetation cover

Typical XRF analysis of hardpan/cements

SiO2 %	Al2O3 %	Fe2O3 %	Fe %	MnO %	MgO %	CaO %	K2O %	TiO2 %	P2O5 %	SO3 %
59.5	15.2	6.53	4.60	0.05	2.80	2.83	3.22	0.63	0.33	2.69
S %	Ba ppm	Ce ppm	Co ppm	Cr ppm	Cu ppm	Ga ppm	La ppm	Ni ppm	Pb ppm	Rb ppm
1.08	2410	75	5	95	40	25	105	25	155	155
Sr ppm	Th ppm	U ppm	V ppm	Y ppm	Zn ppm	Zr ppm				
175	40	15	110	25	40	130				

4.2.1.1 Tailings Dam History

The Brukunga mine site has a single tailings dam located to the east of Dawesley Creek, containing approximately 3.5MT of flotation tailings (EGI report, 1993). The starter dam was built from earth and rock directly onto the natural valley floor. Deposition took place via edge spigots on the perimeter of the dam wall. The spigots were irregularly extended to deposit tailings centrally in the impoundment (B.Bradshaw, pers. comm., 1994). Large grain size variations were produced resulting in predominantly coarse tailings at the front of the dam, with slimes deposited at the back of the impoundment (Agnew, 1994). Blesing et al. (1974) reported 1.4 S% for the tailings occurring predominantly as pyrrhotite, however up to 4% total S was observed by Agnew (1994), mainly as pyrite. The tailings dam has been covered using waste rock, soil and neutralisation sludge. A large portion of the area has been revegetated using native species. Seepage from the tailings dam together with that from the mine benches and waste rock dumps is collected continuously and is treated via a lime slurry neutralisation plant. Neutralised water is released back to the near-by Dawesley Creek, while the by-product sludge is deposited in holding ponds at the back of the dam.

4.2.1.2 Sampling Description

This mine was the focus of a previous study in 1994 (Agnew, 1994) at which time examinations of 7 sites were undertaken. Recent investigations have been restricted to Holes 4, 5 and 7 which occur at the front of the dam and pass through the predominantly coarse grained tailings fraction (Fig 4.1).

4.2.1.3 Tailings Mineralogical Description

At Hole 4, oxidation has taken place down to 1m depth. Oxidation of pyrite is essentially complete within this zone, so that little or no pyrite is present and only secondary minerals formed during this process, along with degraded gangue minerals, remain. Below 1m, cement layers have developed to approximately 1.4m depth below which unoxidised tailings persist.

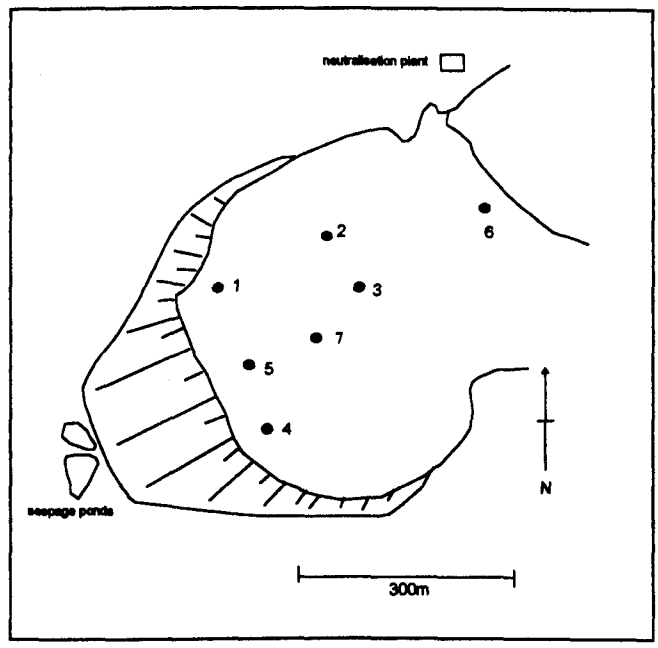

FIG 4.1 MAP OF BRUKUNGA TAILINGS DAM

4.2.1.3.1 Gangue mineralogy

Gangue minerals were found in varying amounts throughout the tailings profile (XRD and XRF analysis). The gangue minerals present in all samples were quartz, anorthite, albite, phlogopite and muscovite, while clinochlore was present in all but a few. Tremolite was found irregularly down the profile, mainly in the deeper levels. Calcite was identified in rocks from the waste rock dump, however was not detected in significant amounts in any of the tailings samples, and may have been already depleted by neutralisation reactions.

4.2.1.3.2 Sulfide mineralogy

Only negligible quantities of pyrite were found within the highly oxidised zone stretching from the surface down to 1.4 m. However, pyrite contents increased sharply directly below this zone and, together with pyrrhotite, was identified in all subsequent samples below this (Sulfide % 1.6-3.5). Sphalerite was also found only below 1.4m with maximum Zn concentrations of 1110 ppm at 3.69-3.76m depth, but was less abundant than pyrrhotite, because of its low concentration in the ore bodies (Zn concentrations of 14-106 ppm within waste rocks (Agnew, 1994)).

4.2.1.4 Secondary Mineralogy and Morphology

The oxidised zone near the surface was marked by the presence of ferrihydrite and jarosite. These secondary minerals were observed, using the SEM, as thick coatings upon grains of gangue material, down to approximately 1m, and were largely responsible for the brown and yellow colors of this zone. Ferrihydrite was not found below 1.4 m except within the basement soil, and jarosite was only detected elsewhere in a palaeo-surface.

Gypsum was also found within the oxidised zone, as well as slightly below 1.4m. It was not in sufficiently high concentrations to be detected by XRD below 1.6 m, but it was often observed in the SEM as a minor constituent of samples at lower depths.

4.2.1.5 Cemented Layers

The cemented layers observed at the base of the oxidised zone exist as numerous thin horizons of approximately 0.5cm thickness. The cement has a reddish brown appearance and forms colloform aggregates and coatings around discrete mineral grains. Iron is the predominant element in this zone although patches of S associated with Fe were detected by SEM/EDX between aggregates and identified as jarosite. Hydrogen, C and O are not detected by EDX but their presence is assumed in association with Fe in the absence of signatures of other expected combinations such as S.

The minerals responsible for cohesion between particles are ferrihydrite, jarosite, gypsum, siliceous material and minor alunite and schwertmannite. Throughout the profiles the morphologies of these cements vary depending on the surrounding grains and the geochemical conditions of the immediate environment. Jarosite and alunite exist as well-developed small rhombohedral crystals which make up

the bulk of cements (EMG 4.1), while schwertmannite was present only as small groups of crystals. Gypsum was also present in large quantities and displayed fibrous morphologies. Ferrihydrite was widespread and developed a hygroscopic morphology covering many grains (EMG 4.2). SEM/EDX investigations also indicated the presence of opal A as a major cementing agent. This siliceous material did not exist as skeletal fragments of highly degraded gangue minerals, but rather it appears to have precipitated from solution, coating both gangue and sulfide minerals alike (EMG 4.3 & 4.4).

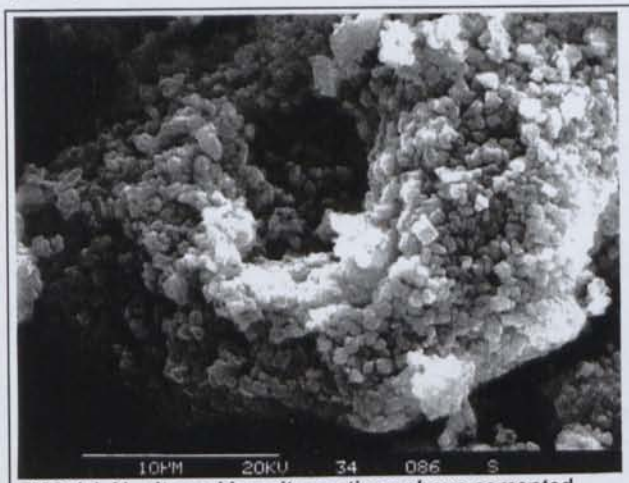

EMG 4.1 Alunite and jarosite coatings above cemented layer at 1.37m depth, Brukunga

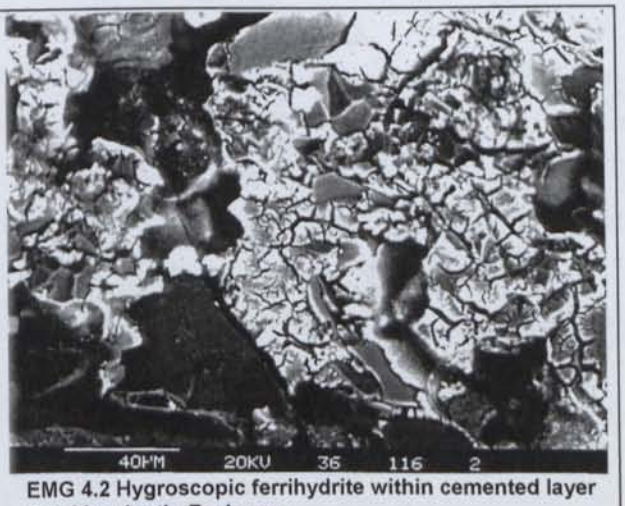

EMG 4.2 Hygroscopic ferrihydrite within cemented layer at 1.09m depth, Brukunga

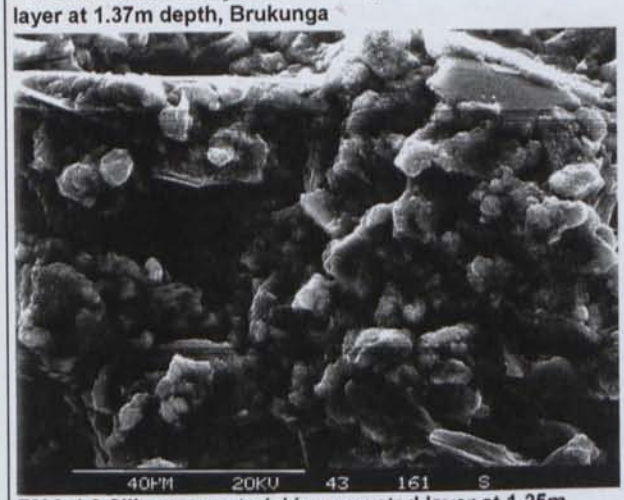

EMG 4.3 Siliceous material in cemented layer at 1.25m depth, Brukunga

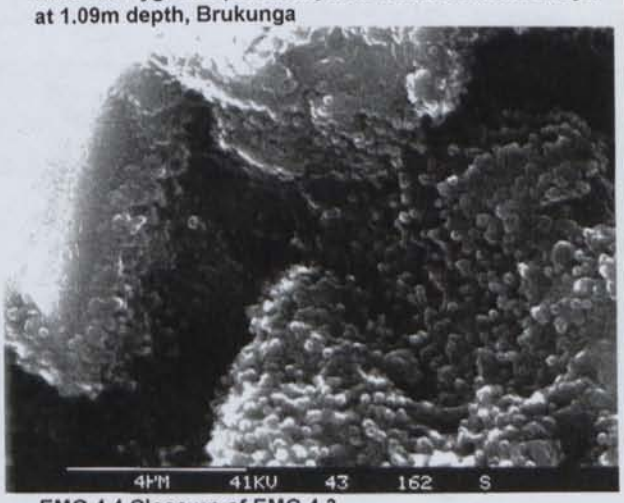

EMG 4.4 Close up of EMG 4.3

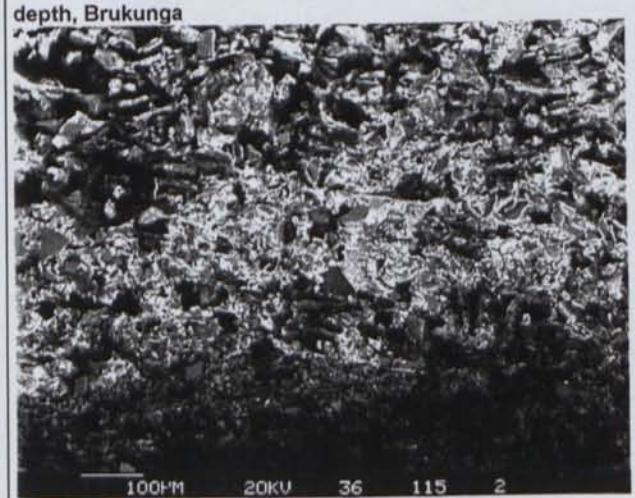

EMG 4.5 Cements developed above textural change at 1.09m depth, Brukunga

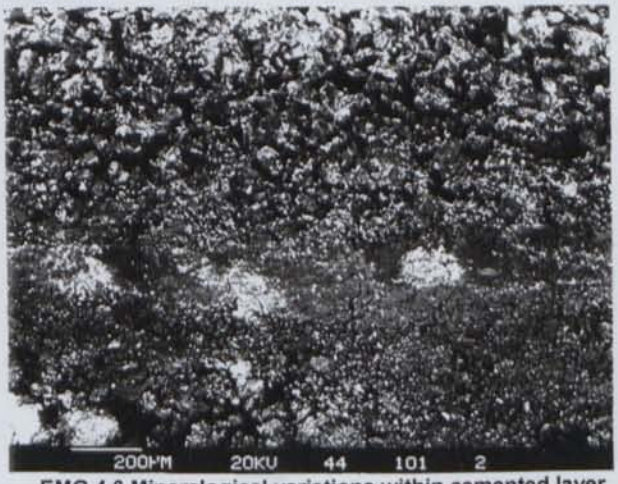

EMG 4.6 Mineralogical variations within cemented layer at 1.37m depth, Brukunga

SEM/EDX investigations suggest that cementing by secondary minerals is dictated by textural changes down the profile. Marked irregularities exist within micro environments as graded bedding and changes in depositional regimes e.g. coarse tailings deposited on fine tailings producing sharp textural contrasts indicative of a hiatus in deposition (EMG 4.5). These sites may act as initial environments for the subsequent in-filling of interaggregate pores through variations in permeability and thus concentration of solute.

The cement that makes up the boundary layer between oxidised and unoxidised tailings varies in composition horizontally (EMG 4.6). Variations are thought to occur in response to infiltrating water, flushing material downward and depositing it in channels and spaces between skeletal grains. Intermittent and repetitive infiltration appears to have alternated with times of evaporation, which initiated the precipitation of secondary minerals. Variations in precipitation may be simply due to the prevailing conditions, solution saturation with respect to each mineral, and the flow path available for its movement. SEM/EDX investigations indicated the cement present at this boundary is a mixture of Fe oxyhydroxide, minor jarosite and alunite. K-alpha X-ray imaging across the boundary layer showed increased levels of Fe and S above the cemented band and an abrupt decrease directly below. This would suggest that the initially precipitated ferrihydrite may be effectively plugging the horizon allowing the subsequently leached Fe and S to concentrate above it as a result of decreased permeability, resulting in jarosite precipitation. This cemented layer also shows elevated concentrations of Al, Si, Ca & K, in response to minor alunite, gypsum and siliceous cement precipitation in this zone.

4.2.2 Disused Kanmantoo Cu Mine

Dam	Only one dam present - on crest with two rock walls covered with soil and native vegetation
Original tailings mineralogy	(pyrite) quartz, phlogopite, biotite, andalusite, clinochlore, almandine, magnesite, calcite
Tailings grain size distribution	coarse sand 4-36% silt 1-27% fine sand 60% clay 1-6%
Hardpan/Cemented Layers/No cements	No cements
Period of exposure	24 years
Hardpan/cement depth in profile	N/A
Lateral extent of hardpan/cemented layers	N/A
Thickness of hardpan / cemented layers	N/A
Cement mineralogy	jarosite
Surface Salt mineralogy	N/A Soil cover

Typical XRF analysis of tailings

Site 1 (50-60cm)

SiO2 %	Al2O3 %	Fe2O3 %	Fe %	MnO %	MgO %	CaO %	K2O %	TiO2 %	P2O5 %	SO3 %
42.7	12.1	42.2	29.5	0.80	1.50	0.16	0.48	0.42	0.11	2.34
S %	Ba ppm	Ce ppm	Co ppm	Cr ppm	Cu ppm	Ga ppm	La ppm	Ni ppm	Pb ppm	Rb ppm
0.94	40	60	30	71	560	15	30	15	0	25
Sr ppm	Th ppm	U ppm	V ppm	Y ppm	Zn ppm	Zr ppm	Sb ppm	Cd ppm	As ppm	
5	0	0	145	60	155	125	0	0	15	

Site 1 (2.5-2.6m)

SiO2 %	Al2O3 %	Fe2O3 %	Fe %	MnO %	MgO %	CaO %	K2O %	TiO2 %	P2O5 %	SO3 %
59.7	14.4	20.6	14.4	0.44	2.41	0.18	1.42	0.51	0.13	3.29
S %	Ba ppm	Ce ppm	Co ppm	Cr ppm	Cu ppm	Ga ppm	La ppm	Ni ppm	Pb ppm	Rb ppm
1.32	120	70	135	90	1240	15	40	35	10	85
Sr ppm	Th ppm	U ppm	V ppm	Y ppm	Zn ppm	Zr ppm	Sb ppm	Cd ppm	As ppm	
10	15	10	70	35	220	140	0	0	5	

4.2.2.1 Tailings Dam History

During processing at the Kanmantoo mine, all tailings were pumped to a single dam spanning two hills across the mouth of a valley, 1.5 miles from the mill (SADME 1972). The dam is an earth-cored rock fill embankment, built mainly from waste rock from the mine (SADME, 1985). The average ore was 1% Cu, with a waste to ore ratio of approximately 5:1. Ore levels up to 2.7% Cu were encountered however this was diluted with waste rock, to allow processing. The resultant sulfidic content of the tailings was very low due to low pyrite content (SADME, 1972). The deposition method is uncertain, however textural variations within the dam suggest deposition was via edge spigots placed predominantly on the perimeter of the dam wall, with coarse tailing deposited near the wall and finer fractions to the back of the impoundment. The total area of the dam is 19.4 ha. During 1985, 65% of the dam was covered with soil and now supports indigenous and imported grasses, trees and shrubs. The pH 1.5 seepage water from the dam is collected immediately downstream from the dam wall and is disposed of via evaporation (SADME, 1985).

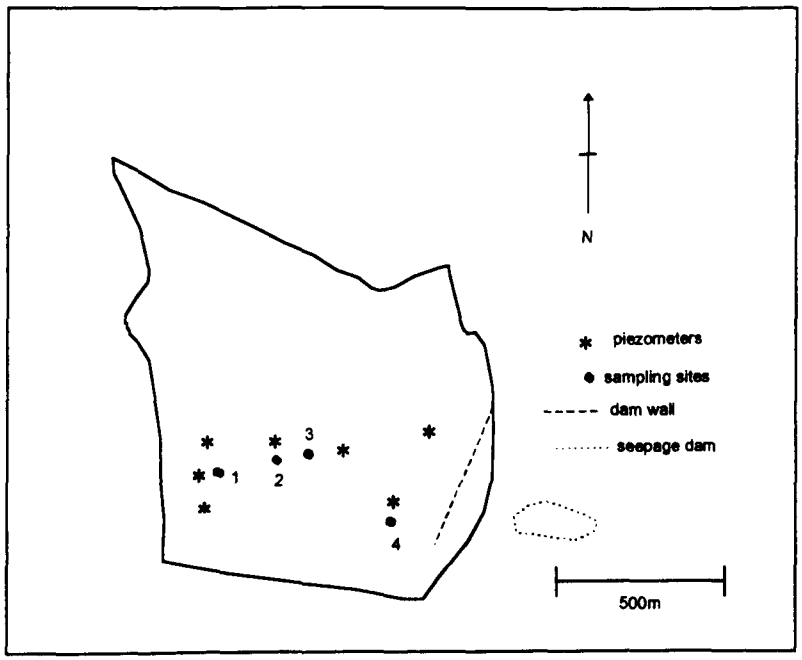

FIG 4.2 MAP OF KANMANTOO TAILINGS DAM SHOWING SAMPLING LOCATIONS

4.2.2.2 Sampling Description

Four locations spanning the width of the tailings dam were investigated to a depth of 4m using hand auguring procedures. These sampling sites were located close to the existing piezometers so that they could be easily relocated on subsequent trips (Fig 4.2). Samples were removed at intermittent depths for mineralogical analysis.

4.2.2.3 Gangue and Sulfide Mineralogy

The tailings gangue mineral assemblage includes quartz, phlogopite, muscovite, clinochlore, almandine, andalusite, hercynite, magnetite, magnesite and minor calcite. The sulfide content of the tailings is between 0.5-1% and consists of pyrite.

4.2.2.4 Secondary Mineralogy and Morphology

The surface of the dam has been covered with a thin layer of soil and so surface salts were not observed or identified. However samples at depth contained jarosite, halite and sylvite. These secondary minerals were not in quantities great enough to develop cementing characteristics.

4.2.2.5 Discussion

No cemented layers or hardpans were identified at this site. The very low sulfide content of the tailings has resulted in limited amounts of oxidation, acid generation, neutralisation and degradation reactions taking place. In response to this the by-product development has also been limited, thus cementation was unable to occur.

4.3 Willyama Block, N.S.W

4.3.1 Broken Hill, Pb, Zn, Ag Mine

Dam	**Alpine Country Dam** - egde spigot deposition, tailings walls, covered with calcrete
Original tailings mineralogy	sphalerite, (pyrite) quartz, clinochlore, muscovite, fluorite, microcline, calcite, (almandine, spessartine)
Tailings grain size distribution	coarse sand 0-6% silt 23-55% fine sand 5-56% clay 0-15%

Typical XRF analysis of basal tailings

SiO2 %	Al2O3 %	Fe2O3 %	Fe %	MnO %	MgO %	CaO %	K2O %	TiO2 %	P2O5 %	SO3 %
49.9	6.03	5.97	4.2	6.15	0.5	14.24	1.69	0.22	0.5	4.53
S %	Ba ppm	Ce ppm	Co ppm	Cr ppm	Cu ppm	Ga ppm	La ppm	Ni ppm	Pb ppm	Rb ppm
1.8	270	160	45	30	135	25	35	10	8780	90
Sr ppm	Th ppm	U ppm	V ppm	Y ppm	Zn ppm	Zr ppm	Sb ppm	Cd ppm	As ppm	
60	10	20	35	25	24800	105	175	145	815	

Hardpan/Cemented Layers/No cements	Cemented layers
Period of exposure	approx. 77 years
Hardpan/cement depth in profile	0-1m depth
Lateral extent of hardpan/cemented layers	Discontinous through out dam
Thickness of hardpan / cemented layers	5mm-15cm
Cement mineralogy	hemimorphite, gypsum
Surface Salt mineralogy	N/A soil cover

Typical XRF analysis of hardpan/cements

SiO2 %	Al2O3 %	Fe2O3 %	Fe %	MnO %	MgO %	CaO %	K2O %	TiO2 %	P2O5 %	SO3 %
43.6	4.79	8.13	5.7	6.96	0.5	13.03	0.94	0.2	0.59	10.36
S %	Ba ppm	Ce ppm	Co ppm	Cr ppm	Cu ppm	Ga ppm	La ppm	Ni ppm	Pb ppm	Rb ppm
4.1	105	145	40	40	255	20	35	10	9950	50
Sr ppm	Th ppm	U ppm	V ppm	Y ppm	Zn ppm	Zr ppm	Sb ppm	Cd ppm	As ppm	
35	25	35	40	30	60260	90	145	175	895	

Dam	**Marlboro Country Dam** - egde spigot deposition, tailings walls, cover with calcrete
Original tailings mineralogy	quartz, clinochlore, muscovite, fluorite, microcline, calcite
Hardpan/Cemented Layers/No cements	No cements
Period of exposure	approx. 57 years
Cement mineralogy	very minor gypsum & hemimorphite
Surface Salt mineralogy	N/A soil cover

Typical XRF analysis of hardpan/cements

SiO2 %	Al2O3 %	Fe2O3 %	Fe %	MnO %	MgO %	CaO %	K2O %	TiO2 %	P2O5 %	SO3 %
56	19.1	6.5	4.5	0.066	2	2.6	3.87	0.79	0.048	0.23
S %	Ba ppm	Ce ppm	Co ppm	Cr ppm	Cu ppm	Ga ppm	La ppm	Ni ppm	Pb ppm	Rb ppm
0.1	535	60	20	60	55	25	40	15	45	155
Sr ppm	Th ppm	U ppm	V ppm	Y ppm	Zn ppm	Zr ppm	Sb ppm	Cd ppm	As ppm	
115	10	10	60	30	115	230	220	85	10	

Dam	**Site A/B** - egde spigot deposition, tailings walls, covered with soil and vegetation
Original tailings mineralogy	sphalerite, (galena), quartz, clinochlore, muscovite, fluorite, microcline, calcite, almandine, spessartine, tremolite (siderite)
Tailings grain size distribution	coarse sand 1-2% silt 24-54% fine sand 26-62% clay 1-6%

Typical XRF analysis of basal tailings

SiO2 %	Al2O3 %	Fe2O3 %	Fe %	MnO %	MgO %	CaO %	K2O %	TiO2 %	P2O5 %	SO3 %
43.9	5.66	9.88	6.9	8.02	1	13.02	1.23	0.22	0.53	7.17
S %	Ba ppm	Ce ppm	Co ppm	Cr ppm	Cu ppm	Ga ppm	La ppm	Ni ppm	Pb ppm	Rb ppm
2.9	120	170	70	140	610	20	35	70	7435	70
Sr ppm	Th ppm	U ppm	V ppm	Y ppm	Zn ppm	Zr ppm	Sb ppm	Cd ppm	As ppm	
50	20	30	45	25	30220	60	150	155	920	

Period of exposure	23 years
Cement mineralogy	Goethite and gypsum
Surface Salt mineralogy	N/A soil cover

Typical XRF analysis of hardpan/cements

SiO2 %	Al2O3 %	Fe2O3 %	Fe %	MnO %	MgO %	CaO %	K2O %	TiO2 %	P2O5 %	SO3 %
50.7	4.57	7.31	5.1	9.82	0.6	9.13	0.89	0.17	0.459	7.14
S %	Ba ppm	Ce ppm	Co ppm	Cr ppm	Cu ppm	Ga ppm	La ppm	Ni ppm	Pb ppm	Rb ppm
2.9	110	210	35	40	270	30	35	10	21020	50
Sr ppm	Th ppm	U ppm	V ppm	Y ppm	Zn ppm	Zr ppm	Sb ppm	Cd ppm	As ppm	
45	20	30	40	30	25790	65	195	395	790	

Dam	**Site C** - edge spigot deposition, tailings wall
Original tailings mineralogy	sphalerite, (galena), quartz, clinochlore, muscovite, fluorite, microcline, calcite, almandine, spessartine, tremolite, siderite
Tailings grain size distribution	coarse sand 40-73% silt 0-4% fine sand 20-50% clay 1-2%

Typical XRF analysis of basal tailings

SiO2 %	Al2O3 %	Fe2O3 %	Fe %	MnO %	MgO %	CaO %	K2O %	TiO2 %	P2O5 %	SO3 %
45.6	7.12	16.7	11.7	8.98	0.9	5.57	0.44	0.16	0.456	7.61
S %	Ba ppm	Ce ppm	Co ppm	Cr ppm	Cu ppm	Ga ppm	La ppm	Ni ppm	Pb ppm	Rb ppm
3.0	30	360	140	45	560	35	35	10	25110	15
Sr ppm	Th ppm	U ppm	V ppm	Y ppm	Zn ppm	Zr ppm	Sb ppm	Cd ppm	As ppm	
10	10	15	45	40	22200	60	125	155	3900	

Hardpan/Cemented Layers/No cements	Cemented layers
Period of exposure	12 years
Hardpan/cement depth in profile	0-1.5m depth
Lateral extent of hardpan/cemented layers	probably over entire dam
Thickness of hardpan / cemented layers	5mm-25cm
Cement mineralogy	gypsum and goethite

Typical XRF analysis of hardpan/cements

SiO2 %	Al2O3 %	Fe2O3 %	Fe %	MnO %	MgO %	CaO %	K2O %	TiO2 %	P2O5 %	SO3 %
51.8	6.7	13.86	9.7	5.91	0.8	4.4	0.8	0.2	0.67	9.23
S %	Ba ppm	Ce ppm	Co ppm	Cr ppm	Cu ppm	Ga ppm	La ppm	Ni ppm	Pb ppm	Rb ppm
3.7	30	190	30	30	815	20	35	10	7390	25
Sr ppm	Th ppm	U ppm	V ppm	Y ppm	Zn ppm	Zr ppm	Sb ppm	Cd ppm	As ppm	
20	10	10	55	25	36560	50	100	190	1550	

Dam	Site D - edge spigot deposition, tailing walls
Original tailings mineralogy	galena quartz, clinochlore, muscovite, fluorite, calcite, almandine, spessartine, tremolite
Tailings grain size distribution	coarse sand 40% silt 2% fine sand 56% clay 1%

Typical XRF analysis of original tailings

SiO2 %	Al2O3 %	Fe2O3 %	Fe %	MnO %	MgO %	CaO %	K2O %	TiO2 %	P2O5 %	SO3 %
62.4	5.25	9.02	6.30	6.51	0.8	5.9	0.62	0.19	0.315	1.8
S %	Ba ppm	Ce ppm	Co ppm	Cr ppm	Cu ppm	Ga ppm	La ppm	Ni ppm	Pb ppm	Rb ppm
0.70	105	85	35	25	90	15	35	10	1240	25
Sr ppm	Th ppm	U ppm	V ppm	Y ppm	Zn ppm	Zr ppm	Sb ppm	Cd ppm	As ppm	
25	10	10	25	25	5360	115	30	80	540	

Hardpan/Cemented Layers/No cements	No cements
Period of exposure	In use
Hardpan/cement depth in profile	N/A
Lateral extent of hardpan/cemented layers	N/A
Thickness of hardpan / cemented layers	N/A
Cement mineralogy	N/A
Surface Salt mineralogy	N/A
Typical XRF analysis of hardpan/cements	N/A

4.3.1.1 Tailings Dam History

The history of many of the tailings impoundments in the Broken Hill region is unknown to the present Pasminco staff. Only 5 of the numerous dams were investigated, ranging from the oldest through to the present day impoundments, including Alpine Country, Marlboro Country, Site A/B, Site C and Site D (Figs 4.3 and 4.4). The history of the Alpine Country and Marlboro Country dams is unknown however it is suggested that the former was deposited between approximately 1900-1920. Marlboro Country is the younger of the two and is suggested to have been deposited between approximately 1920-1940. The tailings were supplied from the South mine. These dams were covered with approximately 20-25cm thick layer of calcareous soil to reduce dusting problems during 1994. It is understood that Site A/B was deposited during 1940-1974, while Site C was deposited between 1974-1985. Deposition into Sites A/B, C & D were via the edge spigot method, with the coarsest fractions of the tailings being utilised to build the dam walls. At present the tailings are being deposited into Site E. Each of the impoundments vary in mineralogy, due to variations in the ore bodies being mined and the ore processing techniques utilised at the time.

During the life of the mine, mineralisation has changed from more calcitic lodes to more siliceous lodes. During this period a complex history of tailings deposition has occurred with tailings being produced from the NBHC and ZC mills and a retreatment plant. Between 1906-1939 tailings were heaped near the metallurgical plant, in what was known as Mt Keast. In 1939 the ZC mill began processing the calcitic

lodes of the ZC and Freeman shafts. The tailings were pumped directly to Site A. Then during 1952 the NBHC mill came into production, processing the primarily siliceous NBHC shaft ore. Between 1952-1976 tailings from both the ZC and NBHC tailings were combined in the ZC Residue Plant prior to its deposition in Site B which was combined with Site A and is now known as Site A/B. During 1976 tailings deposition began into Site C consisting of tailings from the ZC and NBHC mills and included tailings from the Mt Keast Retreatment Plant. This continued until 1986 when the ZC mill was closed. All ore was then processed in the NBHC mill and deposited directly into Site D and E which continues today.

4.3.1.2 Sampling Description

During 1995 sampling was undertaken at all 5 dams. Three holes were sampled across the Alpine Country dam, along with 4 locations across Marlboro Country (Fig 4.3). Because of time constraints only three single locations were sampled in Site A/B, Site C and D. These sites were sampled again in 1996, along with 2 additional sites in Dam A/B and 7 additional sites in Dam C (Fig 4.4)

4.3.1.3 Gangue & Sulfide Mineralogy

Alpine and Marlboro Country dams contained varying quantities of quartz, clinochlore, muscovite, fluorite, microcline and calcite. Almandine and spessartine were also identified at depth in Alpine Country. Site A/B and Site C contain all of the above mentioned minerals along with tremolite and minor siderite. The sulfide content of all tailings is very low (0.1-0.8%). Alpine Country contains sphalerite and minor pyrite, while no sulfides where identified in Marlboro Country. Site A/B and C also contain sphalerite, along with minor galena. Galena was also identified in Site D.

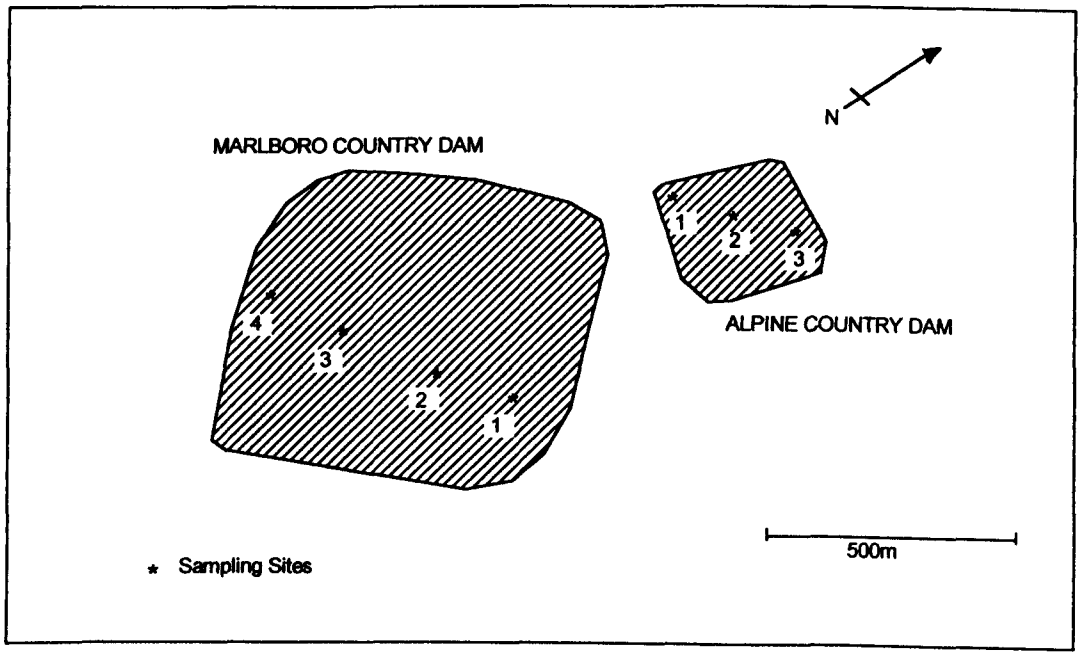

FIG 4.3 SAMPLING SITES IN ALPINE AND MARLBORO COUNTRY DAMS, BROKEN HILL

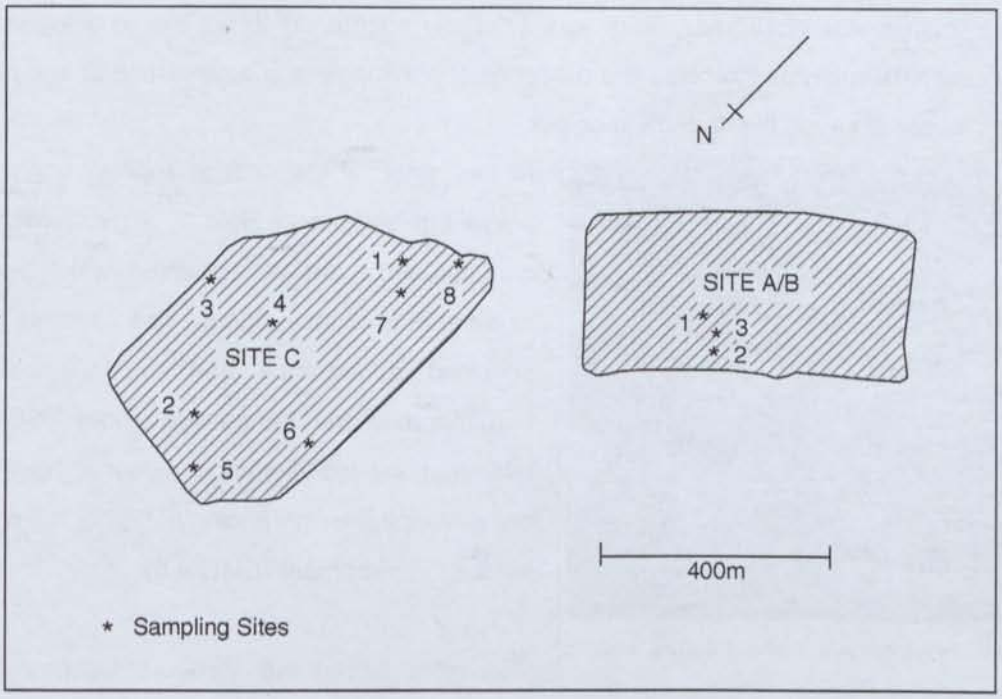

FIG 4.4 SAMPLE LOCATION MAP OF SITE A/B AND C

4.3.1.4 Secondary Mineralogy and Morphology

4.3.1.4.1 Alpine and Marlboro Country

The cementing within the Alpine Country dam has assumed different morphologies depending on the locations within the dam. Holes 1 and 3 were located on the periphery of the dam in coarser tailings than the centrally located Hole 2. In the outer zones, the cements have developed as layers approximately 1.5-2cm thick between 0-40cm depth. Below this down to 70cm consolidated layers have developed but are less cemented.

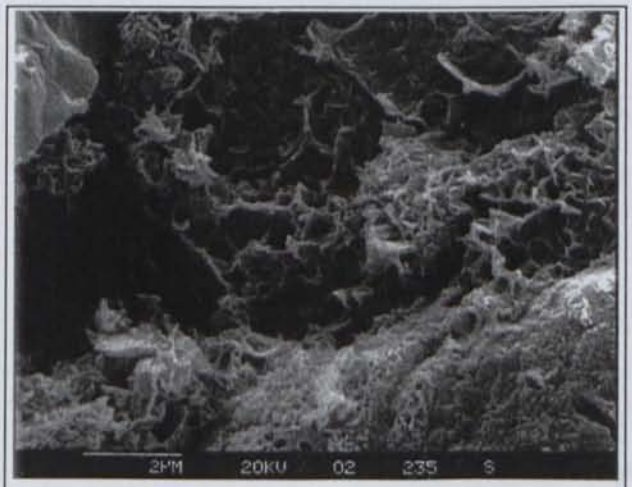

EMG 4.7 Mn and Fe oxide cement, Alpine Country, Hole 1, Broken Hill

XRD analysis indicated that the main cementing agent in the coarse tailings is hemimorphite, a secondary mineral developed as a by-product of sphalerite oxidation. SEM-EDX analysis was also undertaken to observe the morphology of the developing cements. During this examination it was observed that the cements were in fact a combination of hemimorphite, iron oxy-hydroxides and manganese oxides. XRD was unable to detect the oxides presence because of their amorphous nature (EMG 4.7).

Within the depth range 70-240cm little or no variations in texture or cementation were observed. Between 40 and 240cm depth sphalerite was also present, suggesting that the oxidation front was at approximately 40cm depth, where the sphalerite is yet to be converted to hemimorphite. Such a shallow depth appears unlikely for a dam which has been exposed for such a long time, however the dry nature of the site combined with the highly cemented surface may have prevented further oxidation. At 205cm

depth a colour change was observed. This was originally suggested to be the oxidised/unoxidised boundary, however XRD analysis indicated the presence of almandine and spessartine at and below this depth which is thought to cause the change in colour.

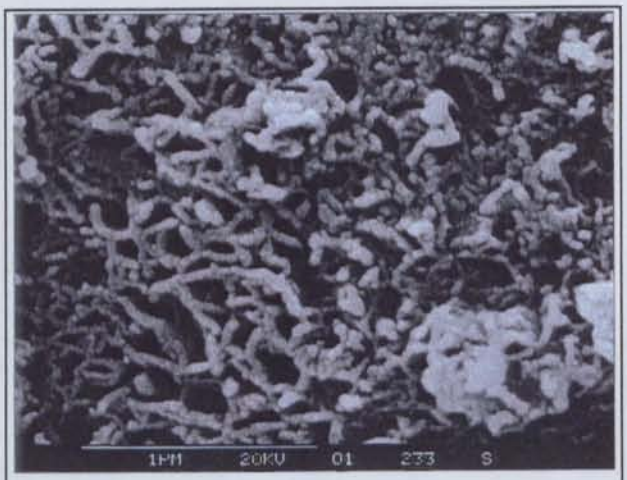

EMG 4.8 Mn and Fe oxide cement, Alpine Country, Hole 2, Broken Hill

At the center of the dam at approximately 3-4cm below the surface in Hole 2, an extremely hard continuous cement was observed, which persisted to a depth of at least 35cm. The cements have a speckled appearance and are a mixture of hemimorphite and manganese oxides. SEM-EDX examinations indicated the cements have taken on a vermiform morphology, typical of a highly leached environment (EMG 4.8).

Cementing within the Marlboro Country dam is only very minor. Minor hemimorphite and gypsum cements were observed at the surface of Hole 2 and again at 48cm depth.

4.3.1.4.2 Site A/B and Site C

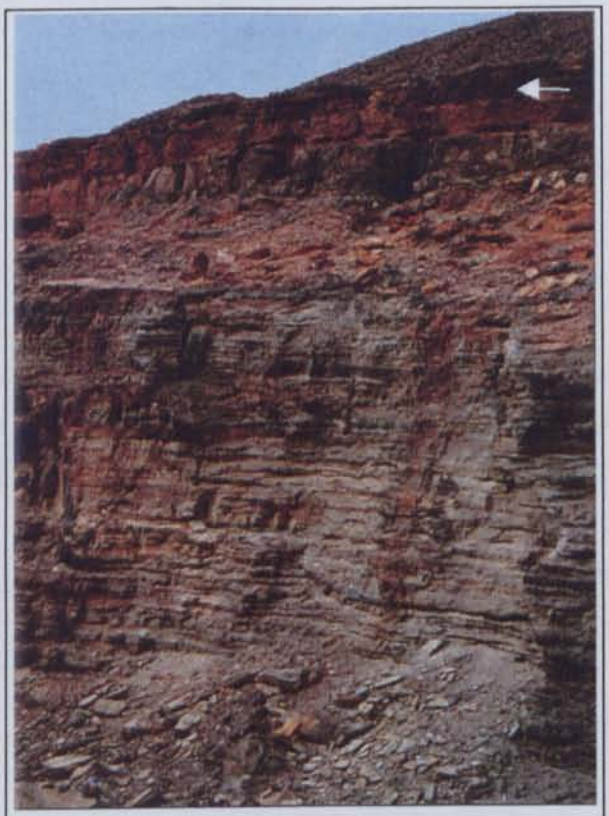

Photo 4.1 Broken Hill, Site C open pit in tailings, cementation in upper 1-2m. Arrow represents cemented region

Site A/B has been used intermittently as disposal locations for mine waste, while in the past tailings from Site C have been recovered for back-fill. These practices have resulted in large open pits within the dams. These locations were the initial focus of cementing examinations in 1995. During 1996 additional small holes were made for profile examination. Cements in both dams were of similar style, position in the profile and coloring. However, Site C cementing was noticeably more widespread, harder and more continuous, especially within the upper 1-2m within the coarse peripheral tailings (photo 4.1). Cementing was also more prevalent in coarse peripheral tailings of Site A/B, compared with the central tailings.

The exposed profiles showed the highly variable nature of the tailings including structures of cross bedding, graded bedding and hiatus in deposition. These structures have strongly influenced the location of oxidation and cementing by gypsum and goethite identified by XRD.

Photo 4.2 Cemented layers in upper 1-2m tailings, Site C, Broken Hill.

In sections of predominantly coarse grained tailings where cross- and graded-bedding texture were dominant, cementation had developed along the fine-grained layers (photo 4.2). This is probably due to transport of solutes through localised 'unsaturated flow' within the finer layers (Newman et al, 1997). During subsequent evaporation and concentration, secondary salts have precipitated, preferentially cementing these regions. EMG 4.9 shows the development of micro scale cementing preferentially within the finer grained Site C tailings. EMGs 4.10 and 4.11 display higher magnifications of the fine-grained cemented region. Very fine secondary minerals have developed as a coating on the primary tailings. Degraded gypsum was observed, along with widespread fine spherical cements which consists predominantly of Fe and Si with lesser amounts of Zn, Mn and Al. The morphology and EDX signature of these cements suggest that this may be a mixture of Fe oxides and siliceous cement intimately mixed with variable quantities of hemimorphite and manganese oxide. Most of these minerals were verified by XRD analysis but the siliceous material remained unidentified.

EMG 4.9 Cement deposition on textural boundary, Site C, Broken Hill

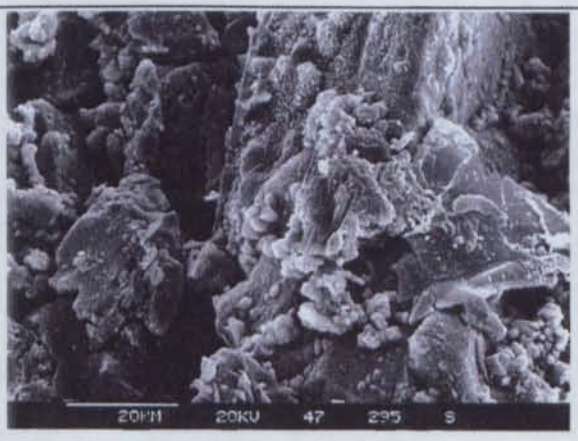

EMG 4.10 Close-up of EMG 4.9 fine-grained region

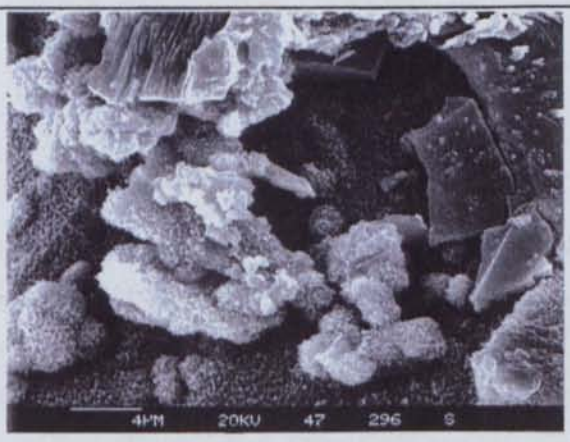

EMG 4.11 Close-up of EMG 4.9 Fe oxide and siliceous cement

In locations where pockets of very fine-grained tailings overlie coarse-tailings or visa versa, saturation of the tailings has dictated oxidation and cementation. The very fine-grained tailings (slimes) have maintained levels of water saturation such that oxidation has not taken place, whereas the surrounding coarse-grained tailings have become unsaturated through drainage or evaporation resulting in oxidation and secondary mineral precipitation (photo 4.3 & 4.4).

Photo 4.3 Broken Hill Site C profile showing tailings of varying oxidation states

Photo 4.4 Close-up of Photo 4.4

4.3.1.5 Discussion

The morphologies of the Alpine Country Dam cements are not consistent through-out the dam, suggesting different modes of formation. At the edge of the dam the texture is predominantly coarse-medium sands allowing both increased water and oxygen penetration resulting in increased oxidation reactions. The oxidation reactions produce large quantities of by-products which are then available for concentration through evaporation and subsequent cementation results. At the edge of the dam the cements have developed in the top coarse tailings and are quite dark in colour.

The central cements are in more clay/silt sized tailings with small black speckles of cements developing in a very pale brown matrix. The fine-grained nature of the central tailings may in fact be reducing oxidation through elevated saturation levels associated with substantial matrix and osmotic suction. These central cements may have developed through redistribution processes from the coarse edge tailings. This redistribution would probably be restricted to surface runoff, as the center is the lowest section of the dam. Additionally SEM investigations showed leached morphologies indicating surface inflow and potential flushing.

The historical differences between Alpine and Marlboro Country dams is unknown, however cementation of the tailings is very different. Alpine Country is older and may have undergone a more primitive processing, resulting in higher original sulfide content. Likewise variations in geology/mineralogy of the lodes may have resulted in variations of sulfide content being processed. Whatever the reason behind the variations in the original tailings mineralogy, cementation has developed preferentially in Alpine Country and consists of hemimorphite, manganese and iron oxides.

The history of tailings deposition at Broken Hill is complex with variations in mill processing and lodes being mined. Further investigations in the surface tailings of Sites A/B and C revealed that during the final stages of deposition in Site A/B tailings were sourced from both the ZC and NBHC mills. During the 1985-86 period when Site D was commissioned, tailings from the NBHC mill (primarily siliceous ore) were pumped into the new impoundment, while the final tailings from the ZC mill continued to be deposited in Site C.

This has resulted in the Site C surface tailings being more calcitic than those in Site A/B. Cementation of Site C appears to be generally more pronounced in the upper 1-2m of tailings. The release of Ca associated with calcite dissolution would have also enhanced the precipitation of gypsum cements. The elevated pH conditions and different ore being processed may have promoted the development of Fe oxides.

4.4 Lachlan Fold Belt, N.S.W

4.4.1 Elura Zn-Pb-Ag Mine

Dam	**Present Tailings Dam 3** – triple point, modified central spigotting technique, rock walls
Original tailings mineralogy	pyrite, pyrrhotite, (galena, sphalerite), quartz, siderite, muscovite
Tailings grain size distribution	coarse sand 0% silt 32% fine sand 56% clay 7%

Typical XRF analysis of original tailings

SiO2 %	Al2O3 %	Fe2O3 %	Fe %	MnO %	MgO %	CaO %	K2O %	TiO2 %	P2O5 %	SO3 %
9.9	1.1	53.6	37.5	0.38	0.8	0.59	0.28	0.073	0.076	69.4
S %	Ba ppm	Ce ppm	Co ppm	Cr ppm	Cu ppm	Ga ppm	La ppm	Ni ppm	Pb ppm	Rb ppm
27.80	680	130	25	55	425	20	480	10	13550	10
Sr ppm	Th ppm	U ppm	V ppm	Y ppm	Zn ppm	Zr ppm	Sb ppm	Cd ppm	As ppm	
15	10	35	10	5	18420	20	195	130	6830	

Dam	**Dam 1** - triple point, modified central spigotting technique, rock walls, covered with rock, soil and native vegetation
Hardpan/Cemented Layers/No cements	Laterally Extensive Surface Hardpan
Period of exposure	9 years
Hardpan/cement depth in profile	Surface and palaeo-hardpans
Lateral extent of hardpan/cemented layers	Over entire dam
Thickness of hardpan / cemented layers	3-7cm
Cement mineralogy	gypsum, goethite, natrojarosite, (jarosite)
Surface Salt mineralogy	sulfur, rozenite, melanterite
Tailings grain size distribution	coarse sand 3-16% silt 20-30% fine sand 24-44% clay 8-12%

Typical XRF analysis of hardpan/cements

SiO2 %	Al2O3 %	Fe2O3 %	Fe %	MnO %	MgO %	CaO %	K2O %	TiO2 %	P2O5 %	SO3 %
8.6	0.9	50.7	35.4	0.2	0.5	0.2	0.2	0.1	0.1	64.6
S %	Ba ppm	Ce ppm	Co ppm	Cr ppm	Cu ppm	Ga ppm	La ppm	Ni ppm	Pb ppm	Rb ppm
25.9	510	260	25	50	1190	10	365	10	12560	10
Sr ppm	Th ppm	U ppm	V ppm	Y ppm	Zn ppm	Zr ppm	Sb ppm	Cd ppm	As ppm	
25	25	50	20	5	27600	20	230	135	4200	

Dam	**Dam 2** - triple point, modified central spigotting technique, rock walls
Hardpan/Cemented Layers/No cements	Laterally extensive surface hardpan
Period of exposure	Used intermittently with exposure periods up to 18 months
Hardpan/cement depth in profile	Surface and palaeo-hardpans
Lateral extent of hardpan/cemented layers	Over entire dam
Thickness of hardpan / cemented layers	3-5 mm - 3-5 cm depending on exposure time
Cement mineralogy	gypsum, goethite, natrojarosite, (jarosite)
Surface Salt mineralogy	sulfur, rozenite, blodite, melanterite, (alunite)
Tailings grain size distribution	coarse sand 5-12% silt 20-34% fine sand 45-50% clay 5-7%

Typical XRF analysis of hardpan/cements

SiO2 %	Al2O3 %	Fe2O3 %	Fe %	MnO %	MgO %	CaO %	K2O %	TiO2 %	P2O5 %	SO3 %
6.6	0.4	54.1	37.8	0.2	0.5	0.4	0.2	0.0	0.1	62.5
S %	Ba ppm	Ce ppm	Co ppm	Cr ppm	Cu ppm	Ga ppm	La ppm	Ni ppm	Pb ppm	Rb ppm
25.03	1070	140	15	55	760	15	570	40	13250	10
Sr ppm	Th ppm	U ppm	V ppm	Y ppm	Zn ppm	Zr ppm	Sb ppm	Cd ppm	As ppm	
15	20	40	15	5	8025	20	95	65	2180	

4.4.1.1 Tailings Dam History

There are 3 tailings dams present at the Elura Mine site and a location has been determined for a fourth dam. The dams have been constructed in a sub-circular arrangement, on the flat lying topography, the walls having been made of waste rock and clay soils. Dam 1 is the oldest of the three and has been completed for 9 years. These tailings were deposited from the northern end and the majority of seepage drained into a separate pond at the southern end. A small revegetation trial has been undertaken on this dam, to determine the appropriate close-out method. Dams 2 & 3 are utilised intermittently, using central spigot methods, with irregular exposure times of up to 18 months. The tailings water is combined with plant water and recycled back through the mill. Deposition into Dam 4 will commence in 1998. Pasminco are presently considering retreatment of the tailings in Dams 1 to 3.

4.4.1.2 Sampling Description

During 1995 surface hardpan samples were removed from Sites 1 - 4 in Dam 1 and sites 6 and 7 in Dam 2. At this time, deposition was taking place in Dam 3 and a sample of the recently deposited tailings was removed from Site 9 (Fig 4.5).

At the southern end of Dam 1, a section of the retaining wall between the tailings and the seepage dam had collapsed exposing a profile (Site 1). The slightly eroded hardpan at this site was investigated via core sampling down to 50cm depth. Coring was also attempted in Dam 2 at this time but was unsuccessful due to the hardness of the cements encountered. In 1996 additional investigations of all sites were undertaken and cores removed from Site 5 in Dam 1 and Sites 6 and 7 in Dam 2. During 1997, samples from two additional sites (Site 10 & 11) were removed for isotopic analysis and permeability tests undertaken, these results are discussed fully in Chapter 7.

4.4.1.3. Gangue and Sulfide Mineralogy

The gangue mineralogy in each dam is similar with varying quantities of quartz, siderite and muscovite present. Pyrite and pyrrhotite are the most common sulfides throughout the tailings, with lesser amount of galena and sphalerite (sulfide content = 29-31%).

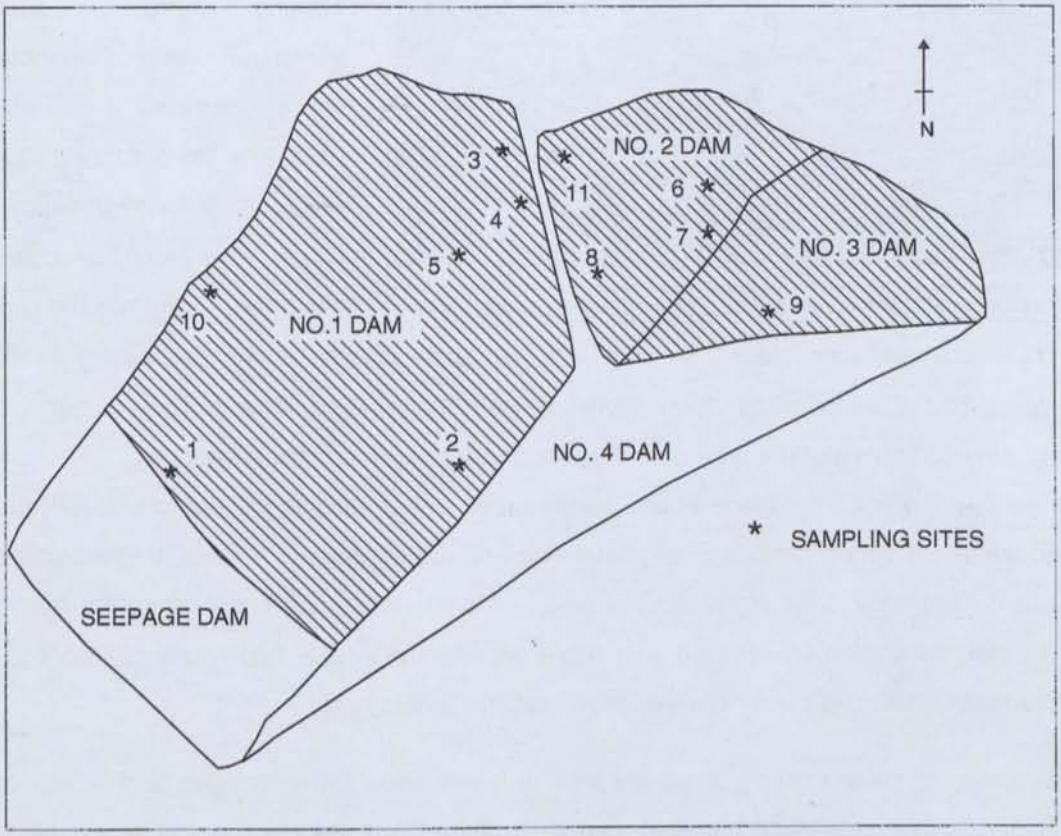

FIG 4.5 SAMPLING SITES AT THE ELURA TAILINGS DAMS.

4.4.1.4 Secondary Mineralogy and Morphology

During 1995 it was observed that a well-developed laterally extensive surface hardpan 3-10cm thick had developed over the entire surface of Dam 1 (photo 4.5) and of areas in Dam 2 that had been exposed for approximately 12-18 months (photo 4.6). The type and quantity of secondary minerals within this hardpan varied at each site depending of the period and condition of exposure. Varying amounts of melanterite, rozenite, goethite, gypsum, blodite and alunite were identified by XRD.

Photo 4.5 Elura Dam 1, Site 3 hardpan (1995)

Photo 4.6 Elura Dam 2, Site 6 hardpan (1995)

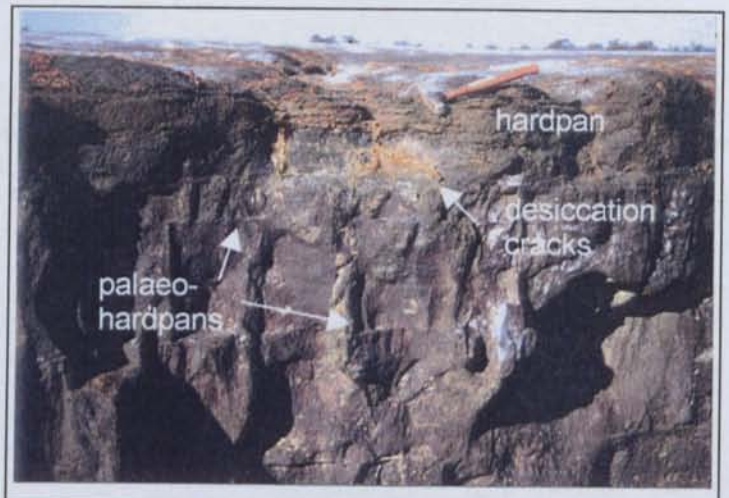

Photo 4.7 Elura Dam 1, Site 1, cells observed in wash away zone

At Site 1 where the retaining wall had collapsed exposing a profile, 3 different types of cementation were observed; a surface hardpan, palaeo-hardpans and desiccation crack cements. Palaeo-hardpans were formed during previous periods of exposure, which were long enough for oxidation, neutralisation and degradation reactions to take place, producing by-products available for hardpan formation. Subsequent deposition of fresh tailings then covered these layers. Desiccation crack cements also formed during periods of exposure when the surface dried and cracks developed. The same geochemical reactions which took place at the surface also occurred along these cracks producing cements. Additionally, if during periods of exposure the surface hardpan is eroded, surface cements may have been redistributed down these cracks adding to their integrity. It was apparent from this profile (Site 1) that the formation of such cements can effectively seal fresh tailings into cell-like structures, potentially protecting them from oxidation reaction (photo 4.7).

Further examinations of Dam 1 during the 1996 visit revealed substantial changes to the previously identified laterally continuous surface hardpan. Approximately 1/3 of the dam, in the raised eastern-central region, had developed a surface unlike that observed elsewhere in the dam. The surface had taken on a much lighter colour, was much softer with no desiccation cracks and a generally lumpy morphology. It was initially thought that this material was freshly deposited tailings and had never formed a hardpan surface. This material had distinct boundaries where the still-intact hardpan at the north and south ends of the dam could be traced beneath. Even within the center of the material, the remnant hardpan could be observed at depth. A core was removed from this site (Site 5) to compare the materials. Discussions with staff on site indicated that there had been no additional tailings deposition and XRD/XRF analyses supported that this material had very similar mineralogy, but were in different quantities to that of the fresh hardpan. Discussions with mine staff and mineralogical analysis indicated that this material was in fact the break down products of hardpan observed in 1995. During an additional review of Dam 1 in 1997, residual hardpans could still be located but the breakdown surface was more widespread.

The Dam 2 surface hardpan was still competent in 1996 and displayed a range of cement morphologies. 'Pop-up' or 'teepee' structures had developed in some areas in response to volume increases during secondary mineral precipitation and hydration reactions (photo 4.8 & 4.9). In other regions, cements remained flat with thin layers of surface salts (photo 4.10), whilst elsewhere disc-like structures had formed (photo 4.11).

Photo 4.8 Pop-up structures along side flat lying hardpan, Elura Dam 2, (1995)

Photo 4.9 Minor pop-up structures, Elura Dam 2, 1996

Photo 4.10 Flat lying hardpan, Elura Dam 2 (1996) (1996)

Photo 4.11 Disc-like structures in hardpan, Elura Dam 2

SEM investigations of the Elura hardpan at different stages of development were undertaken to further understand the processes taking place. EMG 4.12 presents a general view of the 12 month old hardpan developed in Dam 2, Site 8. On close inspection degrading Fe sulfide and galena grains were observed in a matrix of fine fibrous/needle like cements. These needle/fibrous cements contain equal quantities of Fe and S and in places grade into smooth cements which consist of very fine sub-circular particles of predominantly Fe oxides (EMG 4.13).

EMG 4.14 shows a general view of the 7 year old intact cements developed in Dam 1 (Site 4). Cements have developed throughout, producing a low porosity structure. EMG 4.15 shows a close up of columnar gypsum cements, tubes and particles of Pb sulfate and fine-grained fibrous Fe oxides

Cements with a minor S content (EMG 4.16). In general these cements are less fibrous / acicular like than those in the younger hardpan.

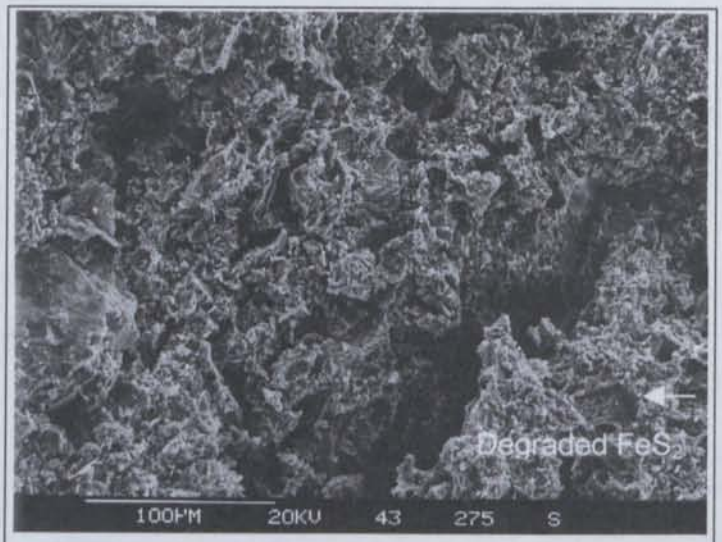

EMG 4.12 General view of 12 month old hardpan, Elura Dam 2

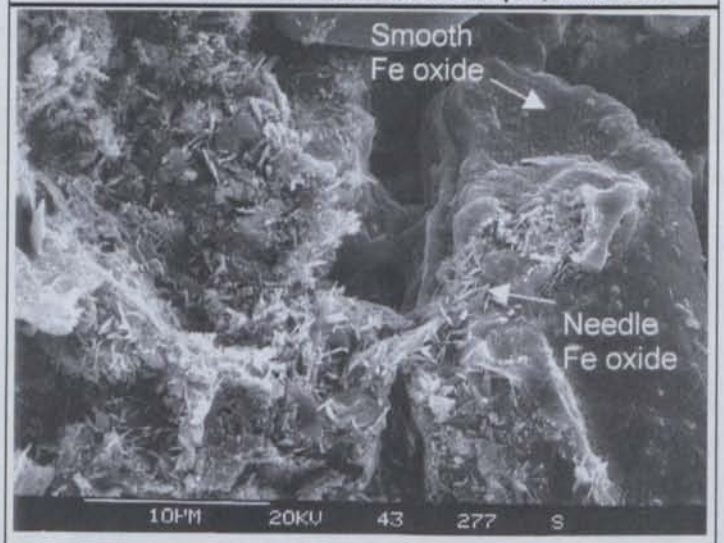

EMG 4.13 Close-up of EMG 4.12 Needle like Fe sulfate grading to smooth Fe oxide cements

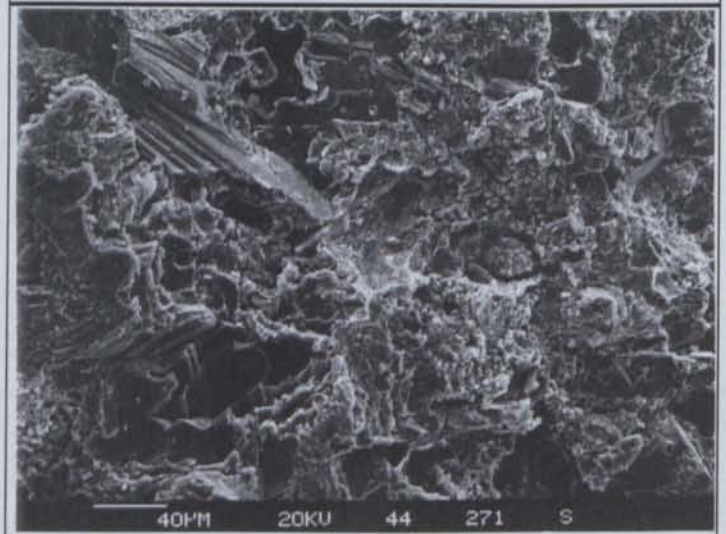

EMG 4.14 General view of cements in intact 7 year old hardpan, Elura Dam 1 Site 3)

A sample of a more degraded hardpan from Dam 1 (Site 3) was also investigated. It appears that an amount of primary and secondary grain dissolution has occurred, developing a generally more porous structure (EMG 4.17). Within this hardpan the cements are dominated by Fe oxides cements with lesser amounts of S present as gypsum and Fe sulfate. Sulfur may have been leached from this surface region. EMGs 4.18 and 4.19 show a close up of the Fe oxide cements coating many of the larger grains. The smaller angular grains throughout the sample have a signature of equal quantities of Fe and S, which together with their morphology suggests they are in fact sulfide grains. Generally the cements are widespread and have maintained a structure, but the sulfides appear to be more exposed through the dissolution of cement. An investigation of the breakdown hardpan observed in Dam 1 (Site 5), indicates the material has less structure and thus less porosity (EMG 4.20). The cements are a mixture of sub-angular particles and smooth coatings. The particles may be the breakdown of the smooth coating, or the smooth coating may be developing through the recombination of the particles (EMG 4.21). These materials consist of Fe and S most probably as a Fe sulfate and minor mobile SiO_2. Widespread primary mineral degradation is apparent. EMG 4.22 shows the

degradation of a Fe sulfide grain and the resultant Fe sulfate and siliceous reaction rim.

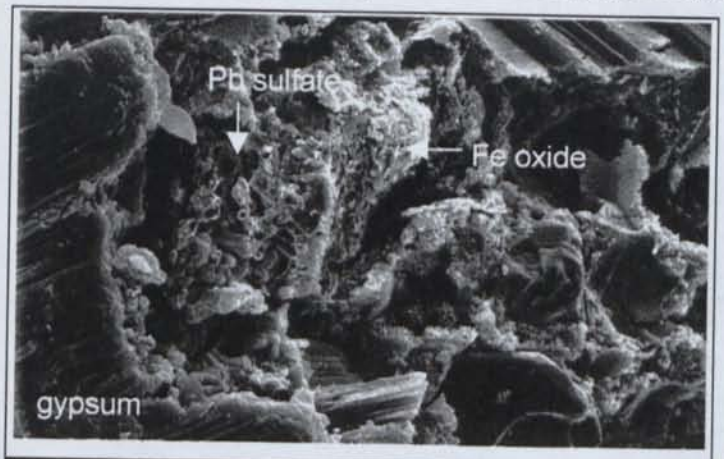

EMG 4.15 Close up of EMG 4.14, column gypsum, tubes of lead sulfate and fine grained Fe oxide 1cm = 10μm.

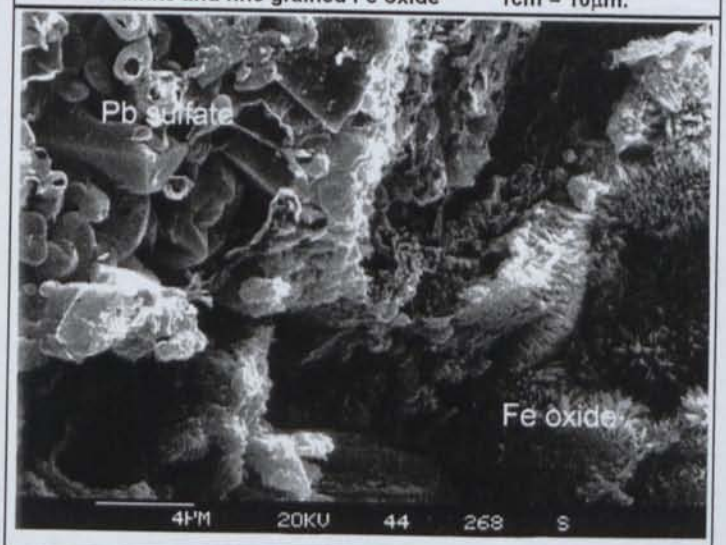

EMG 4.16 Close up of EMG 4.15

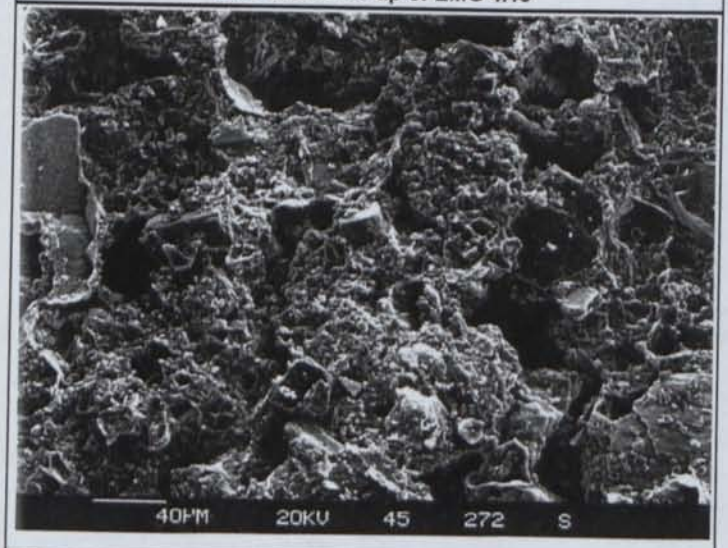

EMG 4.17 General view of degrading 7 year old Elura hardpan (Site 4)

This SEM review suggests a series of morphological changes associated with hardpan development, re-organisation and final degradation and possible redevelopment. Initially needle-like soluble sulfate cements and columnar gypsum have precipitated, in-filling many of the pore spaces (EMG 4.12 & 4.14). As the cements evolve the various sulfate cements degrade, with much of the Fe sulfate altering to Fe oxide as the sulfate is leached from the upper surface (EMG 4.17 & 4.19). The result is a more porous structure and the re-exposure of sulfide grains and ultimately the redevelopment of sulfate cements (EMG 4.21).

4.4.1.5 Discussion

Hardpan development at the Elura site occurs rapidly upon exposure of tailings to oxygen and water, due to the highly reactive pyrrhotite content of the tailings. Once exposed, these tailings react rapidly developing high concentrations of soluble surface salts which alter over time to less soluble and eventually insoluble cements. The hardpan which forms contains residual pyrite, pyrrhotite, quartz and siderite encapsulated by a range of secondary mineral coatings. The dynamic nature of the hardpan surface has been seen in the Elura tailings dams. During secondary mineral precipitation, large increases in volume/mass occur resulting in pop-up structures which eventually erode producing a flat lying continuous hardpan which may alter over time. The mature hardpans in Dam 1 exhibit various alteration/breakdown structures. At Site 1 the hardpan was mechanically eroded, while at Site 5 the hardpan appeared to be chemically eroded.

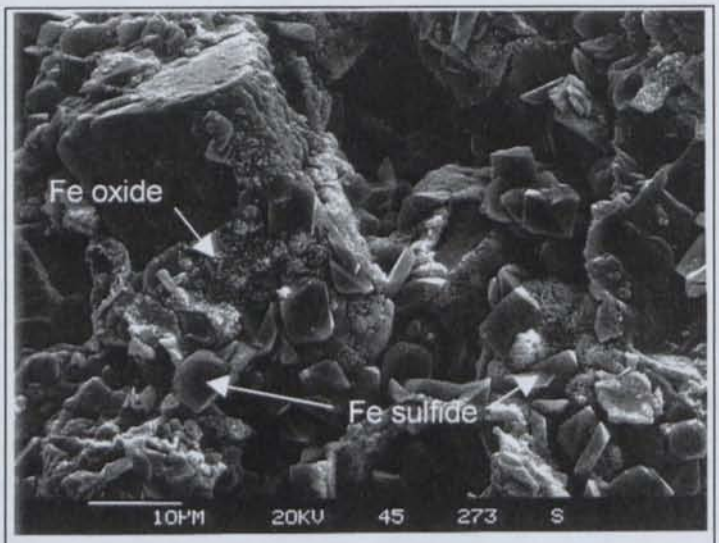

EMG 4.18 Close up of EMG 4.17 Fe oxide coatings on large primary grains, with uncoated fine grained Fe sulfides

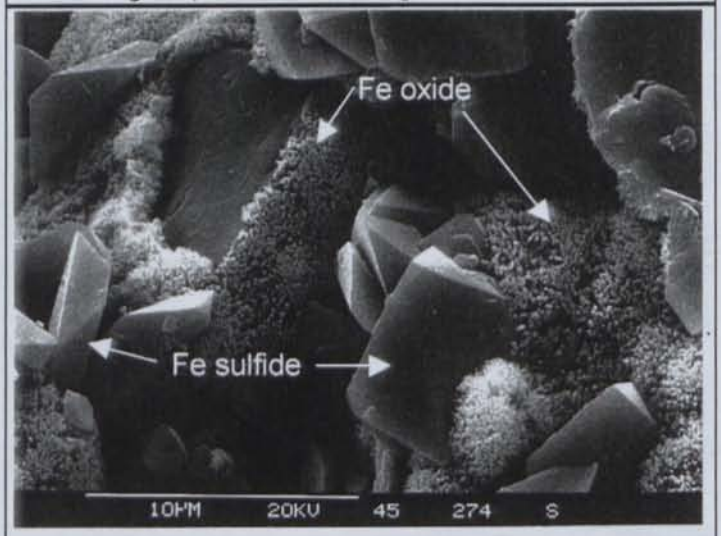

EMG 4.19 Close up of EMG 4.18

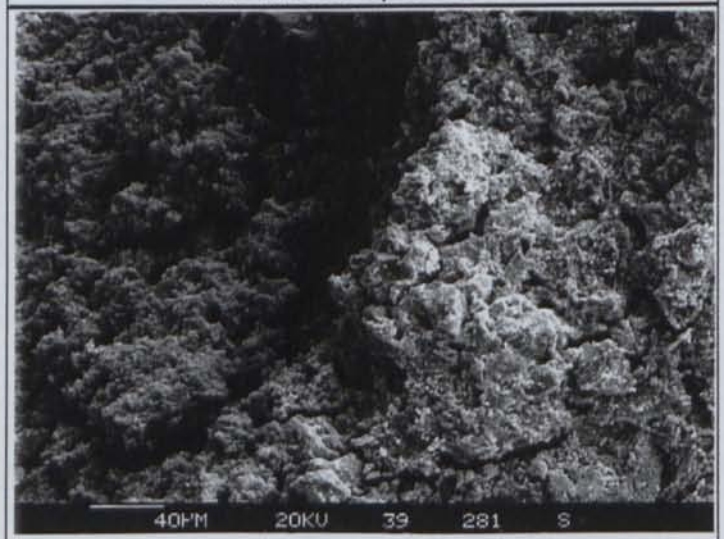

EMG 4.20 General view of degrading cement at Elura Dam 1, Site 5

This breakdown (Site 5) may have been enhanced in this topographically elevated region where rapid water runoff occurs. Erosion and re-exposure of the cements and sulfides has produced conditions where sulfide oxidation and the associated acid generation has limited the stability of the previously precipitated cements. Additionally the siderite which makes up 30-40% of the tailings may be having a secondary effect. Initially siderite is involved with neutralisation reactions, releasing Fe^{2+} into the system. As this oxidises, the resultant Fe^{3+} becomes involved in the oxidation reactions producing a more rapidly reacting system. The consumption of the neutralising minerals and the release of Fe^{2+} together produce a more acid environment, potentially effecting the stability of the cements and may result in the eventual breakdown of the hardpan. Once the hardpan has broken-down, erosion may take place re-exposing the underlying tailings which react and again cause hardpan development.

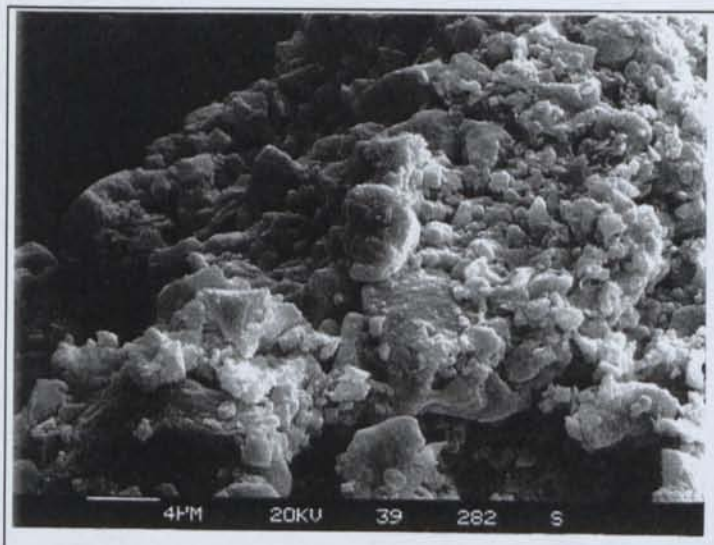

EMG 4.21 Close up of EMG 4.20 Fe sulfate cement

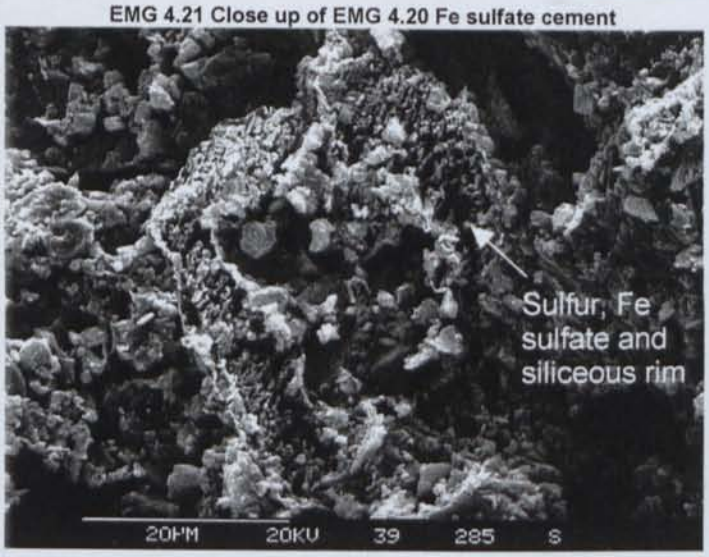

EMG 4.22 Close up of 4.20 Degraded sulfide grain consisting mainly of sulfur, Fe Sulfate and Siliceous material

4.4.2 CSA Cu-Pb-Zn Mine

Dam	**North Dam** - egde spigot deposition, rock and soil walls
Original tailings mineralogy	pyrite, pyrrhotite, (galena, sphalerite chalcopyrite) quartz, clinochlore, muscovite
Tailings grain size distribution	coarse sand 41% silt 15% fine sand 11% clay 8%

Typical XRF analysis of original tailings

SiO2 %	Al2O3 %	Fe2O3 %	Fe %	MnO %	MgO %	CaO %	K2O %	TiO2 %	P2O5 %	SO3 %
58.4	7.8	19.6	13.7	0.203	4.1	0.85	0.18	0.26	0.082	15.7
S %	Ba ppm	Ce ppm	Co ppm	Cr ppm	Cu ppm	Ga ppm	La ppm	Ni ppm	Pb ppm	Rb ppm
6.30	50	75	70	155	485	20	35	60	980	5
Sr ppm	Th ppm	U ppm	V ppm	Y ppm	Zn ppm	Zr ppm	Sb ppm	Cd ppm	As ppm	
30	25	25	40	20	1780	120	15	20	115	

Hardpan/Cemented Layers/No cements	Laterally Extensive Surface Hardpan
Period of exposure	15 years
Hardpan/cement depth in profile	Surface
Lateral extent of hardpan/cemented layers	Probably over entire dam

Thickness of hardpan / cemented layers	5-10cm
Cement mineralogy	goethite, jarosite, natrojarosite, gypsum
Surface Salt mineralogy	sulfur, halite, hexahydrite

Typical XRF analysis of hardpan

SiO2 %	Al2O3 %	Fe2O3 %	Fe %	MnO %	MgO %	CaO %	K2O %	TiO2 %	P2O5 %	SO3 %
34.8	2.89	39	27.3	0.11	1.8	0.54	0.16	0.2	0.085	16.1
S %	Ba ppm	Ce ppm	Co ppm	Cr ppm	Cu ppm	Ga ppm	La ppm	Ni ppm	Pb ppm	Rb ppm
6.45	30	85	15	35	1500	10	40	10	2590	5
Sr ppm	Th ppm	U ppm	V ppm	Y ppm	Zn ppm	Zr ppm	Sb ppm	Cd ppm	As ppm	
35	30	25	35	15	2910	95	15	30	220	

Dam	**South Dam** - egde spigot deposition, rock and soil walls
Original tailings mineralogy	pyrite, (galena, sphalerite chalcopyrite) quartz, clinochlore, muscovite, calcite
Tailings grain size distribution	coarse sand <1% silt 82% fine sand 9% clay 4%

Typical XRF analysis of original tailings

SiO2 %	Al2O3 %	Fe2O3 %	Fe %	MnO %	MgO %	CaO %	K2O %	TiO2 %	P2O5 %	SO3 %
67.2	9.5	14.2	9.91	0.202	2.7	0.9	1.21	0.44	0.101	4.2
S %	Ba ppm	Ce ppm	Co ppm	Cr ppm	Cu ppm	Ga ppm	La ppm	Ni ppm	Pb ppm	Rb ppm
1.68	220	60	45	50	625	20	60	10	120	50
Sr ppm	Th ppm	U ppm	V ppm	Y ppm	Zn ppm	Zr ppm	Sb ppm	Cd ppm	As ppm	
40	20	15	40	25	345	160	70	45	20	

Hardpan/Cemented Layers/No cements	Surface salts only
Period of exposure	5 years
Surface Salt mineralogy	Gypsum, halite, halotrichite, pickeringite, hexahydrite, kaolinite, rozenite

Typical XRF analysis of oxidised tailings

SiO2 %	Al2O3 %	Fe2O3 %	Fe %	MnO %	MgO %	CaO %	K2O %	TiO2 %	P2O5 %	SO3 %
65.2	6.92	16.7	11.70	0.168	2.4	0.75	0.7	0.36	0.08	9.2
S %	Ba ppm	Ce ppm	Co ppm	Cr ppm	Cu ppm	Ga ppm	La ppm	Ni ppm	Pb ppm	Rb ppm
3.68	105	55	45	45	1220	15	35	10	690	30
Sr ppm	Th ppm	U ppm	V ppm	Y ppm	Zn ppm	Zr ppm	Sb ppm	Cd ppm	As ppm	
40	35	20	35	15	1040	130	45	35	120	

4.4.2.1 Tailings Dam History

The CSA mine has two tailings dams, the North and the South dams, both of which are approximately 35yrs old. Both dams are still in use and during the period of this investigation the South Dam had the oldest surface. Initially deposition of tailings was via the center spigot method, but was subsequently changed to the edge method to allow increased water containment. As a result of this, a raised western region (Site 1) and a central region (Site 2) have been exposed for up to 12-15 years within the Northern Dam (Fig 4.6). These locations were the focus for examination of well-developed laterally-continuous surface hardpan. There is no recycling of the water back to the mine at this site and therefore the only means of water removal are through a central drainage line, seepage and evaporation. Drainage is collected in two collecting ponds and allowed at evaporate.

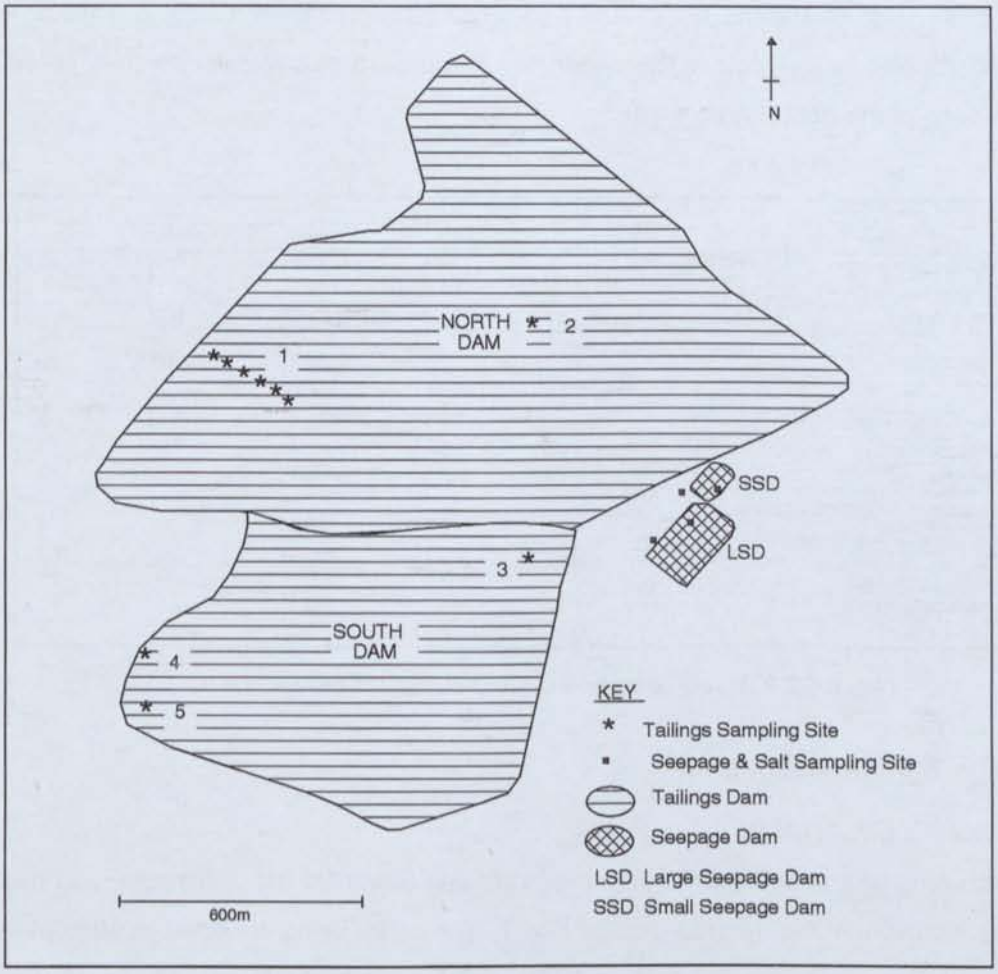

FIG 4.6 SAMPLING SITES AT THE CSA TAILINGS DAMS

4.4.2.2 Seepage Dam Investigations

The two decant ponds in which tailings water is collected (large seepage dam (LSD) & small seepage dam (SSD)) (Fig 4.6) were also investigated to measure solute concentrations and precipitation of salts typical of this geochemical system. Water did not appear to be collected in the SSD at the time of sampling, however the residual water (pH 3.9) was collected.

Photo 4.12 CSA Large seepage dam

Analysis for major and trace element composition of this water indicated high concentrations of Ca, Mg, and S, (Table 4.2). Both natrojarosite and gypsum had precipitated from this solution along the dam wall. Secondary minerals were also removed from pipes near SSD and LSD and the mineralogy was determined as natrojarosite, jarosite and gypsum. Water samples were also removed from the LSD which collects seepage from the North Dam. Direct seepage had a pH of 4.2, while the ponded water had a pH of 3. Both had increased

levels of Al, Ca, Fe, Mg, S, Na and Mn (Table 4.2). The salts precipitated from this water included pickeringite, kalinite and hexahydrite. The water had taken on a red colour with pale yellow slimes forming on the base of the dam (Photo 4.12).

	pH	EC	Al	Ca	Cd	Co
		mS/cm	mg/L	mg/L	mg/L	mg/L
Direct North Dam water	4.2--3.07	9.57	145	432.5	0.1	0.2
small seepage dam	3.9--3.34	1.56	36.7	144.2	<0.1	0.2
large seepage dam	3--2.53	10.69	368.2	609.1	0.1	0.5
	Cu	Fe	K	Mg	Mn	Mo
	mg/L	mg/L	mg/L	mg/L	mg/L	mg/L
Direct North Dam water	1.3	2218	36.3	872.0	63.9	<0.1
small seepage dam	0.9	0.6	8.9	61.4	7.9	<0.1
large seepage dam	1.1	1747	8.5	1191	93.7	<0.1
	Na	Ni	P	Pb	S	Zn
	mg/L	mg/L	mg/L	mg/L	mg/L	mg/L
Direct North Dam water	354.8	<0.1	2.6	0.7	3582	17.8
small seepage dam	9.9	<0.1	<0.1	<0.1	312.6	17.5
large seepage dam	452.6	0.2	3.9	0.2	4571	46.3

TABLE 4.2 ICP ANALYSIS FOR CSA DRAINAGE/SEEPAGE DAMS.

4.4.2.3 Tailings Dam Investigations

4.4.2.3.2 Sampling Description

During 1995 sampling was undertaken in both the North and South Dams. A traverse was made from the edge of the North Dam into fresh tailings at Site 1, with cores being collected at 40m intervals. A single site in the NE corner of the South Dam (Site 3) was sampled as this was suggested to be the oldest surface available (18 months-2 years old at the time of sampling).

In 1996 Site 1 was re-examined and additional cores at CSA 20 and CSA 180 (Fig 4.7) were removed for an annual geochemical comparison (Chapter 5). Additional samples were removed from the west side and the SW corner in the South Dam (Site 4 and Site 5 respectively) for comparison with Site 3. Samples were removed at 5m and 50m from the edge at Site 5 capturing both surface and palaeo-cements. A single core was removed from Site 4 where surface cements were again only minimal.

In 1997 Site 1 in the North Dam had been substantially covered with new tailings, however a hardpan region in the center of the dam (Site 2) was accessible. Samples for isotopic analysis were removed from this region and permeability tests undertaken. These results are discussed fully in Chapter 7.

4.4.2.2.3 Gangue and Sulfide Mineralogy

Both the North and South Dams contain varying amounts of quartz, muscovite and clinochlore. Calcite was also identified in the South Dam tailings. The North Dam tailings contains both pyrite and pyrrhotite with lesser amounts of galena, sphalerite and chalcopyrite (sulfide % 1.5-1.8). The South Dam has similar sulfide content but contains little or no pyrrhotite.

4.4.2.2.4. Secondary Mineralogy and Morphology

North Dam

Generally the tailings profile at Sites 1 and 2 consist of a 3-7cm thick surface hardpan (photo 4.13) underlain by a 10-30cm mottled zone which consists of both oxidised and unoxidised tailings with extensive development of cements in desiccation cracks in response to preferential redistribution of surface oxidation by-products. Below this, unoxidised tailings exist. The orange cements consist of goethite, jarosite, natrojarosite and gypsum. These cements also incorporate residual pyrite, quartz, chlorite and muscovite.

Fig 4.7 is a schematic diagram showing the locations of the cores samples from the Site 1 traverse. Below this is a brief description of each core.

FIG 4.7 SIDE VIEW OF SAMPLING LOCATIONS AT SITE 1, NORTH DAM

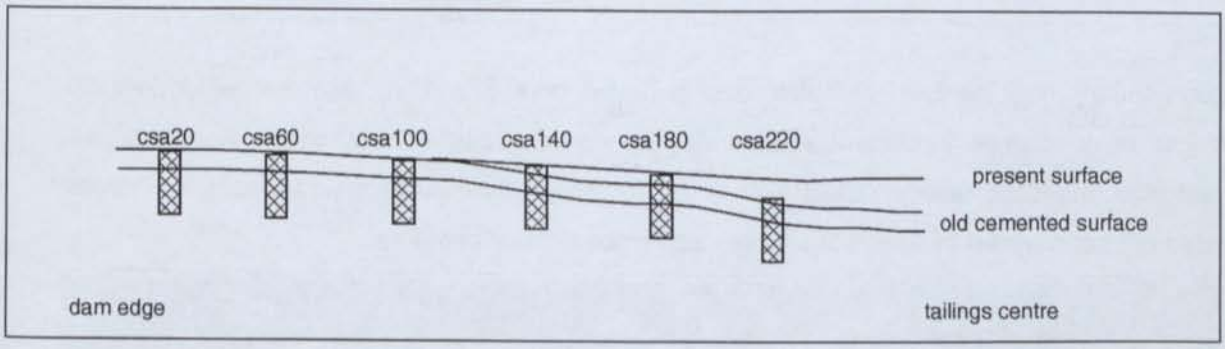

Distance from edge	depth of core	description of core contents
20m	0-45cm	hardpan at surface, unoxidised tailings directly below
60m	0-50cm	hardpan at 15cm depth, uncemented oxidised tailings above and unoxidised tailings below
100m	0-50cm	mottled crumbly cement mixed with unoxidised tailings to 10cm, below unoxidised tailings
140m	0-50cm	new tailings to 6.5cm, oxidised tailings to 25cm, cements to base
180m	0-50cm	new tailings to 3cm only, cements below
220m	66-116cm	slightly oxidised new tailings, cements at 67cm depth

In 1996 this region was still uncovered and had changed little, however erosion had removed much of the surface cements leaving residual desiccation crack cements (photo 4.14). In regions where new tailings had been deposited on old hardpan, the integrity of the cement was not compromised.

Photo 4.13 CSA North Dam Site 1 (CSA20) hardpan (1995)

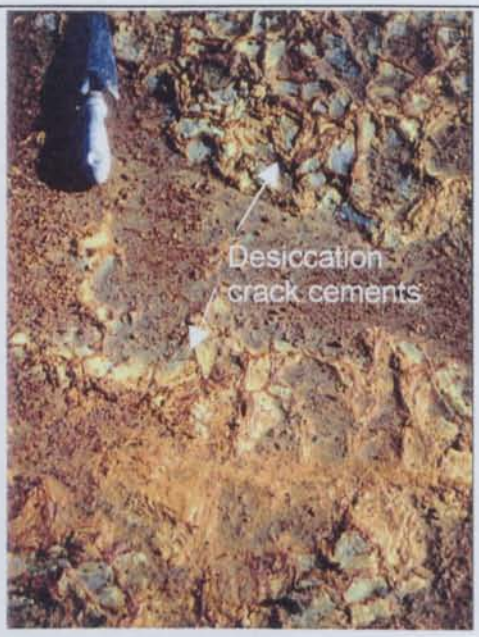

Photo 4.14 CSA CSA North Dam Site 1 (CSA20) dessciation cement (1996)

SEM examinations of 2 hardpan samples, one removed from Site 1 in 1995, the other in 1996, showed little or no change in cement and primary mineral degradation over time. Cements have developed throughout the tailings (EMG 4.23 & 4.24). Large pure sulfur crystals have developed, surrounded but not covered by fine cubes, fibers and smooth basal cements.

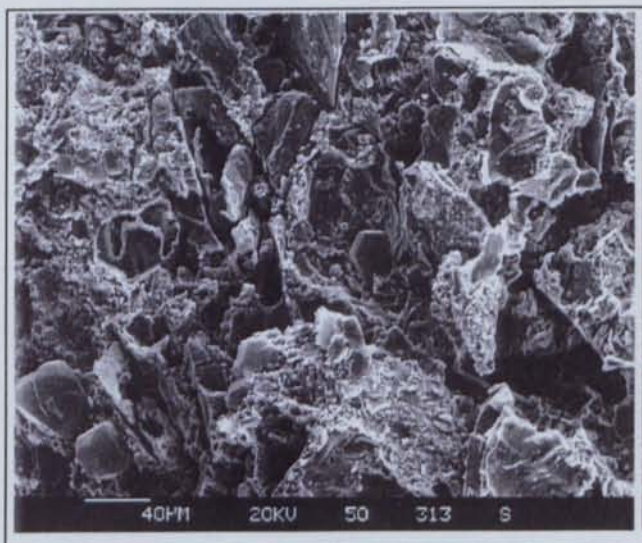

EMG 4.23 General view of CSA North Dam cement

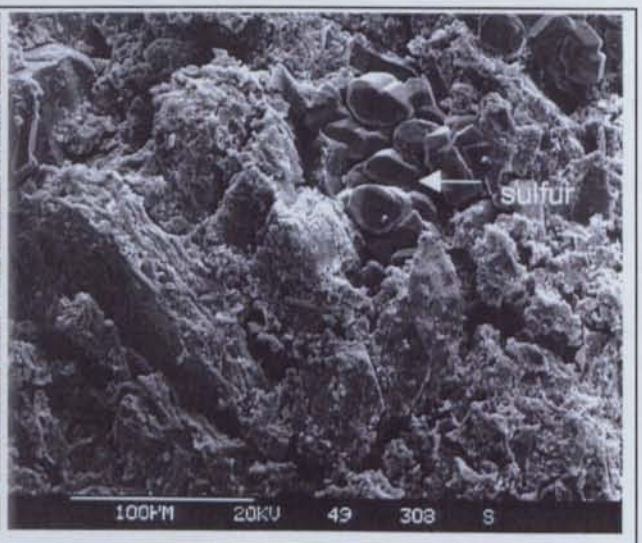

EMG 4.24 General view of CSA North Dam cement including pure sulfur crystals

EMG 4.25 shows the development of a large bridging column gypsum cement, fibrous Al sulfate minerals containing minor Fe (possibly halotrichite), and cubic Fe minerals containing variable quantities of S, Si and Al. EMG 4.26 shows a close-up of this cubic cement, producing multiple coats on primary mineral grains. This Fe oxide is probably goethite as identified through XRD, with minor additives of S as sulfate. A Si signature was observed throughout much of the cement, suggesting Si is relatively mobile within the system.

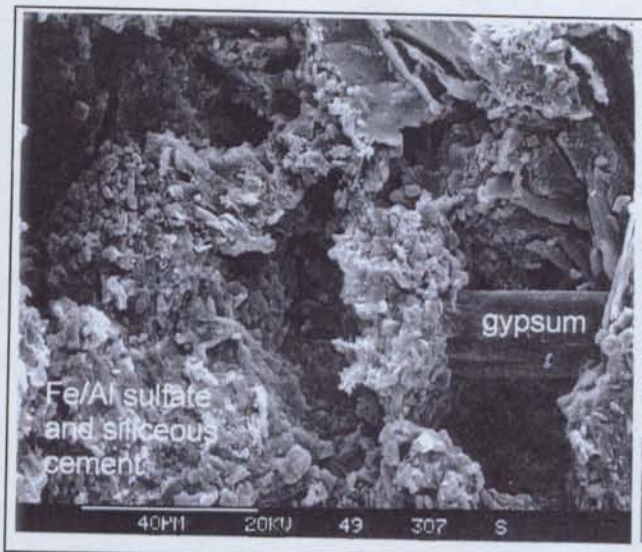

EMG 4.25 Bridging gypsum crystals, variable Al/Fe sulfate and siliceous cements of CSA North Dam hardpan

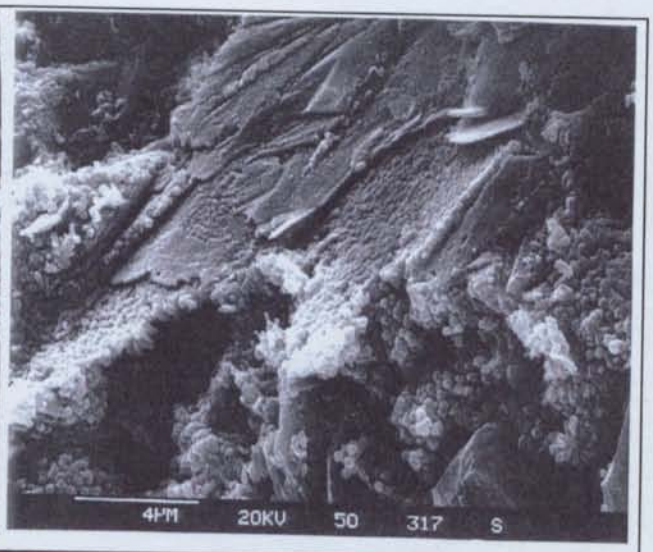

EMG 4.26 Multiple coatings of Fe mineral with variable S, Si and Al on primary grains, CSA North Dam hardpan

South Dam

In 1995 observations of Site 3 showed an oxidised region had developed down to a depth of 3cm. The secondary minerals present within this zone were characterised as minor goethite and gypsum. No surface hardpan had developed. However the secondary salts halotrichite, pickeringite, hexahydrite, kalinite and rozenite were identified on the surface (photo 4.15). Some minor cements intimately mixed with the unoxidised tailings at depth are thought to be desiccation crack cements.

Photo 4.15 Surface Salt CSA South Dam Site 3, (1995)

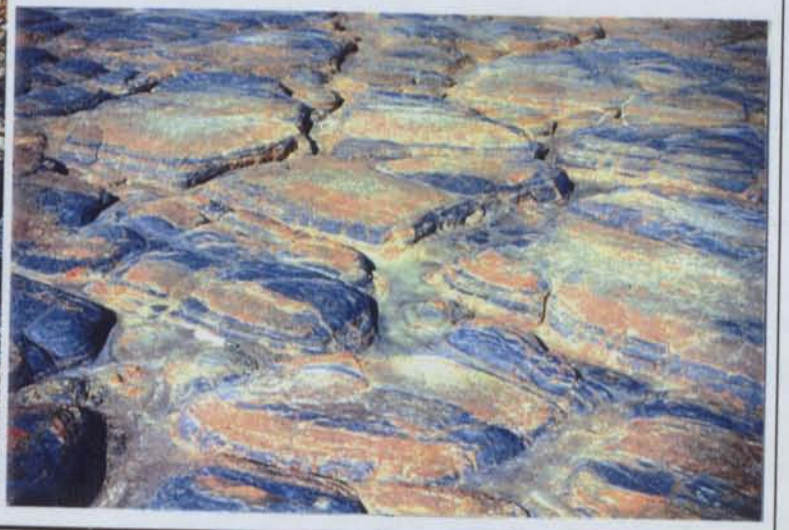

Photo 4.16 Minor surface cements, CSA South Dam, Site 4 (1996)

In 1996 the surface of the dam at this site had changed very little, however less surface salt crusts were present. At this time it was suggested by staff that the region previously examined may have been disturbed by traffic during dam wall construction and therefore may not be representative of the

entire dam. Cores from the SW corner (Site 5) and west side (Site 4) were obtained for comparison. Site 4 showed very different surface morphology compared to Site 3, with minor surface cements developing (photo 4.16).

4.2.2.4 Discussion

The surface cements observed in the North Dam are extremely hard and in most cases a mottled zone exists directly beneath and is underlain by unoxidised tailings. The mottled zone consists of desiccation crack cements produced during periods of exposure through the same geochemical reactions that have taken place at the surface. These cements may have been enhanced through the redistribution of soluble secondary minerals from the surface into these preferential flow paths during rainfall or subsequent tailings deposition.

The development of these hardpans is very much slower than those produced in highly sulfidic tailings. These tailings contain only 1.5-2% total sulfide, thus acid generation associated with sulfide oxidation is limited and degradation of gangue minerals is reduced, resulting in diminished by-products available for cementation.

The South Dam showed very limited sulfide oxidation and hardpan development after 5 years of exposure. This may simply reflect the lower sulfide content and thus the slow formation of hardpans associated with this type of tailings.

However, the characteristics of the tailings have changed over time, so that the tailings are now physically and mineralogically different. When tailings were initially deposited in the dams, the coarse fraction of the tailings were also released. Now the tailings are sized with the coarse fraction retained for back-filling. Thus the South Dam contains only the finer fraction of the tailings which may be inhibiting hardpan development through increased water holding capacity. At these elevated saturation levels, oxygen diffusion into the tailings is limited and thus oxidation reactions and the associated geochemical reactions are also substantially inhibited.

Another difference between the tailings in the North and South dams is the mineralogy, which is dictated by the ore being processed at the time. XRD analysis indicated that the South Dam tailings contained additional calcite but little or no pyrrhotite compared with the old North Dam tailings. The lack of reactive pyrrhotite reduces the amount of Fe available for cementing, while the additional calcite may be maintaining elevated pH conditions not optimal for sulfide oxidation and may be potentially limiting secondary mineral precipitation.

4.4.3 Peak Au Mine

Dam	only one dam present – central spigot into drainage chanel, no walls
Original tailings mineralogy	pyrrhotite, pyrite, (sphalerite) quartz, muscovite, microcline, clinochlore, calcite,
Tailings grain size distribution	coarse sand 11% silt 26% fine sand 52% clay 6%

Typical XRF analysis of original tailings

SiO2 %	Al2O3 %	Fe2O3 %	Fe %	MnO %	MgO %	CaO %	K2O %	TiO2 %	P2O5 %	SO3 %
75.7	6.95	9.07	6.34	0.088	2.5	0.19	1.77	0.26	0.074	6.16
S %	Ba ppm	Ce ppm	Co ppm	Cr ppm	Cu ppm	Ga ppm	La ppm	Ni ppm	Pb ppm	Rb ppm
2.47	280	50	20	25	2445	15	35	10	1550	80
Sr ppm	Th ppm	U ppm	V ppm	Y ppm	Zn ppm	Zr ppm	Sb ppm	Cd ppm	As ppm	
25	10	10	25	15	2760	120	110	60	80	

Hardpan/Cemented Layers/No cements	Surface salts only
Period of exposure	still in use - study site approx. 12 month exposed
Hardpan/cement depth in profile	N/A
Lateral extent of hardpan/cemented layers	N/A
Thickness of hardpan / cemented layers	N/A
Cement mineralogy	N/A
Surface Salt mineralogy	gypsum, halite, blodite

Typical XRF analysis of hardpan/cements

SiO2 %	Al2O3 %	Fe2O3 %	Fe %	MnO %	MgO %	CaO %	K2O %	TiO2 %	P2O5 %	SO3 %
62.9	5.57	7.65	5.35	0.1045	2.45	0.63	1.66	0.23	0.0695	13.34
S %	Ba ppm	Ce ppm	Co ppm	Cr ppm	Cu ppm	Ga ppm	La ppm	Ni ppm	Pb ppm	Rb ppm
5.34	220	50	40	30	2180	15	35	10	2305	70
Sr ppm	Th ppm	U ppm	V ppm	Y ppm	Zn ppm	Zr ppm	Sb ppm	Cd ppm	As ppm	
30	15	15	25	10	2280	110	105	75	130	

4.4.3.1 Tailings History

The tailings dam at Peak Gold Mine was started in early 1992 and thus is only 6 years old. It has a central spigot system so that the majority of coarse tailings are deposited in the center, the fine fraction being transported to the periphery. Tailings seepage mixes with fresh water run off in a seepage dam down-slope of the tailings facility.

4.4.3.2 Sampling Description

In 1995 a general review of the tailings dam was undertaken and a single core removed from the center of the dam (Site 1, Fig 4.8). During 1996, 4 additional sites were investigated and surface samples removed. Three cores were also removed at this time, one was a re-core of Site 1 and contained freshly deposited tailings. Another was removed from Site 5, adjacent to an open excavation in the tailings, and the third from Site 3 where the surface was suggested to be the oldest available (1 year exposed).

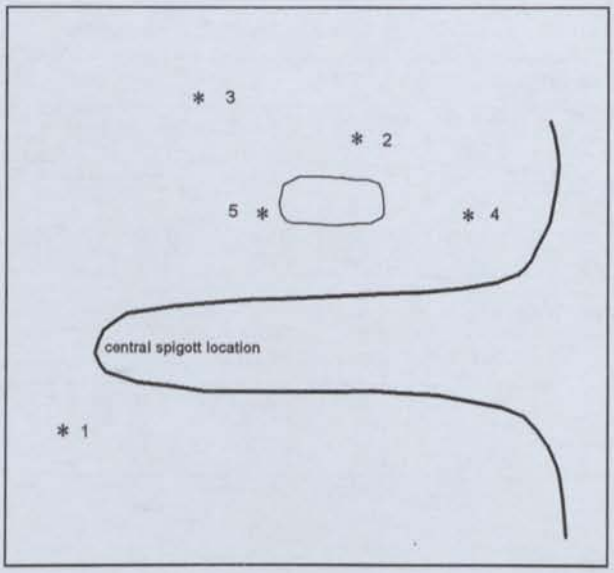

FIG 4.8 SAMPLING LOCATIONS IN THE PEAK TAILINGS DAM

4.4.3.3 Gangue and Sulfide Mineralogy

XRD analysis indicated that the tailings mineralogy is a mixture of quartz, muscovite, microcline, clinochlore, pyrite, sphalerite, pyrrhotite and calcite. Laboratory analysis of the tailings suggested levels of 2-2.4% total sulfide, however discussions with staff on site indicate concentrations of up to 6-7%.

4.4.3.4 Secondary Mineralogy and Morphology

Photo 4.17 Surface salts, Peak Site 1, (1995)

Salt crusts rather than cements have developed on the surface of this dam (photo 4.17). These have been identified as gypsum, halite and blodite. In some locations (Site 2 and 3) the tailings appear to have oxidised to 3-4cm depth, shown by a red/orange surface compared with the underlying light grey tailings. Photos 4.18 and 4.19 shows the surface at Site 3. The oxidation by-products appear to have bound the surface together, resisting wind and water erosion and resulting in an undercut surface. SEM examinations of this material indicated that the tailings remain only loosely cemented. EMG 4.27 shows a general view of the cements. Much of the

fine-grained material was identified as primary aluminosilicates rather than secondary cements. Upon closer inspection, very fine-grained sub-spherical grains of Fe oxides were identified covering may of the primary grains (EMG 4.28).

Photo 4.18 Fe oxide cements within the upper 3-5cm of Peak tailings (Site 3) (1996)

Photo 4.19 Fe oxide cements resisting wind and water erosion at Peak Site 3 (1996)

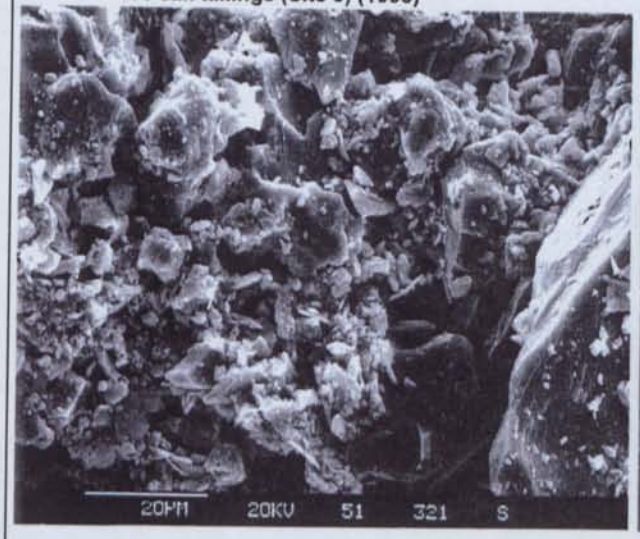

EMG 4.27 General view of Peak Site 3 cements

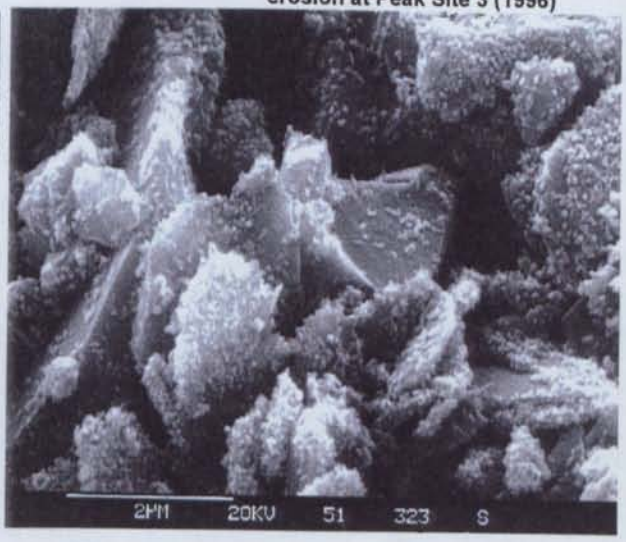

EMG 4.28 Close up of EMG 4.27 Fine grained Fe oxide cements coating primary grains

4.4.3.5 Discussion

As the Peak site is very new and tailings deposition occurs continuously into the one dam, there has been no opportunity to observe tailings exposed for any great length of time. It is for this reason that investigations of this site have focused more on the laboratory experiments than field observations.

4.4.4 Disused Chesney Au-Cu Mine

Dam	**Upper Dam** - single spigot deposition, tailings walls
Original tailings mineralogy	Unknown, present tailings mineralogy includes: (pyrite, pyrrhotite) quartz, clinochlore, muscovite, magnetite
Tailings grain size distribution	coarse sand 55-60% silt 6-13% fine sand 22-30% clay 3-9%

Typical XRF analysis of present uncemented tailings

SiO2 %	Al2O3 %	Fe2O3 %	Fe %	MnO %	MgO %	CaO %	K2O %	TiO2 %	P2O5 %	SO3 %
72.3	5.07	13.5	9.41	0.086	2	0.001	0.23	0.27	0.06	0.89
S %	Ba ppm	Ce ppm	Co ppm	Cr ppm	Cu ppm	Ga ppm	La ppm	Ni ppm	Pb ppm	Rb ppm
0.36	40	20	25	65	1270	20	700	60	105	5
Sr ppm	Th ppm	U ppm	V ppm	Y ppm	Zn ppm	Zr ppm	Sb ppm	Cd ppm	As ppm	
20	10	10	30	15	50	115	20	20	30	

Hardpan/Cemented Layers/No cements	Laterally Discontinous Surface Hardpan
Period of exposure	Uncertain approx. 77 years
Hardpan/cement depth in profile	Surface
Lateral extent of hardpan/cemented layers	Only in seepage zone
Thickness of hardpan / cemented layers	approx. 1m
Cement mineralogy	goethite, natrojarosite, hydrobasaluminite

Typical XRF analysis of hardpan/cements

SiO2 %	Al2O3 %	Fe2O3 %	Fe %	MnO %	MgO %	CaO %	K2O %	TiO2 %	P2O5 %	SO3 %
70.4	3.02	18.3	12.80	0.048	0.9	0.001	0.21	0.26	0.066	0.87
S %	Ba ppm	Ce ppm	Co ppm	Cr ppm	Cu ppm	Ga ppm	La ppm	Ni ppm	Pb ppm	Rb ppm
0.35	45	20	15	35	1740	20	350	10	220	5
Sr ppm	Th ppm	U ppm	V ppm	Y ppm	Zn ppm	Zr ppm	Sb ppm	Cd ppm	As ppm	
20	30	10	30	10	30	115	200	10	45	

Dam	**Lower Dam** - single spigot deposition, tailings walls
Original tailings mineralogy	Unknown, present tailings mineralogy includes: (pyrite, pyrrhotite) quartz, clinochlore, muscovite, magnetite
Tailings grain size distribution	coarse sand 2% silt 58% fine sand 23% clay 13%

Typical XRF analysis of present uncemented tailings

SiO2 %	Al2O3 %	Fe2O3 %	Fe %	MnO %	MgO %	CaO %	K2O %	TiO2 %	P2O5 %	SO3 %
57.4	9.4	18.3	12.80	0.15	4.033	0.022	0.52	0.307	0.064	1.39
S %	Ba ppm	Ce ppm	Co ppm	Cr ppm	Cu ppm	Ga ppm	La ppm	Ni ppm	Pb ppm	Rb ppm
0.56	70	35	20	55	1600	10	20	10	150	30
Sr ppm	Th ppm	U ppm	V ppm	Y ppm	Zn ppm	Zr ppm	Sb ppm	Cd ppm	As ppm	
20	15	0	115	15	135	80	5	0	35	

Hardpan/Cemented Layers/No cements	Cemented layers
Period of exposure	Uncertain approx. 45 years
Hardpan/cement depth in profile	discontinuously within at least upper 50cm
Lateral extent of hardpan/cemented layers	uncertain
Thickness of hardpan / cemented layers	1-5mm

4.4.4.1 Tailings History

The history of processing has been compiled from a number of reports however the literature often contradicts other references (Carne, 1908, Andrews, 1911, Rayner, 1969, Mele, 1995). There are 5 small tailings impoundments located down hill from the disused mine workings (Fig 4.9).

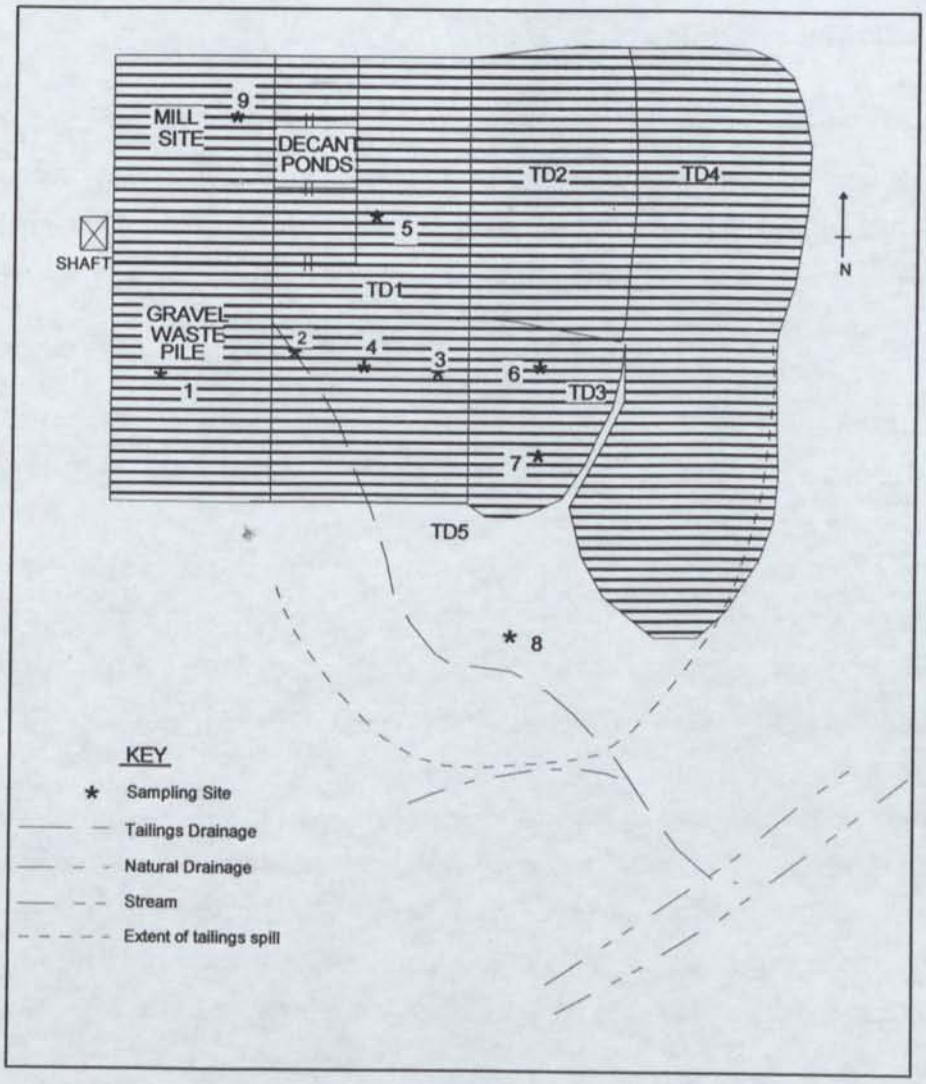

FIG 4.9 SAMPLING LOCATIONS AT THE CHESNEY TAILINGS DAMS

The tailings history is not well known however the textures and mineralogy reflects at least 2 or 3 separate periods of deposition. Between 1888-1899 Au ore was mined at Chesney, however no discussions on processing have been located. The mine underwent extensive development in 1899 when Cu was encountered at 46m. As the Cu content increased with depth, difficulties associated with the separation of free-milling Au ores from Cu ore resulted in the Chesney mine being absorbed by the Great Cobar Company in 1903. During 1904 to 1910 primary Au-Cu ores were mostly blended as a siliceous flux at The Great Cobar smelters. Some of the original tailings from Chesney were also smelted during this period.

When rich Cu shoots were encountered at depth in 1910-1911, a plant was built to concentrate ore by jigs and mineral separation, to replace transporting the ore to the Great Cobar smelter. The mine was closed in 1920 not to be reopened until 1943 under New Occidental Gold Mines. The mine was closed in 1952. A new shaft was sunk in 1971-72, however promising discoveries at CSA and Peak took precedence. The deposit has recently been re-investigated and production is due to start next year, under the Peak Gold Mine.

From this review, 3 periods of tailings deposition are likely, including: 1888-1899 free-milling Au ore resulting in coarse-grained waste 2-5mm on the upper slopes; 1910-1920 Au-Cu concentrator tailings resulting in coarse sand fractions with minor medium-fine sand size fractions in the upper dams; and 1943-1952 Au-Cu concentrator tailings potentially forming the finer wastes in the low dams. It is suggested that the tailings were deposited similarly between 1910-1952, with grain size differentiation only occurring due to tailings deposition method rather than processing style. The coarser grained tailings may have dropped out of the slurry on the upper slopes and dams, while fines would have been carried to the lower dams.

Deposition of the 2-5mm tailings from the free milling Au ore produced during 1888-1899 is thought to have occurred on the upper slopes of the mine site (Site 1). It is suggested that during processing via jig and mineral separation between 1910-1920 that the tailings were simply allowed to run down slope from the mill site developing grain size fractionation during transport (Fig 4.10a).

It may have been during the period of operation between 1943-52 that the dam wall construction was performed. It is suggested that the previously deposited gravel tailings and coarse tailings were used to construct these walls. Three decant ponds are present in the upper-most region below the mill site. Down slope from these decant ponds, three tailings dams have been constructed. A fourth tailings region further down slope appears to be in no way contained and is thought to be a spill way (Fig 4.10b).

Tailings were observed in a gully beside of the tailings impoundments as well as along the edges of Lake Jackson (south of the tailings). It is uncertain as to whether these tailings are from spills during mine operation or whether they are erosion/runoff since mine closure.

4.4.4.2 Sampling Description

In 1995 surface samples were removed from many sites through-out the tailings impoundments, gravel heaps and spillway areas. Coring was undertaken at Site 2 in Dam 1 where natural drainage had developed a series of rills in well-cemented tailings. A second uncemented site (Site 3) further down slope within Dam 1 was also cored for comparison. During 1996 an additional 4 sites were sampled, Sites 4, and 5 in Dam 1 and 6 and 7 in Dam 2. Site 2 was re-cored, as was Site 3.

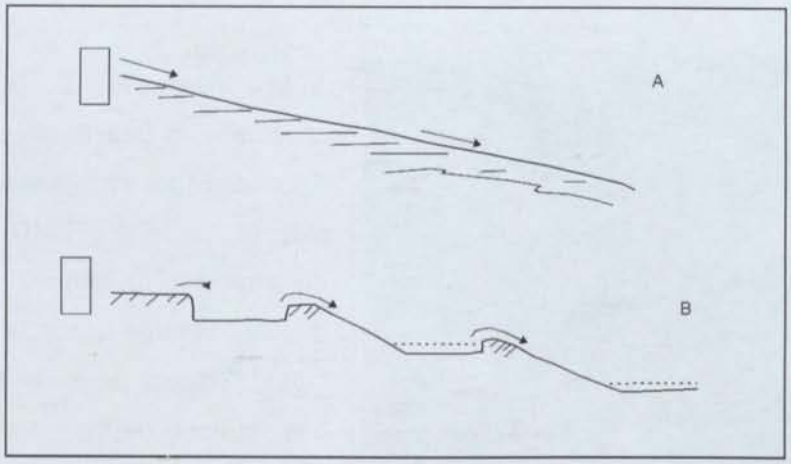

FIG 4.10A & B SUGGESTED DEPOSITION STYLES AT THE CHESNEY SITE

4.4.4.3 Gangue and Sulfide Mineralogy

The original tailings mineralogy is unknown for this location however the present primary mineralogy consists of quartz, clinochlore, muscovite, magnetite with minor pyrite, chalcopyrite, pyrrhotite and traces of sphalerite and galena. The total sulfur content of the tailings at present is approximately 1-2%.

4.4.4.4 Secondary Mineralogy and Morphology

Cements have not developed universally at this site. Cementing was observed only within the gravels at Sites 1 and 9 (photo 4.20) and in the upper coarse tailings in Dam 1 at Sites 2 and 5 (photo 4.21). These regions have developed a well layered stratigraphy with cements of goethite, natrojarosite and hydrobasaluminite developing at the boundary of the coarse and fine fractions. XRD analysis of the tailings at the non-cemented Site 3, indicated that there were no detectable sulfides and that the gangue minerals were the same as those observed at Site 2.

Photo 4.20 Cements within coarse grained gossaniferous fragments and fine tailings, Site 9 (1996)

Photo 4.21 Cements within coarse grained tailings, TD1, Site 2 Chesney (1995)

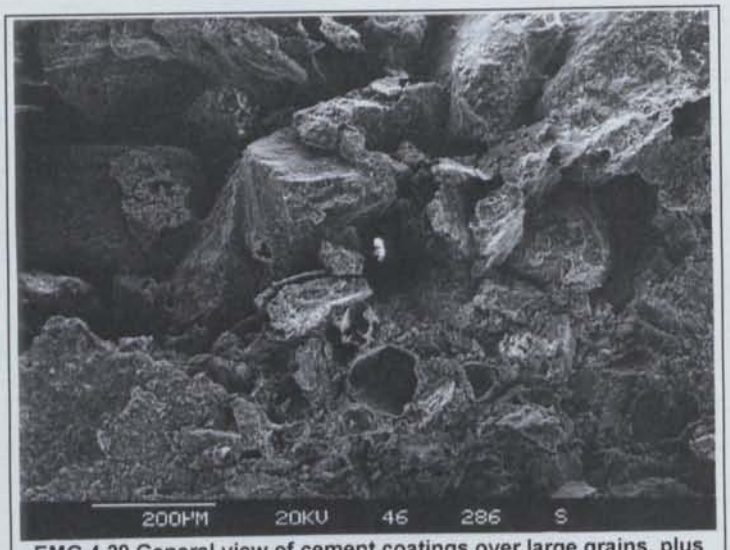

EMG 4.29 General view of cement coatings over large grains, plus bridging and cutan cements in fine grained tailings, Site 2, Chesney

SEM investigations of the hardpan developed at Site 2 indicate the large role Fe oxides (goethite) and siliceous cements play at this site. EMG 4.29 shows the development of cement coatings on the majority of large grains, while bridging and cutan cements have developed within the finer grained region. EMG 4.30 shows a close up of the more fine-grained region, showing the multiple cement morphologies. The cutan cements may have originally developed as a grain coating and the grain has now dissolved or may have developed as a pore coating. EMG 4.31 shows the main sub-angular cement consisting of alternating Fe and Si signatures developed throughout the hardpan. The Fe oxides may have incorporated Si into their structures, however only 0-5% incorporation has been previous identified (Carlson & Schertmann, 1981). Equal EDX signatures of Fe and Si suggest the development of discrete Fe oxides and siliceous material.

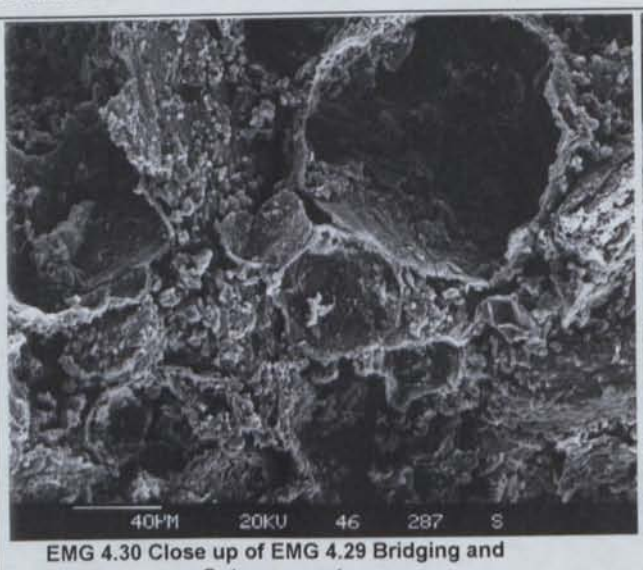

EMG 4.30 Close up of EMG 4.29 Bridging and Cutan cements

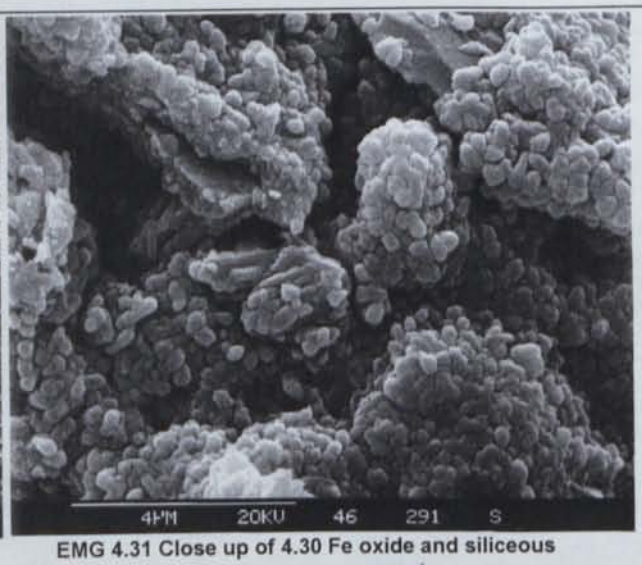

EMG 4.31 Close up of 4.30 Fe oxide and siliceous cements

4.4.4.5 Discussion

The review of the site suggests that the tailings cements were developed through a leaching mechanism. The hill above TD1 has a scree slope of coarse waste material (gravel sized). It is proposed that the gravel waste rock has weathered and oxidised over time releasing Fe and other elements into the surrounding environment. As a consequence of the natural drainage of the area, iron oxides and other compounds have been relocated into the tailings below. The result is a large gully developed at the base of the hill which has remnant cementing structures.

It is suggested that the moist finer tailings observed further from the base of the hill in TD1 have less potential for cementation. In general the tailings within 20cm of the surface were puggy/very fine sand/silt and very moist. The fine textured tailings present appear to have an increased moisture retaining capacity, and as a result, any Fe-rich seepage reaching this area is not evaporated thus reducing the formation of cements.

The rainfall run-off from the surrounding ridges appears to channel through the gully area within the coarse tailings and then infiltrates the finer tailings eventually seeping from the dam wall to the lower lying TD5. Excess run-off from these lower uncemented tailing have also resulted in gully erosion (site 8). In this lower gully region the eroded tailings have been interbedded with other eroded material from the surrounding natural landscape. At this point the tailings have become cemented in discrete layers. This site may also be prone to Fe-rich waters from higher in the landscape and thus cements have resulted through similar mechanisms observed in TD1. An alternative to this mechanism is that the cements may have developed as direct by-product of the in-situ oxidation of tailings. It is suggested that it is more likely that the cements observed here are in fact developed in-situ as palaeo-surfaces rather than the leaching effects observed elsewhere. The main reason for this is the well-bedded nature of the soils and tailings cements.

4.4.5 Woodlawn Cu-Pb-Zn Mine

Dam	**South Dam** - egde spigot deposition, rock walls
Original tailings mineralogy	pyrite, (sphalerite) muscovite, quartz, siderite, talc, calcite, clinochlore
Tailings grain size distribution	coarse sand 1-7% silt 15-31% fine sand 51-75% clay 4-9%

Typical XRF analysis of original tailings

SiO2 %	Al2O3 %	Fe2O3 %	Fe %	MnO %	MgO %	CaO %	K2O %	TiO2 %	P2O5 %	SO3 %
35.9	5.11	28.7	20.1	0.139	5.8	0.69	0.72	0.21	0.106	57
S %	Ba ppm	Ce ppm	Co ppm	Cr ppm	Cu ppm	Ga ppm	La ppm	Ni ppm	Pb ppm	Rb ppm
22.8	8635	45	55	50	3925	25	35	10	12190	35
Sr ppm	Th ppm	U ppm	V ppm	Y ppm	Zn ppm	Zr ppm	Sb ppm	Cd ppm	As ppm	
80	40	30	20	5	22650	60	120	190	870	

Hardpan/Cemented Layers/No cements	Surface salts only
Period of exposure	8 years
Hardpan/cement depth in profile	N/A
Lateral extent of hardpan/cemented layers	N/A
Thickness of hardpan / cemented layers	N/A
Cement mineralogy	N/A
Surface Salt mineralogy	gypsum, natrojarosite, hexahydrite

Typical XRF analysis of hardpan/cements

SiO2 %	Al2O3 %	Fe2O3 %	Fe %	MnO %	MgO %	CaO %	K2O %	TiO2 %	P2O5 %	SO3 %
31.3	3.67	26.7	18.7	0.092	4.1	1.47	0.69	0.25	0.114	44.2
S %	Ba ppm	Ce ppm	Co ppm	Cr ppm	Cu ppm	Ga ppm	La ppm	Ni ppm	Pb ppm	Rb ppm
17.7	12620	65	50	45	1125	20	190	10	6920	30
Sr ppm	Th ppm	U ppm	V ppm	Y ppm	Zn ppm	Zr ppm	Sb ppm	Cd ppm	As ppm	
125	30	25	15	5	3610	65	80	75	695	

4.4.5.1 Tailings Dam History

The Woodlawn mine has three tailings facilities, North, South and West Dams (Fig 4.11). The tailings in the North Dam have recently been retreated, and were not investigated. The West Dam was being used at the time of sampling. Tailings were deposited in the South Dam between 1982-88 and as this was the oldest surface present at the site, this dam was the focus of the investigation. All tailings were deposited via the edge spigot method. Seepage from the tailings and other parts of the mine site is pumped to an evaporation pond distant from the tailings dams.

4.4.5.2. Sampling Description

Surface samples were removed from a gully site (Site 1) developed at the northern edge of the South Dam as well as a hole site (Site 2) where active excavation for reprocessing was taking place in July 1995 (Fig 4.11). A single core was removed from each location to determine variations in mineralogy with depth and the developing geochemical trends. Unfortunately because of the puggy nature of the tailings at the hole site, a core of only 12cm could be obtained. Sampling at the gully site was more successful and a core down to 48cm was obtained. Water samples were also removed from the South Dam and the base of the gossan dump.

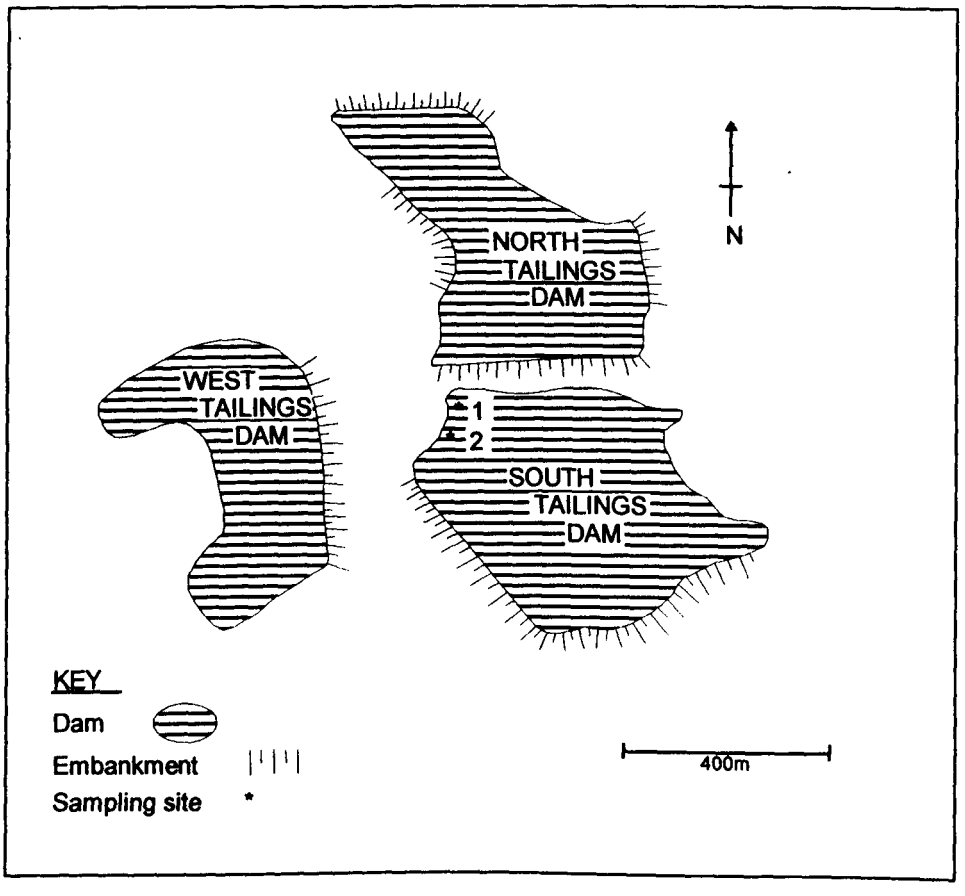

FIG 4.11 SAMPLING SITES AT THE WOODLAWN TAILINGS DAMS

4.4.5.3 Gangue and Sulfide Mineralogy

XRD analysis indicates that gangue mineralogy included quartz, muscovite, siderite, talc and clinochlore, with pyrite and sphalerite constituting the 21-23% sulfide component.

4.4.5.4 Secondary Mineralogy and Morphology

On the surface, sulfide oxidation has taken place producing a crust 0.5-1cm thick over the entire dam (Photos 4.22 & 4.23). This crust consists of natrojarosite, gypsum and hexahydrite.

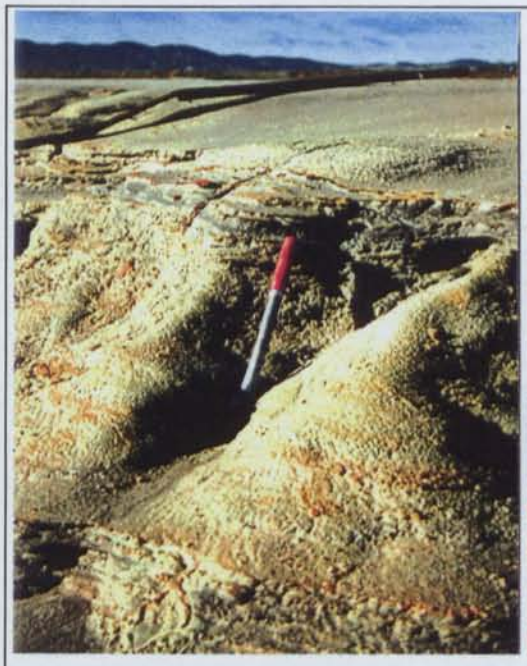

Photo 4.22 General surface salts, Woodlawn South Dam (1995)

Photo 4.23 Surface salts, Woodlawn, South Dam, Site 1 (1995)

Photo 4.24 Salts exposed on a vertical profile at Site 2, Woodlawn, South Dam (1995)

Retreatment of the South Dam had just commenced at the time of the visit and excavation had exposed a vertical tailings profile. Large quantities of salts had precipitated at different levels on an excavated profile which had been exposed for only 2 days (Photo 4.24). The salt crusts observed were 1-5mm thick with unoxidised tailings immediately below. The notable difference in the two day old profile covered with salt and the 8 year old surface with less than 1mm salt in some locations suggest that the tailings must be saturated with many salts but these are not accessed through surface evaporation. Samples of this material where removed for characterisation which revealed a mixture of natrojarosite and gypsum.

4.4.5.5 Water Investigations

Water samples were taken from different locations around the site to obtain an understanding of the processes occurring in the tailings and associated waters. Samples were removed from the South Dam - pH 5.1 and at a seepage area west of the North Dam near the gossan dump - pH 3.4. ICP analysis of these waters indicates high levels of Al, Ca, Cu, Fe, Mg, Mn, Na, S and Zn especially within the seepage (Table 4.3). The low pH observed and the elevated levels of solutes supports the suggestion that this is a very reactive system.

	pH	EC	Al	Ca	Cd	Co
		mS/cm	mg/L	mg/L	mg/L	mg/L
south dam water	5.1--3.64	3.04	23.9	264.4	1.8	0.3
seepage pond	3.4--2.72	19	1257	377.2	66.2	4.6
	Cr	Cu	Fe	K	Mg	Mn
	mg/L	mg/L	mg/L	mg/L	mg/L	mg/L
south dam water	<0.1	12.9	4.4	1.4	177.7	15.8
seepage pond	0.5	500.1	542.2	<0.1	1195	175.9
	Na	Ni	P	Pb	S	Zn
	mg/L	mg/L	mg/L	mg/L	mg/L	mg/L
south dam water	223.0	0.4	<0.1	2.4	820	236.1
seepage pond	20.5	3.9	8.8	0.6	10725	3489

TABLE 4.3 ICP ANALYSIS OF WATER FROM WOODLAWN SITE

4.4.5.6 Discussion

The fact that 7 years of exposure has produced less than 1cm of surface crust and that a 2 day old vertical profile produces just as much secondary mineral formation indicates that the climate and physical properties of the tailings are playing a large role. It is suggested that many of the oxidation by-products forming at the surface are in fact being relocated vertically before they are able to precipitate out as surface salts. This has been verified through ICP solute analysis (Chapter 5).

This mine is in a slight rainfall deficit and thus has a negative water balance. These conditions should promote drying of the surface, allowing reactions to take place at rapid rates. It is however the fine-grained nature of the tailings that is limiting oxidation, through their high water holding capacity. The maintenance of elevated levels of saturation limits oxygen diffusion into the tailings and thus reduces oxidation, by-product development and cementing. These combined with the leaching action of the rainfall, has produced a profile of surface salts, oxidation to a depth of only 3cm below which unoxidised tailings persist.

4.5 Pine Creek Inlier, N.T

4.5.1 Ranger U Mine

Dam	only one dam present - edge spigot deposition, rock walls
Original tailings mineralogy	(pyrite) quartz, muscovite, clinochlore, halloysite, hematite
Tailings grain size distribution	coarse sand 17% silt 18% fine sand 48% clay 14%

Typical XRF analysis of original tailings

SiO2 %	Al2O3 %	Fe2O3 %	Fe %	MnO %	MgO %	CaO %	K2O %	TiO2 %	P2O5 %	SO3 %
56.5	11.8	10.8	7.34	0.145	11.4	1.1	0.52	0.48	0.464	2.07
S %	Ba ppm	Ce ppm	Co ppm	Cr ppm	Cu ppm	Ga ppm	La ppm	Ni ppm	Pb ppm	Rb ppm
0.83	55	20	50	70	410	35	35	70	645	30
Sr ppm	Th ppm	U ppm	V ppm	Y ppm	Zn ppm	Zr ppm	Sb ppm	Cd ppm	As ppm	
25	10	550	105	35	70	205	25	25	10	

Hardpan/Cemented Layers/No cements	No cements
Period of exposure	In use at time of study
Hardpan/cement depth in profile	N/A
Lateral extent of hardpan/cemented layers	N/A
Thickness of hardpan / cemented layers	N/A
Cement mineralogy	N/A
Surface Salt mineralogy	gypsum, boussingaultite, wattevillite, hexahydrite, rozenite

Typical XRF analysis of salts

SiO2 %	Al2O3 %	Fe2O3 %	Fe %	MnO %	MgO %	CaO %	K2O %	TiO2 %	P2O5 %	SO3 %
38.1	10.56	6.38	4.46	0.96	11.1	3.65	1.2	0.35	0.323	18.6
S %	Ba ppm	Ce ppm	Co ppm	Cr ppm	Cu ppm	Ga ppm	La ppm	Ni ppm	Pb ppm	Rb ppm
7.45	195	20	55	120	260	35	35	125	935	60
Sr ppm	Th ppm	U ppm	V ppm	Y ppm	Zn ppm	Zr ppm	Sb ppm	Cd ppm	As ppm	
40	20	325	75	35	55	190	55	40	30	

4.5.1.1 Tailings History

Production at the Ranger Mine started in 1981 with the tailings being deposited in a single tailings impoundment. Deposition was via the edge spigot method, initially sub-aqueously but was changed to sub-aerial deposition to increase consolidation rates. Presently tailings are being deposited into the disused open pit, while research is being undertaken to determine the appropriate method of closure of the tailings dam.

4.5.1.2 Sampling Description

At the time of the site visit the majority of the tailings dam was water saturated with only one area being available for sampling (Fig 4.12). Several sites were sampled in this region both for original tailings and secondary salts. Core sampling was difficult because of the moist nature of the tailings, however 2 cores were obtained. The first core removed tailings from the surface to 20cm depth and the deeper core contained tailings from 1-1.5m depth (Site 1) where variations in texture were observed.

4.5.1.3 Gangue and Sulfide Mineralogy

Large variations in colour and texture occurring as very discrete zones were formed principally by differences in particle size, with fine gravels deposited upon fine sand and silt-sized particle layers. The gravels were a dark grey-black colour while the finer fractions were a reddish-pink-brown colour. XRD analysis carried out on these cores indicated that sulfides were very rare (sulfide 0.2%) and that the gangue mineralogy consists of quartz, clinochlore, halloysite, muscovite, and hematite.

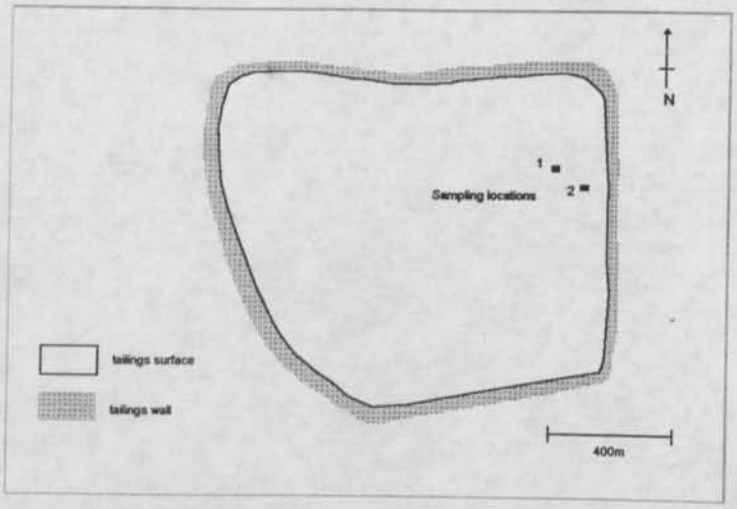

FIG 4.12. RANGER TAILINGS DAM SHOWING SAMPLING LOCATION.

4.5.1.4 Secondary Mineralogy and Morphology

Several samples of salts and surface crusts were removed and analysed. The secondary minerals consisted of gypsum, boussingaulitite, wattevillite, hexahydrite and minor rozenite. Sulfur components of these secondary minerals is sourced from the sulfuric acid utilised during processing

The morphology of these salts varied depending on their location. Salts were removed from a disused spigot hole (Site 1) (photo 4.25) where salts graded from white near the surface to a darker grey near the base (photo 4.26). This colour variation appeared to be a function of the gangue mineral content incorporated in the salt. Similar salts were recognised and sampled from the gully leading from the spigot hole (Site 2). These salts were very coarse and well crystalline. Additionally yellow surface salts of similar mineralogy were observed at Site 2 (photos 4.27 & 4.28).

Photo 4.25 Surface Salts, Ranger, Site 1 (1995)

Photo 4.24 Close up of Photo 4.25

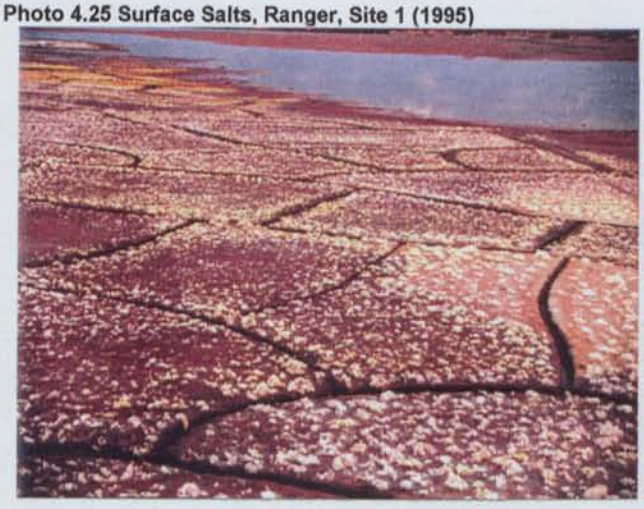

Photo 4.27 Surface Salts, Ranger, Site 2 (1995)

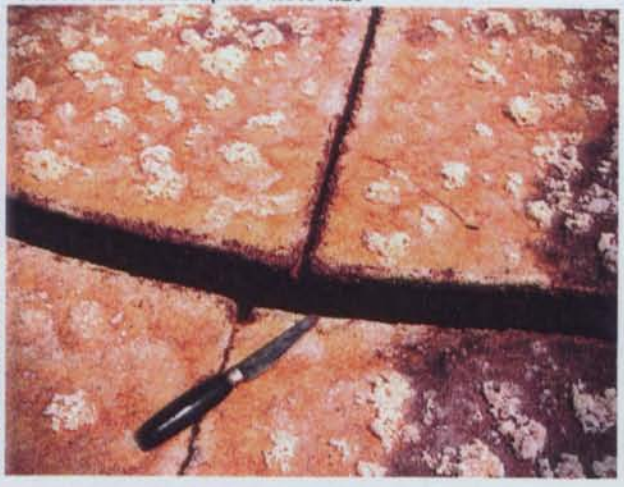

Photo 4.28 Close up of Photo 4.27

4.5.1.5 Discussion

Generally secondary salts had precipitated over much of the exposed surface. Very coarse well crystalline white salts of gypsum, boussingaulitite, wattevillite and hexahydrite were concentrated in lower lying zones e.g. Sites 1 and 2. Yellow more continuous salts had developed in other regions, some of which were continuous surface features and others present as surface clods. The overall secondary mineralogy did not vary and thus colour variations are suggested to result from differences in the individual mineral concentrations present or incorporation of tailings.

The exposed surface had dried out, however water was observed in the desiccation cracks. The true cementing ability of these salts cannot be realised under these moist conditions. However it is suggested that the soluble nature of these salts may restrict their ability to cement and thus unless they convert naturally to less soluble forms during desiccation, the integrity of any cement formed from these minerals would be extremely limited.

4.5.2 Woodcutters Pb-Zn Mine

Dam	**TD1** - edge spigot deposition, rock walls, rock cover
Original tailings mineralogy	pyrite, pyrrhotite, (galena, sphalerite) muscovite, quartz, dolomite, cerrussite, kaolinite, rutile
Tailings grain size distribution	coarse sand <1-5% silt 8-65% fine sand 24-80% clay 4-8%

Typical XRF analysis of original tailings

SiO2 %	Al2O3 %	Fe2O3 %	Fe %	MnO %	MgO %	CaO %	K2O %	TiO2 %	P2O5 %	SO3 %
17.1	3.70	32.8	22.9	0.07	3.90	5.37	0.84	0.16	0.09	50.50
S %	Ba ppm	Ce ppm	Co ppm	Cr ppm	Cu ppm	Ga ppm	La ppm	Ni ppm	Pb ppm	Rb ppm
20.2	55	15	95	75	410	75	0	30	22380	45
Sr ppm	Th ppm	U ppm	V ppm	Y ppm	Zn ppm	Zr ppm	Sb ppm	Cd ppm	As ppm	
45	0	0	155	0	20850	105	2490	140	19280	

Hardpan/Cemented Layers/No cements	Laterally discontinuous surface hardpan
Period of exposure	3 years
Hardpan/cement depth in profile	surface
Lateral extent of hardpan/cemented layers	only in seepage zone
Thickness of hardpan / cemented layers	1-5cm
Cement mineralogy	anglesite, gypsum, hexahydrite, alunite, hematite,
Surface Salt mineralogy	melanterite, beudantite, rozenite, sulfur

4.5.2.1 Tailings Dam History

The Woodcutters mine has two tailings dams (TD1 & TD2). TD1 contains 9 year's of tailings deposition and was completed in 1992 at which time TD2 (the active dam) was commissioned. At the time of the site visit, one third of TD1 was covered with waste rock, with capping due for completion in mid 1996. The present deposition technique at the mine is via the edge spigot method.

4.5.2.2 Sampling Description

The majority of sampling was carried out on TD1 and 4 different locations were investigated, site 1 - *the central* site, site 2 - *the gully* site, site 3 - *the seepage* site and site 4 - *20m from the seepage site* (Fig 4.13). Cores and surface samples were removed from each site. Freshly deposited tailings were also removed from TD2 for comparison. Additionally tailing water and ponded surface waters were sampled at Site 3.

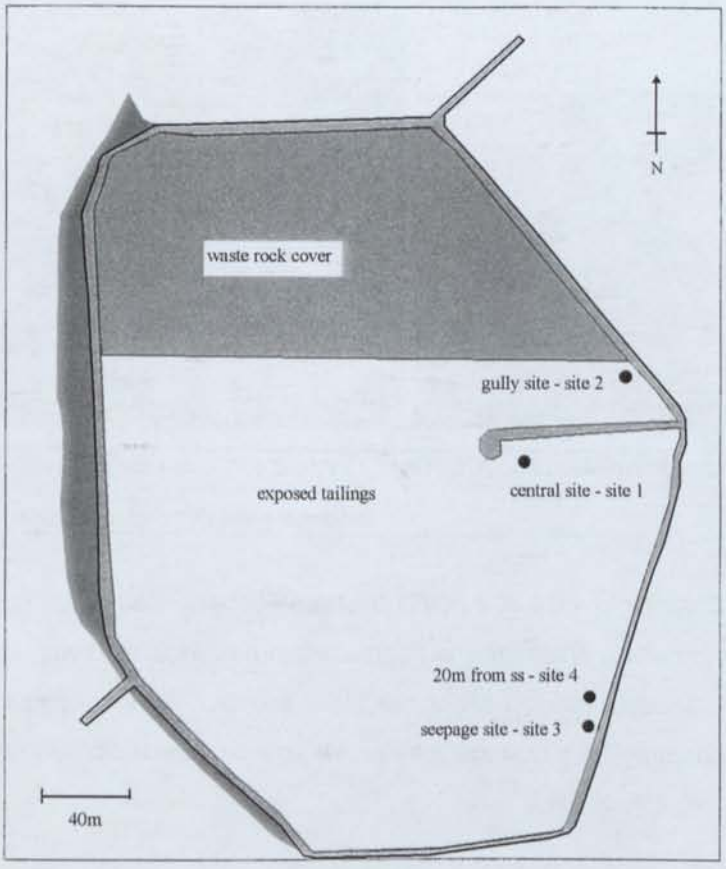

FIG 4.13 LOCATIONS OF SAMPLING SITES AT WOODCUTTERS TAILINGS DAM 1

4.5.2.3 Gangue and Sulfide Mineralogy

The primary mineralogy of the tailings varied from site to site however quartz, dravite (tourmaline), cerussite, dolomite, pyrite, galena and sphalerite were present throughout. The sulfide content makes up 22-28% of the total tailings.

4.5.2.4 Secondary Mineralisation and Morphologies, and associated Water Investigations

Cements/hardpans were observed within TD1, but did not form uniformly over the dam. Site 1 was located in the central part of the dam, where the tailings were very fine. Surface salts of gypsum and anglesite had formed, but were not identified at depth. Site 2 was located near a gully at the edge of the capping. Here layers of cements were observed in the profile and consisted of gypsum, anglesite and beudantite (Photos 4.29 and 4.30).

Tertiary mineral precipitation occurred when the cores from this location were exposed to the atmosphere and allowed to dry. The main mineral developed was hexahydrite, indicating the high concentrations of Mg and SO_4^{2-} present in pore water. This is discussed in detail later (Chapter 5).

Photo 4.29 General view of Site 2, Woodcutters, TD1, (1995) Arrow

Photo 4.30 Close up of Photo 4.29 Cemented profile. indicates cemented region (Vertical height approx. 30cm)

Site 3 is located at the SE corner of TD1 at a position where seepage was draining from the dam wall. The origin of the water is uncertain however it is suggested to be associated with the recent raising of the tailings wall which included covering part of the older tailings. This seepage was sampled and analysed. The solution contained high concentrations of solutes (electrical conductivity 4.61mS/cm) Ca, Mg, SO_4^{2-} and Zn (Table 4.4) at pH 5.

The cements developed at this location were more widespread and thicker than those at Site 2, with the surface hardpan at least 3cm thick. The majority of cement had developed an orange appearance with a slight green tinge. XRD analysis of this region indicated the secondary mineralogy included gypsum, anglesite, native sulfur, beudantite and melanterite.

SEM examinations of this hardpan showed a variety of morphologies which differ depending on depth. EMG 4.32 shows the general view of cements developing near the surface of the hardpan. Coatings cover the majority of the primary grains, leaving only uncovered sulfur crystals. EMG 4.33 shows fibrous gypsum and Fe sulfate crystals along with the continuous coating ranging from pure Fe sulfate including quantities of Ca and Mg and minor Si. EMG 4.34 shows the more fibrous cements developed deeper in the hardpan. As before, the fibers consist of Fe and Ca sulfate, while the coating consist of Fe sulfate with Ca and Mg (EMG 4.35).

Unlike the other sites examined, secondary minerals had developed at depth in the profile suggesting that this is a more active region, probably due to the influx of large pollutant loads associated with the seepage. The core hole at this site filled rapidly with tailings pore water. A sample was removed from this hole with pH 1.8 and high levels of Ca, Fe, Mg, Pb, S and Zn (Table 4.4). For comparison, ponded surface water of pH 6 was also removed for analysis and showed much lower levels of Ca, Pb, Mg, Fe, S and Zn. Presumably this sample was ponded rain water containing only soluble salts previously precipitated at the surface.

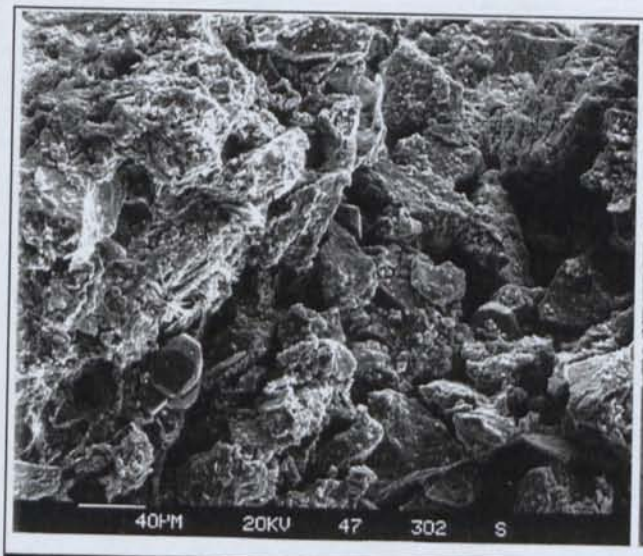

EMG 4.32 General view of cements, Site 3, Woodcutters TD1 gypsum, Fe sulfate crystals, along with a continuous coating ranging from pure Fe sulfate to Fe sulfate containing Ca, Mg and Si

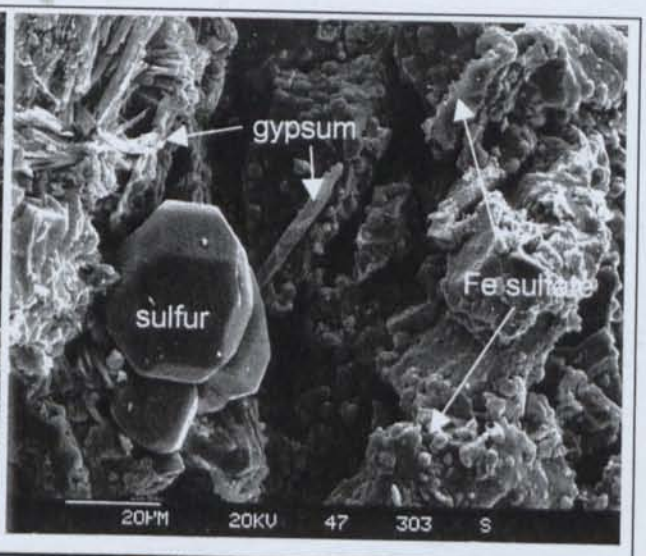

EMG 4.33 Close up of 4.32 pure sulfur crystals, fibrous

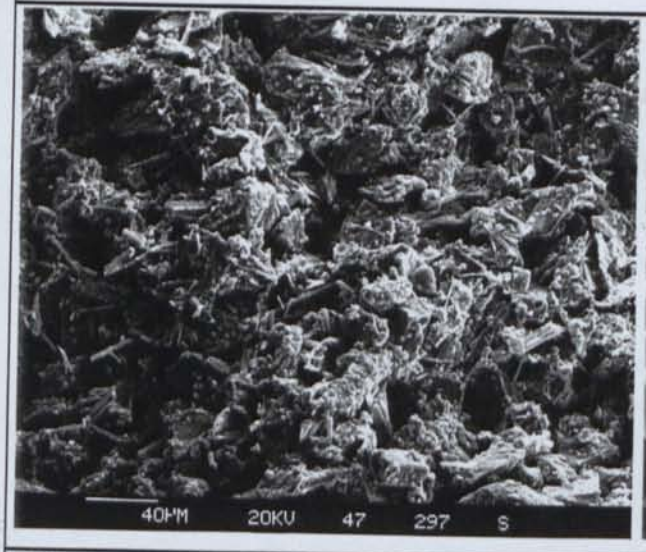

EMG 4.34 More fibrous cements developing deeper in the Woodcutter hardpan, Site 3.

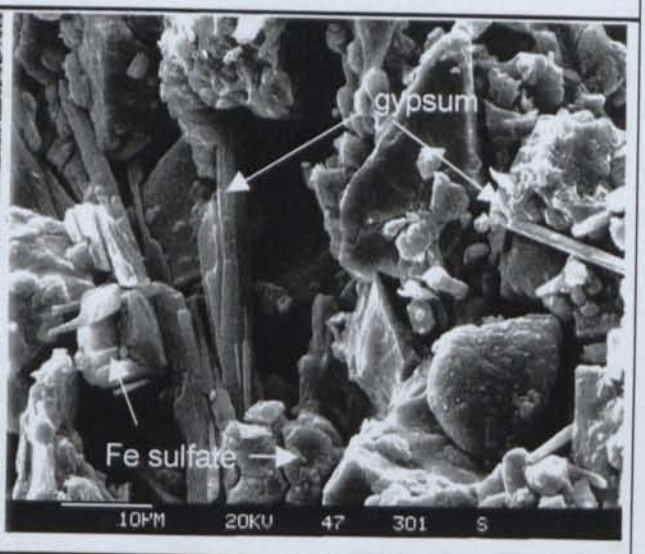

EMG 4.35 Close up of 4.34, fibers of Fe and Ca sulfate with continuous coat of Fe sulfate with Ca and Mg.

The large variations in the water chemistry of samples taken from this site are to be expected because of their different origins. The pH 5 seepage from the dam wall indicates that the dolomite present in the waste rock used in the wall construction has sufficient neutralising capacity so that the acid developed by sulfide oxidation is to some extent neutralised. However the high solute content of this solution indicates the system is very active and oxidation and metal release are extensive. The pH 6 ponded water had low solute levels in comparison with the other samples, presumably because it has not contacted tailings for any length of time. The pore water at pH 1.8 however suggests that the tailings may be developing a very different system. It appears that this very low pH may be localised and is a function of increased dissolved O_2 levels in the waters draining through the tailings, promoting increased oxidation and thus decreased pH. Comparisons of tailings geochemistry at different locations in the dam will be discussed in detail Chapter 5.

	pH	EC	Al	B	Ca	Cd
		mS/cm	mg/L	mg/L	mg/L	mg/L
surface ponded water	6.19	1.68	<0.1	0.1	47	0.3
wall seepage	5.09	4.61	1.3	0.2	552	2.6
tailings pore water	1.8	31	48.0	1.6	589	18.3
	Co	Cu	Fe	K	Mg	Mn
	mg/L	mg/L	mg/L	mg/L	mg/L	mg/L
surface ponded water	<0.1	<0.1	0.2	0.3	5.4	0.3
wall seepage	0.2	0.2	0.7	2.6	500	8.5
tailings pore water	0.4	67.1	22517	<0.1	1213	34.8
	Na	Ni	P	Pb	S	Zn
	mg/L	mg/L	mg/L	mg/L	mg/L	mg/L
surface ponded water	2.0	<0.1	<0.1	0.2	53	25
wall seepage	4.7	0.5	0.7	1.6	1404	712
tailings pore water	2.2	1.4	17.1	60.2	18057	1656

TABLE 4.4 ICP ANALYSIS OF SEEPAGE, PORE AND PONDED WATER AT SITE 4.

While examining the extent of the hardpan developed at Site 3 another hardpan of similar morphology but different colour was observed 20m away (Site 4). At this location the cements formed were confined to the surface and showed little discoloring from the original tailings. Much of the olive coloring observed was not due to oxidation of the sulfides present but the presence of fresh sulfide tailings. The hardpan cements developing at this site included gypsum, anglesite and minor sulfur. This same secondary mineralogy continued down to 7cm but at lesser concentrations and thus does not exhibit substantial cementing properties. Beneath the cemented layers secondary mineralogy decreases, with gypsum present to 25cm only. Again when samples were exposed to the atmosphere in the laboratory, hexahydrite precipitation occurred.

4.5.2.5 Discussion

It would appear that at least four very different geochemical environments have developed within TD1. The Central Site (site 1) has low levels of secondary mineral formation and it is suggested that it is the very fine nature of the tailings at this location that has dictated these conditions. During sampling it was noted that the region was very moist indicative of the large water retention capacity of a fine-grained system. As the tailings are water saturated, limited oxygen diffusion can occur reducing the sulfide oxidation and thus acid generation. This, combined with the presence of fine-grained dolomite with increased surface area available for neutralisation reactions, has helped preserve the elevated pH of the system.

The large washout formed at the Gully Site (Site 2) has exposed sulfides to increased oxygen and has resulted in enhanced elemental transport by rapidly moving water. This has resulted in oxidation of the sulfides present in this region and the development of secondary cements.

As mentioned previously, the Seepage Site (site 3) has developed a very low pH of approx. 2, very different from that of the other sites examined. The site is leached with pH 5 water containing high levels of Ca, Mg, S, Zn and probably increased dissolved oxygen levels. As a consequence, increased

oxidation has occurred in response to the greater oxygen levels and lower pH porewater. The potential neutralising capacity of this region would also be reduced because of the already acid water entering the system. It may be the increased activity of this area that has promoted the development of a hardpan surface however the continual saturation of the site would be reducing the ability of the tailings to concentrate soluble salts at the surface through evaporation. Thus the most effective and well developed hardpan may form once the seepage has stopped and the site allowed to dry.

The hardpan observed 20m away (Site 4) may also at some stage have come under the influence of seepage from the dam wall. However the present variations in colour and thus mineralogy do not support this. The hardpan at this location contains only gypsum, anglesite, sulfur and residual sulfides and gangue minerals whereas the Seepage Site (Site 4) hardpan contains beudantite and melanterite. The present variations in mineralogy between Site 3 and Site 4 may be due to the solubility of these sulfate salts in which case the hardpans at Site 4 may have originally developed under seepage conditions and now the soluble surface salts are being removed by rainfall.

If in fact the hardpan at Site 4 did form without any external input, it suggests that the tailings mineralogy is capable of hardpan development. The fact that this hardpan is not widespread indicates that the physical properties of the dam i.e. grain size and thus moisture-holding capacity may play a major role. The Site 4 hardpan is located near the perimeter of the dam and is generally of larger grain size than the Site 1 (Central site) where there is also no external input but cements are not developing.

The dolomite content of the tailings is substantial and may limit the development of a hardpan by maintaining elevated pH conditions not optimal for sulfide oxidation and thus by-product development. It is suggested that at present, the hardpan development at Site 3 has been enhanced by the seepage. However when the dolomite content of the tailings in general in used up through neutralisation reaction, sulfide oxidation will be more rapid and cementing maybe more widespread.

4.5.3 Pine Creek Au Mine

Dam	**TD3** - edge spigot deposition, rock walls, oxide tailings cover
Original tailings mineralogy	Sulfide Tailings (pyrite) muscovite, quartz, kaolinite, orthoclase, calcite
Tailings Grain size distribution	coarse sand 7% silt 33% fine sand 44% clay 15%

Typical XRF analysis of original tailings

SiO2 %	Al2O3 %	Fe2O3 %	Fe %	MnO %	MgO %	CaO %	K2O %	TiO2 %	P2O5 %	SO3 %
71.4	11.8	7.03	4.92	0.053	1.5	0.55	3.85	0.33	0.096	3.61
S %	Ba ppm	Ce ppm	Co ppm	Cr ppm	Cu ppm	Ga ppm	La ppm	Ni ppm	Pb ppm	Rb ppm
1.45	335	185	25	30	280	30	35	10	600	185
Sr ppm	Th ppm	U ppm	V ppm	Y ppm	Zn ppm	Zr ppm	Sb ppm	Cd ppm	As ppm	
45	10	10	30	30	880	240	215	80	3670	

Dam	**TD1 & TD2** - edge spigot deposition, oxide tailings cover, rock walls
Original tailings mineralogy	Oxide Tailings (pyrite) muscovite, quartz, kaolinite, orthoclase, calcite

Typical XRF analysis of original tailings

SiO2 %	Al2O3 %	Fe2O3 %	Fe %	MnO %	MgO %	CaO %	K2O %	TiO2 %	P2O5 %	SO3 %
67.1	13.17	10.85	7.59	0.084	1.1	0.33	3.69	0.34	0.142	0.39
S %	Ba ppm	Ce ppm	Co ppm	Cr ppm	Cu ppm	Ga ppm	La ppm	Ni ppm	Pb ppm	Rb ppm
0.16	520	92	24	37	346	27	358	19	358	262
Sr ppm	Th ppm	U ppm	V ppm	Y ppm	Zn ppm	Zr ppm	Sb ppm	Cd ppm	As ppm	
57	13	10	37	33	579	203	210	86	1257	

Hardpan/Cemented Layers/No cements	No cements
Period of exposure	Unknown 1-4 years
Cement mineralogy	gypsum, jarosite
Surface Salt mineralogy	*possibly* thiocynate, Cu-Fe cyanide, Cd-Fe cyanide hydrate, Cu ammine W oxide

Typical XRF analysis of hardpan/cements

SiO2 %	Al2O3 %	Fe2O3 %	Fe %	MnO %	MgO %	CaO %	K2O %	TiO2 %	P2O5 %	SO3 %
63.2	11.5	6.31	4.41	0.066	1.6	3.37	3.73	0.32	0.104	8.16
S %	Ba ppm	Ce ppm	Co ppm	Cr ppm	Cu ppm	Ga ppm	La ppm	Ni ppm	Pb ppm	Rb ppm
3.27	415	105	45	30	330	25	35	15	410	185
Sr ppm	Th ppm	U ppm	V ppm	Y ppm	Zn ppm	Zr ppm	Sb ppm	Cd ppm	As ppm	
40	20	10	25	25	1190	205	200	70	2015	

4.5.3.1 Tailings History

During mine life, sulfide tailings were deposited in 3 dams, TD1, TD2 and TD3 which is an up-stream lift above the other two dams. As the mining came to a close previously stock-piled oxide ore was processed and deposited as a capping on all dams. It was proposed that this cover would reduce sulfide contact with both oxygen and water, thus reducing AMD generation.

4.5.3.2 Sampling Description

The investigations of the site had to be undertaken through the use of surface samples only, as the tailings were too moist to obtain cores with the equipment available. Surface oxide tailings were removed from Dams 1 and 2. Access to sulfide tailings was restricted because of the widespread oxide covering. The only location which allowed observations of sulfide tailings was at the base of Dam 3 where a seepage site had developed allowing sulfide tailings to channel from the elevated Dam 3 onto the surface of Dam 1 (Site 1-Fig 4.14). This site is representative of the reactions which may have developed, had the oxide coating not been deposited.

A sample of the freshly deposited oxide tailings was removed from Dam 3. Seepage water samples from Site 1 were collected for comparison with ponded water sampled from the surface of Dam 1 at Site 2 (Table 4.5).

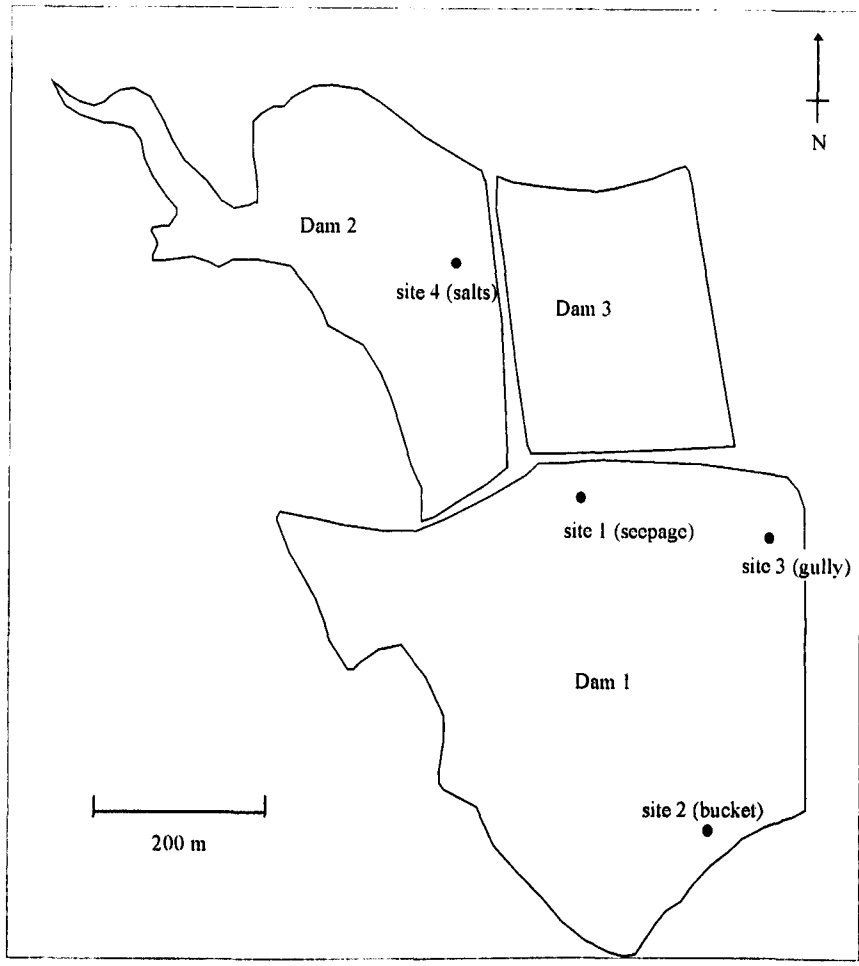

FIG 4.14 SAMPLING LOCATIONS AT THE PINE CREEK TAILINGS DAMS

	pH	EC	Al	Ca	Co
		mS/cm	mg/L	mg/L	mg/L
Site 1 seepage water	5.72	6.33	0.22	575.72	1.16
Site 2 ponded water	6.3	0.33	<0.1	292.30	<0.1
	Cu	Fe	K	Mg	Mn
	mg/L	mg/L	mg/L	mg/L	mg/L
Site 1 seepage water	6.77	18.86	132.48	169.02	26.97
Site 2 ponded water	<0.1	<0.1	25.34	30.98	2.44
	Na	Ni	P	S	Zn
	mg/L	mg/L	mg/L	mg/L	mg/L
Site 1 seepage water	953.50	0.97	0.99	1566.33	8.50
Site 2 ponded water	85.14	<0.1	0.22	345.88	0.72

TABLE 4.5 ICP ANALYSIS OF SEEPAGE AND PONDED WATER AT SITES 1 AND 2

4.5.3.3 Gangue and Sulfide Mineralogy

XRD analysis of the sulfide tailings from Site 1 indicated that the main sulfide in the underlying tailings is pyrite, within a matrix of quartz, muscovite, kaolinite, orthoclase, albite and clinochlore. The same gangue mineral assemblage was observed in the upper oxide tailings with very minor pyrite (0.07-0.16%).

4.5.3.4 Secondary Mineralogy and Morphology

The secondary minerals developed at Site 1 where sulfidic tailings were exposed included jarosite and gypsum. The oxide surface at Sites 2 and 4 have developed orange, red and brown ripple mark and mud crack morphologies, along with green and pale yellow salts (photos 4.31 & 4.32). Gypsum was the main salt identified along with minor hexahydrite. The gypsum was not in sufficient quantities to cement the surface in any way. At Site 3 (gully site), very fine tailings have developed black and brown layering containing cyanide complexes (photo 4.33 & 4.34). The XRD analysis of this material produced a very diffuse pattern giving several possible combinations of compounds including copper thiocyanate, copper iron cyanide, cadmium iron cyanide hydrate, copper ammine tungsten oxide or copper chromium oxide. These compounds did not significantly cement the surface tailings (photo 4.33 & 4.34).

Photo 4.31 Surface ripple marks in oxide tailings Site 2, Pine Creek, 1995

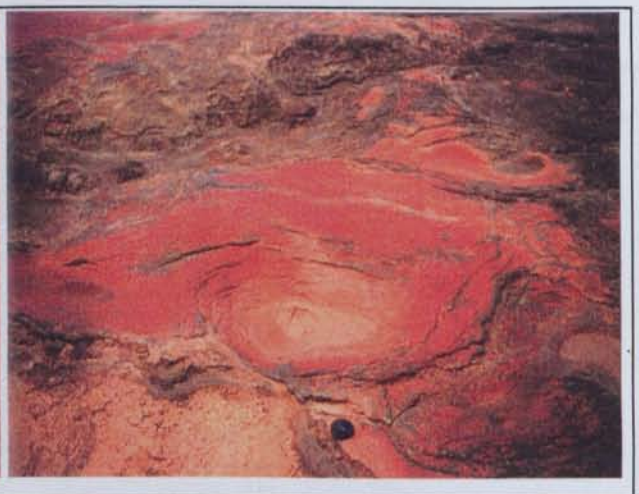

Photo 4.32 Red cements developed in oxide tailings Site 4, Pine Creek, 1995

Photo 4.33 Fine surface cyanide cements with mud crack morphology, Site 3, Pine Creek, 1995

Photo 4.34 Layered tailings containing cyanide complexes, Site 3, Pine Creek, 1995

The effect of this surface on the reduction of AMD at this mine was not assessed. Hardpan development has not occurred within the oxide tailings due to the lack of sulfide oxidation reactions and thus by-product development. These tailings where sourced from the oxidised region of the deposit and thus the reactions required for hardpan development have occurred prior to the mining. At the time of sampling the tailings were very wet. This situation would substantially decrease oxygen diffusion into the tailings. If these conditions persisted throughout the year, oxidation of the minimal sulfides would be reduced, further inhibiting hardpan development.

4.6 Dundas Trough, Tas.

4.6.1 Renison Bell Sn Mine

Dam	**Dam A** - edge spigot deposition, rock walls, CFT cover
Original tailings mineralogy	pyrrhotite, pyrite (arsenopyrite, chalcopyrite) quartz, siderite, chlorite, talc, calcite
Tailings grain size distribution	coarse sand 0% silt 15% fine sand 87% clay 1% (Jones et al., 1997)
Hardpan/Cemented Layers/No cements	Laterally extensive surface hardpan
Period of exposure	17 years
Hardpan/cement depth in profile	surface and palaeo-hardpans
Lateral extent of hardpan/cemented layers	probably over entire dam
Thickness of hardpan / cemented layers	1-10cm
Cement mineralogy	lepidocrocite, goethite, sulfur
Surface Salt mineralogy	N/A CFT Cover

Typical XRF analysis of hardpan/cements

SiO2 %	Al2O3 %	Fe2O3 %	Fe %	MnO %	MgO %	CaO %	K2O %	TiO2 %	P2O5 %	SO3 %
11.1	1.20	60.3	42.1	0.18	1.46	0.41	0.13	0.06	0.24	57.19
S %	Ba ppm	Ce ppm	Co ppm	Cr ppm	Cu ppm	Ga ppm	La ppm	Ni ppm	Pb ppm	Rb ppm
22.9	10	10	0	5	100	10	0	0	620	25
Sr ppm	Th ppm	U ppm	V ppm	Y ppm	Zn ppm	Zr ppm	Sb ppm	Cd ppm	As ppm	
10	0	10	20	15	1320	50	15	0	4970	

Dam	**Dam B** - edge spigot deposition, rock walls, CFT cover
Original tailings mineralogy	pyrrhotite, pyrite (arsenopyrite, chalcopyrite) quartz, siderite, chlorite, talc, calcite
Tailings grain size distribution	coarse sand 1-3% silt 1-3% fine sand 89-92% clay 1-2% (Jones et al., 1997)
Hardpan/Cemented Layers/No cements	Laterally extensive surface hardpan
Period of exposure	16 years

Hardpan/cement depth in profile	surface and palaeo-hardpans
Lateral extent of hardpan/cemented layers	probably over entire dam
Thickness of hardpan / cemented layers	1-10cm
Cement mineralogy	lepidocrocite, goethite, sulfur
Surface Salt mineralogy	N/A CFT cover

Typical XRF analysis of hardpan/cements

SiO2 %	Al2O3 %	Fe2O3 %	Fe %	MnO %	MgO %	CaO %	K2O %	TiO2 %	P2O5 %	SO3 %
17.6	1.33	48.7	34.0	0.13	1.95	0.07	0.29	0.08	0.07	29.12
S %	Ba ppm	Ce ppm	Co ppm	Cr ppm	Cu ppm	Ga ppm	La ppm	Ni ppm	Pb ppm	Rb ppm
11.7	15	10	0	3	320	10	10	0	50	75
Sr ppm	Th ppm	U ppm	V ppm	Y ppm	Zn ppm	Zr ppm	Sb ppm	Cd ppm	As ppm	
10	0	0	20	10	45	50	2	0	4480	

Dam	**Dam C** - edge spigot deposition, rock walls, intermittant CFT cover
Original tailings mineralogy	pyrrhotite, pyrite (arsenopyrite, chalcopyrite) quartz, siderite, chlorite, talc, calcite
Tailings grain size distribution	coarse sand 0% silt 2% fine sand 92% clay 6% (Jones et al., 1997)
Hardpan/Cemented Layers/No cements	Surface hardpan
Period of exposure	In use
Hardpan/cement depth in profile	surface
Lateral extent of hardpan/cemented layers	in regions of exposure for 2-3 months
Thickness of hardpan / cemented layers	1-5cm
Cement mineralogy	lepidocrocite, goethite, sulfur

Typical XRF analysis of hardpan/cements site 1

SiO2 %	Al2O3 %	Fe2O3 %	Fe %	MnO %	MgO %	CaO %	K2O %	TiO2 %	P2O5 %	SO3 %
9.07	1.08	59.5	41.6	0.12	1.66	0.27	0.20	0.11	0.09	50.59
S %	Ba ppm	Ce ppm	Co ppm	Cr ppm	Cu ppm	Ga ppm	La ppm	Ni ppm	Pb ppm	Rb ppm
20.3	5	5	0	10	1320	15	0	15	210	65
Sr ppm	Th ppm	U ppm	V ppm	Y ppm	Zn ppm	Zr ppm	Sb ppm	Cd ppm	As ppm	
10	0	0	35	10	840	35	3	0	6100	

Typical XRF analysis of CFT site 2

SiO2 %	Al2O3 %	Fe2O3 %	Fe %	MnO %	MgO %	CaO %	K2O %	TiO2 %	P2O5 %	SO3 %
36.7	5.4	35.0	24.5	0.21	3.00	0.70	0.45	0.29	0.24	30.45
S %	Ba ppm	Ce ppm	Co ppm	Cr ppm	Cu ppm	Ga ppm	La ppm	Ni ppm	Pb ppm	Rb ppm
12.2	20	35	20	50	1030	15	20	15	85	110
Sr ppm	Th ppm	U ppm	V ppm	Y ppm	Zn ppm	Zr ppm	Sb ppm	Cd ppm	As ppm	
30	0	3	85	25	175	105	5	0	4720	

4.6.1.1 Tailings Dam History

Three tailings dams have been utilised during mine operation; Dam A is the oldest dam commissioned in 1968 and completed in 1979, Dam B was operated between 1970-1980, while Dam C contains tailings from the period 1979-present. During 1992 Dam A was covered with cassiterite flotation tailings (CFT) which contain lower concentrations of sulfides than the tailings. This CFT cover was implemented to inhibit oxidation of the underlying tailings. In 1994 Dam B was covered using the same material. Dam C has been intermittently covered with CFT during the recent years of operation.

4.6.1.2 Sampling Description

Two locations within each dam were selected for sampling, each site having minimal CFT covering. The new and only slightly oxidised tailings of Dam C were compared with locations in Dams A and B where hardpans had developed almost 17 years previously. Cores from all 6 sites were removed along with numerous hardpan samples from these sites and the surface in general.

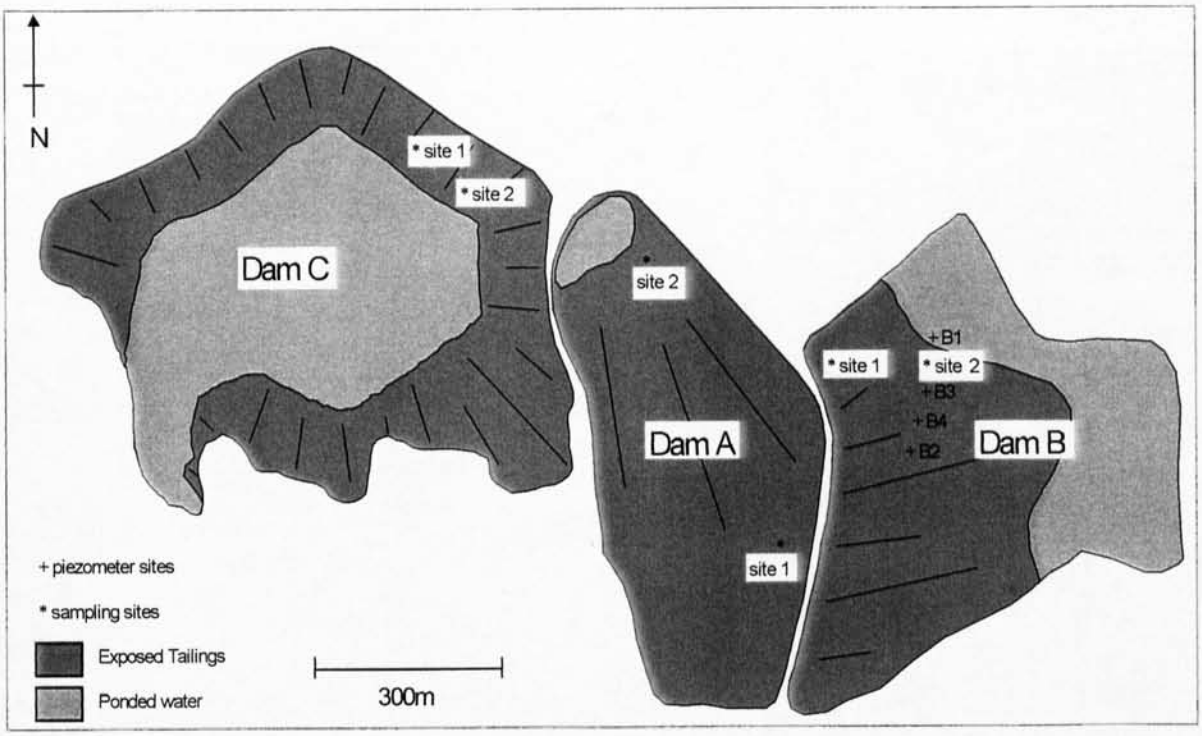

FIG 4.15 RENISON BELL TAILINGS DAMS INDICATING SAMPLING SITES

4.6.1.3 Gangue and Sulfide Mineralogy

The gangue mineralogy in each dam consists of varying quantities of quartz, siderite, dravite, chlorite, talc and calcite. The sulfide content is approximately 21-23% and consists of mainly pyrrhotite and pyrite with lesser amounts of arsenopyrite and chalcopyrite.

4.6.1.4 Secondary Mineralogy and Morphology.

4.6.1.4.1 Dam A

Two sites were investigated in Dam A, one at each end of the dam. The two locations have developed very different physical and geochemical characteristics since deposition was completed in 1979. Both locations show palaeo-surfaces at depth where oxidation and cementing have occurred during previous periods of exposure. The morphology of these layers are dramatically different from each other. These variations are expected with tailings dams because of changes in deposition location and styles resulting in periods of exposure between depositional cycles.

Site 1

Site 1 is located at the Northern end of Dam A. At the time of examination the residue surface was only observable as pop-up structures beneath the CFT covering (photo 4.35). It is assumed that a hardpan

surface has developed over the entire dam and at locations where lateral expansion has been restricted during cementation, pop-up structures have developed. At this location the relic hardpan surface now appears to be degrading. Beneath this however a more substantial hardpan at least 10cm thick has developed at 20cm depth (photo 4.36). This hardpan is regarded as a palaeo-hardpan, developed during a previous deposition cycle. Coring could not be achieved below this massive hardpan and thus geochemical profiles of soluble salt extracts could only be obtained for the top 15cm of the profile.

Photo 4.35 Raised hardpan surface, with minor CFT cover, Rension Bell, Dam A, Site 1 (1996)

Photo 4.36 Massive hardpan at 20cm depth, covered by oxidised tailings, Renison Bell, Dam A, Site 1 (1996)

XRD analysis undertaken on samples from the surface hardpan and palaeo-hardpan at depth indicated they consist of the same mineralogy. The secondary minerals include goethite, sulfur, jarosite and lepidocrocite, in a matrix of quartz, talc, dravite and clinochlore. There was a notable absence of sulfides in both samples. Upon air drying at room temperature, the palaeo-hardpan developed surficial rozenite suggesting relatively high levels of soluble Fe and S within its structure, probably leached from the surface.

The profile observed at this location is unlike all other locations investigated and it is suggested that it is not representative of the entire dam. Tailings deposition may have been very sporadic at this location. The final hardpan appears to have developed on oxidised tailings above the palaeo-hardpan suggesting long periods of exposure before new tailings deposition. Another explanation for the variation in this profile is that it has been disrupted by earth moving equipment used during the excavation of the drainage trench north of this site. This would also explain why the surface has pop-up structures, whereas at Site 2 the hardpan is flat-lying.

Site 2

Photo 4.37 Hole showing paleo-surface at 10-15cm depth within unoxidised tailings, Renison Bell, Dam A, Site 2 (1996)

This site, located in the south of the dam, is perhaps more representative of the usual deposition of tailings. Here a 3-5cm thick hardpan surface has developed, directly below which unoxidised tailings prevail. Palaeo-surfaces of oxidised tailings 3-4cm thick are present at 10 and 15cm depth, however cementing is limited. Below these layer unoxidised tailings are present (photo 4.37). The surface hardpan mineralogy is essentially the same as that observed at Site 1. Within the palaeo-surfaces at 10 and 15cm depth similar secondary minerals are present however jarosite has not developed and both pyrite and pyrrhotite are still present. Both siderite and calcite are present, affirming that acid generation has been mainly restricted to the surface. Quartz and dravite were also observed at depth. This profile shows how a well-developed hardpan capping may have prevented oxidation of the underlying highly reactive tailings which have been deposited for 17 years. The surface hardpan again appears to be breaking down through wind and water erosion.

4.6.1.4.2 Dam B

Two sites were investigated in Dam B however after discussions with staff it was determined that Site 1 at the northern edge of the dam was possibly disturbed during excavation of a trench near that location. Investigations have therefore been concentrated on Site 2 which is approximately 2m from the B3 piezometer.

Site 2

Photo 4.38 Degrading surface hardpan at Renison Bell, Dam B, Site 2 (1996)

The profile developed at this location is very similar to Dam A -Site 2 with oxidation restricted to the immediate surface resulting in a hardpan 4-6cm thick. A palaeo-cemented surface was encountered at 2m depth. Similar to the hardpan surface texture observed elsewhere in Dam A, cements appear to be breaking down (photo 4.38 & 4.39), however, the amount of degradation varies depending on location. In regions of higher gradient where rapid water runoff and subsequent erosion occurs, the hardpan is sometimes only millimeters thick, whereas in lower lying areas where water is sometimes ponded and erosion limited, the hardpan is up to 10cm thick.

Photo 4.39 Close up of Photo 4.38

Both the surface hardpan and desiccation crack cements were sampled for XRD analysis. Again the main secondary minerals of the surface hardpan were goethite, sulfur, jarosite and lepidocrocite. The desiccation crack cement is slightly different as natrojarosite has developed while lepidocrocite has not.

4.6.1.4.3 Dam C

Again two locations were investigated in Dam C but coring problems were encountered at Site 1 because of the hardness of the hardpan. Site 2 was located in an area of recent deposition and thus only slight surface oxidation had taken place which made coring much easier.

Photo 4.40 Blistered hardpan surface, Renison Bell, Dam C, Site 1

Site 1 On first inspection the tailings surface appeared blistered and fragile. On closer examination the hardpan development is substantial after exposure of only 2-3 months (photo 4.40). Surface hardpans of up to 5-6cm thick have been uplifted because of expansion during cementing. When the tailings beneath become exposed, they oxidise, resulting in secondary hardpan formation.

Photo 4.41 Hole showing blister surface hardpan 4-6cm thick, underlain by flat lying hardpan of unknown thickness, Renison Bell, Dam C, Site 1 (1996)

The overall profile which has therefore developed is an uplifted surface hardpan of 4-6cm thickness underlain by a flat-lying hardpan of unknown thickness (at least 10cm) (photo 4.41).

Both the pop-up surface hardpan and secondary hardpan consist of goethite, sulfur, lepidocrocite, metahohmanite, with residual pyrite, pyrrhotite, siderite, dravite, clinochlore, and quartz.

Site 2

Photo 4.42 Initial focus of intensive oxidation and by-product concentration along dessication cracks, Renison Bell, Damc C, Site 2 (1996)

Site 2 gives an indication of the initial focus of oxidation and resultant hardpan development (photo 4.42). It appears that intensive oxidation occurs along the edges of large desiccation structure i.e. in the cracks. Insitu oxidation by-products develop and cementing starts. This cementing eventually results in expansion, causing pop-up structures, again exposing the underlying tailings which in turn oxidise and cement (Fig 4.16). The primary and secondary minerals at this site are the same as those observed at Site 1, however calcite was also detected. It should be noted that both calcite and siderite have neutralising potential, however calcite is more reactive and thus is the first to be utilised under these conditions. The fact that it is still present, indicates sulfide oxidation and thus acid generation is only in the incipient stages of development.

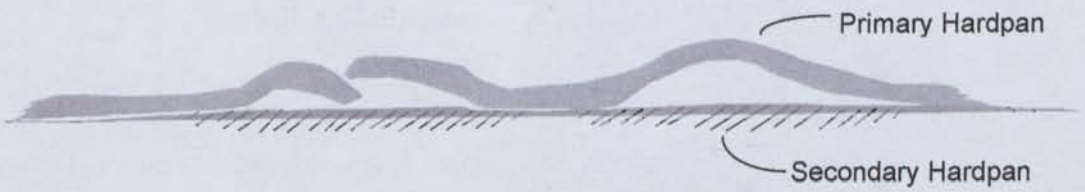

FIG 4.16: SCHEMATIC REPRESENTATION OF SURFACE HARDPAN FORMATION.

SEM investigations were undertaken to observe the change in hardpan over time. Two samples were removed from Dam C, Site 1, a surface hardpan and the hardpan present at 7-13cm depth. These fresh hardpans were compared with the older hardpans of Dam A, sampled from both sites 1 and 2.

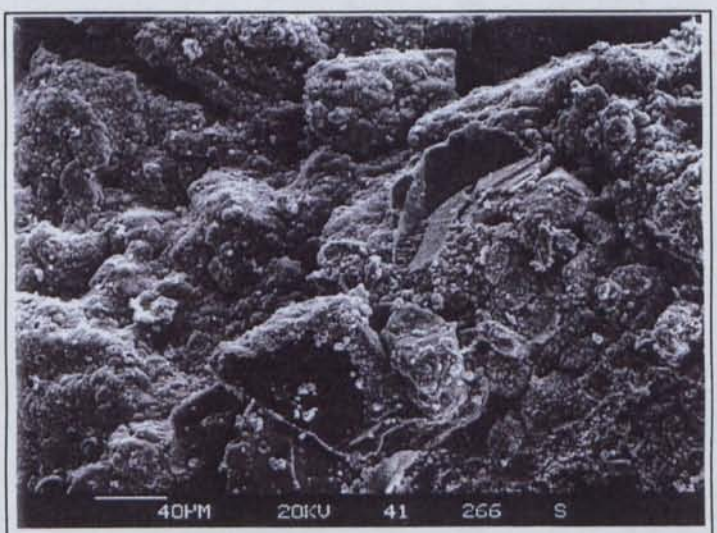

EMG 4.36 Continuous coating and bridging cements of Renison Bell, Dam C, surface hardpan

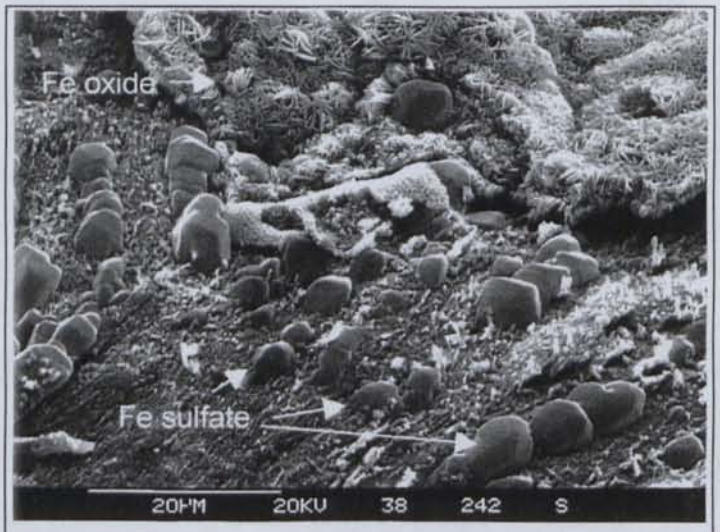

EMG 4.37 Sub-rounded Fe sulfate crystals and Fe oxide needles/plates of hardpan at 7-13cm depth, Site 1, Dam C, Renison Bell.

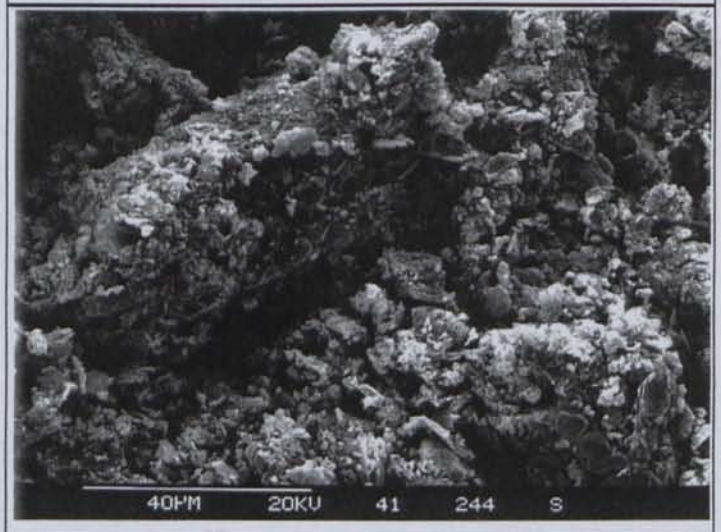

EMG 4.38 Fragmented surface cements of surface hardpan, Dam C, Renison Bell.

The young cements of Dam C are continuous, coat and bridge primary grains and in-fill the majority of pores (EMG 4.36). The hardpan present at 7-13cm depth has a more fibrous nature with sub-rounded Fe sulfate crystals grading into the widespread Fe oxides needle/plates (EMG 4.37). The cements within the surface region, although still slightly fibrous, have a generally more fragmented nature (EMG 4.38) with some regions taking on a smooth appearance, covering primary and secondary minerals alike (EMG 4.39) or sub-angular cubic morphology of the Fe oxide (EMG 4.40).

The morphology of the older cements in Dam A vary dramatically on a centimeter scale. EMG 4.41 (Site 2) shows a well developed continuous Fe oxide cement covering all grains (EMG 4.42). EMG 4.43 (Site 1) however shows a more complicated cementing morphology with uni-directional fibers, sub-angular particles and very fine-grained spherical cementing (EMG 4.44). Both hardpans show a variety of degrading structures. EMG 4.45 (Site 2) displays a degraded aluminosilicate behind an equally degraded Fe sulfide consisting predominantly of sulfur particles (EMG 4.46). EMG 4.47 (Site 1) shows a similar sulfide degradation, along with the development of cubic Fe sulfate (possibly jarosite) as a by-product, along with a basal cement consisting of very small Fe oxide particles which in some region bridge primary grains (EMG 4.48).

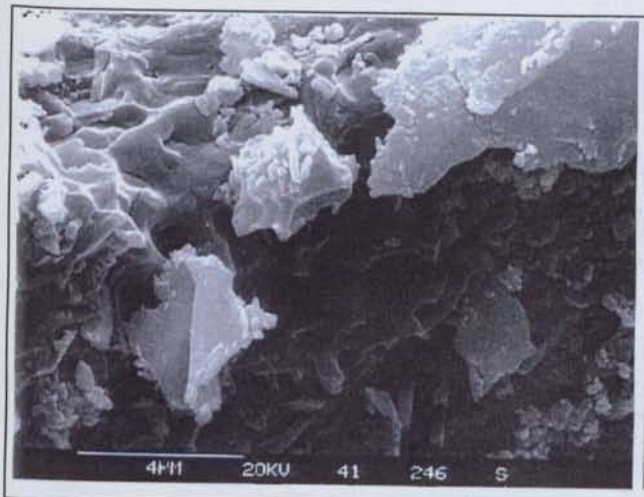

EMG 4.39 Fe oxide cements containing minor S, Dam C, Site 1, Rension Bell

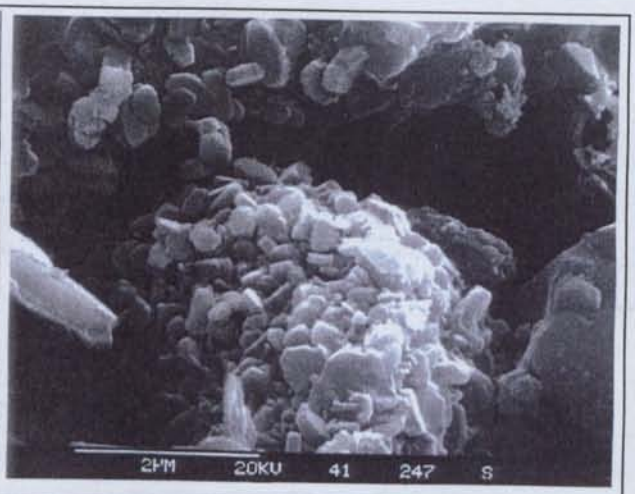

EMG 4.40 Sub angular grains of Fe oxide, Dam C, Site 1, Renison Bell

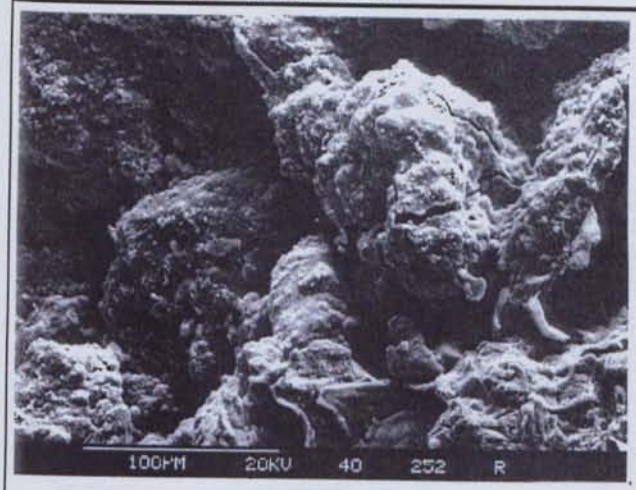

EMG 4.41 General view of cements Dam A, Site 2, Renison Bell

EMG 4.42 Close up of 4.41 Continuous coating of Fe oxide cement

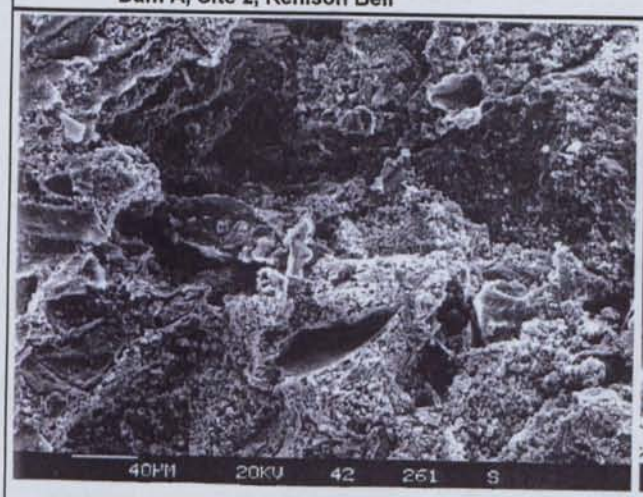

EMG 4.43 General view of cements, Dam A, Site 1, Renison Bell

EMG 4.44 Close up of 4.43 Unidirectional fibers (◀), subangular particles and very fine grained spherical cements (◀) all Fe Sulfate, with varying Si and Mg content

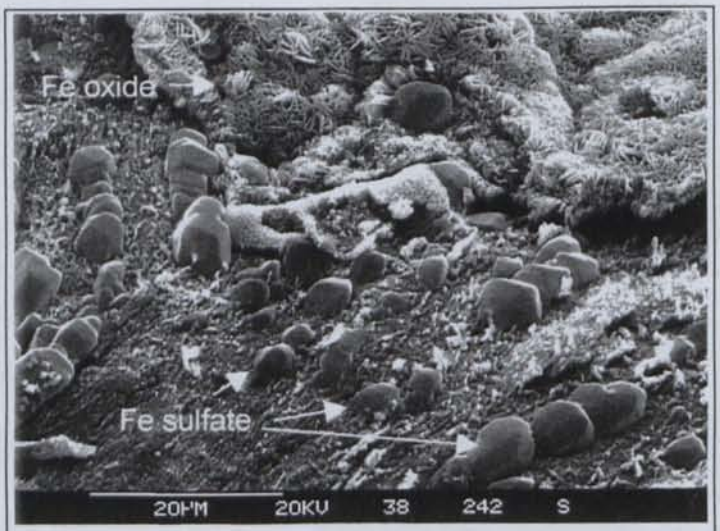

EMG 4.37 Sub-rounded Fe sulfate crystals and Fe oxide needles/plates of hardpan at 7-13cm depth, Site 1, Dam C, Renison Bell.

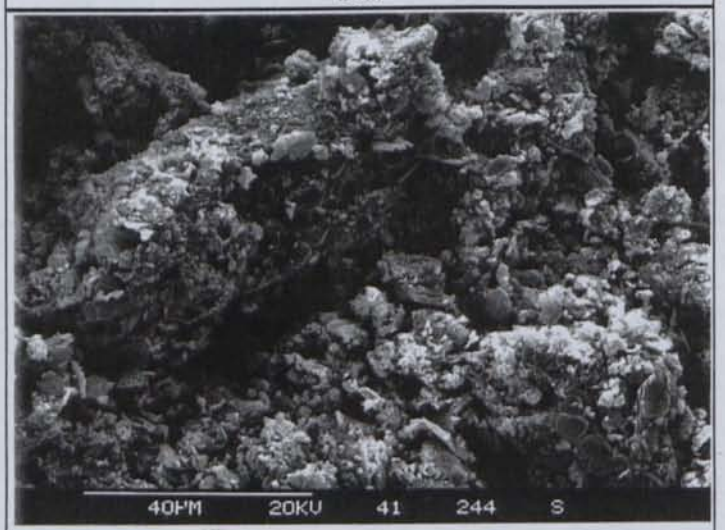

EMG 4.38 Fragmented surface cements of surface hardpan, Dam C, Renison Bell.

The young cements of Dam C are continuous, coat and bridge primary grains and in-fill the majority of pores (EMG 4.36). The hardpan present at 7-13cm depth has a more fibrous nature with sub-rounded Fe sulfate crystals grading into the widespread Fe oxides needle/plates (EMG 4.37). The cements within the surface region, although still slightly fibrous, have a generally more fragmented nature (EMG 4.38) with some regions taking on a smooth appearance, covering primary and secondary minerals alike (EMG 4.39) or sub-angular cubic morphology of the Fe oxide (EMG 4.40).

The morphology of the older cements in Dam A vary dramatically on a centimeter scale. EMG 4.41 (Site 2) shows a well developed continuous Fe oxide cement covering all grains (EMG 4.42). EMG 4.43 (Site 1) however shows a more complicated cementing morphology with uni-directional fibers, sub-angular particles and very fine-grained spherical cementing (EMG 4.44). Both hardpans show a variety of degrading structures. EMG 4.45 (Site 2) displays a degraded aluminosilicate behind an equally degraded Fe sulfide consisting predominantly of sulfur particles (EMG 4.46). EMG 4.47 (Site 1) shows a similar sulfide degradation, along with the development of cubic Fe sulfate (possibly jarosite) as a by-product, along with a basal cement consisting of very small Fe oxide particles which in some region bridge primary grains (EMG 4.48).

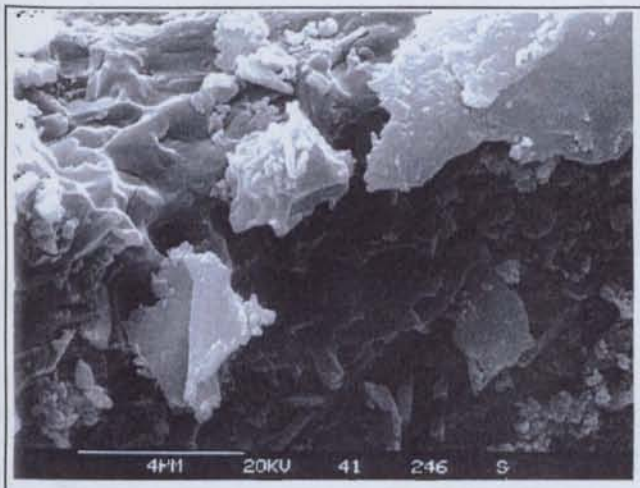

EMG 4.39 Fe oxide cements containing minor S, Dam C, Site 1, Rension Bell

EMG 4.40 Sub angular grains of Fe oxide, Dam C, Site 1, Renison Bell

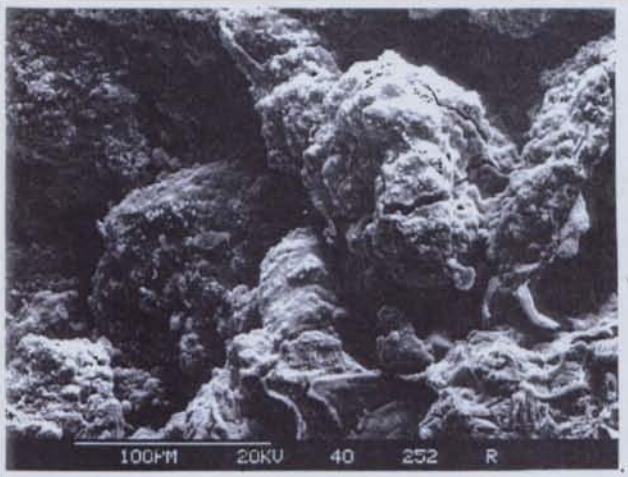

EMG 4.41 General view of cements Dam A, Site 2, Renison Bell

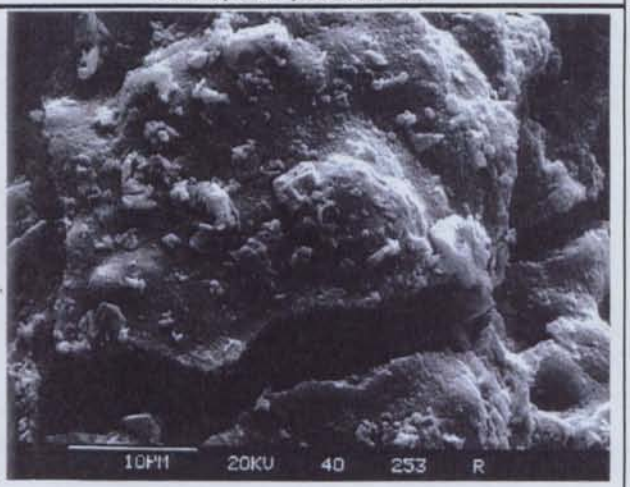

EMG 4.42 Close up of 4.41 Continuous coating of Fe oxide cement

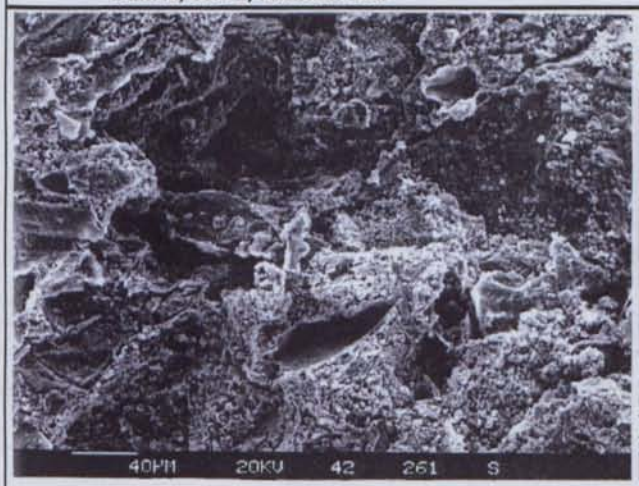

EMG 4.43 General view of cements, Dam A, Site 1, Renison Bell

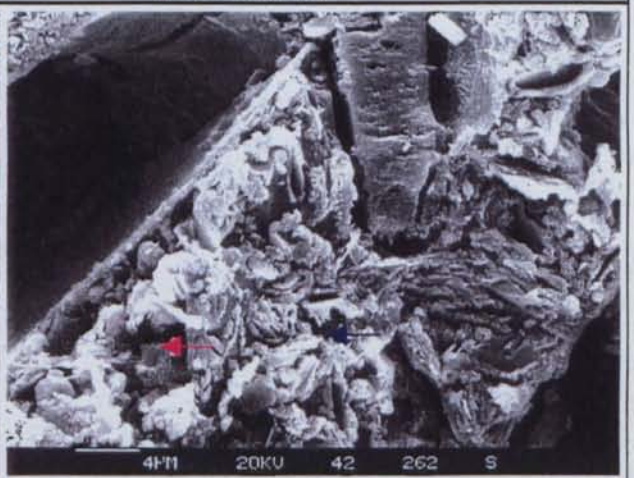

EMG 4.44 Close up of 4.43 Unidirectional fibers (◀), subangular particles and very fine grained spherical cements (◀) all Fe Sulfate, with varying Si and Mg content

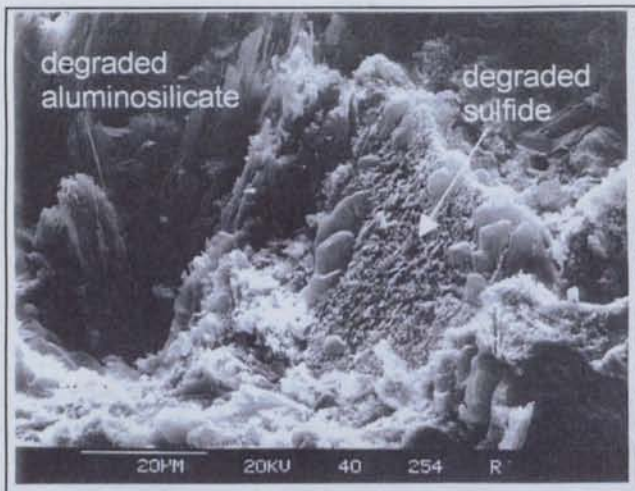

EMG 4.45 Degraded aluminosilicate and Fe sulfide Dam A, Site 2, Renison Bell

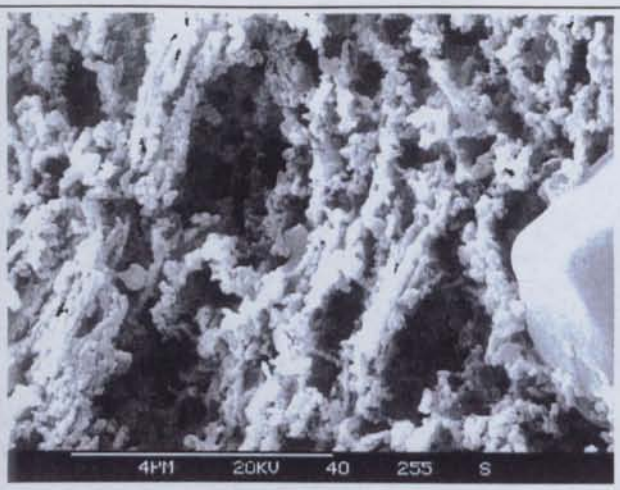

EMG 4.46 Close up of EMG 4.45 Degraded sulfide grain consisting of sulfur particle

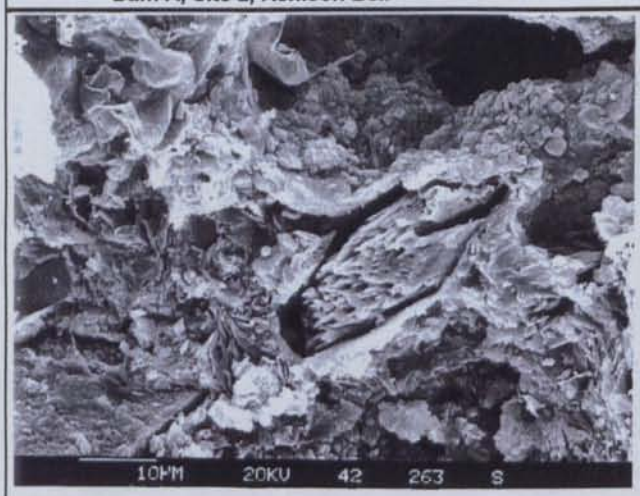

EMG 4.47 Sulfide degradation, cubic Fe sulfate (possibly jarosite) and basal cements of very fine Fe oxide

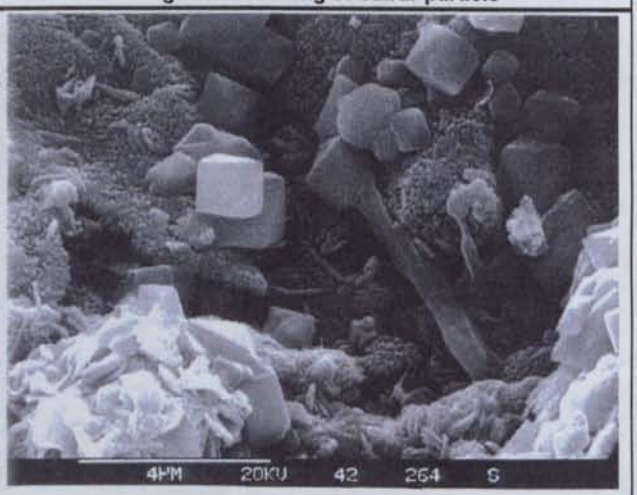

EMG 4.48 Close up of 4.47 spherical Fe oxide basal cement and cubic Fe sulfate

This investigation shows the gradual change of cements associated with hardpan development and degradation. The cements at depth in Site C have taken on a more fibrous appearance which may reflect the precipitation of tertiary minerals upon drying, whereas the young surface hardpan from Dam C has continuous cementing, coating the majority of grains. The Dam A hardpans show a variety of morphologies but are generally less fibrous and show degradation of both primary and secondary minerals.

4.6.1.5 Discussion

It is suggested that the hardpans now observed in Dams A & B are in fact hardpans developed beneath an initially blistered surface which has now eroded leaving a flat-lying cemented surface. The mineralogical and geochemical profiles which have developed beneath these cemented surfaces are evidence that hardpans potentially reduce sulfide oxidation through the inhibition of oxygen and water penetration into the underlying tailings. This statement can be illustrated through a comparison of sites where hardpans are intact, and areas where the hardpan has been disturbed.

In locations where the hardpan is unbroken a pH of 5.5-6 has developed in the underlying tailings and is associated with the presence of calcite and siderite. These relatively high pH conditions and presence of neutralising minerals indicate acid generation has been substantially reduced beneath the hardpan surface. In locations where the hardpan surface has been disrupted through excavation, the pH is acid (pH 2.4) and elevated solute loads have developed (see Chapter 5).

Generally the hardpans appear to have a good resistance to chemical disintegration, even in highly acidic conditions. The palaeo-hardpan developed in Dam A - Site 1, 20cm below the surface is massive and substantial. The hardpan is overlain by tailings of pH 2.2-2.5 and yet the secondary minerals of the hardpan appear to be unaffected by acid attack.

Hardpans were also observed in the adjacent Argent River and appear to have considerable resistance to mechanical erosion. These were developed during the period of mining when Renison tailings were discharged from the Battery Mill directly into the river. The hardpans are still intact, beneath which unoxidised tailings persist. It is suggested that even at these sites, hardpans are helping to reduce pollutant generation.

The hardpan surfaces observed in Dams A and B maybe the secondary cemented surfaces developed under an initially blistered surface or whether they represent a completely new surface developed through a series of cyclical degradation and development since initial formation. During the degradation of the hardpan the whole of the dam surface would not be exposed, as different areas are obviously eroded at different rates, depending on water runoff and exposure to wind. Thus the acid generated and increased solute concentrations would be localised before cementing takes place once again, sealing the system. The solute loads now observed below the surface would have developed during former periods of exposure. It is assumed that this solute release would be limited, however large contaminant loads are released through seepage from the dams. The contaminated seepage may be attributed to this process of hardpan degradation and subsequent sulfide oxidation, however the dam walls are also suggested to be a source of contamination.

Seepage of contaminated waters from the dam is potentially not the only complication associated with hardpan degradation. The transportation off-site of eroded hardpan cements by water and wind could be a problem depending on the rate of breakdown and thus the total amount of degraded cements produced.

It should be noted that the conditions of pH 5-6 and the presence of calcite may be to some extent due to the presence of the hardpans however it must be remembered that the Renison Dams are in a high rainfall zone and preservation of the sulfides may also be due to continual elevated levels of saturation. Under these conditions oxygen diffusion is inhibited and thus oxidation reactions are reduced, preserving the tailings.

4.8 Conclusions

Of the twelve sites selected for investigation, varying sulfide and gangue mineralogy and content, groundwater chemistry, physical characteristics and climate, controlled the nature and extent, of hardpan formation. As a result of these variations, hardpan development differs in depth of formation within the profile, thickness, lateral extent and composition.

Hardpans are defined as relatively hard impervious layers of soil lying at or just below the surface, produced as a result of cementation of particles by precipitation of relatively insoluble materials such as silica, iron oxide, calcium carbonate and organic matter (American Geological Institute, 1997). This definition could encompass surface hardpans developed in tailings except that calcium carbonate and organic matter play little or no role in the cementing process.

The ***hardpans*** described in this Chapter occur at the surface of the tailings where secondary minerals bind both sulfide and gangue minerals into a continuous sheet of cement. The thickness of these surface hardpans range from <1cm to >10cm depending on age and thus extent of development. The ***cemented layers*** are distinct from surface hardpans as they occur deeper in the tailings profile. In these cases, secondary mineral precipitation occurs only along selected layers, usually dictated by textural boundaries produced during tailings deposition. The thickness of these cemented layers range from <0.5cm to >5cm.

Some hardpans and cemented layers form uniformly over entire dams either as a surface cement or at some depth and have been termed ***laterally extensive hardpans/cemented layers.*** **Laterally extensive surface hardpans** have developed at CSA and Elura (NSW) and Renison Bell (Tas) tailings impoundment, while **laterally extensive cemented layers** have developed at depth within the tailings profile, at Broken Hill (NSW) and Brukunga (SA).

Other hardpans have developed only in locations of concentrated seepage, and have been termed ***laterally discontinuous hardpans.*** **Laterally discontinuous hardpans** have developed at the Chesney (NSW) and the Woodcutters (NT) impoundment. In these dams, widespread hardpan development has been restricted by mineralogy, grain size or climate, and hardpan formation has been enhanced in seepage zones in low lying regions. When these tailings are exposed to seepage waters laden with heavy metals and sulfate, additional elemental loads become available for secondary mineralisation, while increased levels of Fe^{2+} can promote enhanced oxidation and thus accelerate hardpan development.

Chapter 5 presents geochemical descriptions for each of the sites examined. The observation made in Chapters 4 and 5 have been combined so that aspects of hardpan formation including, modes of formation and parameters effecting hardpan development are fully outlined in Chapter 8.

Chapter 5 : Tailings Dam Geochemistry

5.1 Introduction

Investigations of solute concentrations within surface hardpans, underlying tailings and cemented layers were undertaken to determine the effect of hardpan and cemented layer generation on solute concentrations within the upper tailings profiles. This information gives an indication of contaminant generation and its availability for leaching into the surrounding environment. Hardpans have the potential to reduce solute concentration by three main mechanisms. 1) The secondary minerals within the cements can incorporate a variety of elements into their structures either through co-precipitation or adsorption. 2) Additionally the cements coat the reactive sulfides thus reducing direct oxidation and pollutant generation. 3) As the cements develop they are believed to form an effective low-permeability barrier to vertically moving water and oxygen thus inhibiting the effects of leaching and oxidation at depth. The effect hardpans have on the geochemical evolution of tailings was determined through comparisons between new and old tailings dams and annual reviews of similar sites. Investigations of old and new tailings examined the effect *developing* hardpans have on newly exposed tailings, while annual comparisons of *well-developed* hardpans gave insight into hardpan stability and the overall effect hardpans have on the underlying tailings over time.

Descriptions of primary and secondary mineralogy (outlined in Chapter 4), together with solute concentration (1:5 extracts), pH, electrical conductivity (EC) and redox potential (Eh) conditions within the tailings have been undertaken to gain an understanding of the type and extent of geochemical reactions occurring. Section 5.2 describes the general geochemical reactions involved in the near-surface zones of the tailings and the development of secondary minerals which, when concentrated sufficiently, cause cementing either as a surface hardpan or as cemented layers within the tailings profile. Discussions and comparisons of individual sites are presented in Sections 5.4.

The geochemistry of tailings dams is complex. Mineralogical reactions can be either inhibited or enhanced by the physical characteristics of the tailings and their environment. Grain-size distribution, deposition style, matrix and osmotic suction potentials can all influence tailings reactivity through effecting moisture saturation levels, which in turn effect gas diffusion properties and ultimately sulfide oxidation and by-product generation. These properties along with others including the climatic setting of the mine can dictate the geochemical evolution of the tailings. Chapter 5 explores these issues with regards to solute generation and the potential for hardpan development and pollutant generation (Section 5.3).

5.2 Geochemical Reactions of Hardpan/Cement Formation

The development of hardpans and cemented layers within tailings, takes place through a series of geochemical reactions which produce by-products available for secondary mineral precipitation. This section outlines the main processes involved, including sulfide oxidation, acid and solute generation, the

associated neutralisation reactions, gangue mineral degradation and secondary and tertiary mineral precipitation. The effect varying geochemical conditions have on secondary mineral precipitation is also investigated.

5.2.1 Sulfide Oxidation, Acid Generation/Neutralisation and Selected Secondary Mineral Precipitation Reactions

Sulfide oxidation reactions are an integral step in the natural development of hardpans and cemented layers in tailings. As a result of these reactions, by-products become available for secondary mineral precipitation, while the acid produced causes additional solutes to form as a result of gangue mineral degradation. Table 5.1 presents typical oxidation reactions and potential precipitation equations.

TABLE 5.1 SULFIDE OXIDATION AND SUBSEQUENT PRECIPITATION EQUATIONS

pyrite oxidation	
$FeS_2 + {}^{7}/_{2}O_2 + H_2O \Leftrightarrow Fe^{2+} + 2SO_4^{2-} + 2H^+$	(5.1)
precipitation reaction	
$FeS_2 + {}^{15}/_{4}O_2 + {}^{7}/_{2}H_2O \Leftrightarrow Fe(OH)_3 + 2SO_4^{2-} + 4H^+$	(5.2)
pyrrhotite oxidation	
$Fe(1-x)S + (2-x/2)O_2 + xH_2O \Leftrightarrow (1-x)Fe^{2+} + SO_4^{2-} + 2xH^+$	(5.3)
chalcopyrite oxidation	
$CuFeS_2 + 4O_2 \Leftrightarrow Fe^{2+} + 2SO_4^{2-} + Cu^{2+}$	(5.4)
precipitation reaction	
$CuFeS_2 + {}^{17}/_{4}O_2 + H_2O \Leftrightarrow Fe(OH)_3 + Cu^{2+} + 2SO_4^{2-} + 2H^+$	(5.5)
sphalerite oxidation	
$ZnS + O_2 \Leftrightarrow Zn^{2+} + SO_4^{2-}$	(5.6)
where the Zn^{2+} cannot oxidise and ZnO_2 will only precipitate if it reaches an alkaline environment.	
galena oxidation	
$PbS + O_2 \Leftrightarrow Pb^{2+} + SO_4^{2-}$	(5.7)
precipitation reaction	
$PbS + {}^{5}/_{2}O_2 + H_2O \Leftrightarrow PbO_2 + SO_4^{2-} + 2H^+$	(5.8)

Oxidation of different sulfides have distinct outcomes in terms of acid and solute generation. Thornber and Taylor (1992) explained that the chemical reactions at the cathode and anodes of the weathering sulfides can be written as follows, where M*r*S is a base metal sulfide with the metal / sulfur ratio = *r*.

cathode: $O_2 + 2H_2O + 4e^- \Leftrightarrow 4OH^-$ (5.9)

anode: $MrS + 4H_2O \Leftrightarrow rM^{2+} + SO_4^{2-} + 8H^+ + (6+2r)e^-$ (5.10)

which combines to give:

$2MrS + (3+2r)H_2O + (3+r)O_2 \Leftrightarrow 2rM^{2+} + 2SO_4^{2-} + 4H^+ + 4rOH^-$ (5.11)

If

1) $r<1$, such as in pyrite (FeS_2), marcasite (FeS_2), pyrrhotite (Fe_7S_8) and violarite ($(FeNi)_3S_4$) acid is produced.

2) r=1, such as galena (PbS), sphalerite (ZnS) or chalcopyrite ($CuFeS_2$) the reaction is neutral and the overall pH will not change i.e. there is no hydrolysis of the metals and
3) r>1, such as for chalcocite (Cu_2S) and pentlandite ($(Ni,Fe)_9,S_8$), OH^- is in excess and the reaction may even be alkaline.

The outcomes of these sulfide oxidation reactions drives the geochemical evolution of the tailings. Usually, the main sulfidic component of tailings consists of pyrite and pyrrhotite. Depending on the type of sulfides present, acid generation varies and the type of cations available for precipitation reactions also differs. Acid generation drives neutralisation reactions involving carbonates, aluminosilicates and oxy-hydroxides, which also supply cations and anions for precipitation reactions. Morin (1988), Morin and Cherry (1988) and Morin et al. (1988 a,b) explain that as sulfide oxidation proceeds at the surface of tailings, the pore water pH decreases over time in a series of steps, each of which represents the dissolution of specific neutralising species present at that pH. The mineral species believed responsible for each pH plateau are presented in Table 5.2 (Morin and Cherry, 1988).

TABLE 5.2: pH PLATEAUS DEVELOPED THROUGH THE PRESENCE OF SPECIFIC MINERAL SPECIES.

Mineral Species	pH Plateau
calcium-based carbonate	pH 5.5-6.4
aluminum hydroxide	pH 4.3-5
iron hydroxide and jarosite	pH 3-3.7
aluminosilicates	pH<3

Calcite and dolomite contents vary from site to site, and thus their impact differs.

$$H^+ + CaCO_3 \Leftrightarrow Ca^{2+} + HCO_3^- \quad (5.12)$$
calcite

$$2H^+ + CaMg(CO_3)_2 \Leftrightarrow Mg^{2+} + Ca^{2+} + 2HCO_3^- \quad (5.13)$$
dolomite

$$H^+ + FeCO_3 \Leftrightarrow Fe^{2+} + HCO_3^- \quad (5.14)$$
siderite

Siderite may also initially act as a neutralising mineral however it has a double effect. As the Fe^{2+} is released, it may oxidise and the product Fe^{3+} may then play a role in the sulfide oxidation reactions causing increased acid and solute production (Ptacek and Blowes, 1994).

As with carbonates, the neutralising potential and cation production varies with the aluminosilicate being degraded by the acid conditions. Kaolinite is a common end product of aluminosilicate degradation. Kaolinite can be formed principally via the weathering of feldspars, feldspathoids and other silicates, e.g. muscovite and pyrophyllite, possibly as:

$$2NaAlSi_3O_8 + H^+ + {}^9/_2H_2O \Leftrightarrow {}^1/_2Al_2Si_2O_5(OH)_4 + Na^+ + 2Si(OH)_4 \quad (5.15)$$
albite kaolinite

$$CaAl_2Si_2O_8 + 2H^+ + H_2O \Leftrightarrow Ca^{2+} + Al_2Si_2O_5(OH)_4 \quad (5.16)$$
anorthite kaolinite

$$KAlSi_3O_8 + H^+ + {}^9/_2H_2O \Leftrightarrow K^+ + 2H_4SiO_4 + {}^1/_2Al_2Si_2O_5(OH)_4 \quad (5.17)$$

k-feldspar kaolinite

$$Al_4Si_8O_{20}(OH)_4 + 10H_2O \Leftrightarrow 2Al_2Si_2O_5(OH)_4 + 4Si(OH)_2 \quad (5.18)$$

pyrophyllite kaolinite

$$K(Mg,Fe)_3(Si_3Al)O_{10}(OH,F)_2 + 4Al^{3+} + 3H_2O + 2H^+$$

biotite

$$\Leftrightarrow 3Al_2Si_2O_5(OH)_4 + 2K^+ + 3Fe^{2+} + 3Mg^{2+} \quad (5.19)$$

kaolinite

The chlorite, clinochlore has a strong neutralising capacity because of its brucite-like ($(MgAl)_6(OH)_{12}$) interlayers, and the dissolution of this mineral has a significant effect on the acidity and thus elemental mobility within the tailings pore waters (Fordham, 1993).

Both jarosite ($KFe_3(SO_4)_2(OH)_6$) and alunite ($KAl_3(SO_4)_2(OH)_6$) have been identified as cementing agents within the hardpans. Their impact on acidity and thus mobility also dictates the conditions in which secondary minerals precipitated. Jarosite may be precipitated by the reaction

$$K^+ + 3Fe^{3+} + 2SO_4^{2-} + 6H_2O \Leftrightarrow KFe_3(SO_4)_2(OH)_6 + 6H^+ \quad (5.20)$$

jarosite

producing 6 moles of acid for every mole of K^+ from the weathering, for example, of muscovite

$$2KAl_3Si_3O_{10}(OH)_2 + 3H_2O + 2H^+ \Leftrightarrow 3Al_2Si_2O_5(OH)_4 + 2K^+ \quad (5.21)$$

muscovite kaolinite

Alunite precipitates through a similar process, where Al^{3+} is derived from the decomposition of aluminosilicate minerals.

$$K^+ + 3Al^{3+} + 2SO_4^{2-} + 6H_2O \Leftrightarrow KAl_3(SO_4)_2(OH)_6 + 6H^+ \quad (5.22)$$

alunite

These minerals produce acidity during their precipitation, but they may play a further role after most of the sulfide has oxidised. If the system is then leached with rainwater, some of the soluble SO_4 is removed, $Fe(OH)_3$ is precipitated releasing more acid

$$KFe_3(SO_4)_2(OH)_6 + 3H_2O \Leftrightarrow 3Fe(OH)_3 + K^+ + 2SO_4^{2-} + 3H^+ \quad (5.23)$$

jarosite

On the other hand, if there is any residual acid (perhaps retained on the mineral surfaces), then the jarosite and alunite could have a neutralising effect by the reaction of H^+ with their hydroxyl groups

(Jambor and Blowes, 1994). However, this effect might only be temporary, since Fe^{3+} in solution could later be re-precipitated as $Fe(OH)_3$ and again add acid. Thus the effect of jarosite on the system is finely balanced to external conditions. Similarly the precipitation of elemental sulfur, detected in the Elura and CSA tailings, has the potential to effect the near surface geochemistry during precipitation and subsequent oxidation. Nordstrom (1982) explains the formation of sulfur as a loss of ferrous ions from lattice sites of pyrite, leaching an unstable sulfur-rich surface which eventually disrupts and re-organises into elemental sulfur. The possible precipitation reaction is:

$$FeS_2 + O_2 + 4H^+ \Leftrightarrow 2Fe^{2+} + 4S^\circ + 2H_2O \quad (5.24)$$

pyrite sulfur

The subsequent oxidation of sulfur again creates more acidity. This may be written as:

$$2S^\circ + 3O_2 + 2H_2O \Leftrightarrow 2SO_4^{2-} + 4H^+ \quad (5.25)$$

sulfur

Goethite, hematite and ferrihydrite have in some cases formed either in conjunction with or instead of sulfates, presumably because sulfate concentrations have been reduced through leaching.

$$Fe^{3+} + 3H_2O \Leftrightarrow Fe(OH)_3 + 3H^+ \quad (5.26)$$

$$2Fe(OH)_3 \xrightarrow{\text{dehydration}} Fe_2O_3 + 3H_2O \quad (5.27)$$

Additionally melanterite and rozenite, were identified through XRD, appearing as white crystals on the tailings surface.

$$Fe^{2+} + 4H_2O + SO_4^{2-} \Leftrightarrow FeSO_4.4H_2O \quad (5.28)$$

rozenite

Halotrichite forms in a similar manner to rozenite, however was only identified as a tertiary mineral developed upon drying of the samples:

$$Fe^{2+} + 2Al^{3+} + 4SO_4^{2-} + 22H_2O \Leftrightarrow FeAl_2(SO_4)_4.22H_2O \quad (5.29)$$

halotrichite

The occurrence of siliceous cements as either opal A as stringers or precipitates with other secondary minerals (e.g. ferrihydrite) is common within many of the hardpans. Siliceous cements are thought to exist as residues after the dissolution of a pre-existing mineral phases. Evidence is provided by opal pseudomorphing mica where all other constituents of the mica have been leached leaving only the framework of silica. Additional siliceous material was observed with little or no structure. This may have formed though direct precipitation from a silica-rich solution. Widespread siliceous cements were observed in the:

- cemented layers at Brukunga and Broken Hill
- leached system of the Chesney seepage hardpan
- slowly formed surface hardpan of CSA, and
- breakdown surface at Elura - Dam 1 (as outlined in Chapter 4)

The siliceous cements appear to develop in the more mature systems where the more soluble sulfate cements have been leached from the system. Brukunga, Broken Hill and Chesney cements may have possibly developed through the translocation of solute loads and their subsequent precipitation. Aluminosilicates may have become unstable in acidic conditions releasing SiO_2 into the surrounds for incorporation into the already precipitated cements.

The CSA hardpan and Elura breakdown material represents the mature end of the cement evolution (Chapter 4), where many of the sulfates have been re-mobilised and SiO_2 has been released due to the acidic conditions and subsequent in-situ re-precipitation.

5.2.2 Conditions of Secondary Mineral Precipitation

The development of the secondary minerals which make up cements within tailings dams have been studied extensively (Fanning and Fanning 1989; Nordstrom, 1982; McSweeney and Madison, 1988; Bigham et al. 1990, 1992; Alpers et al. 1994 and Jambor, 1994). Secondary minerals form as a result of weathering when solubility products are exceeded so that conditions of saturation or super saturation are achieved (Alpers et al. 1994). Nordstrom (1982) and Fanning and Fanning (1989) suggested a series of intermediate steps that may occur prior to the development of iron oxy-hydroxides and sulfates. Nordstrom (1982) explained that the precursor secondary soluble sulfate minerals are most commonly formed during dry periods as evaporation promotes the rise of sub-surface waters to the upper-most surface of tailings by capillary action. As these waters reach the upper portion of the tailings, they become progressively more concentrated and finally precipitate various hydrated soluble salts. This is thought to be an important intermediate step preceding the precipitation of the more common insoluble iron minerals e.g. jarosite, ferrihydrite and goethite.

Fanning and Fanning (1989) explained that both ferrous sulfate and sulfuric acid are very soluble and are normally dissociated in water. Then under desiccation conditions (e.g. at the surface) different $FeSO_4$ minerals may form depending on conditions. Nordstrom (1982) indicated that melanterite ($FeSO_4.7H_2O$) is the first to precipitate, then under continued dryness, melanterite dehydrates to either rozenite ($FeSO_4.4H_2O$) or szomolnokite $FeSO_4.H_2O$. Ferrohexahydrite ($FeSO_4.6H_2O$) may precipitate at this stage but is less common as it has very limited stability. If these minerals are still in contact with water or humid air and warm temperatures, they oxidise to copiapite ($Fe^{2+}Fe^{3+}(SO_4)_6(OH)_2.2H_2O$). Then if Fe becomes fully oxidised it may eventually reach saturation with respect to jarosite. Eventually as jarosite weathers or is exposed to dilute solutions with higher pH, it gradually decomposes to ferrihydrite or goethite.

Nordstrom (1982) also explained that these secondary minerals precipitate at different locations in the profile. The soluble hydrated sulfates form during periods of dry weather near the vicinity of oxidising pyrite in the unsaturated profile, while ferrihydrite, goethite and jarosite are spatially distributed further away from the pyrite under saturation conditions.

It should be noted that the presence of the soluble hydrated sulfates is not a precursor to the less soluble iron bearing minerals (e.g. jarosite or ferrihydrite) and were not always observed during this study. However the reactions and conditions that must take place before Fe oxy-hydroxides and sulfates precipitate are consistent with the formation of these minerals. The reactions include the oxidation of sulfides, oxidation of the resultant Fe^{2+}, saturated conditions with respect to sulfate and Fe and in some cases hydrolysis.

All these studies indicate that the formation of secondary minerals in any system can be complicated. Nordstrom (1982) and Fanning and Fanning (1989) have demonstrated the development of jarosite and less soluble salts through a series of steps, each one depending on the conditions of the surrounding environment. Bigham et al. (1992) have attempted to build on this, integrating the information to produce a tentative biogeochemical model for mineral formation from mine drainage. They stated that under conditions of low pH, high dissolved SO_4 (3000-4000 μg/mL) and sustained bacterial activity, jarosite or related basic ferric sulfates will form, provided suitable cations (e.g. K, Na) are also available. In many cases K and Na would be present from the breakdown of feldspars, chlorites and micas during acid attack.

Bigham et al. (1992) explained that schwertmannite forms most readily within a narrow pH range of 3-4. While the mineral can form in the presence of excess SO_4, concentrations in the range of 1000-3000 μg/mL appear to be optimal. Whereas at pH>5, the dominant mineral product is ferrihydrite, as the abiotic oxidation of Fe^{2+} can proceed rapidly under these conditions. Precipitation of this mineral seems fairly insensitive to SO_4 concentration, while its stability varies depending on its composition. Carlson and Schwertmann (1981) illustrated that once formed, natural ferrihydrite seems to resist transformation to more stable forms for a longer period than it does when produced in pure, but otherwise comparable, synthetic systems, where it converts to goethite and/or hematite within months or years. Stability in this case is due to dissolved ions which have a high affinity for the ferrihydrite surface. Impurities are chemically absorbed and not only suppress ordering of the ferrihydrite, but also inhibit the formation of hematite or goethite. Chemically absorbed silica is one of the main stabilising molecule (Carlson & Schwertmann, 1981).

Many combinations of secondary minerals have been observed acting together to cement tailings, despite their stability fields being considerably different. For example it is explained that jarosite is typically stable at lower pH values than ferrihydrite however McSweeny and Madison, (1988) indicated that the two can coexist with an estimated pH of 3. Further to this, these authors suggested that the pH of the solution in the intra-aggregate pores could be slightly more acidic than that in the bulk solution,

because the smaller pores are in immediate contact with or in very close proximity to a source of oxidisable S. This condition would then favor the formation of jarosite rather than ferrihydrite. In locations further away from sulfides, the pH may be higher and precipitation of ferrihydrite would be favored. As the progressive cementation of the inter-aggregate pores occurs, this reduces permeability of the horizon to downward flow and enhances capillary flow through the intra-aggregate pores, improving the conditions likely for the formation of potentially soluble Fe-sulfates.

Little appears to have been written about the role of siliceous cements in the tailings environment. In the case of many mature hardpans it appears that the siliceous cements are the products of acid dissolution of aluminosilicate minerals present in the tailings. The exact pH and Eh conditions for crystallisation is not completely understood, however the close relationship of silica with jarosite, ferrihydrite and other Fe oxides suggests similar conditions of formation, particularly if they are precipitated in a similar time frame.

With increased acidity, aluminosilicate degradation may be promoted releasing additional SiO_2 available for precipitation. Silica may also co-precipitated with other metals. For this to occur a pH>2 would have to be maintained, as the point of zero charge occurs at pH 2 (Parks, 1967). The negative charge of silica at pH>2 promotes adsorption of metal ions, whereas, the low pH of most sulfidic tailings increases the positive charge due to H^+ ions on silica surfaces, thus hindering adsorption of metal ions and eventual co-precipitation.

5.3 Overview of the Processes Influencing the Geochemical Evolution and Final Morphology of Tailings and Cements

5.3.1 Deposition Style

Tailings are generally pumped to the dams as slurries and deposited via spigots. The deposition method and design of the dams can to some extent dictate the tailings geochemistry that will develop. Deposition via the edge spigot method results in deposition of coarse tailings closest to the dam edge, while fines are deposited furthest from the spigot. Central spigotting results in opposite conditions with the coarsest fractions deposited centrally and the finest fraction near the edge. These grain size variations alter the physical conditions resulting in either promotion or impedance of chemical reactions. Coarse tailings may allow increased loss of pore water via drainage and evaporation, which in turn allows increased gas diffusion and thus oxidation of the unsaturated sulfides. Finer tailings however retain their initial pore waters for extensive periods of time, reducing the oxygen influx and thus reducing the potential for sulfide oxidation, despite the higher surface area and potential reactivity.

Variations in spigot location may result in generalised grain size distributions however each location within the dam has unique sedimentary sequences dictating the geochemistry of that location. As tailings are deposited, gullies are formed which influence the direction of slurry flow. The general sedimentary sequence is not unlike that of braided stream systems, which result in highly heterogeneous

stratigraphy. As mentioned previously, the grain-size controls the water holding capacities and gas diffusion rates but also can control the mineralogical distribution and thus reactivity of the tailings. The reactivity of a mineral is an intrinsic property and is strongly effected by grain-size (surface area), oxygen and water availability. Depending on the metallurgical processes employed, the minerals can be allotted into grain size ranges due to their resistance to grinding/crushing, where the grinding/crushing procedures are determined by the grain size of the ore to be liberated. The final grain-size will in turn influence the reactivity of the minerals, where the large surface area of the fine-grained tailings have greater potential reactivity.

5.3.2 Palaeo-surfaces

The development of palaeo-surfaces also effect mineralogy and geochemistry of the profile. Palaeo-surfaces develop when tailings are exposed for a period of time prior to further tailings deposition. During prolonged exposure, partial evaporation or drainage of the pore water may occur, desiccation cracks may develop and oxidation of the sulfides present can occur. The resultant acid generation, gangue mineral degradation and neutralisation reactions that take place, result in major changes in geochemistry. Depending on the length of exposure and the resultant geochemical conditions, secondary minerals may precipitate at the surface and/or along desiccation cracks. The type of secondary precipitate is dictated by the pH and Eh conditions of the system along with the nature and concentration of elements available. Additionally the moisture content of the tailings may determine the degree of hydration of secondary minerals. Thus a range of soluble and insoluble secondary minerals may form including Fe oxide/oxy-hydroxides, sulfates, sulfur and siliceous material. The type of mineral precipitated will in turn dictate the overall solute concentrations of pore waters within the profile. The more insoluble minerals (oxides, jarosites) have the potential to incorporate contaminants in their structures for extended periods. When rainfall occurs or fresh tailings are deposited on these surfaces, the soluble secondary minerals may be dissolved, resulting in the redistribution of the solutes down the profile. Conversely, the less soluble or insoluble secondary minerals will remain, resulting in the formation of a palaeo-surface and cements.

Palaeo-surfaces and variations in grain size also have the potential to effect the transportation and redistribution of solutes within the profile. In tailings with large grain size, the final sedimentary sequence can strongly dictate water movement and thus leaching potential. Chapter 4 showed profiles through Broken Hill Site C, where oxidation, water movement and leaching has resulted in the precipitation of secondary minerals along fine-grained layers. These fine-grained layers may act as channels for unsaturated water flow, which allows the concentration of oxidation by-products and precipitation of cements. Palaeo-surfaces may also dictate the geochemical profiles because of the scavenging ability of the previously precipitated secondary minerals. The palaeo-surfaces themselves may also retain soluble elements produced during their formation, adding to elemental concentrations at depth.

5.3.3 Final Surface Morphology

The final morphology of the dam also effects the geochemistry that develops. In tailings dams that have been filled to capacity, process waters or rainfall can pond in low lying regions. If the water cover

remains for extended period of time, these saturated conditions may reduce sulfide oxidation through the slow rate of oxygen diffusion through water. Additionally, depending on the origin of the ponded water, solute loads in the saturated upper tailings may be effected. Ponded rainwater may promote the dissolution and leaching of previously concentrated solutes, while ponded process water (often pH>7) may already contain high solute concentrations promoting precipitation from saturated solutions.

5.3.4 Implications and Complications

Thus investigations of the geochemical profiles within tailings can give an indication of the extent to which reactions are occurring and of the contaminants which are available for release, or precipitation as secondary minerals. However, solute concentrations within the profiles can be effected by many mechanisms that preclude a detailed understanding of each site. Additional complications are associated with sampling frequency i.e. increased sampling usually produces increased variability.

Solute concentration, pH and EC profile comparisons on a yearly basis can be useful, however variable sedimentary stratigraphy, the presence and extent of palaeo-surfaces and desiccation crack, salts and cements can produce large variations in the profile causing difficulties in interpretation. In many cases a comparison of similar locations on a yearly basis show great variations in solute loads. For example a surface decrease in Al, S, Pb, Fe etc. may reflect one or a combination of at least three processes:

1) leaching from the surface down the profile,
2) precipitation of insoluble cements,
   and/or
3) mechanical removal of surface salts and tailings by wind or water erosion.

Where possible, microscopic examinations, SEM-EDX, microprobe, XRF and XRD analysis has been utilised to determine the main mechanisms taking place.

5.4 Geochemistry of Solutes from tailings profiles

Geochemical analyses were carried out on core samples from each of the sites investigated. The most valuable information was sourced from sites where two or more dams of varying age were present. It is for this reason that data from Broken Hill, CSA, Elura, Chesney and Renison Bell are presented below, along with discussions on how the hardpans have effected the geochemistry at each site. Woodcutters data is also included in this chapter because of the useful information on seepage hardpans and the subsequent geochemistry that results. The elemental concentrations presented in this section have been derived from batch leaching experiments and thus do not represent the solute concentrations in the original tailings pore waters (Method Section 1A.3.1). The 1:5 batch leaching allowed removal and thus quantification of solutes present in the residue pore waters and those available as soluble salts. This type of extraction gives an insight into the total quantities of elements available for release from the tailings during rainfall events. Tables containing elemental data are presented at the end of each site discussion. Data and discussions on the Brukunga, Kanmantoo, Peak, Woodlawn, Ranger, and Pine Creek tailings are presented in Appendix 2A.

5.4.1 Willyama Block, N.S.W

5.4.1.1 Broken Hill

5.4.1.1.1 Alpine and Marlboro Country Dams

A review of the solute concentration in the Alpine and Marlboro Country dams has been consolidated as similar processes appear to be taking place, except that the Alpine Country Dam is well cemented while Marlboro is not. The review indicates that Ca and S are the main mobile elements present and precipitation of these elements occurs at varying depths down the profile (Table 5.3). XRD verified the main precipitate as gypsum. As much of the textural and colour information has been lost due to problems during extrusion of the cores, it is difficult to assess the relation of these concentrations to oxidation levels and textures.

Sodium, Zn, Mg and K are also present throughout the profiles (Fig 5.3, 5.4, 5.5, 5.10, 5.11 & 5.12) but in lower concentrations than for Ca and S (Fig 5.2, 5.4, 5.9 & 5.11). Potassium appears to follow similar trends to those of Ca and S and it is suggested that K is either absorbing on or co-precipitating with gypsum or is precipitating as a discrete secondary mineral with gypsum through similar mechanisms (Figs 5.5 & 5.12). XRD and SEM investigations did not determine which mechanism was occurring. Generally, elevated concentrations of Na and Mg were observed in the surface regions, but again XRD did not detect an associated secondary mineral (Figs 5.4, 5.5, 5.11 & 5.12). It is therefore suggested that their concentrations are obtained through adsorption, substitution processes or as direct precipitation of amorphous secondary minerals undetectable by XRD. Additionally, crystalline secondary minerals may have precipitated in quantities too low for XRD detection.

Soluble Mn is generally in low concentrations or absent at the surface of the Marlboro Dam and the edge holes of the Alpine Country Dam (Figs 5.6 & 5.13). These concentrations increase with depth. The central Hole 2 in Alpine Country however shows greater quantities of 50-200mg/kg within the upper 30cm of the profile. It is assumed that the Mn has precipitated as insoluble Mn oxides within the surface regions of Holes 1 and 3 and to a lesser extent in Hole 2. At depth Mn mineralogy may have changed, resulting in greater Mn mobility.

Re-coring of the Alpine Country Dam in 1996 showed increased surface concentrations of Cu, Fe, Pb, Si and Zn in the central hole compared with the previous year. This variation is unlikely to be due to increased oxidation between the sampling periods as the dams are up to 60 year old. It is suggested however that slight differences in sampling locations may be responsible.

pH results for the Alpine and Marlboro Dams are presented in Figs 5.1 & 5.8. Although there are slight variations down the profile, pH remains generally between 6 and 8. At some locations a slight decrease is observed at the surface in response to sulfide oxidation, however this is only a minor change as the tailings have a low sulfide content and considerable calcite content which buffers the

pH. Other profiles show slight increases in pH in the surface region, which is attributed to the calcrete soil placed on the surface.

The EC results for the Alpine and Marlboro Country Dams are presented in Figs 5.1 and 5.8. Results vary between 0.5-3 mS/cm, not including the surface calcrete soils. Within the Marlboro Country tailings, the overall EC variations are very minor. Some of the more prominent increases may be a result of palaeo-surfaces where increased exposure time has resulted in increased quantities of oxidation by-products, or increases may occur in response to textural variations throughout the profile. The Alpine Country Dam EC profiles vary more than those of the Marlboro Dam, with the 1996 sampling showing generally lower surface EC results. Larger variations have developed in response to the diversity of cementing throughout the profile, unlike the Marlboro Country Dam which exhibits no cementing properties.

It appears that the main soluble salt producing any cementing qualities is gypsum which has precipitated at various levels down the profile. Other cementing agents are insoluble and have not been detected in this analysis, except as noticeable deficiencies in the surface regions i.e. Zn and Mn depletions developed through precipitation of hemimorphite and Mn oxides.

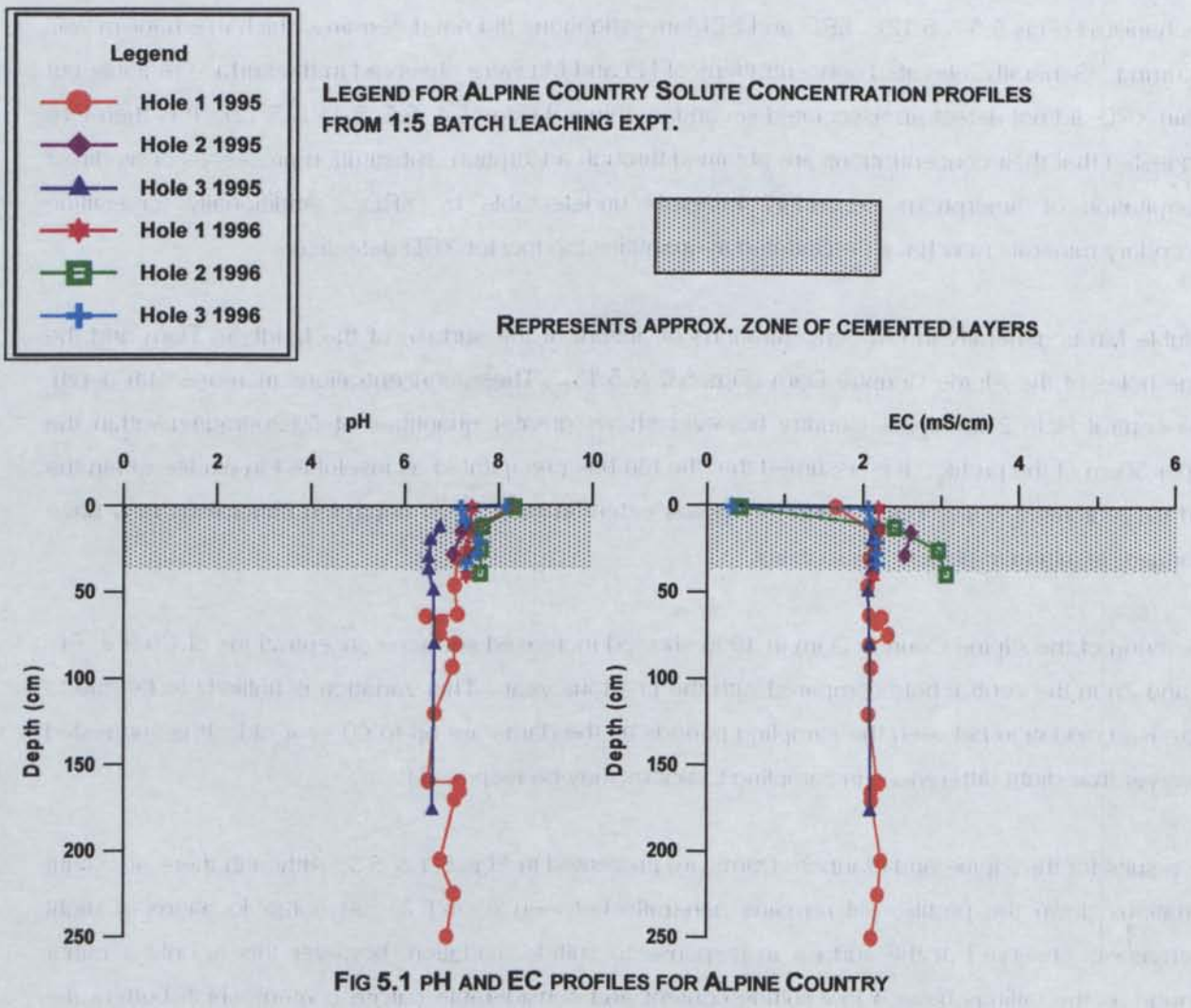

FIG 5.1 pH AND EC PROFILES FOR ALPINE COUNTRY

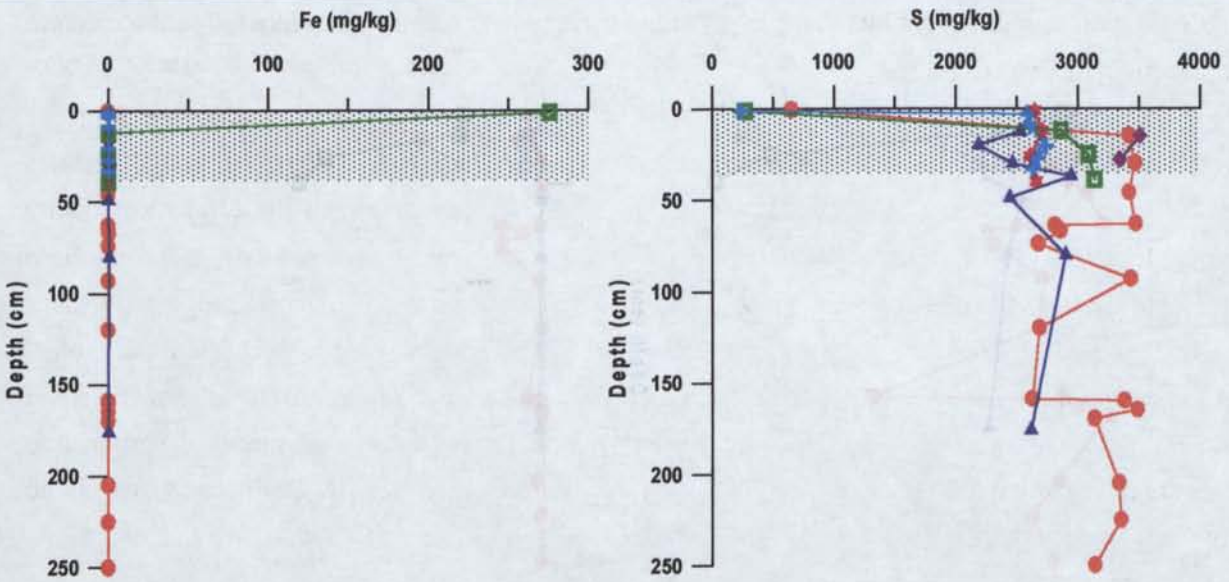

FIG 5.2 FE AND S PROFILES FOR ALPINE COUNTRY

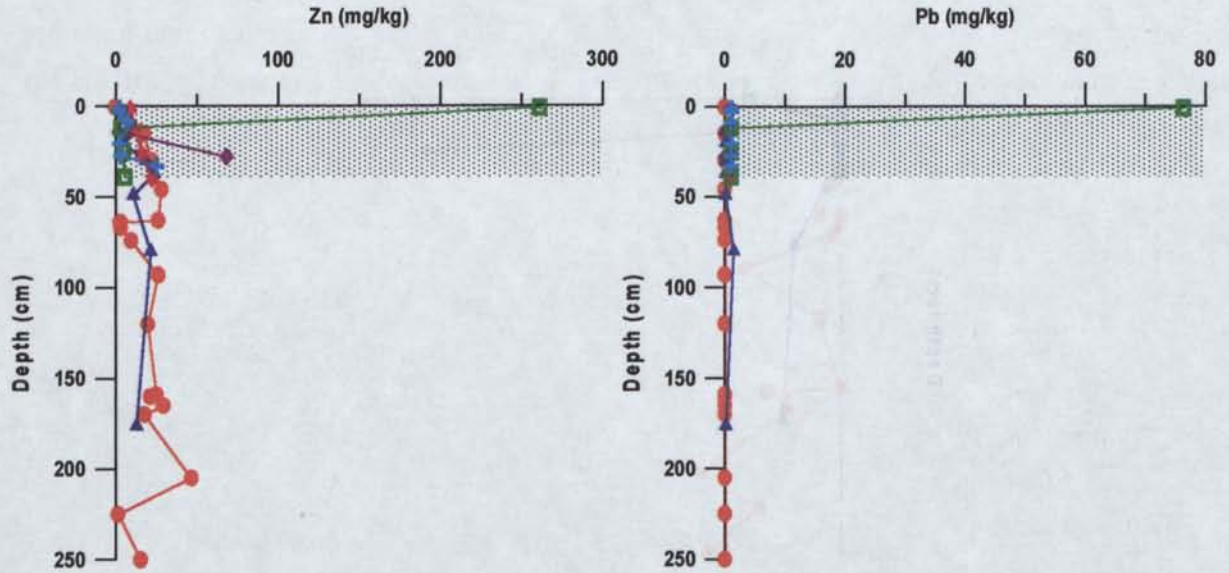

FIG 5.3 ZN AND PB PROFILES FOR ALPINE COUNTRY

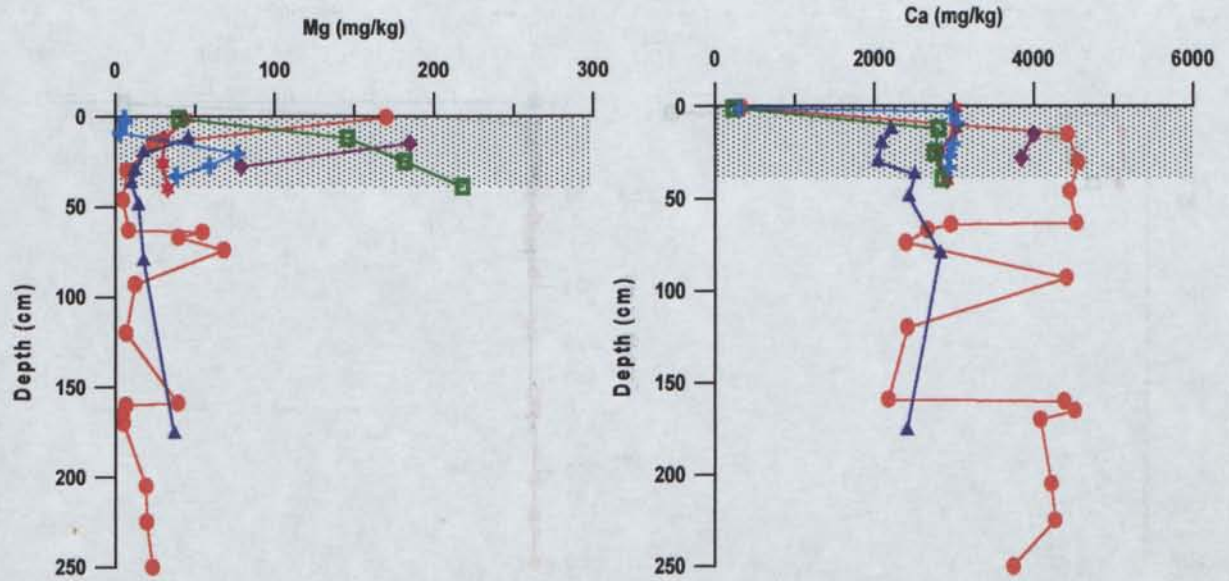

FIG 5.4 MG AND CA PROFILES FOR ALPINE COUNTRY

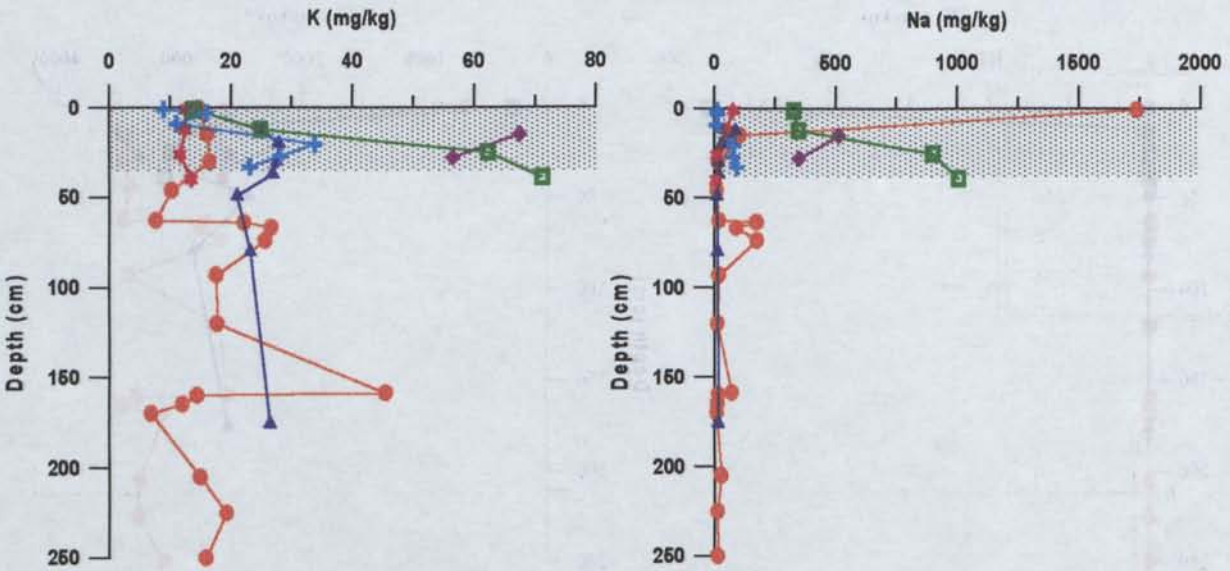

FIG 5.5 K AND NA PROFILES FOR ALPINE COUNTRY

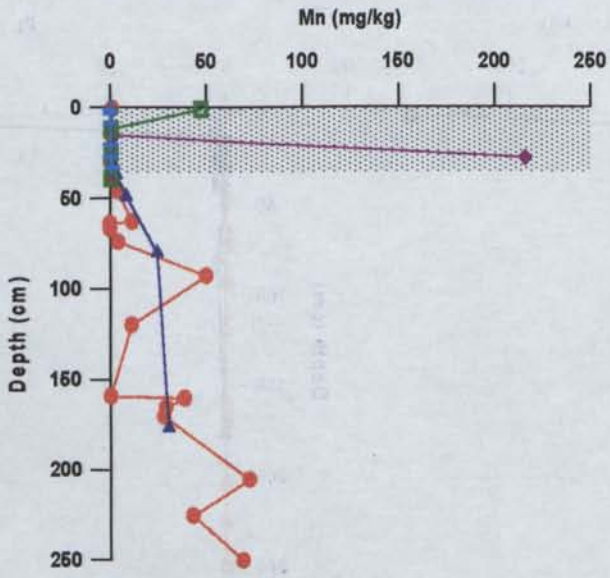

FIG 5.6 MN PROFILE FOR ALPINE COUNTRY

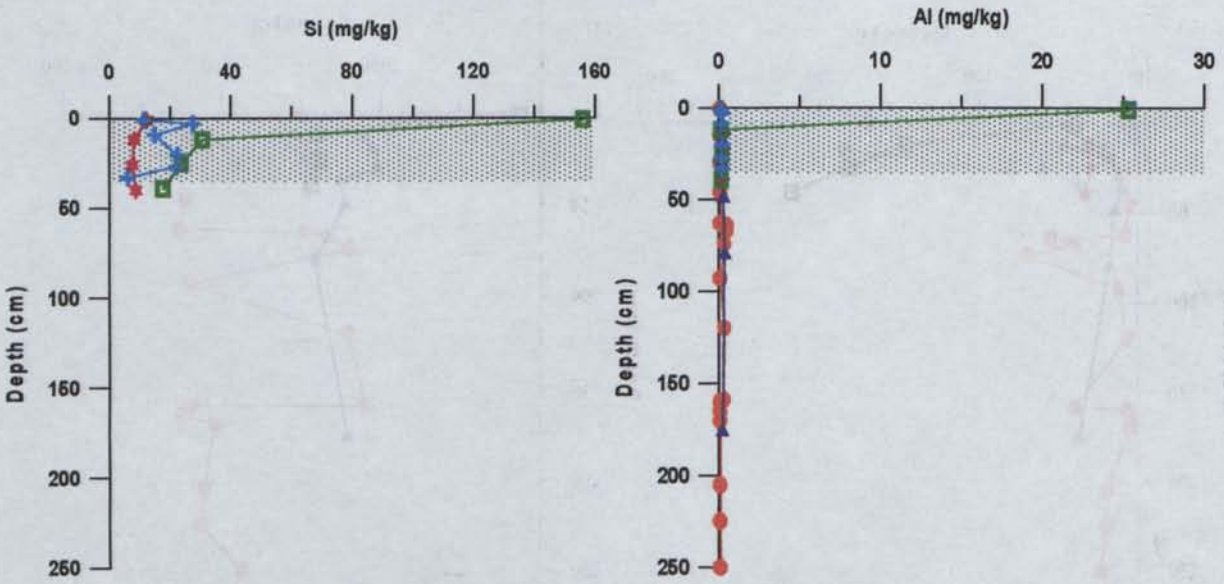

FIG 5.7 SI AND AL PROFILES FOR ALPINE COUNTRY

LEGEND FOR MARLBORO COUNTRY SOLUTE CONCENTRATION PROFILES FROM 1:5 BATCH LEACHING EXPT.

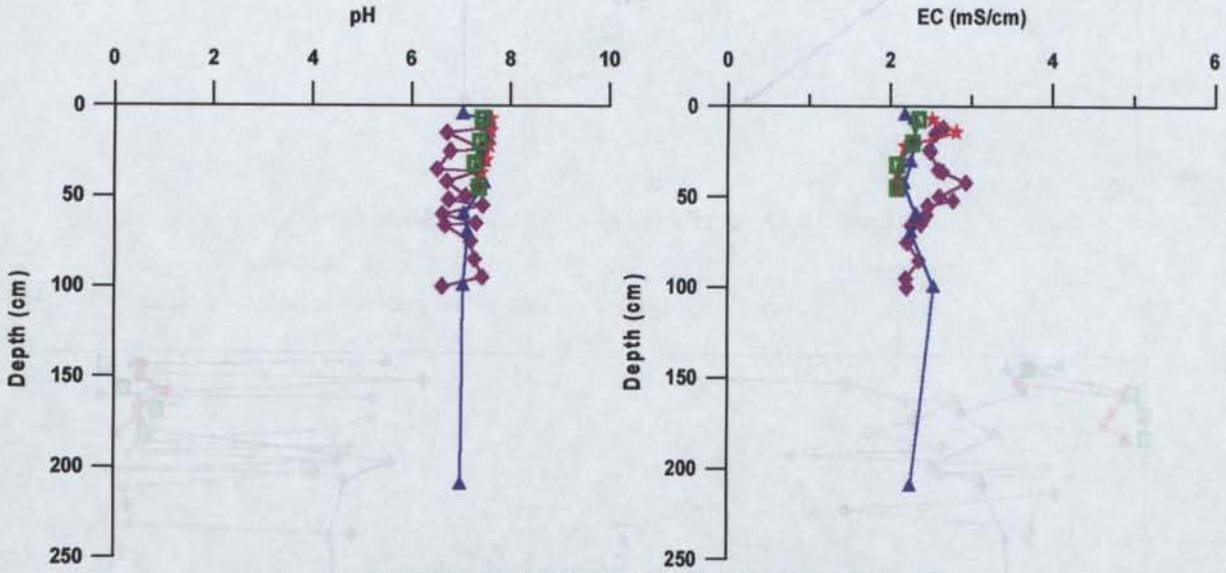

FIG 5.8 pH AND EC PROFILES FOR MARLBORO COUNTRY

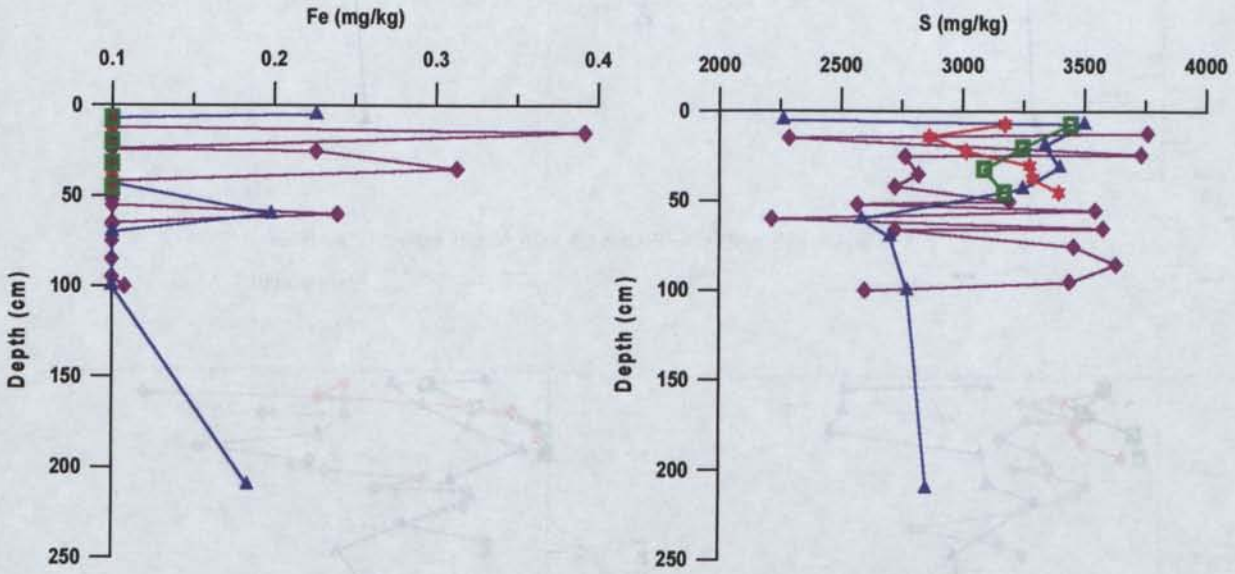

FIG 5.9 FE AND S PROFILES FOR MARLBORO COUNTRY

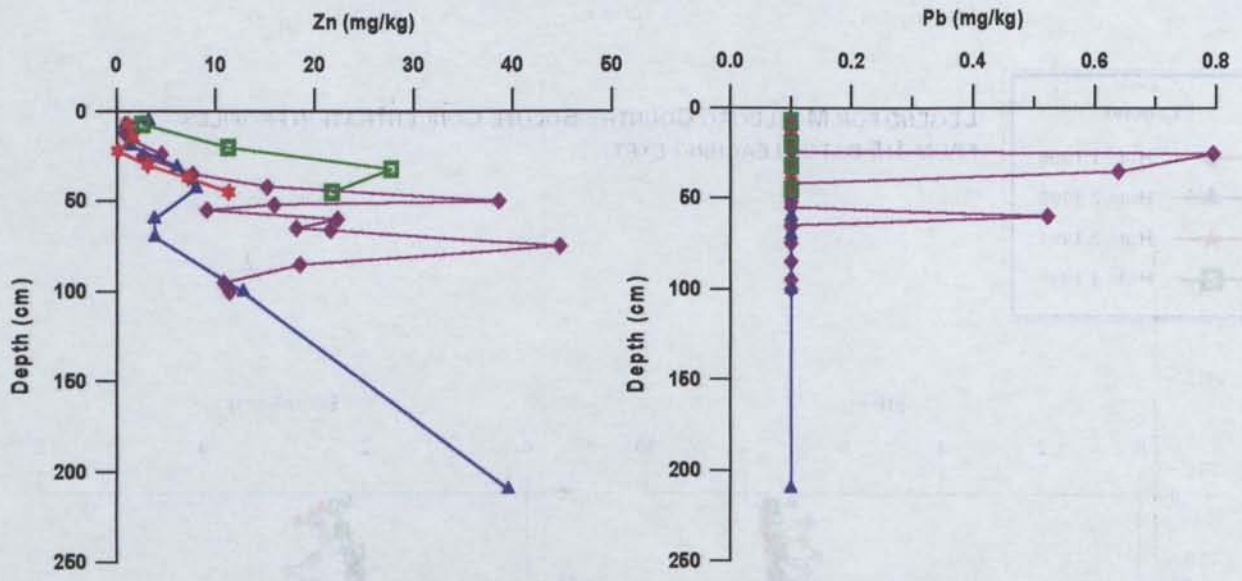

FIG 5.10 ZN AND PB PROFILES FOR MARLBORO COUNTRY

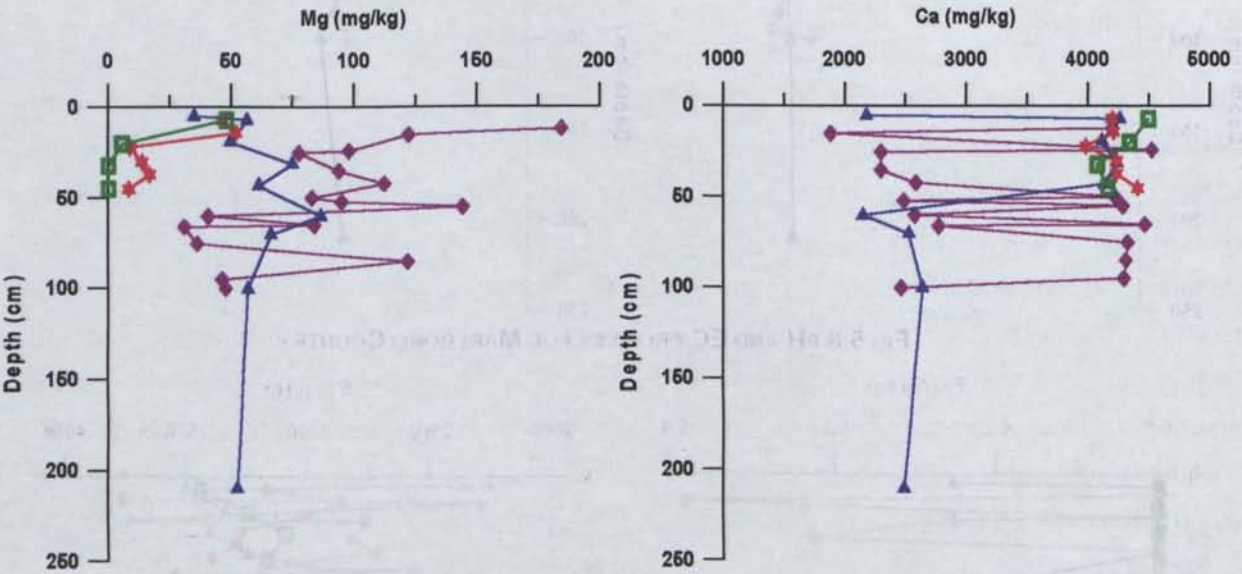

FIG 5.11 MG AND CA PROFILES FOR MARLBORO COUNTRY

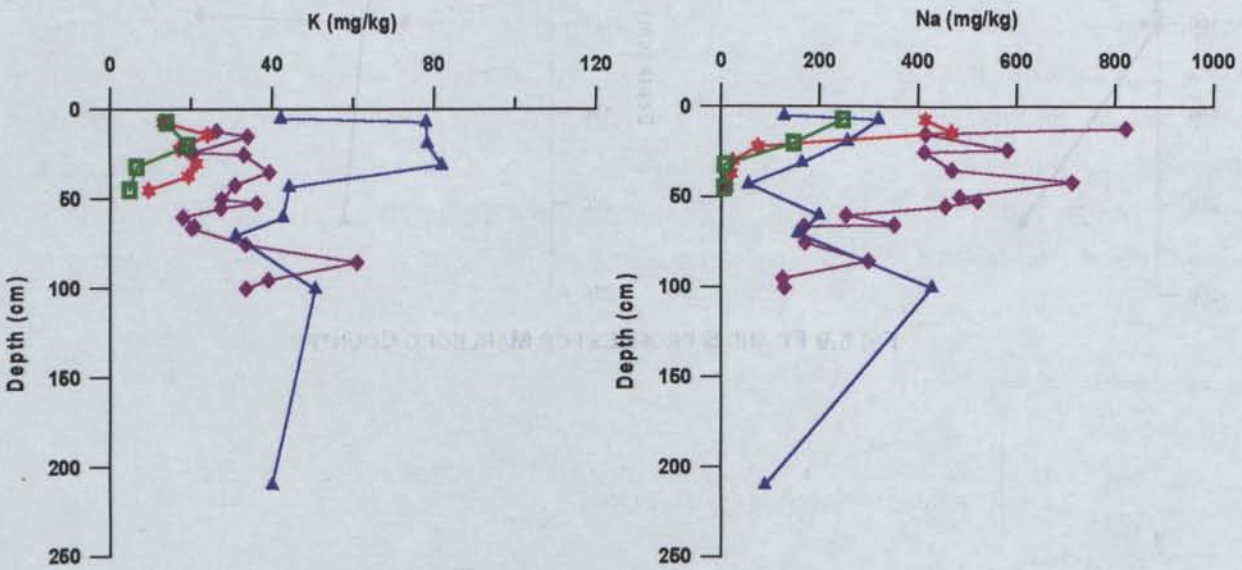

FIG 5.12 K AND NA PROFILES FOR MARLBORO COUNTRY

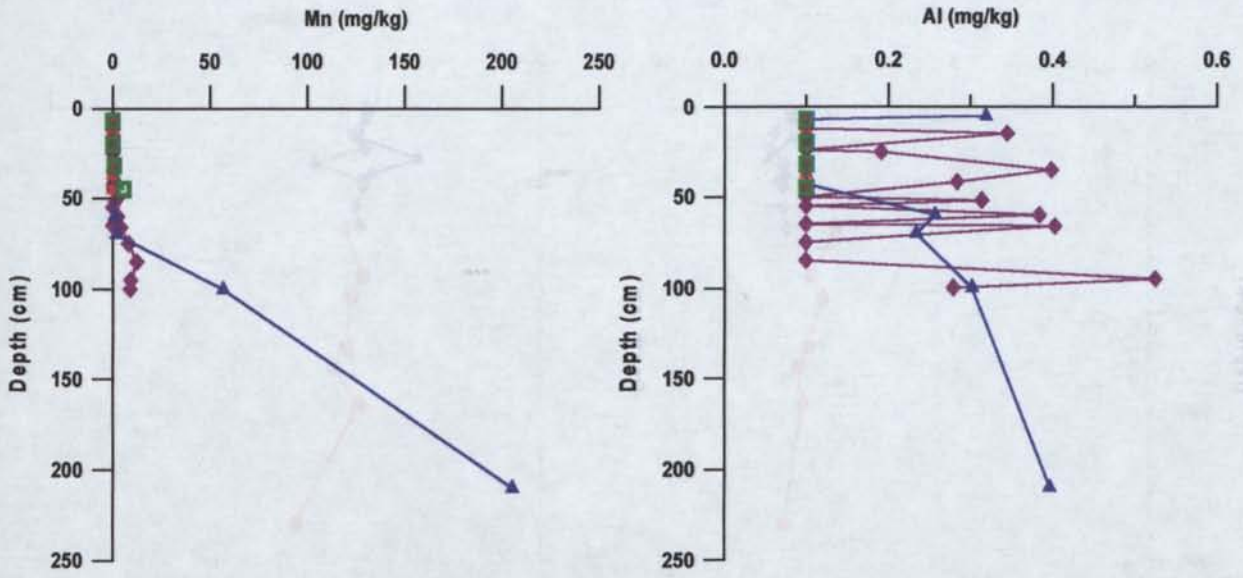

FIG 5.13 MN AND AL PROFILES FOR MARLBORO COUNTRY

5.4.1.1.2 Site A/B

As mentioned in Chapter 4 the surface zones of the Site A/B tailings is highly heterogeneous, with minimal gypsum and goethite cement. In 1995 cores were removed from Site 1 over a depth range of 80-275cm, incorporating tailings of varying grain size and oxidation state (palaeo-surfaces and unoxidised tailings). Then in 1996 additional sampling of the upper 50cm at Sites 2 and 3 were undertaken for comparison (see Chapter 4 for sampling locations). Both of these sites had slightly higher pH of between 7 and 8 compared with Site 1 which ranged from 6 to 7 (Fig 5.14). The EC values at all sites were similar ranging from 1-3 m*S*/cm showing a slight increase with depth, suggesting downward leaching has occurred, concentrating many soluble salts at depth within consolidated silt layers. Other minor increases in EC higher in the profile are associated with solute build-up in the oxidised surface region and palaeo-surfaces (Fig 5.14).

The Site A/B tailings solute concentrations consist mainly of Ca, K, Na, Mg, Mn, Zn and S (Table 5.3). Concentrations of these elements occur at the surface and at depth within palaeo-surface regions. Surface concentrations include elevated levels of Mg, Ca, K and S (Fig 5.15, 5.17 & 5.18), while Ca, Cd, Pb and Zn concentration occur at 100cm depth (Fig 5.16 & 2.17) and K, Na and Mg concentrate further down the profile at 175-250cm depth (Fig 5.17 & 5.18). As the only soluble secondary mineral identified through XRD has been gypsum, the solute concentrations must be attributed to mineral phases in levels too low for XRD detection, or co-precipitation with or absorption on gypsum and goethite.

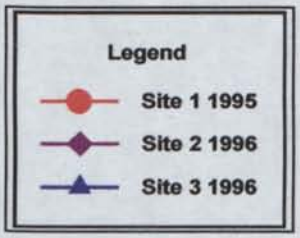

LEGEND FOR SITE A/B SOLUTE CONCENTRATION PROFILES FROM 1:5 BATCH LEACHING EXPT.

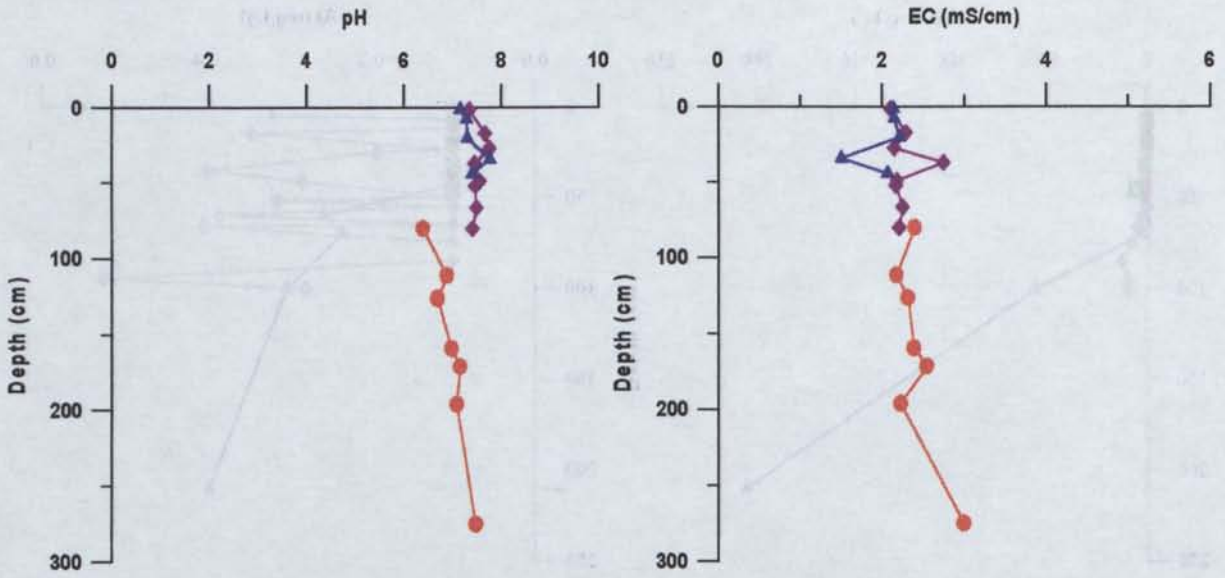

FIG 5.14 pH AND EC PROFILES FOR SITE A/B

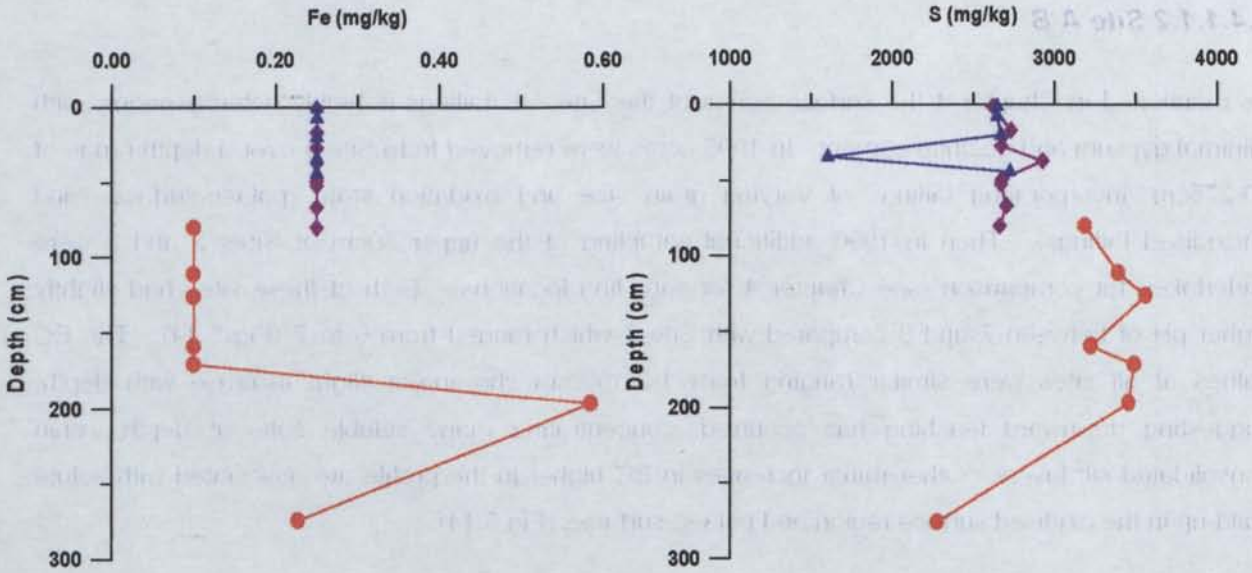

FIG 5.15 FE AND S PROFILES FOR SITE A/B

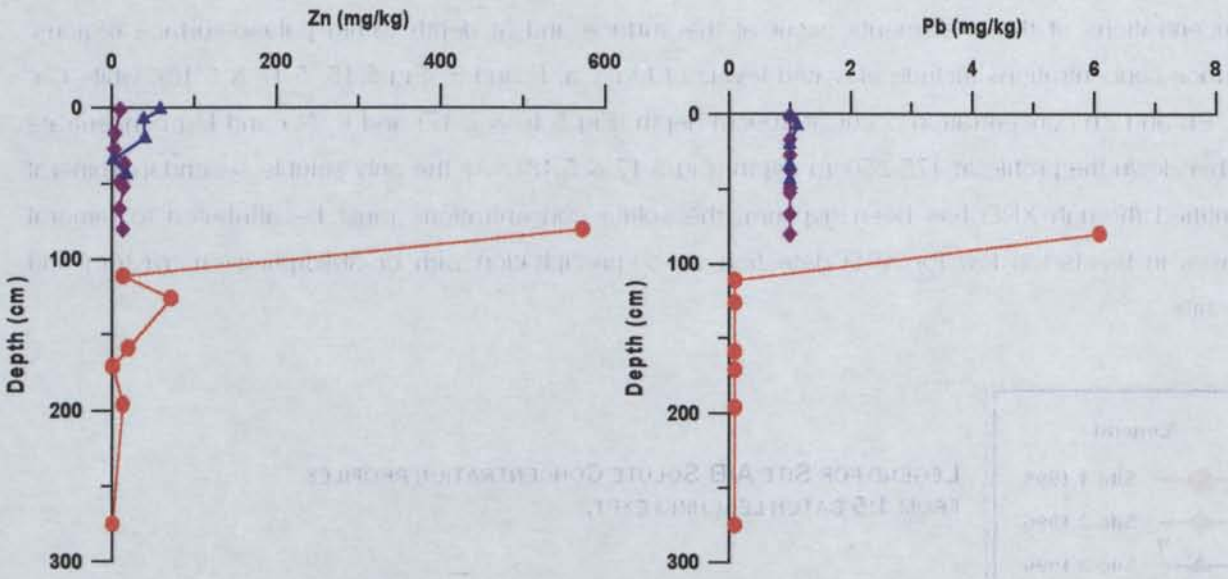

FIG 5.16 ZN AND PB PROFILES FOR SITE A/B

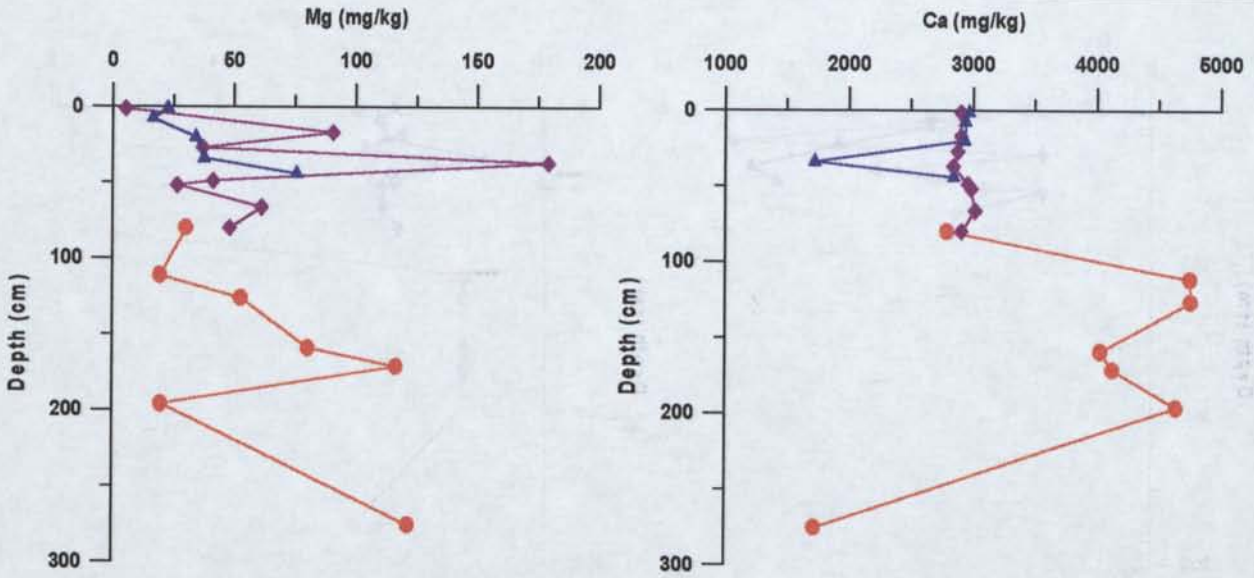

FIG 5.17 MG AND CA PROFILES FOR SITE A/B

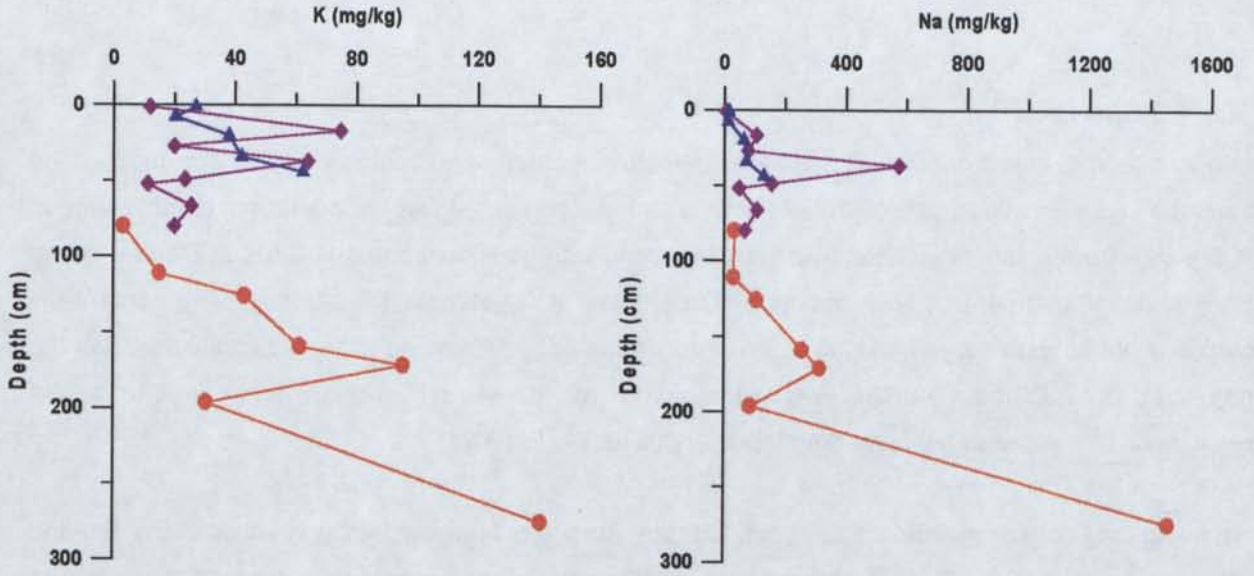

FIG 5.18 K AND NA PROFILES FOR SITE A/B

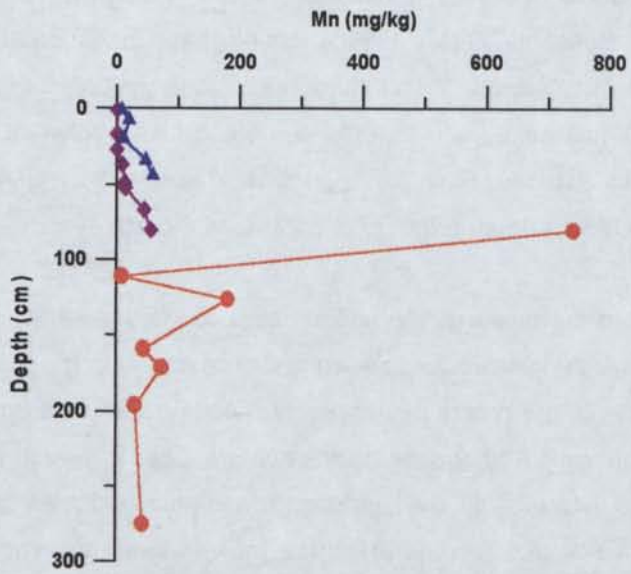

FIG 5.19 MN PROFILE FOR SITE A/B

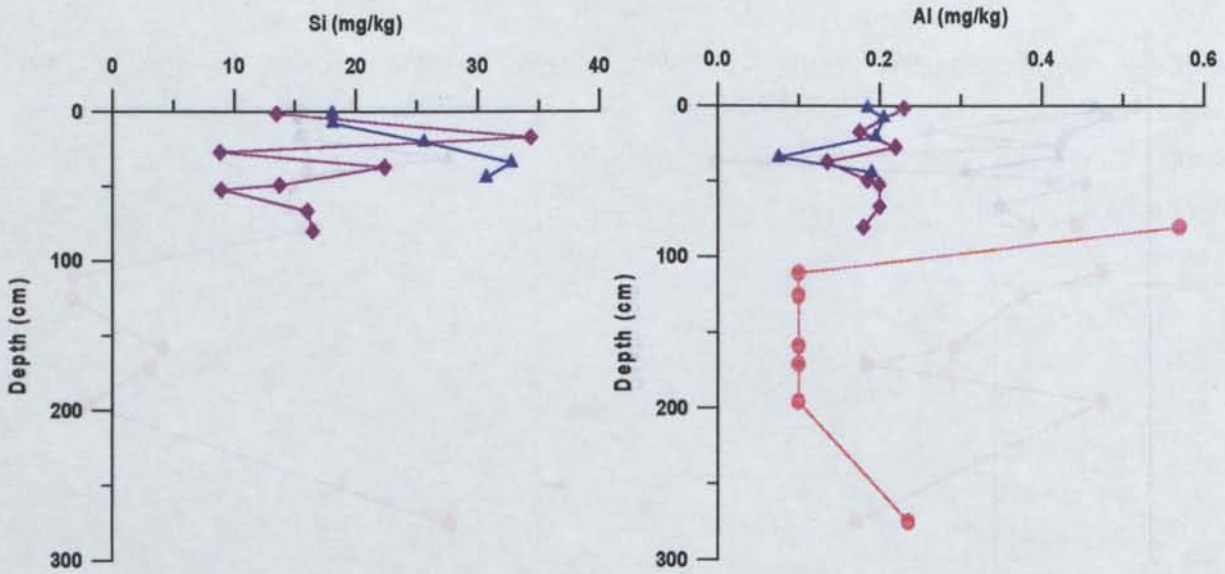

FIG 5.20 SI AND AL PROFILES FOR SITE A/B

5.4.1.1.3 Site C

A single site was cored in 1995 in a well-developed cemented layer region down to 2m depth. The cemented layers exist between 60-150cm, with a strongly cemented layer at 80-120cm depth. Then in 1996 a core from a similar location was sampled along with additional cores at Sites 2, 3 and 4 where less well developed cement was present. (See Chapter 4 for sampling locations). The general pH conditions of this dam range from 3.5 to 7.5, the surface at Site 1 having lower pH conditions than the other sites investigated. Another low pH region exists between 80-120cm depth in Site 1 and corresponds to the cemented layer developed at this depth (Fig 5.21).

The solute load consist mainly of Ca, K, Na, Mg, Mn, Zn and S however elevated levels of Zn, Mn and S are also present (Table 5.3). Additionally Al, Cd, Cu and Pb are generally greater than those at Site A/B. There are some general associations within each profile. Firstly, most elements appear to be concentrated at the surface. Secondly, at Site 1 there is a dramatic reduction of solutes directly above the first cemented layer at 80cm depth. The third main observation is that a large increase in concentration has developed just below or within the cemented layer, between 85-125cm depth (Site 1). For some of the solutes (Cd, Zn, Pb, Co, Fe, Mg, P, Mn and S) a second large increase in concentration occurs at 150-185cm depth (Figs 5.22, 5.23, 5.24 & 5.26).

The main variation throughout the profile is the buildup of secondary minerals (gypsum and goethite, minor hemimorphite, Mn oxide and siliceous material) and cementation. It appears that the cemented layers are playing a large role in the profile development, allowing the build up of soluble salts below them, probably through occlusion. Additionally the cements appear to be causing a depletion above the layers, possibly through lateral fluid flow induced via diminished vertical flow as a result of cementation. Additionally this depletion may reflect the incorporation of some of these elements as insoluble cements in this region.

The EC values of these profiles are also highly variable ranging from 1-3.5 mS/cm (Fig 5.21). The EC results for Site 1 show the effect of the cemented layer at 80-120cm depth, and simply reinforces the assumption that as a direct result of the cemented layer an increase of soluble salts has occurred below the hardpan, and a deficiency has developed above it.

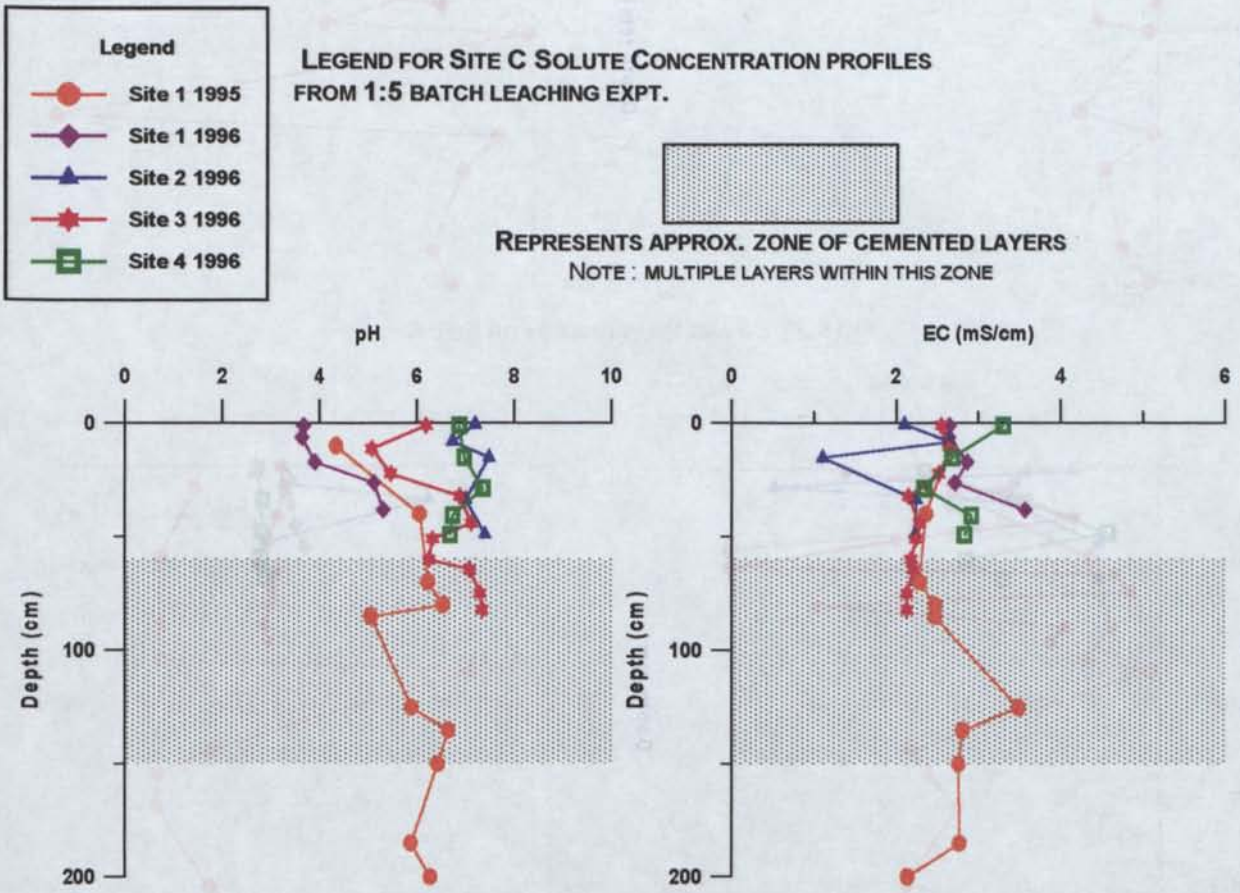

FIG 5.21 pH AND EC PROFILES FOR SITE C

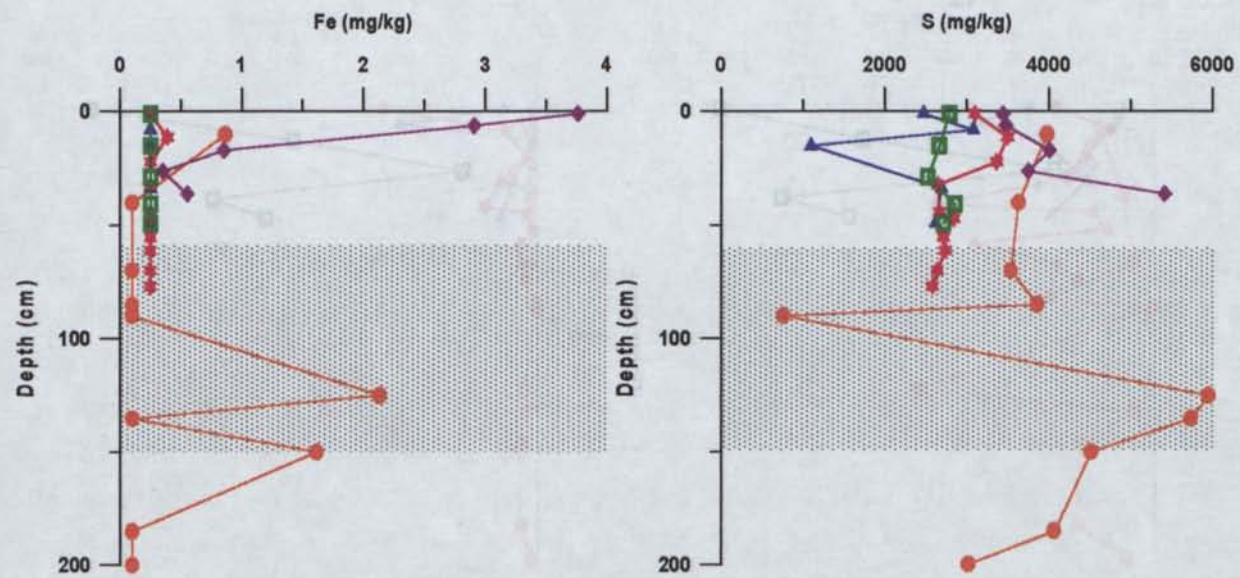

FIG 5.22 FE AND S PROFILES FOR SITE C

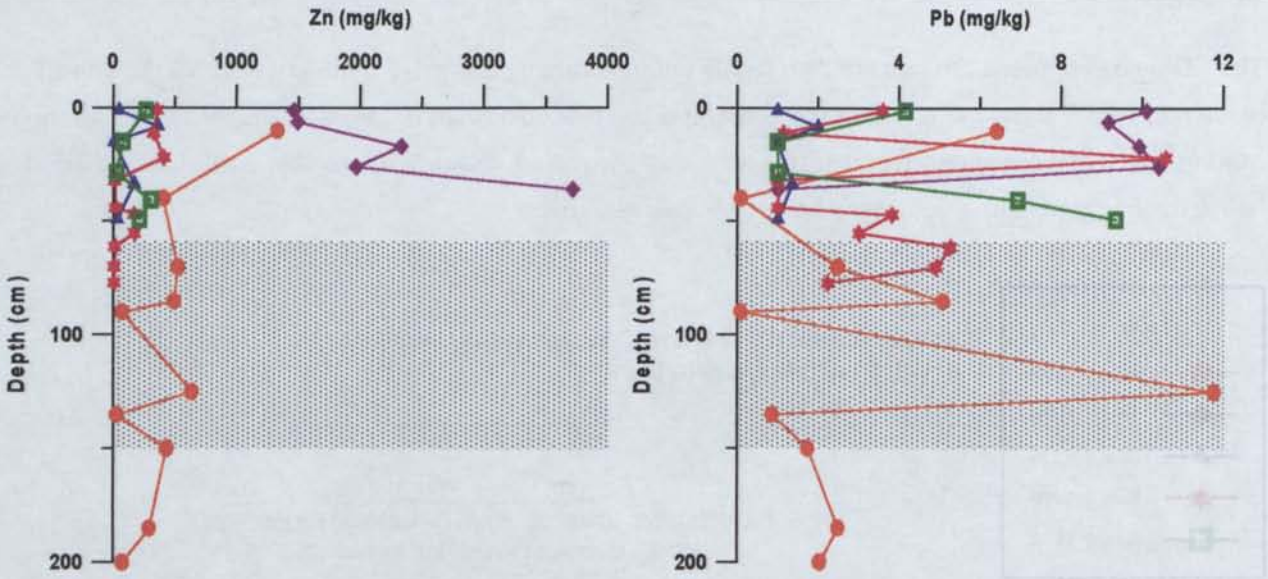

FIG 5.23 ZN AND PB PROFILES FOR SITE C

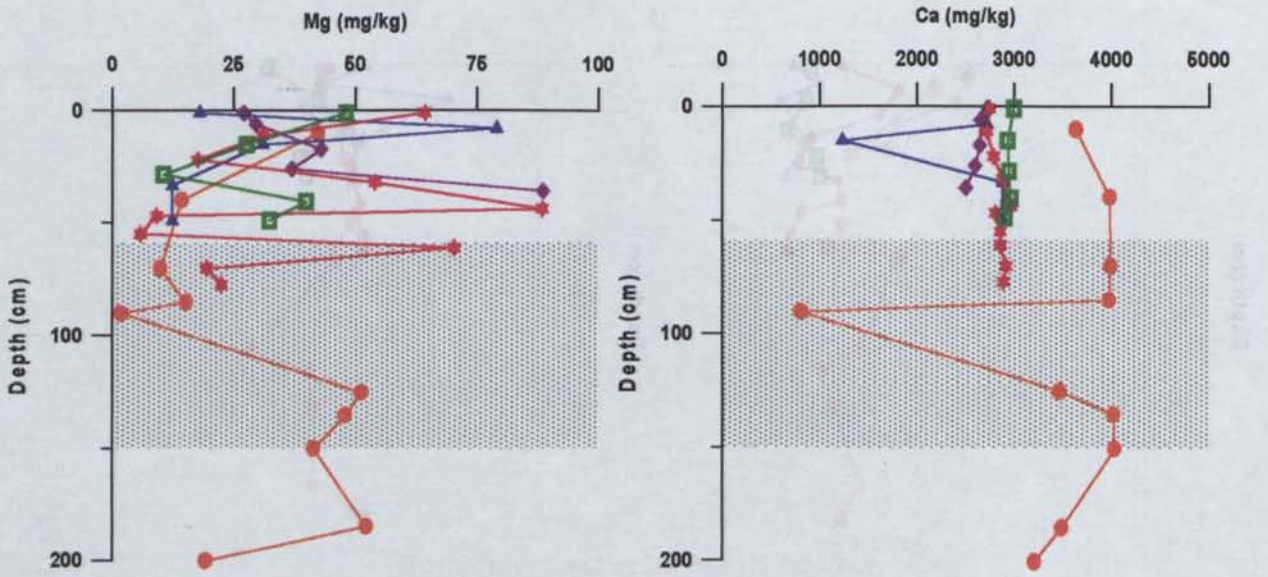

FIG 5.24 MG AND CA PROFILES FOR SITE C

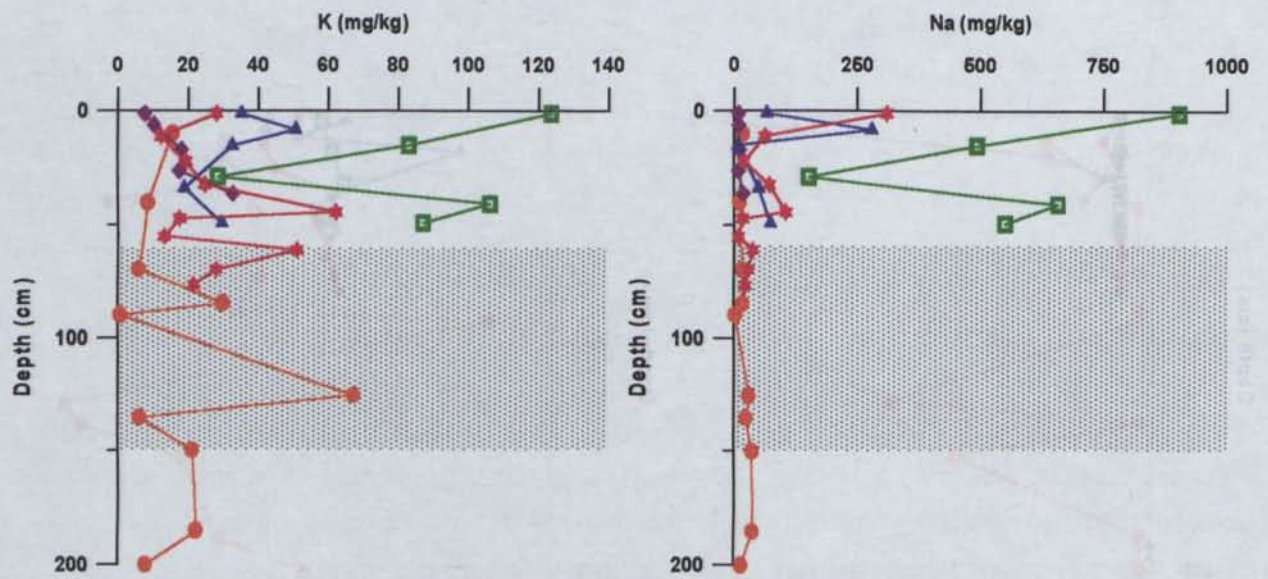

FIG 5.25 K AND NA PROFILES FOR SITE C

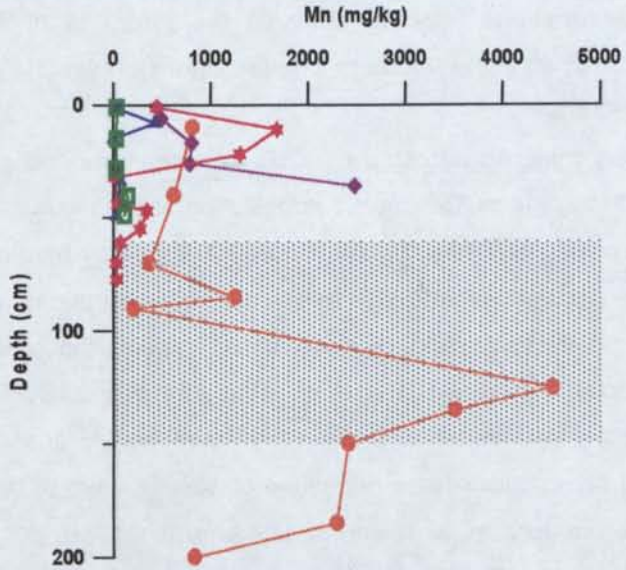

FIG 5.26 MN PROFILE FOR SITE C

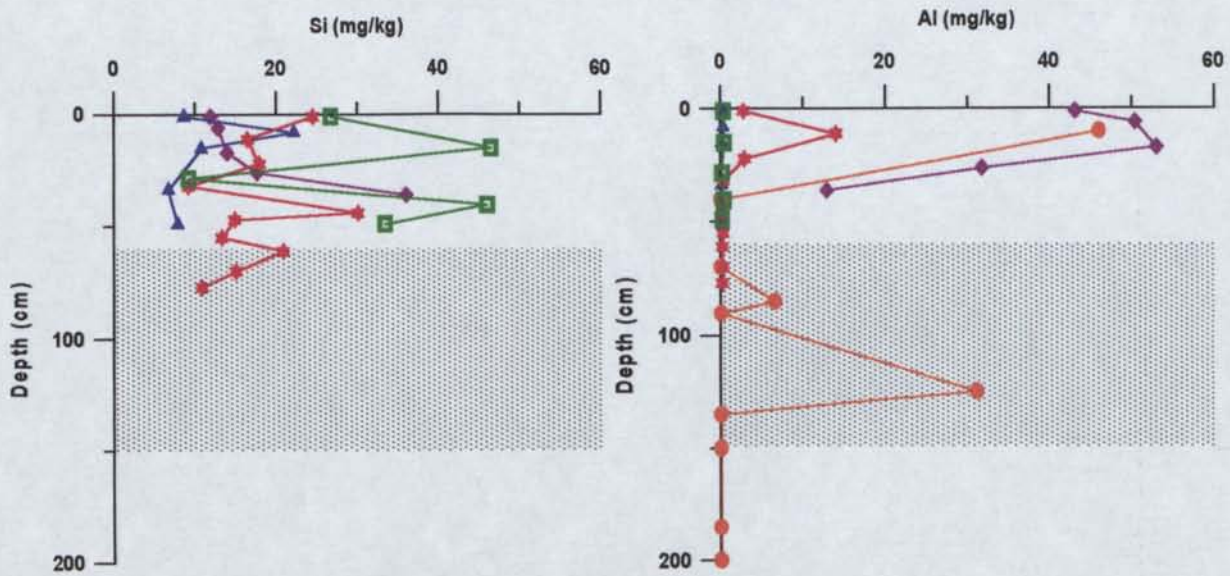

FIG 5.27 SI AND AL PROFILES FOR SITE C

5.4.1.1.4 Discussion

Three different geochemical systems appear to be developing with regards to soluble salt precipitation and the effect they are having on cementation. Firstly in the Alpine and Marlboro Country Dams, the main solutes produce gypsum cements which have precipitated at various levels down the profile. At these locations it is suggested that the other main cementing agents are insoluble and have not been detected in this analysis, except as noticeable deficiencies in the surface regions i.e. Zn and Mn.

A different situation has developed at Site A/B as only minimal cements have formed, XRD did not detect any potential cementing agents apart from gypsum and minor goethite. The soluble elements observed at this site appear to have become incorporated into the oxidised region of the profiles through adsorption and substitution processes with the secondary mineral present or through precipitation of discrete amorphous mineralogical phases undetectable by XRD. At this site however it

is suggested that textural variations may be affecting the locations of these concentrations, a relationship unable to be examined in the Marlboro Country Dam samples.

At Site C the only secondary minerals detected by XRD were goethite and gypsum. SEM and EDX investigations suggested that some adsorption or substitution mechanisms have occurred with fine grained cements observed consisting of Fe, Si, Zn, Mn and Al (possibly hemimorphite, Mn oxides and siliceous material). It is assumed that other elemental concentrations have occurred through adsorption or substitution on these secondary minerals or through the precipitation of amorphous secondary minerals undetected through XRD or in quantities too low for XRD detection. The effect that cemented layers have on the elemental profiles has been readily observed within this dam. It appears that the cemented layers allow large quantities of soluble salts to persist below them, while above, salts are depleted possibly as a result of lateral drainage or incorporation as insoluble secondary minerals within the cemented layers.

	Al	B	Ca	Cd	Fe	K	Mg	Mn	Na	Ni	Pb	S	Zn	Si
	mg/kg	mg/kg	mg/kg	mg/kg	mg/kg	mg/kg	mg/kg	mg/kg	mg/kg	mg/kg	mg/kg	mg/kg	mg/kg	mg/kg
BH Alpine Country Hole 1 (1995)														
<0.5	<0.1	3.91	338	<0.1	<0.1	14.8	170	1.32	1739	<0.1	<0.1	654	<0.1	
15	<0.1	0.69	4432	<0.1	0.770	16.1	23.9	<0.1	105.5	<0.52	<0.1	3423	17.5	
30	<0.1	0.67	4567	0.73	1.090	16.5	7.49	<0.1	15.3	<0.1	<0.1	3473	22.3	
46	<0.1	0.62	4457	1.06	<0.1	10.3	5.02	3.92	10.3	<0.1	<0.1	3422	28.5	
63	<0.1	0.63	4539	<0.1	<0.1	7.7	8.55	11.4	19.4	<0.1	<0.1	3475	26.6	
64	0.50	0.58	2967	0.18	0.163	22.2	54.9	<0.1	174	<0.1	<0.1	2815	2.98	
67	0.48	0.62	2677	0.09	0.392	26.7	40.0	0.11	91.6	<0.1	<0.1	2861	3.19	
74	0.37	0.83	2404	0.35	0.264	25.6	68.5	4.17	176	<0.1	<0.1	2677	9.7	
93	<0.1	0.59	4416	<0.1	<0.1	17.6	12.68	50.0	20.0	<0.1	<0.1	3434	26.3	
120	0.37	0.67	2420	0.10	0.275	17.8	7.03	11.24	13.8	<0.1	<0.1	2685	20.0	
159	0.31	0.66	2184	0.47	0.293	45.5	39.5	0.24	72.2	<0.1	<0.1	2631	25.3	
160	<0.1	0.56	4391	<0.1	<0.1	14.5	7.04	38.8	16.0	<0.1	<0.1	3383	21.7	
165	<0.1	0.56	4523	<0.1	<0.1	12.0	4.97	29.1	12.7	<0.1	<0.1	3491	29.4	
170	<0.1	0.63	4095	<0.1	<0.1	6.9	5.19	28.1	10.8	<0.1	<0.1	3138	17.9	
205	<0.1	1.00	4228	0.54	<0.1	15.0	19.4	72.6	28.2	<0.1	<0.1	3343	46.8	
225	<0.1	0.84	4277	<0.1	<0.1	19.3	19.9	43.3	13.8	<0.58	<0.1	3357	1.71	
250	<0.1	0.95	3754	0.70	<0.1	16.0	23.6	69.0	14.8	<0.1	<0.1	3145	15.7	
BH Alpine Country Hole 2 (1995)														
15	<0.1	0.75	4006	<0.1	<0.1	67.5	185	1.56	515	0.50	0.10	3511	7.27	
28	<0.1	0.80	3845	1.73	<0.1	56.5	79	216	349	<0.1	<0.025	3345	68.4	
BH Alpine Country Hole 3 (1995)														
12.5	0.37	0.70	2214	<0.1	0.313	25.2	45.8	<0.1	87.7	<0.1	<0.1	2534	1.47	
20	0.34	0.59	2089	0.28	0.291	27.9	17.7	0.20	31.8	<0.1	<0.1	2187	4.84	
30	0.21	0.64	2049	0.74	0.334	27.6	12.1	1.06	15.6	<0.1	<0.1	2466	18.4	
37	0.28	0.66	2510	0.76	0.321	26.9	10.1	3.07	17.3	<0.1	<0.1	2947	23.9	
49	0.28	0.49	2437	0.20	<0.166	21.0	14.5	8.28	10.4	<0.1	<0.1	2443	10.9	
80	0.38	0.60	2832	0.17	0.661	23.2	17.8	24.3	13.2	<0.1	1.50	2902	21.6	
176	0.22	0.60	2416	0.12	0.205	26.4	37.2	30.3	14.7	<0.1	<0.1	2616	13.0	
BH Alpine Country Hole 1 (1996)														
1	0.12	<0.025	3021	0.28	<0.25	12.7	43.7	0.09	77.9	<0.25	1.0	2652	9.10	12.4
12	0.13	<0.025	3023	0.67	<0.25	12.5	30.8	0.16	50.2	<0.25	1.0	2713	12.02	8.16
26	0.15	<0.025	2807	0.75	<0.25	11.7	29.9	0.36	10.3	<0.25	1.0	2611	16.32	7.67
40	0.17	<0.025	2914	0.80	<0.25	13.5	33.0	0.36	7.55	<0.25	1.0	2661	22.37	8.79
BH Alpine Country Hole 2 (1996)														
1	25.3	0.00	229	0.00	276	13.9	39.8	47.3	327	<0.25	76.4	270	261	156
12	0.14	1.48	2807	0.06	<0.25	24.9	146	0.24	347	<0.25	1.0	2864	3.24	30.6
25	0.21	0.64	2755	0.08	<0.25	62.3	182	0.28	899	<0.25	1.0	3084	4.52	23.7
39	0.16	0.38	2850	0.11	<0.25	71.2	218	0.32	1004	<0.25	1.0	3137	5.48	17.6
BH Alpine Country Hole 3 (1996)														
1	0.12	<0.025	307	<0.05	<0.25	9.0	5.78	0.11	10.7	<0.25	1.0	240	2.16	11.5
3	0.20	<0.025	2967	<0.05	<0.25	16.0	6.07	0.14	13.1	<0.25	1.0	2592	2.35	27.6
9	0.16	<0.025	3044	0.29	<0.25	11.0	2.84	0.12	7.39	<0.25	1.0	2609	7.66	14.9
20.5	0.18	<0.025	2985	0.06	<0.25	33.8	76.7	0.19	79	<0.25	1.0	2737	2.60	22.4
27	0.18	0.06	2931	0.14	<0.25	28.1	58.9	0.12	75	0.28	1.0	2671	3.28	22.1
33	0.21	<0.025	2935	1.02	<0.25	23.2	38.3	0.90	92	<0.25	1.0	2635	25.04	6.08

TABLE 5.3A BROKEN HILL ALPINE COUNTRY SOLUTE CONCENTRATIONS (1:5 BATCH LEACHING)

Depth	Al	B	Ca	Cd	Fe	K	Mg	Mn	Na	Ni	P	Pb	S	Zn
(cm)	mg/kg	mg/kg	mg/kg	mg/kg	mg/kg	mg/kg	mg/kg	mg/kg	mg/kg	mg/kg	mg/kg	mg/kg	mg/kg	mg/kg
BH Marlboro Country Hole 1 (1995)														
12	<0.1	1.04	4203	<0.1	<0.1	26.4	185	<0.1	823	<0.1	<0.1	<0.1	3761	0.79
15	0.35	0.78	1885	<0.1	0.392	34.1	122	0.37	416	<0.1	<0.1	<0.1	2289	1.28
24	<0.1	0.77	4527	<0.1	<0.1	20.4	98.1	<0.1	582	<0.1	<0.1	<0.1	3735	4.53
25	0.19	0.66	2302	0.23	0.226	33.2	77.8	<0.1	413	0.24	<0.1	0.80	2764	2.63
35	0.40	0.64	2301	0.32	0.313	39.4	94.2	0.26	469	0.20	<0.1	0.64	2818	7.67
42	0.28	0.43	2590	0.91	<0.1	30.9	113	0.25	712	<0.1	<0.1	<0.1	2723	15.2
50	<0.1	0.50	4225	1.77	<0.1	27.5	83.0	2.18	484	0.52	<0.1	<0.1	3191	38.6
52	0.31	0.53	2486	0.90	<0.1	36.1	95.1	1.37	521	<0.1	<0.1	<0.1	2568	15.9
55	<0.1	1.01	4288	<0.1	<0.1	27.4	144	<0.1	456	<0.1	<0.1	<0.1	3547	9.11
60	0.38	0.31	2576	0.96	0.239	18.0	40.7	2.52	253	<0.1	<0.1	0.52	2215	22.3
65	<0.1	0.73	4473	0.73	<0.1	20.8	84.0	<0.1	352	<0.1	<0.1	<0.1	3578	18.2
66	0.40	0.46	2776	0.79	<0.1	20.2	31.0	4.25	168	<0.1	<0.1	<0.1	2722	21.6
75	<0.1	0.66	4329	1.31	<0.1	33.6	36.3	8.22	170	<0.1	11.26	<0.1	3457	44.8
85	<0.1	0.65	4316	<0.1	<0.1	61.1	122	12.5	300	<0.1	<0.1	<0.1	3633	18.5
95	0.53	0.63	4298	<0.1	<0.1	39.2	46.5	9.29	124	<0.1	<0.1	<0.1	3442	10.8
100	0.28	0.50	2467	0.19	0.108	33.6	47.9	8.98	129	<0.1	<0.1	<0.1	2600	11.4
BH Marlboro Country Hole 2 (1995)														
5	0.32	0.68	2180	<0.1	0.226	42.2	35.0	0.19	128	<0.1	<0.1	<0.1	2263	3.22
7	<0.1	0.90	4265	<0.1	<0.1	78.2	56.6	<0.1	320	0.53	<0.1	<0.1	3501	0.84
19	<0.1	0.68	4121	<0.1	<0.1	78.4	49.7	<0.1	257	<0.1	<0.1	<0.1	3338	1.41
31	<0.1	0.63	4243	<0.1	<0.1	81.9	75.1	<0.1	164	<0.1	<0.1	<0.1	3400	6.08
43	<0.1	0.58	4137	<0.1	<0.1	44.2	61.3	<0.1	54.2	<0.1	<0.1	<0.1	3246	8.00
60	0.26	0.65	2149	<0.1	0.198	42.7	86.7	1.00	199	<0.1	<0.1	<0.1	2583	3.79
70	0.23	0.53	2530	<0.1	<0.1	31.1	66.4	1.97	155	<0.1	<0.1	<0.1	2701	3.84
100	0.30	0.56	2640	0.13	<0.1	50.8	57.0	56.7	428	<0.1	<0.1	<0.1	2773	12.8
210	0.40	0.65	2490	0.40	0.184	40.1	52.7	206	89.30	0.14	<0.1	<0.1	2852	39.6
BH Marlboro Country Hole 3 (1995)														
7	<0.1	0.78	4203	<0.1	<0.1	13.2	46.6	<0.1	416	<0.1	<0.1	<0.1	3175	1.10
14	<0.1	0.68	4212	<0.1	<0.1	24.2	52.0	<0.1	469	<0.1	<0.1	<0.1	2863	1.61
22	<0.1	<0.55	3986	<0.1	<0.1	17.2	8.83	<0.1	74.9	<0.1	<0.1	<0.1	3016	<0.1
30	<0.1	0.59	4237	<0.1	<0.1	21.3	13.8	<0.1	23.6	<0.1	<0.1	<0.1	3277	3.11
37	<0.1	0.64	4237	<0.1	<0.1	19.3	16.9	<0.1	20.3	<0.1	<0.1	<0.1	3289	7.19
45	<0.1	0.56	4411	<0.1	<0.1	9.49	8.41	<0.1	11.7	<0.52	<0.1	<0.1	3396	11.3
BH Marlboro Country Hole 4 (1995)														
7	<0.1	0.69	4499	<0.1	<0.1	14.0	48.2	<0.1	247	<0.1	<0.1	<0.1	3444	2.60
20	<0.1	0.57	4345	<0.1	<0.1	19.2	5.51	<0.1	148	<0.1	<0.1	<0.1	3247	11.23
32	<0.1	<0.1	4077	0.61	<0.1	6.52	<0.1	0.69	6.56	<0.1	<0.1	<0.1	3088	27.73
45	<0.1	<0.1	4165	0.54	<0.1	4.72	<0.1	5.48	5.17	<0.1	<0.1	<0.1	3170	21.73
BH Nth Mine No. 3 slimes dam (1996)														
1	0.15	0.18	3139	0.06	<0.25	142	479	0.22	3571	<0.25	0.59	1.00	3402	4.12
12	0.19	<0.025	2769	0.10	<0.25	26.5	42.9	0.16	265	<0.25	<0.5	1.00	2402	7.39
23	0.16	0.06	2939	0.11	<0.25	36.9	114	0.39	682	<0.25	<0.5	1.00	2634	6.47
33	0.22	0.08	2920	0.09	<0.25	42.1	126	0.31	646	<0.25	<0.5	1.00	2643	5.45
49	0.26	<0.025	1113	0.08	<0.25	13.6	18.11	9.36	82.23	<0.25	<0.25	1.00	972	11.8

TABLE 5.3B BROKEN HILL - MARLBORO COUNTRY SOLUTE CONCENTRATIONS (1:5 BATCH LEACHING)

	Al	B	Ca	Cd	Fe	K	Mg	Mn	Na	Ni	P	Pb	S	Zn	Si
	mg/kg	mg/kg	mg/kg	mg/kg	mg/kg	mg/kg	mg/kg	mg/kg	mg/kg	mg/kg	mg/kg	mg/kg	mg/kg	mg/kg	mg/kg
BH Site A/B Site 1 (1995)															
80	0.57	0.55	2790	6.95	<0.1	3.26	30.3	741	34.3	<0.1	<0.1	6.10	3189	573	
111	<0.1	0.88	4753	0.73	<0.1	15.2	19.7	8.47	32.1	<0.1	2.32	<0.1	3396	13.8	
126	<0.1	0.94	4756	1.04	<0.1	43.3	53.0	181	108	<0.1	2.15	<0.1	3562	72.2	
159	<0.1	1.14	4029	<0.1	<0.1	61.4	80.6	44.4	257	<0.1	1.98	<0.1	3224	20.3	
171	<0.1	1.11	4130	<0.1	<0.1	95.4	117	73.7	316	<0.1	2.27	<0.1	3492	1.29	
196	<0.1	0.85	4644	<0.1	0.585	30.5	20.0	30.8	86.4	<0.1	2.19	<0.1	3458	13.3	
275	0.24	0.95	1724	<0.1	0.227	141	122	43.1	1460	<0.1	<0.1	<0.1	2280	0.62	
BH Site A/B Site 2 (1996)															
1	0.23	0.06	2902	0.73	<0.25	12.1	5.27	0.25	5.67	<0.25	<0.5	1.00	2621	<0.15	13.5
17	0.18	0.34	2900	0.06	<0.25	74.7	90.7	0.20	106	<0.25	<0.5	1.00	2731	3.61	34.4
27	0.22	<0.025	2876	<0.05	<0.25	20.1	37.1	0.25	79.6	<0.25	<0.5	1.00	2671	2.97	8.84
37	0.14	0.08	2841	<0.135	<0.25	64.0	179	8.97	574	<0.25	<0.5	1.00	2926	15.2	22.4
49	0.19	<0.025	2960	<0.05	<0.25	23.5	41.4	12.89	156	<0.25	<0.5	1.00	2676	9.58	13.8
52	0.20	<0.025	2985	<0.11	<0.25	11.3	26.5	14.38	49.0	0.30	<0.5	1.00	2672	13.9	8.97
66.5	0.20	<0.025	3017	<0.15	<0.25	25.5	61.3	45.1	108	<0.25	0.56	1.00	2705	9.43	16.0
80	0.18	<0.025	2904	<0.05	<0.25	20.0	48.2	55.9	68.2	<0.25	<0.5	1.00	2662	13.2	16.5
BH Site A/B Site 3 (1996)															
1	0.19	0.12	2967	2.76	<0.25	27.0	22.6	8.48	15.3	0.26	<0.5	1.00	2647	59.1	18.1
7.5	0.21	0.06	2937	0.40	<0.25	20.3	16.6	19.8	11.6	<0.25	<0.5	1.12	2647	38.8	18.1
20	0.20	0.12	2930	0.97	<0.25	37.9	34.1	10.8	63.3	0.26	<0.5	1.00	2669	40.0	25.6
34	0.08	0.16	1720	<0.05	<0.25	42.1	37.5	46.8	71.6	0.34	<0.5	1.00	1602	1.80	32.8
44	0.19	0.20	2841	<0.05	<0.25	62.3	75.7	59.2	129	<0.25	<0.5	1.00	2726	17.7	30.7

TABLE 5.3C BROKEN HILL - SITE A/B SOLUTE CONCENTRATIONS (1:5 BATCH LEACHING)

	Al	Ca	Cd	Co	Cu	Fe	K	Mg	Mn	Na	Ni	Pb	S	Zn	Si
	mg/kg	mg/kg	mg/kg	mg/kg	mg/kg	mg/kg	mg/kg	mg/kg	mg/kg	mg/kg	mg/kg	mg/kg	mg/kg	mg/kg	mg/kg
BH Site C Site 1 (1995)															
10	46.0	3633	4.44	2.63	8.1	0.865	15.5	42.3	815	17.3	1.18	6.43	3981	1334	
40	<0.1	3985	1.98	3.23	<0.1	<0.1	8.52	14.3	623	10.4	1.12	<0.1	3634	408	
70	<0.1	3991	3.16	1.48	<0.1	<0.1	5.95	9.86	373	16.6	0.71	2.49	3544	529	
85	6.64	3976	3.41	5.22	<0.53	<0.1	30.0	15.3	1251	17.2	1.63	5.10	3866	497	
80	<0.1	809	0.71	1.13	<0.1	<0.1	0.78	1.81	206	2.64	0.66	<0.1	765	72.4	
125	31.21	3469	7.92	23.8	1.255	2.135	67.2	51.3	4518	30.5	21.15	11.8	5956	640	
135	<0.1	4024	<0.1	6.80	<0.1	<0.1	6.05	48.0	3511	24.6	1.73	0.87	5740	31.5	
150	<0.1	4038	1.52	12.29	<0.1	1.620	21.2	41.5	2413	36.7	2.09	1.74	4522	434	
185	<0.1	3489	1.09	5.36	<0.1	<0.1	22.2	52.2	2295	37.8	1.07	2.50	4072	296	
200	<0.1	3211	0.28	1.53	<0.1	<0.1	7.83	19.3	834	14.6	0.77	2.04	3023	76.3	
BH Site C Site 1 (1996)															
1	43.2	2738	7.51	1.80	13.4	3.765	7.6	27.0	450	8.62	0.67	10.1	3445	1464	11.9
6	50.4	2653	7.62	2.08	16.1	2.910	10.3	29.5	502	9.08	2.36	9.16	3479	1496	12.9
17	53.0	2645	10.68	3.34	22.6	0.855	18.2	43.0	808	10.7	2.77	9.93	4010	2336	14.0
26	31.8	2597	8.78	4.55	4.405	0.350	17.5	36.9	783	9.37	2.63	10.4	3750	1968	17.7
36	12.9	2502	14.95	15.64	0.320	<0.555	32.8	88.5	2475	18.25	5.24	1.00	5416	3719	36.1
BH Site C Site 2 (1996)															
1	0.18	2717	0.74	0.14	<0.025	<0.25	35.2	18.0	13.1	66.0	0.85	1.00	2473	50.6	8.64
8	0.31	2720	5.42	3.11	0.115	<0.25	50.7	79.0	432	280	6.56	2.01	3077	366	22.2
15	0.11	1230	<0.05	<0.05	<0.025	<0.25	32.6	30.9	0.2	7.9	<0.25	1.00	1095	8.5	10.8
33.5	0.14	2880	1.42	<0.58	0.045	<0.25	18.9	12.3	68.7	50.1	<0.25	1.36	2689	169	6.74
49	0.22	2870	0.30	0.15	0.030	<0.25	29.6	12.3	29.8	73.8	<0.25	1.00	2618	32.1	7.91
BH Site C Site 3 (1996)															
1	2.80	2741	0.66	2.99	0.305	<0.25	28.1	64.3	446	310	0.97	3.60	3096	355	24.5
11	14.04	2717	1.88	7.52	0.555	0.390	12.3	30.8	1684	62.5	1.52	1.15	3499	330	16.5
22	2.92	2789	1.88	5.06	0.165	<0.25	19.4	17.6	1305	20.1	1.57	10.6	3365	412	17.9
32	0.31	2883	0.26	0.07	<0.025	<0.25	24.8	54.0	13.9	71.7	<0.25	1.00	2645	11.7	9.22
44	0.14	2970	1.03	0.80	<0.025	<0.25	62.2	88.4	40.5	105	0.35	1.00	2667	21.4	30.1
47	0.32	2808	1.52	3.12	0.075	<0.25	17.5	9.09	345	16.7	0.58	3.83	2841	170	14.9
55	0.33	2859	1.00	2.97	0.060	<0.25	13.2	5.8	273	8.08	0.66	3.01	2715	173	13.3
61	0.25	2861	0.06	1.45	<0.025	<0.25	51.0	70.3	71.6	37.5	1.22	5.28	2738	14.5	20.9
70	0.29	2914	0.46	0.07	<0.025	<0.25	28.0	19.4	31.3	28.5	<0.25	4.92	2640	10.9	15.1
77	0.21	2890	0.70	<0.05	<0.025	<0.25	21.5	22.5	34.3	23.1	<0.25	2.24	2583	11.1	10.9
BH Site C Site 4 (1996)															
1	0.34	2994	0.74	0.35	0.360	<0.25	124	48.0	36.2	904	0.37	4.16	2786	264	26.7
15	0.41	2929	0.35	0.16	0.180	<0.25	83.1	27.6	33.5	493	<0.25	1.00	2661	78.8	46.5
28.5	0.15	2945	0.31	0.18	<0.025	<0.25	28.5	10.5	30.3	151	<0.25	1.00	2522	28.0	9.21
40.5	0.39	2960	2.53	0.91	0.165	<0.25	106	39.8	148	657	<0.25	6.93	2851	303	46.0
49	0.21	2902	3.76	0.54	<0.11	<0.25	87.0	32.3	112	549	<0.25	9.34	2711	213	33.4

TABLE 5.3D BROKEN HILL - SITE C SOLUTE CONCENTRATIONS (1:5 BATCH LEACHING)

5.4.2 Lachlan Fold Belt, N.S.W

5.4.2.1 Elura Zn-Pb-Ag Mine

The geochemistry of the tailings at the Elura Mine has been investigated over a period of 3 years. In 1995 a single core was removed from Site 1 in Dam 1 (Fig 4.5). Additional coring was tried in Dam 2 at this time but was unsuccessful due to the hardness of the cements. During the period between field visits in 1995 and 1996, tailings deposition was carried out in both Dams 2 and 3. Thus during the 1996 visit the hardpan surface of Dam 2 was less developed and coring was achieved at Sites 6 and 7. An additional core was recovered from the North end of Dam 1 at Site 5 at this time. The upper section of this core represents the break-down of surface hardpan previously noted in Chapter 4. During the 1997 visit, active deposition was again occurring in Dam 2, Site 1 at the southern end of Dam 1 had been fully eroded, while the northern end was being covered by a revegetation trial. Thus an additional site, Site 10 was sampled for isotopic and Cl analysis, where the residual hardpan was still intact. Hence the geochemical data presented here is from a number of different sites over a number of years. The significance is however that all the profiles from Dam 1 are substantially older (up to 8 years) than those from Dam 2, which are less than 1 year old.

The tailings pH conditions range from 3 to 7, the older Dam 1 having a generally lower surface pH which increases with depth (Fig 5.28). The newly deposited tailings of Dam 2 has pH conditions ranging from 5 to 7 throughout the profile. The most acidic conditions were observed at the break-down surface at Site 5 in Dam 1 and were associated with EC levels up to 8mS/cm. The EC of the pore waters at the other sites ranges from 2 to 4 mS/cm (Fig 5.28).

The main solute components in Dam 1 include Ca, Fe, Mg, Mn, Zn and S, while As, Cu, Al, Pb and Ni are present at lower levels (Table 5.4). Aluminum, Ca, Fe, Mn, As, Mg and S have accumulated within or just below the hardpan surface, and concentrations generally decrease with depth (Figs 5.29, 5.31, 5.32, 5.34 & 5.35). Similar trends occur within Sb, Ba, B, Cd, Cr, Li, Ti, Mo and P profiles however these elements play only a minor role in the geochemistry of these tailings and the profiles are not presented. The elevated EC values observed at Site 5 within the break-down surface were due to accumulations of soluble Al, Ca, Cu, Fe, Mg, Mn and S. It should be noted that the Site 10 profile sampled in 1997 had considerably lower solute loads than those observed at Sites 1 and 5. Iron speciation was also determined for this site which indicated that the main mobile Fe cation was Fe^{2+} (940 mg/kg).

Generally the main solute loads of Dam 2 consists of Ca, Fe, Mg, Mn, Na, S and Zn, with lower levels of K, Pb, Ni (Table 5.4). The profiles for Dam 2 are highly variable and reflect numerous palaeo-surfaces developed during deposition. For example at approximately 15-20cm depth at Site 2 a drop in pH has occurred which correlates with an increase in EC (Fig 5.28). This increase occurs via elevated Al, Ca, K, Mg, Pb and S concentrations.

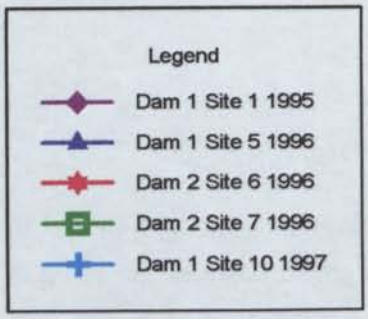

LEGEND FOR ELURA DAMS 1 & 2 SOLUTE CONCENTRATION PROFILES FROM 1:5 BATCH LEACHING EXPT.

REPRESENTS APPROX. ZONE OF HARDPAN

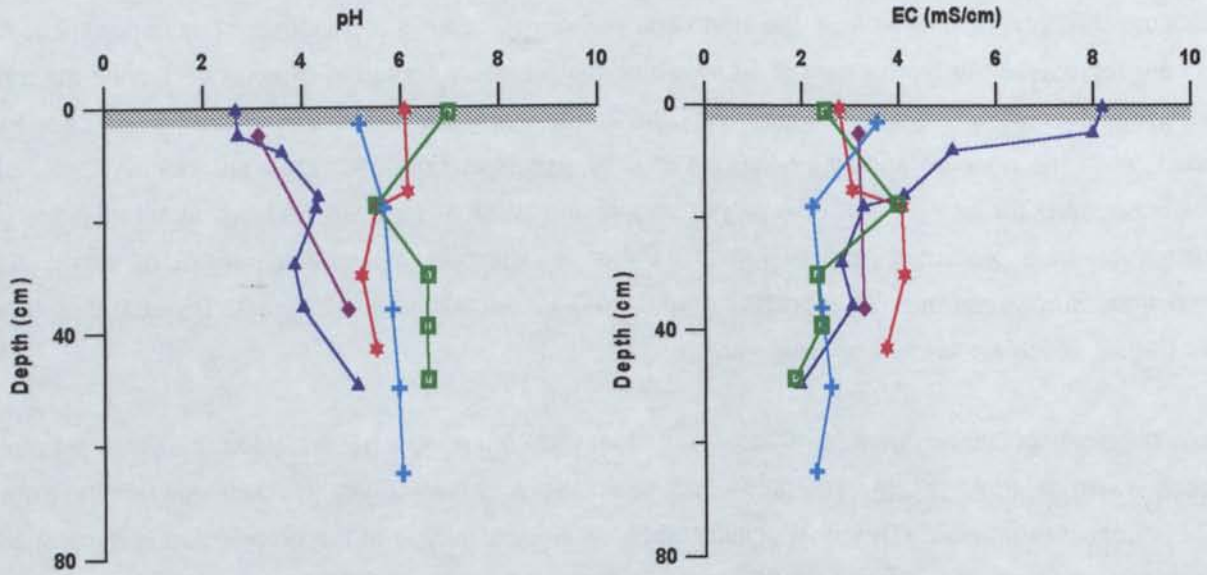

FIG 5.28 pH AND EC PROFILES FOR ELURA

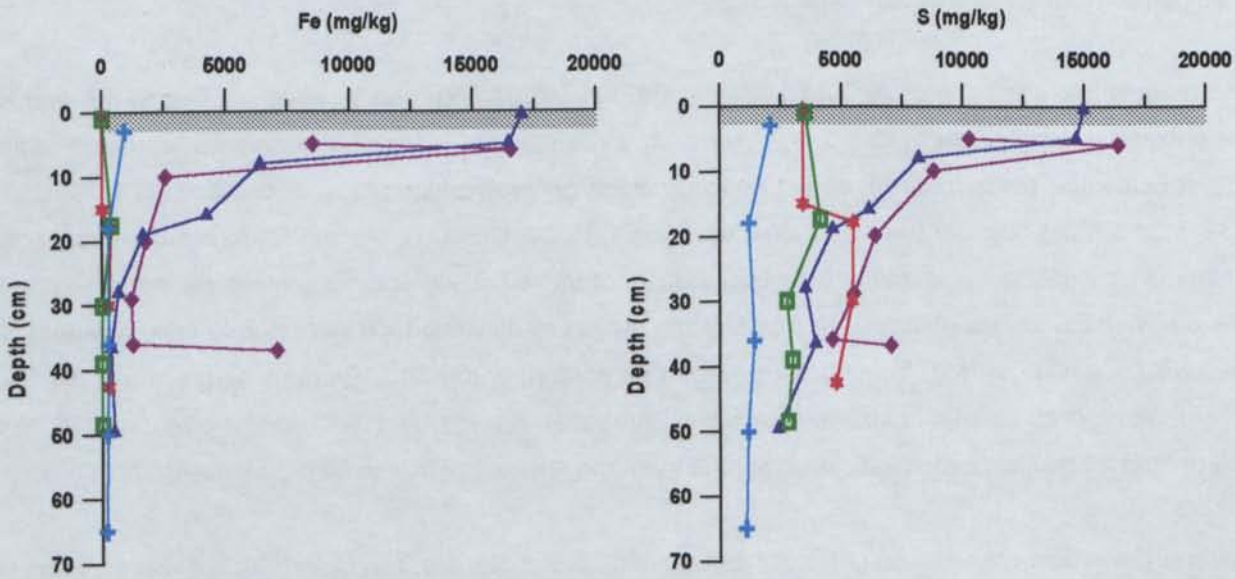

FIG 5.29 FE AND S PROFILES FOR ELURA

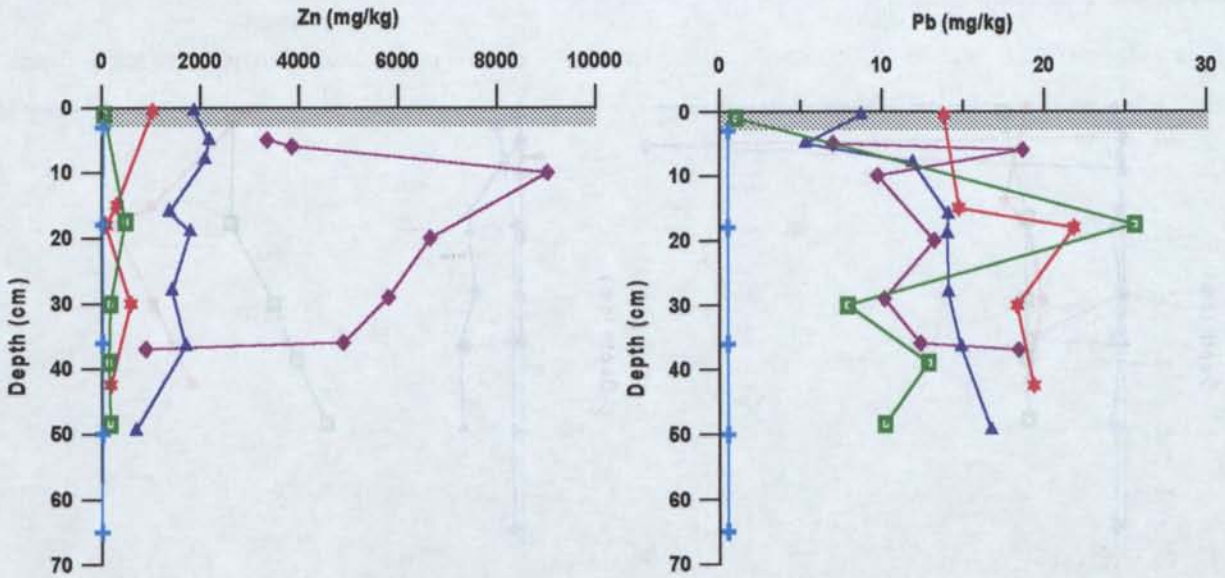

FIG 5.30 ZN AND PB PROFILES FOR ELURA

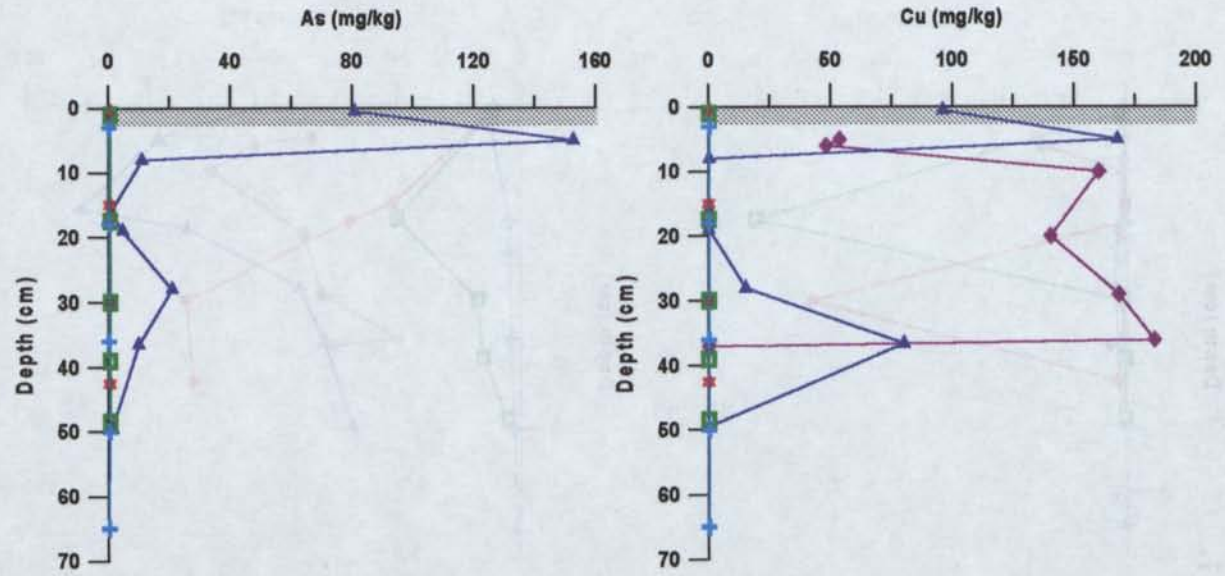

FIG 5.31 AS AND CU PROFILES FOR ELURA

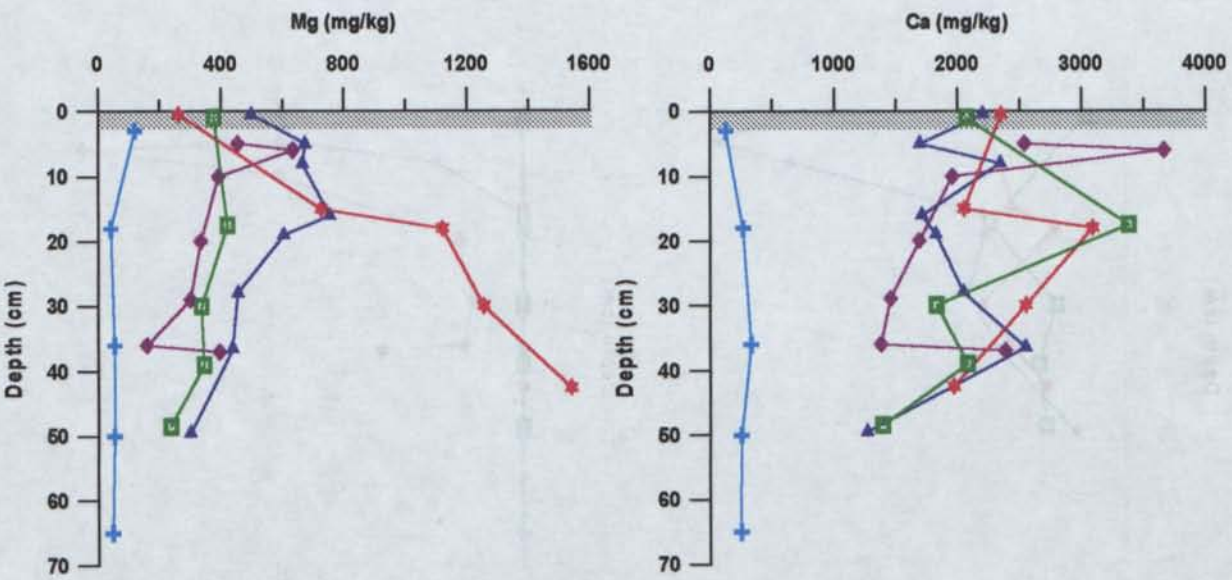

FIG 5.32 MG AND CA PROFILES FOR ELURA

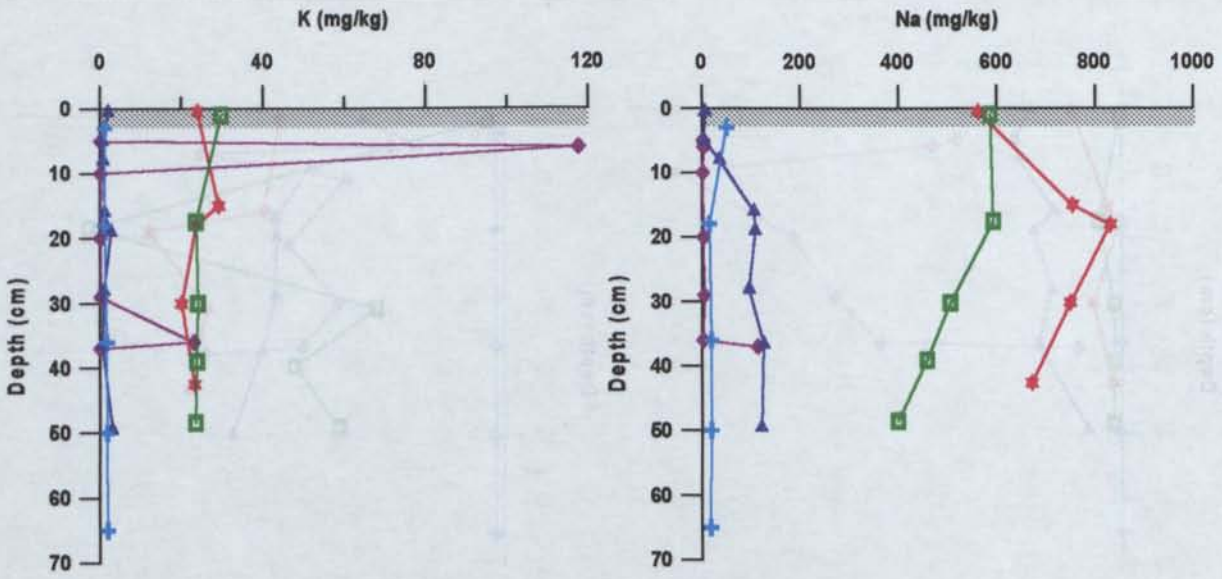

FIG 5.33 K AND NA PROFILES FOR ELURA

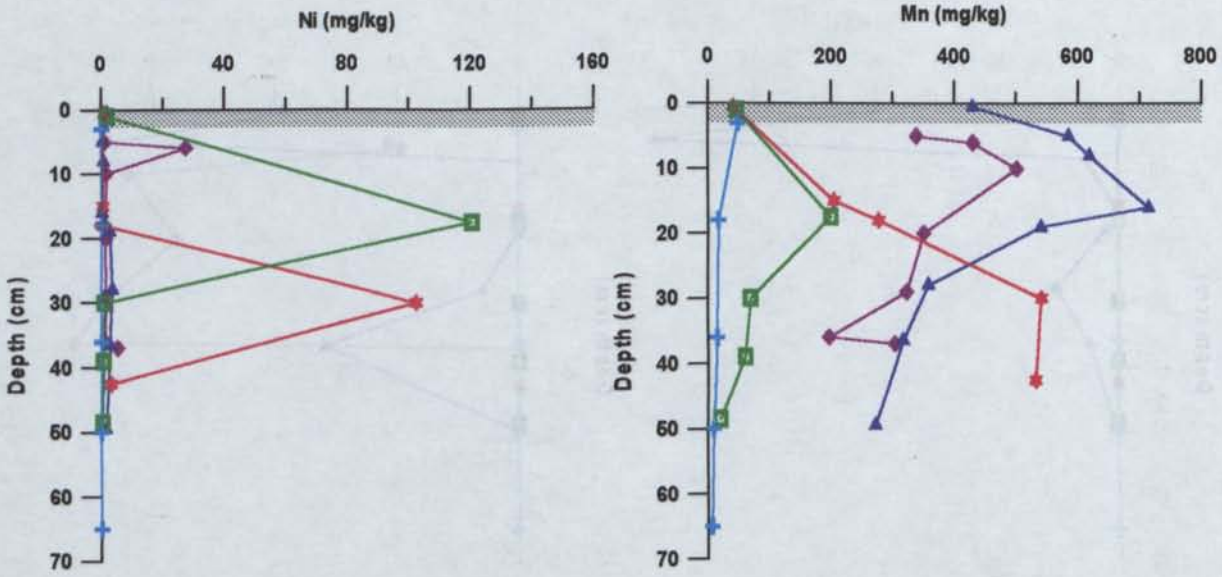

FIG 5.34 NI AND MN PROFILES FOR ELURA

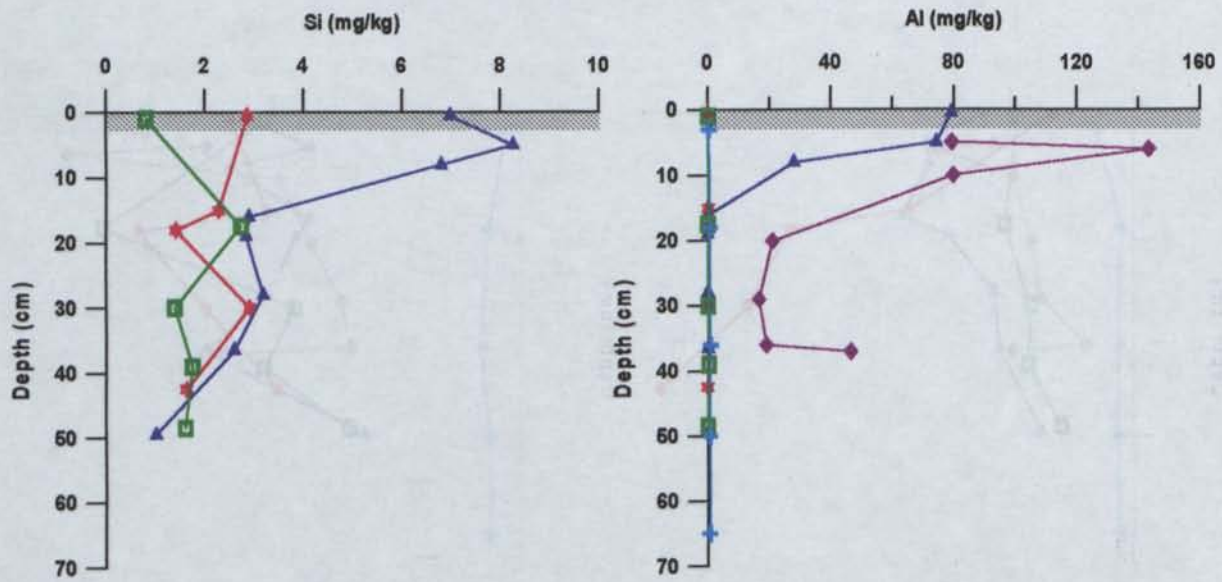

FIG 5.35 SI AND AL PROFILES FOR ELURA

5.4.2.1.1 Discussion

In general, Dam 2 has accumulated lower levels of Al, Cu, Fe, K, Mn, Si, Zn and S, compared with Dam 1, however Ca concentrations are similar, while Na, Mg, Ni and Pb are present in greater concentrations. The annual comparison shows similar Ca content over time, suggesting that Ca has very limited mobility in this system. The calcite content of the tailings is low and thus the majority of Ca is thought to be derived from lime additions during processing. Sodium is also present through metallurgical processing, however Na is more mobile and has been lost from the system in Dam 1.

In general the EC values of Dam 2 are lower than those for Dam 1. However, a comparison of the intact hardpan surface at Site 10 (Dam 1), with degraded hardpan surfaces at Sites 1 and 5 (Dam 1), shows that pH and EC levels are lower and more alkaline in the underlying tailings. These results are very similar to the newly exposed tailings at Sites 6 and 7 (Dam 2). The elevated levels of Al, Cu, Fe, K, Mn, Si, Zn and S within Dam 1 (Sites 1 and 5) compared with Dam 2, simply reflect the maturity of the system and degradation of the hardpan, where longer periods of sulfide oxidation, acid generation and gangue mineral dissolution have caused elevated solute concentrations. The higher levels of Mg, Ni and Pb in the recently deposited Dam 2 tailings may reflect a variation in the primary mineralogy of the ore, where there is potentially increased levels of primary Pb sulfide, dolomite and/or Mg - chlorites, and variations in Ni impurities of the sulfides.

The results observed for Dam 1 Site 5 and to a lesser extent Site 1 support the hypothesis that the hardpan is in fact degrading, resulting in increased levels of soluble salt formation possibly produced through the re-exposure of sulfide and siderite grains as the cements become degraded. SEM investigations presented in Chapter 4 and porosity and permeability measurements in Chapter 7 support this hypothesis. Degradation of mature hardpans may be promoted in high runoff regions where mechanical erosion, dissolution and lateral transport are promoted. Site 5 is located on a topographical high, while Site 1 is located in a low lying region next to a collapse in the dam wall. Degradation at these sites may have been enhanced while the flat lying hardpans at Sites 3, 4 and 10 have remained intact and have suppressed the development of additional solutes for many years.

	Al	Ca	Cd	Co	Cr	Cu	Fe	K	Mg	Mn	Na	Ni
	mg/kg	mg/kg	mg/kg	mg/kg	mg/kg	mg/kg	mg/kg	mg/kg	mg/kg	mg/kg	mg/kg	mg/kg
D2 S6 (1996)												
0.5	0.07	2349.9	4.285	0.7	<0.025	0.205	0.6	23.925	261.19	40.68	562.58	0.88
15	0.095	2050.1	2.16	0.265	<0.025	0.03	0.8	29.195	726.16	204.02	754.73	0.46
18	<0.01	3089.4	<0.01	0.05	<0.025	<0.025	356.6	23.58	1121.03	276.65	831.23	0.37
30	<0.01	2552.4	<0.01	1.095	<0.025	<0.025	251.8	20.04	1256.18	540.72	749.94	102.5
42.5	<0.01	1967.3	<0.01	0.29	<0.025	<0.025	272.1	23.29	1540.53	530.80	672.35	3.10
D2 S7 (1996)												
1	0.115	2067.5	0.26	0.17	<0.025	<0.025	0.5	29.715	376.37	46.24	586.42	1.785
17.5	0	3380.3	0	0.98	<0.025	<0.025	377.6	23.525	420.75	198.55	593.31	120.5
30	0.055	1827.7	0.37	0.05	<0.025	<0.025	0.3	24.01	336.20	68.63	505.41	1.04
39	0.23	2080.0	0.72	0.12	<0.025	<0.025	0.4	23.815	344.84	59.71	458.57	0.64
48.5	0.06	1392.8	0.7	0.13	<0.025	0.03	0.4	23.445	235.59	19.64	399.11	0.51

	Pb	S	Zn	As	Ba	Be	Li	Sb	Si	Sr	Ti	V
	mg/kg	mg/kg	mg/kg	mg/kg	mg/kg	mg/kg	mg/kg	mg/kg	mg/kg	mg/kg	mg/kg	mg/kg
D2 S6 (1996)												
0.5	13.80	3410.3	1027.7	<0.5	0.065	<0.01	0.19	<0.5	2.87	0.73	<0.025	<0.025
15	14.73	3404.0	302.6	<0.5	0.05	<0.01	0.265	<0.5	2.28	0.99	<0.025	<0.025
18	21.83	5475.1	77.3	<0.5	<0.025	<0.01	0.31	<0.5	1.415	0.84	<0.025	<0.025
30	18.33	5428.3	580.0	<0.5	<0.025	<0.01	0.33	<0.5	2.91	0.49	<0.025	<0.025
42.5	19.36	4775.2	174.5	<0.5	<0.025	<0.01	0.3	<0.5	1.63	0.58	<0.025	<0.025
D2 S7 (1996)												
1	1	3500.4	45.5	<0.5	0.085	<0.01	0.15	<0.5	0.81	0.96	<0.025	<0.025
17.5	25.57	4124.2	472.4	<0.5	<0.025	<0.01	0.19	<0.5	2.73	1.29	<0.025	<0.025
30	7.90	2736.4	160.7	<0.5	0.045	<0.01	0.15	<0.5	1.39	0.66	<0.025	<0.025
39	12.88	2976.9	136.8	<0.5	0.045	<0.01	0.14	<0.5	1.75	0.99	<0.025	<0.025
48.5	10.20	2786.3	161.3	<0.5	0.065	<0.01	0.12	<0.5	1.61	0.78	<0.025	<0.025

TABLE 5.4A ELURA - DAM 2 SOLUTE CONCENTRATIONS (1:5 BATCH LEACHING)

	Al	Ca	Cd	Co	Cr	Cu	Fe	K	Mg	Mn	Na	Ni	Pb	S	Zn
	mg/kg	mg/kg	mg/kg	mg/kg	mg/kg	mg/kg	mg/kg	mg/kg	mg/kg	mg/kg	mg/kg	mg/kg	mg/kg	mg/kg	mg/kg
D1 S1 (1995)															
5	79.3	2539	3.38	0.18	<0.1	53.8	8531	<0.1	455	338	2.03	1.00	6.98	10272	3343
6	144	3668	8.15	0.56	5.02	48.2	16569	117.68	633	430	3.53	27.5	18.7	16401	3854
10	79.8	1958	16.9	0.53	0.10	160	2561	<0.1	392	501	1.89	1.71	9.73	8801	9024
20	21.1	1689	10.6	0.45	<0.1	140	1768	<0.1	333	350	2.84	1.39	13.2	6383	6650
29	16.7	1458	8.73	0.31	<0.1	168	1186	<0.1	301	322	4.56	1.45	10.1	5503	5798
36	19.0	1380	8.50	0.38	<0.1	183	1241	23.153	158	196	2.86	1.28	12.4	4614	4883
37	46.5	2384	0.78	<0.1	<0.1	<0.1	7090	0.1	396	303	114	5.31	18.42	7032	886
D1 S10 (1997)															
3	0.30	126	<0.1	<0.25	<0.05	<0.05	917	1.069	119	47.8	49.6	<0.1	<0.5	2070	15.6
18	0.56	265	<0.1	<0.25	<0.05	<0.05	245	1.01	40.8	16.0	14.5	<0.1	<0.5	1180	11.5
36	0.72	330	<0.1	<0.25	<0.05	<0.05	244	1.597	53.3	14.1	19.0	<0.1	<0.5	1410	8.3
50	0.64	250	<0.1	<0.25	<0.05	<0.05	205	1.733	52.2	8.56	19.0	<0.1	<0.5	1140	5.8
65	0.62	249	<0.1	<0.25	<0.05	<0.05	171	1.862	46.6	6.05	17.8	<0.1	<0.5	1050	1.6
D1 S5 (1996)															
0.5	79.2	2202	<0.01	0.07	4.25	96.2	17011	1.965	499	429	5.34	2	8.69	14981	1867
5	74.3	1695	<0.01	0.125	4.42	168	16484	0.45	673	585	3.91	0.53	5.28	14668	2169
8	28	2347	<0.01	0.23	0.11	0.15	6396	0.66	666	619	35.7	0.81	11.9	8177	2083
16	<0.01	1708	<0.01	0.05	<0.025	<0.025	4226	1.11	754	715	106	0.25	14.1	6124	1361
19	<0.01	1822	<0.01	0.13	<0.025	<0.025	1653	2.655	604	540	108	2.83	14.0	4630	1788
28	<0.01	2045	<0.01	0.095	<0.025	15.0	641	0.835	455	357	96.0	3.65	14.1	3498	1409
36.5	<0.01	2550	<0.01	0.26	<0.025	80	363	0.575	438	317	126	2.69	14.9	3920	1697
49.5	<0.01	1267	<0.01	0.05	<0.025	0.05	484	2.885	300	271	121	1.64	16.7	2376	683
	As	Ba	Be	Li	Sb	Si	Sr	Ti	V	Fe (II)					
	mg/kg	mg/kg	mg/kg	mg/kg	mg/kg	mg/kg	mg/kg	mg/kg	mg/kg	mg/kg					
D1 S5 (1996)															
0.5	80.9	0.06	<0.01	0.23	1.885	6.99	0.03	0.03	<0.025						
5	153	0.09	<0.01	0.305	1.29	8.27	0.03	<0.025	<0.025						
8	10.9	0.04	<0.01	0.36	<0.5	6.8	0.52	<0.025	<0.025						
16	0.775	<0.025	<0.01	0.255	<0.5	2.89	0.03	<0.025	<0.025						
19	4.7	<0.025	<0.01	0.22	<0.5	2.84	0.35	<0.025	<0.025						
28	20.8	<0.025	<0.01	0.18	<0.5	3.19	0.03	<0.025	<0.025						
36.5	9.83	<0.025	<0.01	0.16	<0.5	2.60	0.12	<0.025	<0.025						
49.5	1.24	<0.025	<0.01	0.1	<0.5	1.02	0.05	<0.025	<0.025						
D1 S10 (1997)															
3	0.1	<0.05	<0.01	<0.055	<0.1		0.03	<0.05	<0.05	937					
18	0.20	<0.05	<0.01	<0.05	<0.1		0.06	<0.05	<0.05	251					
36	0.15	<0.05	<0.01	<0.05	<0.1		0.09	<0.05	<0.05	251					
50	0.33	<0.05	<0.01	<0.05	<0.1		0.07	<0.05	<0.05	212					
65	0.22	<0.05	<0.01	<0.05	<0.1		0.09	<0.05	<0.05	179					

TABLE 5.4B ELURA - DAM 1 SOLUTE CONCENTRATIONS (1:5 BATCH LEACHING)

5.4.2.2 CSA Cu-Pb-Zn Mine

Tailings pore waters from both the North and South Dams have been analysed for pH, EC and elemental concentrations over a 3 year period. The locations of the sites investigated have been outlined in Chapter 4. Six sites in the North Dam were cored in 1995 and then CSA20 and CSA180 were repeated in 1996. Unfortunately this area was unavailable for investigation in 1997 and so a central site (Site 2) was investigated where a similar well-developed surface hardpan existed. Three sites were investigated in the South Dam: Site 3 was cored in 1995 and repeated in 1996 during which time additional cores were removed from Sites 4 and 5 for comparison.

5.4.2.2.1 North Dam

The elements analysed can be grouped into two categories based on their concentrations in the profile. Group 1 consists of those which occur mainly in cemented or oxidised zones, while Group 2 includes those which are concentrated at depth in the mottled or unoxidised zones. Group 1 includes Al, Fe, P, S, B and Ca, all of which are generally concentrated in the surface regions but also persist to some degree in the buried cements.

In the cores removed during 1995 it was observed that increased Al and S concentrations occurred in the cements of CSA20, & 60, and the oxidised tailings of CSA100 & 140, resulting in the precipitation of natrojarosite, hexahydrite, native S and gypsum identified through XRD and possibly halotrichite as detected via SEM/EDX investigations (Table 5.5). However at the CSA180 & 220 sites where new tailings deposition had taken place, Al and S appeared to have been leached into the unoxidised tailings below (Fig 5.37, 5.39, 5.44 & 5.50). Repeat coring at CSA20 & 180 in 1996, showed a substantial decrease in surface Al and S. The Al and S contents at both locations may have been leached from the surface or may have been incorporated as insoluble secondary minerals although no discrete phases were identified at CSA 180. Erosion from the CSA20 site may also be responsible for Al and S reductions. The levels of both S and Al observed in the 1997 central site were much lower than those observed in the 1995 and 1996 sites. The central profile showed elevated Al and S levels within the mottle zone (10cm), with levels decreasing with depth.

The 1995 profiles indicated that the Fe concentrations also generally occurred in the cemented zones (e.g. CSA20, 140, & 220) (Figs 5.37 & 5.44). However elevated levels were also detected within palaeo-surfaces (CSA60) and in mottled regions below (CSA100). Not unlike Al, some redistribution of Fe into the underlying unoxidised tailings may have occurred through leaching when additional tailings were deposited on the surface (CSA180). The poorly soluble Fe salts determined by XRD included natrojarosite and jarosite. Much of the Fe has been removed from solution as it has precipitated out as insoluble goethite, one of the main cementing agents at this mine.

The 1996 repeat coring showed much greater total Fe concentrations at 15cm depth in the unoxidised tailings at CSA20, suggesting leaching has occurred or oxidation is occurring at this depth. The repeat profile at CSA180 showed a similar profile. The 1997 central profile was investigated for both Fe^{2+} and Fe^{3+} concentrations. Analysis indicated that Fe^{2+} was mobile with levels up to 500mg/kg observed at 30cm depth (Fig 5.37).

Group 2 includes a larger group of elements which are concentrated deeper in the tailings profile, mainly in the unoxidised zones or mottled regions. Elements included here are Pb, Cu, Zn, Ni, Mg, Mn Na, Co, and Cd. Many of the elements in this group are at very low concentrations and do not greatly effect the geochemical system. However in many cases elevated levels of Cu, Mg, Mn, Na, Ni and Zn were observed at depth (Figs 5.38 to 5.49). It is suggested that this suite is in soluble form, is not playing a role in the cementation of the tailings at the surface but is in fact being leached from the surface. A proportion of these elements may already be incorporated into the insoluble cements at the surface, however SEM/EDX investigations gave limited indications of this. At depth, concentrations can be attributed to the formation of natrojarosite (Na) and hexahydrite (Mg) as elevated levels of S were also observed over this depth range. The concentration of Cu, Mn, Ni, and Zn have not resulted in the precipitation of any discrete secondary mineral phases at depth and again it is suggested that adsorption, coprecipitation and substitution must play a role.

It should be noted that the large increase in concentration of Zn, Ni, Co, Cr and Cd at depth observed in the 1995 was not detected in the 1996 re-coring at CSA20 & 180 (Figs 5.45 & 5.49). This may reflect a slight variation in sampling site, a leaching effect, or incorporation of these elements as insoluble cements. Whatever the reason, a general increase in concentration with depth was still evident in 1996. The 1997 central site sampling also showed elemental concentrations deeper in the profile at approximately 30cm depth, at the base of the mottled zone. This region represents the zone of active oxidation, resulting in elevated solute concentrations (in particular Fe^{2+}) and a drop in pH from 5 to 3 across this boundary (Fig 5.36). Eh measurements presented in Chapter 7 also support this.

The 1995 and 1996 results for pH and EC at each sampling location are presented in Figs 5.36 and 5.43. Locations CSA20, 60, 100 and 140, show a general increasing pH trend with depth. This simply reflects the near-surface oxidation and production of acid. The fact that the pH does not increase greatly with depth reflects the low neutralising potential of the tailings sampled, or that the neutralising potential has been all but utilised. Locations CSA180 & 220 show slightly different trends. CSA220 shows a general pH decrease with depth responding to the newly deposited tailings above the old hardpan. CSA180 on the other hand has a varied profile reflecting the exposure time of each layer and the development of palaeo-surfaces i.e. longer exposure - lower pH conditions obtained.

The 1995 EC results again group CSA20, 60, 100, 140, with a general decreasing trend with depth which again reflects the oxidation taking place at the surface and the solutes produced. At depth oxidation is less or absent and therefore by-product formation is also reduced. Re-coring of CSA20 showed that the solute content at the surface has decreased with time whereas at CSA180 oxidation of the newly

deposited tailing has produced solute concentrations greater than that previously observed. The 1995 CSA220 EC profile is substantially diminished as less oxidation has taken place at the surface of the newly deposited tailings at the time of sampling. The varying results reflect the dynamic nature of the hardpan surface. The effects of mechanical erosion, dissolution and leaching have produced changes in concentrations, while solute incorporation into cements has added complexity to the system

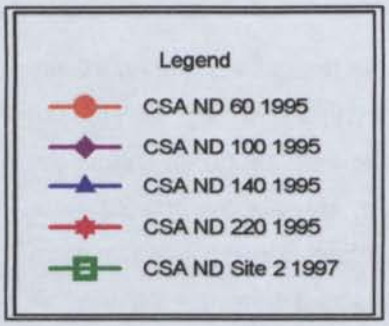

LEGEND FOR CSA NORTH DAM SOLUTE CONCENTRATION PROFILES FROM 1:5 BATCH LEACHING EXPT.

REPRESENTS APPROX. ZONE OF HARDPAN

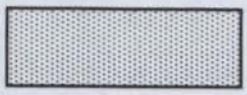

REPRESENTS APPROX. ZONE OF OXIDATION

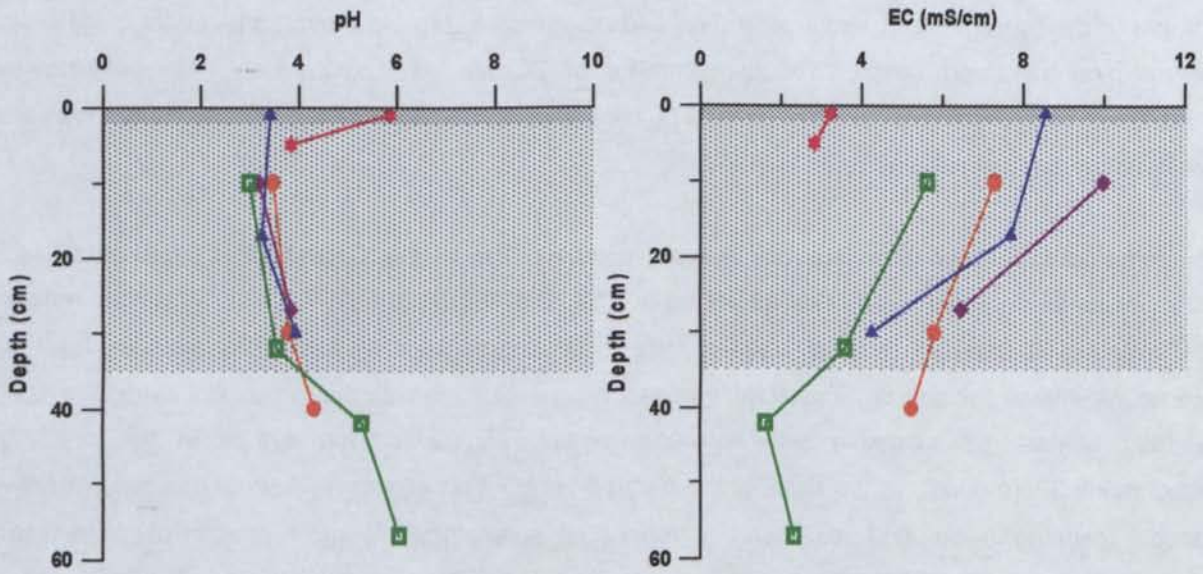

FIG 5.36 pH AND EC PROFILES FOR CSA NORTH DAM

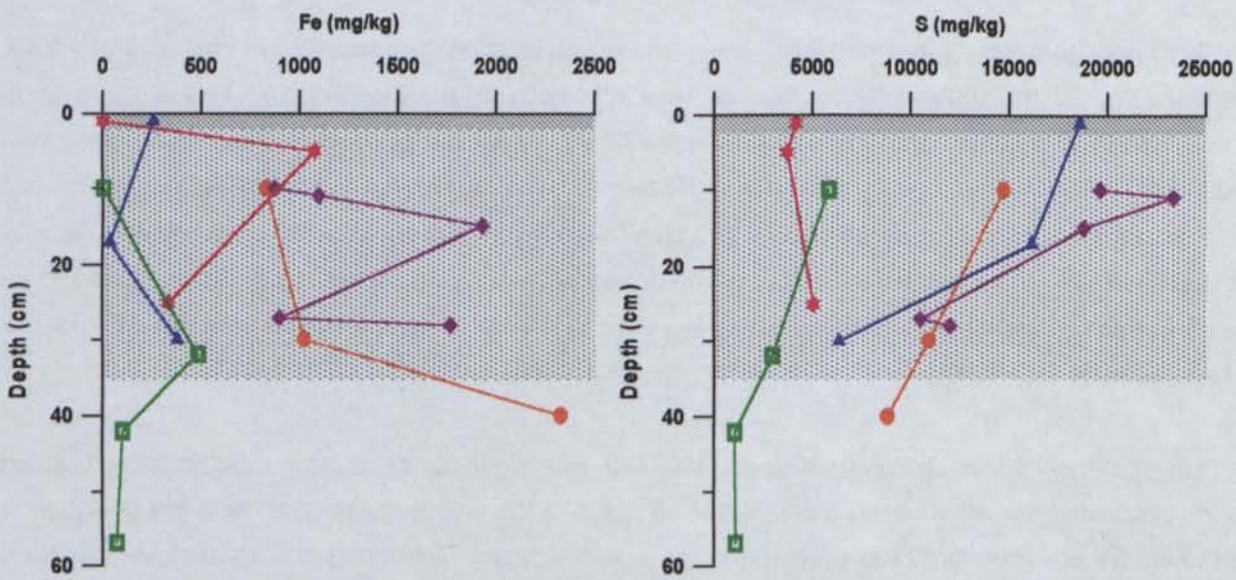

FIG 5.37 FE AND S PROFILES FOR CSA NORTH DAM

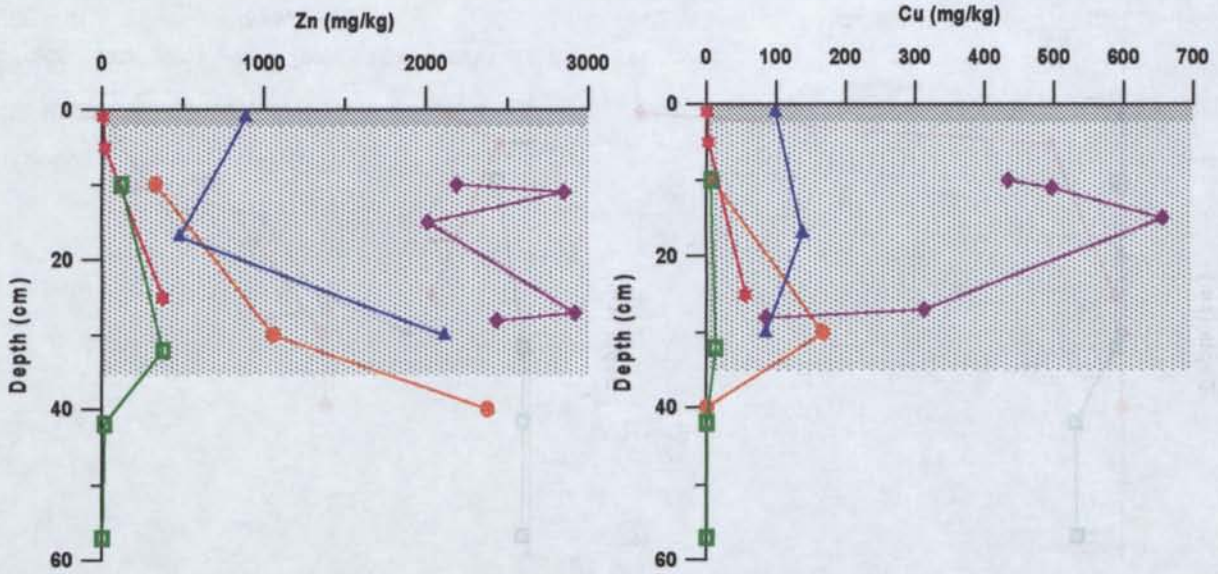

FIG 5.38 ZN AND CU PROFILES FOR CSA NORTH DAM

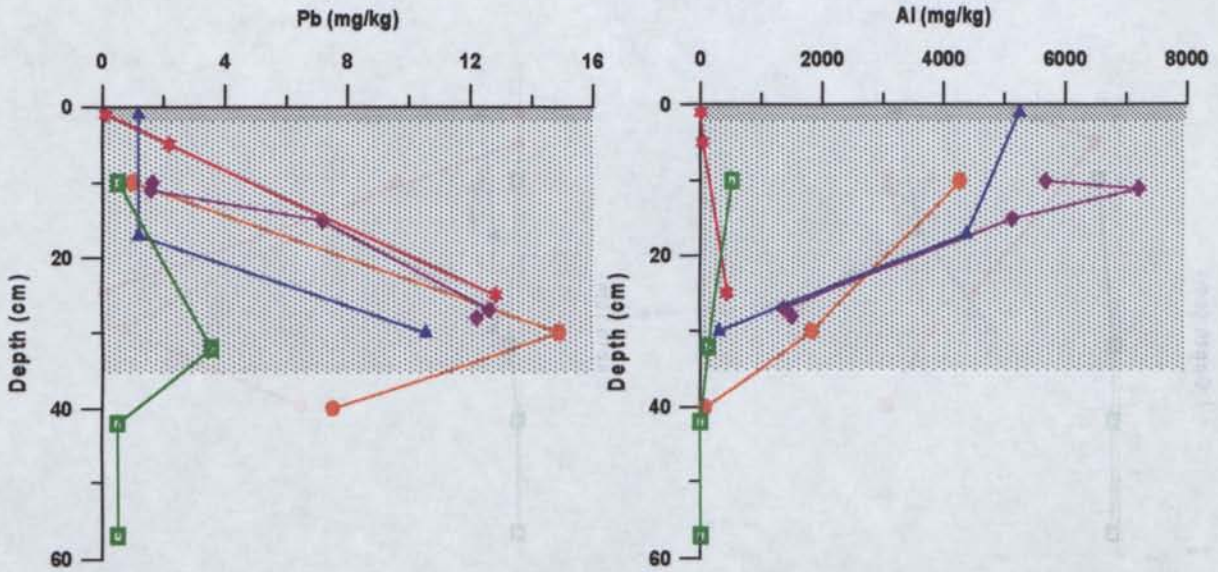

FIG 5.39 PB AND AL PROFILES FOR CSA NORTH DAM

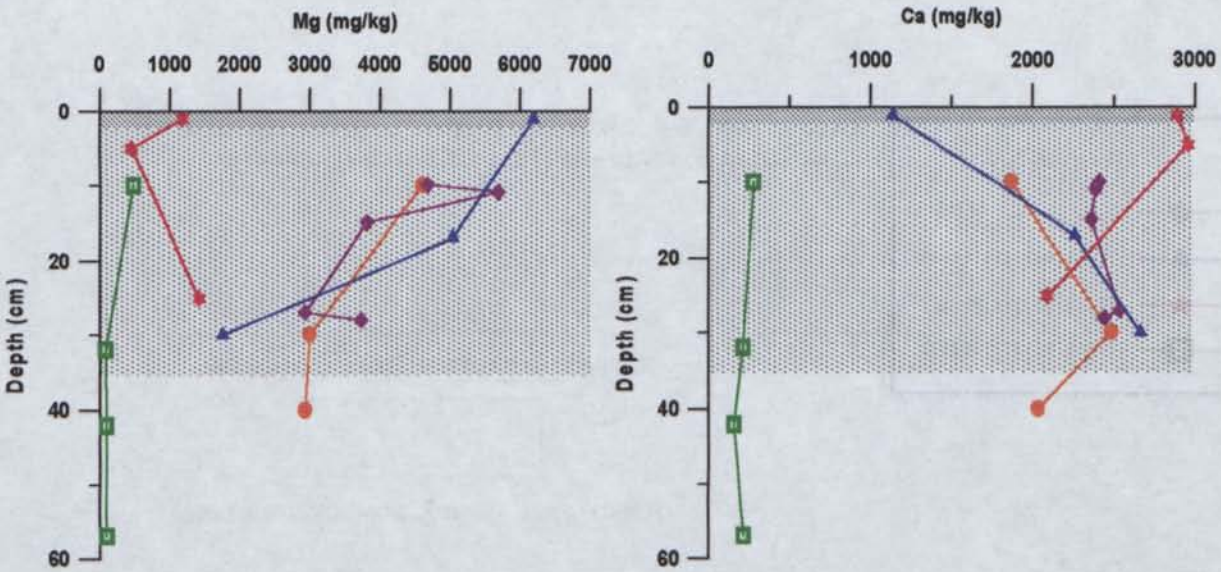

FIG 5.40 MG AND CA PROFILES FOR CSA NORTH DAM

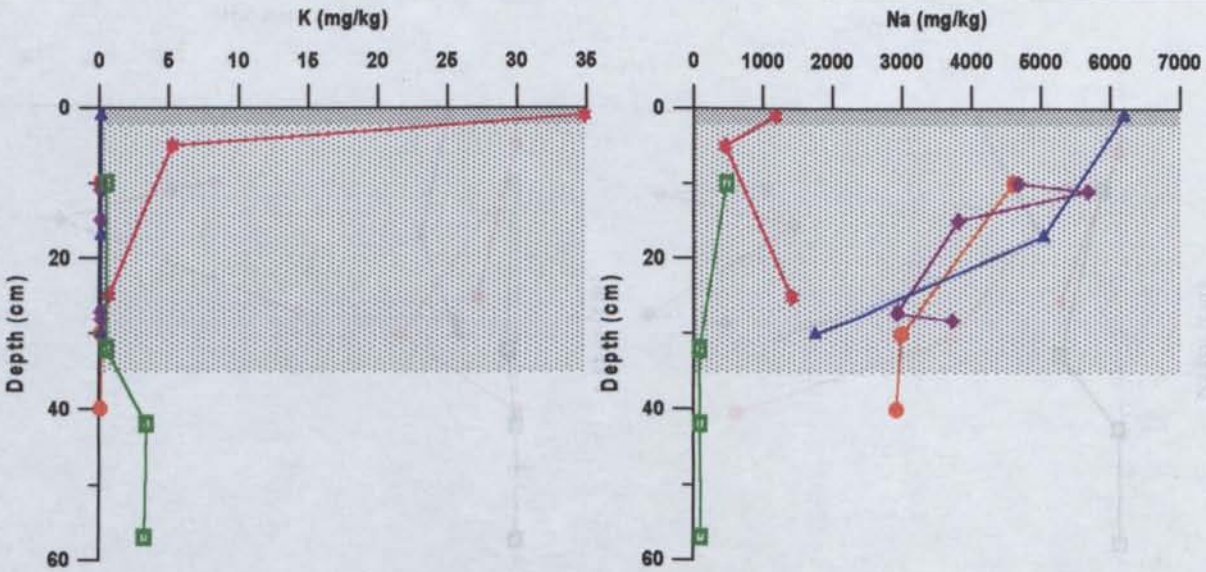

FIG 5.41 K AND NA PROFILES FOR CSA NORTH DAM

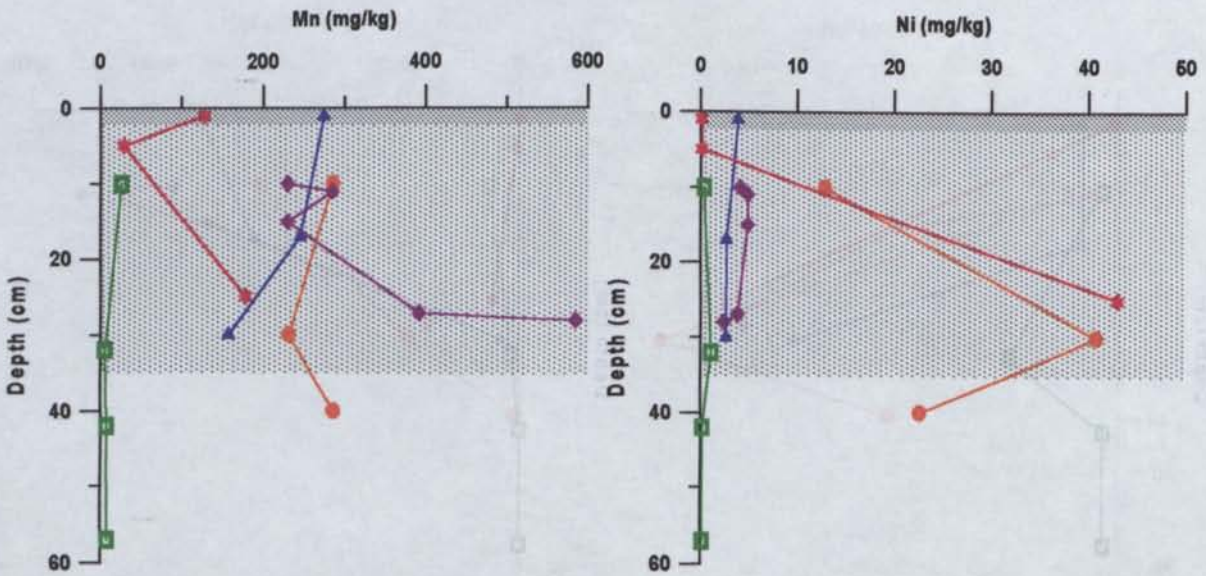

FIG 5.42 MN AND NI PROFILES FOR CSA NORTH DAM

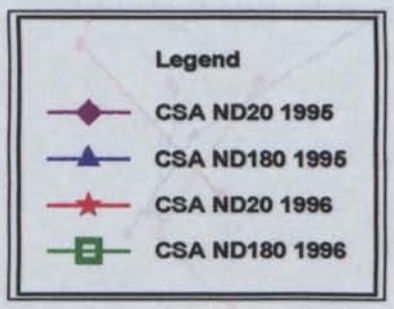

LEGEND FOR CSA NORTH DAM ANNUAL COMPARISON SOLUTE CONCENTRATION PROFILES FROM 1:5 BATCH LEACHING EXPT.

REPRESENTS APPROX. ZONE OF HARDPAN

REPRESENTS APPROX. ZONE OF OXIDATION

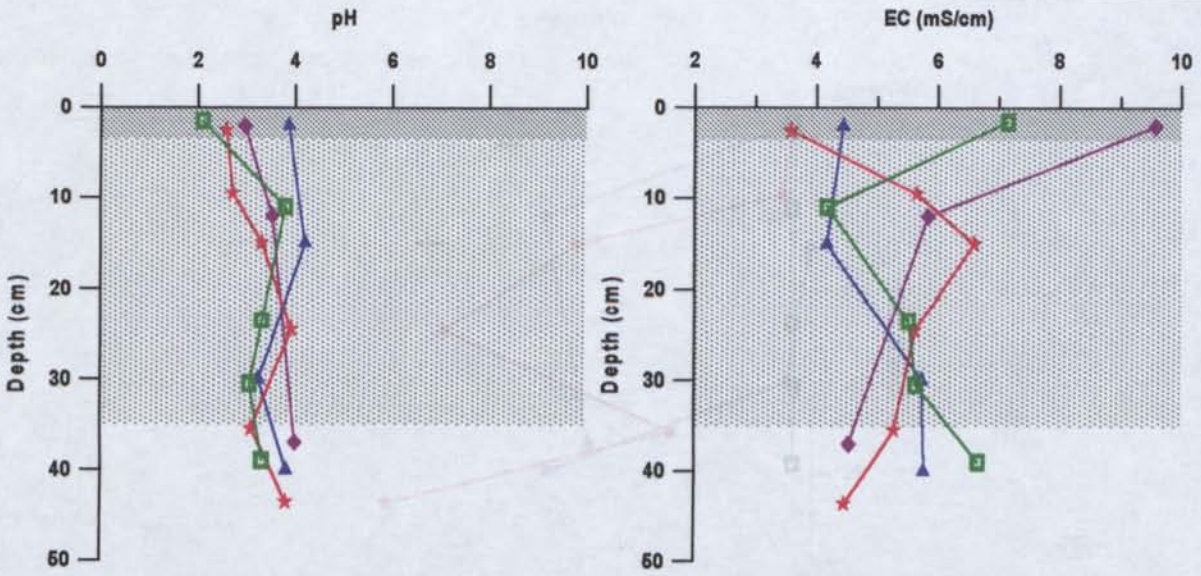

FIG 5.43 PH AND EC PROFILES FOR CSA NORTH DAM ANNUAL COMPARISON

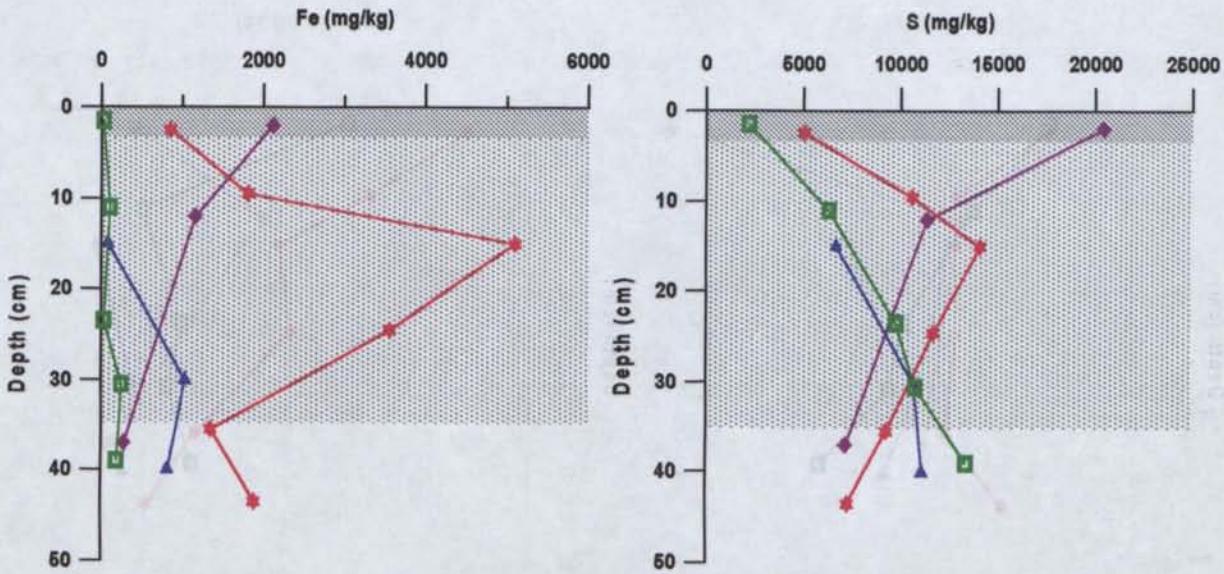

FIG 5.44 FE AND S PROFILES FOR CSA NORTH DAM ANNUAL COMPARISON

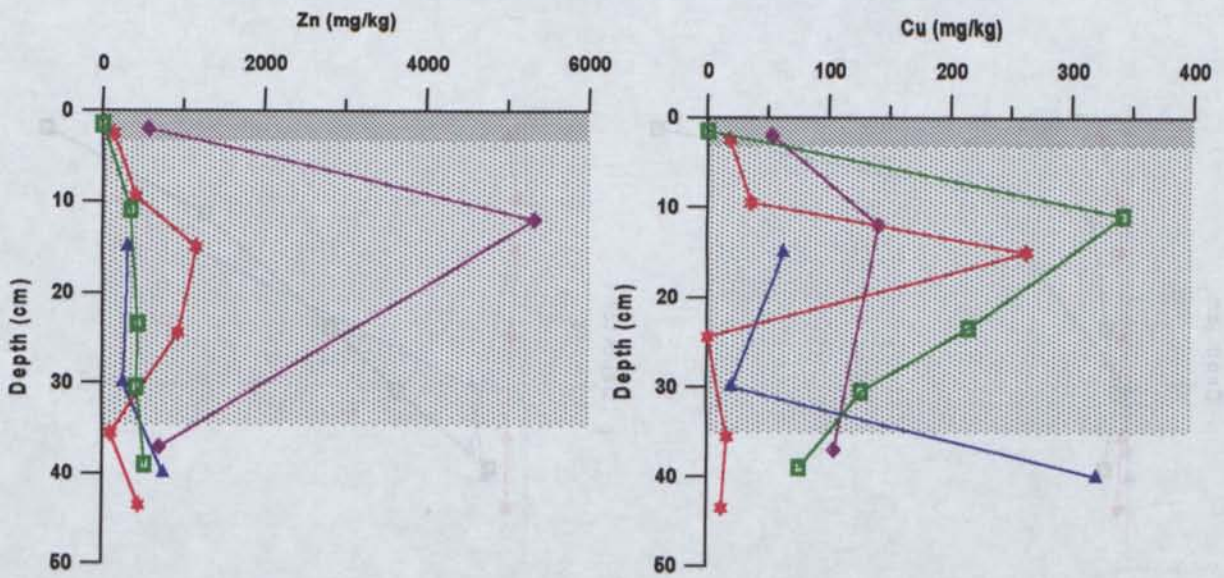

FIG 5.45 ZN AND CU PROFILES FOR CSA NORTH DAM ANNUAL COMPARISON

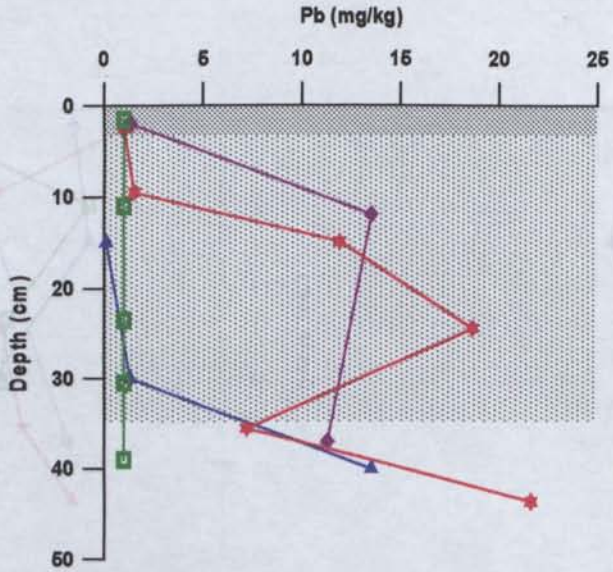

FIG 5.46 PB PROFILE FOR CSA NORTH DAM ANNUAL COMPARISON

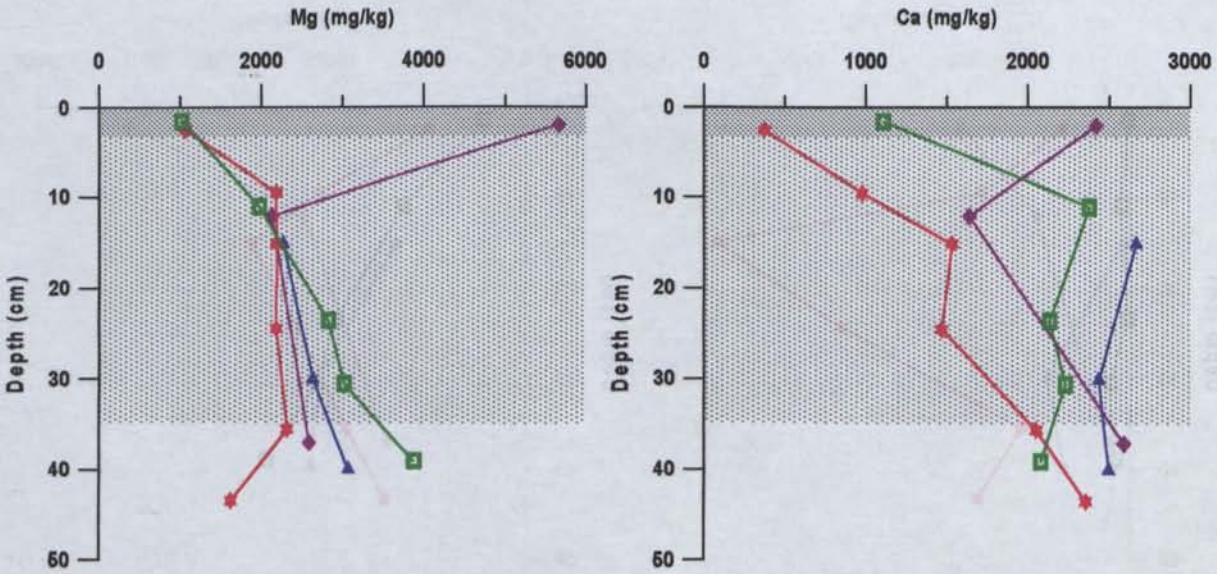

FIG 5.47 MG AND CA PROFILES FOR CSA NORTH DAM ANNUAL COMPARISON

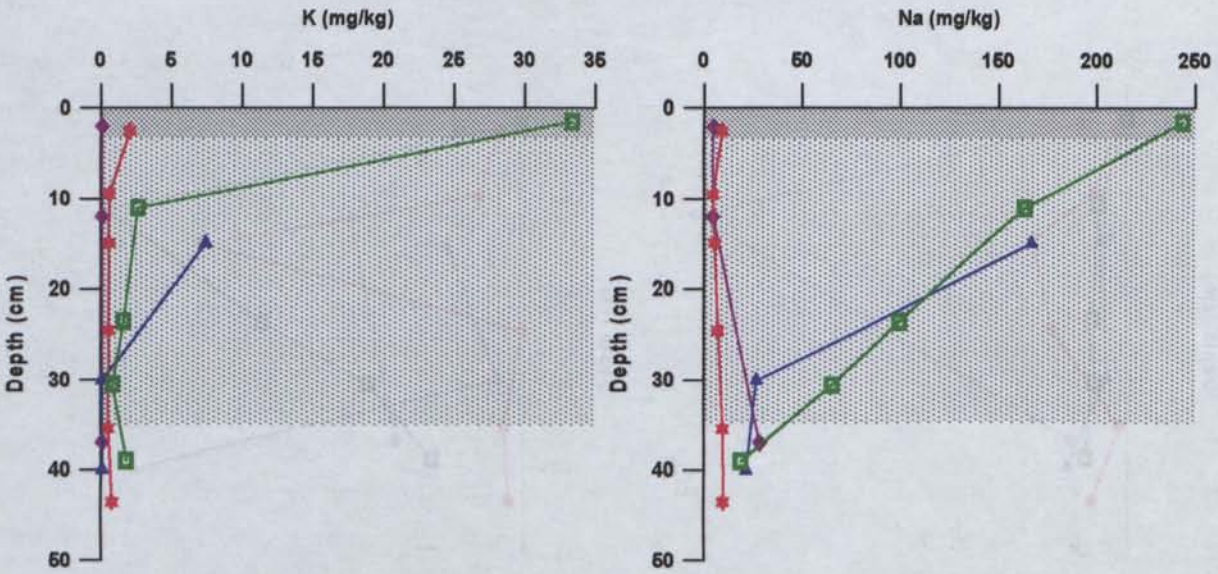

FIG 5.48 K AND NA PROFILES FOR CSA NORTH DAM ANNUAL COMPARISON

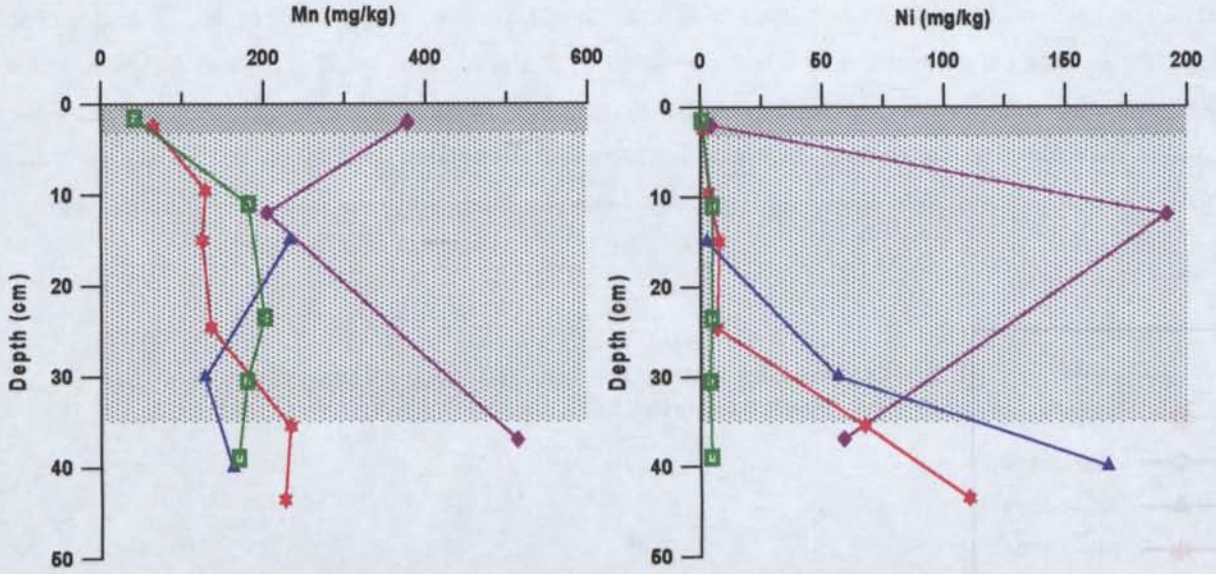

FIG 5.49 MN AND NI PROFILES FOR CSA NORTH DAM ANNUAL COMPARISON

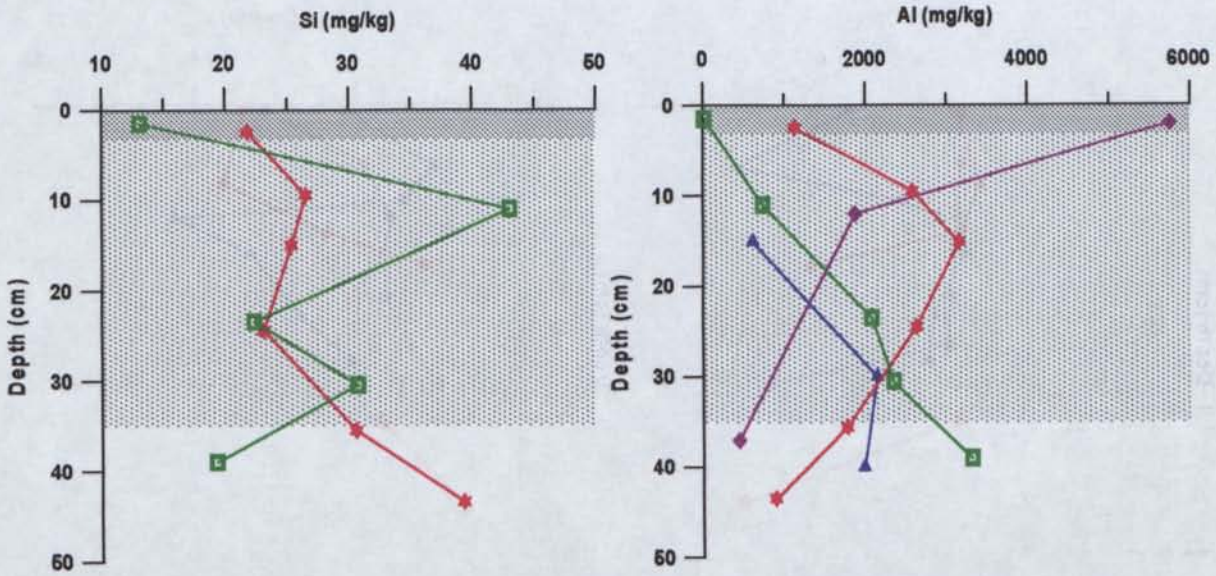

FIG 5.50 SI AND AL PROFILES FOR CSA NORTH DAM ANNUAL COMPARISON

5.4.2.2.2 South Dam

The pH profiles for the sites investigated in the South Dam are highly variable ranging from pH 3 to 8 (Fig 5.51). 1995 and 1996 measurements at Site 3 indicate that the site has maintained pH levels of approximately 3 down to 40cm depth, which increased to approximately 7 at 50cm depth. During the 1996 visit, staff indicated that this site had been compacted/disturbed by previous traffic and is thus not representative of the entire dam. Additional sites (Site 4 and 5) were cored for comparison. The pH measurement from Sites 4 and 5 on the opposite side of the dam were inconclusive. Site 4 exhibited an increase to pH 7.5 at 15cm depth which decreased to pH 4 for the remainder of the profile, while at Site 5, pH 3 conditions persisted down to 25cm depth at which depth the pH abruptly increased to 6. The EC profiles were also highly variable with Site 3 and 5 showing general decreases in EC with depth, while Site 4 showed a large increase in EC at 20cm associated with a well developed palaeo-surface (Fig

5.51). The solutes at this depth consisted of Al, Ca, Co, Cr, Cu, Fe, K, Mg, Mn, Na, Ni, Zn and S (Table 5.5), while surface concentrations at Site 5 consisted of S, Zn, Ni, Mn, Fe, Cu, Ca and Al. Here tailings have produced very limited cementing since exposure. Surface salts and palaeo-surfaces were identified consisting of halotrichite, pickeringite, hexahydrite, kalinite and rozenite. These salts have formed through minor sulfide oxidation, by-product development and evaporation of process waters to the surface.

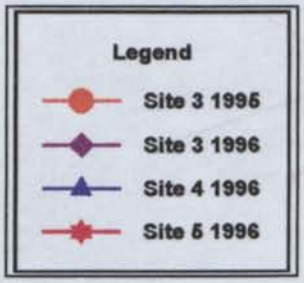

LEGEND FOR CSA SOUTH DAM SOLUTE CONCENTRATION PROFILES FROM 1:5 BATCH LEACHING EXPT.

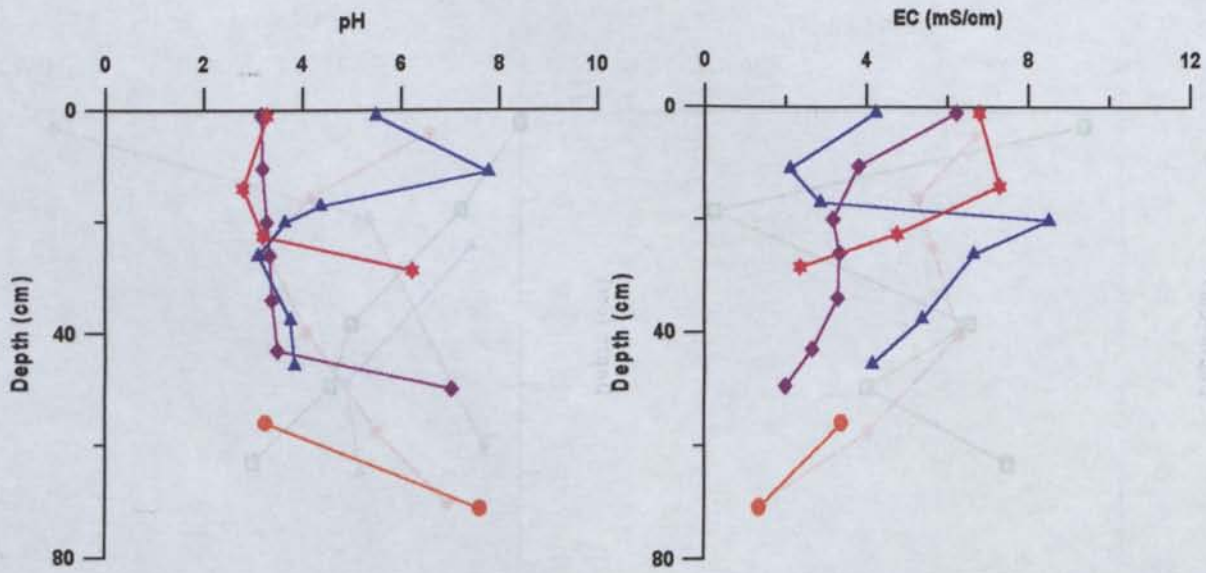

FIG 5.51 pH AND EC PROFILES FOR CSA SOUTH DAM

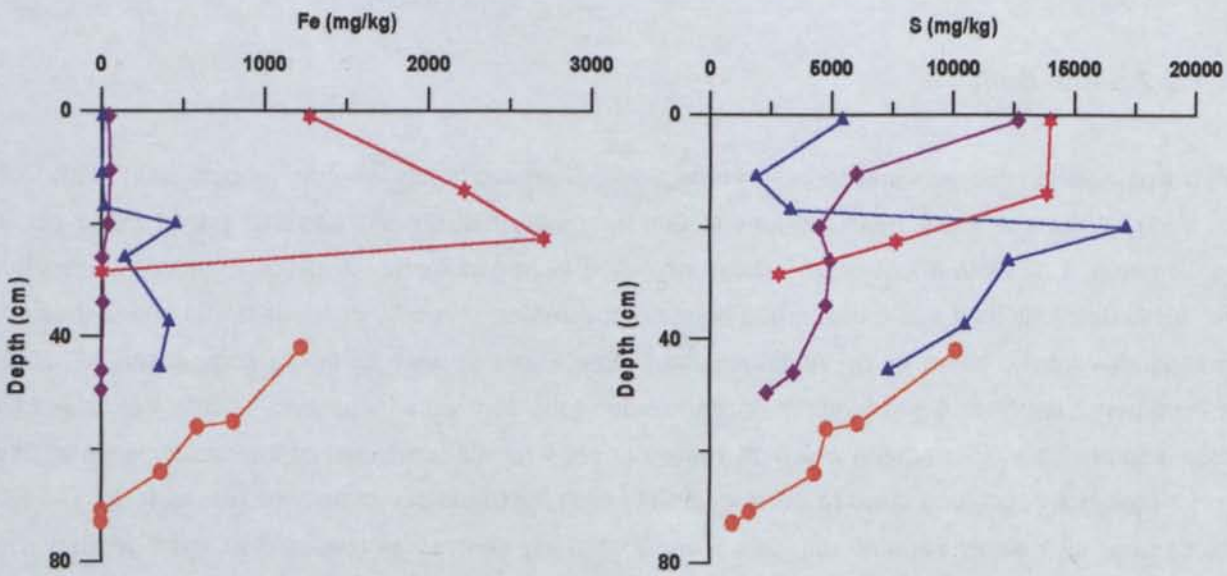

FIG 5.52 FE AND S PROFILES FOR CSA SOUTH DAM

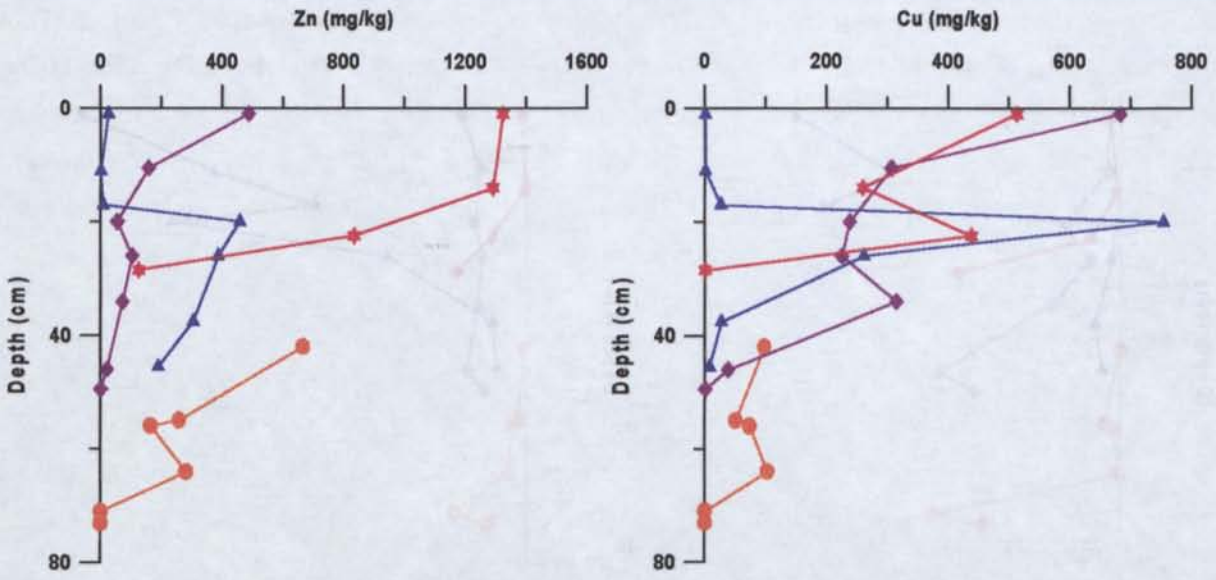

FIG 5.53 ZN AND CU PROFILES FOR CSA SOUTH DAM

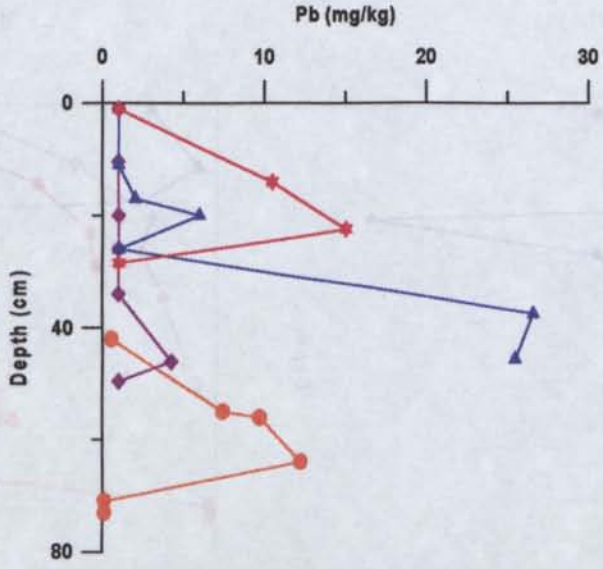

FIG 5.54 PB PROFILE FOR CSA SOUTH DAM

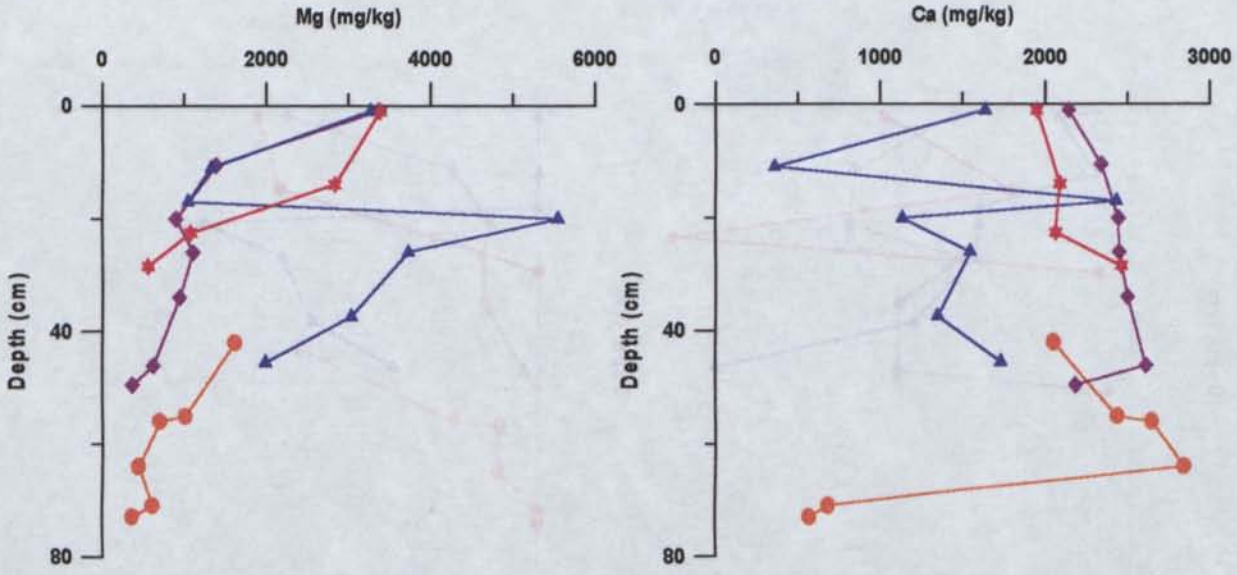

FIG 5.55 MG AND CA PROFILES FOR CSA SOUTH DAM

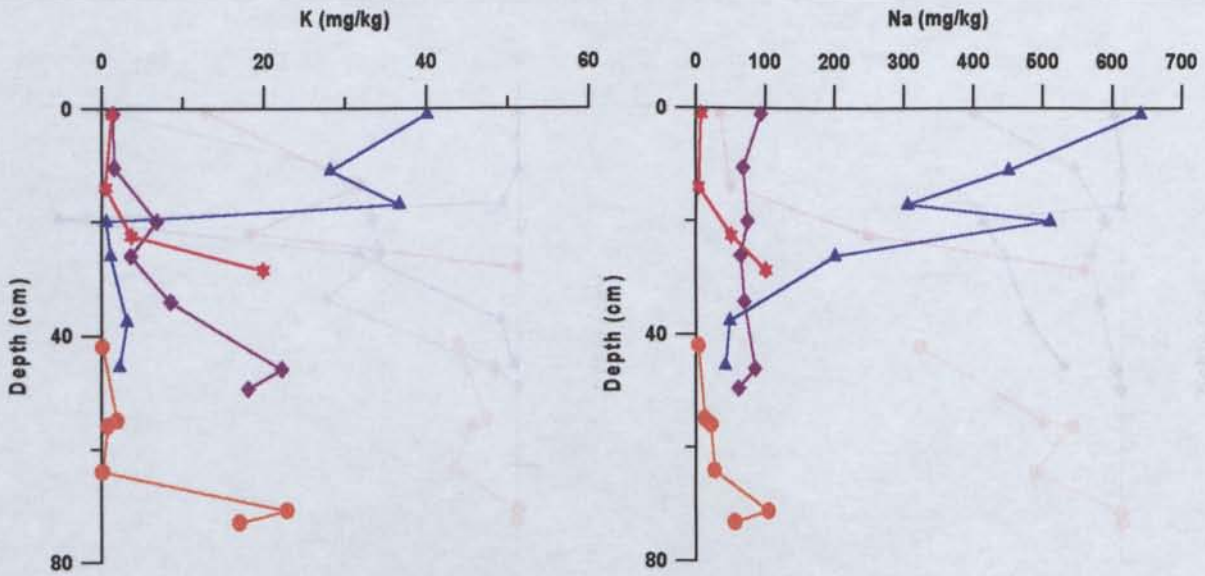

FIG 5.56 K AND NA PROFILES FOR CSA SOUTH DAM

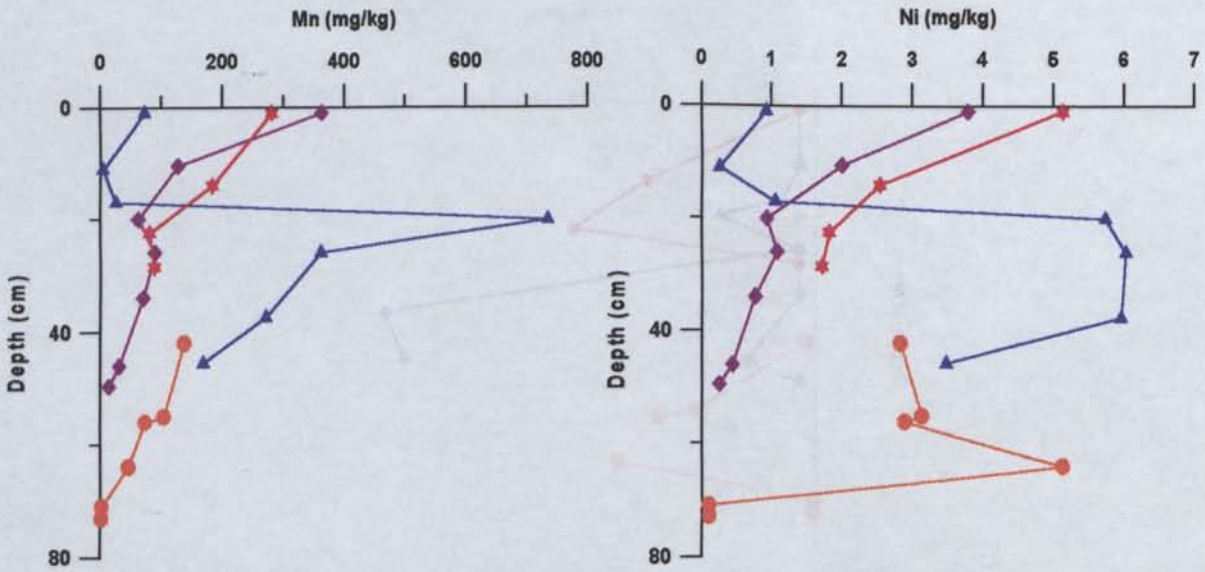

FIG 5.57 MN AND NI PROFILES FOR CSA SOUTH DAM

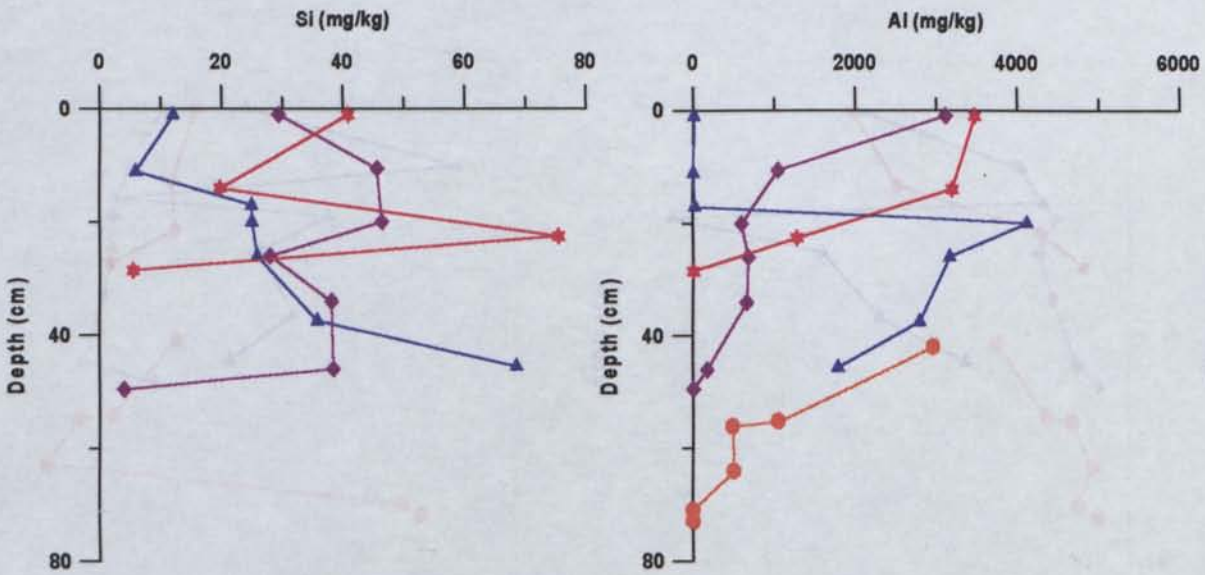

FIG 5.58 SI AND AL PROFILES FOR CSA SOUTH DAM

5.4.2.2.3 Discussion

A review of this information reveals the highly heterogeneous nature of tailings in general, which causes difficulties in interpreting the geochemistry but simply reflects the dynamic nature of the hardpan and tailings surface. At all of the sites investigated in the North Dam, large variations in concentration have developed down the profile. These variations occur in response to tailings cementation, exposure time (palaeo-surface development) and new tailings deposition. The water associated with new tailings deposition has the potential to leach soluble salts from their location of precipitation, causing concentrations deeper in the profile. Additionally, cements scavenge elements into their structures as insoluble salts, thus reducing the solute concentration near the surface.

The solute concentrations of the South Dam have been influenced less by elemental incorporation into insoluble mineral phases, as limited cementing has developed. Here surface solute concentrations have developed in response to minor sulfide oxidation and gangue mineral dissolution, which have combined with process water additives and contaminants. Additionally palaeo-surfaces have dictated geochemistry as outlined in Section 5.3.2.

A comparison of the oldest hardpan surface CSA20 (Site 1) in the North Dam, with Site 5 in the South Dam, indicates that pH is marginally more acidic and solute levels are only slightly elevated beneath the 15 yr old hardpan compared with the newly exposed tailings. Levels of Al, Ca, Mn, Pb, S and Zn are similar in both dams. The newly exposed tailings of the South Dam contain elevated levels of the more mobile K and Na, while the hardpan surface has high concentrations of Cr, Fe and Ni.

Thus solute concentrations within both tailings dams are comparable, indicating that hardpan formation has the ability to inhibit additional solute development over time, i.e. the 15 years exposure of tailings in the North Dam has not resulted in solute levels significantly greater than those observed in the more recently exposed South Dam tailings. The slightly elevated solute levels beneath the North Dam hardpan (compared with the South Dam) are potentially associated with hardpan breakdown and re-exposure of the tailings and re-mobilisation of previously precipitated secondary minerals. The South Dam solute levels are more centralised on mobile elemental loads yet to be leached from the surface.

	Al	Ca	Co	Cr	Cu	Fe	K	Mg	Mn	Na	Ni	P	Pb	S	Zn
	mg/kg	mg/kg	mg/kg	mg/kg	mg/kg	mg/kg	mg/kg	mg/kg	mg/kg	mg/kg	mg/kg	mg/kg	mg/kg	mg/kg	mg/kg
ND S1 20 (1995)															
2	5756	2418	4.55	3.89	52.8	2115	<0.1	5658	378	4.62	4.38	11.6	1.4	20409	568
12	1869	1637	74.0	46.6	140	1155	<0.1	2136	205	4.55	191.6	6.74	13.5	11334	5328
37	437	2592	4.82	1.38	104	278	<0.1	2588	513	28.5	58.8	4.85	11.3	7143	700
ND S1 20 (1996)															
2.5	1128	372	1.92	0.61	18.06	846	2.05	1063	64.13	9.17	0.81	0.50	1.0	5016	134
9.5	2578	977	5.16	1.15	35.4	1807	0.59	2182	128	4.64	3.33	0.50	1.5	10556	403
15	3151	1531	8.10	0.68	262	5104	0.57	2184	125	5.38	7.50	0.50	11.9	14054	1156
24.5	2628	1469	3.72	0.32	0.31	3555	0.55	2182	135	7.24	6.46	0.50	18.6	11645	932
35.5	1771	2052	1.42	80.6	15.85	1345	0.49	2315	233	9.58	67.4	0.50	7.2	9235	95
43.5	890	2358	3.20	104	12.15	1889	0.79	1621	226	9.89	110.1	2.19	21.6	7266	446
ND S1 60 (1995)															
10	4260	1865	4.79	18.2	9.21	830	<0.1	4604	286	2.87	12.78	7.41	1.0	14717	330
30	1834	2488	10.9	27.7	168	1024	<0.1	2996	231	6.74	40.7	5.86	14.9	10905	1059
40	81.2	2035	3.04	<0.1	0.90	2329	<0.1	2931	286	42.0	22.5	5.05	7.5	8810	2382
ND100 S1 (1995)															
10	5667	2410	23.9	0.51	434	874	<0.1	4676	230	6.72	4.06	20.2	1.6	19607	2185
11	7206	2389	29.7	0.1	496	1097	<0.1	5683	285	3.96	4.84	14.3	1.6	23343	2852
15	5118	2363	21.3	0.44	656	1928	<0.1	3815	230	3.41	4.84	16.9	7.2	18799	2009
27	1367	2539	11.1	<0.1	313	898	<0.1	2934	392	10.4	3.75	1.51	12.6	10472	2920
28	1506	2445	5.55	<0.1	85.0	1768	<0.1	3733	585	14.5	2.36	9.72	12.2	12000	2436
ND 140 S1 (1995)															
1	5246	1136	20.3	0.67	98.6	258	<0.1	6193	274	5.62	3.82	10.4	1.2	18605	886
17	4361	2260	15.6	0.57	138	35.8	<0.1	5039	245	4.06	2.64	9.50	1.2	16145	480
30	304	2668	8.82	<0.1	84.9	379	<0.1	1753	157	77.4	2.60	3.96	10.5	6349	2112
ND S1 180 (1995)															
2	448	2539	12.4	<0.1	121	135	4.79	2450	232	374	2.72	4.01	0.1	6697	373
15	608	2668	13.0	<0.1	62.3	76.2	7.43	2267	233	167	2.56	3.65	0.1	6640	309
30	2141	2437	9.83	26.8	19.8	1030	<0.1	2632	127	26.9	56.3	6.20	1.3	10630	256
40	1979	2499	18.2	38.4	320	818	<0.1	3071	162	21.5	167	6.10	13.5	11082	750
ND S1 180 (1996)															
1.5	10.58	1106	0.075	0.03	0.07	23.5	33.4	1011	41.0	244	0.25	0.50	1.0	2178	0.4
11	732	2377	16.0	0.05	342	98.9	2.62	1972	181	163	4.78	0.50	1.0	6281	344
23.5	2075	2135	18.0	0.12	214	25.9	1.61	2829	201	99.42	4.43	0.50	1.0	9738	433
30.5	2343	2229	15.8	0.75	127	243	0.84	3022	179	65.20	3.73	0.50	1.0	10716	417
39	3307	2079	14.8	1.80	75.67	185	1.78	3879	169	18.66	4.28	0.50	1.0	13341	518
ND S1 220 (1995)															
1	0.1	2893	0.76	<0.1	0.10	0.1	34.83	1180	128	436	0.10	2.33	0.1	4161	5.5
5	36.1	2961	0.62	<0.1	2.14	1079	5.23	451	28.14	183	0.10	2.33	2.2	3705	15.8
25	440	2090	2.275	<0.1	55.2	333	0.65	1419	178	78.4	42.9	3.65	12.8	5042	373
ND S2 (1997)															
10	510	273	1.03	0.08	6.07	1.8	0.5	472	25.0	2.74	0.31	0.2	0.5	5780	117
32	119	211	1.53	0.13	12.7	483	0.5	80.1	4.93	3.35	1.04	0.2	3.55	2930	375
42	0.35	154	0.25	0.05	0.05	101	3.40	93.5	6.62	18.1	0.13	0.2	0.5	1040	13.919
57	0.46	214	0.25	0.05	0.05	71.5	3.23	98.0	7.54	20.5	0.1	0.2	0.5	1070	0.641
	As	Ba	Be	Li	Sb	Si	Sr	Ti	V	Fe (II)					
	mg/kg	mg/kg	mg/kg	mg/kg	mg/kg	mg/kg	mg/kg	mg/kg	mg/kg	mg/kg					
ND S1 20 (1996)															
2.5	<0.5	<0.025	0.015	1.14	<0.5	21.8	0.21	0.1	<0.025						
9.5	<0.5	<0.025	0.03	2.15	<0.5	26.5	0.55	0.0	<0.025						
15	<0.5	<0.025	0.04	2.27	<0.5	25.3	1.07	<0.025	<0.025						
24.5	<0.5	<0.025	0.05	2.53	<0.5	23.1	0.43	<0.025	<0.025						
35.5	<0.5	<0.025	0.03	1.27	<0.5	30.6	1.92	0.0	<0.025						
43.5	0.58	<0.025	0.02	0.60	1.34	39.3	0.84	0.1	<0.025						
ND S1 180 (1996)															
1.5	<0.5	0.1	0.01	0.04	<0.5	13.1	3.90	0.0	<0.025						
11	<0.5	<0.025	0.05	1.17	<0.5	43.0	4.59	0.1	<0.025						
23.5	<0.5	<0.025	0.08	2.23	<0.5	22.3	4.14	<0.025	<0.025						
30.5	<0.5	<0.025	0.05	2.25	<0.5	30.7	1.42	<0.025	<0.025						
39	<0.5	<0.025	0.04	2.52	<0.5	19.3	1.80	<0.025	<0.025						
ND S2 (1997)															
10	<0.1	<0.05	<0.01	0.69	<0.1		0.20	0.1	<0.05	1.2					
32	0.11	<0.05	<0.01	0.26	<0.1		0.0601	0.1	<0.05	497					
42	<0.1	<0.05	<0.01	0.05	<0.1		0.35	0.1	<0.05	103					
57	<0.1	<0.05	<0.01	0.05	<0.1		0.50	0.1	<0.05	78					

TABLE 5.5A CSA - NORTH DAM SOLUTE CONCENTRATIONS (1:5 BATCH LEACHING)

	Al	Ca	Co	Cr	Cu	Fe	K	Mg	Mn	Na	Ni	P	Pb	S	Zn
	mg/kg	mg/kg	mg/kg	mg/kg	mg/kg	mg/kg	mg/kg	mg/kg	mg/kg	mg/kg	mg/kg	mg/kg	mg/kg	mg/kg	mg/kg
SD S3 (1995)															
42	2962	2054	10.5	0.225	97.3	1222	<0.1	1618	138	3.57	2.83	0.35	0.5	10117	667
55	1050	2440	3.6	1.39	50.7	809	1.92	1012	104	12.8	3.14	0.25	7.5	6065	259
56	488	2650	2.43	1.855	73.8	586	0.69	701	73.2	21.5	2.89	3.58	9.7	4791	165
64	506	2845	11.9	0.616	103	364	0.1	443	45.8	27.0	5.13	0.10	12.2	4302	282
71	0.8	686	<0.1	<0.1	0.10	0.84	22.86	617	1.48	105	0.10	1.18	0.1	1637	0.1
73	0.22	571	<0.1	<0.1	0.10	0.10	16.97	365	1.13	56.0	0.11	0.10	0.1	950	0.1
SD S3 (1996)															
1	3111	2145	18.3	0.24	682	45.8	1.39	3370	363	94.2	3.79	0.50	1.0	12691	488
10.5	1046	2339	6.765	0.15	306	52.4	1.51	1383	127	67.9	2.00	0.50	1.0	5989	157
20	595	2448	3.27	0.10	238	43.8	6.74	900	62.1	74.2	0.93	0.59	1.0	4494	55.5
26	675	2451	4.87	0.07	225	4.07	3.57	1103	88.8	64.6	1.08	0.53	1.0	4927	103
34	659	2501	3.635	0.11	315	8.13	8.49	939	69.6	69.7	0.76	0.85	1.0	4741	72.6
46	173	2616	1.215	0.04	38.0	3.03	22.2	624	30.9	85.5	0.44	0.54	4.2	3442	21.1
49.5	0.225	2186	0.05	0.03	0.03	0.46	18.07	369	13.4	61.6	0.25	0.50	1.0	2325	0.3
SD S4 (1996)															
1	3.39	1635	2.11	0.025	0.12	10.18	40.08	3265	72.3	641	0.92	0.50	1.0	5428	25.5
11	0.43	357	0.05	0.025	0.03	0.88	28.16	1322	3.60	451	0.25	0.50	1.0	1861	0.3
17	18.4	2434	2.18	0.025	25.8	16.8	36.6	1047	25.4	305	1.05	0.58	2.0	3298	8.7
20	4122	1134	21.8	0.22	754	455	0.50	5550	735	510	5.74	0.50	6.0	17133	459
26	3161	1546	22.7	0.36	261	143	1.11	3729	362	201	6.03	0.50	1.0	12274	386
37.5	2795	1350	20.2	0.16	27.0	411	3.09	3027	271	48.4	5.96	1.06	26.6	10460	305
45.5	1789	1735	13.6	0.22	7.49	358	2.18	1989	168	42.4	3.48	1.19	25.5	7325	189
SD S5 (1996)															
1	3470	1950	29.94	0.96	513	1272	1.25	3385	281	7.41	5.14	0.50	1.0	14002	1324
14	3199	2090	21.49	1.86	260	2219	0.39	2830	183	3.24	2.54	0.50	10.5	13849	1291
22.5	1279	2066	9.99	1.11	439	2710	3.64	1079	80.2	51.0	1.82	0.90	15.0	7660	835
28.5	0.34	2463	2.55	0.03	0.03	0.99	19.9	557	88.0	101	1.71	0.50	1.0	2808	125

	As	Ba	Be	Li	Sb	Si	Sr	Ti	V
	mg/kg	mg/kg	mg/kg	mg/kg	mg/kg	mg/kg	mg/kg	mg/kg	mg/kg
SD S3 (1996)									
1	<0.5	<0.025	0.14	4.35	<0.5	29.3	4.65	0.05	<0.025
10.5	<0.5	<0.025	0.05	1.78	<0.5	45.7	6.00	0.105	<0.025
20	<0.5	<0.025	0.03	0.73	<0.5	46.5	8.30	0.08	<0.025
26	<0.5	<0.025	0.035	1.10	<0.5	28.0	6.78	<0.025	<0.025
34	<0.5	0.1	0.035	0.85	<0.5	38.2	7.23	<0.025	<0.025
46	<0.5	0.07	0.015	0.23	<0.5	38.5	9.35	<0.025	<0.025
49.5	<0.5	0.08	<0.01	0.03	<0.5	3.98	6.28	<0.025	<0.025
SD S4 (1996)									
1	<0.5	0.045	<0.01	0.61	<0.5	12.0	11.65	<0.025	<0.025
11	<0.5	0.09	<0.01	0.03	<0.5	5.89	3.03	<0.025	<0.025
17	<0.5	0.05	<0.01	0.55	<0.5	25.0	7.71	<0.025	<0.025
20	<0.5	0.04	0.28	3.53	<0.5	25.0	3.57	<0.025	<0.025
26	<0.5	<0.025	0.14	3.07	<0.5	25.9	3.27	0.03	<0.025
37.5	<0.5	<0.025	0.07	2.56	<0.5	35.8	2.28	0.03	<0.025
45.5	<0.5	<0.025	0.045	1.60	<0.5	68.7	2.85	0.19	<0.025
SD S5 (1996)									
1	<0.5	0.03	0.095	2.69	<0.5	40.78	1.47	0.19	<0.025
14	<0.5	0.045	0.06	3.24	<0.5	19.82	4.07	0.07	<0.025
22.5	<0.5	0.035	0.045	1.29	<0.5	75.52	3.05	0.21	<0.025
28.5	<0.5	0.08	<0.01	0.52	<0.5	5.41	5.71	<0.025	<0.025

TABLE 5.5B CSA - SOUTH DAM SOLUTE CONCENTRATIONS (1:5 BATCH LEACHING)

5.4.2.3 Disused Chesney Au-Cu Mine

Geochemical investigations at the Chesney Mine were centered around the upper coarse-grained tailings dam (TD1) in which a hardpan had developed in a zone of seepage and TD3 a fine-grained tailings impoundment at the base of the slope.

In 1995 a single core profile was investigated within Dam 1 at Site 2 where a hardpan had developed on the west side of the dam. In 1996 Site 2 was re-cored and additional cores were removed from Sites 3 and 4. All sites are located directly down slope from Site 1, thus the grain size at Site 3 is much finer than at Site 2. These sampling locations were examined to investigate the influence grain size distribution has on solute concentrations and hardpan development.

In 1995, Site 2 solute concentration profiles exhibited similar trends for Al, Ca, Na, S, Zn and Cu (Table 5.6). Aluminum, S and Ca had almost identical profiles with elevated concentrations occurring at the surface, 51cm and 83cm depth and low levels at 45 and 70cm (Figs 5.60, 5.62, & 5.65). The similarities observed in the Al and S profiles were attributed to the precipitation of hydrobasaluminite at different depths. Likewise Ca profiles corresponding with S distribution result from the precipitation of gypsum. Zinc and Na profiles also mimicked the S distribution. The core removed in 1996 showed similar levels of most elements, however Ca, Zn, Fe, Na and to a lesser extent S were noticeably less concentrated, potentially due to incorporation as cements, leaching or slight variations in sampling location and thus tailings morphology (see Section 5.3.4).

The general similarity of solute concentrations can be observed in the EC profiles (Fig 5.59). The EC for this dam ranges from 0.1-2mS/cm, with Site 4 having higher EC values than Sites 2 and 3. Site 4 has greater levels of Al, Cu, Fe, Mn, Mg, Zn and S, while Site 3 has greatest surface accumulations of Ca and Na. The pH varies little down the profiles, with a consistent level of approximately 4 with slight increases to pH 6 at depth at Site 3 (Fig 5.59).

The increase in solute concentrations further from the dam wall (at site 4) can be interpreted in a number of ways. For example, the hardpan developed at Site 2 may have incorporated much of the solute concentrations developed at this site into the insoluble cements. Or the hardpan developed within these coarse tailings may have promoted the lateral transport of solute loads produced from this site and from the upper slopes, in particular to Site 4, 15m down slope.

It is suggested that the variation in grain size, along with the addition of added solute loads from the upper slope, have dictated where the hardpan has developed within this dam. Solute loads are available for secondary mineral development in the finer tailings down slope, in particular at Site 4, but have not resulted in cementation. It is thought the these loads have not been concentrated through evaporation because of the fine grain nature of the tailings, resulting in larger suction potentials and ultimately elevated moisture contents.

The pH of the finer grained Dam 3 is also acidic (pH 4-5), but in general is slightly more alkaline than Dam 1. The EC ranges from 1-5mS/cm which is substantially higher than the coarser tailings in Dam 1, Sites 2 and 3. The EC trends show an increase at approximately 20cm depth in both profiles, and in particular at Site 6 which is associated with cemented layers (palaeo-surfaces). The solute concentrations at this depth consist mainly of Na, Mg, Mn, Zn and S (Figs 5.60 to 5.64), and to a lesser extent Al and Cu (Figs 5.61 & 5.65). The surface accumulations within this dam are dictated by Ca, Fe, S, Mg, Mn and Cu (Figs 5.60 to 5.64).

The Dam 3 has greater concentrations of Ca, Cu, Fe, K, Na, Mg, Si, Zn and S compared with Dam 1. This may reflect the natural drainage of the dams and or the fine-grained nature of the tailings in these lower dams and thus their increased reactivity when exposed to non-saturated conditions. The solute levels in Dam 3, are comparable to Site 4 in Dam 1 where solutes are available for cementing but have not resulted in hardpan development.

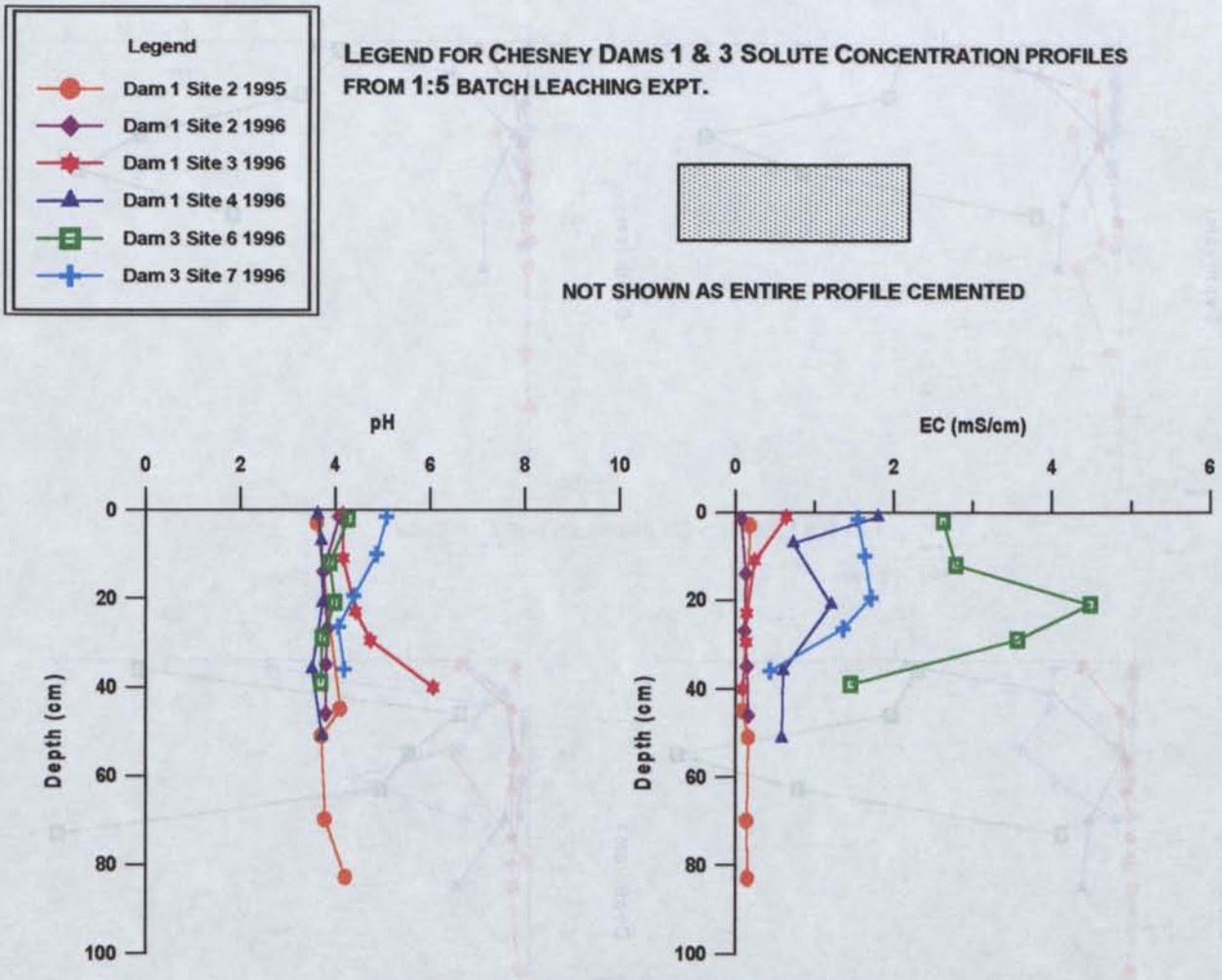

FIG 5.59 pH AND EC PROFILES FOR CHESNEY

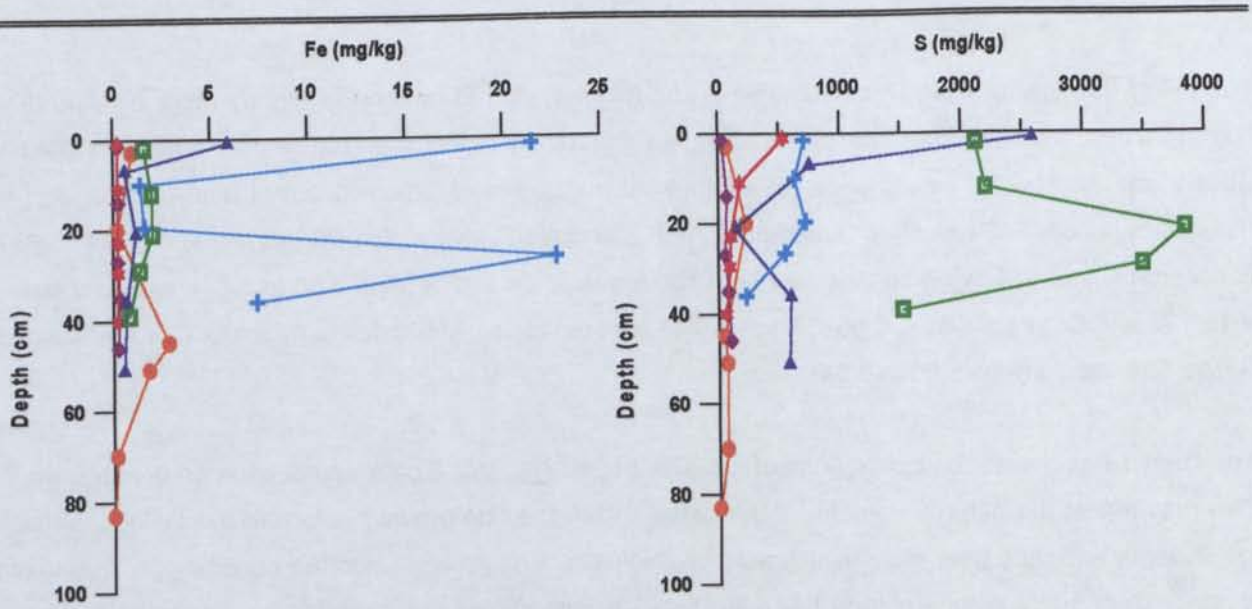

FIG 5.60 FE AND S PROFILES FOR CHESNEY

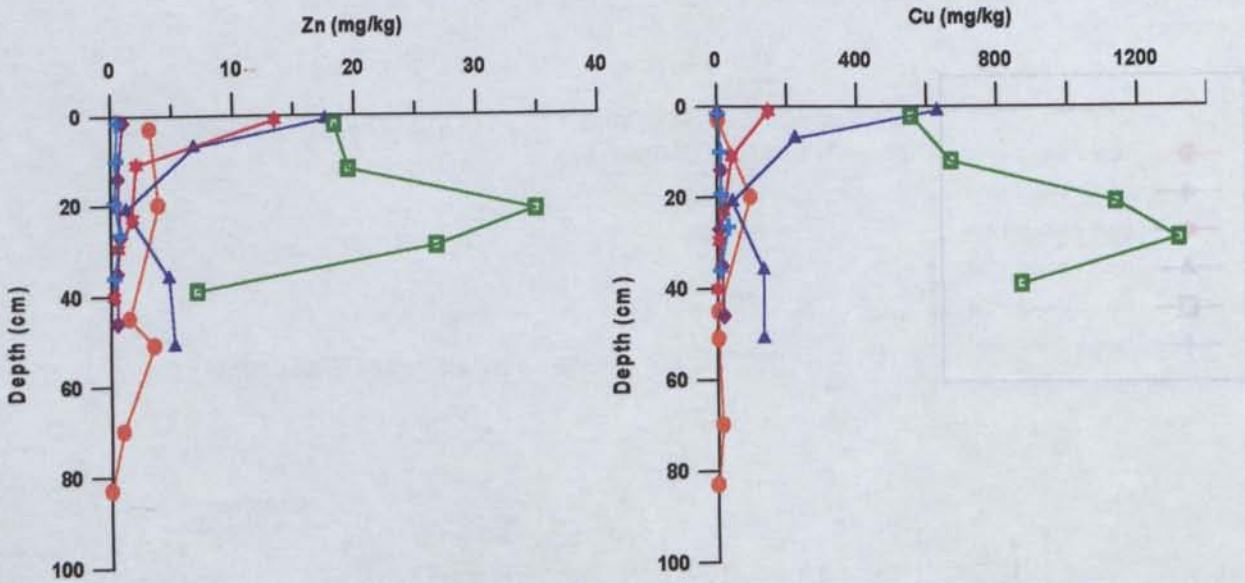

FIG 5.61 ZN AND CU PROFILES FOR CHESNEY

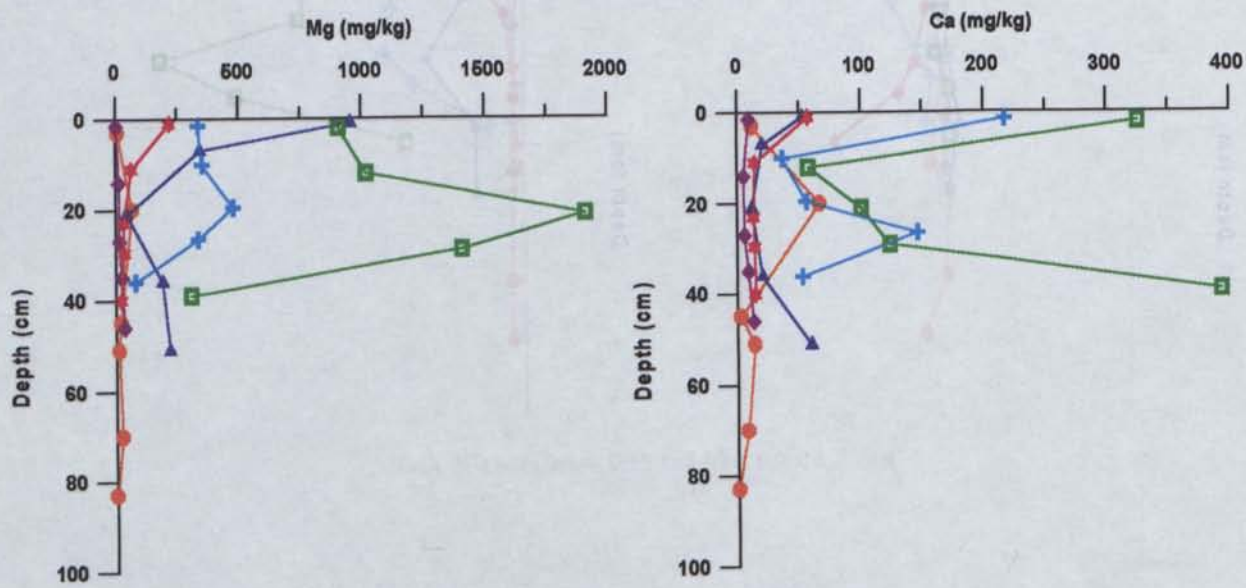

FIG 5.62 MG AND CA PROFILES FOR CHESNEY

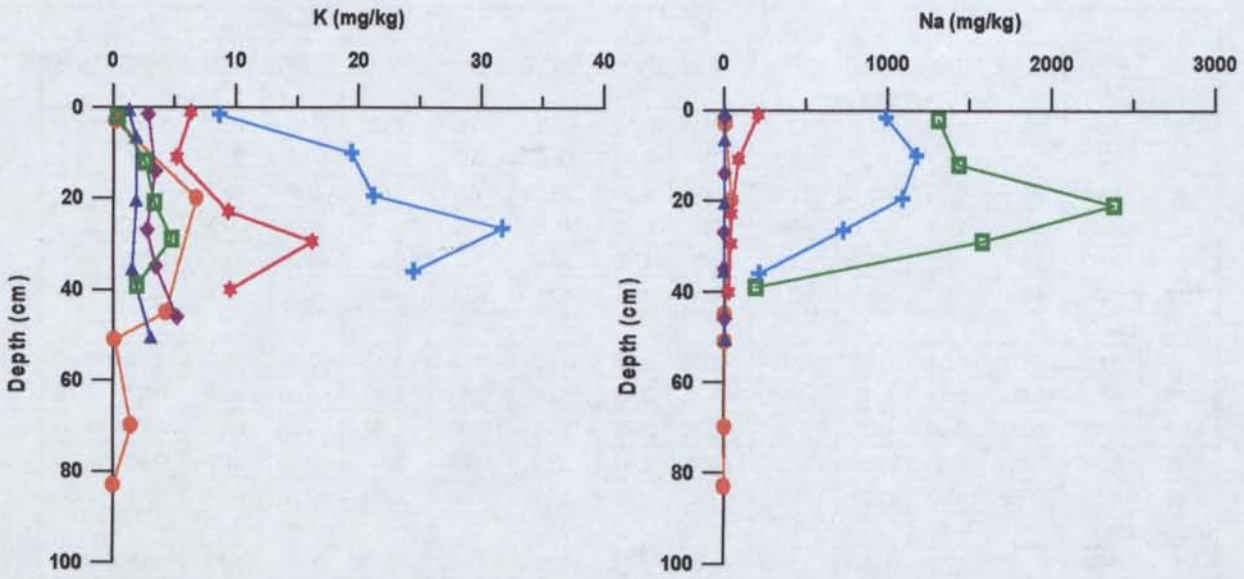

FIG 5.63 K AND NA PROFILES FOR CHESNEY

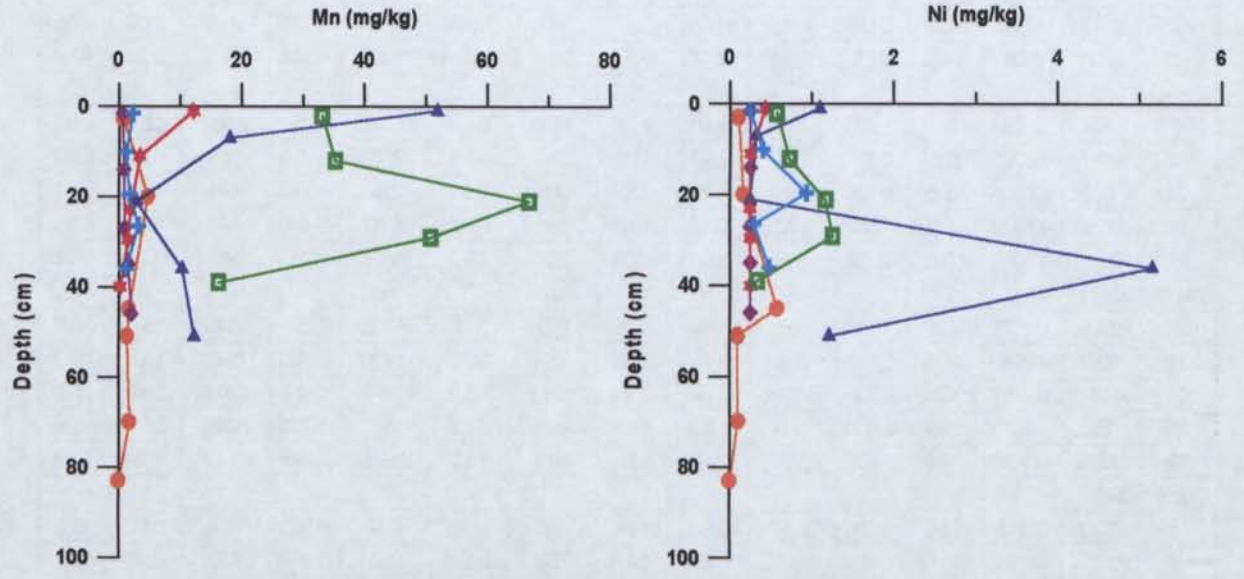

FIG 5.64 MN AND NI PROFILES FOR CHESNEY

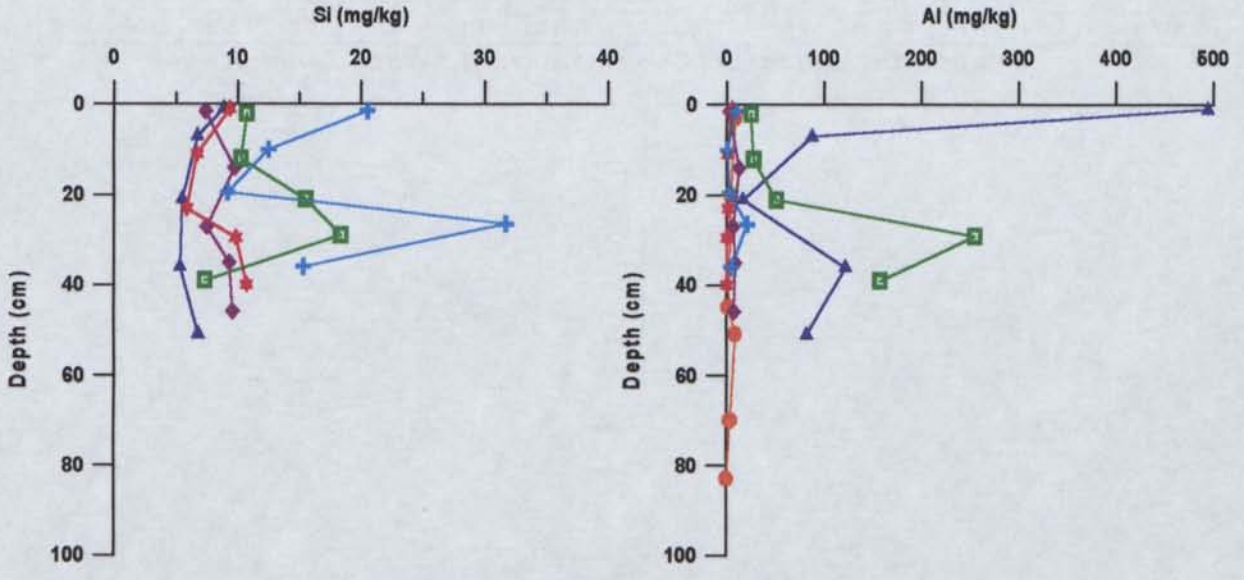

FIG 5.65 SI AND AL PROFILES FOR CHESNEY

	Al	B	Ca	Co	Cu	Fe	K	Mg	Mn	Na	Ni	S	Zn	Si
	mg/kg	mg/kg	mg/kg	mg/kg	mg/kg	mg/kg	mg/kg	mg/kg	mg/kg	mg/kg	mg/kg	mg/kg	mg/kg	mg/kg
Site 2 (1995)														
3	8.39	<0.1	11.8	<0.1	3.14	1.0	0.22	9.21	0.8	7.02	0.10	70.3	3.19	
20	4	0.4	66.7	0.2	96.8	0.2	6.79	66.0	4.8	45.3	0.17	230	3.92	
45	1.74	<0.1	2.76	<0.1	2.80	2.9	4.29	20.0	1.6	3.90	0.6	49.1	1.49	
51	8.85	<0.1	13.4	<0.1	4.04	1.8	0.10	11.6	1.4	4.25	<0.1	69.5	3.55	
70	3.63	<0.1	8	<0.1	13.8	0.2	1.48	24.6	1.7	5.61	<0.1	71.0	0.97	
83	0	<0.1	0	<0.1	<0.1	<0.1	<0.1	<0.1	<0.1	<0.1	<0.1	<0.1	<0.1	
Site 2 (1996)														
1.5	2.59	<0.025	9.04	0.05	1.92	<0.25	2.85	3.52	0.55	3.57	<0.25	33.5	0.98	7.40
14	12.9	<0.025	5.11	0.05	11.38	<0.25	3.42	13.4	0.84	2.38	<0.25	69.9	0.57	9.76
27	6.68	<0.025	5.68	0.05	7.28	<0.25	2.79	15.3	0.96	1.62	<0.25	58.1	0.78	7.50
35	8.57	<0.025	8.87	0.055	13.9	0.34	3.47	25.9	1.565	2.09	<0.25	81.9	0.48	9.33
46	7.62	<0.025	13.0	0.06	18.8	<0.25	5.21	34.1	2.08	2.70	<0.25	99.1	0.51	9.60
Site 3 (1996)														
1	5.59	0.065	57.1	0.485	147	<0.25	6.34	220	12.1	209.05	0.43	536	13.5	9.35
11	0.87	0.03	14.0	0.14	42.2	<0.25	5.15	64.1	3.37	86.0	<0.25	175	2.10	6.72
23	1.50	<0.025	12.8	0.06	20.7	<0.25	9.39	32.7	1.935	44.4	<0.25	102	1.78	5.88
29.5	0.11	<0.025	13.9	0.05	6.43	<0.25	16.2	34.0	1.515	41.9	<0.25	94.8	0.62	9.85
40	0.09	0.04	14.3	0.05	0.05	<0.25	9.53	21.8	0.215	27.6	<0.25	62.3	0.25	10.7
Site 4 (1996)														
1	494	0.03	52.7	2.405	630	5.91	1.28	956	51.8	5.47	1.095	2582	17.6	8.87
7	87.7	<0.025	20.1	0.83	223	0.605	1.86	345	18.0	3.17	0.315	751	6.82	6.73
21	16.3	<0.025	11.5	0.13	45.2	1.18	1.84	44.82	2.89	2.87	<0.25	141	1.27	5.51
36	122	<0.025	20.5	0.5	132	0.68	1.53	191	10.27	2.32	5.155	598	4.73	5.35
51	82.2	<0.025	60.0	0.505	133	0.525	3.06	219	12.3	3.71	1.215	578	5.22	6.81
Site 6 (1996)														
2	24.9	0.175	326	1.61	555	1.58	0.37	907	33.0	1308	0.57	2119	18.3	10.7
12	27.7	0.14	57.6	1.825	668	1.97	2.60	1019	35.2	1432	0.725	2196	19.5	10.3
21	50.7	0.175	100	3.335	1136	2.03	3.34	1911	66.8	2378	1.17	3836	34.9	15.5
29	255	0.2	124	2.405	1317	1.375	4.76	1408	50.8	1577	1.255	3490	26.7	18.4
39	158	0.105	394	0.725	867	0.815	1.93	307	16.2	193	0.33	1517	7.04	7.33
Site 7 (1996)														
1.5	8.92	0.315	218	0.04	1.57	21.5	8.65	337	2.23	987	<0.25	706	0.50	20.5
10	0.89	0.175	36.6	0.05	8.96	1.385	19.4	353	1.195	1174	0.395	630	0.42	12.5
19.5	2.68	0.135	56.0	0.08	12.4	1.59	21.2	479	1.77	1088	0.935	720	0.33	9.17
26.5	20.9	0.315	146	0.095	31.6	22.7	31.7	336	3.22	728	0.295	551	0.74	31.7
36	4.36	0.165	52.8	0.05	7.87	7.38	24.5	80.63	1.13	215	0.48	226	0.26	15.3

TABLE 5.6 CHESNEY SOLUTE CONCENTRATIONS (1:5 BATCH LEACHING)

5.4.3 Pine Creek Inlier, N.T

5.4.3.1 Woodcutters Pb-Zn Mine

Four sites were targeted for investigation at the Woodcutters site. Site 1 is located in the fine-grained central tailings, Site 2 in a gully, Site 3 at a seepage site where a hardpan was developing and Site 4, 20m way from Site 3 where a hardpan had formed to a lesser extent.

The Site 1 (Central Site) profiles show generally low levels of solute concentrations, with many elements below detectable limits (Table 5.7). Calcium, Cd, Mg, Pb, S and Zn all exhibit similar profiles of increased concentrations at the surface and a rapid decrease with depth (Figs 5.67 to 5.70). These concentrations have resulted from the precipitation of gypsum and anglesite at the surface. Magnesium may be present as minor traces of hexahydrite not detected by XRD, while Cd and Zn are probably concentrated through absorption or coprecipitation reactions with the minerals already discussed.

Potassium and Na are present in low concentrations and show a similar decrease with depth but prevail to lower depths in the profile (Figs 5.71). Manganese is also present in low concentrations but has developed a variable profile and generally increases with depth (Fig 5.72). This pattern is not observed at other sites where Mn concentrations exhibit a decrease with depth similar to the majority of other elements.

The Site 2 (Gully Site) profiles have greater concentrations of most solutes than those observed in Site 1 except for Fe. Higher levels of Mg, Mn, S and Zn are present with minor increases in Ni, Pb, P and Cd (Table 5.7). The majority of elements show increased levels at the surface which then decrease with depth (Figs 5.67 to 5.72). Calcium shows a slight increase at 25cm at the depth of a palaeo-surface, while Cd, Mg, Mn, Ni, S and Zn show increases at 42cm depth, which is again associated with secondary mineral development at a palaeo-surface.

Lead, K and Na are also concentrated deeper in the profile and may also be associated with this palaeo-surface. The low levels of Pb, K and Na at the surface may be attributed to a number of factors. Firstly low levels may be due to original levels in the gangue and weathering characteristics of the minerals. Additionally levels can be simple function of element mobility under these conditions which have resulted in leaching from surface regions. Low levels could also be due to precipitation of insoluble salts within the hardpan surface and thus elements may not be available for this type of analysis. This site is located closer to the dam wall and contains slightly coarser material which has been exposed due to gully erosion. These conditions have promoted oxidation of the sulfides and gangue mineral degradation, and thus elevated solute levels.

The Site 3 (Seepage Site) profiles exhibit the largest solute concentrations of all sites examined (Table 5.7). Again the majority of elements show a general decrease in concentration with depth except for high concentrations at a palaeo-surface at 20cm depth. An important difference at this location is the increased amount of Fe present with maximum concentration of 15000 mg/kg and associated large increases in Zn, S, Mg and minor increases in Al, Ca, Cd, Co, Cu, Mn, Ni, P and Pb occurring at 20cm. Much of this increase can be attributed to the precipitation of gypsum, anglesite, sulfur, beudantite and melanterite and the coprecipitation and absorption reactions associated with their formation. These elevated concentrations have developed in response to added solute input from seepage water and the enhanced conditions of sulfide oxidation and gangue mineral degradation induced by this seepage.

The profile at Site 4, 20m away shows similar decreases in all elements with depth. The majority of elements are in similar or greater concentrations than those at Site 2 but lower concentrations than those at Site 3 (Table 5.7). This site is thought to represent a previous zone of seepage in which hardpan development has been promoted. If this is correct it would suggest that the solute levels within the tailings at the seepage zone (Site 3) will subside once the seepage stops. The reduction may occur in response to the development of insoluble cements.

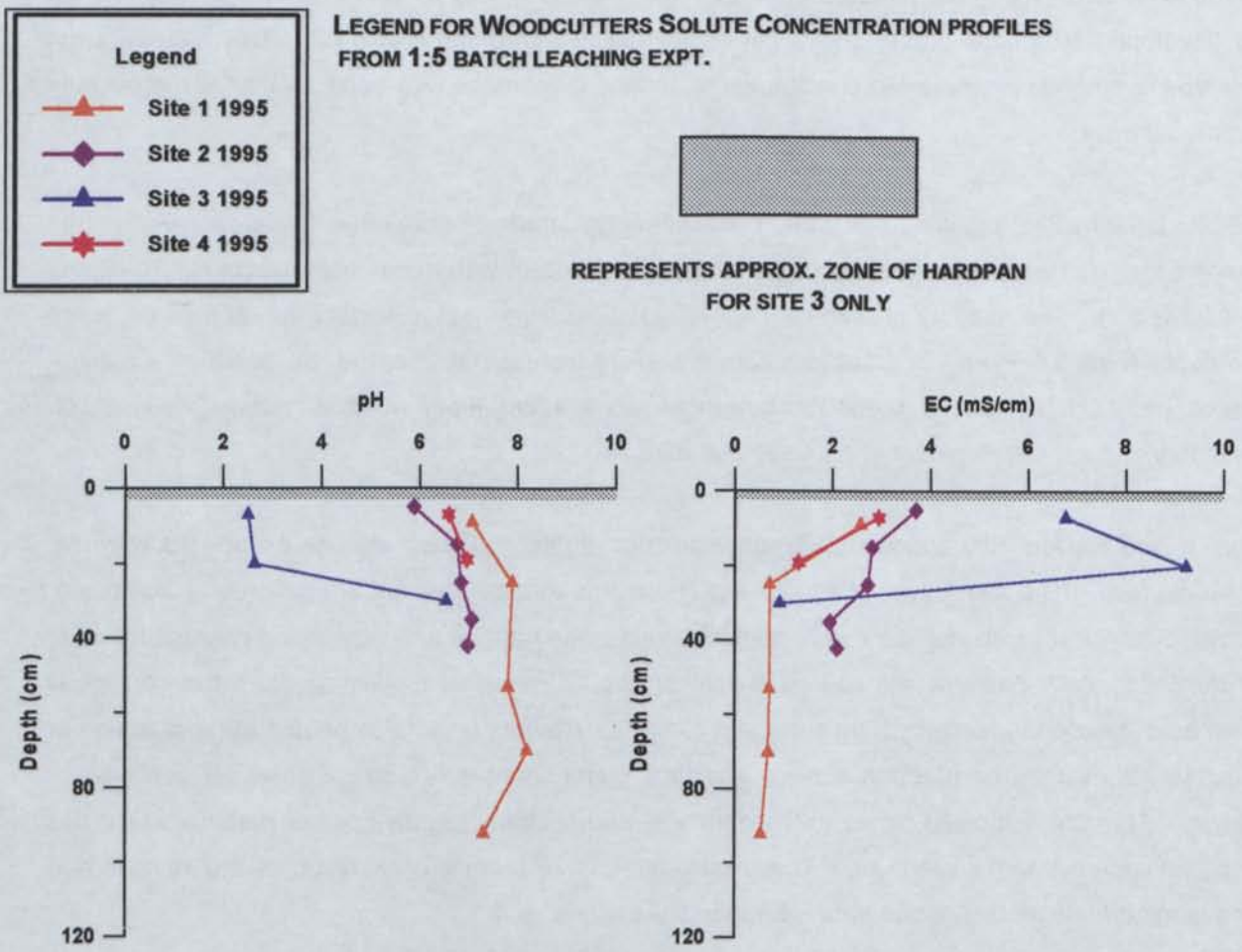

FIG 5.66 pH AND EC PROFILES FOR WOODCUTTERS

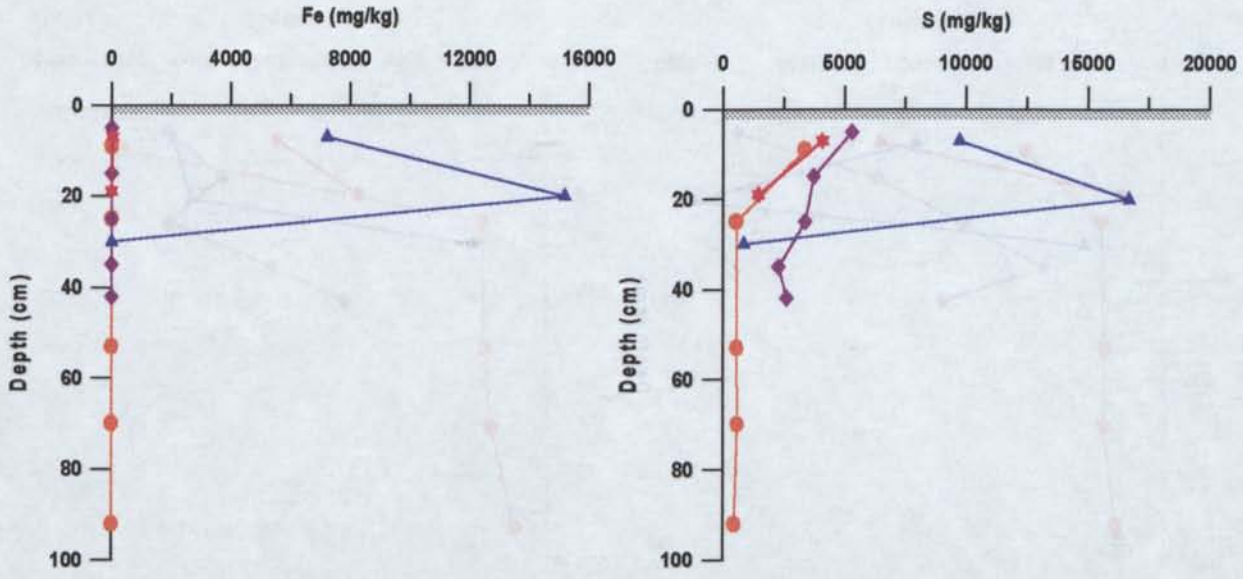

FIG 5.67 FE AND S PROFILES FOR WOODCUTTERS

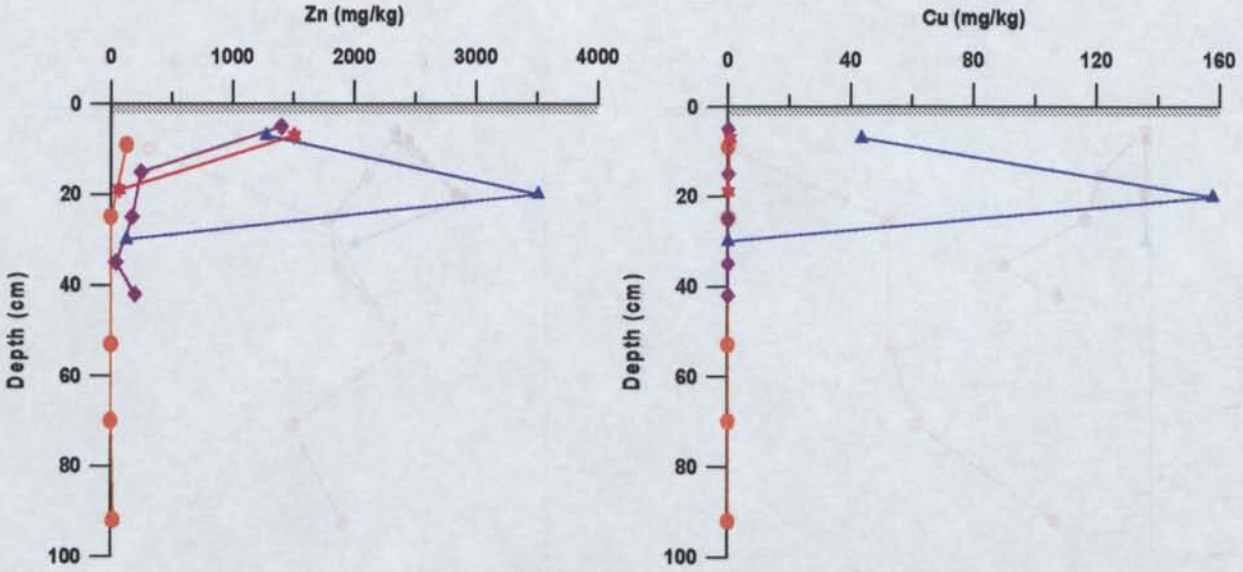

FIG 5.68 ZN AND CU PROFILES FOR WOODCUTTERS

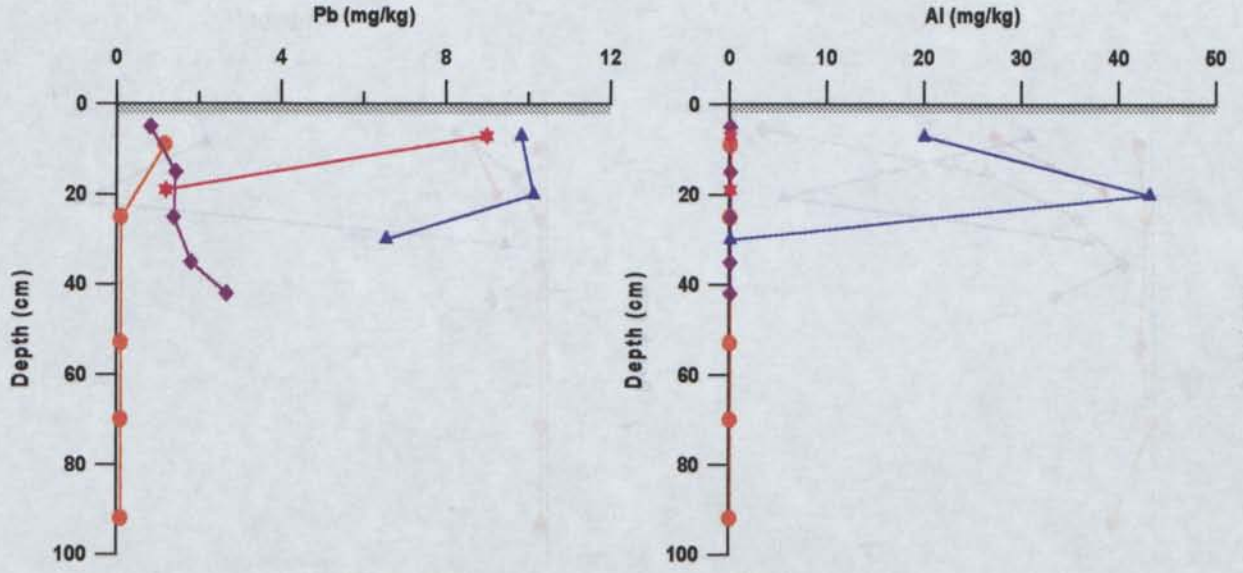

FIG 5.69 PB AND AL PROFILES FOR WOODCUTTERS

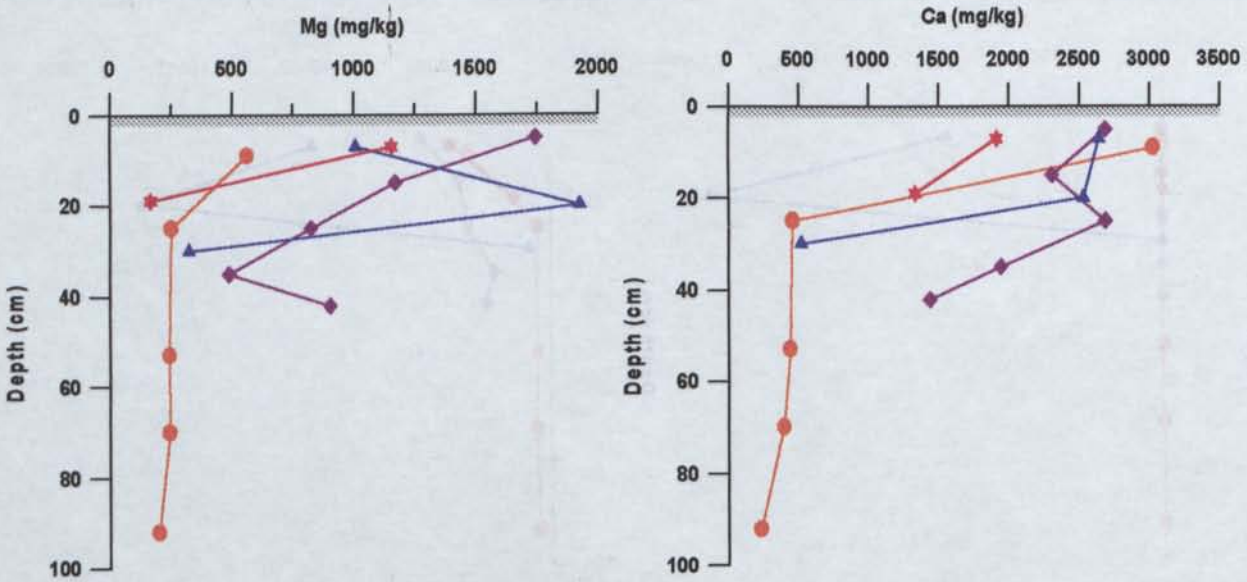

FIG 5.70 MG AND CA PROFILES FOR WOODCUTTERS

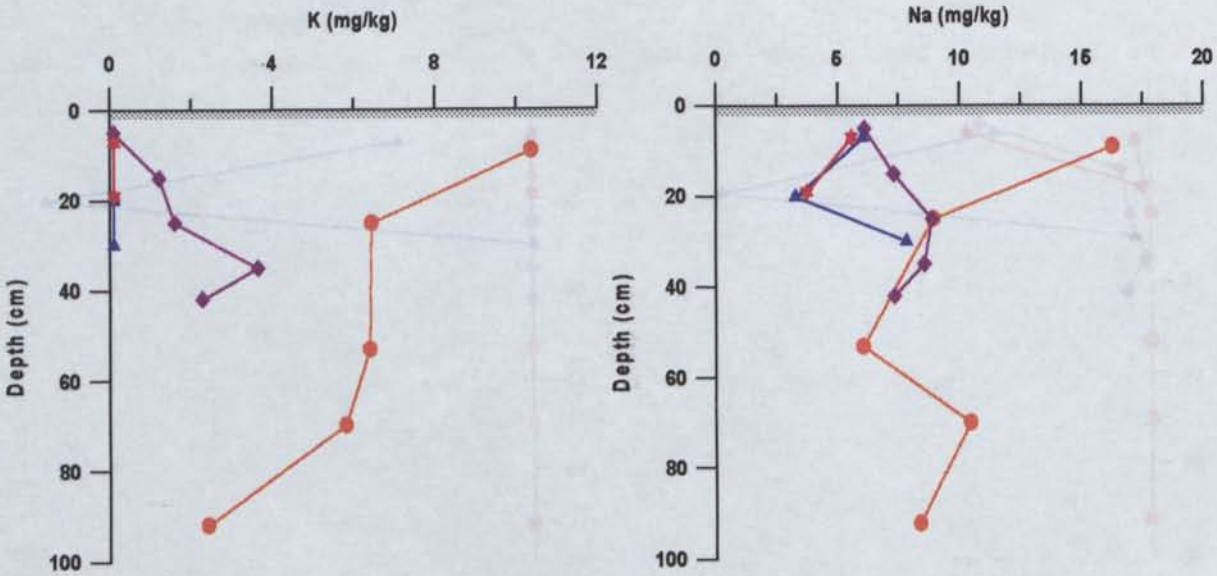

FIG 5.71 K AND NA PROFILES FOR WOODCUTTERS

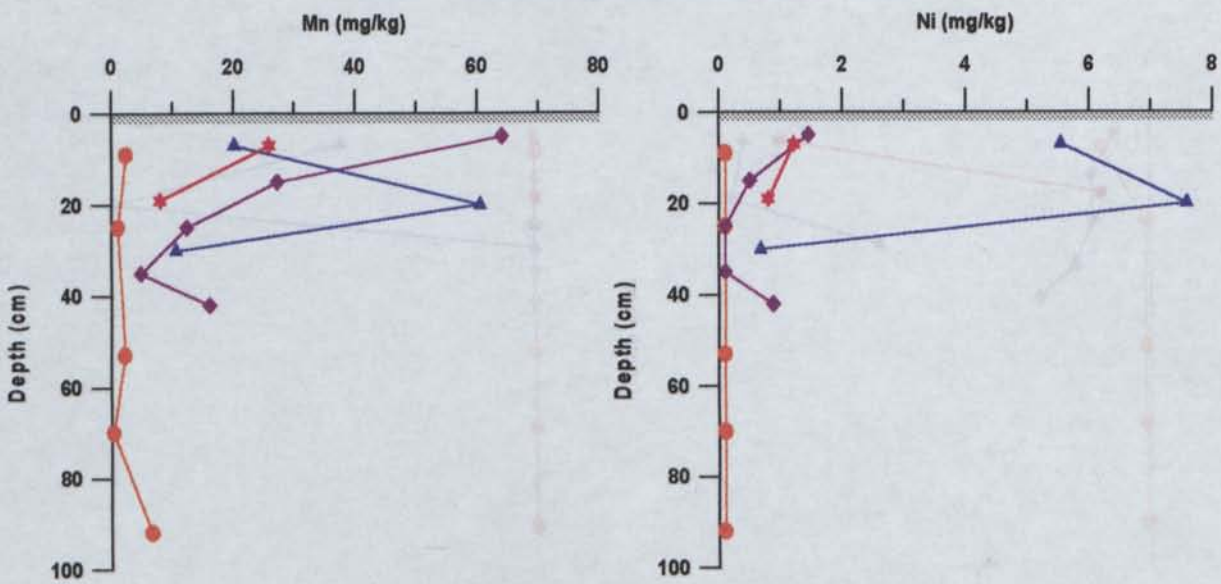

FIG 5.72 MN AND NI PROFILES FOR WOODCUTTERS

5.4.3.1.1 Discussion

As mentioned in Chapter 4, it would appear that at least four very different geochemical environments have developed within TD1. The Central Site (site 1) has low solute concentrations and very limited secondary mineral formation along with a generally high pH of between 7 and 8. It is suggested that it is the very fine nature of the tailings at this location that has dictated these conditions through elevated saturation levels, reducing oxygen diffusion, and thus reduced oxidation reaction.

The large washout formed at the Gully Site (Site 2) has exposed sulfides to increased oxygen, enhanced sulfide oxidation and by-product development and has potentially resulted in increased elemental transport by rapidly moving water. As mentioned previously the Seepage Site (Site 3) has developed a very low pH of approx. 2, considerably different from that of the other sites examined. This site has been continuously leached with pH 5 water containing high levels of Ca, Mg, S, Zn and probably increased dissolved oxygen levels. As a result, sulfide oxidation has been promoted, by-product development enhanced and hardpan formation has occurred. A comparison with the Site 4 hardpan, thought to have developed under similar conditions, suggests solute levels will subside once seepage is excluded, potentially through the development of insoluble cements.

	Al	Ca	Cd	Co	Cu	Fe	K	Mg	Mn	Na	Ni	Pb	S	Zn
	mg/kg	mg/kg	mg/kg	mg/kg	mg/kg	mg/kg	mg/kg	mg/kg	mg/kg	mg/kg	mg/kg	mg/kg	mg/kg	mg/kg
Site 1														
9	<0.1	3027	3.105	<0.1	<0.1	<0.1	10.4	563	2.36	16.3	<0.1	1.17	3353	126
25	<0.1	456	<0.1	<0.1	<0.1	<0.1	6.45	249	1.08	8.93	<0.1	<0.1	551	1.215
53	<0.1	439	<0.1	<0.1	<0.1	<0.1	6.4	243	2.22	6.06	<0.1	<0.1	556	1.855
70	<0.1	395	<0.1	<0.1	<0.1	<0.1	5.81	244	0.34	10.5	<0.1	<0.1	591	0.59
92	<0.1	231	<0.1	<0.1	<0.1	<0.1	2.41	199	6.68	8.38	<0.1	<0.1	447	18.66
Site 2														
5	<0.1	2688	11.2	<0.1	<0.1	<0.1	<0.1	1747	64.1	6.11	1.45	0.82	5306	1400
15	<0.1	2305	0.81	<0.1	<0.1	<0.1	1.22	1171	27.2	7.29	0.50	1.43	3726	246
25	<0.1	2685	1.21	<0.1	<0.1	<0.1	1.61	824	12.3	8.88	<0.1	1.38	3388	173
35	<0.1	1942	<0.1	<0.1	<0.1	<0.1	3.65	489	4.80	8.57	<0.1	1.8	2279	39.32
42	<0.1	1438	2.95	<0.1	<0.1	<0.1	2.28	903	16.1	7.34	0.88	2.67	2613	196
Site 3														
7	20	2641	12.1	<0.1	43.48	7223	<0.1	1008	20.1	6.05	5.54	9.83	9732	1275
20	43.2	2529	41.2	0.69	158	15190	<0.1	1927	60.5	3.27	7.58	10.13	16673	3510
30	<0.1	520	<0.1	<0.1	<0.1	<0.1	<0.1	323	10.6	7.83	0.68	6.55	856	125
Site 4														
7	<0.1	1913	2.45	<0.1	0.58	37.98	<0.1	1156	25.8	5.57	1.21	8.99	4086	1505
19	<0.1	1332	1	<0.1	<0.1	<0.1	<0.1	166	7.98	3.73	0.80	1.19	1453	67.5

TABLE 5.7 WOODCUTTERS SOLUTE CONCENTRATIONS (1:5 BATCH LEACHING)

5.4.4 Dundas Trough, Tas.

5.4.4.1 Renison Bell Sn Mine

The effectiveness of hardpans as sulfide oxidation inhibitors at this mine was investigated through geochemical comparisons between young and old tailings surfaces where hardpan development was at different stages. The young surface of Dam C-Site 2 where surface tailings have only begun to oxidise and hardpan development is yet to occur was compared with Dam A - Site 2 and Dam B - Site 2 which have been exposed for 17 and 16 year respectively and have mature hardpan development.

A geochemical investigation of the profile developed at Dam A -Site 1 has also been undertaken. This site shows a profile which possibly does not represent the bulk of the tailings surface as the surface has been highly fractured, causing the exposure and subsequent oxidation of the underlying tailings. However, it does give an indication of the potential of the tailings to produce very acidic conditions and potentially large pollutant loads.

5.4.4.1.1 Dam A - Site 1

The solute concentrations observed at this site are some of the highest levels detected within the Renison tailings system (Figs 5.74 to 5.79, Table 5.8). This has resulted from sulfide oxidation taking place down to 20cm depth due to the fractured hardpan surface. This oxidation has produced acidic conditions of pH 2.2-2.4 (Fig 5.73). As a consequence of this, total soluble Fe contents of up to 4080 mg/kg and S levels of up to 4510 mg/kg have developed. Additionally Cu, Ni and Zn levels, although minimal, are higher than the other locations investigated. In response to these acidic conditions the breakdown of gangue minerals has accelerated resulting in marginally elevated Al contents. Magnesium and Na levels although elevated in comparison with Dam A -Site 2 and Dam B -Site 2 are significantly lower than the profile developed at Dam C-Site 2.

The massive hardpan at 20cm depth below this acidic tailings surface appeared competent and thus is seemingly unaffected by these low pH conditions. It is expected that below this massive hardpan, tailings are unoxidised and thus do not contain potential pollutant loads. If however the underlying tailings are in fact oxidised as a result of previous exposure, the soluble elemental load developed in this zone would perhaps not be susceptible to leaching by water because of the low permeability of the massive overlying hardpan.

5.4.4.1.2 Dam A -Site 2 & Dam B -Site 2

A comparison of the geochemical profiles developed at Dam A -Site 2 & Dam B -Site 2 beneath well-developed hardpans show that Dam A generally has slightly lower values of the main solutes in this system, Fe, Mn, Mg, S and Ca, compared with Dam B (Figs 5.74, 5.76 & 5.78, Table 5.8). These lower

levels can be attributed to gradual leaching from the surface with time, incorporation in surface cements, or slight variations in the primary mineral concentrations. The pH of 5-6 of these surface profiles is quite remarkable considering the acid producing potential of these tailings particularly as they contain such a high sulfide content (Fig 5.73). The main point of interest however is the large variation in the geochemical profiles developed under these hardpans compared with the freshly exposed surface at Dam C-Site 2.

5.4.4.1.3 Dam C -Site 2

The Dam C geochemical profile, developed in an area where hardpans are yet to form, gives an indication of potential solute load in leachate if hardpans did not develop. Results also give insight into the scavenging potential of the hardpan cements produced within the older dams. The values of Fe, S, Mg, Mn and K within the Dam C profile are up to twice that in Dam A -Site 2 and Dam B -site 2 (Figs 5.74 to 5.78). Maximum values are observed at *either* the surface or near the base of the oxidised zone. Lower surface levels, compared with levels near the base of the oxidised zone have developed either as a result of leaching from the surface or alternatively, the reduction in solute load at the surface may be due to incorporation into insoluble surface cements (goethite and lepidocrocite).

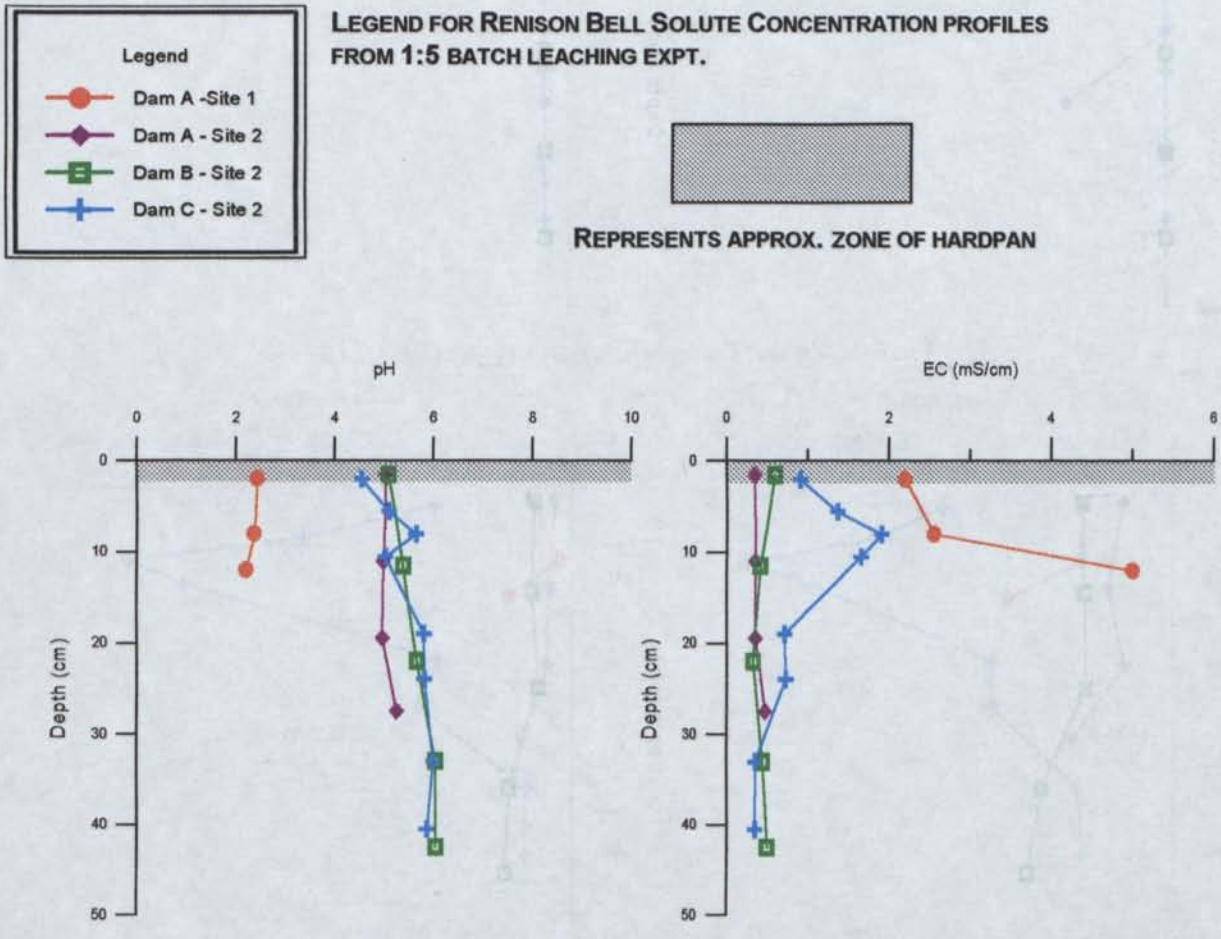

FIG 5.73 pH AND EC PROFILES FOR RENISON BELL

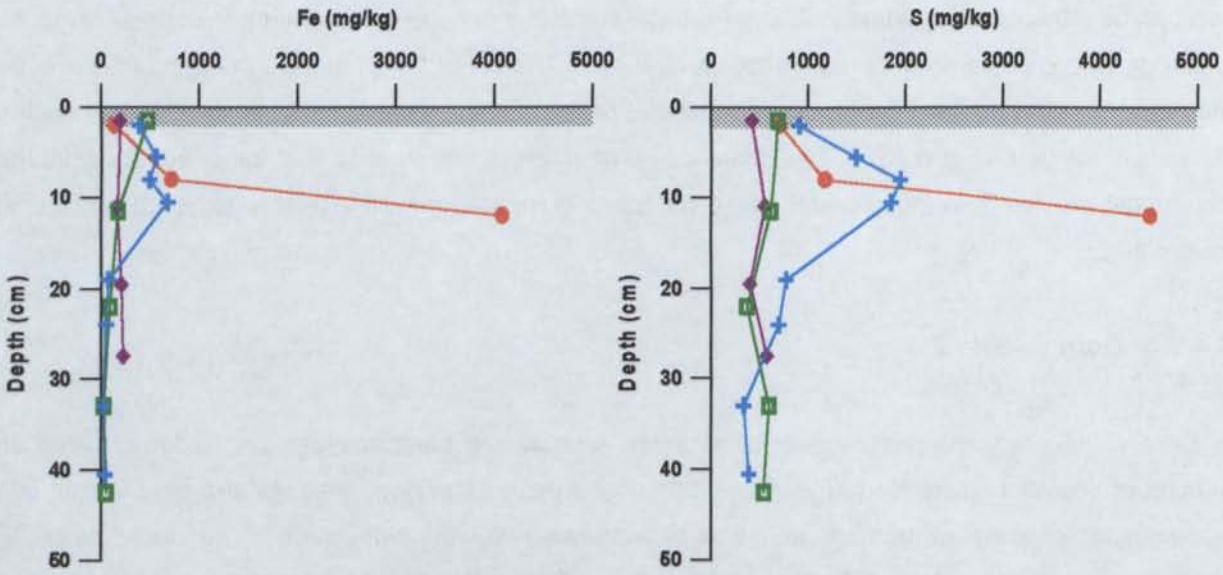

FIG 5.74 FE AND S PROFILES FOR RENISON BELL

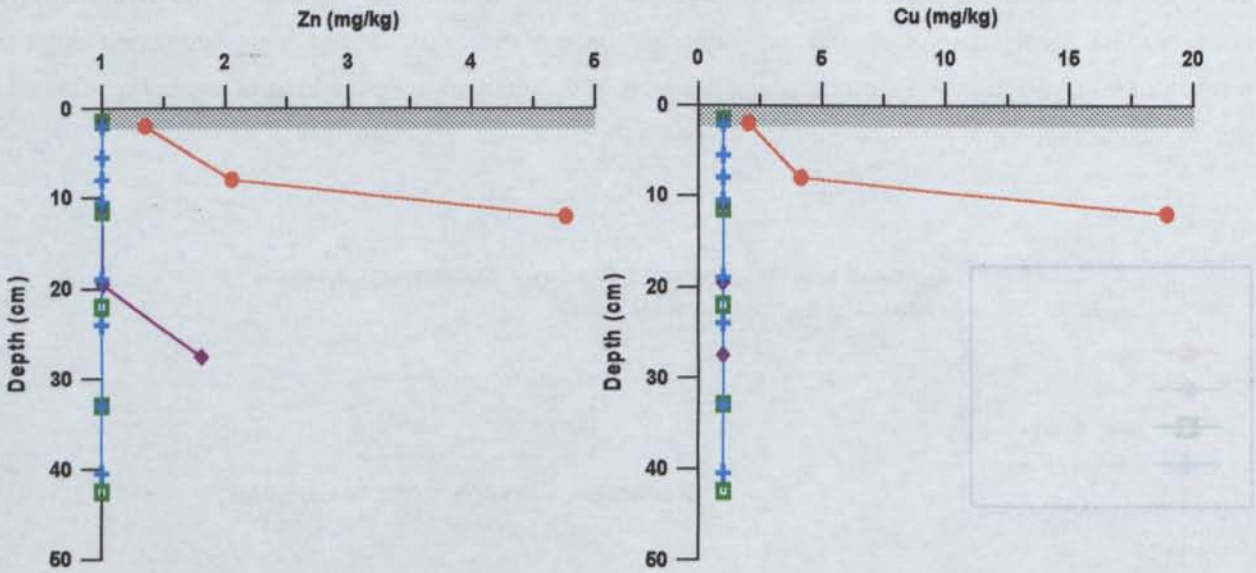

FIG 5.75 ZN AND CU PROFILES FOR RENISON BELL

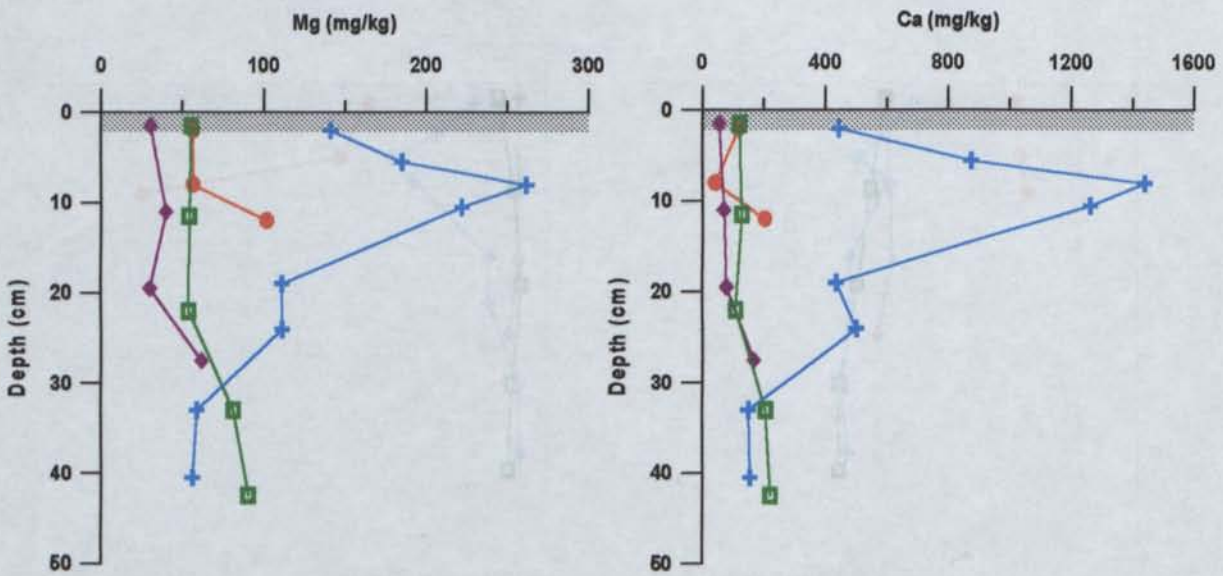

FIG 5.76 MG AND CA PROFILES FOR RENISON BELL

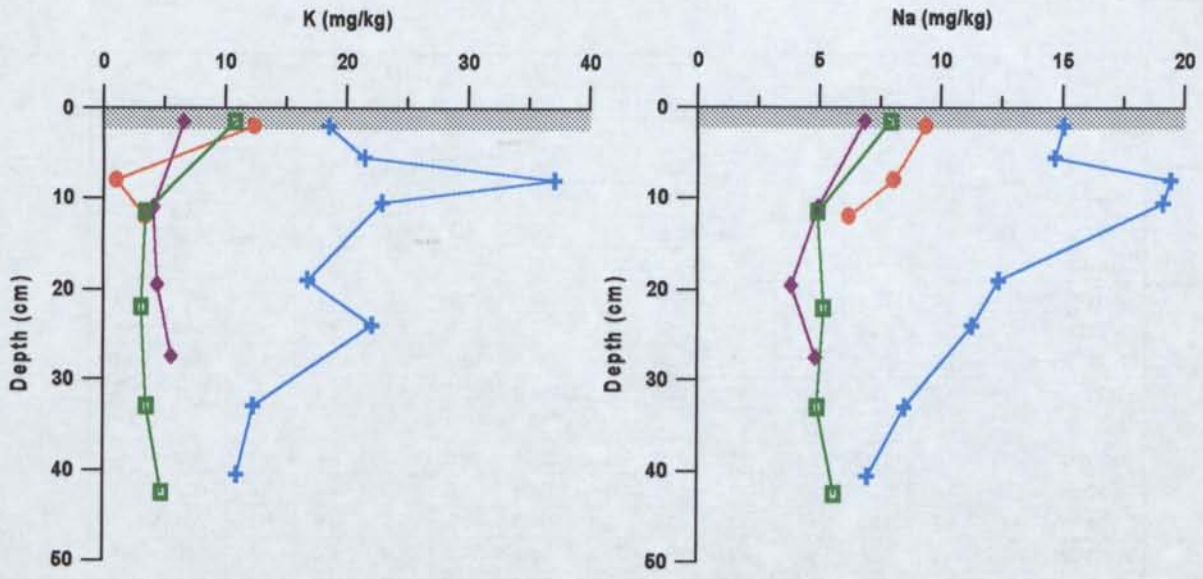

FIG 5.77 K AND NA PROFILES FOR RENISON BELL

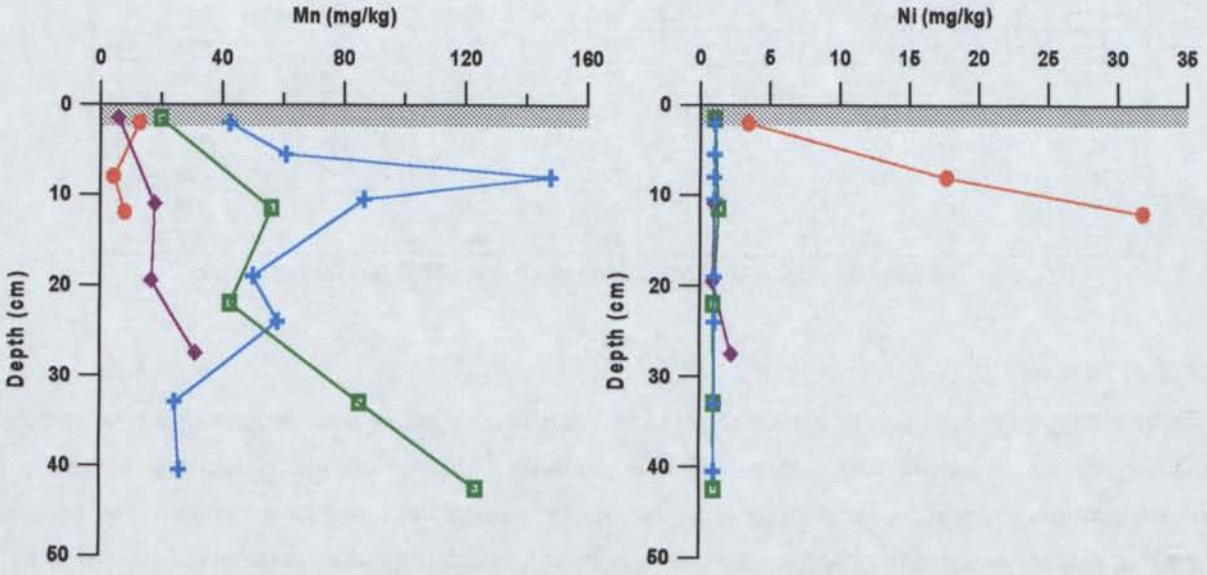

FIG 5.78 MN AND NI PROFILES FOR RENISON BELL

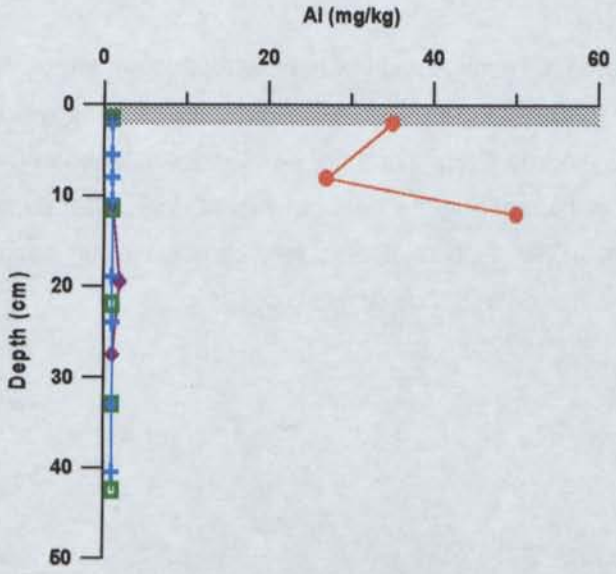

FIG 5.79 AL PROFILE FOR RENISON BELL

	Al	B	Ca	Co	Cu	Fe	K	Mg	Mn	Na	Ni	Pb	S	Zn
	mg/kg	mg/kg	mg/kg	mg/kg	mg/kg	mg/kg	mg/kg	mg/kg	mg/kg	mg/kg	mg/kg	mg/kg	mg/kg	mg/kg
DA S1														
1-3 cm	35	<1	119	<1	2.0	138	12.4	56.5	12.7	9.4	3.5	<1	710	1.4
7-9 cm	27	<1	41.6	<1	4.2	714	<1	56.6	4.3	8.0	17.7	<1	1166	2.1
11-13 cm	50	<1	204	1.3	18.9	4081	3.4	102	8.0	6.2	31.8	<1	4510	4.8
DA S2														
0-3 cm	<1	1.0	55.1	<1	<1	196	6.6	30.7	5.8	6.9	<1	<1	415	<1
9-13 cm	<1	1.0	69.2	<1	<1	164	4.1	39.8	17.9	5.0	<1	<1	548	<1
18-21 cm	2.0	1.0	79.3	<1	<1	204	4.4	30.0	16.7	3.8	0.9	<1	395	1.0
26-29 cm	<1	1.2	167	<1	<1	226	5.6	61.8	31.4	4.8	2.2	<1	571	1.8
DB S2														
0-3 cm	<1	1.1	120	<1	<1	471	10.8	55.4	19.8	7.9	<1	<1	682	<1
10-13 cm	1.0	1.2	128	<1	<1	173	3.5	54.0	56.2	4.9	1.3	<1	607	<1
20-24 cm	<1	1.2	108	<1	<1	86.2	3.1	53.8	42.6	5.2	0.9	<1	361	<1
31-35 cm	<1	1.2	206	<1	<1	25.8	3.5	81.4	85.2	4.9	1.0	<1	590	<1
40-45 cm	<1	1.2	220	<1	<1	51.0	4.8	90.4	123.5	5.6	<1	<1	539	<1
DC S2														
0-4 cm	<1	<1	443	<1	<1	384	18.5	141	42.3	15.0	<1	<1	904	<1
4-7 cm	<1	1.2	874	<1	<1	560	21.5	185	60.9	14.7	<1	<1	1486	<1
7-9 cm	<1	1.8	1439	<1	<1	490	37.1	262	148	19.4	<1	<1	1939	<1
9-12 cm	<1	1.7	1261	<1	<1	677	22.9	222	86.7	19.1	<1	<1	1844	<1
17-21 cm	<1	1.4	435	<1	<1	72.6	16.8	111	50.1	12.4	<1	<1	767	<1
23-25 cm	<1	1.4	501	<1	<1	50.9	22.1	111	58.4	11.3	<1	<1	689	<1
32-34 cm	<1	1.2	150	<1	<1	20.1	12.3	59.0	24.5	8.5	<1	<1	328	<1
39-42 cm	<1	1.1	155	<1	<1	39.2	11.0	56.1	26.1	7.0	<1	<1	382	<1

TABLE 5.8 RENISON BELL SOLUTE CONCENTRATIONS (1:5 BATCH LEACHING)

5.4.4.1.4 Discussion

In locations where the hardpan is unbroken a pH of 5.5-6 occurs below the hardpan and is associated with the presence of calcite and siderite. These relatively high pH conditions and the presence of neutralising minerals indicate acid generation has been substantially reduced beneath the hardpan surface. In locations where the hardpan surface has been disrupted through excavation, the pH is very low and elevated solute concentrations have developed.

The surface profiles investigated in Dams A and B where hardpans are intact, contain solute levels lower than those beneath ruptured hardpan and are far lower than those developed in regions of initial exposure prior to hardpan development (e.g. Dam C - Site 2). As outlined in Chapter 4, these conditions of pH 5-6 and the presence of calcite may be to some extent due to the presence of the hardpans. It must also be considered that in this high rainfall region, constant water saturated conditions must be playing a role in reducing O_2 diffusion and thus sulfide oxidation.

5.4.5 Geochemical Overview of Site Investigations

The geochemistry of the near surface tailings is a complex and dynamic system influenced by many physical, mineralogical and chemical properties. Each of the sites discussed have unique geochemical characteristic as evidence of these properties. The data displayed within this chapter are testimony to the fact that hardpan and cemented layer development has a dramatic effect on the near surface solute loads.

The cemented layers developed throughout the upper surface of the Broken Hill tailings dams have strongly influenced solute concentrations. Not only do they have the ability to scavenge elements into their mineralogical structures, but once formed can influence the physical properties of the zone, enhancing their own development. Once cementation is initiated, water movement through the profile is effected. As primary skeletal grains become bridged with secondary minerals, the vertical permeability is restricted allowing the build up of water containing solutes. During drying this water is evaporated, some of the solutes may be transported to the surface, however precipitation of solutes also occurs insitu. These soluble salts are then available for cementing and may eventually change to less soluble mineral phases reducing the solute concentrations. Once the cemented layers become an extensive horizon, they may promote lateral movement of water under higher rainfall conditions. Additionally solute concentrations may become elevated beneath the layer through occlusion of vertically leaching waters.

The Chesney tailings dams provide insight into the effect grain size distribution has on solute generation and cement development. At this location the tailings mineralogy does not support hardpan formation. Cement formation is promoted through additional input via solute laden seepage from scree slopes above the dam. Hardpan development has been restricted to the coarse tailings at the edge of the dam. Here solutes have been concentrated through evaporation producing cements to at least 1m depth. Hardpan development has not occurred 15m further down slope in finer tailings even though seepage has resulted in elevated solute concentrations. It is suggested that the finer tailings have maintained greater moisture contents and thus solutes have not been concentrated through evaporation and precipitation as insoluble cements.

In many of the other sites investigated comparisons of solute loads from old hardpan and new tailings profiles were made (Elura, CSA and Renison Bell). Comparable solute concentrations within the various dams at the CSA and Elura sites indicate that constant solute levels can be maintained for some time beneath the hardpan surface. Investigations at the Renison Bell site indicated that the hardpans have the ability to lessen the surface solute loads compared with the freshly exposed tailings. Hardpans therefore have the ability to suppress the development of additional solutes through coatings on sulfide grains, incorporation into cements and potentially the reduction of oxygen and water into the underlying tailings (see Chapter 7).

Solute variations that do develop are associated with the dynamic nature of the hardpan surface. Chapter 4 has outlined the cycles associated with the development and degradation of surface hardpans and these geochemical investigation have supported these finding. Degradation of mature hardpans may be enhanced in high run-off regions where mechanical erosion, dissolution and lateral transport are promoted. Hardpan degradation results in the re-exposure of primary minerals and can result in the dissolution of previously precipitated secondary minerals if pH, EC and Eh conditions change sufficiently. In this situation, the integrity of the hardpan is compromised and susceptible to erosion. Eventually the hardpan is completely eroded and the underlying sulfides become exposed, allowing the production of a fresh hardpan surface.

Through this process it is apparent that hardpan development can suppress solute generation however in most cases this has a finite time frame before hardpan degradation takes place. The effect of this cycling is dependent on the time frame of hardpan development. At Elura and Renison Bell, hardpan formation is rapid and cycling may occur over a matter of months, thus the impact on solute generation may be minimal. In locations where hardpan development takes longer, the time frame may be extended over which solute leaching occurs from the surface (e.g. CSA).

The geochemistry within the Woodcutters tailings dam is strongly dictated by grain size and external seepage input. The seepage hardpan developed at this site also exhibits solute abatement type characteristics. Results indicate that once seepage is excluded solute levels are reduced potentially through precipitation of insoluble cements.

Each of the sites investigated have unique geochemical properties, enhanced or inhibited by the physical nature of the tailings and their surrounds (e.g. climate). It is obvious from this review that hardpans and cemented layers have the ability to suppress solute development for some finite period before degradation and alteration takes place. The extent to which this occurs is influenced by surface morphology and climatic conditions (wind/water), while the effect this has on solute generation is dependent on the reactivity of the tailings and thus how long it takes for hardpan development.

Chapter 6 : Laboratory Simulations of Hardpan Formation and Implications

6.1 Overview

Many of the tailings dams examined during this study have well-developed hardpans, but the time required for their formation varies dramatically. Three preliminary experiments using fresh tailings from each of the sites, were designed to determine the reactivity of each of the tailings, whether hardpan development could be enhanced and which tailings have the fastest observable hardpan formation.

- Experiment 1 - natural enhancement of hardpans

  designed to investigate the development of hardpans through enhancing the processes which occur naturally through regular watering and increased temperatures.
- Experiment 2 - biological and chemical enhancement of hardpans

  investigated the development of hardpans through biological and chemical enhancement via bacterial inoculations and additions of Fe^{2+} solution at pH 3.

The natural enhancement (Expt 1) was compared with the biological and chemical enhancement (Expt 2) to determine the increase in cement development associated with each treatment. The results obtained from these experiments indicated whether or not liquid additives could be used for hardpan enhancement.

- Experiment 3 - tailings leaching characterisation

  leaching experiment to determine the reactivity of the tailings and the effects hardpan development had on leaching characteristics.

From these preliminary experiments, tailings were selected for use in the main experiment which was designed to investigate the effect of several different additives on hardpan formation. Field investigations have shown that naturally formed tailings hardpans are unlikely to be stable to physical and/or chemical break down, as they do not form persistent indurated layers similar to naturally occurring ferricretes, calcretes and silcretes which are both resistant to erosion and have low porosity and permeability. Additives were selected in part to provide Si, Al, and Ca for the formation of such cements. These additives included flyash, lime, limestone and phosphate mixed with the tailings as a surface mixture or as a discrete layer within the tailings profiles. This experiment was conducted over a 1 year period, at which time permeability, porosity and geochemistry examinations were undertaken to determine the successfulness of each additive on hardpan development.

6.2 Preliminary Hardpan Enhancement and Leaching Experiments

6.2.1 Selection and Design of Experimental Parameters

6.2.1.1 Column Design

The columns constructed for these experiments varied in height and diameter, depending on the materials available and the objectives of each experiment. Columns for Experiments 1 and 2 were constructed using 10.5 and 7.5cm diameter PVC tube and bases respectively, while Experiment 3 columns combined 7.5cm diameter PVC and plastic or ceramic funnels. All columns were constructed using PVC glues and sealed with silicone gel. At the base of each column a Geotextile was used to ensure the tailings were not flushed out. Schematic drawings of the column designs are presented in Fig 6.1.

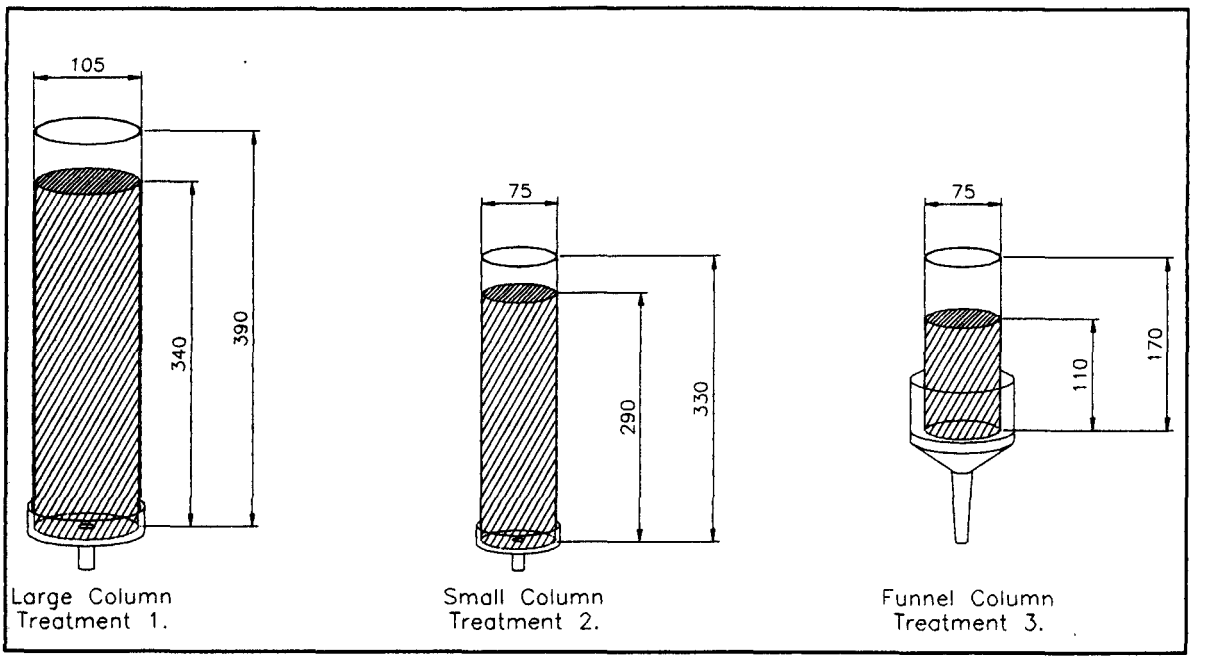

FIG 6.1 PRELIMINARY COLUMN SETUP (ALL MEASUREMENTS IN MM)

6.2.1.2 Column Packing

Samples of fresh tailings from each site were placed in a dough mixer and stirred for a period of approximately 5 minutes to obtain a homogeneous mixture. Distilled water was added to the tailings to obtain a slurry so that packing of the tailings would mimic depositional conditions within an impoundment. Packing of the columns was done in stages to achieve several graded bedding sequences within each column. The supernatant was allowed to drain and the packed columns were then permitted to dry undisturbed for 3 weeks.

6.2.1.3 Determination of Liquid Additive Regime

The volume of liquid added was based upon the rainfall for the locations where well developed hardpans have formed. The optimal average rainfall was determined at 320mm/yr, which corresponds to 6.2mm/wk. The addition required per week to obtain 6.2mm of rainfall was determined for each column size. The rate at which this water moved through the columns was dictated by the physical characteristics of each tailings type.

- Experiment 1 - natural enhancement - large diameter columns (10.5cm) 53ml/wk
- Experiment 2 - biological and chemical enhancement - small diameter columns (7.5cm) 27ml/wk
- Experiment 3 - leaching characterisation - funnel columns (7.5cm)
  1 week of continuous leaching every 3 weeks

6.2.2 Experimental Conditions

6.2.2.1 Experiment 1 - Natural Enhancement of Hardpans

This column experiment was designed to mimic the natural environment within a tailings dam. The study was designed to develop hardpans through enhancing the processes which occur naturally through regular watering and increased temperatures. Each week 53mls of deionised water was added as representative of rainfall. During the week, the columns were exposed to the increased ambient temperatures of the glass house and also to 2 hours (1 hour per day) of increased temperature through the use of heat lamps. Water was not allowed to escape from the base of the column during the life of the experiment.

6.2.2.2 Experiments 2 - Biological and Chemical Enhancement of Hardpans

This experiment investigated the development of hardpans through biological and chemical enhancements. Initially the columns were inoculated with bacteria grown from acidic seepage obtained from the disused Brukunga Pyrite Mine, S.A. Following this, 27mls of 2% Fe^{2+} at a pH of 3 was added to the columns weekly. Again during the week the columns were exposed to the increased temperatures. Water was restricted from flowing from the base of the columns throughout the life of the experiment.

6.2.2.3 Experiment 3 - Leaching Characterisation

This leaching experiment was designed determine the reactivity of the tailings and the effects hardpan development had on leaching characteristics. Batch leaching was conducted every third week and the leachate collected 3 time during that week. This leaching regime allowed an optimum time for oxidation, neutralisation and gangue mineral degradation reactions to take place (Grote, et.al. 1981). Approximately 50 ml of deionised water was added to each column, 3 times during the leaching week. This quantity of liquid caused saturation of the tailing and resulted in ponded water on the tailings

surface. After 1 hour leachate was collected, in some cases additional sampling was required after 6 and 24hrs to remove additional leachate. The samples collected through out the day were combined. Three independent solutions were obtained for the leaching week (Monday, Wednesday and Friday). The leachate was then analysed using ICP-AES to determine the nature and concentration of elements leached from the tailings. Additionally, pH and EC were measured on the leachate.

6.3 Results and Comparisons of Natural Enhancement vs. Biological and Chemical Enhancement of Hardpans

In most trials, secondary mineral precipitation was greater in the biologically and chemically enhanced experiments compared with the natural enhancement. This was in direct response to the increased sulfide oxidation due to the addition of Fe and bacteria. The Fe oxidising bacteria catalysed the sulfide oxidation reactions. The ferrous sulfate solution also acted as a catalyst after oxidising to Fe^{3+} form, and was an additional source of solute (Fe and SO_4^{2-}) available for secondary mineral precipitation. As a consequence of adding pH 3 solutions and enhanced oxidation in Experiment 2, most trials showed a decrease in pH at the surface and down preferential flow paths. In response to lower pH conditions, sulfide oxidation and gangue mineral degradation were also enhanced resulting in increased solute loads. In both Experiment 1 and Experiment 2 potential sources of solutes were present as soluble and less soluble mineral phases (Table 6.1), their site of precipitation dictated by the physical nature of the tailings and nature of cements (Table 6.2).

One of the major observations from these experiments was the recognition of the role of particle size and the correlation with climatic conditions. As mentioned previously, field observations of highly pyritic Woodlawn tailings exposed for 8 years showed evidence of only limited secondary mineral development. Fresh Woodlawn tailings were sampled and treated within this suite of experiments. These tailings treated at a lower rainfall rate and exposed to elevated temperatures, developed large quantities of cement down preferential flow paths, indicating tailings mineralogy favoured cement development. However, within the Woodlawn tailings dams the very fine-grained nature of the tailings has resulted in continuously saturated conditions through large matrix and suction potentials, reducing sulfide oxidation and thus secondary mineral development.

In the majority of cases the addition of acidic Fe-rich solution (Experiment 2) on a weekly basis promoted the development of cements. In the tailings where cementing was not obviously enhanced, ICP-AES analysis of 1:5 tailings/water extractions indicated that oxidation and acid generation was occurring as shown by elevated solute contents. In these cases cements may have formed if the experiment was allowed to continue over a longer period. Results of cements/secondary minerals, pH and EC variations down the profiles and elevated solute loads are presented in Table 6.1. Results and discussions for individual sites are presented in the Appendix 3A (Tables 3A.1 to 3A.37). Two different Brukunga tailings samples were used in these experiments to observe the differences in cementing ability of slightly oxidised tailings which were air dried in the lab prior to packing (B1) and fresh unoxidised tailings

(B2). Both Brukunga trials exhibited greater cementation with biological and chemical enhancement (Expt 2) with the slightly oxidised tailings (B1) showing enhanced cement formation. A comparison of these experiments is outlined in Appendix 3A, Section 3A.1.

TABLE 6.1 SUMMARY OF PRELIMINARY COLUMN EXPERIMENTS

		BRUKUNGA 2	BRUKUNGA 1	ELURA	WOODLAWN	WOODCUTTERS
E1	pH Range	3 - 3.8	3.8 - 3	4.4 - 6.4	6 - 3.2	5 - 6.6
	E.C Range mS/cm	13 - 1	14 - 0.6	22.5 - 2	2.5 - 8	26.6 - 2
	soluble surface concentrations		Zn, Ni, Co, Cd, Mg	Cr, Mg, Na	K	Cd, Co, Ni, Pb, Zn
	Secondary salts	gypsum, jarosite	gypsum, jarosite	gypsum, hexahydite, bianchite boyleite	gypsum, zinc blodite hexahydite basaluminite	gypsum, hexahydite, anglesite
E2	pH Range	3.1 - 3.3	3.1 - 3.2	6 - 4	6 - 4	4.7 - 6.2
	E.C Range mS/cm	18 - 2	15.4 - 2	2.5 - 22.5	3 - 10	28.3 - 3
	soluble surface concentrations	Al, Ca, Cd, Co, Cr, Cu, Fe, Mg, Mn, Ni, P, S, Zn	Al, Cr, Cu, Fe, K, Na, P, Pb, S	Al, Cd, Cu, Fe, Mn, Co, Zn	Al, Cd, Cu, Fe, Mg, Mn, S, Zn	Fe, K, Mg, Mn, Na, S
	Secondary salts	gypsum, jarosite	gypsum, jarosite	gypsum, hexahydite, rozenite, boyleite, mirabilite, szomolnokite	gypsum, zinc blodite, hexahydite, loweite, jarosite	gypsum, hexahydite, anglesite
E3	pH Range	3.8 - 2.5	2.6 - 3.6	7 - 4	8.5-3.2	8 - 6
	E.C Range mS/cm	max 17 final 8	max 12 final 7	initial flush 7.4 final 2 - 2.4	initial flush 11 final 25-30	9 - 10
	Secondary salts	gypsum	gypsum, jarosite	gypsum, hexahydite, wattevilleite, beudantite	gypsum, hexahydite, basaluminite	gypsum, hexahydite, beudantite
		BROKEN HILL	RANGER	PINE CREEK	CSA	PEAK
E1	pH Range	7.7 - 7	6.4 - 7	7.6 - 8.3	4 - 8	5.5 - 4.7
	E.C Range mS/cm	0.6 - 7	32 - 4	13.5 - 0.1	6 - 1	1 - 25
	soluble surface concentrations	B, Ca, K, Mg, Na	Zn, Al	Ca, Co, K	K, Ca, Na	K, Na
	Secondary salts	gypsum	gypsum, hexahydite, wattevilleite, boussingaulttite, hematite	gypsum, goethite	gypsum, hexahydite, goethite	thenardite, blodite, halite
E2	pH Range	7 - 4.7	5 - 7	4.6 - 7.7	3.6 - 4.1	4 - 5
	E.C Range mS/cm	0.6 - 6	41 - 3.6	15.4 - 1	1.7 - 13	1 - 27
	soluble surface concentrations	Al, Cd, Co, Fe, Mn, Ni, Zn, Pb, S	Co, Fe, K, Mg, Mn, Na, Ni, P, S	Al, Cu, Fe, Mg, Mn, Na, Ni, S, Zn	Mg, Mn, P, Cd, Fe, Al, Co, Cu, Ni, Zn, S	Al, B, Co, Cd, Ca, Cu, Fe, Mg, Mn, Ni, P, S, Zn
	Secondary salts	gypsum, jarosite, melanterite	gypsum, wattevilleite, hematite	gypsum, goethite	gypsum, hexahydite, jarosite	jarosite, gypsum
E3	pH Range	7.6 - 6.4	7.5 - 6.5	8.2 - 5.5	8 - 7	6.7-4.9
	E.C Range mS/cm	initial flush 10 final 0.6-0.8	initial flush 27 final 6.5 - 8	initial flush 9 final 1-4	initial flush 4.5 final 2.5-3	initial flush 17.6 final 2-3
	Secondary salts	gypsum	gypsum	gypsum, goethite	gypsum	gypsum

TABLE 6.2 CHARACTERISATION OF CEMENT TYPE AND LOCATION WITHIN PRELIMINARY EXPERIMENTS E1 AND E2

Tailings Type	Cementation Type and Location
Coarse-grained tailings with low sulfide content	Cements developed predominantly at the surface through evaporation and surface concentration
Fine-grained tailings with low sulfide content	Cements developed predominantly down preferential flow paths and along minor textural variations, with oxidation by-products and cements also observed at the surface.
Fine-grained tailings with high sulfide content	Responded differently depending on the sulfide type
pyrrhotitic tailings	Rapidly develop cements on the surface, down desiccation cracks and preferential flow paths.
pyritic tailings	Develop cements predominantly down preferential flow paths through redistribution of secondary by-products.

This overview table describes general cementation in both E1 and E2. In the majority of cases the preferential flow paths were not expressed as a desiccation crack or hole at the surface. These paths exhibited cement development 3-7 cm from the surface and presumably developed as a result of packing and particle size distribution of the tailings. It is suggested that these paths are shear planes developed during the drying and subsequent re-packing of the tailings within the column. Preferential paths such as these develop naturally in dams during drying of the surface zones in response to cohesion and shear strength variations.

6.3.1 Discussion

Although these results showed positive cementing enhancement through the addition of Fe^{2+} solution additions, this line of amelioration was not pursued. Initially it was suggested that tailings dam seepage could be recycled onto the dams thus providing the required elemental load and conditions for enhanced cementation. However, at present there are perceived problems with regulatory authorities associated with such a system. Doherty (1978) explained that after the closure of the Brukunga Pyrite Mine in 1972, the tailings dam became a major source of acidic seepage. To prevent this being released into the surroundings, the seepage was pumped back to the dam surface, thus recycling and concentrating it. Concerns regarding the leaching effect of this water, potentially resulting in piping of the tailings and rapid loss of water were expressed and the practice terminated. Doherty (1978) referred to this as "tailings dam suicide".

It was for this reason that the main column experiment investigated less emotive treatments for promoting hardpan development. This was achieved through the additions of solid additives and distilled water only. These experiments are outlined in Section 6.5.

6.4 Experiment 3 - Leaching Characterisation

Leaching experiments were undertaken to investigate the temporal development of solutes and the effect secondary mineral formation (hardpan development) had on the solute characteristics.

To make comparisons of the highly variable tailings used in this experiment, solute concentrations have been plotted as averages for each week. Figures 6.2 to 6.4 however show the elemental variability in the Brukunga tailings within the weekly cycles through-out the life of the experiment. Within each week's leaching cycle (as shown by the different colours), discrete patterns have developed. The initial leachate collected exhibited high concentration of many solutes as the most soluble salts were flushed from the column. The second and third leachate flushed the less soluble elements or those more readily adsorbed on surfaces of tailings minerals, which took longer to be transported through the column.

Note: first result = initial solute level in the tailings

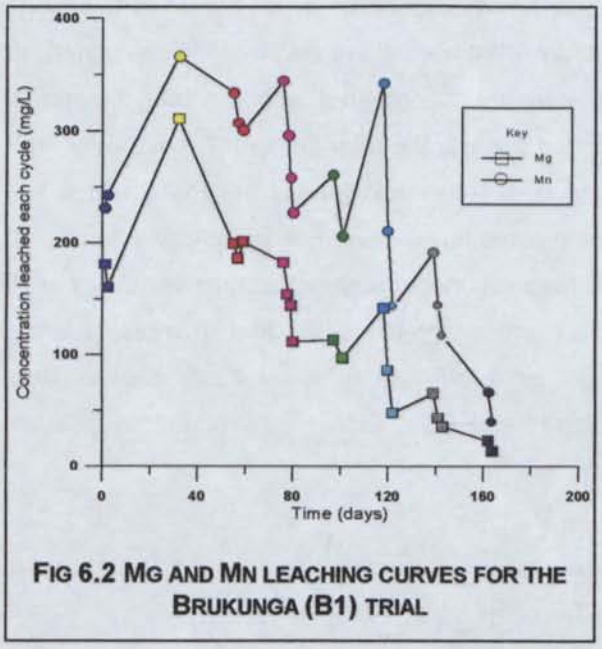

FIG 6.2 MG AND MN LEACHING CURVES FOR THE BRUKUNGA (B1) TRIAL

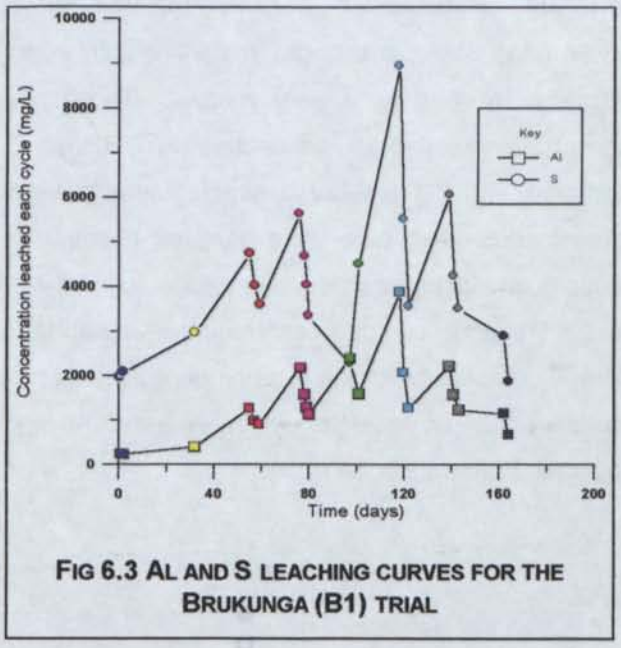

FIG 6.3 AL AND S LEACHING CURVES FOR THE BRUKUNGA (B1) TRIAL

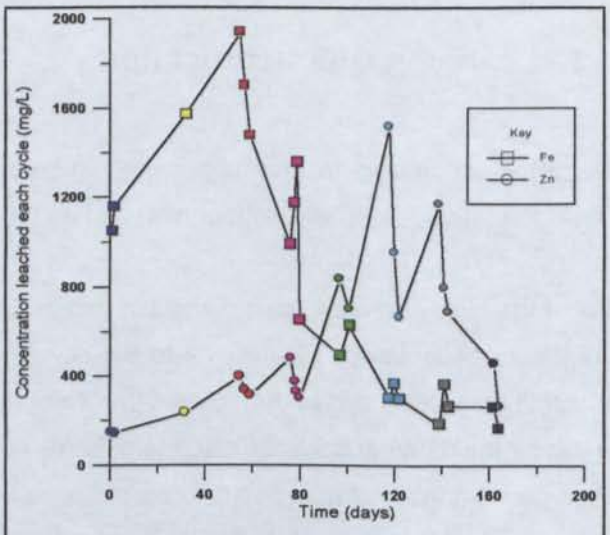

FIG 6.4 FE AND ZN LEACHING CURVES FOR THE BRUKUNGA (B1) TRIAL

Figures 6.5 to 6.14 show for selected elements the average load in milligrams leached per week of all tailings types, along with the cumulative % leached. Large variations in flow rate and storage capacity of the tailings produced differences in the volume of leachate collected. To allow better comparisons between the various tailings, results which were initially obtained as mg/L, were recalculated to milligrams leached on a weekly basis. These results were then compared with the total elemental concentration available to be leached (XRF data) and plotted to show the total amount leached over time compared with the amount available (cumulative % leached). (See additionally section 6.4.2). The elements presented here were selected because of their potential involvement in hardpan formation reactions and included those elements which showed the largest concentrations and most variability in all trials. It can be clearly seen from these graphs that the total percentage leached in most cases is minimal compared with the total amount available. Tables 3A.4 to 3A.39, in Appendix 3A shows actual results (mg/L) for all elements investigated, along with pH and EC. Discussions of these data are presented in Appendix 3A.

where

very low %sulfide - 0-1%
low % sulfide - 1- 5%
high % sulfide - 5- 30%

Legend for Figs 6.5 to 6.16

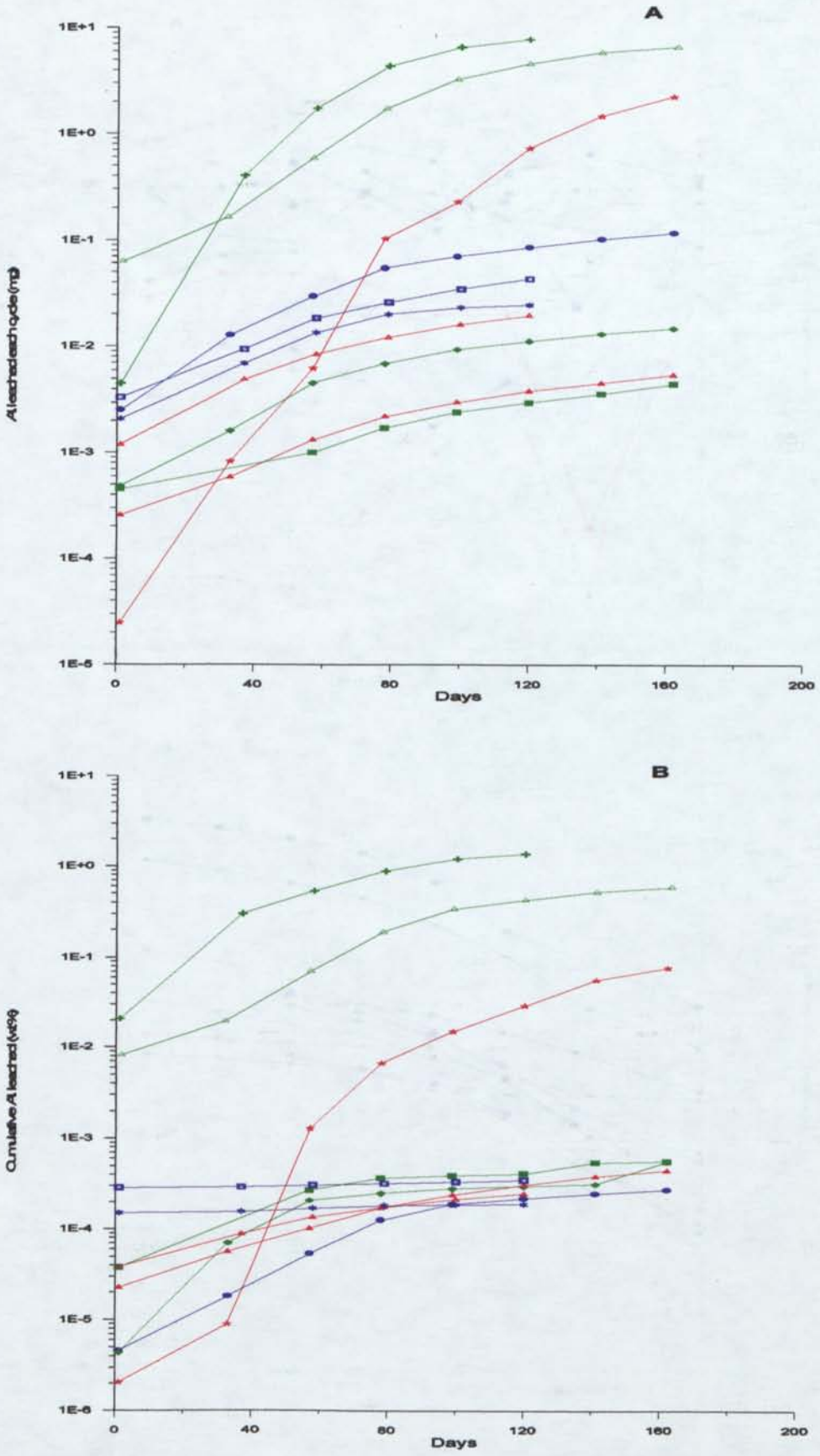

FIG 6.5 ALUMINIUM LEACHED (A) EACH CYCLE (mg) AND (B) CUMULATIVE (WT%)

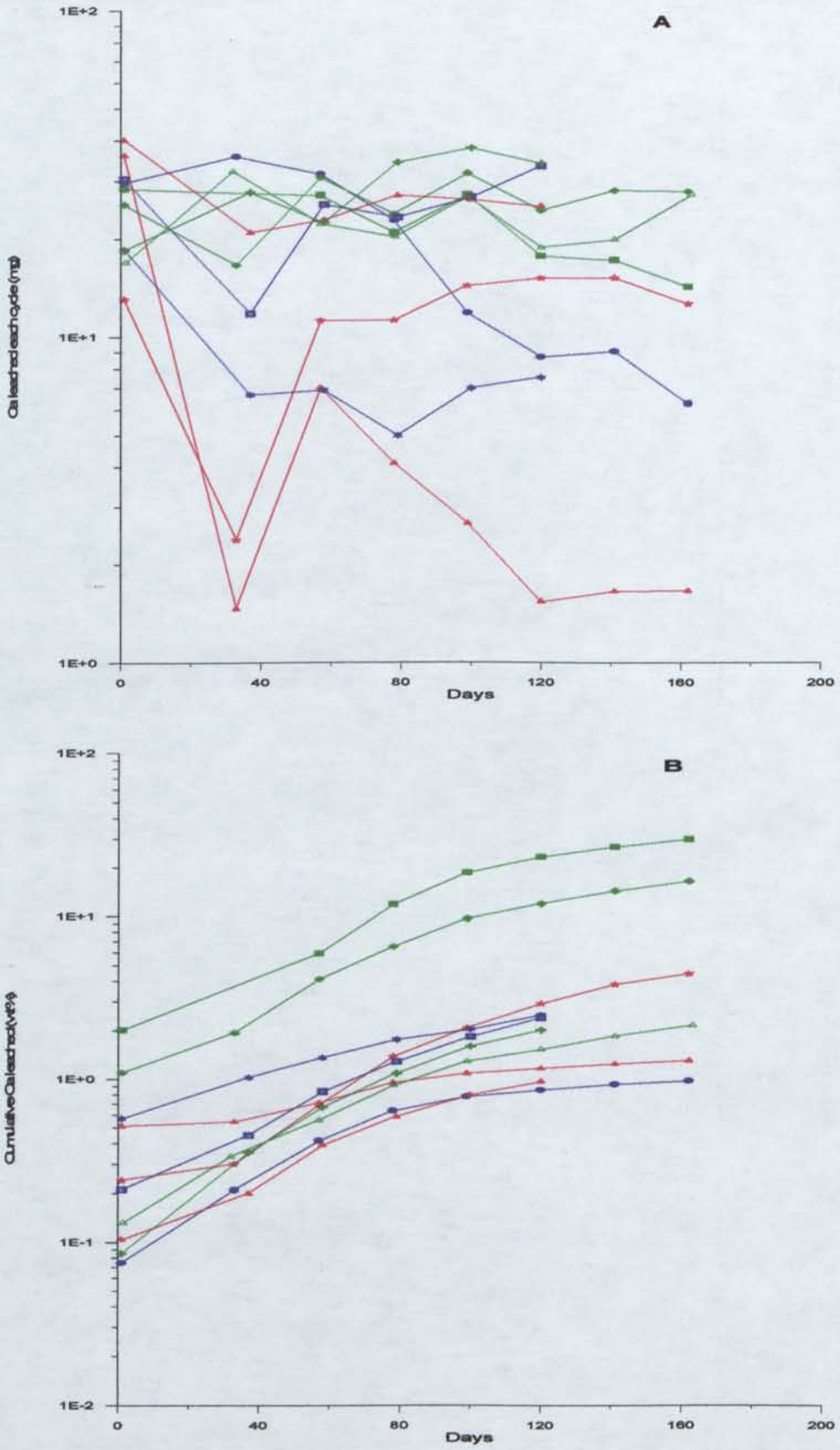

FIG 6.6 CALCIUM LEACHED (A) EACH CYCLE (mg) AND (B) CUMULATIVE (WT%)

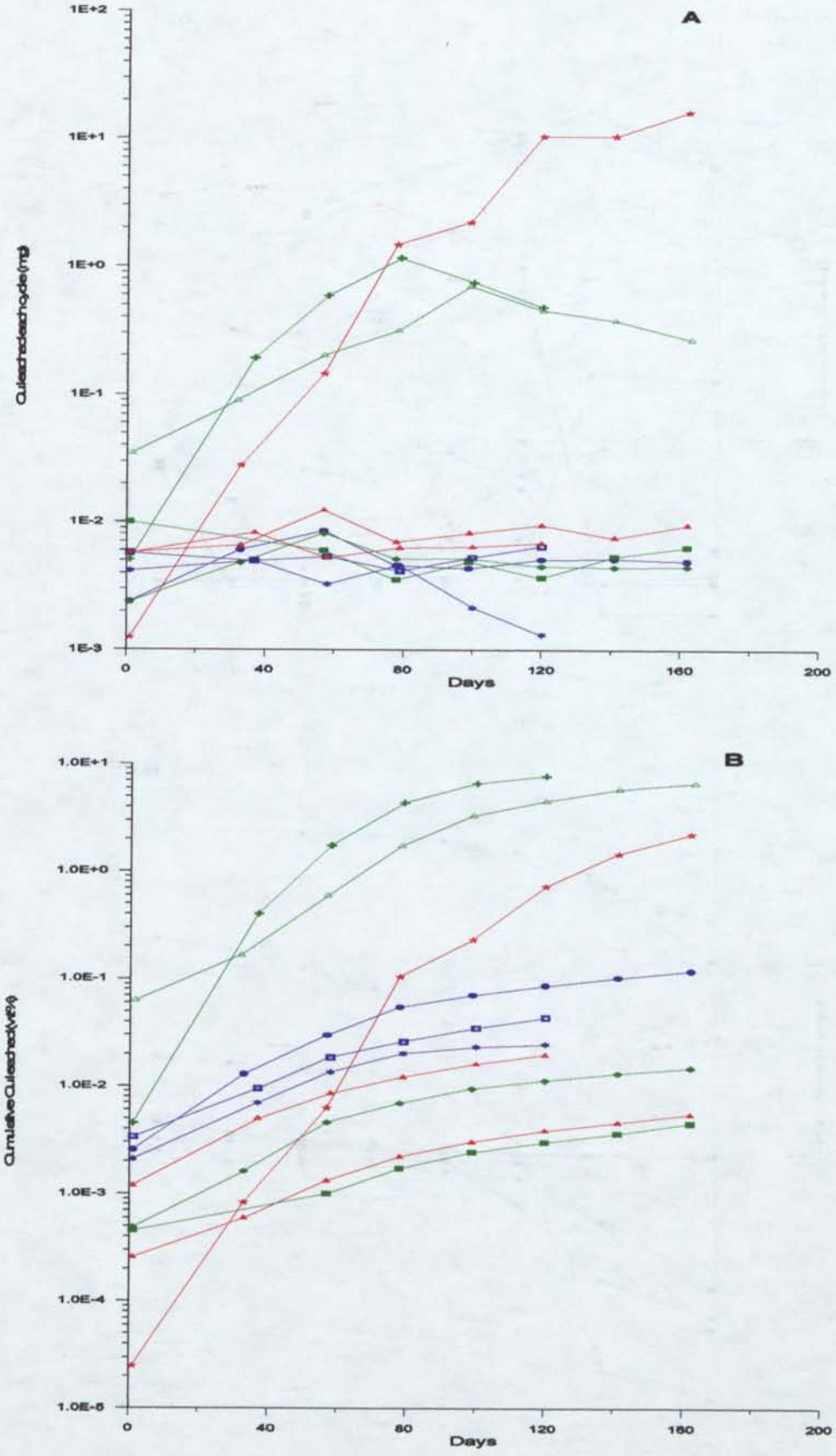

FIG 6.7 COPPER LEACHED (A) EACH CYCLE (mg) AND (B) CUMULATIVE (WT%).

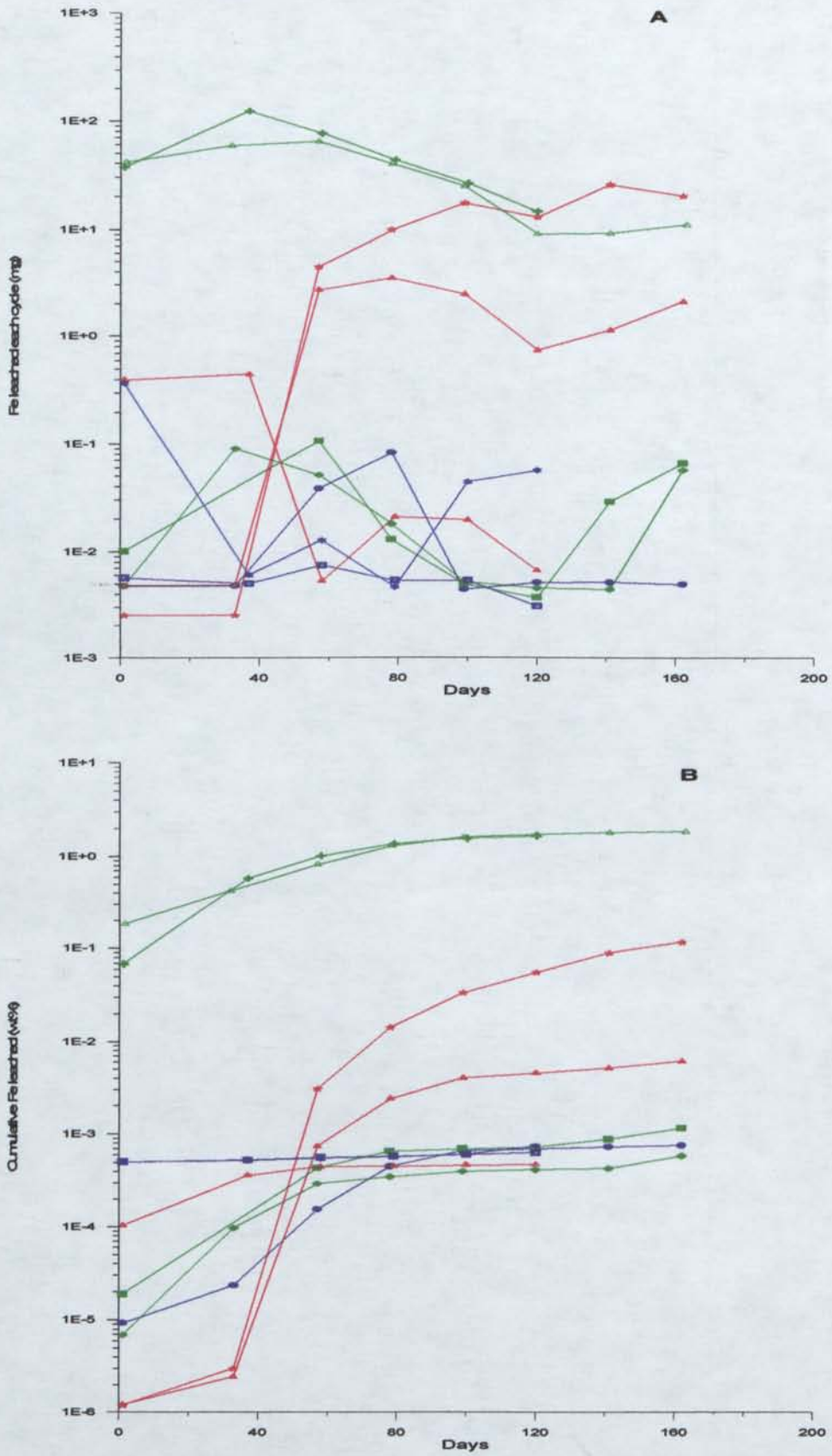

FIG 6.8 IRON LEACHED (A) EACH CYCLE (mg) AND (B) CUMULATIVE (WT%).

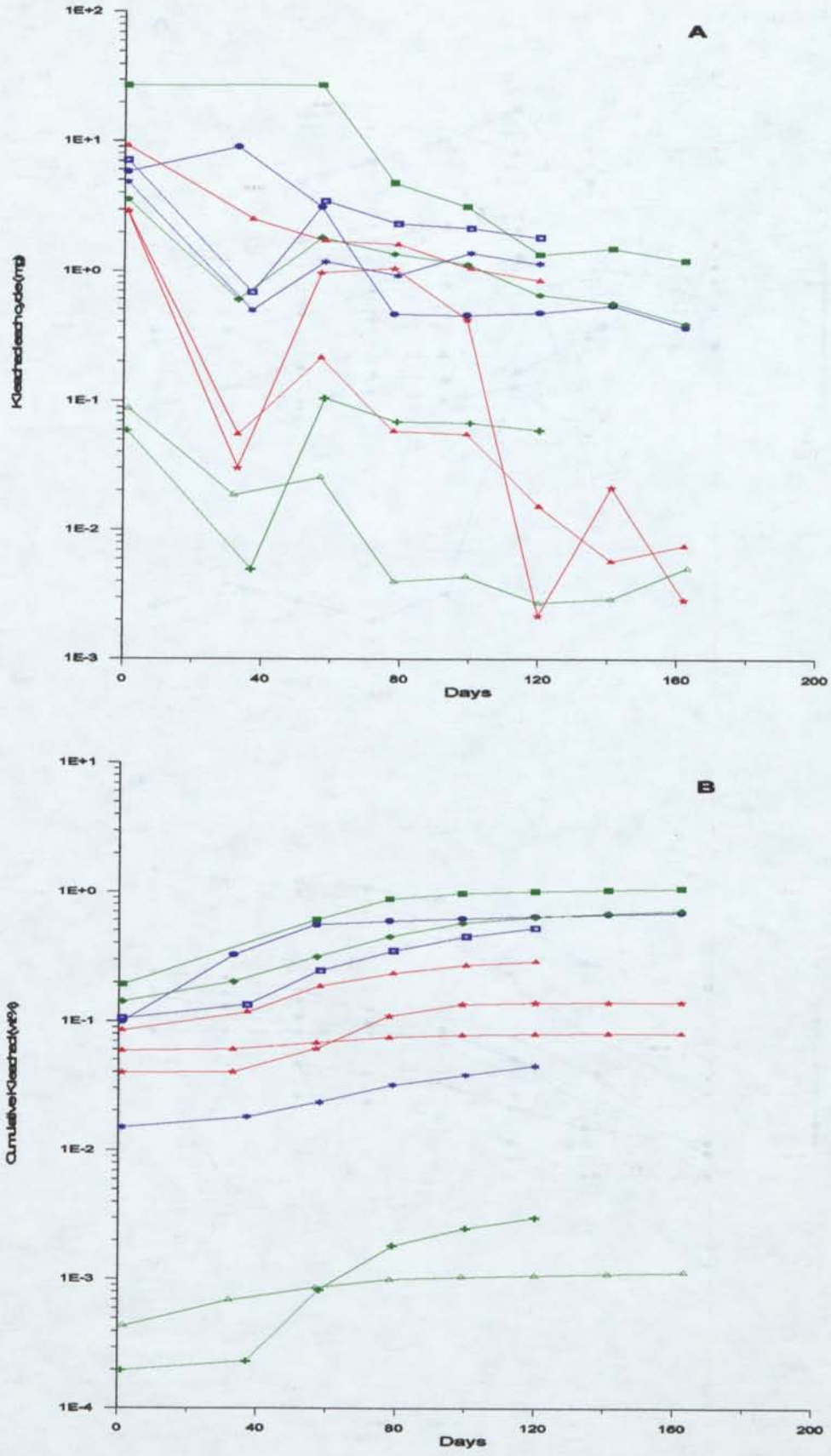

FIG 6.9 POTASSIUM LEACHED (A) EACH CYCLE (mg) AND (B) CUMULATIVE (WT%).

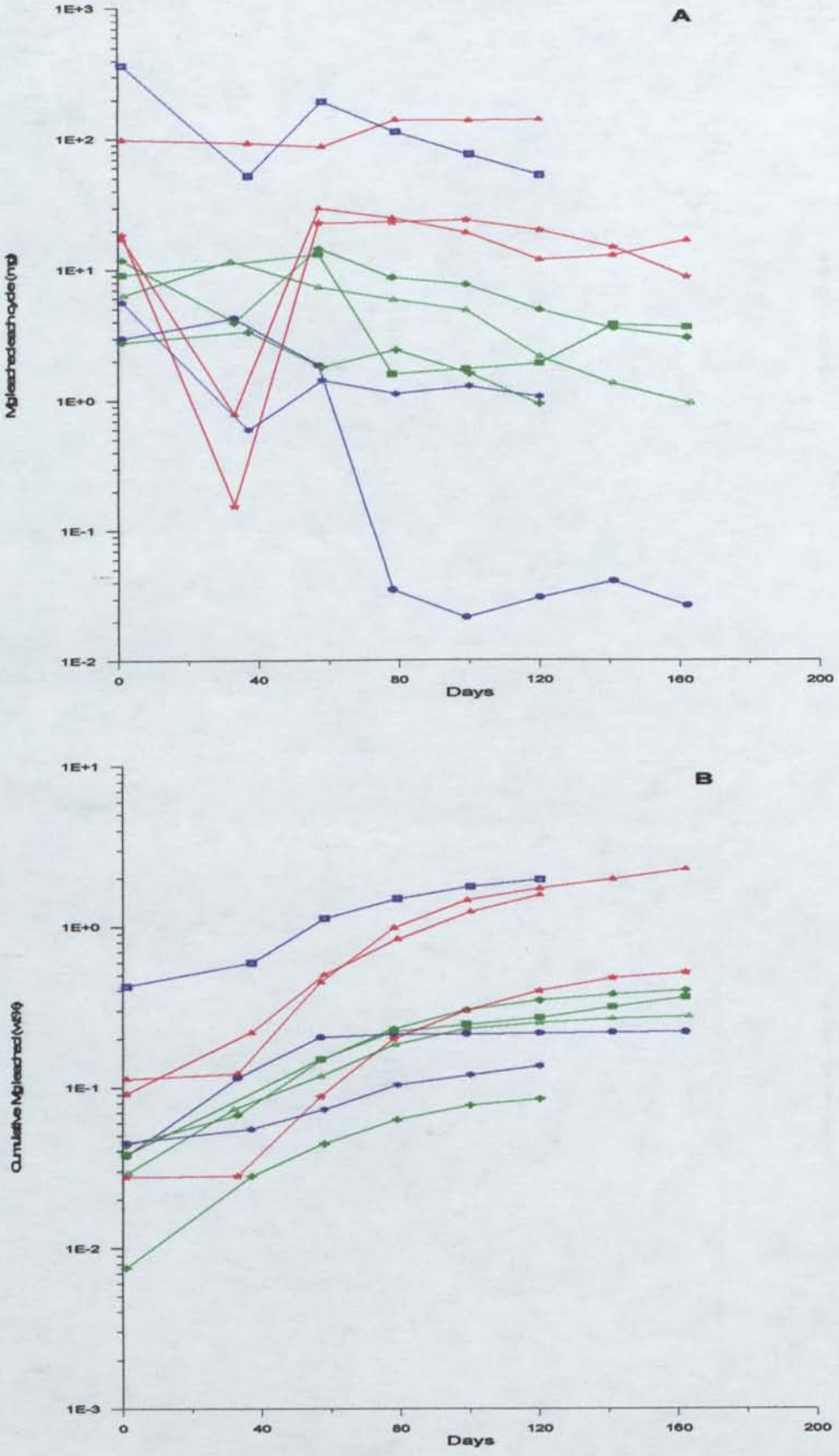

FIG 6.10 MAGNESIUM LEACHED (A) EACH CYCLE (mg) AND (B) CUMULATIVE (WT%).

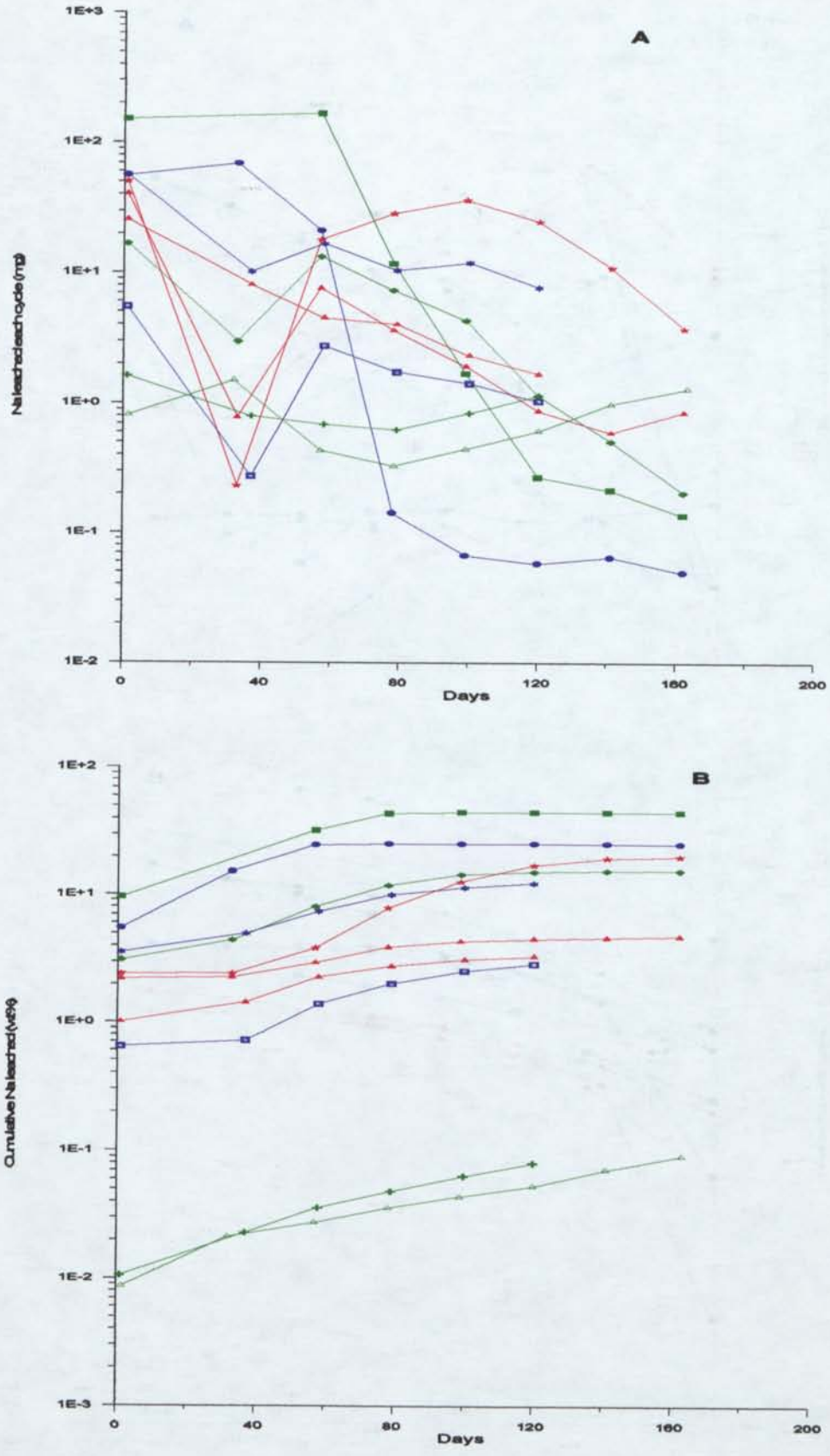

FIG 6.11 SODIUM LEACHED (A) EACH CYCLE (mg) AND (B) CUMULATIVE (WT%).

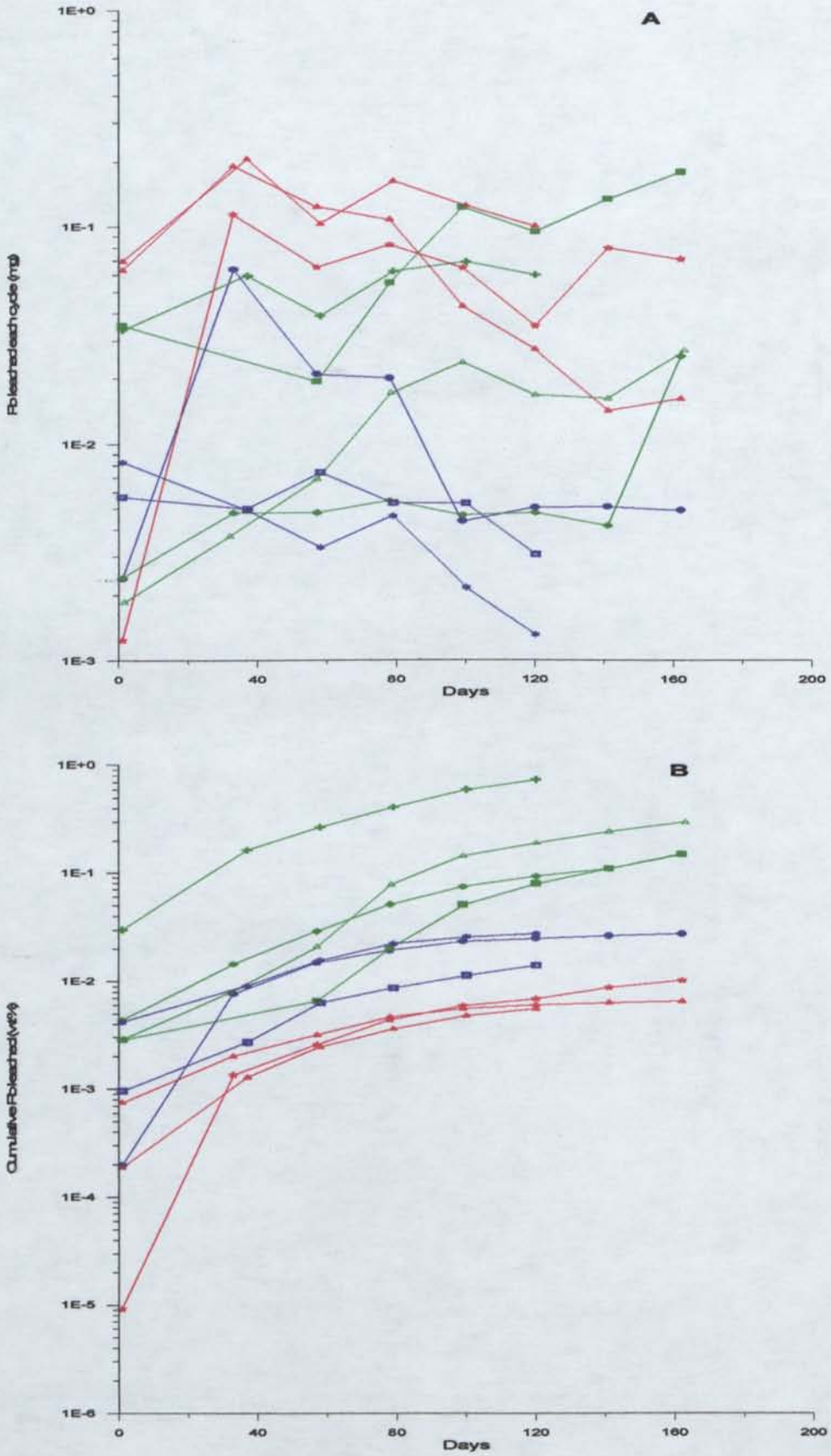

FIG 6.12 LEAD LEACHED (A) EACH CYCLE (mg) AND (B) CUMULATIVE (WT%).

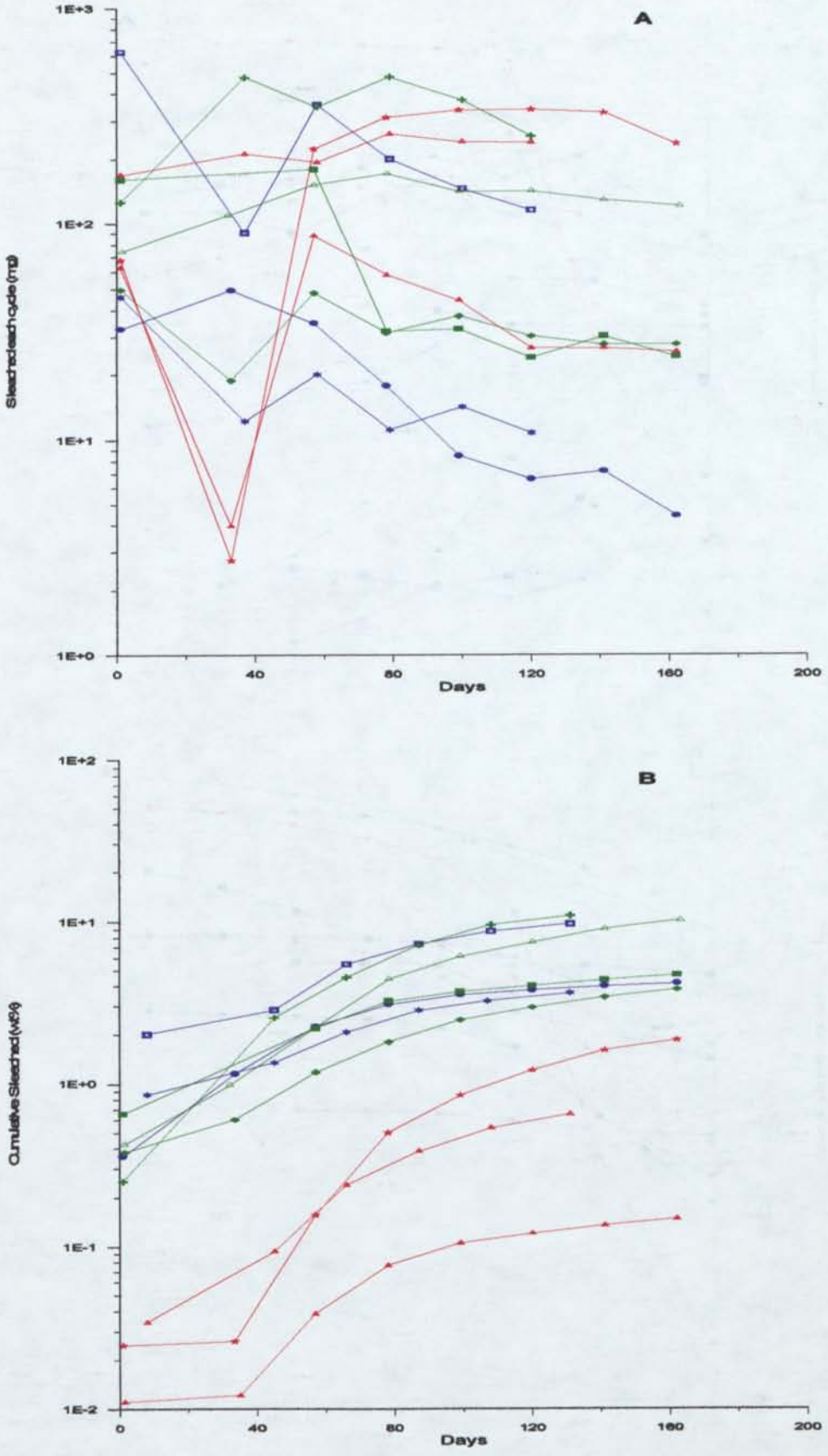

FIG 6.13 SULFUR LEACHED (A) EACH CYCLE (mg) AND (B) CUMULATIVE (WT%).

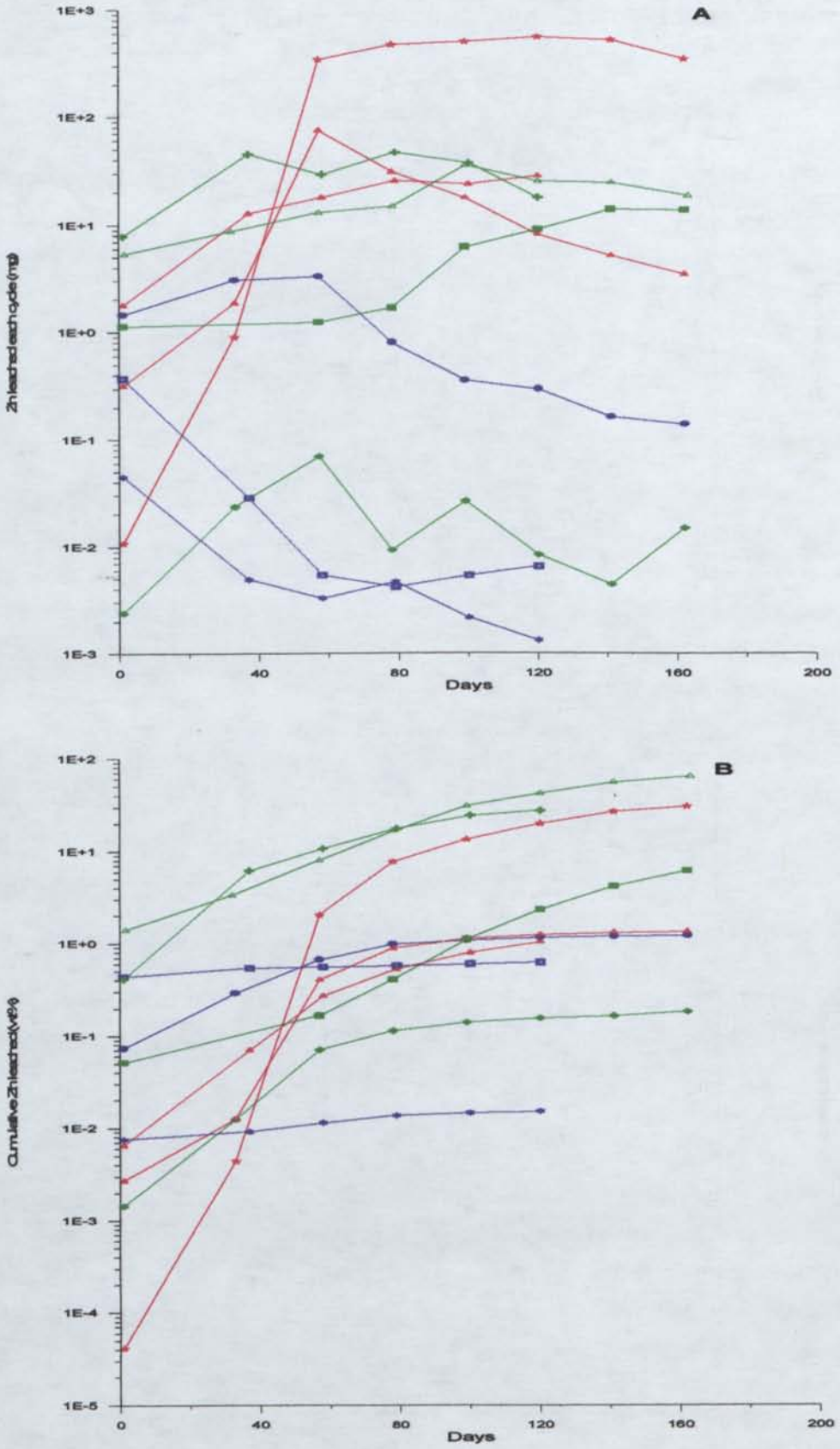

FIG 6.14 ZINC LEACHED (A) EACH CYCLE (mg) AND (B) CUMULATIVE (WT%).

6.4.1 General mineralogical reactions and by-products

In many tailings dams, very reactive tailings when allowed to dry, rapidly oxidise producing an acidic environment. In response to this sulfide oxidation, neutralisation reactions may also occur adding to the solute load of the pore waters. As a consequence of these reactions, high solute concentrations are released often in quantities much greater than those recommended by the ANZECC Australian Water Quality Guidelines for the protection of aquatic ecosystems and livestock watering (1992), and NHMRC/AWRC guidelines for drinking water (1987) (Tables 3A.4 to 3A.39, in Appendix 3A). In less reactive tailings in which sulfide content is low and thus acid generation is limited, release is subdued and in some cases simply reflects elemental loads associated with primary mineral dissolution.

In the highly sulfidic tailings investigated, pyrite, pyrrhotite and sphalerite were the predominant sulfides present with small but significant amounts of chalcopyrite and galena. As these sulfides oxidise, acid, heavy metals and S are released which are then available for in-situ secondary mineral precipitation or leaching away from the surface. Any H^+ released may react with carbonates and other gangue minerals present resulting in a sequence of pH buffering reactions. Blowes and Ptacek (1994) explain that the principal acid neutralising mechanisms in tailings are carbonate mineral dissolution, hydroxide mineral dissolution and alumino-silicate mineral dissolution as the pH decreases.

The leachates observed from all trials show large variations in pH over time (Fig. 6.15). The Ranger, Pine Creek and Broken Hill leachates have an initial pH of approximately 8 and remain that way indicating the lack of acid generating minerals. At Woodcutters, originally high pH of the leachate indicates that dolomite, calcite or siderite are readily available for initial neutralising reactions. These reactions consume carbonate and H^+, release cations (Ca, Mg and Fe) to the tailings pore water and increase pore water alkalinity concentrations. The general order of carbonate depletion begins with calcite which is followed by dolomite and then siderite (Blowes and Ptacek, 1994). In some of the trials (Elura and Woodlawn) the pH dropped dramatically over time from 9 to 3 suggesting that these neutralising minerals are only in very limited supply. Individual results of pH and EC are presented in Appendix 3A. Tables 3A.6 to 3A.38.

As a result of these initial buffering reactions metal hydroxides or hydroxy-sulfates may precipitate. Once the carbonate contents are depleted, these hydroxides may act in neutralisation reactions with eventually alumino-silicate neutralisation reactions occurring once the pH drops sufficiently (pH 4-3). Observations of these processes and the order and extent of their involvement in the tailings were achieved through these leaching experiments.

It should be noted that the secondary mineralogy observed in the field was not always the same as that observed developing through-out this trial. This simply reflects variations in the time constraints in the laboratory experiments compared with the period of exposure of tailings in the field. Once secondary minerals precipitate and are exposed, they alter their structures either through oxidation or dehydration reactions resulting in relatively stable compounds.

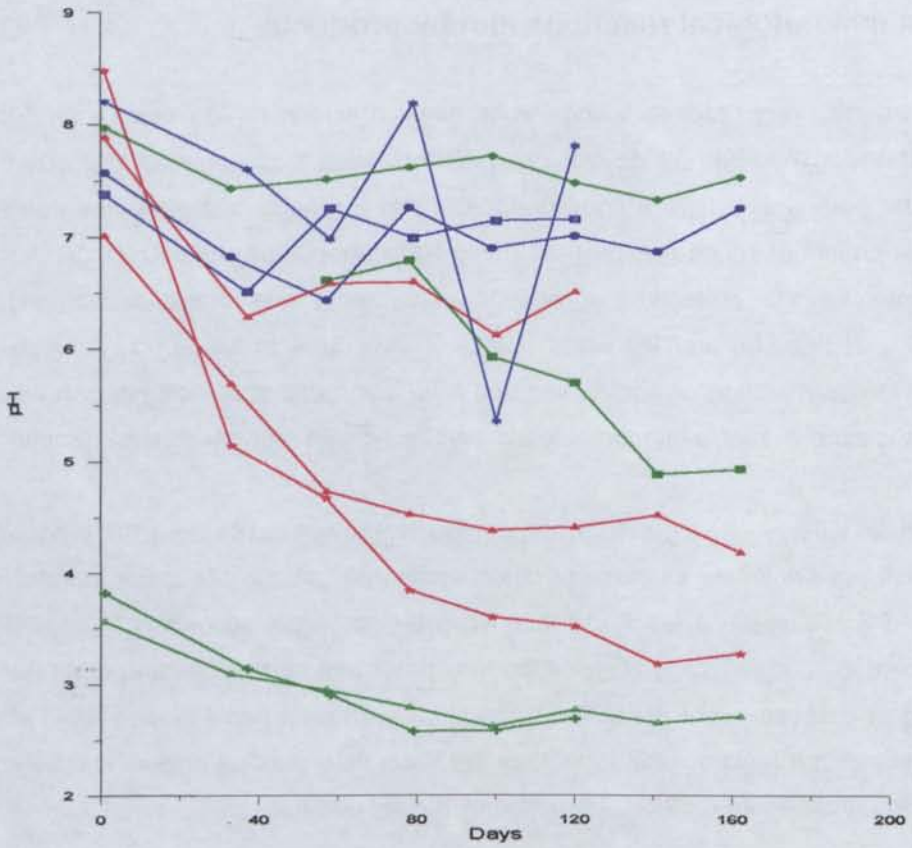

FIG 6.15 LEACHATE PH

6.4.2 Solute Release

Results of ICP-AES analyses of leachates (Tables 3A.4 to 3A.39, Appendix 3A) indicate that the major solutes vary dramatically from site to site and are obviously dictated by the original mineralogy of the ore and the nature of metallurgical processing. Table 6.3 displays selected data on the original elemental quantities available for leaching, the total amount leached and the average, initial and final rate at which this has occurred. Additional information is presented in Table 3A.40, Appendix 3A, which shows data on all of the elements investigated and rates of release. The release rates presented here were determined through by exponential regression analysis of the data.

Rates of release were variable through out the duration of the experiment. In many cases the release rate decreased over time in response to secondary mineral coatings and preferential flow path development. In a number of cases release rates increased with time as dissolution related to acid attack became enhanced. Release and leachate trends are discussed extensively in Section 6.4.3.

The amount of elemental release achieved during the life of the experiment was in many cases minimal (Table 6.3 and 3A.40). Compared with the total amount available, release of Fe and Pb was generally low (0-2%), while in some trials release of Zn and Cu was high (up to 65% of available Zn was released from the Brukunga 1 trial). Such differences are attributed to the original mineralogy of the tailings and thus the variable solubility and reactivity of the primary minerals.

TABLE 6.3 AVAILABILITY, RELEASE AND RATE OF RELEASE FOR SELECTED ELEMENTS - EXPT 3 : LEACHING CHARACTERISATION.

	Total Pb available (mg)	Total Pb leached (mg)	Total Pb leached (%)	Average rate of Pb release mg/day	Initial rate of Pb release mg/day	Final rate of Pb release mg/day	Total Fe available (mg)	Total Fe leached (mg)	Total Fe leached (%)	Average rate of Fe release mg/day	Initial rate of Fe release mg/day	Final rate of Fe release mg/day
Brukunga 2	112	0.85	0.76	$5x10^{-4}x$	$4x10^{-4}x$	$6x10^{-4}x$	53984	872.02	1.62	$1x10^{-3}x$	$1.7x10^{-3}x$	$5x10^{-4}x$
Brukunga 1	96	0.30	0.31	$2x10^{-4}x$	$1x10^{-4}x$	$2x10^{-4}x$	33216	612.70	1.84	$9x10^{-4}x$	$1.6x10^{-3}x$	$3x10^{-4}x$
Elura	22378	1.44	0.01	$3x10^{-6}x$	$5x10^{-6}x$	$9x10^{-7}x$	592850	37.27	0.01	$3x10^{-6}x$	$5x10^{-6}x$	$2x10^{-6}x$
Woodlawn	13625	1.42	0.01	$5x10^{-6}x$	$8x10^{-6}x$	$5x10^{-6}x$	209280	265.63	0.13	$7x10^{-5}x$	$3x10^{-5}x$	$9x10^{-5}x$
Woodcutters	37120	2.07	0.01	$4x10^{-6}x$	$4x10^{-6}x$	$3x10^{-6}x$	382400	1.83	0.0005	$2x10^{-7}x$	$4x10^{-7}x$	$5x10^{-8}x$
Broken Hill	1215	0.33	0.03	$1x10^{-5}x$	$5x10^{-5}x$	$4x10^{-6}x$	51425	0.39	0.0008	$4x10^{-7}x$	$6x10^{-7}x$	$1x10^{-7}x$
Ranger	595	0.09	0.01	$9x10^{-6}x$	$1x10^{-5}x$	$9x10^{-6}x$	51255	0.33	0.0006	$1x10^{-7}x$	$9x10^{-8}x$	$1x10^{-7}x$
Pine Creek	198	0.05	0.03	$2x10^{-6}x$	$2x10^{-6}x$	$1x10^{-6}x$	73656	0.59	0.0008	$2x10^{-7}x$	$8x10^{-8}x$	$4x10^{-7}x$
CSA	83	0.17	0.20	$7x10^{-6}x$	$6x10^{-6}x$	$8x10^{-6}x$	103950	0.62	0.0006	$2x10^{-7}x$	$4x10^{-7}x$	$2x10^{-7}x$
Peak	1239	1.99	0.16	$8x10^{-6}x$	$5x10^{-6}x$	$1x10^{-4}x$	53897	0.67	0.0012	$4x10^{-7}x$	$6x10^{-7}x$	$5x10^{-7}x$
	Total Cu available (mg)	Total Cu leached (mg)	Total Cu leached (%)	Average rate of Cu release mg/day	Initial rate of Cu release mg/day	Final rate of Cu release mg/day	Total Zn available (mg)	Total Zn leached (mg)	Total Zn leached (%)	Average rate of Zn release mg/day	Initial rate of Zn release mg/day	Final rate of Zn release mg/day
Brukunga 2	112	8.93	7.98	$6.7x10^{-3}x$	$4.7x10^{-3}x$	$6.7x10^{-3}x$	1904	512.33	26.91	$2.3x10^{-2}x$	$2x10^{-2}x$	$2.2x10^{-2}x$
Brukunga 1	96	6.53	6.80	$4.2x10^{-3}x$	$2.5x10^{-3}x$	$4.8x10^{-3}x$	576	371.60	64.51	$5.5x10^{-2}x$	$2.5x10^{-2}x$	$8.2x10^{-2}x$
Elura	3173	0.18	0.01	$3x10^{-6}x$	$3x10^{-6}x$	$3x10^{-6}x$	32064	420.09	1.31	$7x10^{-4}x$	$1.4x10^{-3}x$	$2x10^{-4}x$
Woodlawn	5014	125.90	2.51	$1.2x10^{-3}x$	$2x10^{-4}x$	$2.4x10^{-3}x$	26051	8207.14	31.50	$2.1x10^{-2}x$	$1.5x10^{-2}x$	$2.5x10^{-2}x$
Woodcutters	480	0.10	0.02	$1x10^{-5}x$	$1x10^{-5}x$	$1x10^{-5}x$	27520	295.20	1.07	$8x10^{-4}x$	$6x10^{-4}x$	$9x10^{-4}x$
Broken Hill	94	0.12	0.12	$6x10^{-5}x$	$7x10^{-5}x$	$5x10^{-5}x$	1964	23.26	1.18	$4x10^{-4}x$	$1.2x10^{-3}x$	$1x10^{-4}x$
Ranger	170	0.08	0.05	$3x10^{-5}x$	$3x10^{-5}x$	$3x10^{-5}x$	85	0.52	0.62	$8x10^{-5}x$	$1x10^{-4}x$	$7x10^{-5}x$
Pine Creek	198	0.05	0.03	$2x10^{-5}x$	$2x10^{-5}x$	$1x10^{-5}x$	594	0.09	0.02	$6x10^{-6}x$	$7x10^{-6}x$	$4x10^{-6}x$
CSA	743	0.12	0.02	$7x10^{-6}x$	$8x10^{-6}x$	$6x10^{-6}x$	248	0.45	0.18	$9x10^{-5}x$	$1x10^{-4}x$	$4x10^{-5}x$
Peak	2213	0.10	0.005	$2x10^{-6}x$	$2x10^{-6}x$	$2x10^{-6}x$	2213	140.03	6.33	$3.5x10^{-3}x$	$1x10^{-3}x$	$5.8x10^{-3}x$
	Total S available (mg)	Total S leached (mg)	Total S leached (%)	Average rate of S release mg/day	Initial rate of S release mg/day	Final rate of S release mg/day	Total Ca available (mg)	Total Ca leached (mg)	Total Ca leached (%)	Average rate of Ca release mg/day	Initial rate of Ca release mg/day	Final rate of Ca release mg/day
Brukunga 2	50400	5622.12	11.16	$8.3x10^{-3}x$	$8.2x10^{-3}x$	$7.5x10^{-3}x$	21728	451.84	2.08	$1.4x10^{-3}x$	$1.2x10^{-3}x$	$1.7x10^{-3}x$
Brukunga 1	26112	2742.80	10.50	$6x10^{-3}x$	$6x10^{-3}x$	$5.7x10^{-3}x$	19776	439.19	2.22	$1.1x10^{-3}x$	$1.1x10^{-3}x$	$1.1x10^{-3}x$
Elura	581160	877.55	0.15	$8x10^{-5}x$	$1x10^{-4}x$	$5x10^{-5}x$	7181	94.92	1.32	$4x10^{-4}x$	$2x10^{-4}x$	$2x10^{-2}x$
Woodlawn	275443	5386.76	1.96	$1.1x10^{-3}x$	$9x10^{-4}x$	$1.1x10^{-3}x$	5450	257.21	4.72	$2.5x10^{-3}x$	$2x10^{-3}x$	$2.8x10^{-3}x$
Woodcutters	496800	3373.27	0.68	$5x10^{-4}x$	$5x10^{-4}x$	$5x10^{-4}x$	38560	383.54	0.99	$7x10^{-4}x$	$6x10^{-4}x$	$7x10^{-4}x$
Broken Hill	9163	384.94	4.20	$1.6x10^{-3}x$	$3.6x10^{-3}x$	$8x10^{-4}x$	39738	390.40	0.98	$4x10^{-4}x$	$7x10^{-4}x$	$2x10^{-4}x$
Ranger	31110	3103.53	9.98	$6.4x10^{-3}x$	$7.7x10^{-3}x$	$4.9x10^{-3}x$	14450	362.01	2.51	$1.6x10^{-3}x$	$1.2x10^{-3}x$	$2x10^{-3}x$
Pine Creek	5346	201.00	3.76	$2.3x10^{-3}x$	$2.6x10^{-3}x$	$1.8x10^{-3}x$	3267	85.15	2.61	$1.4x10^{-3}x$	$1.4x10^{-3}x$	$1.5x10^{-3}x$
CSA	19635	778.72	3.97	$1.8x10^{-3}x$	$1.9x10^{-3}x$	$1.6x10^{-3}x$	3548	610.60	17.21	$5x10^{-4}x$	$7.6x10^{-3}x$	$8.6x10^{-3}x$
Peak	24603	1178.39	4.79	$1.8x10^{-3}x$	$3.1x10^{-3}x$	$1.2x10^{-3}x$	1416	433.55	30.62	$1.9x10^{-2}x$	$2x10^{-2}x$	$1.6x10^{-2}x$

The major components (>100mg/L) in many of the trials included Ca, Mg, S and Na, some of which can be attributed to mill processing additives. Lime, acid, sodium xanthates (SiBX) and sodium bisulfide (SBS) additives would contribute to Ca, Na and S release, with Ca and S directly related to dissolution of gypsum (precipitated through lime additions) and residual lime after tailings deposition. Magnesium and Ca levels can also be attributed to neutralisation reaction and direct dissolution of calcite and dolomite depending on the original gangue mineralogy. Sulfur, Pb, Zn, Cu and Fe are presumably derived from the oxidation of sulfides. Iron may also be derived by neutralisation reactions of siderite. The increased levels of Al and K must be attributed to the degradation of alumino-silicates, while Mg levels can

partially be attributed to Mg-bearing chlorites (e.g. Ranger). Similarly trace levels (>10 mg/L) of P and B are suggested to have developed through degradation of trace gangue minerals or present as substitution in the major phases. Minor and trace levels (10-100 mg/L) of Mn, Cd, Co, Ni can be attributed to the oxidation of impure pyrite and other sulfides or again directly from gangue mineral degradation. Other chalcophile elements (As, Sb, Bi, Sn, Hg, Se and Tl) were not measured during this experiment as the ICP-AES method employed did not have these capabilities.

All solutes analysed show variations in concentration over time. The tailings used in this experiment were obtained from dams presently in use (except Brukunga and Pine Creek). The majority of these tailings contained readily soluble Na, Ca, K, Mg and S as shown by initially elevated levels in the profiles followed by rapid flushing from the column, shown by a profile decrease. This trend is also shown in many of the EC profiles (Fig 6.16). In all cases the tailings used in the experiment had not been oxidised since deposition as they were obtained from depth but must have contained vertically transported oxidation and neutralisation reaction by-products from the surface region, along with Na and Ca from the mill processing. This was not the case at the disused sites, as many of the more soluble salts had previously been leached from the tailings.

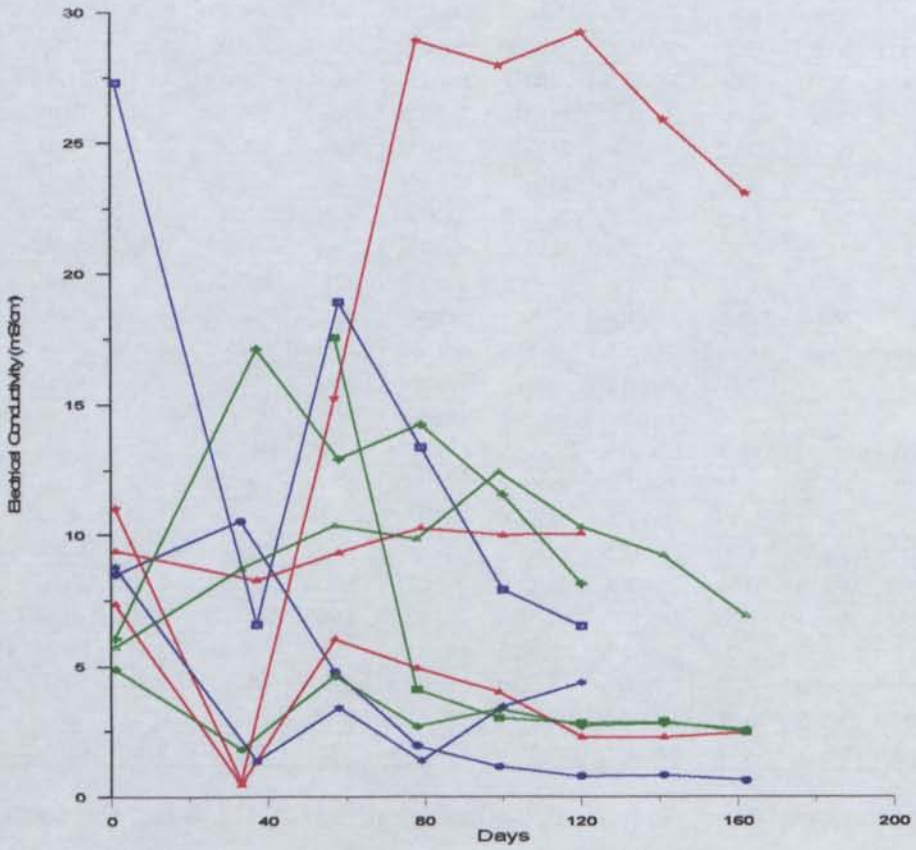

FIG 6.16 LEACHATE ELECTRICAL CONDUCTIVITY

The elemental load released from each of the tailings type is obviously dependent on:

- the percentage of each element initially available
- the mineral stability ie. Mg bound as Mg-chlorite or dolomite, Fe as pyrite, pyrrhotite, siderite or Fe-chlorite.

Such relationships are discussed on an individual basis in Appendix 3A. However obtaining an insight into the processes occurring can be achieved through observations of the general elemental distribution occurring through-out the profiles.

6.4.3 Leachate Trends

The predominant although not marked trend developed during the life of the experiment was that the majority of elements increased to peak concentrations and then decreased. This again is reflected in the overall trend of the EC of many of the leachates (Fig 6.16). This is a general observation regarding the trends and within each of the trials, specific elements did not behave this way.

Solute concentrations peaked at different stages during the experiment. For example galena is one of the most reactive sulfides and thus Pb concentrations in some cases peaked early in the experiment, whereas an initially subdued Cu release may be a function of the lower reactivity of chalcopyrite. Jambor (1994) noted the general reactivity sequence of the common sulfides as:

pyrrhotite>galena-sphalerite>pyrite-arsenopyrite>chalcopyrite

The peak of the other elements attributed to gangue mineral degradation vary depending on their resistance to acid attack. For example Mg from chlorites (eg clinochlore) occurs more rapidly than Al resulting in Mg release into solution and the coeval development of kaolinite, which eventually may break down to silicic acid or opaline silica.

As the experiment progressed the flow rates through many of the tailings (ie. leachate quantity) varied. In some cases leachate quantity decreased suggesting some secondary cementing or variations in the packing/sorting of primary mineralogy resulting in a decreased permeability. Other trials showed rapid through-flow due to the development of preferential pathways equivalent to the desiccation cracks developed naturally in dams. Other trials however showed little or no change in permeability.

In the highly pyrrhotitic tailings of Elura, surface oxidation and preferential flow path oxidation resulted in cementing and thus sealing of the remaining tailings. This effectively reduced the amount of both primary sulfides and gangue minerals available for reaction. Thus the reduction of leachate quantity over time can in this case be directly attributed to secondary mineral precipitation as hardpan cements.

In highly pyritic tailings (eg. Woodlawn) cementing occurred but was not only associated with preferential flow paths. It is suggested in this case that the reduction in observed permeability was due to the precipitation of secondary minerals near the surface, cementing the tailings and effectively plugging the profile. As in the pyrrhotitic tailings, the decreased solute concentrations may be a function of elemental capture associated with secondary mineral precipitation. It could be argued however that the decrease in solute concentration is directly related to the amount of water moving through the profile as a transporting medium. Thus the decreased permeability has resulted in reduced water movement through the profile and thus reduced potential for transport of soluble salts to be collected as leachate. It should

be noted that the results presented here do account for the volume of leachate. Thus a decrease in permeability may show an increase in soluble concentration per volume, however the total amount transported is in fact decreased.

One indication that the latter is perhaps not the case for all tailings dam is the continued increase in Cu concentration at Woodlawn, while the majority of other solute concentrations are decreasing. It would be expected that if elemental concentrations were decreasing because of reduced water flow, Cu would also decrease even if chalcopyrite was continuing to oxidise. Therefore it is suggested that the developing secondary minerals may be coating the sulfides and thus reducing oxidation and acid generation and thus neutralisation reactions resulting in a general decrease in leachate concentrations. However the fact that the Cu is still increasing indicates that sulfides (especially chalcopyrite) must still be exposed to oxygen and water. Thus hardpan cements have probably effected the elemental loads released from these tailings but not to the extent as those observed in the highly pyrrhotitic Elura tailings. Adsorption and co-precipitation reactions may have played a larger role in pollutant capture at Woodlawn.

In the low to very low sulfide content tailings (CSA and Peak), release of solutes to the leachate varied considerably and in many trials the true potential for leachate release and thus secondary cementation was not fully realised because of the time constraint of the experiment. Within the very low sulfide oxide tailings (Pine Creek and Ranger) where acid generation was limited or non-existent, solute release is associated with simple dissolution reactions of both primary and secondary minerals and processing additives.

The low sulfide tailings of the CSA and Peak trials which contained substantial neutralising minerals showed increased levels of Ca and Mg release associated with calcite and dolomite dissolution enhanced by acid generation. Release of Fe, Pb, and Zn showed an increase in the final stages of these experiments. This release and thus increased mobility of the metal ions corresponds to a decrease in pH in the Peak trial. The increased metal release in the CSA trial however does not correspond to a decrease in pH and is suggested to be due to the exhaustion of absorption sites for these ions. These increasing metal ion trends indicate that in these trials a longer experimental period would potentially have shown the true potential of the tailings for solute generation and the final effect of secondary mineralisation on these loads.

Similar observations were made within highly sulfidic tailings which contained high levels of neutralising minerals (Woodcutters). However in these sulfidic tailings, only a very minor decrease in pH was observed and limited variations in Ca and Mg release occurred. In these cases however the release of Pb and Zn remained amongst the highest throughout the life of the experiment, while Fe release increased to some of the highest levels in the final stages. In these trials again, the full pollutant load was not achieved. Once all neutralisation reactions are completed after a long period, base metal release will no doubt increase through the development of more acidic conditions.

Two Brukunga samples were also utilised in this experiment, one air dried prior to packing the other tailings sampled and packed directly from the dam. There appears to be a distinct differences between

the two Brukunga samples based on the solute concentrations. In B1 (air dried sample) much of the acid generation and subsequent neutralisation by gangue minerals must have already started as release of lithophile elements (Al, Mg etc) was more pronounced. Whereas for B2 (unoxidised sample) the major solute releases were due to direct sulfide oxidation. A comparison of the EC trend for both experiments (Fig 6.16) indicates that B2 released greater solute loads with maximum EC levels of 17mS/cm compared with B1 which peaked at 12.5mS/cm. The maximum EC in B2 occurred during the first leach at 37 days while in B1 the maximum EC occurred at 99 days during the 4th leaching cycle. This may indicate that either B2 is more reactive as fresh tailings become exposed or that the B1 release takes longer because of the secondary mineral coatings developed prior to packing and the lag period associated with destabilisation of these coatings.

6.4.4 Leachate Overview

The results obtained in this study should only be used as a comparison between elements and not as the final contaminant load of leachates. This is simply because of the large number of variables which can effect the contaminant load. Doepker (1991) explained that there are significant factors influencing the dissolution and transport of metals, including availability of oxygen, amount of pore water, leachant pH, ionic strength, and type of ions present, leachate contact time (residence/rest time), depth of tailings, volume of leachant, pore water evaporation rate and degree of saturation, and dry tailings "storage" time, humidity and secondary mineral formation. Thus comparisons between tailings from different mines can only be made when experimental parameters remain constant.

The results presented here show the total solute percentage leached in most cases was minimal compared with the total elemental load available. The majority of tailings initially contained readily soluble Na, S, Ca, K and Mg which were flushed from the tailings in the earliest leaching cycles. The subsequent solute release was dictated by the stability of the minerals containing these elements. During the life of the experiment, solute release generally increased to a peak and then decreased over time. Variations in the timing of peak concentrations simply reflected the different solubility and reactivity of the original tailings minerals. In the highly pyrrhotitic and pyritic tailings the decrease in solute concentration was attributed to secondary mineral precipitation similar to hardpan development. In the low sulfide content tailings, much of the solute load was attributed to direct dissolution of both primary and secondary minerals. In a number of cases the true potential for leachate release and thus secondary mineral precipitation was not fully realised because of the time restraints of the experiment.

The solute concentrations developed during this experiment are testimony to the ability of secondary minerals to dictate contaminant loads. This effect was enhanced in the highly sulfidic tailings containing low quantities of neutralising minerals, as they were the most reactive, producing significant solute loads available for secondary mineral formation.

6.5 Use of additives for the enhancement of hardpan formation and integrity

Both field observations and preliminary experiments show that cemented layers and hardpans form at or near the surface of tailings. However, formation processes are often slow and resultant hardpans are not sufficiently stable or impermeable to prevent AMD generation. The main purpose of this research was to develop techniques to enhance the formation of hardpans by use of various additives.

The initial experiments showed additions of Fe at a pH of 3 promoted hardpan development. However, recycling of AMD to the surface of tailings facilities is not presently considered environmentally acceptable, and the use of solid additives was examined.
The objectives of this 1-year long column experiment were therefore:

- selection of appropriate solid additives
- determination of methods of application and mixing
- determination of mineral characteristics of hardpans formed, and
- water/oxygen diffusion as measured by geotechnical parameters

using three different types of tailings

6.5.1 Experimental Design

6.5.1.1 Selection of Tailings

In response to preliminary experimental results, field observations, access and close-out benefits, tailings from three of the mines were selected for detailed testing. Preliminary column results played a crucial role in the selection of tailings but another important factor was to ensure research be undertaken on tailings where the results could be used in decisions regarding real close-out strategies. For this reason, the rehabilitated tailings facilities at Pine Creek, Brukunga and Kanmantoo were excluded. Constraints on continued access restricted the inclusion of Woodcutters, Woodlawn, Renison and Ranger tailings in this work. Broken Hill tailings were not included as closeout methods have already been employed at this site. The three sites selected for the continued research had different mineralogy and degrees of natural and laboratory hardpan development, but came from the same geological and climatic regime. The trial included Elura, CSA and Peak tailings, all originating from the Cobar Super Group metallogenic province in the Lachlan Fold Belt.

Elura tailings showed extensive hardpan development in the field and exhibited rapid formation under laboratory conditions. These tailings were included to determine whether additives have impacts on cementing abilities.

CSA tailings developed hardpans in the field but not as readily as Elura tailings. Laboratory trials showed only slight cementing and these tailings were included to determine whether hardpan development could be enhanced.

Peak tailings formed surface secondary minerals in the field, but had not been deposited for a sufficient period to determine long-term behaviour. Preliminary laboratory experiment showed little or no cementing. Inclusion provided data on the effect of additives on tailings with a potentially low natural cementing ability.

6.5.1.2 Selection of Experimental Parameters

Reviews of previous studies on both leaching and static column tests were undertaken to determine the most appropriate experimental procedures. There appeared to be little or no recommendations regarding column testing techniques, however it was emphasised that the column diameter must be sufficiently larger than the mean particle size of the material being tested. For example, a column experiment using 2mm sand should have a minimum diameter of 60-250mm (Zachara and Streile, 1991). The reviewed studies varied in the quantity of leachate and the presence or absence of saturation zones within the profile depending on the required outcomes of the experiments (Madgwick and Ralph, 1980, Lapakko and Antonson, 1990, Day, 1994, Rose and Darb, 1994, and Chermak and Runnells, 1995).

6.5.1.2.1 Column Design

The columns used in this experiment were approximately 1m high and 150 mm wide, with Suba Seal membranes down one side to allow needle/ syringe extractions of pore waters and gas if required throughout the experiment (Figure 6.17). Dripper heads with surgical needles were placed on top of each column to supply water without disturbing the tailings surface. After each wetting they were removed to allow increased evaporation. A water table was maintained within the column and varied during the wetting and drying cycles mimicking natural seasonal groundwater fluctuations as well as providing a water source for evaporation and elemental transport. When water levels dropped below the desired level, additional water was added directly to the external reservoir bottle which was fixed to the side of the column. At the base of the columns geotextile fabric held the tailings in place but allowed leachate to seep through to the reservoir which controlled the height of the water table.

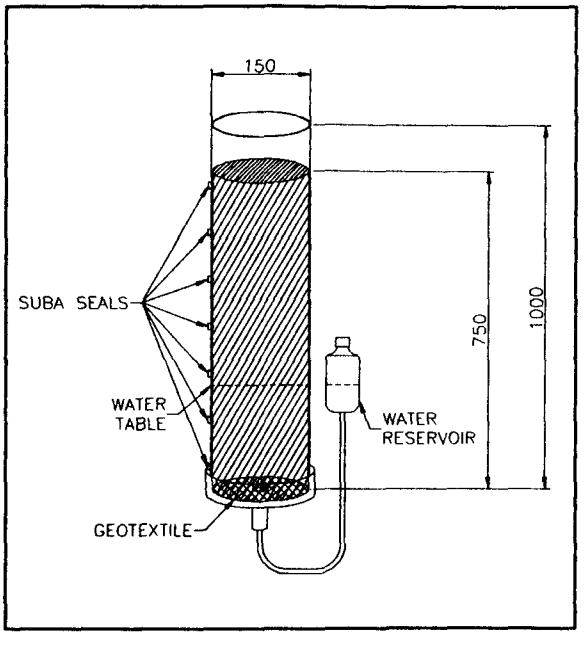

FIG 6.17 SCHEMATIC DIAGRAM OF COLUMN

(ALL MEASUREMENTS IN MM)

Total Volume = 13250 cm^3

Average Porosity of Control trials = 45%

Water addition = 280ml / fortnight

% of added water as function of pore space = 5%

6.5.1.2.1 Tailings Preparation

Tailings were obtained directly from the mill at each site in 44 gallon drums. During transportation the tailings settled so that the water and the tailings fractions required remixing upon arrival. After remixing, $^2/_3$ of each column was filled with tailings slurry and allowed to stand for several hours. Additives were then placed either as a surface mixture with the tailings (1:1 ratio via volume) (Fig 6.18A) or as a 10cm discrete layer, below a 10cm thick surface layer of tailings (Fig 6.18B). These two types of mixing and packing of tailings were utilised to ensure a number of possible cementing mechanisms could be investigated. The surface tailings/additive mixture allowed investigations of the cementation processes taking place through direct sulfide/additive contact, whereas the discrete layer of additive at depth was designed to examine the leaching processes of oxidation by-products down the profile and precipitation associated with pH boundaries.

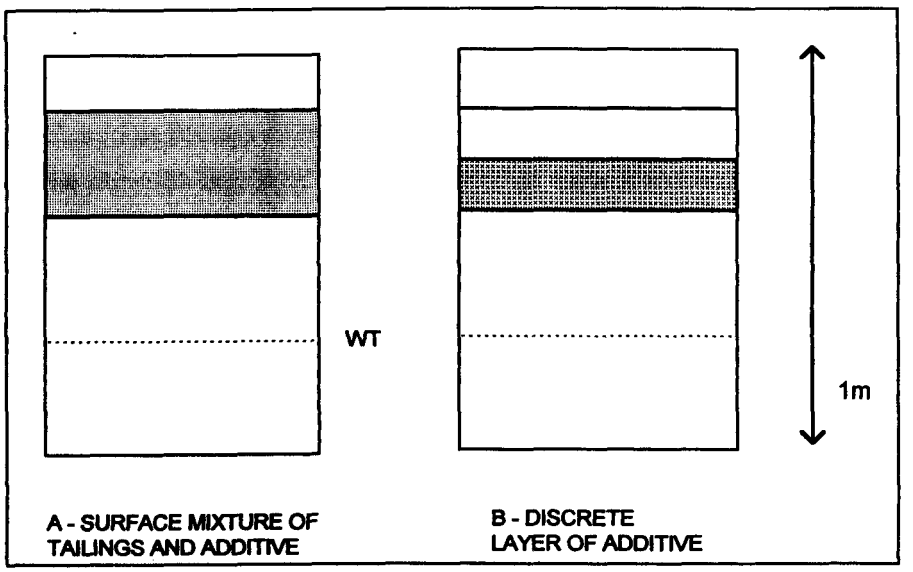

FIG 6.18 SCHEMATIC DIAGRAM OF ADDITIVE TECHNIQUES

6.5.1.2.2 Leaching Regime and Water Supply

As with the preliminary experiments, rainfall simulation was based on that at locations of extensive hardpan development, eg. Broken Hill and Cobar. Rainfall simulations were initially delivered on a fortnightly cycle however concerns regarding the level of water saturation and thus reduced oxidation led to a change to irregular additions of water twice a month.

6.5.1.3 Selection of Additive Types

A literature review was undertaken to select additives which may induce cementing processes in the tailings. The four additives selected were flyash, rock phosphate, limestone and lime. A detailed review of the mechanism of cementation associated with these additions along with previous field and laboratory studies is presented below.

6.5.1.3.1 Lime/limestone

The main objective of the addition of lime/limestone was the development of Fe oxide cements due to neutralisation of acid generated by sulfide oxidation. Rose and Darb (1994) compared lime and limestone for neutralisation processes and indicated lime was better than limestone. They hypothesised that because lime is commonly finer than limestone, it's large surface area can result in greater reactivity and thus may produce more alkaline environments. They suggested that some small volumes (micro environments) in limestone-amended samples lacked significant alkalinity and bacteria were able to metabolise creating acidity and dissolved SO_4^{2-}, Fe^{2+} and Mn^{2+}. Any acidity within the limestone amended samples was largely neutralised resulting in the precipitation of Fe oxides. Such precipitates were not observed in the lime treated samples, as lime completely prevented acid formation.

Thus limestone addition was included for the potential development of Fe oxide cements while lime addition was trialed as a comparison.

6.5.1.3.2 Flyash

Flyash is a by-product of the combustion of pulverised coal in thermal power plants. It is removed by electrostatic precipitation as a fine particulate residue from the combustion gases before they are discharged to the atmosphere. The particle size ranges from 1-150μm, with the majority less than 45μm. More than 85% of flyash comprises minerals (mullite and anorthite) and glasses formed from the elements Si, Al, Fe, Ca and Mg (Malhotra, 1992).

In the acid conditions which prevail in oxidising tailings, Si, Al, Fe, Ca and Mg may be released from the metastable alumino-silicates of the flyash thus becoming available to complex with other ions, resulting in the development of cements. Flyash has also been suggested as a hydraulic inhibitor which may be beneficial through reducing permeability and thus potentially creating longer reaction times to form cements (Bowders et al. 1994).

Although no examples for the direct use of flyash were found, Rao et al. (1991) gives some insight into the processes of silica behavior. They describe bench-scale studies of the coagulation of fine silica, clay slurries, and municipal waste water by AMD. The idea that AMD can cause coagulation in a silica slurry was explored. Results showed that the silica slurry did certainly effect the system through faster settling rates and decreased metal load in residual solutions. The results also indicated that at low pH conditions, the effect on the silica slurry was limited. The adsorption of other elements by silica is pH dependent with the point of zero charge occurring at pH 2 (Parks, 1967). The negative charge of silica at pH>2 promotes adsorption of metal ions, whereas, the low pH of most sulfidic tailings increases the positive charge due to H^+ ions on silica surfaces, thus hindering adsorption of metal ions. This complication was overcome by mixing a buffer (lime) which neutralised the H^+ ions and resulted in increased cation uptake.

The addition of lime as a buffer was suggested to have a double effect, as it causes pozzolanic reactions to occur within flyash. A pozzolan is defined as a siliceous or siliceous and aluminous material which itself possesses little or no cementing properties but which will, in finely divided form and in the presence of moisture, chemically react with $Ca(OH)_2$ at ambient temperatures to form compounds possessing cementitious properties. Thus the metastable alumino-silicates within the flyash can react with Ca^{2+} in the presence of moisture to form calcium silicate hydrates if the pH is sufficiently high (Malhotra, 1992).
Pure flyash additions were included for

- potential cementing produced through the complexing of the elemental constituents of flyash with by-products produced through sulfide oxidation and tailings breakdown
- the elemental scavenging ability of pure flyash
- the inhibiting hydraulic properties which may be beneficial through reduced permeability and thus potentially longer reaction times to form cements

Mixtures of flyash and lime were included for

- maintaining pH levels sufficiently high enough to sustain the scavenging ability of the silica, and
- the development of pozzolanic reactions producing calcium silicate cements

6.5.1.3.3 Rock Phosphate

Phosphate cements are suggested to form when rock phosphate is added in an acidic environment (Meek, 1991). When pyrite begins to oxidise, the pore water within the tailings may potentially become acidic, in which case the phosphate rock will release phosphate ions into solution. The phosphate ions will then complex with the ferrous ions on the pyrite surfaces to coat the reactive surfaces with iron phosphate compounds (Meek, 1991). Phosphate rock may also act as a hydraulic barrier (Bowders & Chiado, 1990).

The application of phosphate rock (apatite) along with other acid preventative measures were investigated in the Upshur Complex, West Virginia (Island Creek Mining) (Meek, 1991). Apatite was placed on the pit floor prior to back filling and blended into acid generating overburden at a rate of 3 tons apatite/1000 tons of spoil. Results were compared with sealing via plastic liners, lime addition and selective handling and placement techniques. None of the techniques attempted were totally successful in preventing AMD. However an evaluation indicated that the most cost-effective acid preventative technique was the apatite admixture (Meek, 1991).

The addition of phosphate using KH_2PO_4 was also reviewed. The main problem identified was that if an addition of acid occurred after the coatings were established, this chemically engineered coating may became unstable and additional KH_2PO_4 is required (Evangelou, 1994 and Huang & Evangelou, 1994). Using phosphate rock, a large quantity of phosphate can be easily added and if the initial coatings are removed due to a decrease in pH, the phosphate ions will again be released from the apatite potentially resulting in the precipitation of another coating.

Huang & Evangelou (1992) and Evangelou (1994) discussed possible complications with Fe phosphate coatings resulting from the pore water saturation. If the degree of saturation of the pore waters is relatively low, the Fe phosphate might not precipitate instantly and thereby exist as a discrete phase. Conversely, if the degree of supersaturation with respect to Fe phosphate is high, Fe phosphate will precipitate as a coating on pyritic surfaces. It was suggested that the use of a buffer reagent would greatly reduce the amount of pyrite oxidised to create the coatings and ensure precipitation of iron phosphate coatings (Evangelou, 1994). Thus trials involving phosphate with both lime and limestone were considered but concerns regarding the lack of acid development in the presence of lime (Rose and Darb, 1994) resulted in the application of phosphate rock with limestone only.

6.5.1.4 Selection from Potential Additives

Potential additives from a range of locations were analysed for mineralogy (XRD), element composition (XRF) and ICP-AES of water extracts at various pH values, to determine the mobility of the potential cementing agents and impurities in the phosphate and flyash samples. Lime, was obtained from a local hardware supplier.

6.5.1.4.1 Limestone

Five samples were removed from the Kleins Point Quarry, Stansbury, S.A. These samples represented the range of limestone available, based on SiO_2 content. A description of these samples is presented in Table 6.4.

TABLE 6.4 DESCRIPTION OF LIMESTONE SAMPLES

Sample	Sample Description
Sample A	fossiliferous-friable
	cream - pale yellow, some deep red staining
	50% Ca, 5% Si
Sample B	fossiliferous-friable
	red - orange
	50% Ca, 3% Si
Sample C	hard - less friable - fossiliferous in some layering only
	50% Ca, 3% Si
Sample D	mainly sand grains - friable but not fossiliferous
	cream - pale yellow, slight red staining
	45% Ca, 15% Si
Sample E	Blend - Content of shipment
	50% Ca, 5% Si

Sample D was determined as the most appropriate sample for use in the trial. XRD analysis indicated that it contained calcite, dolomite and quartz. XRF analysis suggested Sample D had the lowest carbonate content (inferred from the 5-6% lower CaO content) and thus its neutralisation potential was diminished (Table 3A.41, Appendix 3A). However, as the SiO_2 levels were up to 10% higher than the

other samples, it was suggested that enhanced silica mobility under these alkaline conditions may promote siliceous cements.

6.5.1.4.2 Phosphate Rock

Four samples of phosphate rock were obtained from the Pivot Fertilizer Company, Adelaide, S.A. and included phosphate rock from Christmas Island B, Florida, Nauru and a blend of all 3 presently being used at the plant. XRF analysis indicated that the Nauru phosphate rock had the highest CaO and P_2O_5 contents of all investigated and generally lower impurities. Levels of up to 1250 ppm Zn were noted as a possible problem (Table 3A.42, Appendix 3A).

The water extracts at pH values of 6.5, 5.5, 3.5 and 2 indicated that the Christmas Island B sample released the greatest quantities of phosphorus in the lower pH ranges (Table 3A.43, Appendix 3A), which however, were accompanied by elevated levels of impurities (Al, Ca, Cu, Fe, Ni and Zn). The next highest soluble phosphorus content was released from the Nauru phosphate with potassium being the only ion released in any significant quantities. The Zn content of Nauru phosphate detected by XRF is obviously less mobile and thus not a potential pollutant. The Nauru rock phosphate was therefore selected for use in the hardpan trials.

6.5.1.4.3. Flyash

Four samples of flyash were obtained from the Port Augusta Power Station, S.A. These samples represented the various flyash types collected from the electrostatic precipitators and included Unit 1 - Zone 1, Unit 1 - Zone 2, Zone 2-3 and Bottom Ash.

XRF analysis indicated that the Unit 1-Zone 2 flyash would be most appropriate because of its low impurities and high Al content, even though it contained 6% less Si than the Bottom Ash (Table 3A.44, Appendix, 3A). However when subjected to acid extractions, the Al and Si mobility was greatest in the Bottom Ash and the impurities released were not substantially greater than those released from the other samples (Table 3A.45, Appendix, 3A) and was therefore selected for use in the experiments.

6.5.2 Review of Investigations

Enhanced hardpan formation within tailings dams has the potential to reduce water and oxygen penetration into the tailings, and as a result restrict sulfide oxidation and solute generation and transport. Forty three columns consisting of 4 control columns containing pure tailings only (Elura had 2 control columns due to excess tailings), and 39 columns of tailings and additives as surface mixes and discrete layers systems, (Fig 6.18) were treated for 1 year to achieve hardpan formation. Various techniques have been utilised to determine the efficiency of the cements in reducing sulfide oxidation and thus AMD generation.

Permeability investigations

Permeability is a measure of the ability of the cement to reduce the movement of oxygenated water into the underlying tailings thus reducing oxidation reactions and transportation of contaminants. Initial permeability tests were not able to be performed within the columns due to leaks in the initial stages of the experiment. For this reason permeability tests on representative samples were carried out in laboratory oedometer appartus. The discrete layered experiments (Fig 6.18b) could not be simulated using the oedometers, and so permeabilities based on pure amendments and pure tailings were determined. These results were compared with falling head permeability tests carried out in the columns after 1 year of treatment to determined the characterisics of each additive.

CO_2 analysis

After permeability had been determined, the columns were allowed to drain for 1 month, at which time gas samples were removed at 10cm depth intervals within the columns to determine the CO_2 content to ascertain the movement of gas within the profiles. These analyses provided insight into the ability of the cements to restrict O_2 movement and thus restrict oxidation of the underlying tailings.

Chemical Evaluations

After the gas sampling was completed, the columns were opened under anaerobic conditions in an argon filled chamber. Eh and pH measurements and sub-samples taken for soluble Fe^{2+}/Fe^{3+} analysis. This chemical evaluation gave an insight into the extent of oxidation reactions taking place within the columns and the solute loads being produced.

Geotechnical Evaluations

Once removed from the chamber, samples were taken for moisture content, particle density and bulk density measurements. From these results, total porosity, air-filled porosity and degree of saturation were calculated.

6.5.3 Results

6.5.3.1 Permeability

6.5.3.1.1 Initial Permeability and Porosity of the tailings and additives

The initial permeability and porosities of the tailings and additives used in this experiment were determined through laboratory oedometer testing (Method section 1A.4.7.3 Appendix 1A). Saturated tailings were placed in the oedometer apparatus and permeability determined at 7 separate vertically applied stresses. With increased loading the samples consolidated, achieving higher bulk densities and lower porosities. Consolidation rates and porosities were determined at each stage. Table 6.5 presents permeability, bulk density and porosity results at various stresses for the 3 tailings types. Fig 6.19 shows permeability of the samples as a function of stress. From these results, it was determined that after

loadings equivalent to 19.4 kPa stress, the permeability decreased at the same rate as below 19.4 kPa and thus investigations in the higher stress ranges for all mixture and additive tests were not warranted.

FIG 6.19 CONTROL TAILINGS OEDOMETER RESULTS - PERMEABILITY VS. STRESS

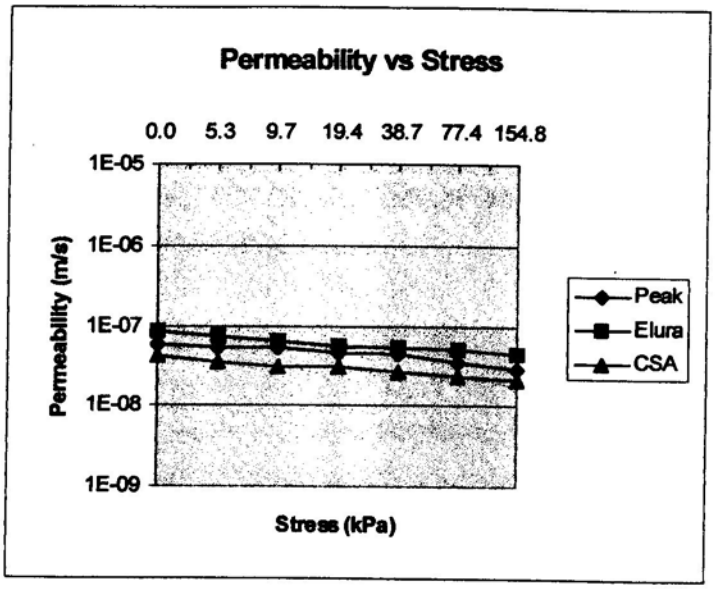

TABLE 6.5 CONTROL TAILINGS OEDOMETER TEST RESULTS

Test No.	Applied Vertical Stress (kPa)	Average Dry Bulk Density (t/m³)	Average Permeability (m/s)	Average Porosity (%)
Peak 1	0.00	1.50	5.91E-08	46.1
2	5.32	1.54	5.29E-08	44.7
3	9.68	1.55	5.34E-08	44.3
4	19.36	1.56	4.69E-08	44.0
5	38.71	1.59	4.53E-08	43.1
6	77.42	1.61	3.57E-08	42.2
7	154.85	1.64	2.89E-08	41.2
Elura 1	0.00	2.30	8.33E-08	45.6
2	5.32	2.42	7.25E-08	42.9
3	9.68	2.45	6.52E-08	42.2
4	19.36	2.49	5.67E-08	41.3
5	38.71	2.51	5.39E-08	40.7
6	77.42	2.55	5.07E-08	39.8
7	154.85	2.59	4.48E-08	38.8
CSA 1	0.00	1.25	4.22E-08	56.5
2	5.32	1.33	3.51E-08	53.9
3	9.68	1.34	3.11E-08	53.5
4	19.36	1.36	3.05E-08	52.7
5	38.71	1.39	2.68E-08	51.8
6	77.42	1.42	2.33E-08	50.7
7	154.85	1.43	2.15E-08	50.2

Pure additives and tailings-additives mixtures were subsequently tested over stress ranges from 0 to 19.4 kPa. Permeability, porosity and bulk density were determined at each stress. Table 6.6 and Figures 6.20 and 6.21 presents a typical set of results. Results of individual tests are presented in Appendix 3A, Tables 3A.46 and 3A.47.

FIG 6.20 PERMEABILITY VS. DRY BULK DENSITY FOR FLYASH AND CSA TAILINGS

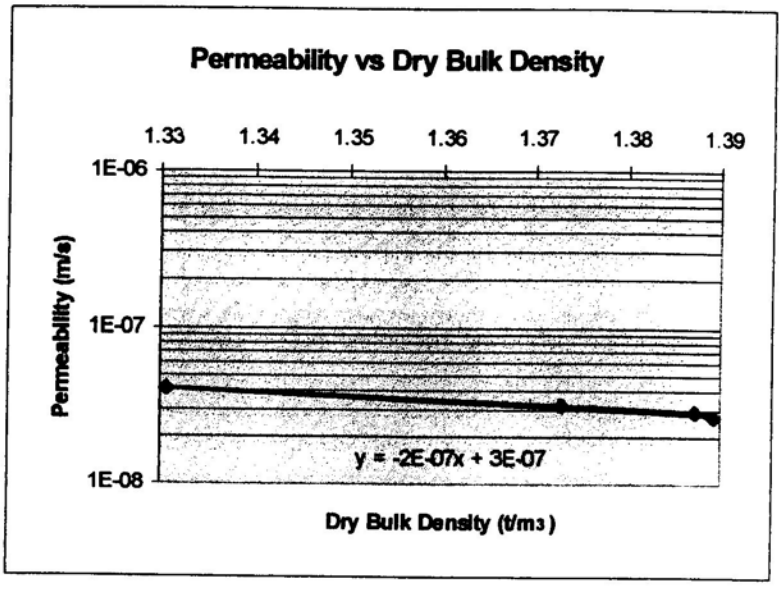

FIG 6.21 POROSITY VS. DRY BULK DENSITY FOR FLYASH AND CSA TAILINGS

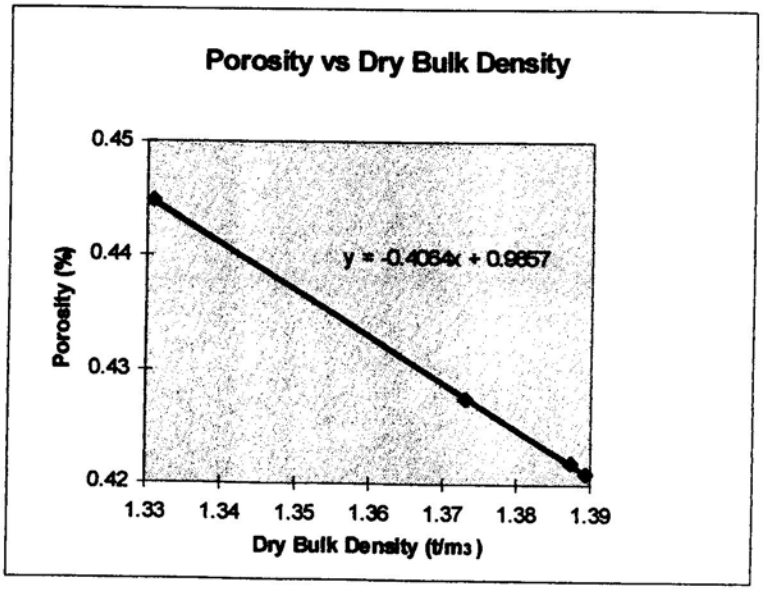

TABLE 6.6 TYPICAL RESULTS FOR OEDOMETER TEST - EXAMPLE OF FLYASH & CSA TAILINGS MIX

Test No.	Applied Vertical Stress (kPa)	Average Dry Bulk Density (t/m^3)	Average Permeability (m/s)	Average Porosity (%)
1	0.00	1.33	4.06E-08	44
2	5.32	1.37	3.20E-08	43
3	9.68	1.39	2.95E-08	42
4	19.36	1.39	2.71E-08	42

6.5.3.1.2 Final Permeability and Porosity Determination and Comparisons

After one year of treatment, permeability testing was carried out on each column using a falling head infiltration method (Method sections. 1A.4.7.1 Appendix 1A). After an additional 1 month period, bulk density profiles (Fig 6.22) and moisture contents (Fig 6.23) of each column were determined and the

loadings equivalent to 19.4 kPa stress, the permeability decreased at the same rate as below 19.4 kPa and thus investigations in the higher stress ranges for all mixture and additive tests were not warranted.

FIG 6.19 CONTROL TAILINGS OEDOMETER RESULTS - PERMEABILITY VS. STRESS

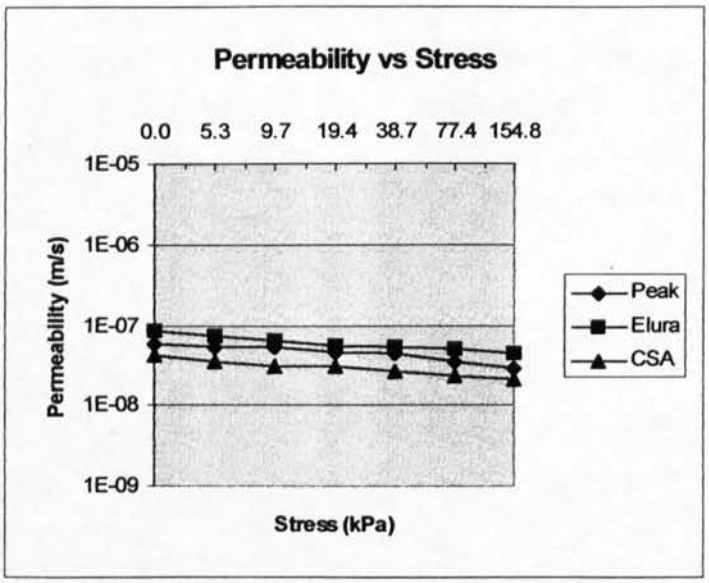

TABLE 6.5 CONTROL TAILINGS OEDOMETER TEST RESULTS

Test No.	Applied Vertical Stress (kPa)	Average Dry Bulk Density (t/m^3)	Average Permeability (m/s)	Average Porosity (%)
Peak 1	0.00	1.50	5.91E-08	46.1
2	5.32	1.54	5.29E-08	44.7
3	9.68	1.55	5.34E-08	44.3
4	19.36	1.56	4.69E-08	44.0
5	38.71	1.59	4.53E-08	43.1
6	77.42	1.61	3.57E-08	42.2
7	154.85	1.64	2.89E-08	41.2
Elura 1	0.00	2.30	8.33E-08	45.6
2	5.32	2.42	7.25E-08	42.9
3	9.68	2.45	6.52E-08	42.2
4	19.36	2.49	5.67E-08	41.3
5	38.71	2.51	5.39E-08	40.7
6	77.42	2.55	5.07E-08	39.8
7	154.85	2.59	4.48E-08	38.8
CSA 1	0.00	1.25	4.22E-08	56.5
2	5.32	1.33	3.51E-08	53.9
3	9.68	1.34	3.11E-08	53.5
4	19.36	1.36	3.05E-08	52.7
5	38.71	1.39	2.68E-08	51.8
6	77.42	1.42	2.33E-08	50.7
7	154.85	1.43	2.15E-08	50.2

Pure additives and tailings-additives mixtures were subsequently tested over stress ranges from 0 to 19.4 kPa. Permeability, porosity and bulk density were determined at each stress. Table 6.6 and Figures 6.20 and 6.21 presents a typical set of results. Results of individual tests are presented in Appendix 3A, Tables 3A.46 and 3A.47.

FIG 6.20 PERMEABILITY VS. DRY BULK DENSITY FOR FLYASH AND CSA TAILINGS

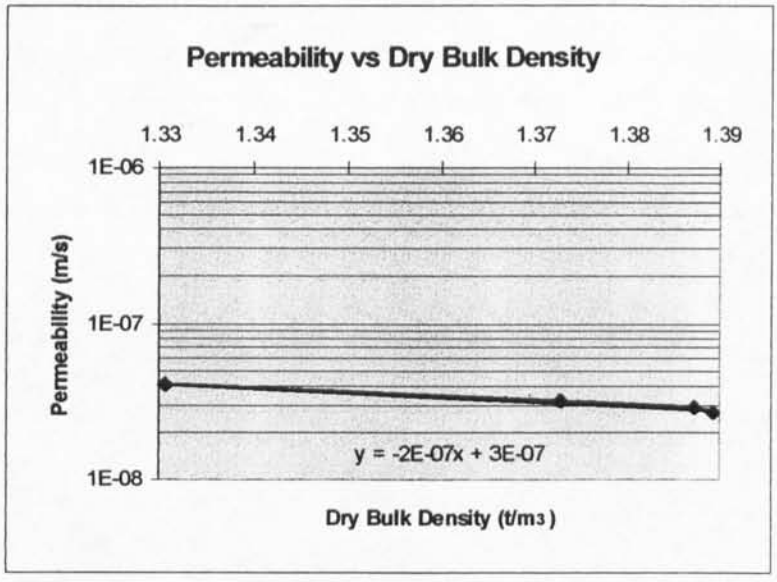

FIG 6.21 POROSITY VS. DRY BULK DENSITY FOR FLYASH AND CSA TAILINGS

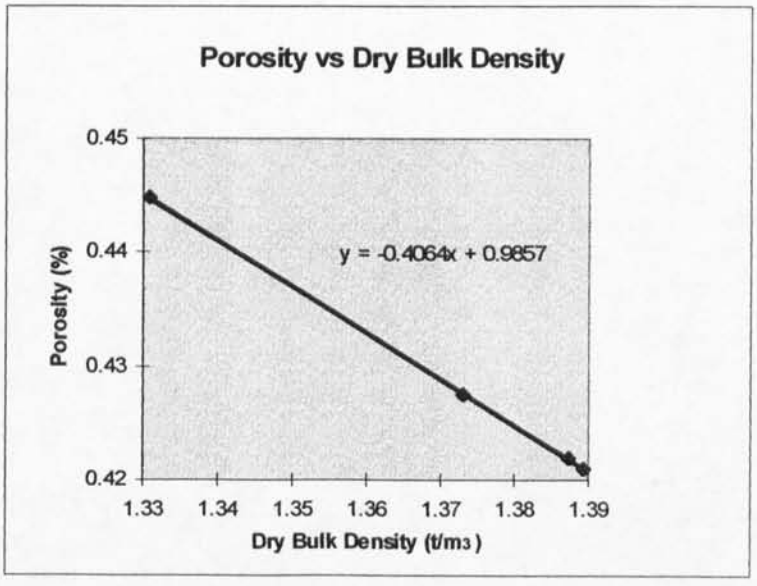

TABLE 6.6 TYPICAL RESULTS FOR OEDOMETER TEST - EXAMPLE OF FLYASH & CSA TAILINGS MIX

Test No.	Applied Vertical Stress (kPa)	Average Dry Bulk Density (t/m^3)	Average Permeability (m/s)	Average Porosity (%)
1	0.00	1.33	4.06E-08	44
2	5.32	1.37	3.20E-08	43
3	9.68	1.39	2.95E-08	42
4	19.36	1.39	2.71E-08	42

6.5.3.1.2 Final Permeability and Porosity Determination and Comparisons

After one year of treatment, permeability testing was carried out on each column using a falling head infiltration method (Method sections. 1A.4.7.1 Appendix 1A). After an additional 1 month period, bulk density profiles (Fig 6.22) and moisture contents (Fig 6.23) of each column were determined and the

porosity, air-filled porosity and degree of saturation calculated (Method sections 1A.4.2 to 1A.4.6 Appendix 1A). Comparisons of initial and final permeability and porosity were accomplished via contrasting the bulk densities achieved during the oedometer testing to those observed at the end of the experiment. Table 6.7 presents the initial and final bulk densities and their corresponding permeabilities and porosities.

TABLE 6.7 ORIGINAL AND FINAL BULK DENSITIES, PERMEABILITIES AND POROSITIES FOR THE MAIN COLUMN EXPERIMENT

Sample	Measured Final Bulk Density (t/m³)	Final Bulk density comparison with initial oedometer tests	Comparable Original Bulk Density (t/m³)	Comparable Stress (kPa)	Extrapolated Original Permeability (m/s)	Measured Final Permeability (m/s)	Extrapolated Total Porosity (%)	Measured Final Total Porosity (%)	Measured Final Air filled Porosity (%)
CC	1.56	greater		>154.8	1.2E-08	1.9E-08	47.2	43.2	2.2
EC	2.44	within	2.45	9.7	6.3E-08	2.7E-08	42	42.1	0
PC	1.63	within	1.64	154.8	2.8E-08	8.3E-08	40.8	40.8	2.6
CFLI	1.03	less	1.08	0	>1.6E-08	5.6E-08	>59	60.7	0
EFLI	0.96	less	1.08	0	>1.6E-08	2.3E-08	>59	63.8	1.3
PFLI	1.08	within	1.08	0	1.6E-08	3.5E-08	59	58	2
CFI	0.97	less	1.47	0	>1.0E-08	2.2E-08	>35	50.2	28.3
EFI	1.17	less	1.47	0	>1.1E-08	1.8E-07	>35	48.1	9.5
PFI	1.24	less	1.47	0	>1.1E-08	5.7E-08	>35	45.2	9.7
CLI	0.9	less	0.95	0	>2.4E-08	3.0E-08	>60	68.7	18.7
ELI	0.66	less	0.95	0	>2.4E-08	1.2E-07	>60	72.3	7.7
PLI	1.02	within	1.02	9.7	2.1E-08	3.9E-08	57	63	0
CPLI	1.11	less	1.38	0	>1.2E-08	1.7E-07	>51	61.1	33
EPLI	1.15	less	1.38	0	>1.2E-08	4.2E-08	>51	59.6	11.1
PPLI	1.22	less	1.38	0	>1.2E-08	2.9E-08	>51	57.9	24.4
CPLSTI	1.27	less	1.52	0	>6.5E-07	1.3E-08	>48	56.5	41.8
EPLSTI	1.24	less	1.52	0	>6.5E-07	2.4E-08	>48	57	27
PPLSTI	1.26	less	1.52	0	>6.5E-07	6.2E-07	>48	57.1	43.9
CPI	1.18	less	1.69	0	>1.0E-08	1.2E-07	>44	46.2	28.5
EPI	1.38	less	1.69	0	>1.0E-08	8.9E-08	>44	54.8	26.6
PPI	1.51	less	1.69	0	>1.0E-08	4.7E-07	>44	50.5	26.7
CLSTI	1.41	greater		>19.4	neg	4.8E-08	46.5	66	46.3
ELSTI	1.41	greater		>19.4	neg	1.4E-08	46.5	66	32
PLSTI	1.41	greater		>19.4	neg	7.5E-08	46.5	66	44.9
CLSTm	1.59	less	1.63	0	>4.7E-08	3.1E-08	>42	43.5	3.8
ELSTm	2.31	greater		>19.4	2.95E-07	3.0E-08	41.5	38.5	0
PLSTm	1.58	less	1.59	0	>4.6E-08	7.5E-08	>42	43.1	17.3
CPLm	1.16	less	1.25	0	>4.9E-08	2.3E-08	>56	59.4	0.5
EPLm	1.87	within	1.87	5.3, 9.7,19.4	3.4E-08	6.1E-08	50.4	49.3	11
PPLm	1.45	within	1.45	19.4	4.5E-08	2.8E-08	49	49	0
CFLm	1.14	within	1.09-1.2	0-5.3	5.7E-08	5.1E-08	58.7	58.7	20.3
EFLm	1.79	greater		>19.4	2.2E-07	4.1E-08	52.6	53.1	9.8
PFLm	1.41	greater		>19.4	1.5E-08	4.8E-08	48.6	48.3	11.7
EPm	1.63	within	1.5-1.68	0-5.3	2.2E-08	3.5E-09	44.7	44.8	9.1
CPm	2.23	greater		>19.4	2.5E-08	7.1E-09	40.9	40.9	2
PPm	1.8	within	1.79-1.83	5.3-9.7	1.4E-08	8.6E-09	37.5	37.9	4.9
CLm	1.04	greater		>19.4	7.2E-08	9.9E-08	62.2	62.2	1.35
ELm	1.77	greater		>19.4	2.2E-08	3.9E-08	54.2	54.2	6.5
PLm	1.41	greater	1.26	>19.4	2.6E-08	8.7E-08	49.3	49	0
CFm	1.23	less	1.33	0	>4.0E-08	8.7E-08	>44	48.7	3.1
EFm	1.74	less	2.1	0	>4.2E-08	1.2E-07	>40	50.5	0.9
PFm	1.51	less	1.55	0	>3.9E-08	3.3E-07	>40	42.1	0.07

Where P = Peak tailings, C=CSA tailings, E = Elura tailings

C=Control, L=lime, F=flyash, LST=limestone, P=phosphate

l=layer, m=mix

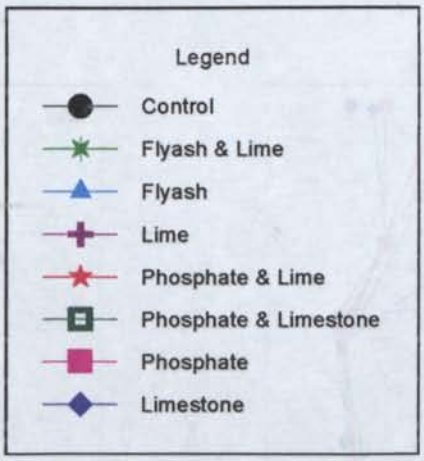

Legend used for Figs 6.22 to 6.25 and 6.28

where **A** = Mix trials

B = Layer trials

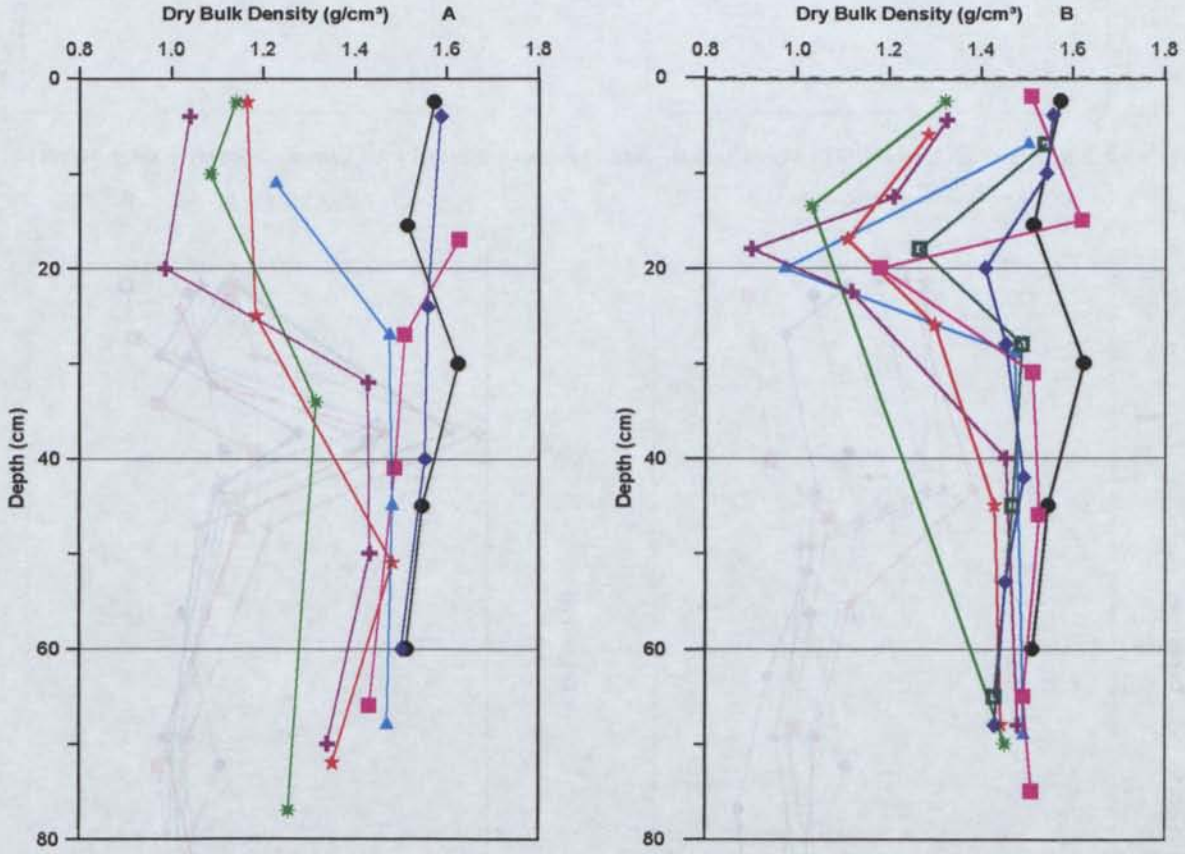

FIG 6.22A : DRY BULK DENSITY FOR CSA - SOLID ADDITIVE HARDPAN ENHANCEMENT EXPERIMENT

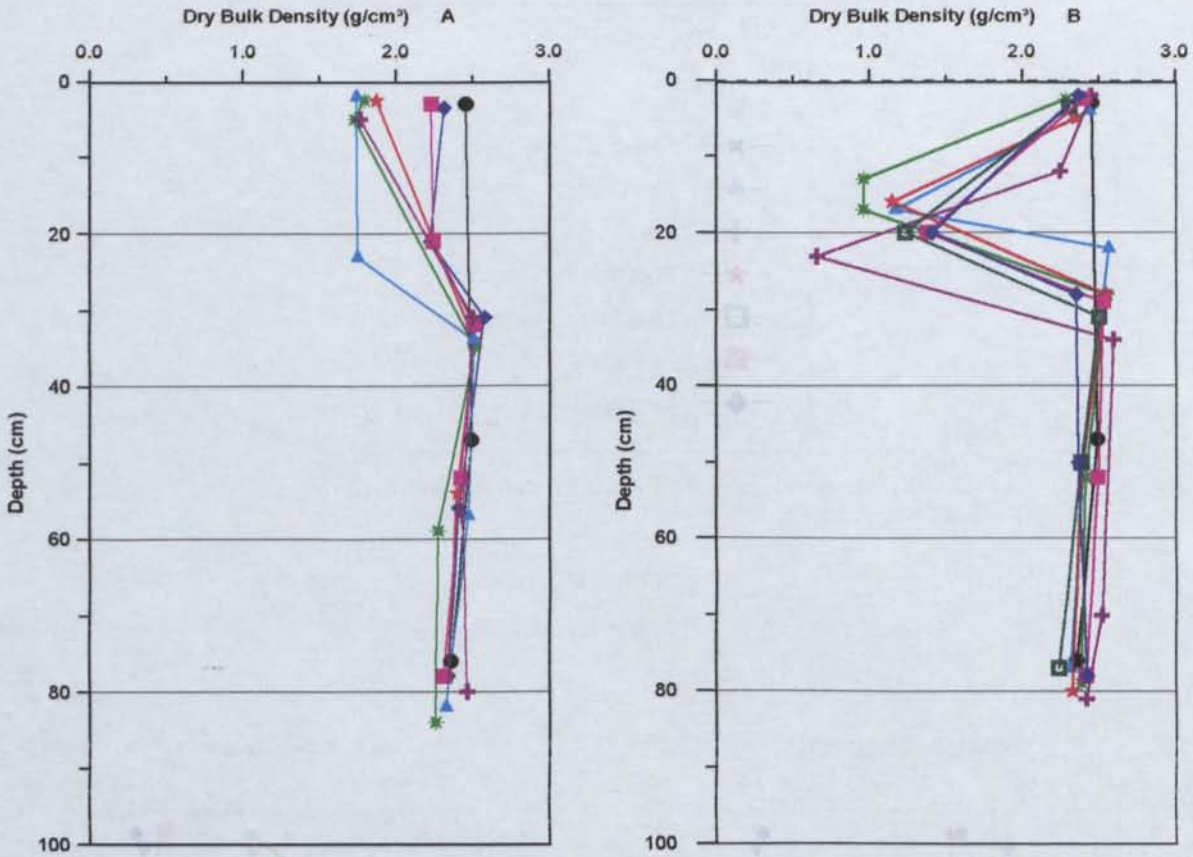

FIG 6.22B : DRY BULK DENSITY FOR ELURA - SOLID ADDITIVE HARDPAN ENHANCEMENT EXPERIMENT

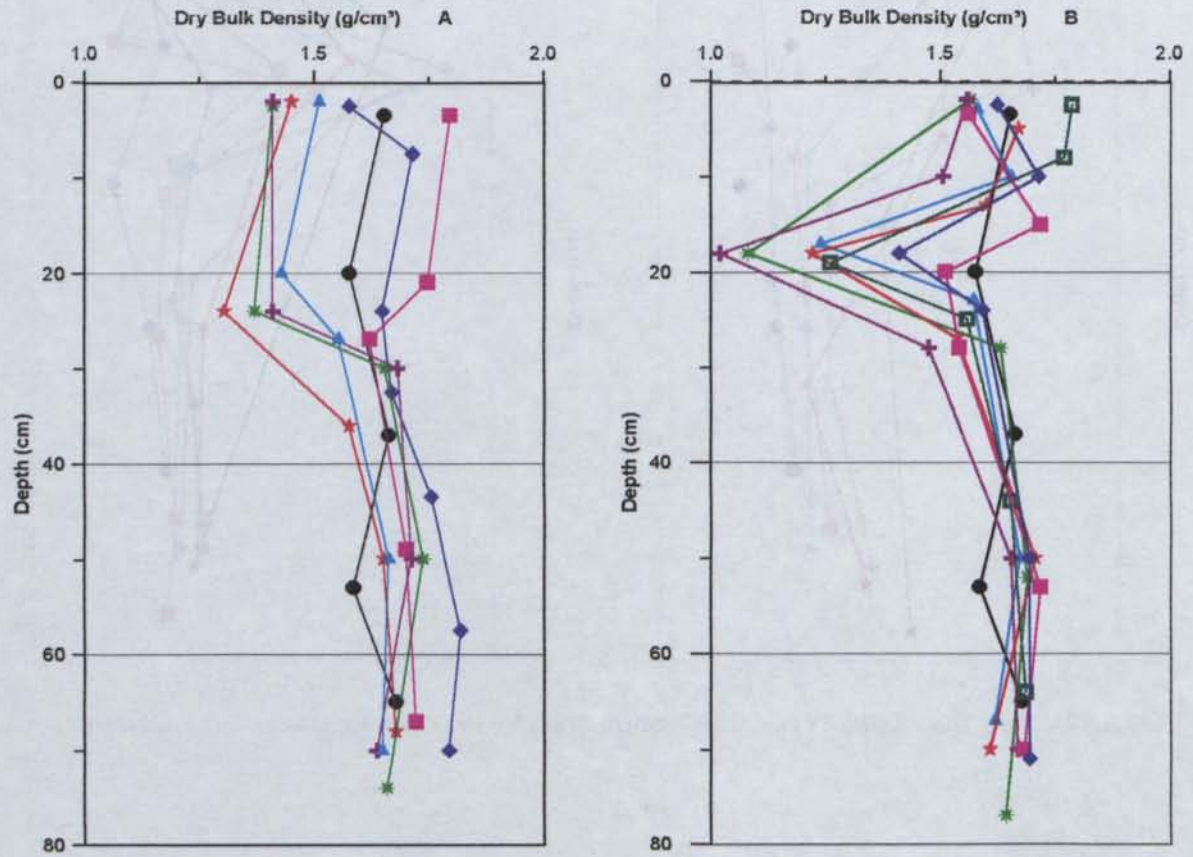

FIG 6.22C : DRY BULK DENSITY FOR PEAK - SOLID ADDITIVE HARDPAN ENHANCEMENT EXPERIMENT

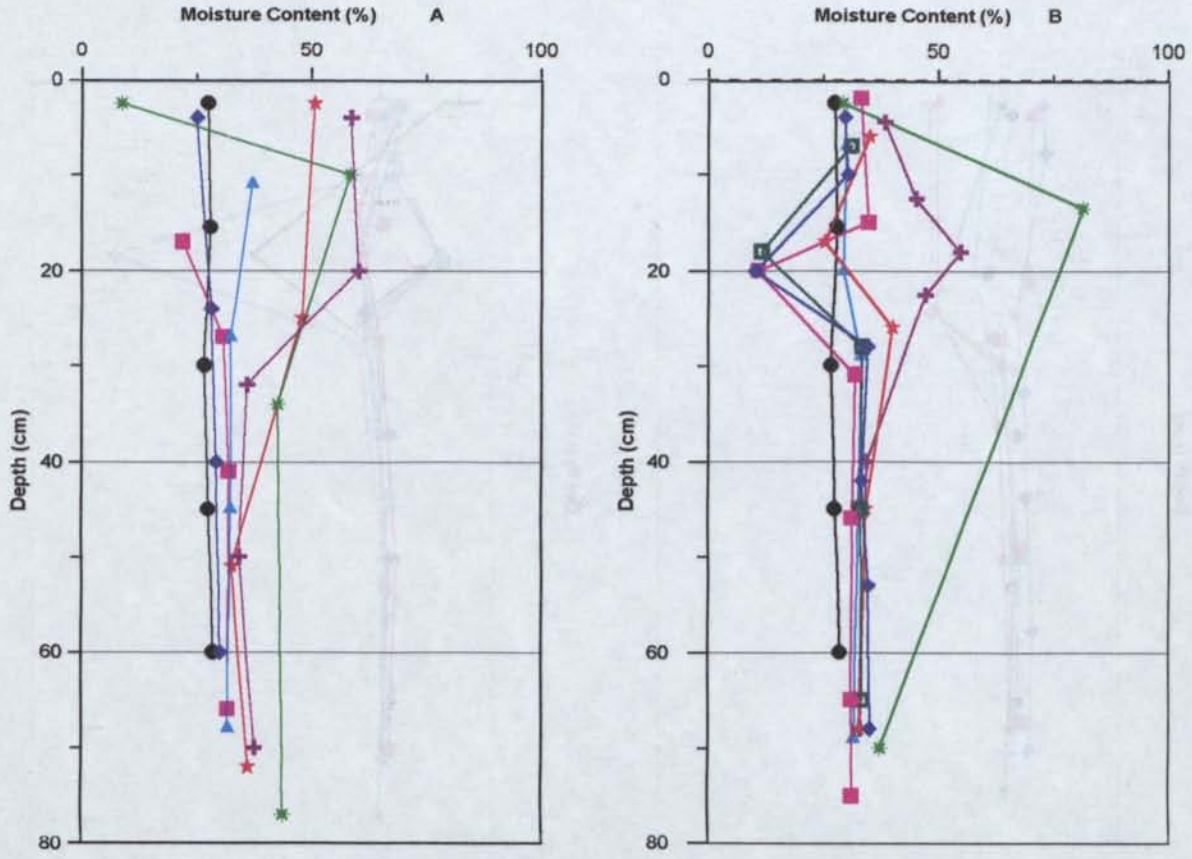

FIG 6.23A : MOISTURE CONTENT FOR CSA - SOLID ADDITIVE HARDPAN ENHANCEMENT EXPERIMENT

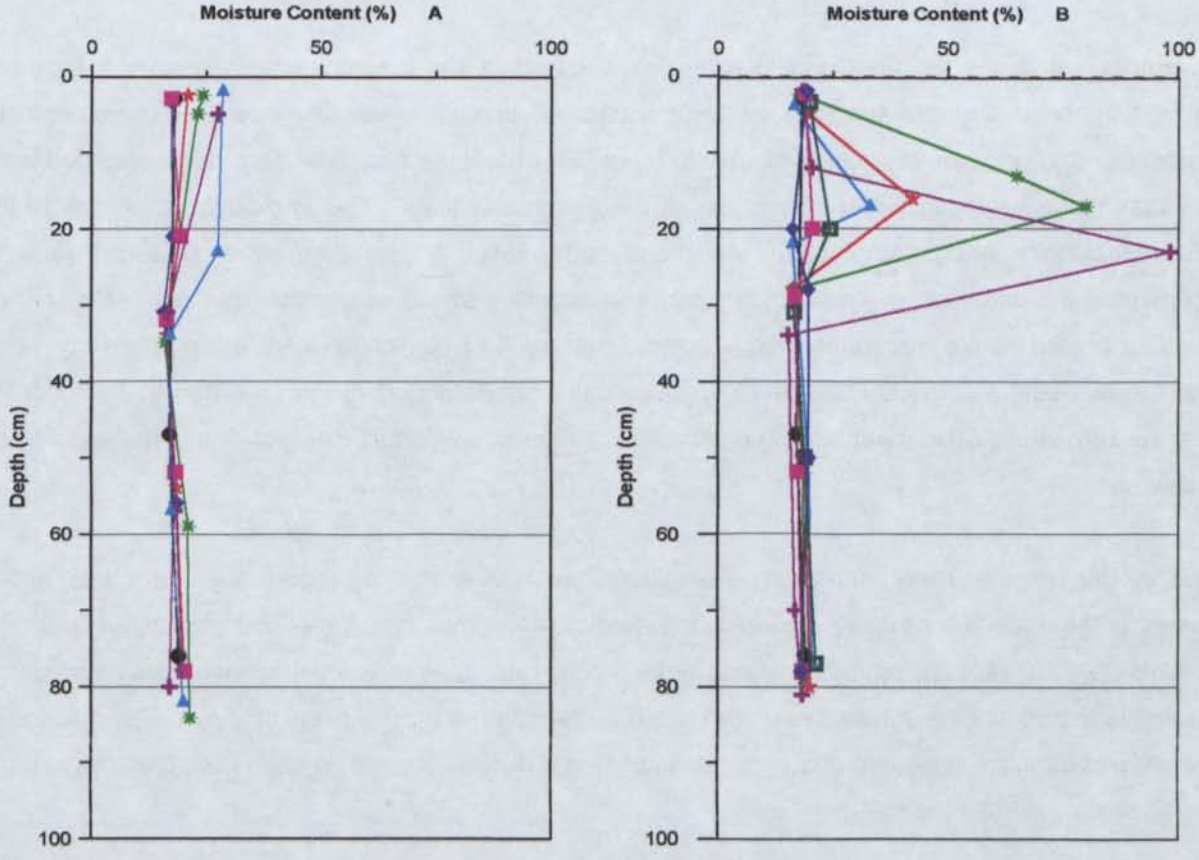

FIG 6.23B : MOISTURE CONTENT FOR ELURA - SOLID ADDITIVE HARDPAN ENHANCEMENT EXPERIMENT

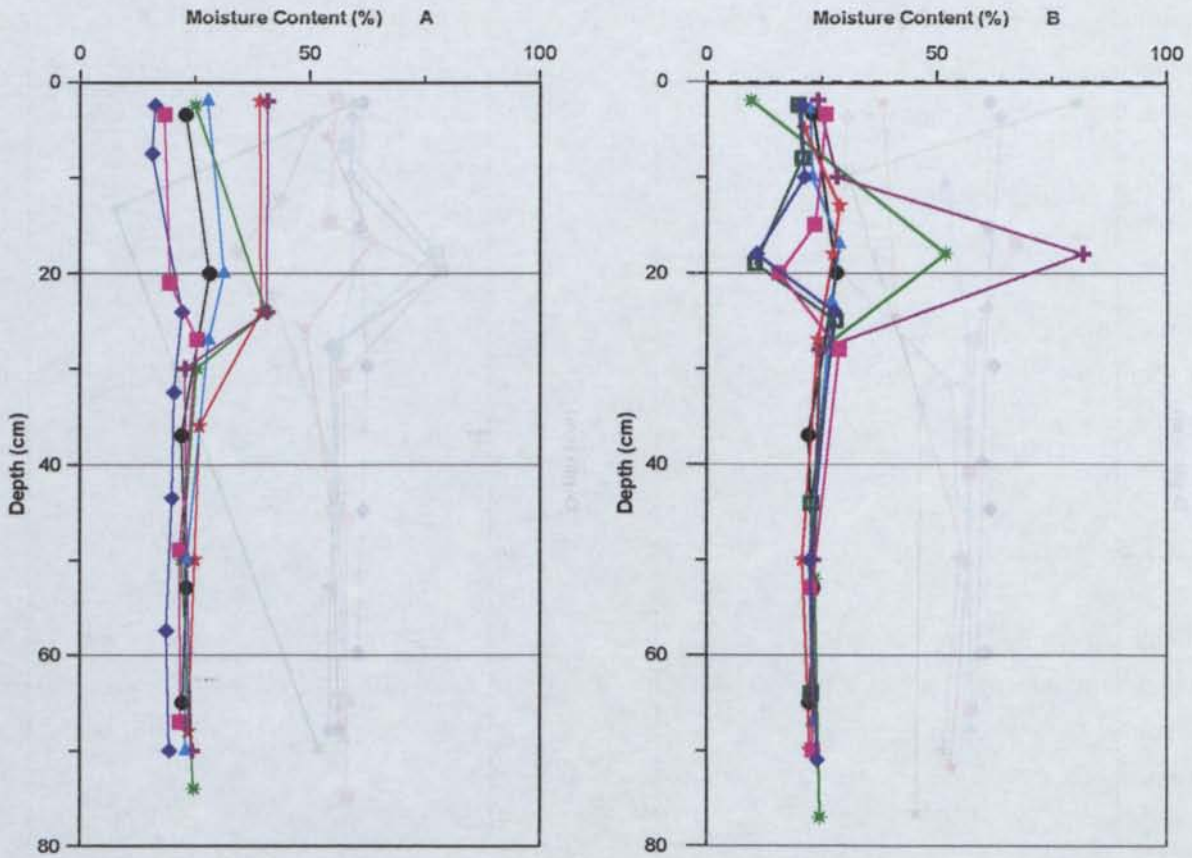

FIG 6.23C : MOISTURE CONTENT FOR PEAK - SOLID ADDITIVE HARDPAN ENHANCEMENT EXPERIMENT

In a number of cases the final bulk densities established in the columns where greater than those achieved in the oedometer testing. In these cases extrapolation was required to determine initial permeability and porosities for comparison. In other layer trials the final bulk densities developed were lower than those achieved under zero stress in the oedometer tests. This is thought to be due to the column packing methods employed. As mentioned previously, samples were saturated prior to placement in the oedometer, whereas, packing of the additive layers was in the dry state. Wet tailings were then placed above the additive layer but did not result in consolidation of the additive layer. In these cases, original permeabilities and porosities can only be stated as greater than those recorded under the zero stress oedometer tests and cannot be further quantified as extrapolation is not appropriate in these cases.

Some of the trials involving mixtures of additives also developed bulk densities lower than those obtained in the oedometer testing, and included the limestone mix, flyash mix and phosphate-lime mix. It is suggested that perhaps minor variations in the mixing rates may have been responsible. However, it is more likely that when the mixtures were placed in the column they set rapidly into a well developed structure and during subsequent drying, consolidation and desiccation forces were not sufficiently strong to significantly increase the bulk densities.

Unfortunately because of the differences encountered in bulk density, absolute quantification of the changes in permeability and porosities could not be attained for all layered trials. In these cases the final permeability of the columns was compared with the final permeabilities of the controls.

6.5.3.1.3 Control Permeability (Tailings Only)

The final permeabilities determined for the three control columns varied as a result of natural cementing potentials and the development of preferential flow paths and desiccation cracks. The permeability of CSA Control increased slightly over the 1 year period, from $1.2x10^{-8}$ to $1.8x10^{-8}$ m/s. The Elura Control had reduced permeability ($6.3x10^{-8}$ to $2.7x10^{-8}$), while the Peak Control permeability increased substantially from $2.8x10^{-8}$ to $8.3x10^{-8}$ m/s.

6.5.3.1.4 Permeability of Layered Additives - Comparisons with Controls

In many cases, the layered additives exhibited decreased permeability simply through their physical properties rather than any significant geochemical reactions producing impervious layers. Again, variations were produced by preferential flow paths and desiccation cracks both of which reflect natural processes.

The only well-cemented layer produced during this experiment was that of a mixture of flyash and lime in which the cements were developed through reactions between the two additives rather than via reactions with the tailings. Both Elura and Peak produced lower, while the CSA trial had an increased permeability. Similar permeability results were observed within the limestone layer trial however no cements were formed, suggesting that the permeability was dictated more by the upper tailings than the additive layer. The phosphate-limestone layer trial also produced a reduction in permeability for two of the trials however it was increased in the Peak trial.

Flyash, lime and phosphate layers all produced lower permeabilities in the Peak trials which appears to be more a function of the preferential flow paths in the Peak control rather than through any cements associated with the additive trials. The phosphate layer trials caused an increase in permeability in all repeats.

6.5.3.1.5 Comparisons of Permeability of Original and Final Mix Trials

The phosphate-tailings mix was the only test which successfully reduced the permeability in all trials. CSA tailings were reduced from an initial permeability of $2.2x10^{-8}$ to a final permeability of $3.5x10^{-9}$, Elura from $2.5x10^{-8}$ to $7.1x10^{-9}$ and Peak from $1.4x10^{-8}$ to $8.6x10^{-9}$ m/s.

Limestone, phosphate-lime, and flyash-lime mixes were successful in reducing permeability for 2 out of the 3 tailings trials: limestone and flyash-lime produced reductions in CSA and Elura, while phosphate-lime mix reduced the permeability of CSA and Peak. The lime mix and flyash mix actually increased the permeability in all trials possibly through the development of preferential flow paths.

6.5.3.1.6 Comparisons of Final Permeability of Mixes and Controls

When compared with the final permeabilities of the controls, the only universally successful reduction was observed with the phosphate mix. The CSA trial was reduced from $1.9x10^{-8}$ to $3.5x10^{-9}$, Elura reduced from $2.7x10^{-8}$ to $7.1x10^{-9}$ and Peak reduced from $8.3x10^{-8}$ to $8.6x10^{-9}$ m/s. The limestone, phosphate-lime and flyash-lime mixes reduced permeability for the Peak tailings only, while the lime and flyash mixes increased permeability in all trials.

6.5.3.1.7 Permeability Summary

The phosphate additive as a surface mixture with tailings was the most successful in reducing permeability by up to an order of magnitude. Thus for the reduction of water infiltration to prevent oxidation and transport of contaminant loads, phosphate addition as a surface mixture with tailings is suggested.

6.5.3.2 Porosity Investigations

A comparison of the initial and final porosities of the trials was undertaken to investigate the potential decrease in gas diffusivity through the development of low porosity cements. The final column total porosity and air-filled porosities are shown in Figures 6.24 and 6.25 respectively.

6.5.3.2.1 Control Porosity

A comparison of the original and final porosity of the control samples indicated that the near-surface porosity of CSA tailings decreased from an original 47% to 43% after one year of treatment, while the Elura and Peak Controls remained very similar at approximately 41% (Table 6.7).

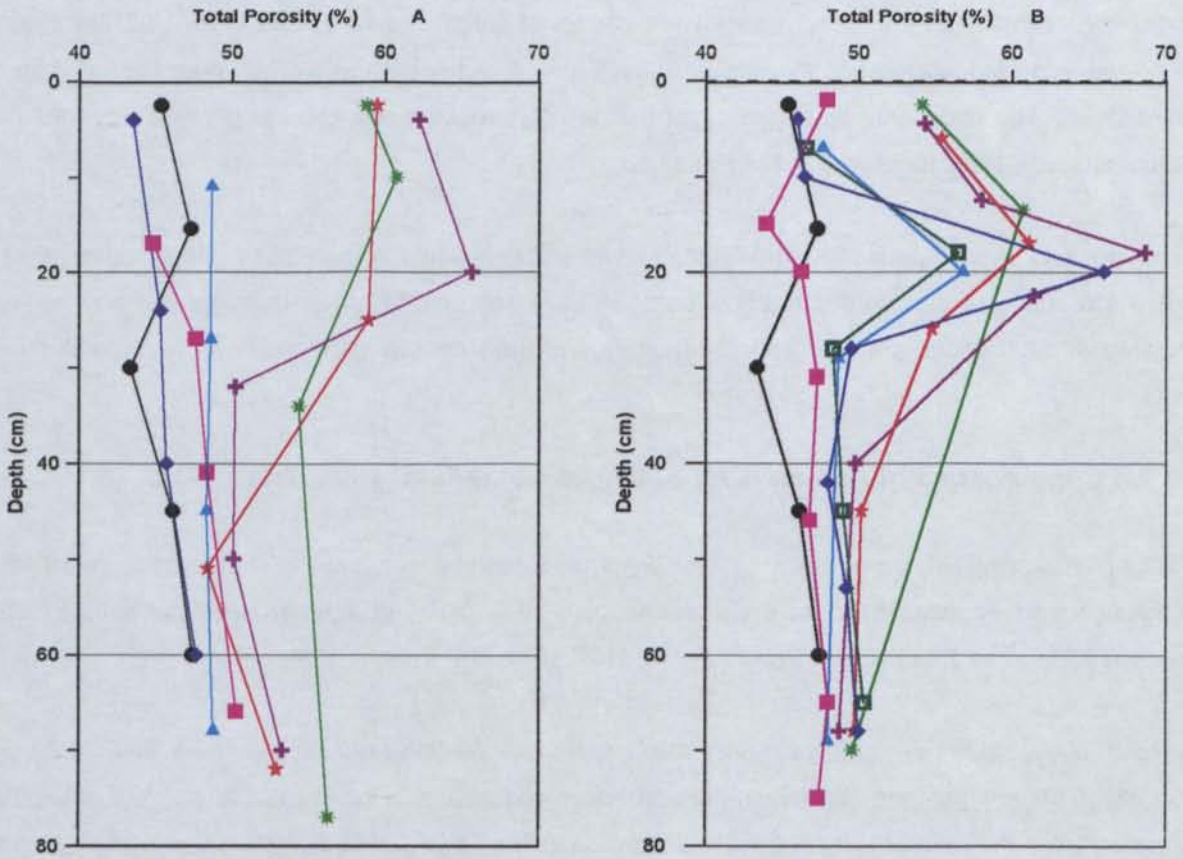

FIG 6.24A : TOTAL POROSITY FOR CSA - SOLID ADDITIVE HARDPAN ENHANCEMENT EXPERIMENT

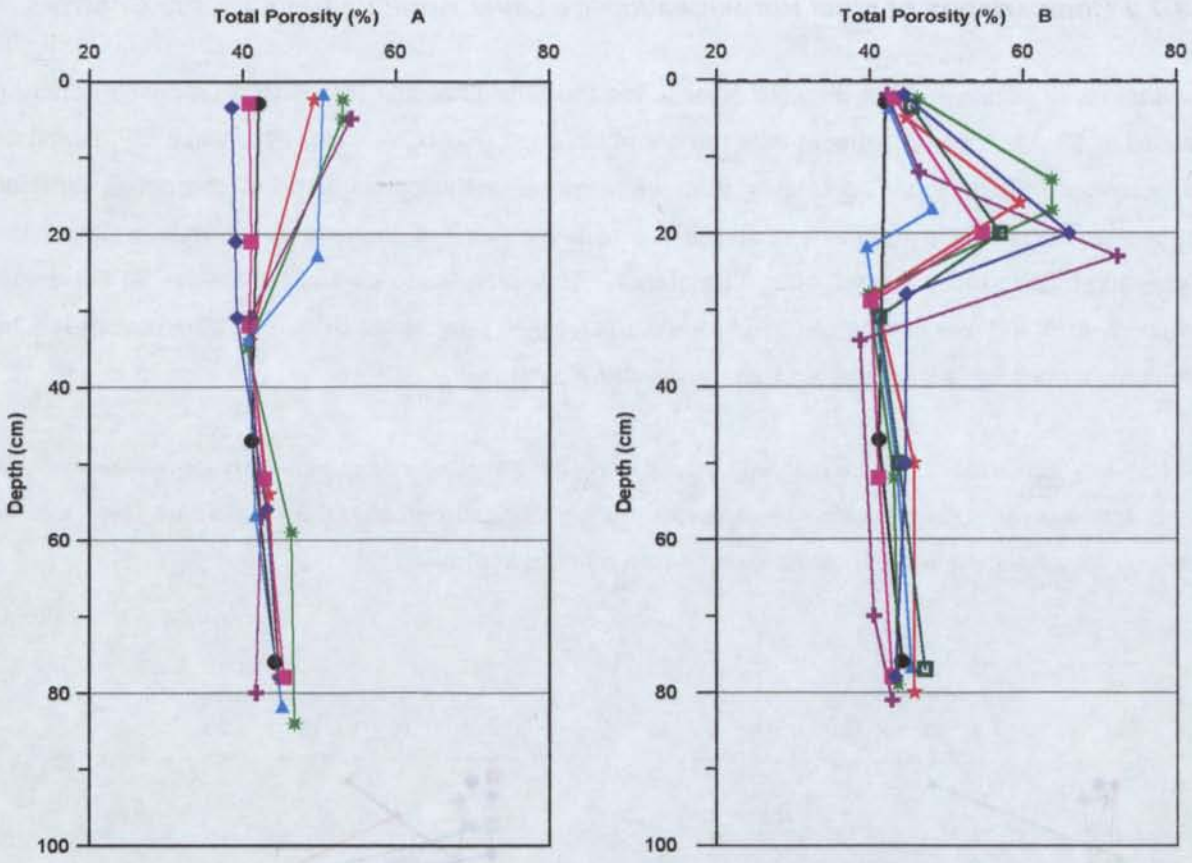

FIG 6.24B : TOTAL POROSITY FOR ELURA - SOLID ADDITIVE HARDPAN ENHANCEMENT EXPERIMENT

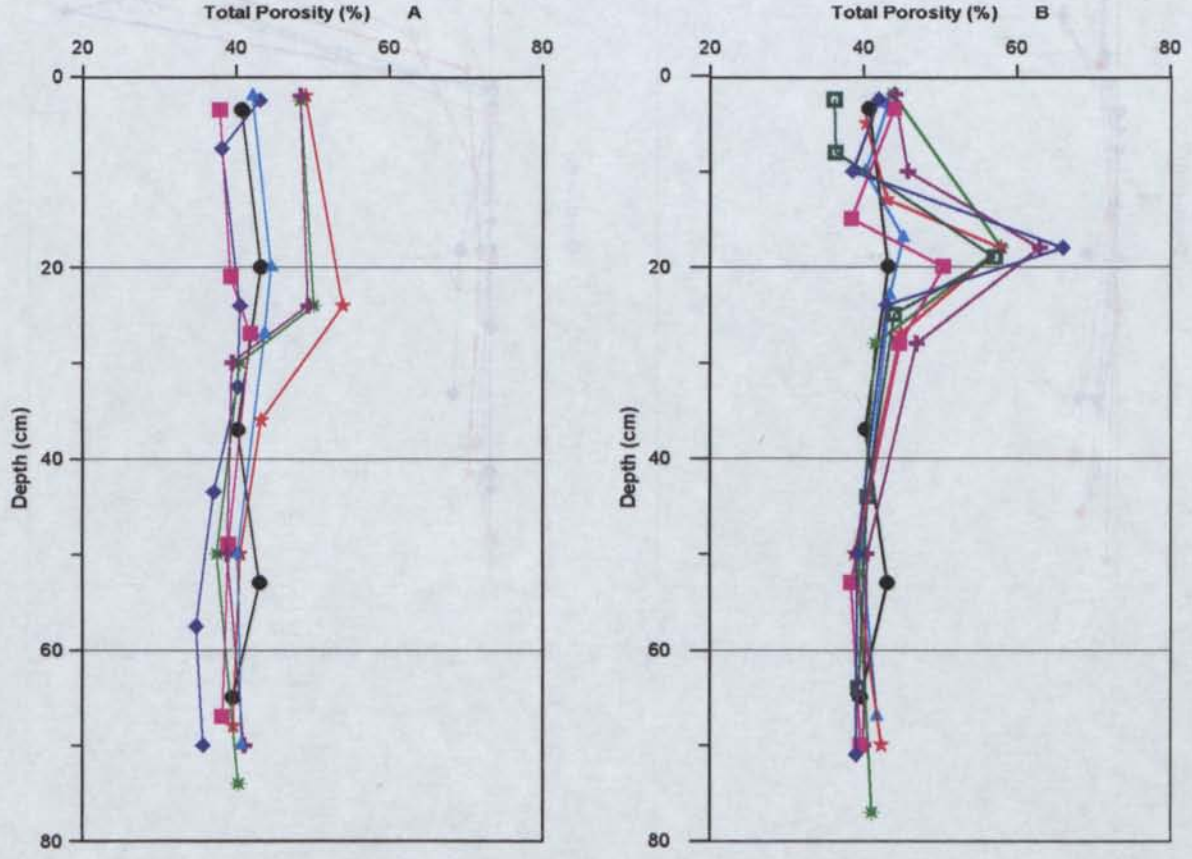

FIG 6.24C : TOTAL POROSITY FOR PEAK - SOLID ADDITIVE HARDPAN ENHANCEMENT EXPERIMENT

6.5.3.2.2 Comparisons of Final Porosities for the Layer Additive trials vs. the Controls.

The additions of additives as a discrete layer within the tailings profile (Fig 6.18b) produced consistent increases in total porosity compared with the control tailings (Fig 6.24). However when comparing air-filled porosities, the flyash - lime layer trials were significantly lower ie. 0-2% compared with total porosities of 58-64% (Fig 6.25). The flyash - lime layer trial has developed a strong water holding capacity and thus reduced oxygen diffusion potential. However, these air-filled porosities do not deviate significantly from the air-filled porosities of the controls, which range from 0-3%. All other layer trials had significantly higher air-filled porosities than those of the controls.

Therefore oxygen diffusion, as calculated by total porosity, has not been inhibited by cements developed in the discrete layer additive trials. However based on air-filled porosity, the flyash-lime layer trial has produced oxygen diffusion coefficients comparable with the controls.

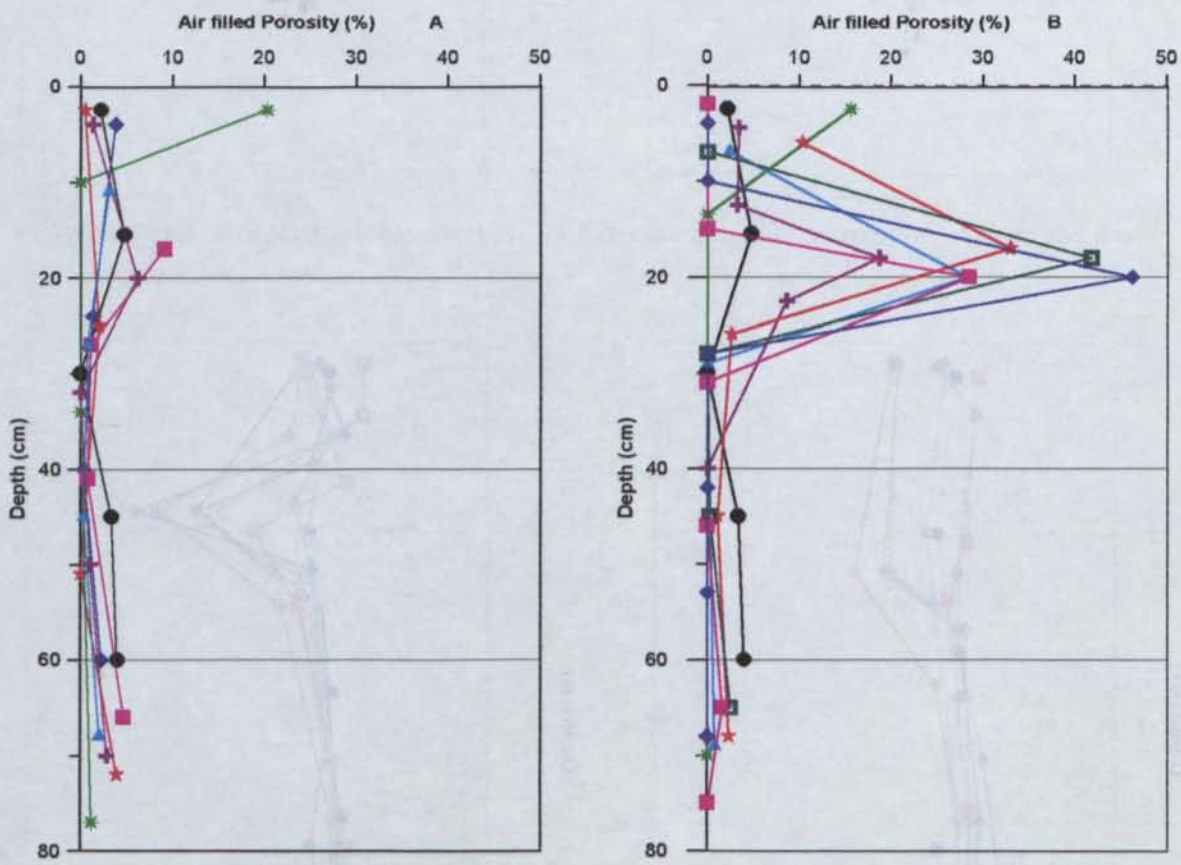

FIG 6.25A : AIR FILLED POROSITY FOR CSA - SOLID ADDITIVE HARDPAN ENHANCEMENT EXPERIMENT

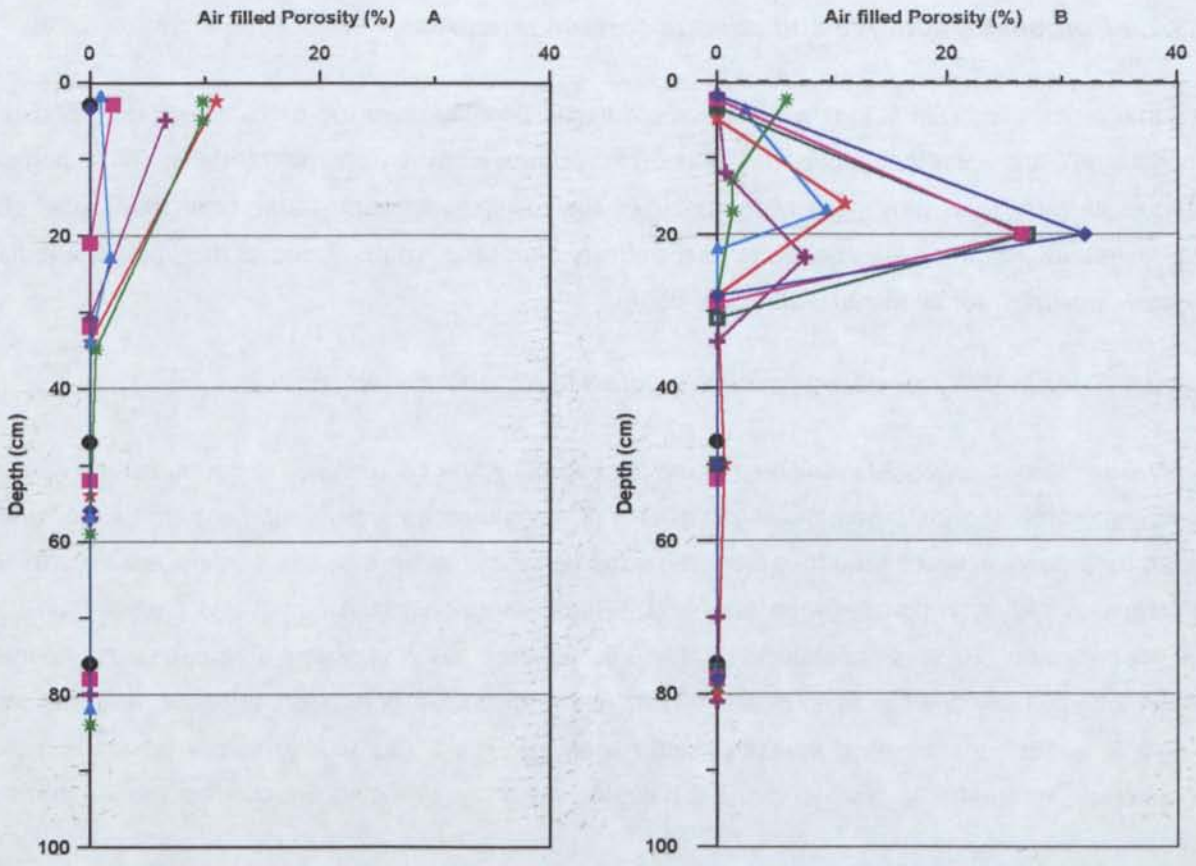

FIG 6.25B : AIR FILLED POROSITY FOR ELURA - SOLID ADDITIVE HARDPAN ENHANCEMENT EXPERIMENT

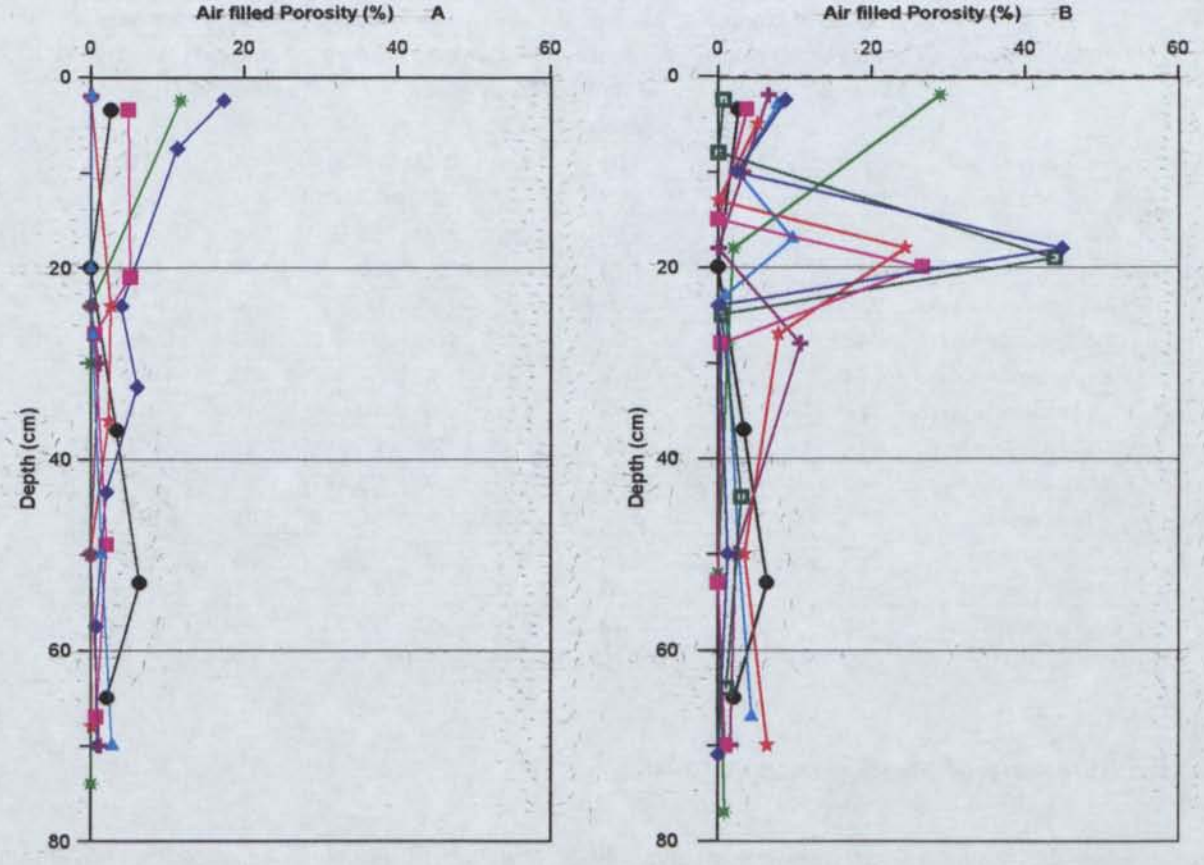

FIG 6.25C : AIR FILLED POROSITY FOR PEAK - SOLID ADDITIVE HARDPAN ENHANCEMENT EXPERIMENT

6.5.3.2.3 Porosity of additive and tailings surface mixtures

The surface mix trials (Fig 6.18a) which decreased total porosity were the Elura limestone mix, Elura phosphate mix and Peak phosphate mix (Fig 6.24). However, when comparing the air-filled porosity properties of these trials with those of the controls, the results were comparable or slightly higher (Fig 6.25). When investigating the change in total porosity over time, comparisons of the original and final porosity were similar for all mix trials (Table 6.7).

6.5.3.2.4 Connectivity of pores within selected layer and mixed trials

As very little or no changes was observed in the total porosity, the connectivity of the pores in a number of the more cemented trials was investigated. Three sample repeats were submerged in water under vacuum for 5 days, at which time they were regarded as saturated. A moisture content was determined and compared with total porosity measurements. Some samples slaked during this process and thus could not be tested. Results are shown in Table 6.8. In some cases very little difference was observed between total porosity and saturated moisture content and thus most pores were regarded as connected. However in some trials, air-filled porosities, after soaking, were up to 10% in some repeats and thus unconnected. The results expressed in Table 6.8 show the range of results obtained for the 3 repeats of each sample investigated.

TABLE 6.8 AVERAGE RESULTS OF PORE CONNECTIVITY TESTS

Sample Name	Average Moisture Content	Average OD density of clod	Average wet density of clod	Ave Particle density	Ave Void Ratio	Porosity Range	Average Degree of Saturation	Air filled porosity Range
	%	g/cm3	g/cm3	g/cm3		%	%	%
Elura control	15.3	2.62	3.03	4.24	0.62	37.3-38.9	100	0.00
Elura phos-lime mix	27.4	1.83	2.33	3.77	1.07	50.5-52.9	97.0	0-2.9
CSA phos-lime mix	44.3	1.29	1.86	2.87	1.23	55.19	100	0.00
Peak phos-lime mix	34.1	1.45	1.94	2.84	0.96	48.8-49.2	100	0-0.7
Elura fly ash-lime mix	27.8	1.79	2.28	3.69	1.06	51-52.2	96.3	1.4-2.8
CSA fly ash-lime mix	54.8	1.06	1.63	2.76	1.62	60.7-62.8	93.8	2.4-5.1
Peak fly ash-lime mix	37.6	1.30	1.79	2.74	1.10	52.2-52.7	93.2	3.1-4
Elura fly ash-lime layer	71.6	1.00	1.71	2.65	1.66	58.5-64.6	100	0-1
CSA fly ash-lime layer	63.4	0.99	1.61	2.63	1.66	61.8-63.1	100	0-3.1
Peak fly ash-lime layer	64.7	1.01	1.66	2.99	1.99	59.3-74.7	100	0-9.6
Elura lime mix	31.6	1.74	2.29	3.85	1.21	54.6-54.9	100	0-0.8
CSA lime mix	50.6	1.17	1.77	2.75	1.35	56.6-58	100	0.00
Peak lime mix	35.9	1.38	1.88	2.76	0.99	49-50.5	100	0-0.9
Elura phosphate mix	14.8	2.37	2.72	3.77	0.59	36-36.1	94.4	1.9-2.2

Samples of Peak and CSA controls and phosphate mixes collapsed during testing

6.5.3.2.5 Summary of Variations in Porosity

Oxygen diffusivity is determined by the porosity, with a reduction in diffusivity being achieved through either a reduction in the total porosity or a continuous reduction in the air-filled porosity. When

comparing results of total porosity, the phosphate mixture trials appear to be most successful in reducing diffusivity (Fig 6.24). However investigations of the air-filled porosity suggest that the high water holding capacity of the lime-flyash layer has the ability to reduce gas diffusivity (Fig 6.25). This is further supported by investigations into pore connectivity, where up to a 10% reduction in connected pores was detected for the lime flyash layer trials. Similarly, significant reductions in pore connectivity were observed in the lime-flyash mix and less in the lime, phosphate-lime and phosphate mixes.

6.5.3.3 Cementation, Eh, pH, Solute Chemistry, Degree of Saturation

So far the measure of success of the trials have been predominantly based on permeability and porosity. In this section the mineralogical and geochemical effects of these additives on the tailings is investigated and results presented. The tailings from the discrete additive layer trials (Fig 6.18b) are referred to in this section as the upper (above the additive layer) and lower (below the additive layer) tailings.

Measurement of pH, solute chemistry and redox potential (Eh) were carried out to achieve an understanding of the geochemical reactions taking place and the extent to which they have occurred. The mineralogy and morphology of cements and degree of saturation are also discussed in this section and are related to porosity and permeability results. Results from both Elura control columns have been included in this section. The physical attributes for Control 2 were not determined and thus not reported in Section 6.4-6.6. The only difference between these columns is the diameter, where the Control 1 diameter is 15cm and the Control 2 diameter 30cm.

6.5.3.3.1 Redox Potential (Eh)

The Eh conditions in all the columns did not vary significantly from those observed in the control columns. In tailings from Peak, Eh ranged from 0 to -400mv, CSA from 200 to -600 mV, while Elura ranged from 50 to -400mv (Fig 6.26). Within the Elura tailings, the most obvious decrease in Eh was associated with layered flyash-lime, lime and phosphate-lime. The most positive Eh conditions were observed within the phosphate layer.

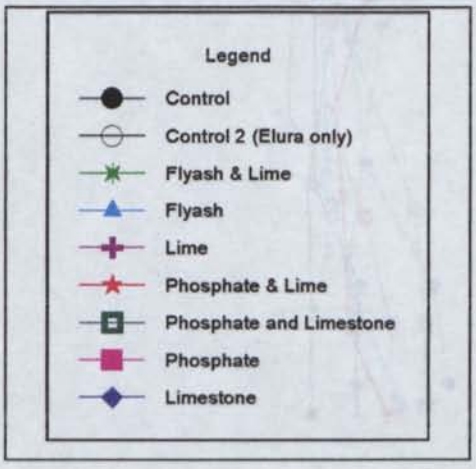

Variations in Eh within the CSA and Peak trials were more subdued, the most negative values associated with the phosphate-lime-tailings surface mixtures. A positive Eh was recorded for the phosphate layer trial within Peak tailings, similar to the Elura trials, however a most positive Eh was recorded in the upper tailings of the lime layer trial of CSA.

Legend used for Figures 6.26 and 6.27
where **A** = Mix trials **B** = Layer trials

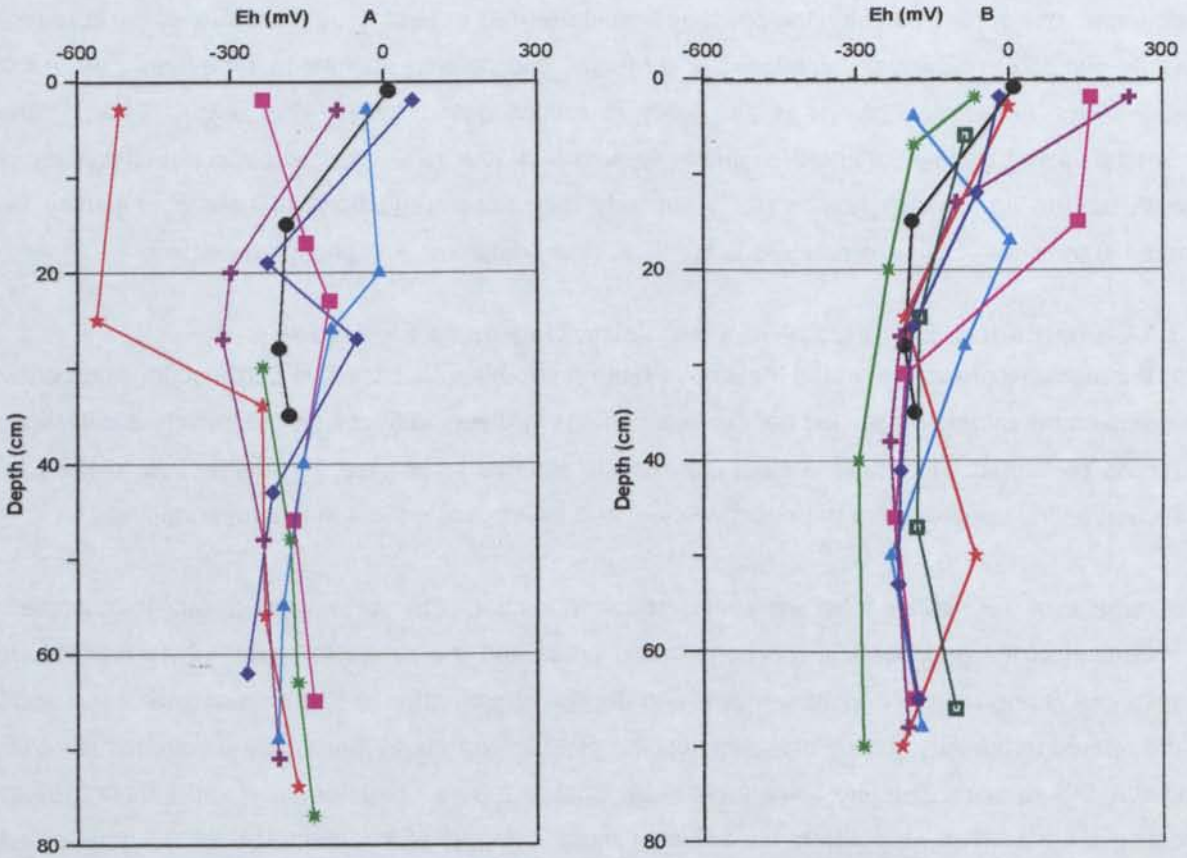

FIG 6.26A : REDOX POTENTIAL (Eh) FOR CSA - SOLID ADDITIVE HARDPAN ENHANCEMENT EXPERIMENT

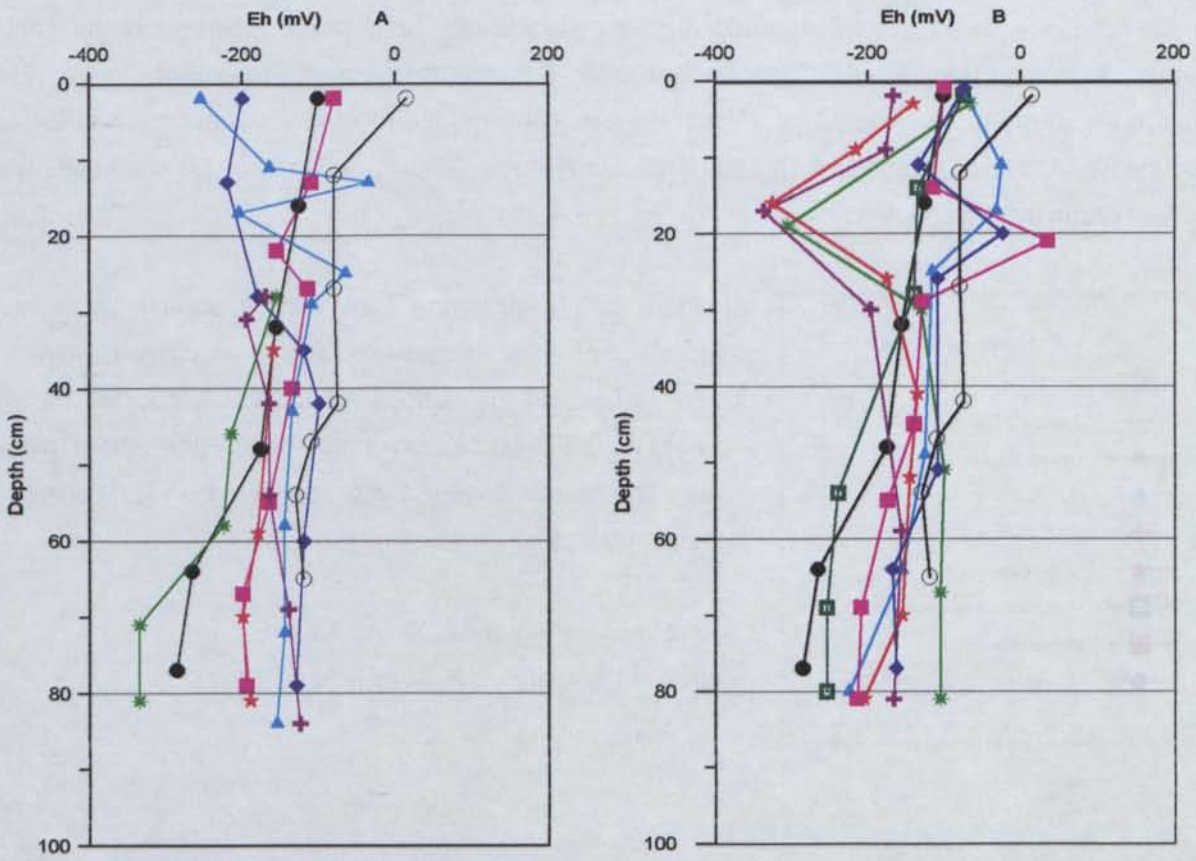

FIG 6.26B : REDOX POTENTIAL (Eh) FOR ELURA - SOLID ADDITIVE HARDPAN ENHANCEMENT EXPERIMENT

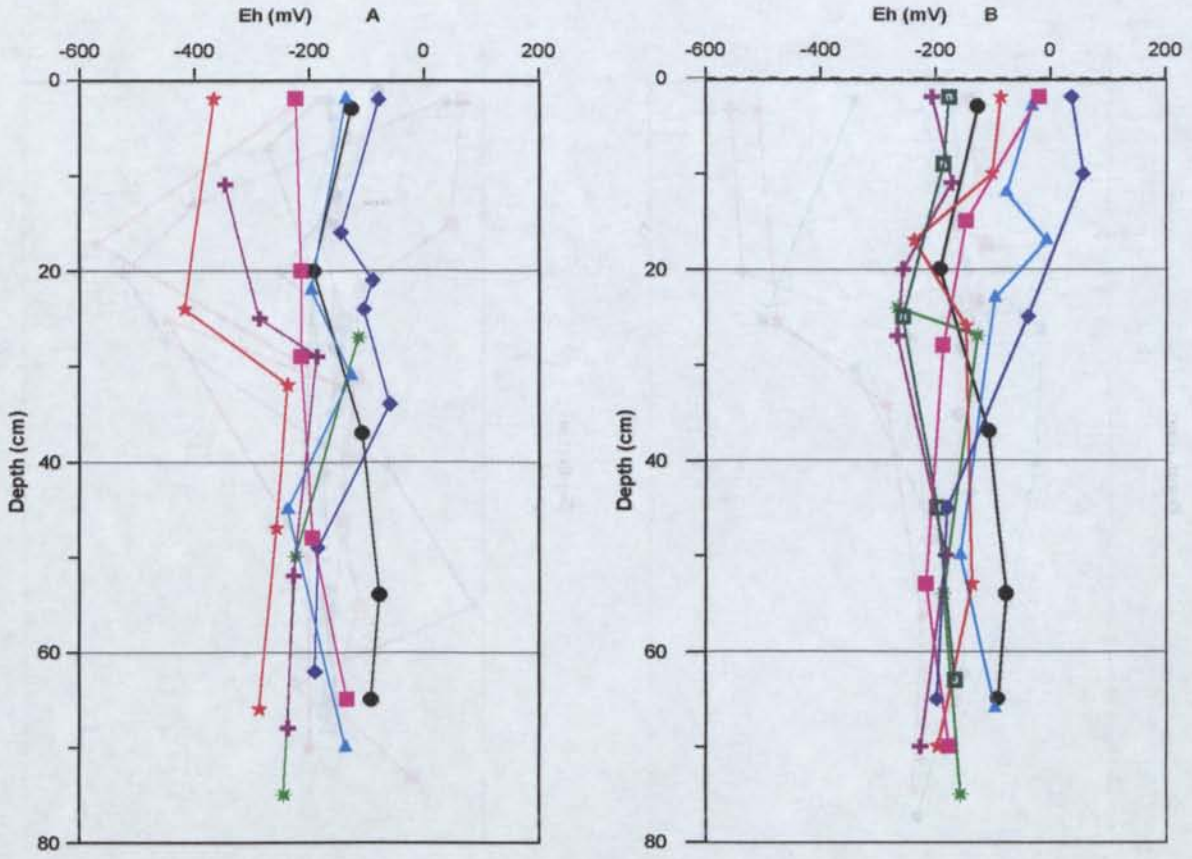

FIG 6.26C : REDOX POTENTIAL (Eh) FOR PEAK - SOLID ADDITIVE HARDPAN ENHANCEMENT EXPERIMENT

6.5.3.3.2 pH

Individual pH results are presented in Table 3A.54, Appendix 3A. Lime, phosphate-lime and flyash-lime mixes produced elevated paste pH conditions within all trials, however were most evident within the CSA and Peak trials (Fig 6.27). Significantly increased pH values in the Elura trials were restricted to the lime mix. The positive Eh observed with the upper tailings of the CSA lime layer was reflected in the low pH (4.5) showing the development of more acidic conditions at the surface than the control tailings suggesting oxidation is occurring in this region. Similarly acidic conditions had developed within the upper tailings of the phosphate layer trial, and were associated with positive surface Eh conditions. pH conditions at depth within the CSA tailings were similar to the control tailings but both the flyash mix and lime layer promoted slightly more acidic conditions at depth which are assumed to be associated with preferential flow paths. Elura tailings exhibited elevated pH conditions with lime additions, but at depth within these columns, conditions were similar to those observed within the controls. As expected, Peak also exhibited increased pH with the lime addition. However, lime additions as layers increased the pH only within the layer, whereas lime as a mix produced an overall increase in pH throughout the profile.

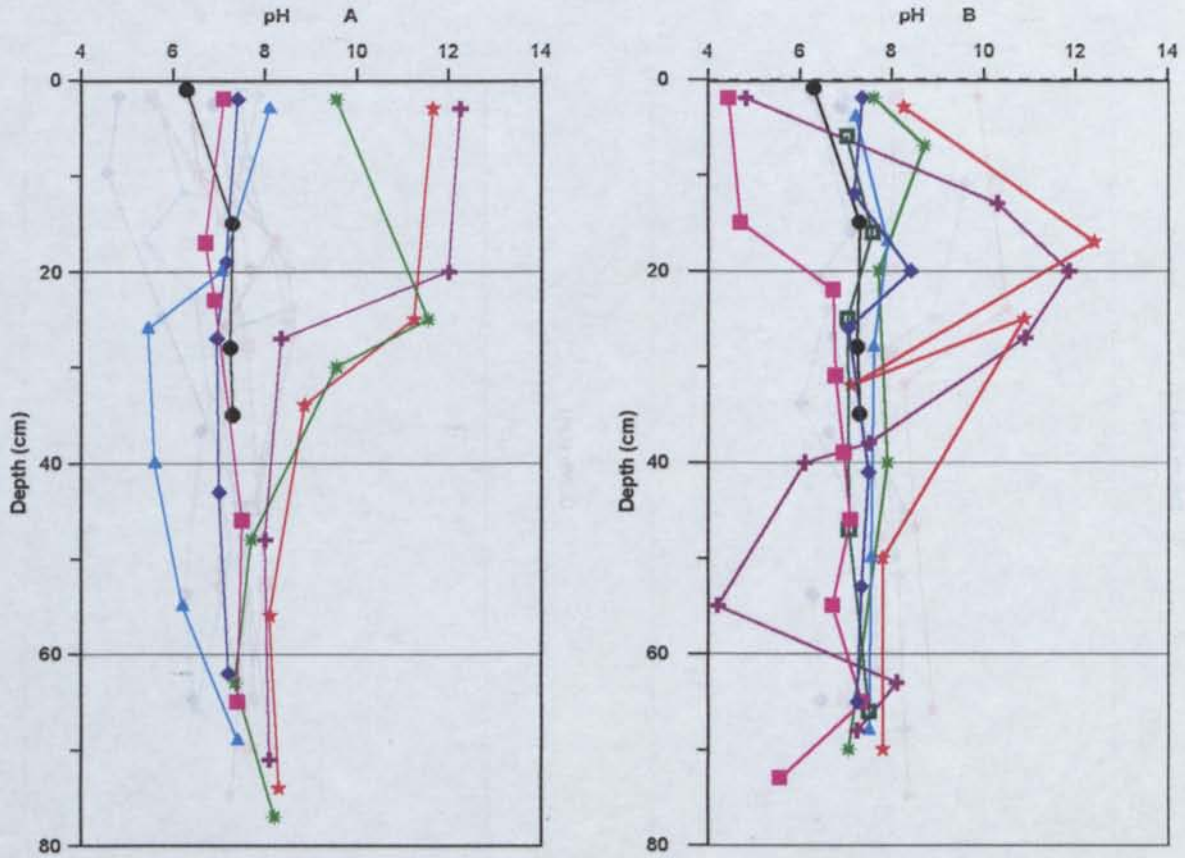

FIG 6.27A : pH PROFILES FOR CSA - SOLID ADDITIVE HARDPAN ENHANCEMENT EXPERIMENT

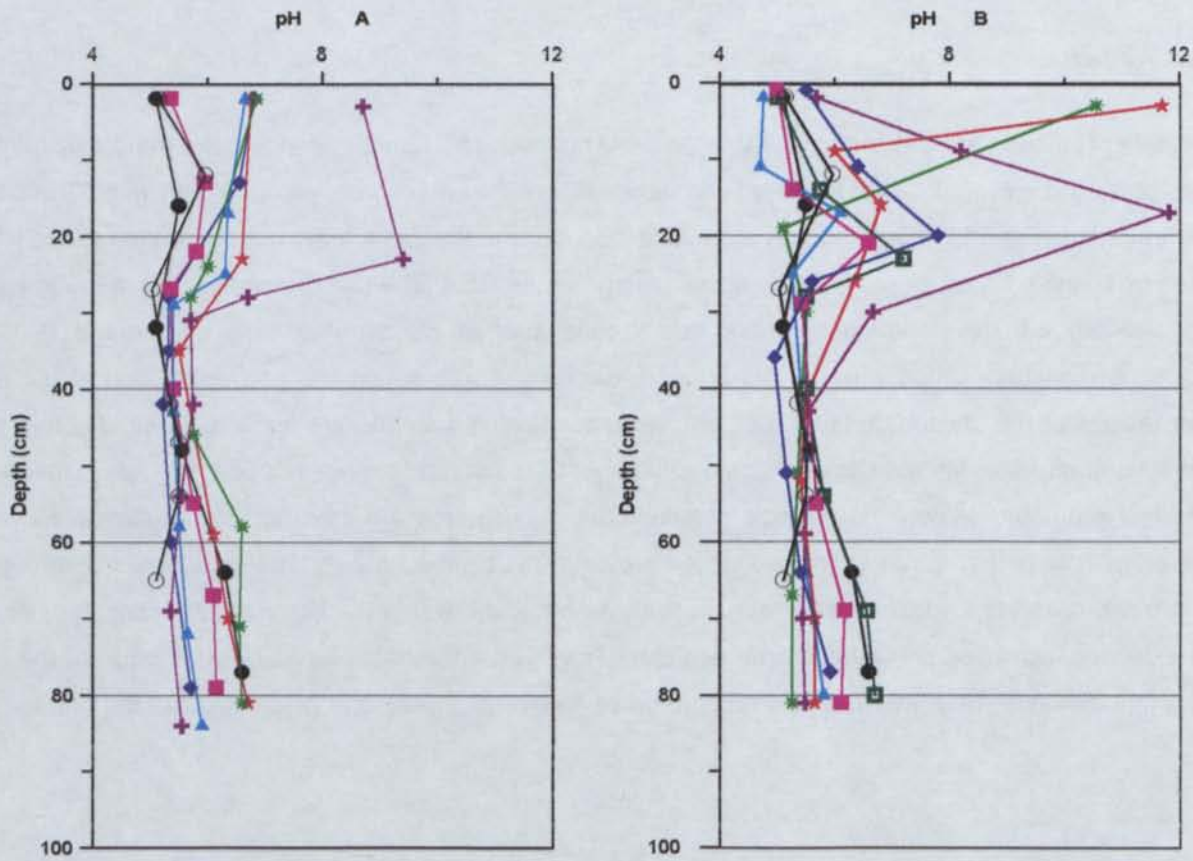

FIG 6.27B : pH PROFILES FOR ELURA - SOLID ADDITIVE HARDPAN ENHANCEMENT EXPERIMENT

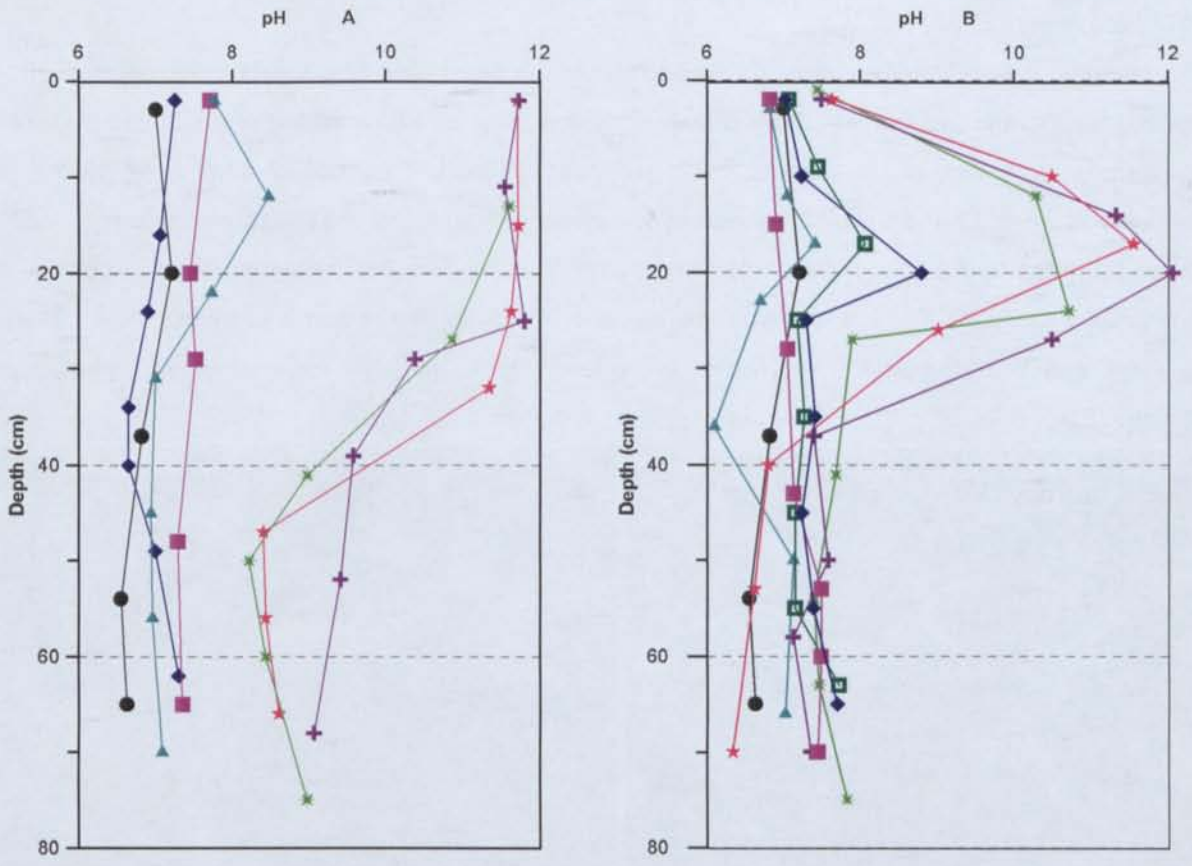

FIG 6.27C : pH PROFILES FOR PEAK - SOLID ADDITIVE HARDPAN ENHANCEMENT EXPERIMENT

6.5.3.3.3 Mineralogy and Morphology of Cements

Once exposed, the hardness of any cements was gauged by the ease of sampling. The flyash and lime mixture produced well-developed cements with the three tailings types, as did the layer trials but these were not as hard. The phosphate and lime mix produced well-developed cements in the Elura tailings and to less extent in the CSA and Peak tailings. Similarly the lime mix produced cements in the Elura tailings but were almost non existent in the CSA and Peak tailings. Table 6.9 shows the classification of the trials based on cementation.

As the flyash and lime mix and layer trials developed the most cementation, SEM investigations were undertaken to examine the morphology and mineralogy of the cements. The phosphate mix trials were also investigated to determine which secondary mineral or physical attributes have supported the development of low permeabilities and porosities. The secondary minerals of the cements and surface salts were also investigated using XRD.

TABLE 6.9 MAIN EXPERIMENT CEMENT CLASSIFICATION

Tailings - Additive Trial	Cementation
Flyash lime mix	cemented in all trials
Flyash lime layer	cemented in all trials but to a lesser extent than flyash-lime mix
Phosphate lime mix	well cemented in Elura tailings and less in CSA and Peak
Lime mix	cemented in Elura tailings but much less in CSA and Peak

All trials not outlined in the above table were regarded as non cemented.

Flyash / lime layer

The morphology of secondary minerals developed within the flyash and lime layers differ depending on their location within the physical structure of the cemented layer and their timing of precipitation. EMG 6.1 shows a general view of the cement. There appears to be two periods of cement development. Initially cements of Al, Si and Ca have formed by the direct interaction of the flyash and lime mix. EMG 6.2 shows a degrading flyash sphere, coated and surrounded by cements containing equal quantities of Al, Si and Ca and minor K, Fe and Mg. This cement is widespread in samples of this type. These cements are very fine-grained, in many cases being less than 0.1μm, and have taken on a wispy type morphology (EMG 6.3).

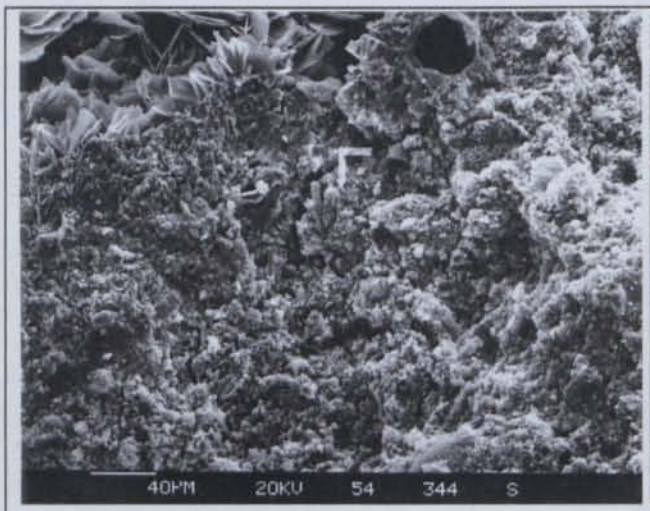

EMG 6.1 General cement of flyash lime layer

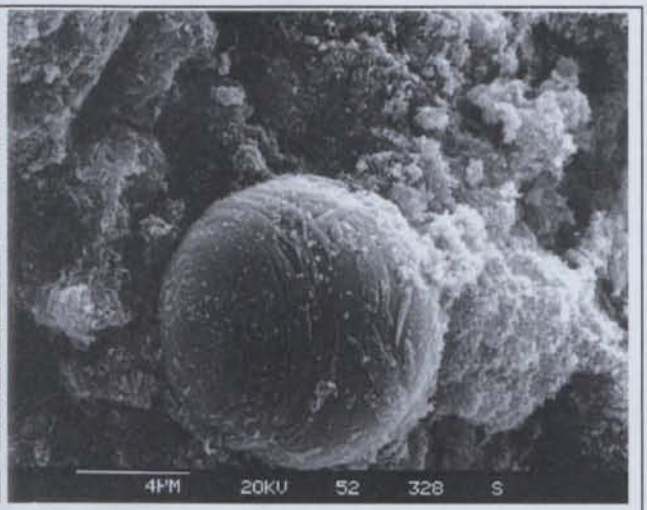

EMG 6.2 Close up of EMG 6.1 Degraded flyash sphere coated and surrounded by cement

Additional cements have precipitated within cavities, along channels and within pores. These appear to have developed subsequent to the original structure allowing precipitation in a variety of morphologies. Fine plates of mainly Ca and approx. 0.5 to 0.25 Al and Si content have developed (EMG 6.4). Additionally fibrous cements of mainly Ca with very minor Al and Si content were observed (EMG 6.5). In many cases these cements have been further coated by smooth layers of Si and Ca minerals containing minor Al. These secondary minerals exhibits desiccation cracks suggesting the it is hydrated (EMG 6.6).

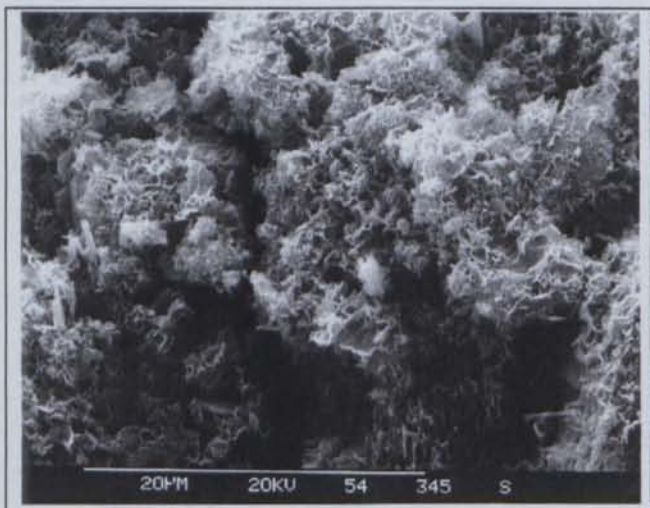

EMG 6.3 Closeup of EMG 6.1 Wispy cements

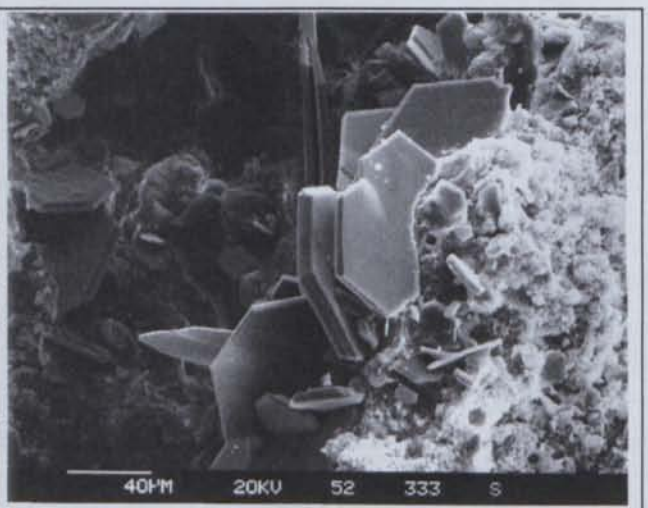

EMG 6.4 Close up of EMG 6.1 Fine plates of Ca cement

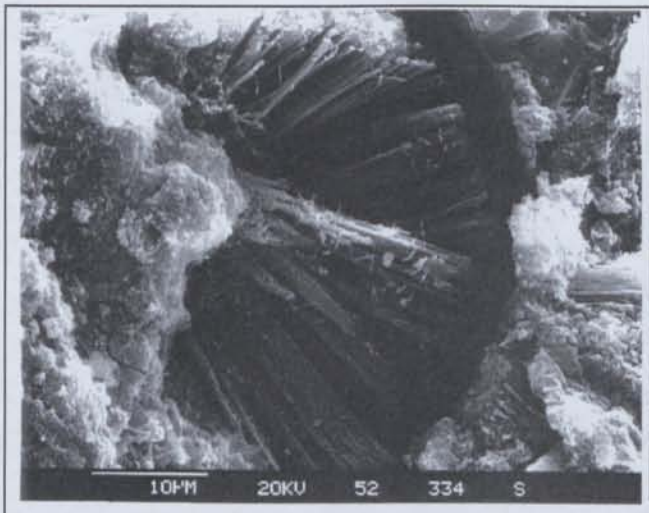

EMG 6.5 Closeup of EMG 6.1 Radiating Ca fibers

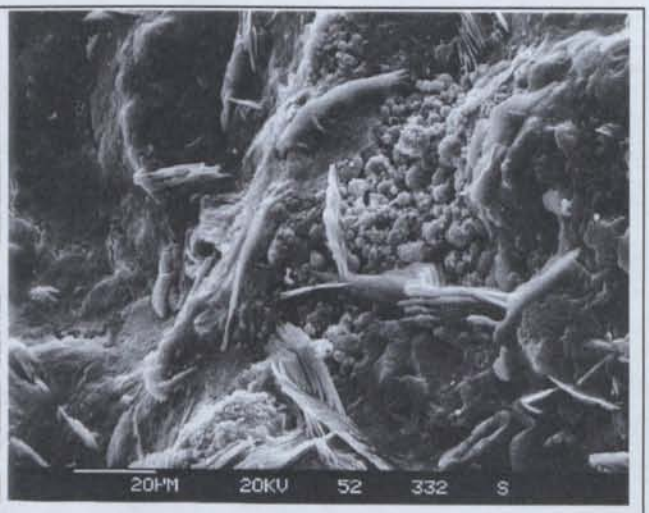

EMG 6.6 Close up of EMG 6.1 Coatings of smooth Ca and Al cements

Identification of these minerals has been hampered by their very fine-grained nature. The microanalyser (EDX-energy dispersive X-ray) associated with the SEM has a beam energy of 20 KeV, with electrons penetrating a sample with density of 2 g/cm^3 to a depth of 4µm. The resultant X-rays emitted will come from a surface of approximately 8µm diameter. Many of the wispy and fibrous cements observed are less than 0.1µm wide, while many of the coatings are potentially thinner than 4µm. Therefore the Al, Si and Ca signature observed may have originated from a single type of cement or from several closely packed phases. Investigations of pure flyash indicate the existence of spheres from less than 1µm up to 100µm. Lime contains lumps up to 20µm with the majority approximately 2µm comprised of sub-micron grains (0.2µm). Thus unreacted additives may be responsible for some EDX signature overlap. An example of this is illustrated in EMGs 6.6 and 6.3 where Al, Si and Ca signatures were detected. The central region of EMG 6.6 probably represents unreacted flyash spheres and lime particles, while the wispy nature shown in EMG 6.3 suggests reactions have occurred resulting in the precipitation of a secondary minerals. Both regions contain Al, Si and Ca however the wispy cements have substantially higher Ca levels.

Sulfur-rich cements were observed precipitating along channels within these samples. This suggests release of SO_4^{2-} from oxidation of sulfidic minerals near the surface and leaching into the layer below.

Flyash and lime Mix

Generally the flyash and lime mix results in cements which are less porous and more tightly packed than the flyash lime layer cements. This structure does not support the widespread development of platey or fibrous secondary minerals as observed within the layer trials. Here the cements are wispy and very-fine grained with minor fibers and plates throughout. EMG 6.7 shows cavities where flyash spheres have

been degraded leaving reaction rims of Al and Si with minor Ca. EMG 6.8 shows the degradation of spheres and subsequent development of Ca, Si and Al wisps around, on and within the sphere.

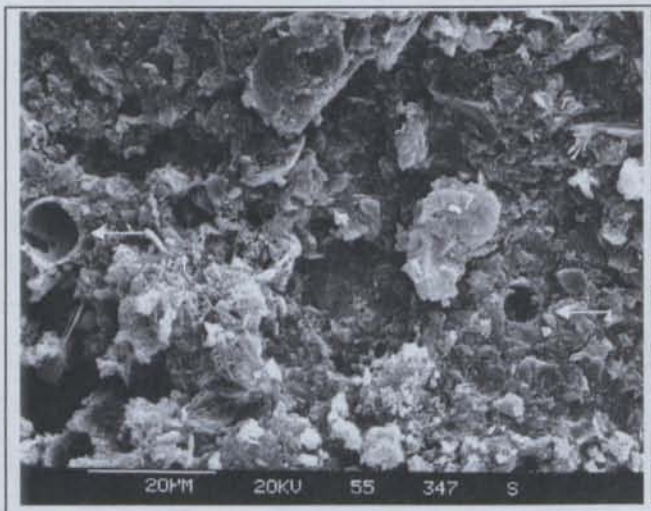

EMG 6.7 General view of flyash and lime mix cements, with flyash sphere replacement structures of Al and Si cement

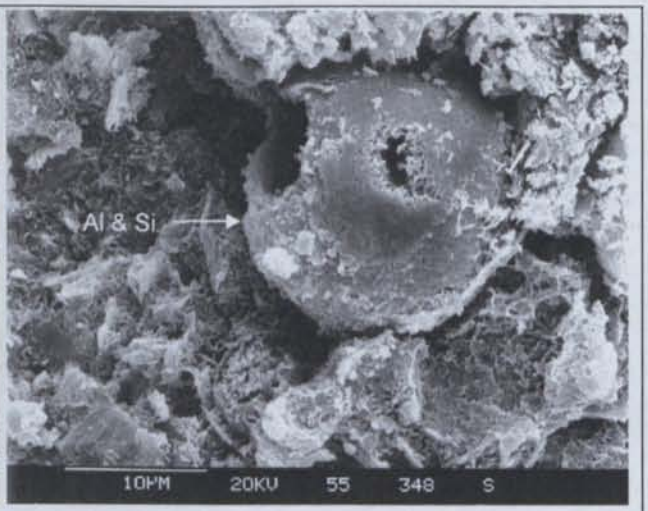

EMG 6.8 Close up of EMG 6.7 Degrading flyash sphere being replaced by Al and Si wispy cements

EMG 3.9 shows a close-up of the wispy cements which have potentially developed between two grains which have subsequently been degraded. They consist mainly of Al and Si and minor Ca.

The tailings within the mixes have influenced the composition of the cements. For example the highly sulfidic tailings from Elura have produced cements containing Zn, Mn, Fe, Na and S whereas the tailings of CSA and Peak have had limited Fe input and only minor Mg and Na additions. Sulfur is absent in both cases. EMG 6.10 shows sulfate-rich cement developed within the Elura flyash-lime mix together with minor Ca, Fe and Si. The more fibrous and undulating secondary minerals in the upper section of EMG 6.10 consists of equal quantities of Fe and S with approximately half as much Al and Si.

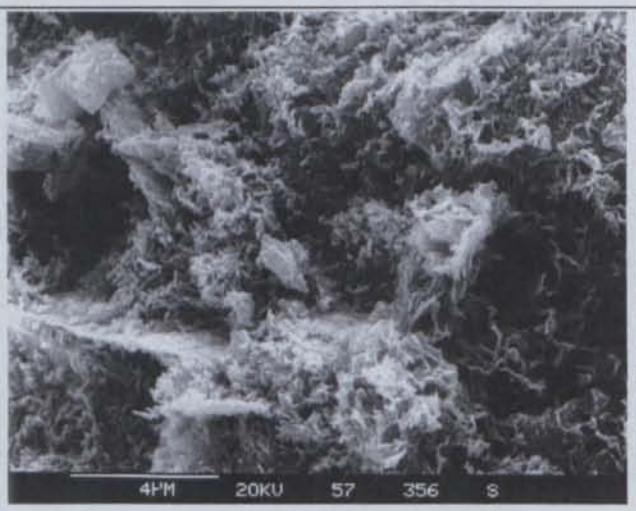

EMG 6.9 Close up of EMG 6.7 Al and Si wispy cement

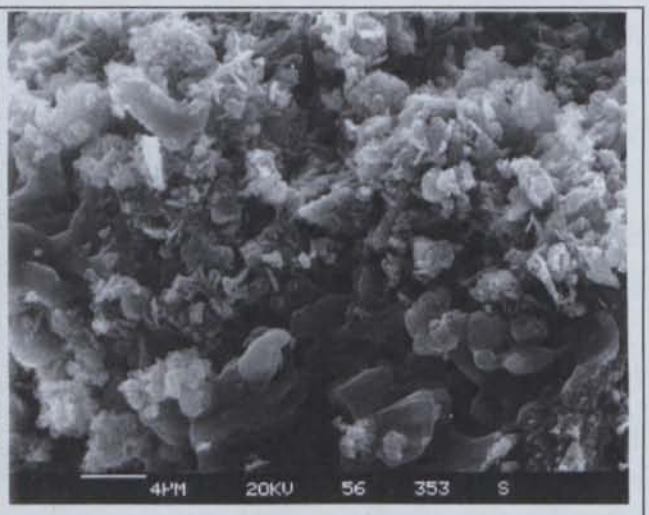

EMG 6.10 Elura flyash/lime mix - sulfate rich cements

Phosphate Mix

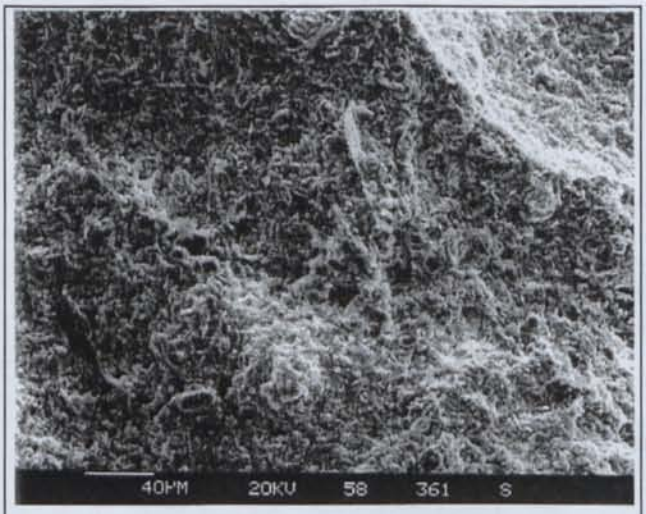

EMG 6.11 Well packed, low porosity phosphate - tailings mix trial

SEM investigations of the phosphate mix showed the development of a well-packed, low porosity material containing no channels (EMG 6.11). Cementation within the material was limited to minor bridging cements and coatings (EMG 6.12), the majority of grains remained unconnected and only slightly covered (EMG 6.13). The contribution of phosphate to this system was very minor and was only observed in association with apatite grains. The Fe signature may have increased at the boundary of these grains but these increases were not sufficiently significant to be identified as Fe phosphate cements.

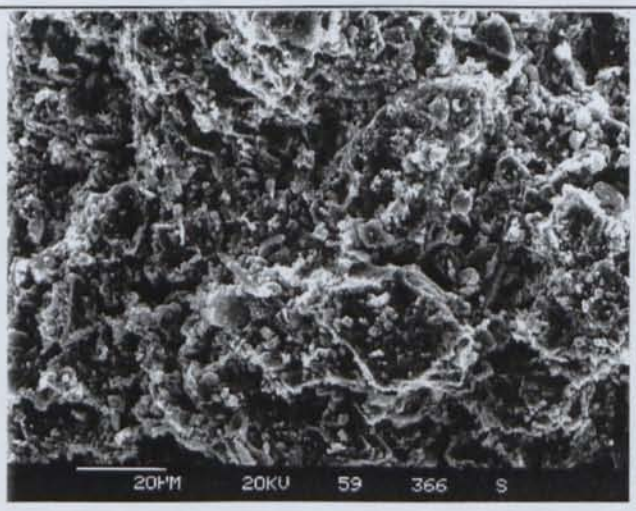

EMG 6.12 Close up of 6.11 Minor briding cements

EMG 6.13 Close up of 6.11 Slight cementing only

Spectral K-alpha scanning was undertaken to verify the development of Fe phosphate cements along the boundary of the apatite grains. Results indicated very limited, if any, co-speciation cements (K-alpha Maps 1 and 2). The scanning of sulfide grains to observed Fe phosphate surface coatings was not undertaken as no P signature was observed in any sulfide locations investigated.

EDX maps of Elura and CSA phosphate mixes. Images modified to show white = max counts

Map 1 - Elura Phosphate Mix

Back Scattered Image | Fe kα line max counts = 71 | P k line max counts = 65 | Background Image

Map 2 - CSA Phosphate Mix

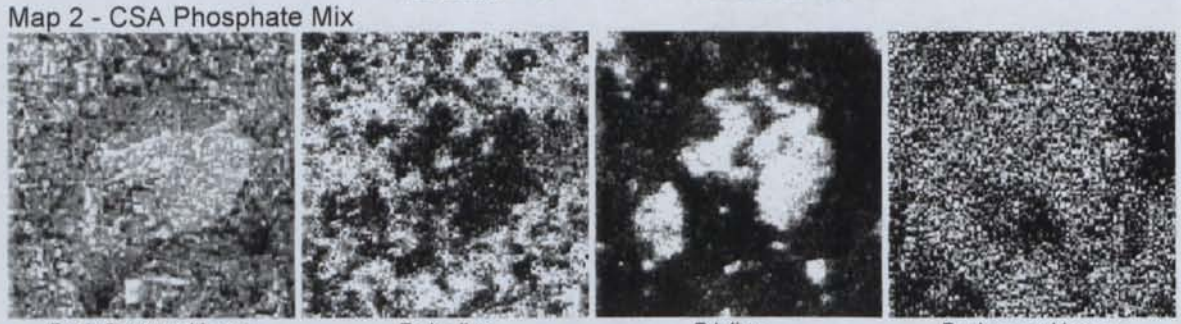

Back Scattered Image | Fe kα line max counts = 20 | P k line max counts = 32 | Background Image

Again the minor cements within the tailings phosphate mix were very fine-grained (<0.2μm) making identification difficult. It could not be ascertained whether the minerals were primary grains of aluminosilicate, sulfide and apatite or cements containing mainly Fe, Ca and S and minor varying quantities of K, Si, P, Al and Mg. Sulfur, Fe and to a lesser Zn, played a larger role in the Elura cements.

6.5.3.3.4 Degree of Saturation

The degree of saturation gives an insight into physical conditions which are dictating the geochemical evolution within the profiles. The degree of saturation is simply the percentage of voids filled with water at the time of sampling (Fig 6.28). These results were also obtained at the end of the 1 year period.

The lowest degree of saturation (ie. highest air-filled porosity) was measured within the layer trials. The degree of saturation increased from phosphate -limestone, phosphate, phosphate-lime, flyash, lime to lime-flyash which had the highest recorded levels. Within all trial of the lime-flyash layers, significant reductions in the degree of saturation had developed within the upper tailings overlying the layer (Fig 6.28). A comparison with the control columns suggests that the water has preferentially moved from the upper tailings into the lime-flyash layer itself. Although not obvious from the pH and Eh profiles for this trial, it is these conditions which promote oxidation through increased oxygen diffusion into the unsaturated overlying tailings. It is for this reason that the flyash-lime layers are not a preferred close out option.

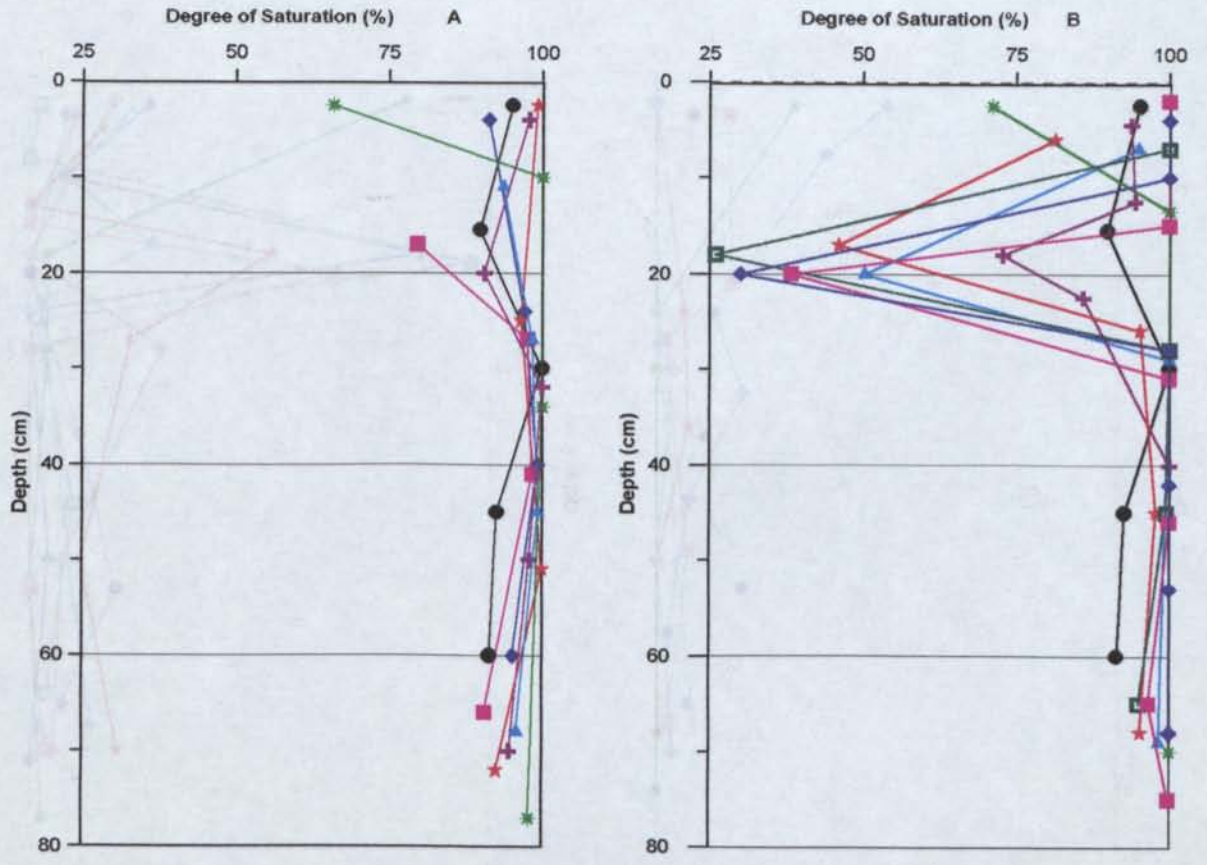

FIG 6.28A : DEGREE OF SATURATION PROFILES FOR CSA - SOLID ADDITIVE HARDPAN ENHANCEMENT EXPT.

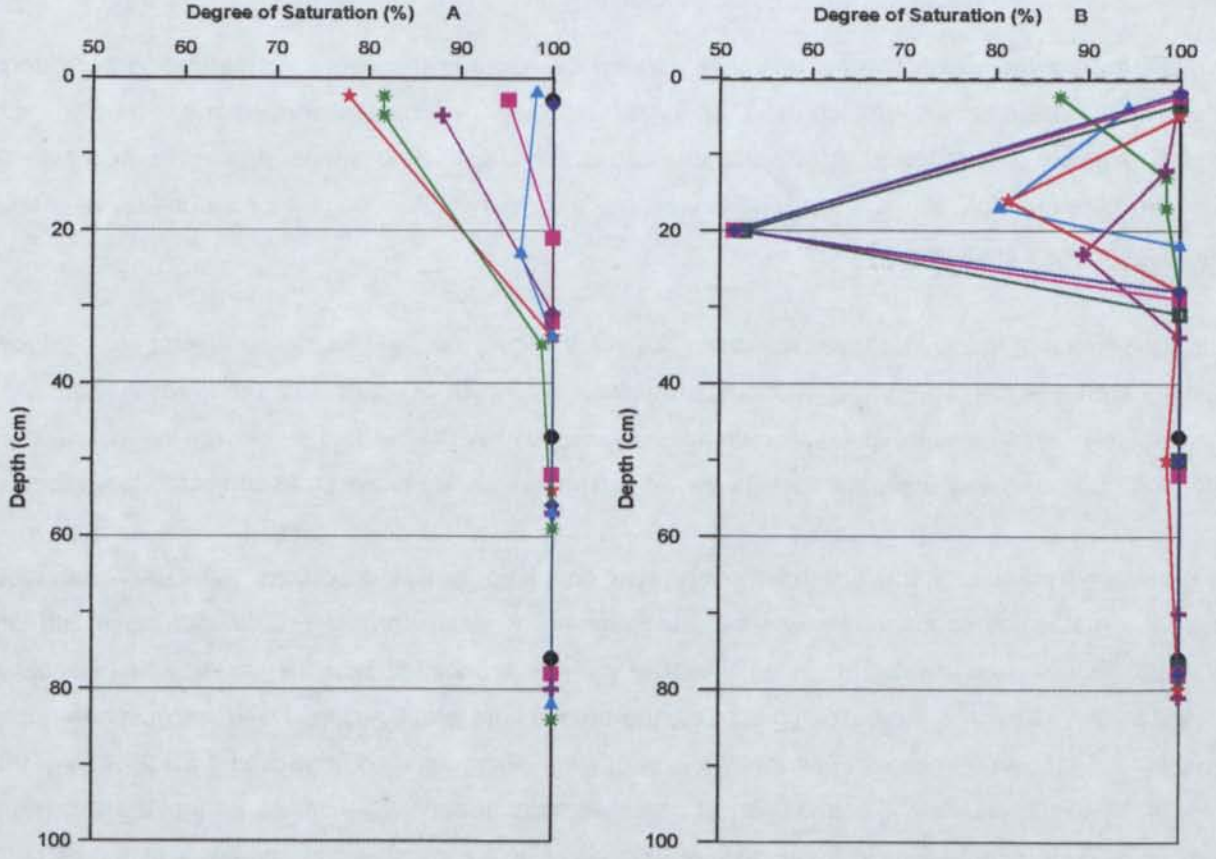

FIG 6.28B : DEGREE OF SATURATION PROFILES FOR ELURA - SOLID ADDITIVE HARDPAN ENHANCEMENT EXPT.

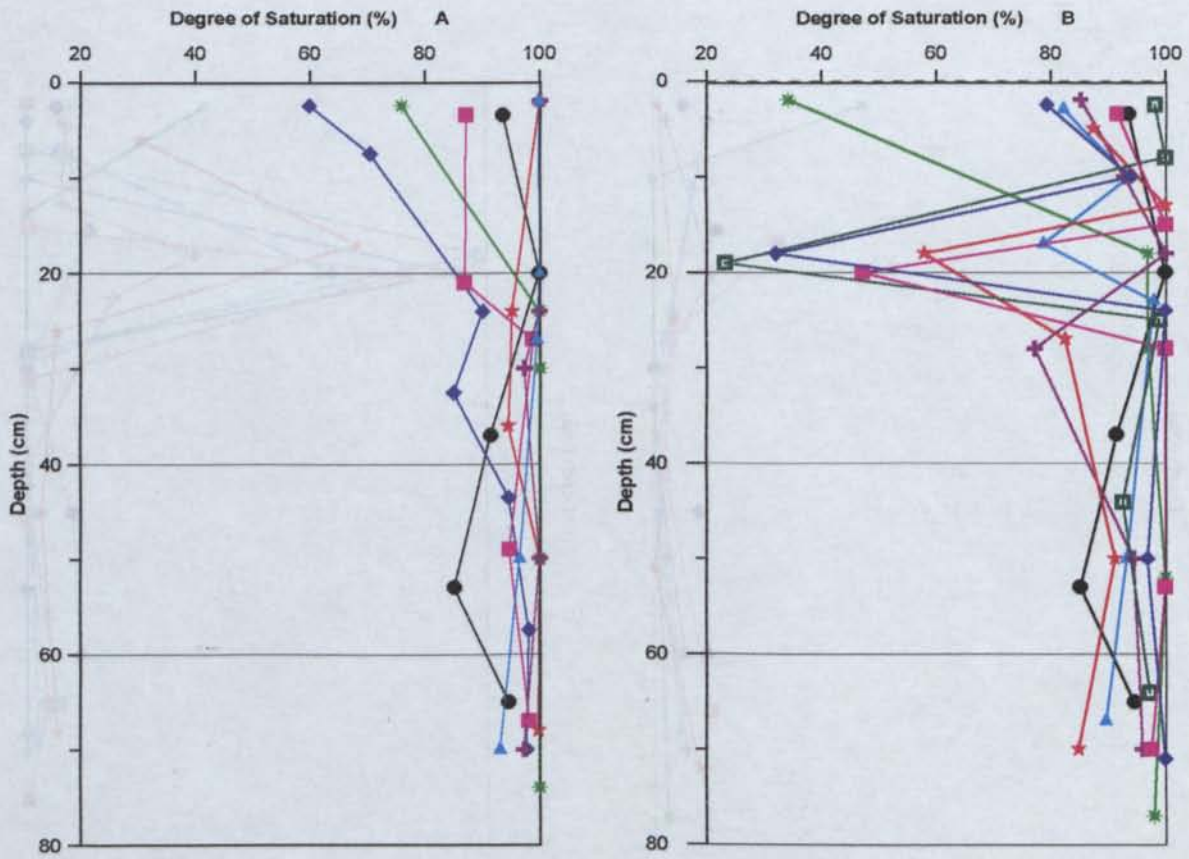

FIG 6.28C : DEGREE OF SATURATION PROFILES FOR PEAK - SOLID ADDITIVE HARDPAN ENHANCEMENT EXPT.

Flyash-lime mix trials also show a universal surface decrease in the degree of saturation but directly below in the tailings, levels increased to 100% saturation. Phosphate-limestone, limestone and phosphate layers (and to lesser extents the lime and flyash layers) show similar profiles for all trials, with up to 100% saturation at the basal additive-tailings boundary. The degree of saturation decreases slightly with depth below this.

The significance of this is that these materials, especially phosphate and limestone layers, are producing capillary breaks within the profiles, reducing the upward migration of water from the lower tailings. As a result of this, highly saturated conditions have formed within the tailings, reducing the potential for oxidation. Unfortunately the upper tailings remain unsaturated and are therefore subject to oxidation.

As mentioned previously the flyash-lime mix also produced similar conditions with 100% saturation below the mix which continues through out the column. A similar profile occurs with the flyash lime layer. In these cases instead of being a capillary break associated with the addition of the coarse-grained additive and thus increased pore sizes, the breaks here are associated with a reduction in pores available for gaseous movement of water via evaporation. As mentioned in Section 6.5.3.2, tests of total porosity, air-filled porosity and connectivity of pores were undertaken which indicated that these cements have up to a 10% reduction in connecting pores. One of the most successful trials in reducing the connecting pores was the flyash-lime mix. This may be a factor in increasing the saturation levels within

the underlying tailings. It should be noted however that the percentage of connected pores in the mix zone was consistently higher than those of the underlying pure tailings.

6.5.3.3.5 Fe^{2+}/Fe^{3+} and Other Solute Chemistry

Solute loads were determined for 6 of the trials, based on cementation, permeability and porosity results and included the flyash-lime layer and mix trials, the phosphate mix, the phosphate-lime mix and lime mix trials. These results were determined through a 1:5 tailings water extractions, followed by ICP-AES analysis. The samples were removed at approximately 20cm intervals down the column and the results compared with control columns and correlated with XRD analysis of surface salts and cements. Results are presented in Tables 3A.48 to 3A.53 Appendix 3A and Figures 6.29 to 6.31. The legend used for these figures is presented below.

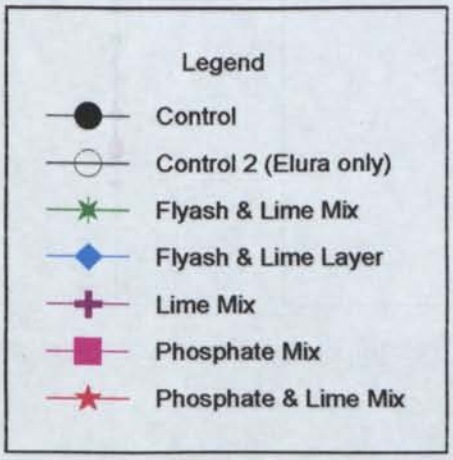

Solute Chemistry in Elura tailings

The Elura phosphate-lime mix trial had the greatest surface concentrations of K, B, Cu, Li, Na P, S and Si with the development of a thick surface salt crust. XRD identified gypsum as the main source of sulfur but did not identify the source of the other solutes. Both the Control (2) and flyash-lime layer trials produced elevated surface concentrations of Zn, Mg, Fe^{2+}, Fe^{3+}, Mn and Ca (Figs 6.29a, b, e, f). It should be noted that Control (1) and Control (2) produced very different profiles, with concentrations deeper in the Control (1) profile. Surface concentrations of gypsum and blodite ($Na_2Mg(SO_4)_2.4H_2O$) were identified in the flyash-lime layer trials.

Increased surface Ca concentrations were also observed within the phosphate-lime and lime mixes produced through the breakdown of lime and resultant precipitation of gypsum as identified by XRD. Rozenite ($FeSO_4.4H_2O$) was also identified at the surface of the lime mix trials. Elevated concentrations of Al were identified at the surface of the flyash-lime mix and at depth within the flyash-lime layer trial. These concentrations can be attributed to the dissolution of amorphous aluminosilicates of the flyash. Elevated levels of Zn, Mg and Mn were observed in the phosphate mix trial but concentrations were lower than those observed in the controls.

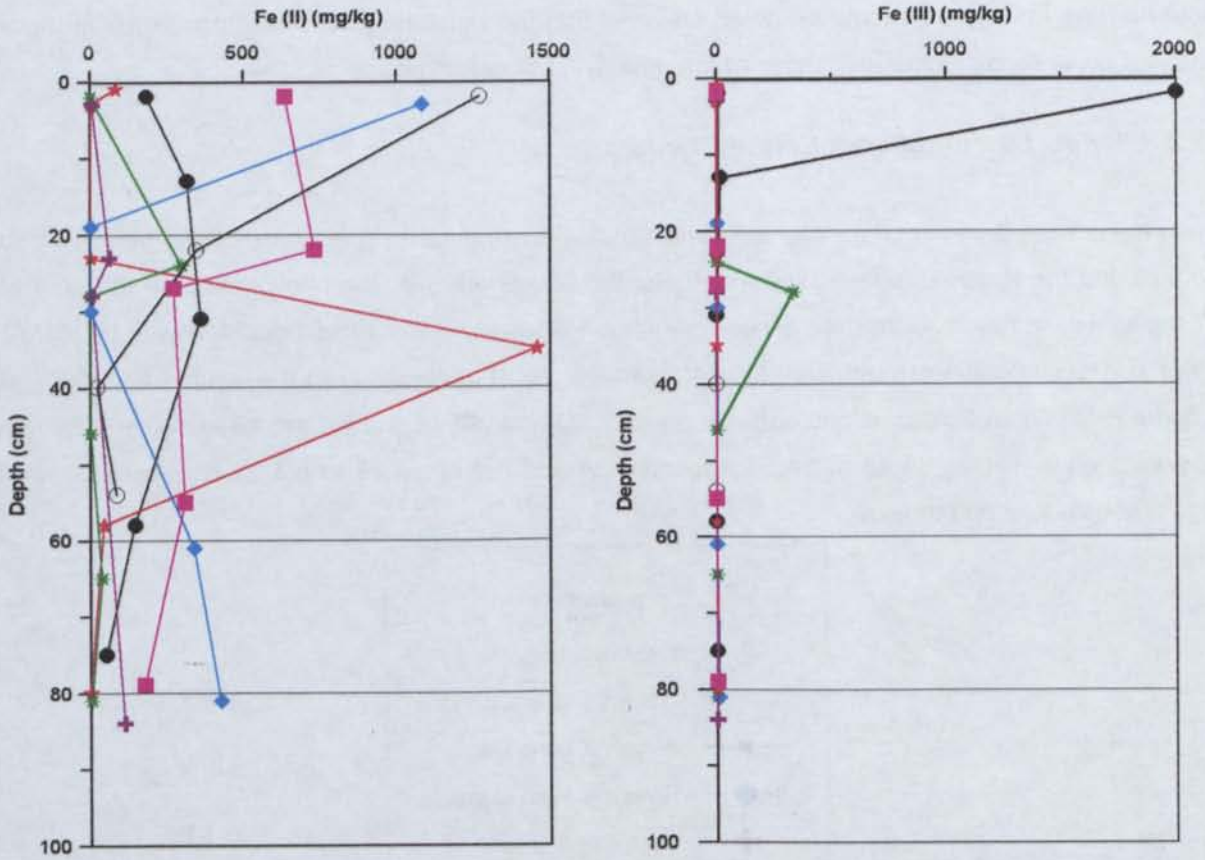

FIG 6.29A SOLUBLE Fe^{2+} AND Fe^{3+} FOR THE ELURA - SOLID ADDITIVE HARDPAN ENHANCEMENT EXPERIMENT

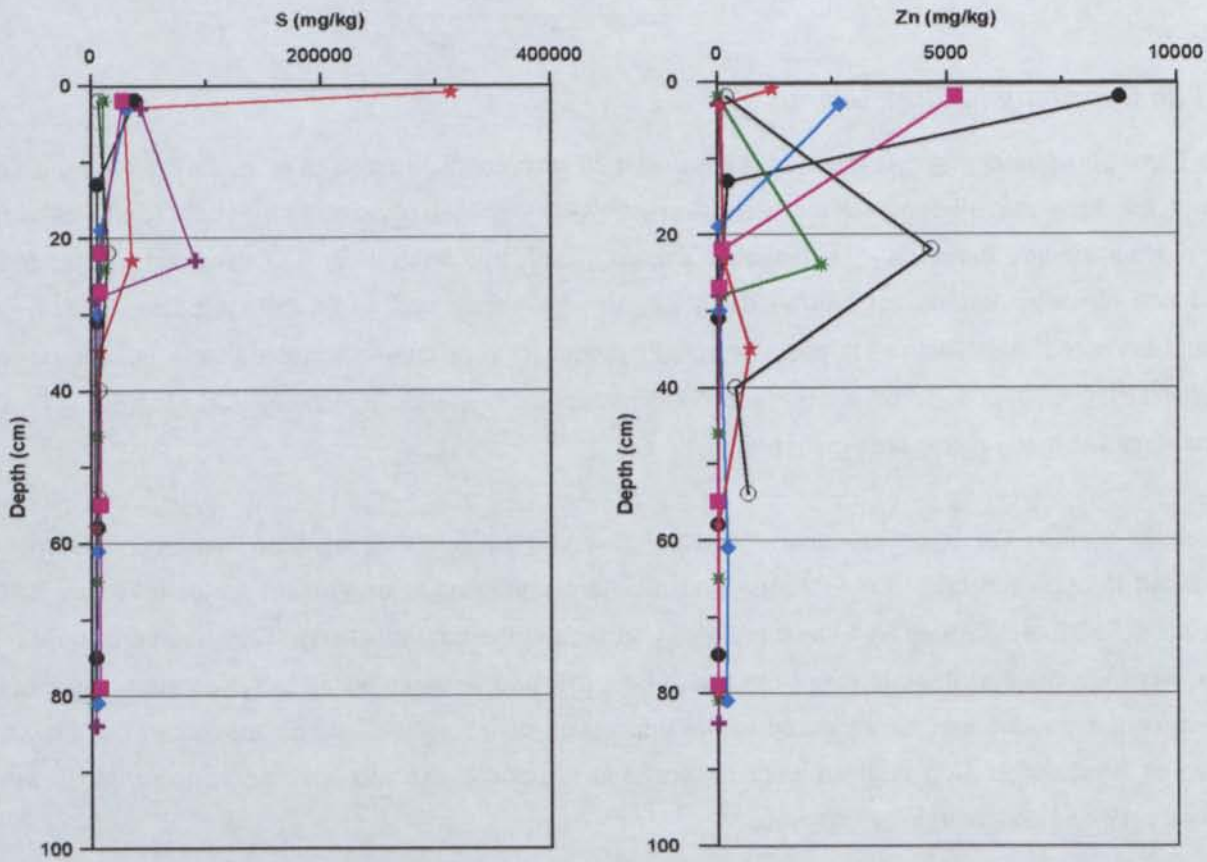

FIG 6.290B SOLUBLE S AND ZN FOR THE ELURA - SOLID ADDITIVE HARDPAN ENHANCEMENT EXPERIMENT

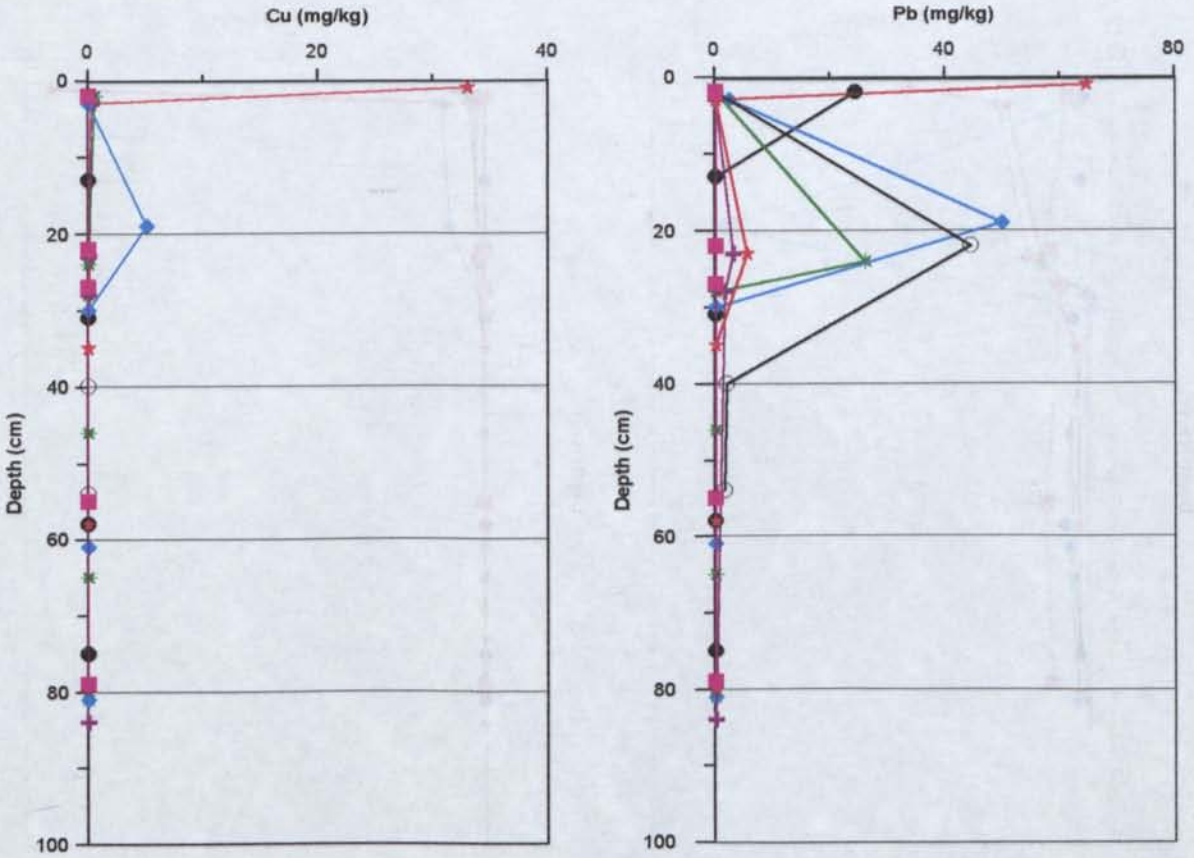

FIG 6.29C SOLUBLE CU AND PB FOR THE ELURA - SOLID ADDITIVE HARDPAN ENHANCEMENT EXPERIMENT

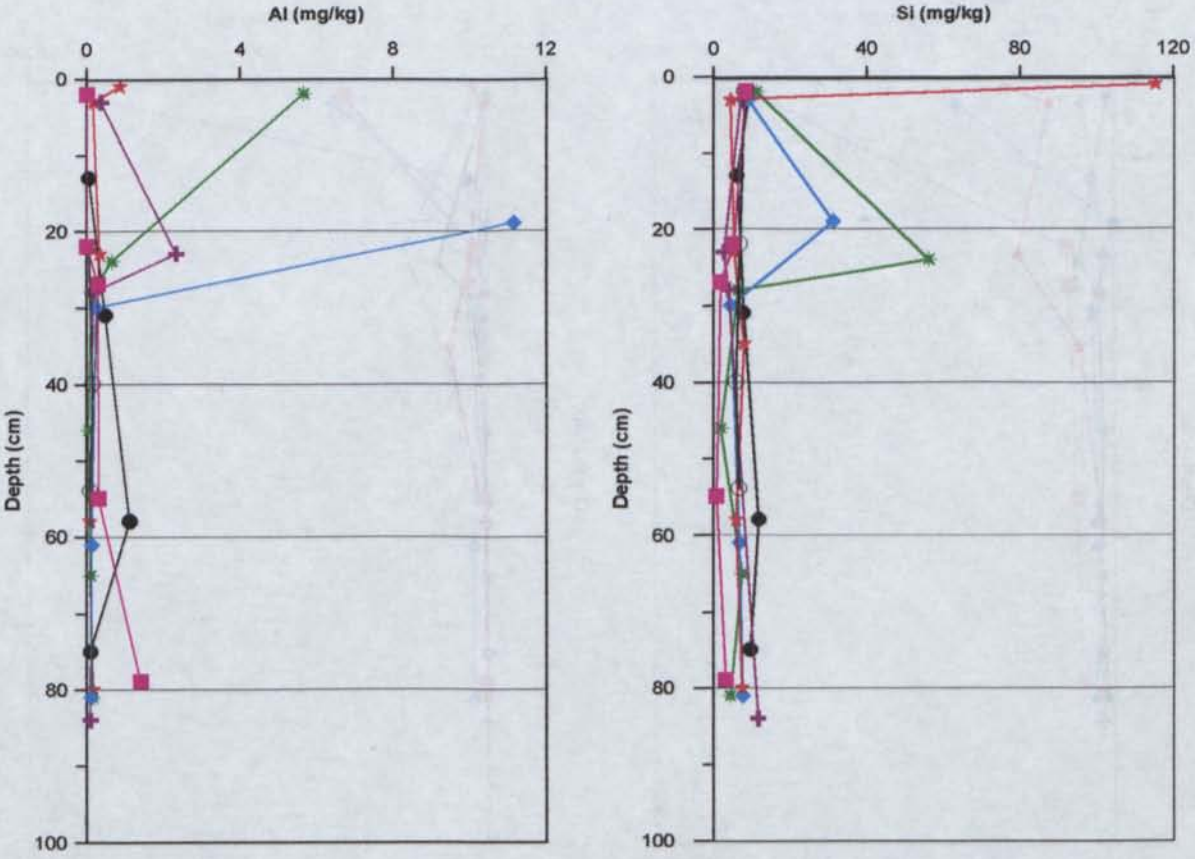

FIG 6.29D SOLUBLE AL AND SI FOR THE ELURA - SOLID ADDITIVE HARDPAN ENHANCEMENT EXPERIMENT

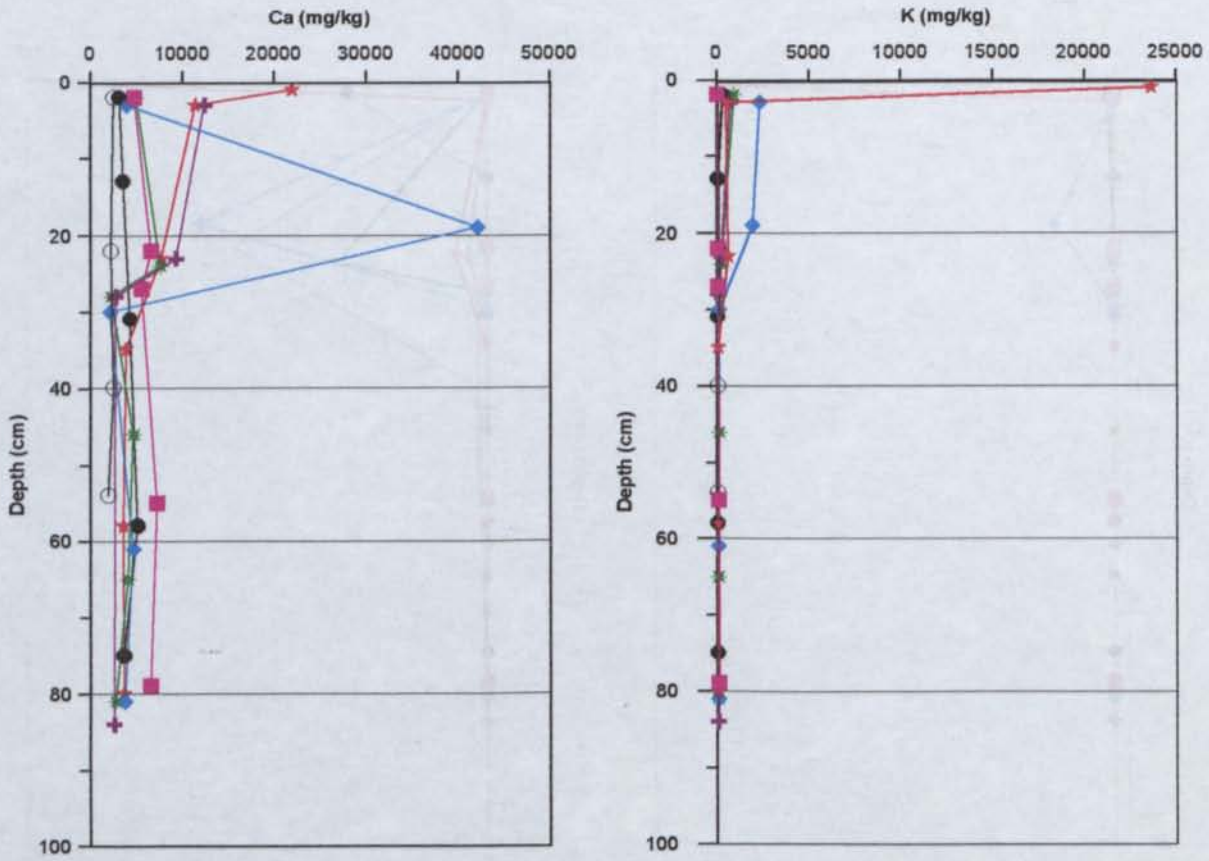

FIG 6.29E SOLUBLE CA AND K FOR THE ELURA- SOLID ADDITIVE HARDPAN ENHANCEMENT EXPERIMENT

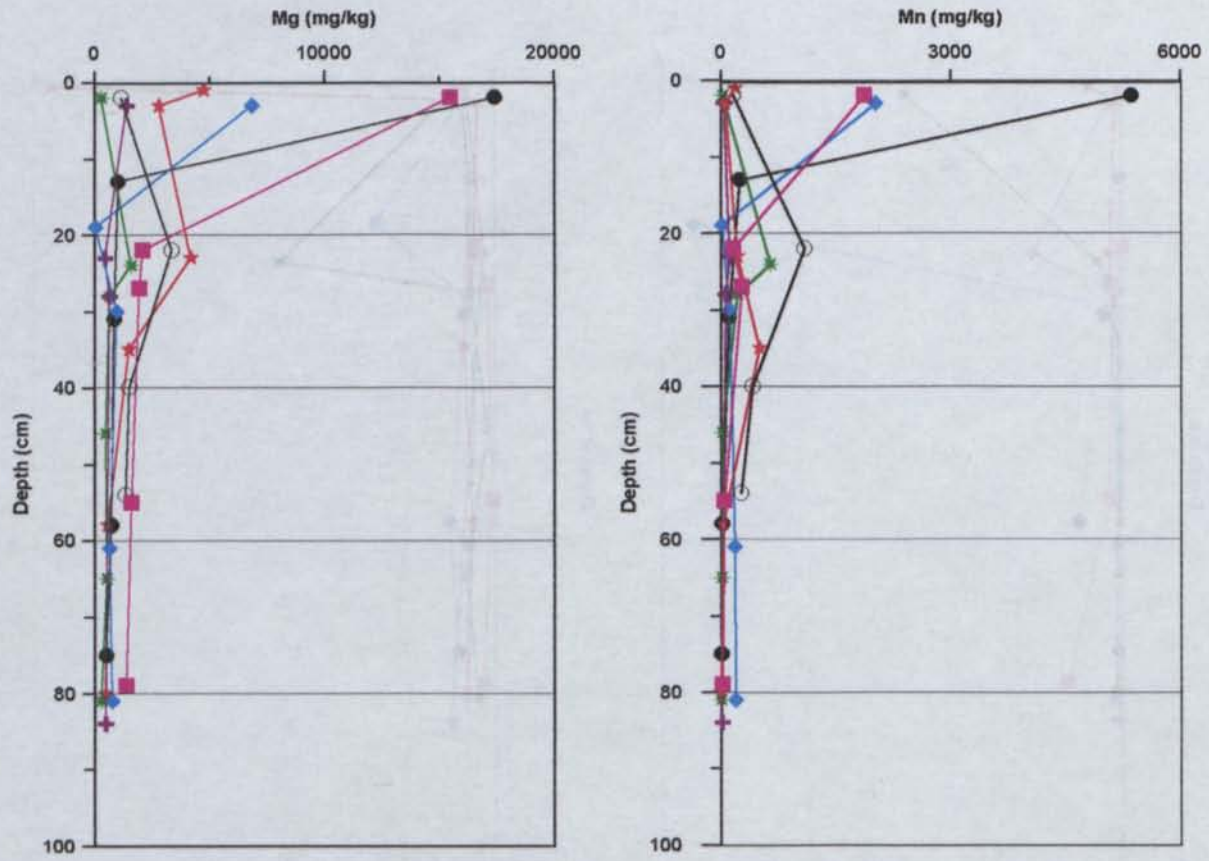

FIG 6.29F SOLUBLE MG AND MN FOR THE ELURA - SOLID ADDITIVE HARDPAN ENHANCEMENT EXPERIMENT

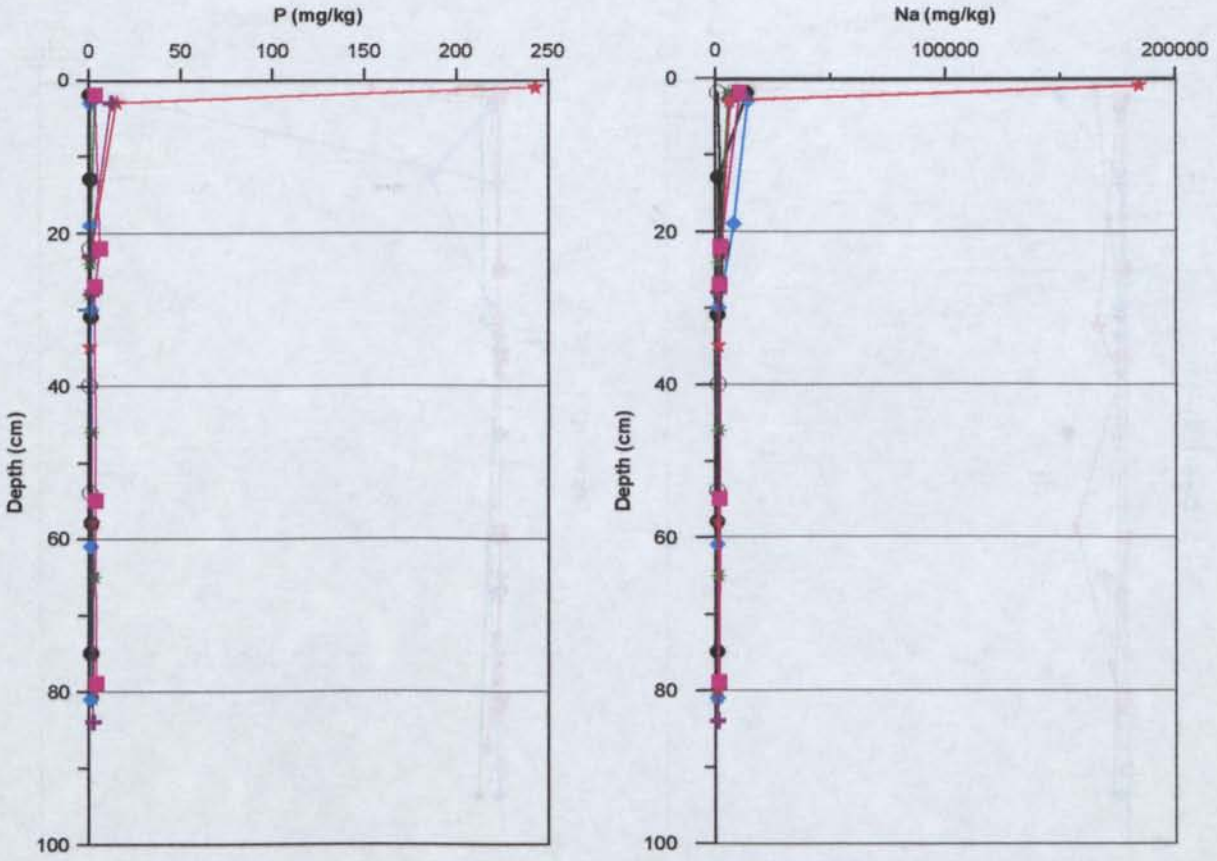

FIG 6.29G SOLUBLE P AND NA FOR THE ELURA - SOLID ADDITIVE HARDPAN ENHANCEMENT EXPERIMENT

Solute Chemistry in Peak tailings

The phosphate-lime mix trial also produced large quantities of surface soluble salts resulting in elevated surface concentrations of Fe^{2+}, Fe^{3+}, Cu, Mo, P, Si, S and Ca (Fig 6.30a, b, c, d, e and g). No discrete phases were identified by XRD techniques. The flyash-lime layer trial also showed elevated levels of all the previously mentioned elements, along with K, Na, Pb, Zn and Li and produced significant amounts of surface salts (Fig 6.30b, c, e and g). This large selection of solutes in the upper tailings of the flyash-lime layer is suggested to have developed through oxidation of the sulfides and the subsequent degradation of the gangue minerals.

The control exhibited elevated surface concentrations of Mg and Mn resulting in the precipitation of blodite, along with thenardite (Fig 6.30f). A concentration of Mn and Mg at 55cm depth correlates with increased Fe^{2+} levels, suggesting leaching from the surface (Fig 6.30a). A similar effect was observed for Pb within the lime mix trials with increased concentrations at 30cm depth (Fig 6.30c). Again elevated concentrations of Ca can be attributed to lime degradation (Fig 6.30e), similarly elevated concentrations of Al are attributed to flyash additions and its subsequent breakdown (Fig 6.30d). The elevated levels of Mg observed in the Elura phosphate mix are repeated here however Mn and Zn are not released.

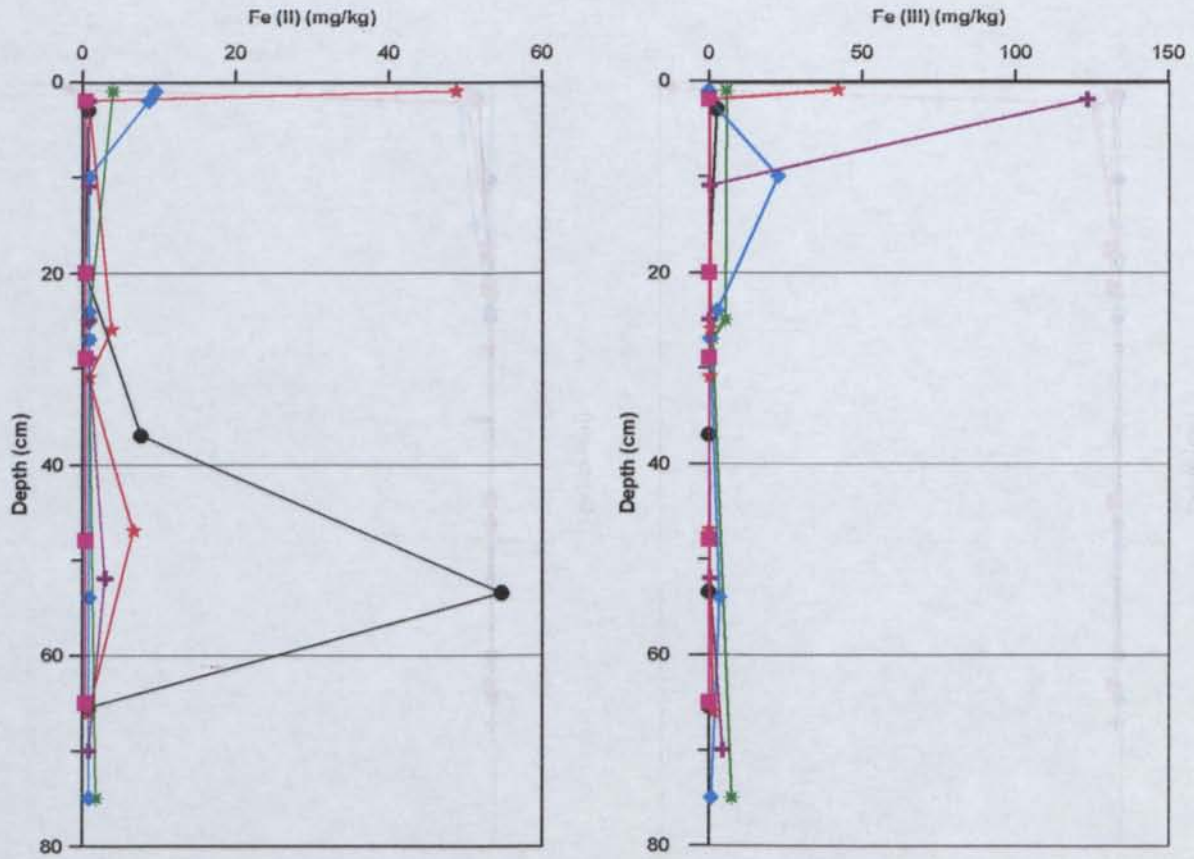

FIG 6.30A SOLUBLE Fe^{2+} AND Fe^{3+} FOR THE PEAK - SOLID ADDITIVE HARDPAN ENHANCEMENT EXPERIMENT

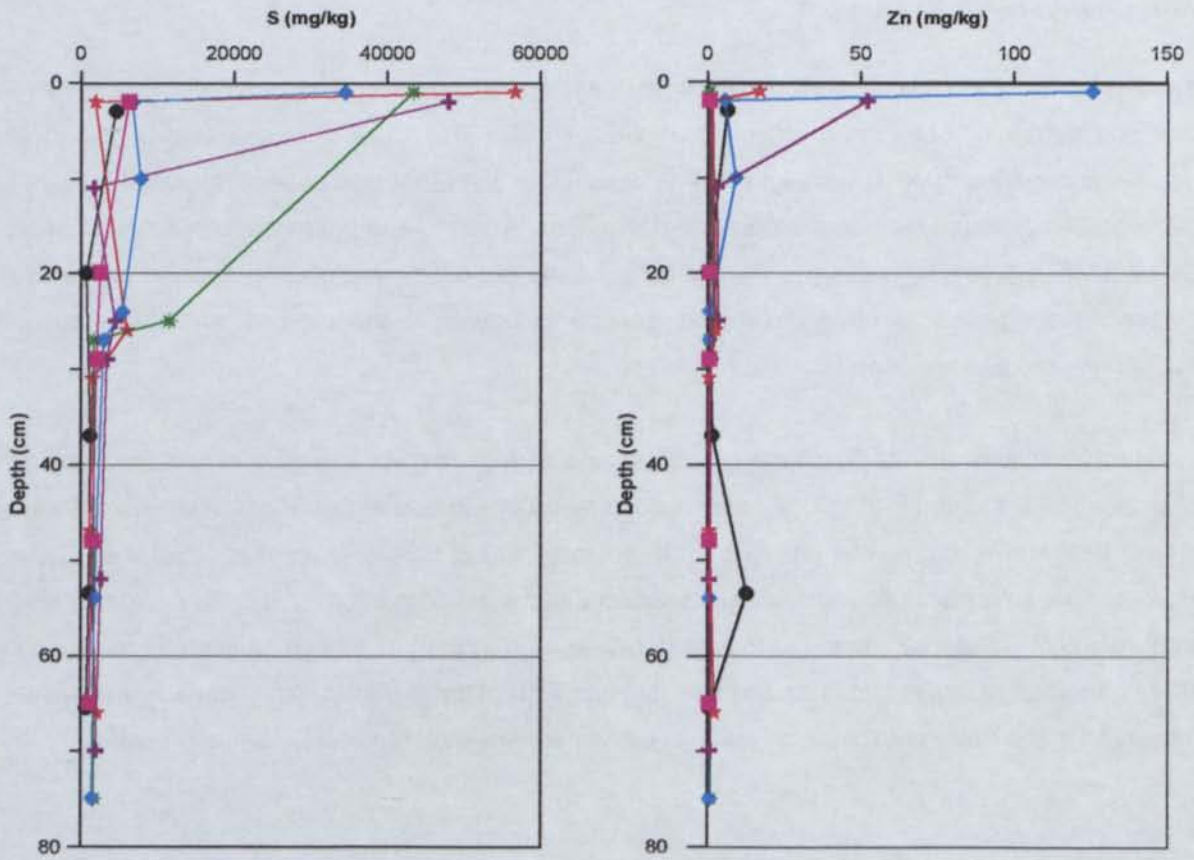

FIG 6.30B SOLUBLE S AND ZN FOR THE PEAK - SOLID ADDITIVE HARDPAN ENHANCEMENT EXPERIMENT

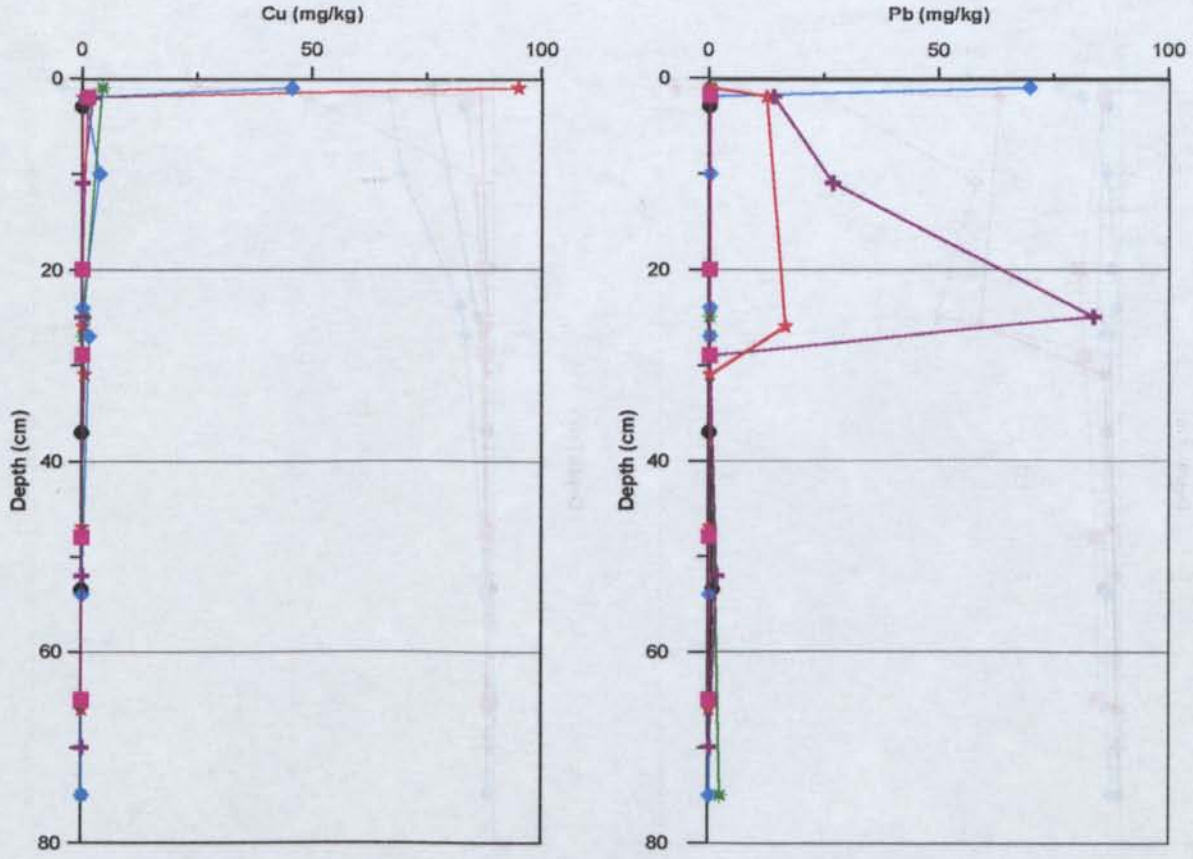

FIG 6.30C SOLUBLE CU AND PB FOR THE PEAK - SOLID ADDITIVE HARDPAN ENHANCEMENT EXPERIMENT

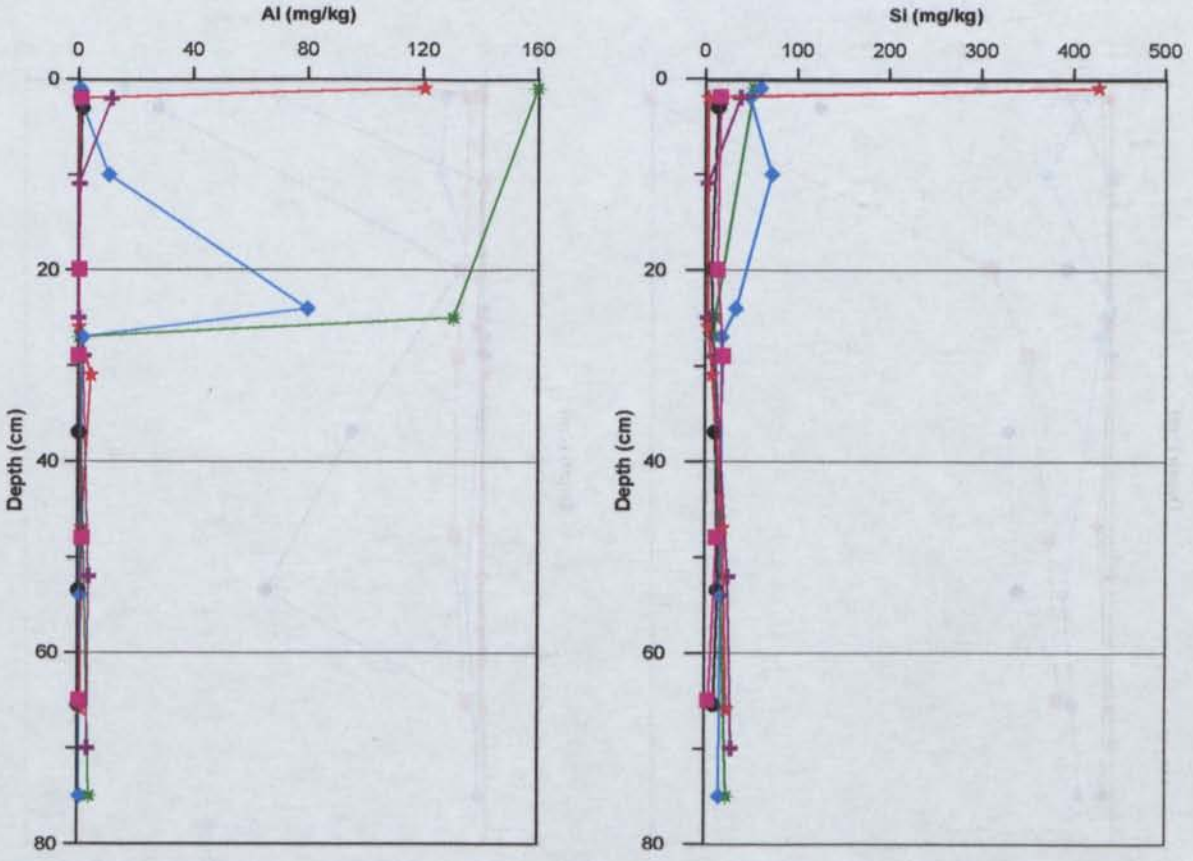

FIG 6.30D SOLUBLE AL AND SI FOR THE PEAK - SOLID ADDITIVE HARDPAN ENHANCEMENT EXPERIMENT

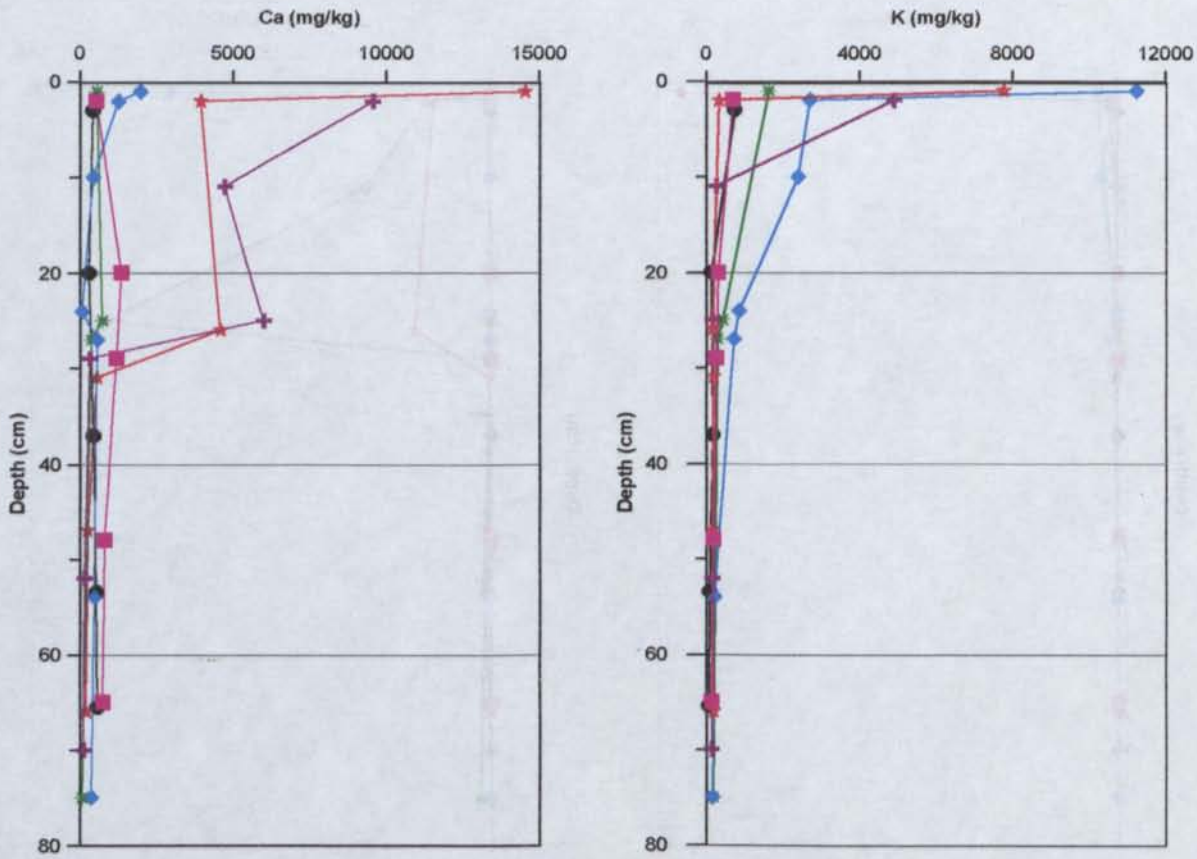

FIG 6.30E SOLUBLE CA AND K FOR THE PEAK - SOLID ADDITIVE HARDPAN ENHANCEMENT EXPERIMENT

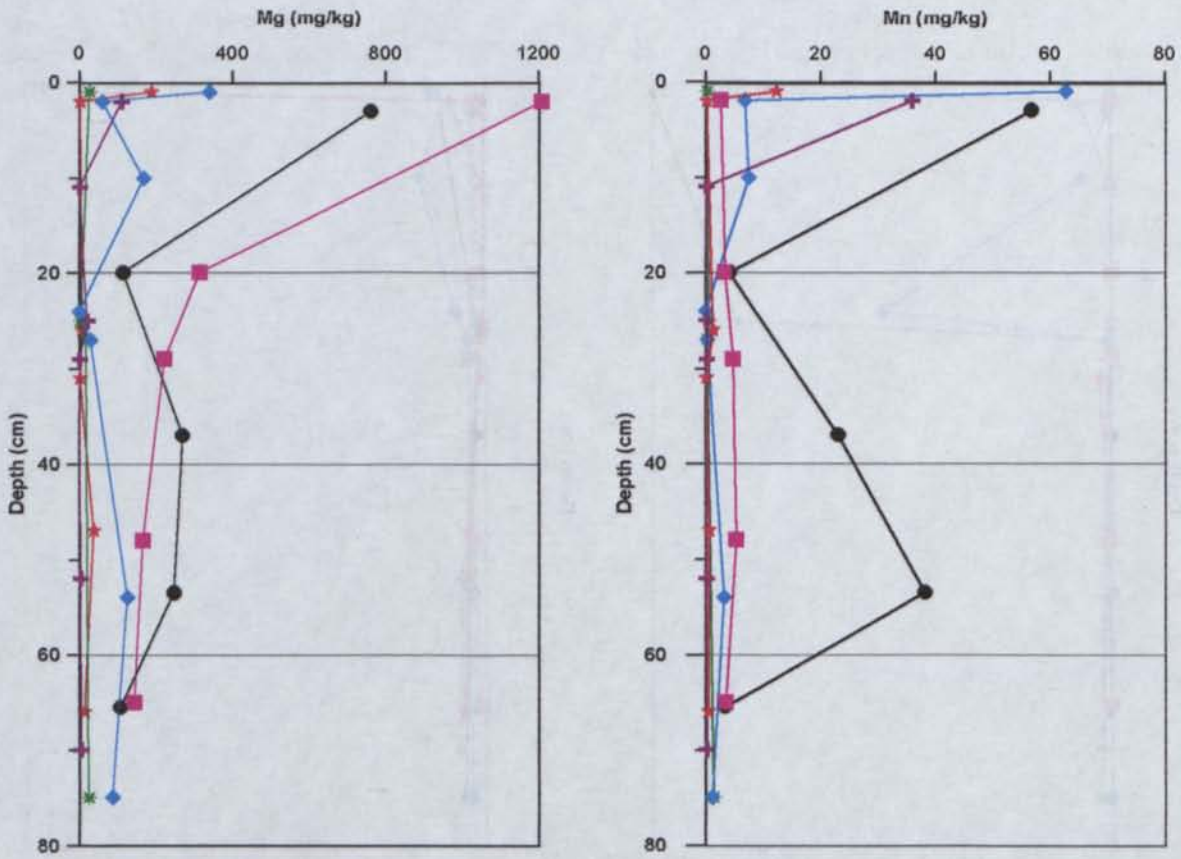

FIG 6.30F SOLUBLE MG AND MN FOR THE PEAK - SOLID ADDITIVE HARDPAN ENHANCEMENT EXPERIMENT

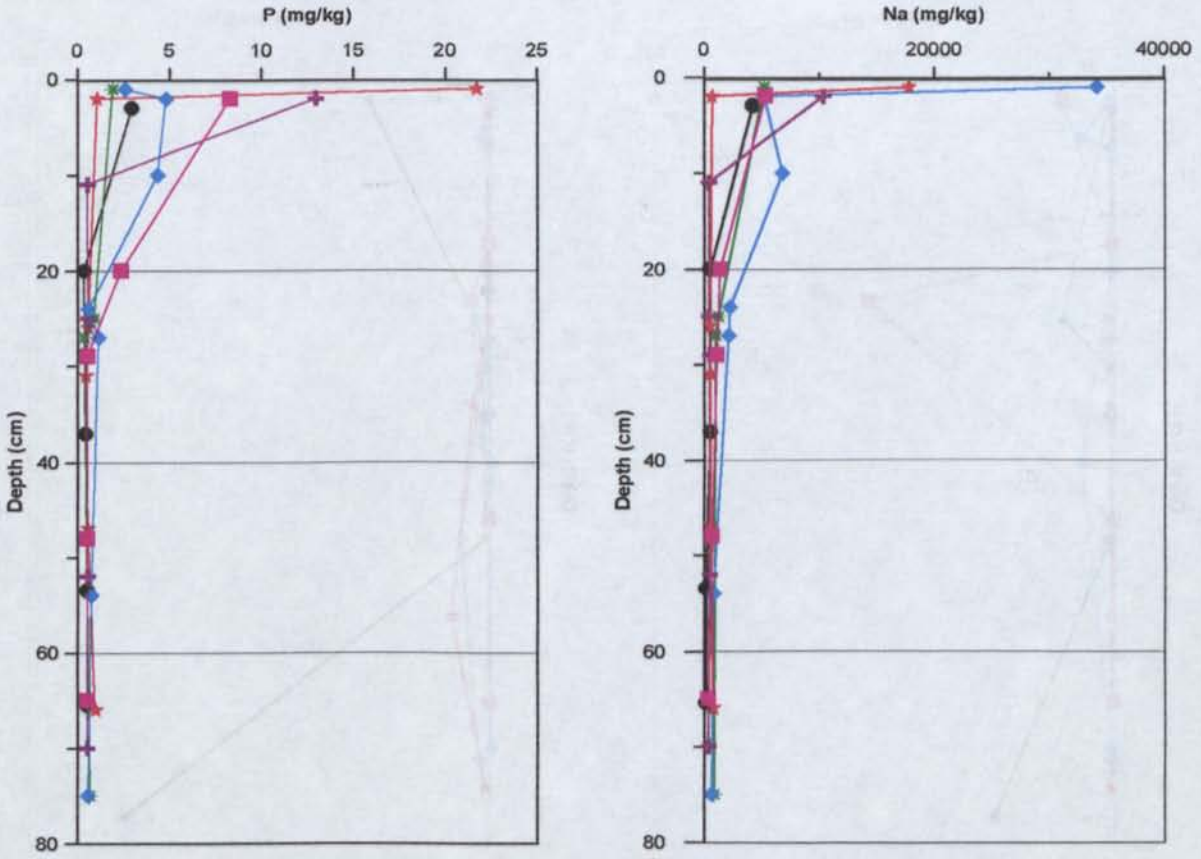

FIG 6.30G SOLUBLE P AND NA FOR THE PEAK - SOLID ADDITIVE HARDPAN ENHANCEMENT EXPERIMENT

Solute Chemistry in CSA tailings

The influence of the phosphate-lime mix trial observed in the Elura and Peak trials has not occurred within the CSA tailings. Instead, it is the flyash-lime mix which has produced elevated concentrations of P, Na, Cu, K, Al, B, Mo, Li, Fe^{3+}, S and Si (Fig 6.31a, b, c, d, e and g). Gypsum was identified at the surface. It should be noted that increased concentrations of Na, Cu, K, Al, S and Si were also identified in the flyash-lime layer occurring as gypsum and thenardite (Fig 6.31b, c, d and g).

Surface concentrations of Fe^{2+}, Mg, Ca, S and Mn developed within the control (Fig 6.31a and f) but only gypsum was identified. Manganese concentrations also increased at approximately 20cm depth and correlated with a minor increase in Pb and Zn (Fig 6.31b and c). Again Ca concentrations were dictated by lime additions. The Ca concentrations were greater throughout the CSA trials suggesting Ca is potentially more mobile within these tailings (Fig 6.31f). Elevated Mg levels are also apparent within the phosphate mix but only low levels of other solutes were observed.

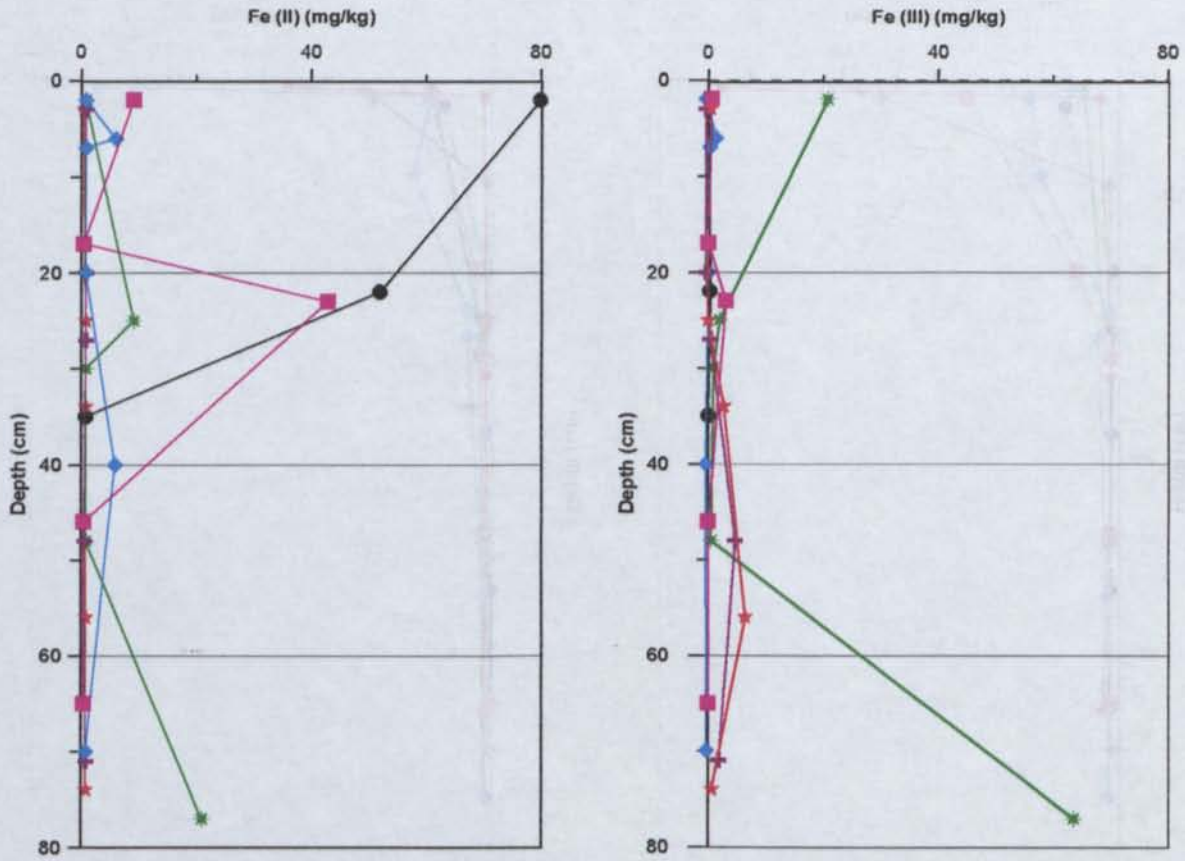

FIG 6.31A SOLUBLE Fe^{2+} AND Fe^{3+} FOR THE CSA - SOLID ADDITIVE HARDPAN ENHANCEMENT EXPERIMENT

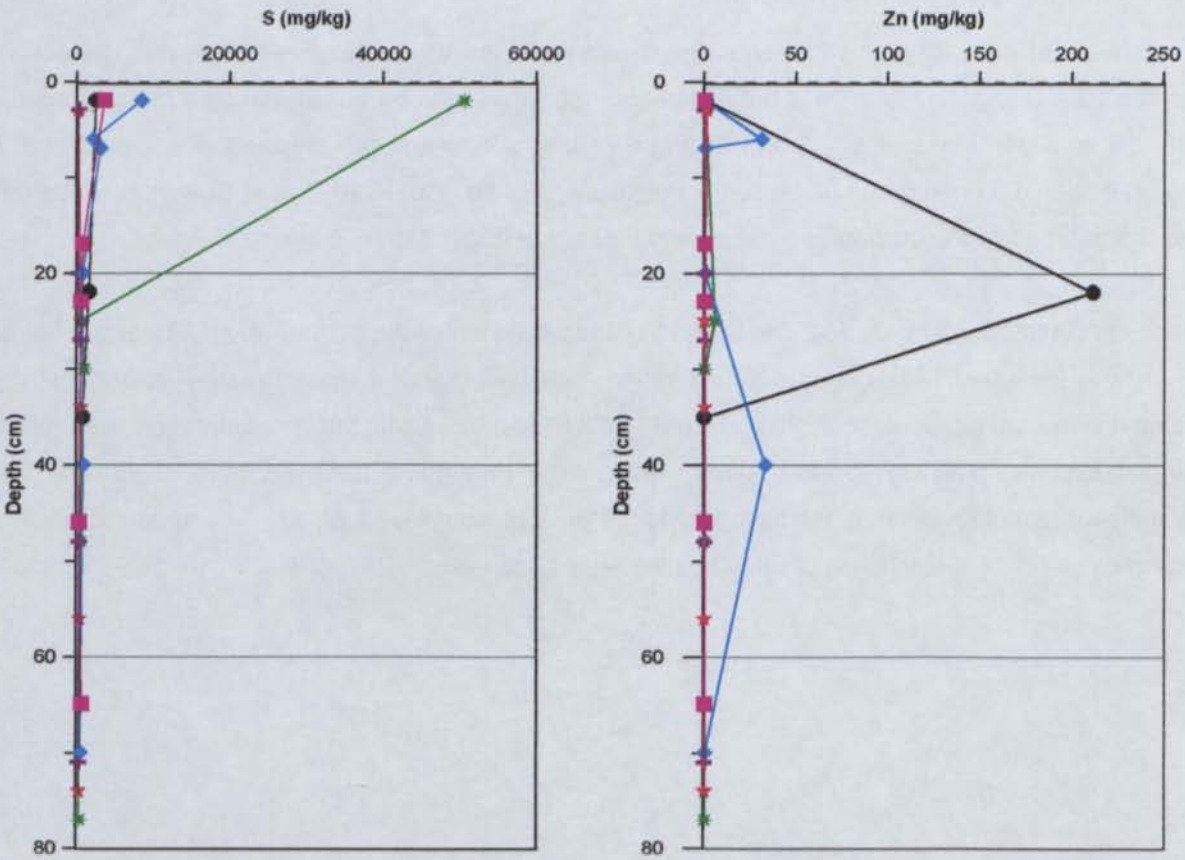

FIG 6.31B SOLUBLE S AND ZN FOR THE CSA - SOLID ADDITIVE HARDPAN ENHANCEMENT EXPERIMENT

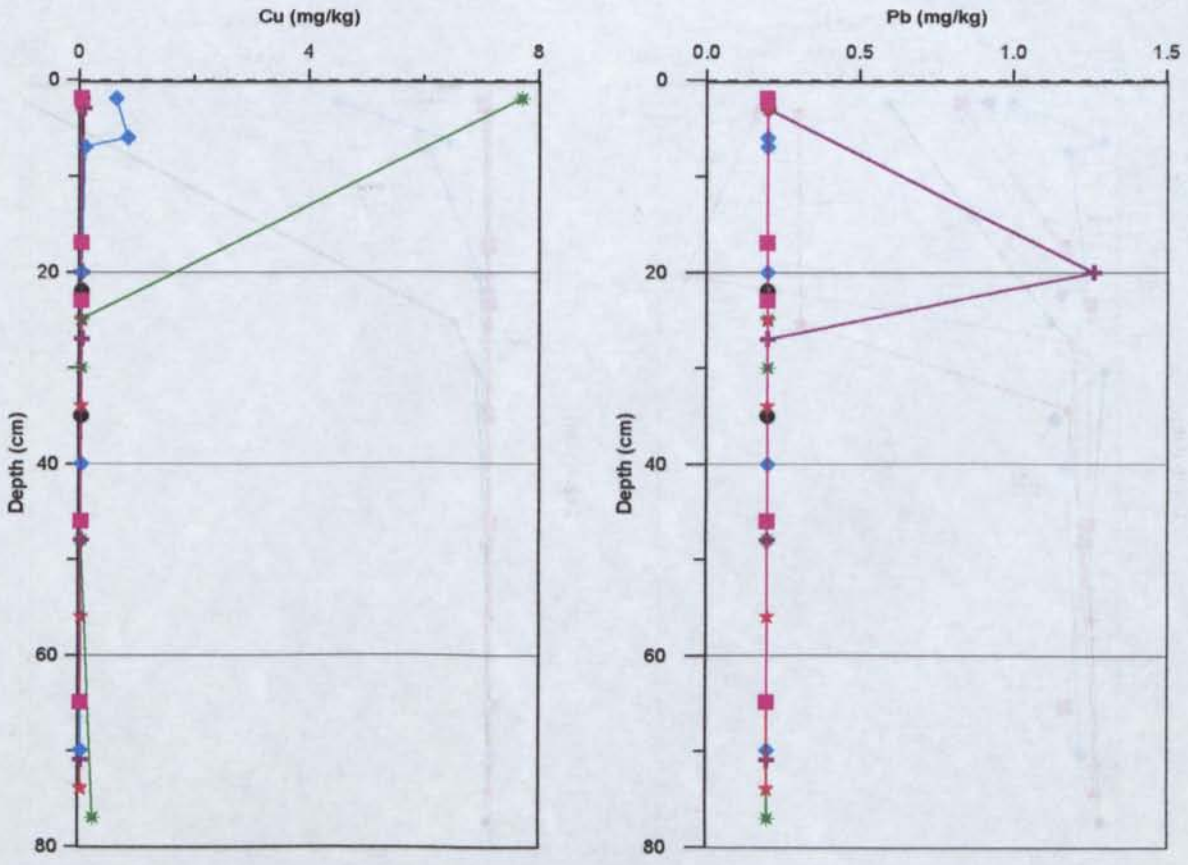

FIG 6.31C SOLUBLE CU AND PB FOR THE CSA - SOLID ADDITIVE HARDPAN ENHANCEMENT EXPERIMENT

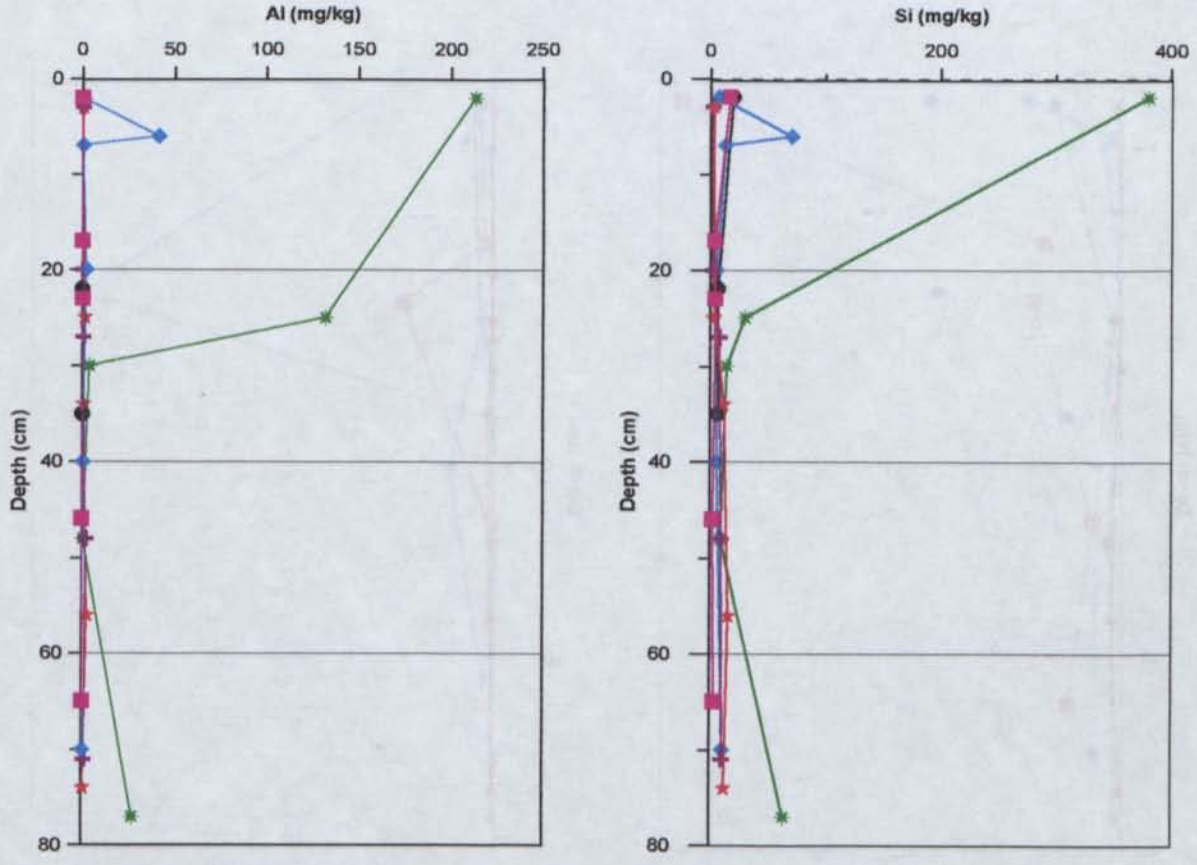

FIG 6.31D SOLUBLE AL AND SI FOR THE CSA - SOLID ADDITIVE HARDPAN ENHANCEMENT EXPERIMENT

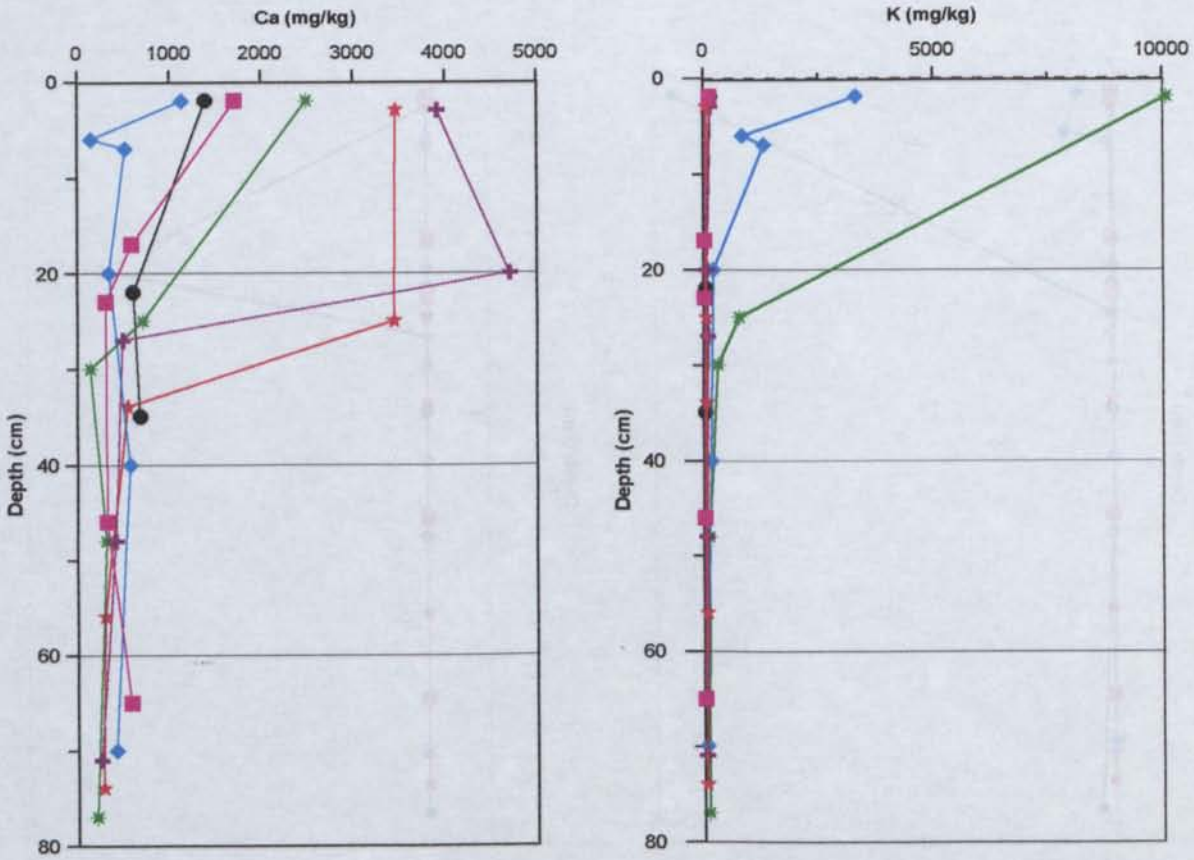

FIG 6.31E SOLUBLE CA AND K FOR THE CSA - SOLID ADDITIVE HARDPAN ENHANCEMENT EXPERIMENT

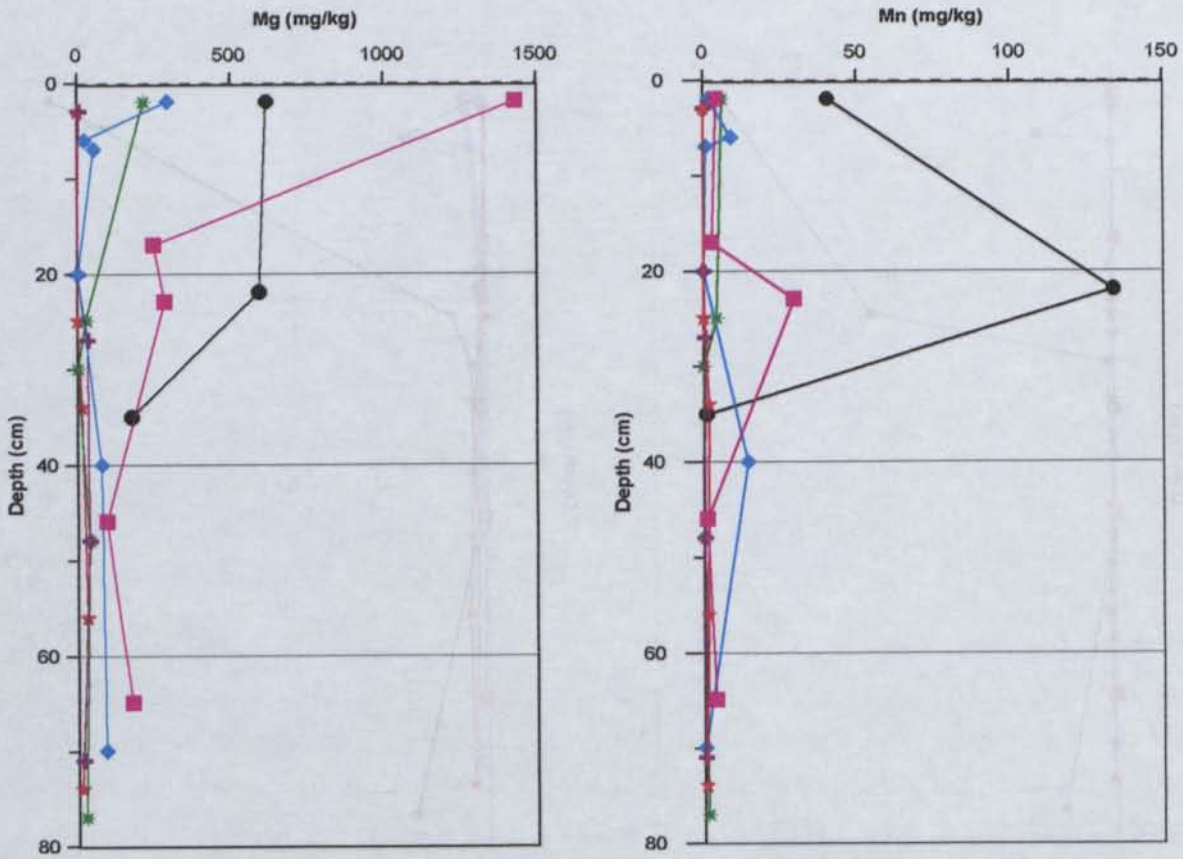

FIG 6.31F SOLUBLE MG AND MN FOR THE CSA - SOLID ADDITIVE HARDPAN ENHANCEMENT EXPERIMENT

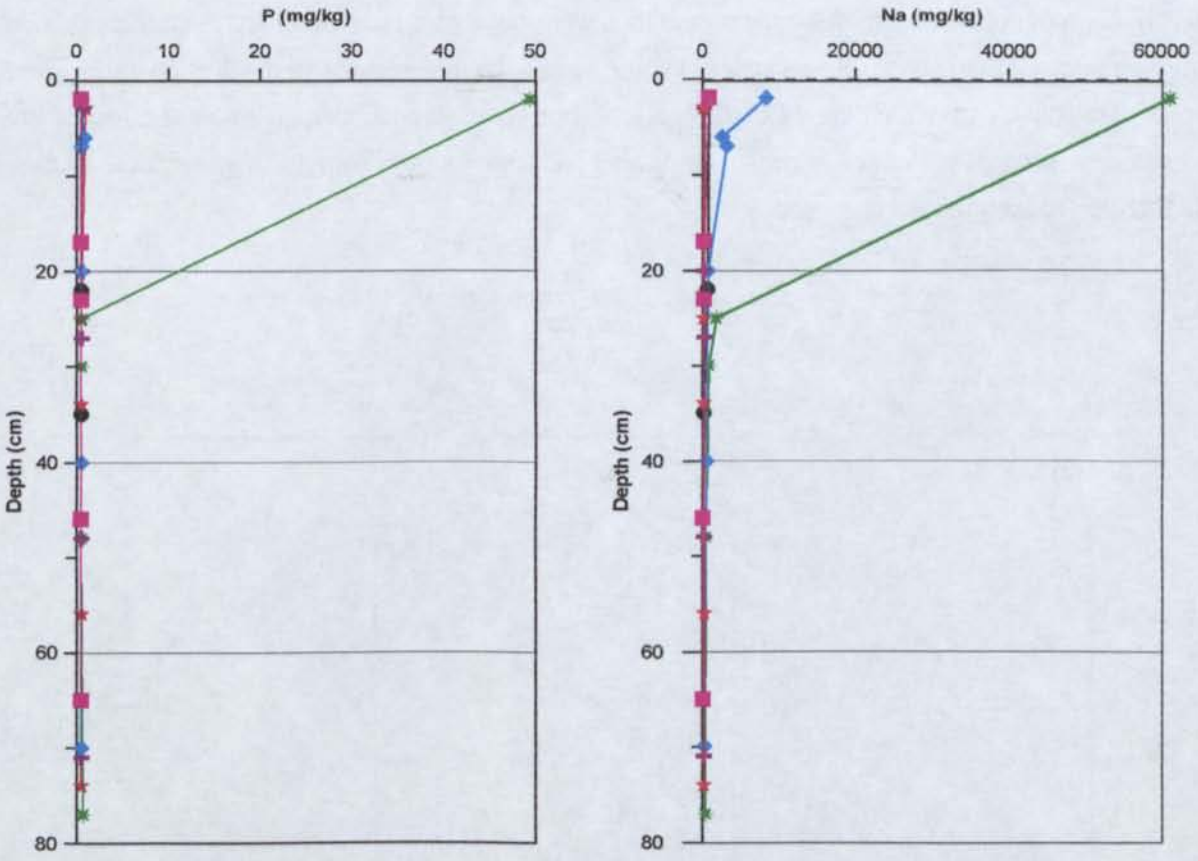

FIG 6.31G SOLUBLE P AND NA FOR THE CSA - SOLID ADDITIVE HARDPAN ENHANCEMENT EXPERIMENT

6.5.3.3.6 Chemistry Summary

The solute chemistry of these profiles has developed in response to direct dissolution of primary tailings and additives, through oxidation of sulfides, acid generation and neutralisation reactions and acid degradation of gangue minerals. The greatest surface concentrations produced through evaporation and precipitation of soluble salts has occurred predominantly within the phosphate-lime mix and the flyash-lime mix and layer trials. Surface concentrations in the mix trials can be attributed to reactions between tailings and additive or direct additive dissolution, while the surface concentrations within the flyash-lime layer must be attributed to oxidation reactions of the tailings. Elevated surface concentrations indicated the lack of stable cementation and thus suggests that these trials may be unsuccessful. It should be remembered however that over time salts may alter from soluble to insoluble due to dehydration.

6.5.3.4 CO_2 Analysis

The CO_2 concentrations within pore gases were determined to further investigate the effect of porosity and to ascertain whether cements with low gas diffusivity properties had developed. Gas sampling was carried out at the end of the 1 year period via the method 1A.5.1, Appendix 1A. The variations in CO_2 concentrations within the trials were compared within the control columns, with a build up of CO_2 below the additive zone indicating a reduction in upward gas diffusion (Figs 6.32 to 6.45). High levels of CO_2 within the limestone additive zones either as mixes or layers were regarded as having formed at those

locations through direct carbonate dissolution, and thus were not a true build-up of CO_2. Carbon dioxide concentrations lower than those observed within the control columns suggested diffusion rates were enhanced. The initial carbonate content of the three tailings types vary significantly so the effect of the additives is discussed as *factors of increase,* compared with the control columns. Figures 6.32 to 6.45 present the CO_2 concentrations observed.

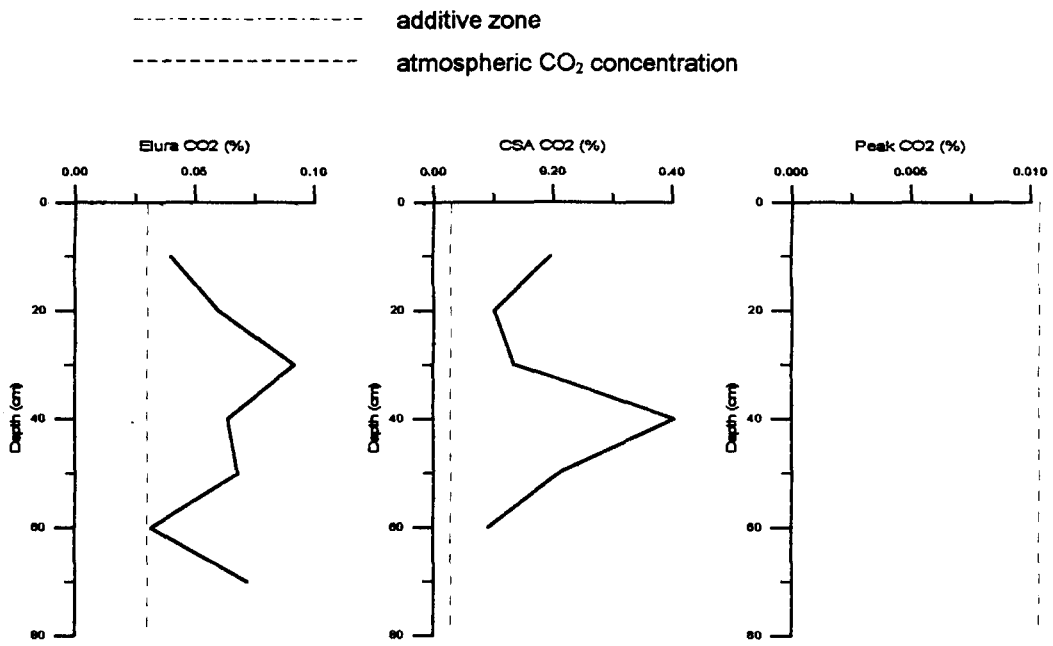

FIG 6.32 CO_2 PROFILES FOR CONTROL TRIALS - SOLID ADDITIVE HARDPAN ENHANCEMENT EXPERIMENT

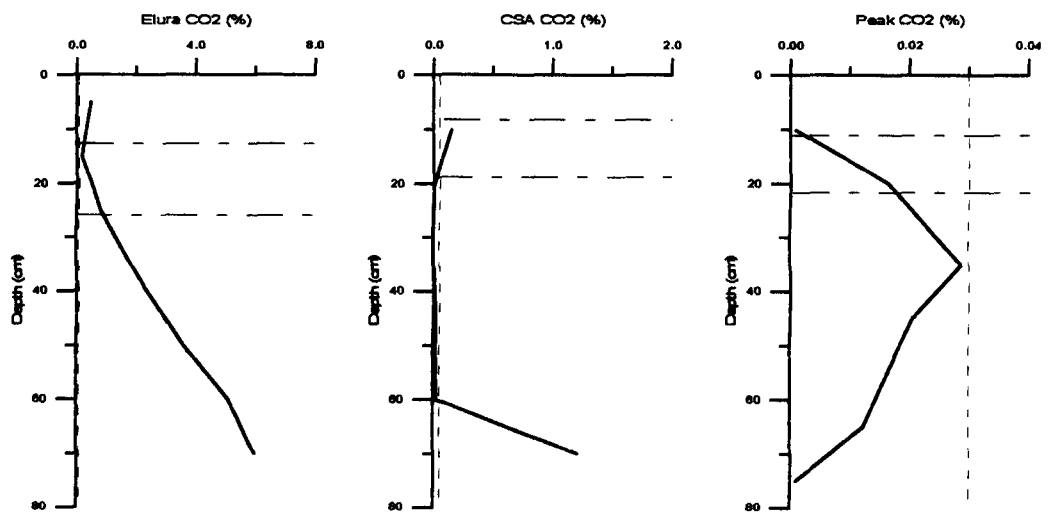

FIG 6.33 CO_2 PROFILES FOR FLYASH-LIME LAYER TRIALS- SOLID ADDITIVE HARDPAN ENHANCEMENT EXPERIMENT

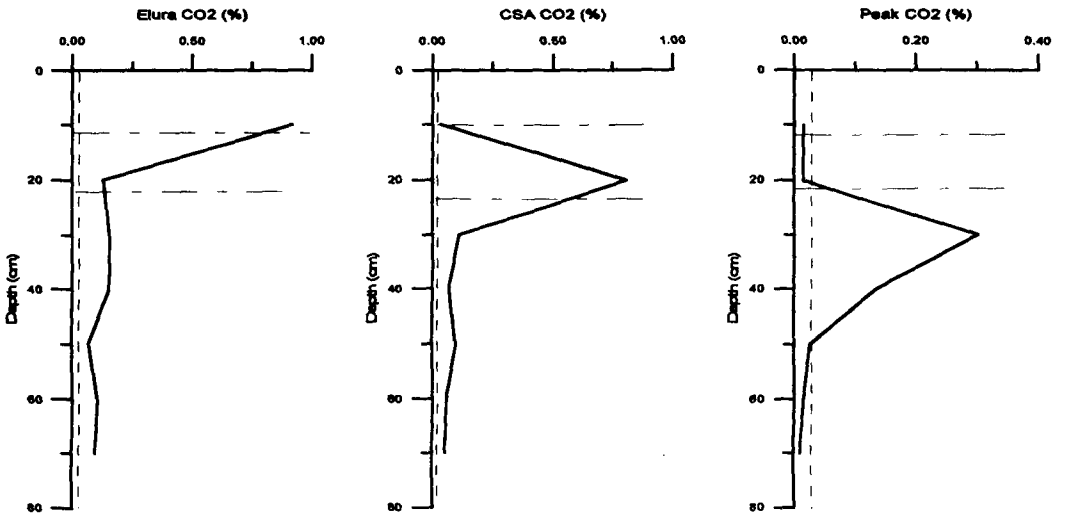

FIG 6.34 CO_2 PROFILES FOR FLYASH LAYER TRIALS- SOLID ADDITIVE HARDPAN ENHANCEMENT EXPERIMENT

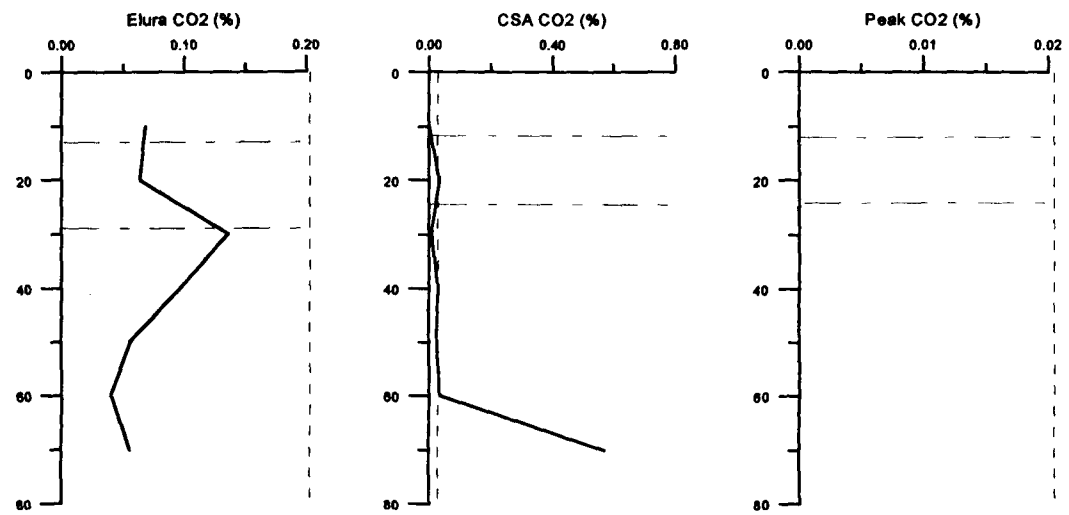

FIG 6.35 CO_2 PROFILES FOR LIME LAYER TRIALS- SOLID ADDITIVE HARDPAN ENHANCEMENT EXPERIMENT

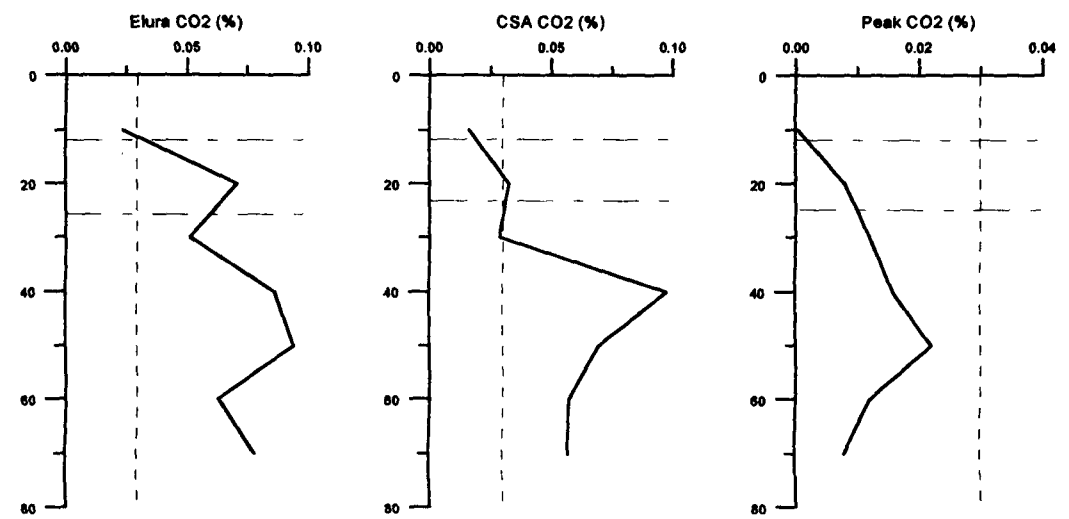

FIG 6.36 CO_2 PROFILES FOR PHOSPHATE-LIME LAYER TRIALS- SOLID ADDITIVE HARDPAN ENHANCEMENT EXPERIMENT

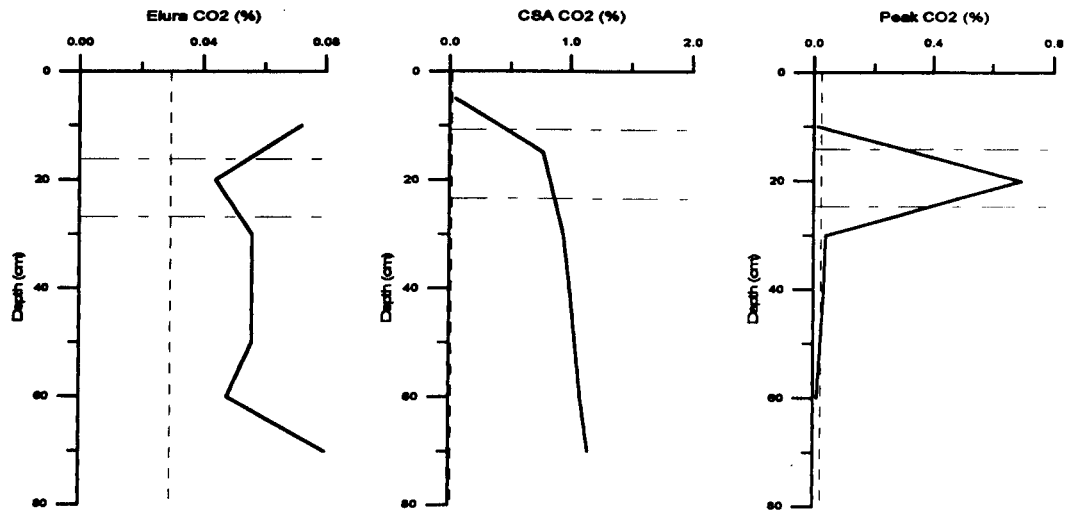

FIG 6.37 CO_2 PROFILES FOR PHOSPHATE-LIMESTONE LAYER TRIALS- SOLID ADDITIVE HARDPAN ENHANCEMENT EXPERIMENT

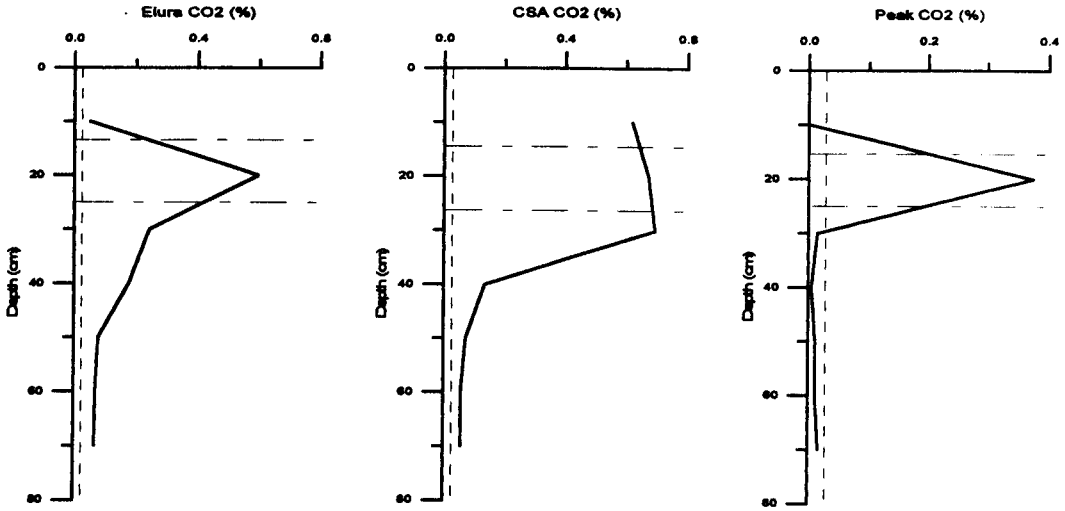

FIG 6.38 CO_2 PROFILES FOR PHOSPHATE LAYER TRIALS - SOLID ADDITIVE HARDPAN ENHANCEMENT EXPERIMENT

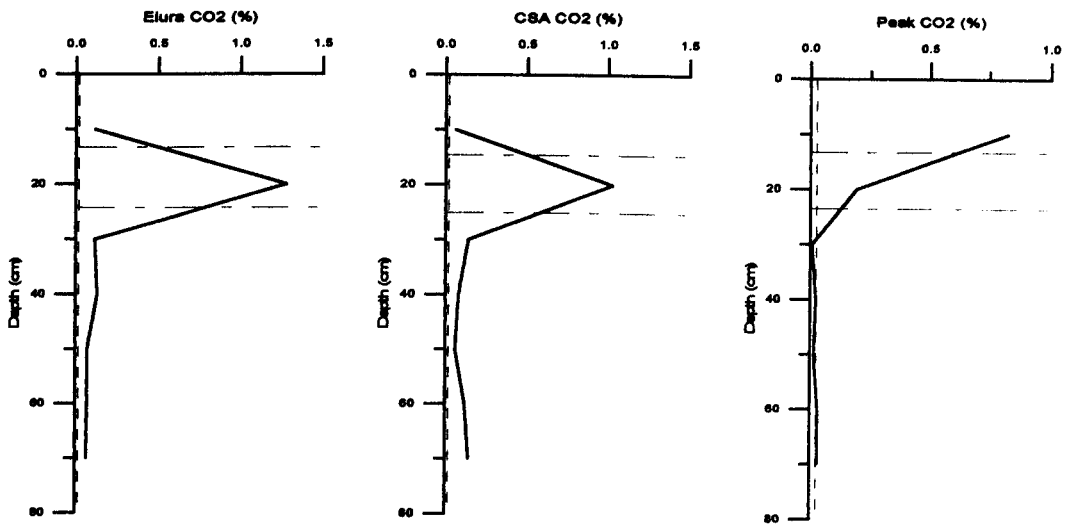

FIG 6.39 CO_2 PROFILES FOR LIMESTONE LAYER TRIALS - SOLID ADDITIVE HARDPAN ENHANCEMENT EXPERIMENT

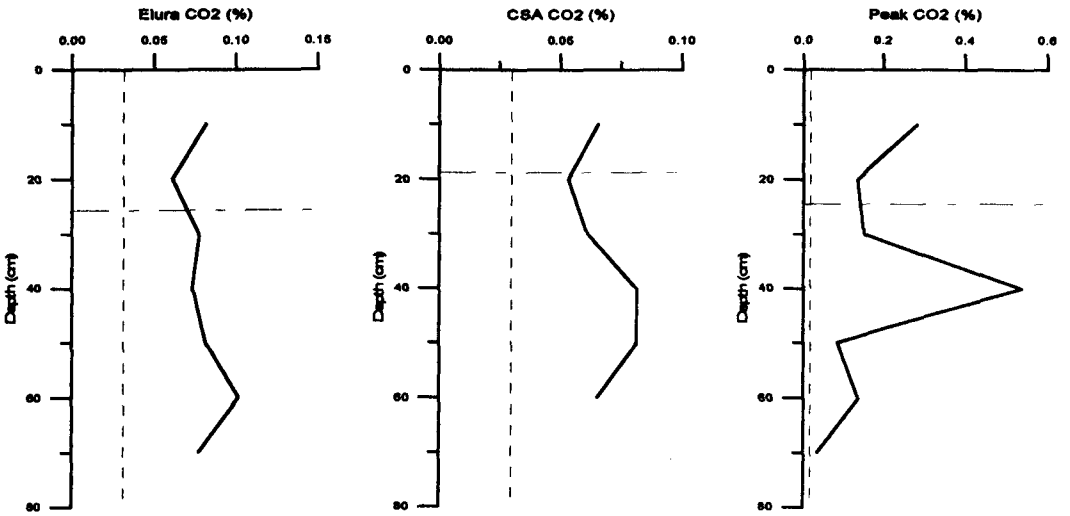

FIG 6.401 CO_2 PROFILES FOR LIMESTONE MIX TRIALS - SOLID ADDITIVE HARDPAN ENHANCEMENT EXPERIMENT

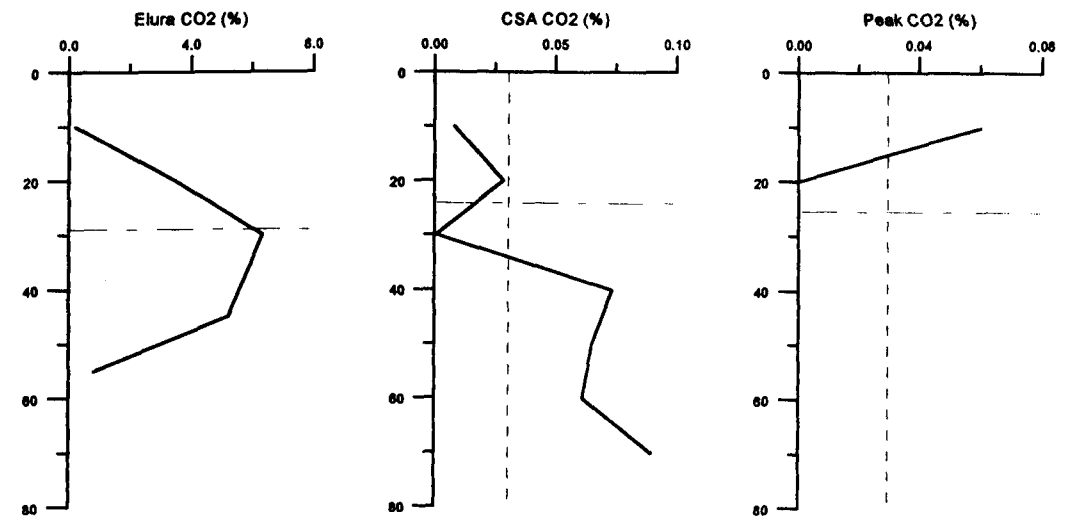

FIG 6.41 CO_2 PROFILES FOR PHOSPHATE-LIME MIX TRIALS - SOLID ADDITIVE HARDPAN ENHANCEMENT EXPERIMENT

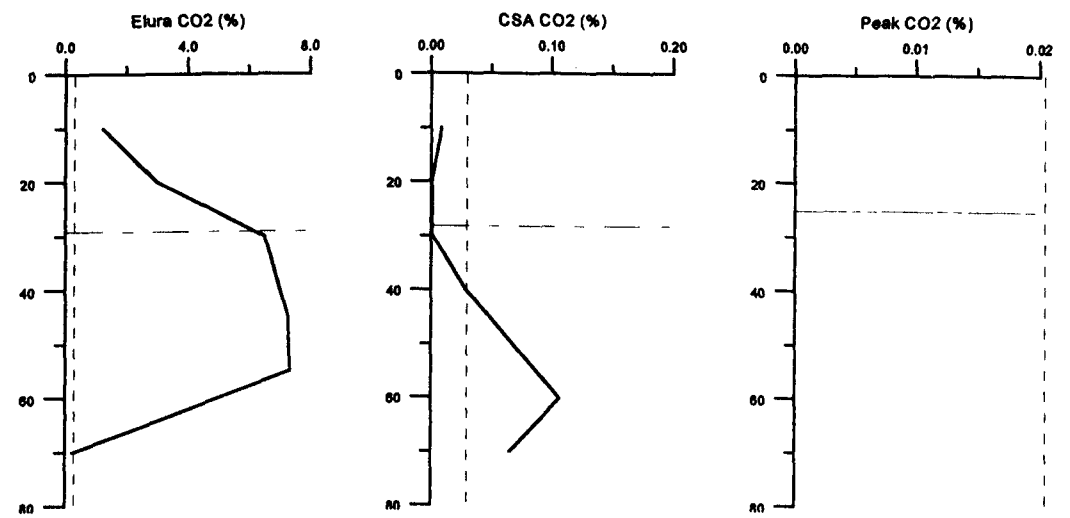

FIG 6.42 CO_2 PROFILES FOR FLYASH-LIME MIX TRIALS - SOLID ADDITIVE HARDPAN ENHANCEMENT EXPERIMENT

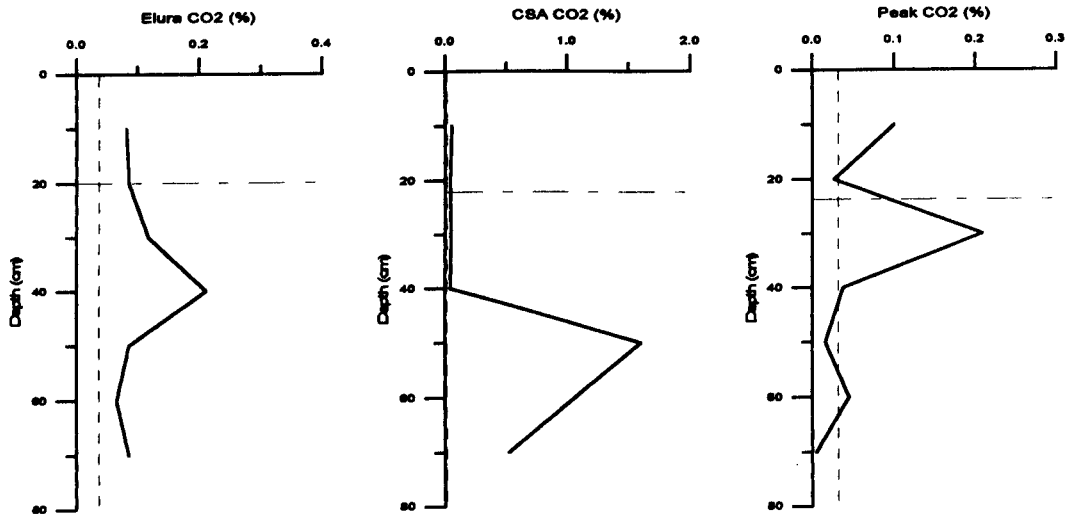

FIG 6.43 CO_2 PROFILES FOR PHOSPHATE MIX TRIALS - SOLID ADDITIVE HARDPAN ENHANCEMENT EXPERIMENT

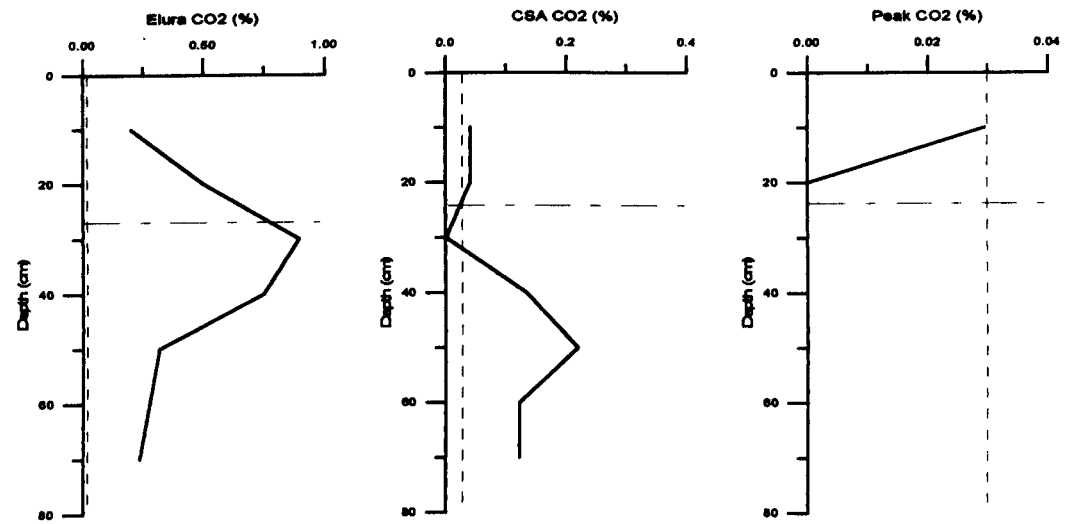

FIG 6.44 CO_2 PROFILES FOR LIME MIX TRIALS - SOLID ADDITIVE HARDPAN ENHANCEMENT EXPERIMENT

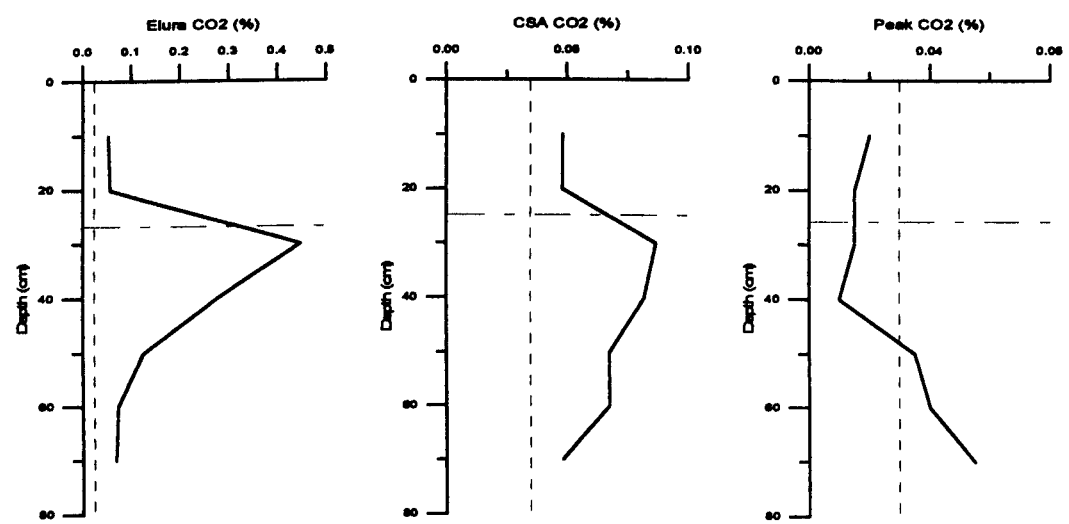

FIG 6.45 CO_2 PROFILES FOR FLYASH MIX TRIALS - SOLID ADDITIVE HARDPAN ENHANCEMENT EXPERIMENT

All trials produced profiles of which at least one of the tailings had CO_2 concentrations greater than the control columns (Fig 6.32 to 6.45). Two additive trials were successful in increasing concentrations within all tailings, indicating a reduction in gas diffusivity. Phosphate mix trials produced CO_2 concentrations greater than atmospheric CO_2 and concentrations higher than the controls for all trials (Fig 6.43). The region of increased concentration varied from directly below the additive zone (30cm) in the Peak to 50cm depth in CSA in which an increase by a factor of 4 was achieved.

The flyash layer also showed universal increases in CO_2, the concentrations occurring below the layer in the Peak tailings and within the layer for CSA and Elura tailings where a 10-fold increase was observed (Fig 6.34). Additionally the flyash-lime layer produced elevated CO_2 concentrations in all trials with up to 60 times increase in Elura. However this increase was not seen in the other tailings (Fig 6.33).

It appeared that of all trials, the Elura tailings exhibited the lowest diffusivity as shown by CO_2 build up. The phosphate-lime mix increased CO_2 concentrations by a factor of 60, whilst the flyash-lime mix produced CO_2 concentrations of 7% compared with the control which obtained levels of 0.1% only, a 70-fold increase. Increased concentrations were also observed in the lime mix, flyash layer, flyash-lime mix, lime layer and phosphate-lime layer trials, but to a lesser extent.

Elevated CO_2 concentrations were also observed in the lime layer and flyash-lime layer in CSA tailings (Figs 6.35, 6.334), whilst increased CO_2 concentrations occurred in the flyash mix and limestone mix within Peak tailings (Figs 6.45, 6.40).

The greater reactivity of the Elura tailings (pyrrhotite and siderite) has produced conditions in which elevated CO_2 concentrations can be more readily formed. This has been achieved through the development of thin cements observed at the boundaries of many of the layered trials and within the mixed surface zones.

6.5.3.4.1 Summary of CO_2 concentrations

These results are consistent with the evidence that the phosphate mix has produced a universal decrease in total porosity and that the flyash-lime layer has developed a strong water holding capacity and reduced the connectivity of some of the pores resulting in elevated degree of saturation in the lower tailings and build up of CO_2.

6.5.4 Overview of Results and Conclusions

The hardness of additives zones within each trial was initially used as a guide for cementation success, with the flyash lime mix rapidly developing cements within all trials, while the flyash lime layer also formed cements within all trials but to a lesser extent. The phosphate-lime mix and lime mix produced cements but not universally. SEM investigations showed the development of very fine-grained Al, Ca and Si cements within both the flyash and lime mix and layer trials, with larger Ca (minor Si and Al) plates and fibers developing in the cavities of the layer trials.

Permeability was investigated to determine which additives significantly reduced the inflow of water, thus inhibiting AMD generation and the transport of contaminants. Phosphate added as a surface mix was the only additive which successfully reduced permeability, which in some cases was by an order of magnitude.

Porosity investigations were undertaken to examine rates of gas diffusion into the tailings, which in turn dictates sulfide oxidation rates. Reductions in total porosity were observed in the Elura and Peak phosphate mix trials while the Elura limestone mix also produced a decrease. The air-filled porosities were also investigated which indicated that the flyash-lime layers had very high moisture holding capacities resulting in reduced air-filled porosity. Gas diffusivity was further investigated by CO_2 content within the tailings profiles, degrees of saturation and connectivity of pores. The flyash-lime layer trials showed a reduction in pore connectivity by up to 10% and produced elevated degrees of saturation in the lower tailings. Additionally significant build up of CO_2 developed below the layer. All of this evidence suggests a reduction in gas diffusivity and preservation of saturation in the underlying tailings.

The degree of saturation within the upper tailing of the flyash and lime layer trial was reduced through preferential movement of water into the additive layer, thus allowing rapid oxidation of the tailings. Similar situations were identified by low pH and positive Eh conditions in the upper tailings of the CSA lime layer and phosphate layer trials. These oxidising conditions have resulted in elevated surface solute loads within the flyash-lime layer trials and thus deem this additive style unsuitable.

The flyash-lime mix trials also produced high degrees of saturation in the underlying tailings and although total porosity remained the same through-out the experiment, the connectivity of these pores was reduced by up to 5 %. The CO_2 concentrations for this trial showed extensive accumulation for the Elura tailings with concentrations up to 70 time that observed in the control column. Unfortunately this was not achieved in all trials, with little or no accumulations observed in the Peak and CSA tailings. Additionally significant quantities of soluble surface salts were observed on the flyash lime mix and thus makes this additive type less than ideal. However, over time these salts may modify to less soluble phases and add to the cementation of the zone.

As mentioned the phosphate mix produced decreases in permeability and total porosity resulting in the build up of CO_2 below the additive zone. A four-fold increase developed within the CSA trial while the Elura trial developed a 2-fold increase compared with their controls. Additionally the degree of saturation was up to 90% within the lower tailings.

The decrease in total porosity and permeability in the phosphate trials is due to packing rather than the development of significant quantities of cements. It would appear that the cements developed within the flyash layers and mixes have developed so rapidly that during dewatering, consolidation and desiccation forces have not been able to take place. In effect, the cements have solidified the tailings mixture into a configuration which contains significant pore structure. In the case of the flyash-lime layer trial these pores have, to a certain extent, been filled and blocked by additional sulfur cements obtained from the upper tailings. This has reduced the pore connectivity by up to 10%.

The phosphate trials however have remained uncemented and have slowly re-orientated/repacked through desiccation and shearing forces. This re-packing has been enhanced in the phosphate mix, compared with the other mixtures which did not cement (limestone, lime and flyash) because of the wide grain size distribution of the additive itself. It is for these reasons that the phosphate tailings mixture is more favorable than the others investigated in this experiment, even though cementation remained undeveloped.

The use of an additive for the development of enhanced hardpans is obviously an economic decision and the use of a rock phosphate additive would only be acceptable if a local, inexpensive source was available. In the case where an immediate source is not available and economic constraints are an issue, the use of a flyash and lime surface mix may be more appropriate, especially if dust suppression is the main priority over AMD generation. At many arid locations around Australia a simple surface application is required which has the ability to store rainfall events, thus inhibiting vertical transportation of contaminants. The addition of flyash and lime mixed with tailings may serve this purpose while remaining resistant to both wind and water erosion. Further investigations of the optimum rate of addition to achieve the best conditions while considering economic prerequisites are required.

Chapter 7 : Effectiveness of Hardpan in the Reduction of AMD and Contaminant Transport

7.1 Overview of Investigations

The effectiveness of hardpans to inhibit AMD generation is dependent on reducing oxygen diffusion and water infiltration. In this Chapter, hardpan permeability and porosity have been compared with those of freshly deposited and uncemented tailings. These results have been combined with isotope and geochemical analyses to determine the physical and geochemical conditions of the laterally extensive surface hardpans at Elura and CSA Mines. These sites were selected for further investigation because of their very different tailings mineralogy (25-35% pyrrhotite and pyrite at Elura vs. 1-2% pyrite at CSA), but identical climatic conditions.

7.2 Permeability Investigations

The movement of oxygenated water through tailings is responsible for AMD generation and the dissolution and transport of contaminants. During this study, the movement of water through naturally occurring hardpans and fresh tailings has been investigated using four different techniques.

At a number of field sites, single ring infiltrometer tests were carried out in triplicate. For this test 500mm diameter steel rings were used. When tests were carried out on fresh tailings this ring was pressed 100mm into the surface, however when testing hardpan surfaces, the ring was sealed to the surface using bentonite clay. Once in place, a cloth was placed over the surface to minimise disturbance, and the ring quickly filled with water. The rate of water infiltration was measured using a calibrated scale and the permeability calculated (Method section. 1A.4.7.1 Appendix 1A). Additional field measurements were made using a Disc Permeameter. The permeameter was filled with water and placed on a sand bed to ensure total hydraulic contact and the rate of infiltration determined. Permeability was then calculated based on the tube and disk diameters (Method section 1A.4.7.2 Appendix 1A).

Two laboratory methods were also employed. Permeability of fresh tailings was measured using the oedometer apparatus previously outlined in Chapter 6 (Method section 1A.4.7.3 Appendix 1A). Permeability on hardpans was determined through shaping the samples into cylinders with radii between 10-15cm, sealing them into P.V.C tubing and measuring flow rates while maintaining a constant head of water (Method section 1A.4.7.4 Appendix 1A).

Laboratory testing of fresh tailings and hardpans were carried out on the majority of sites, however field testing was restricted to Brukunga, Broken Hill, CSA, Renison Bell and Elura tailings dams. The results of these tests are presented in Table 7.1.

TABLE 7.1 SUMMARY OF FIELD AND LABORATORY PERMEABILITY TESTING
(note the results are presented as numbers to the exponent 10^{-7} m/s)

Mine	Site	surface type	Field Infiltrometer Tests (10^{-7} m/s)			Laboratory Oedometer and PVC Tube Tests (10^{-7} m/s)				Field Disc Permeameter Tests (10^{-7} m/s) a=-0.2kPa b=-0.6kPa
			max	min	ave	max		min	ave	ave
Renison	Dam A CFT surface	uncemented	730	330	**560+/-204**	12		11		
Bell	Dam A surface (site 1 & 2)	hardpan				3.6	-	0.15	**1.5+/-1.9**	
	Dam B 7.5-8m depth	uncemented				13		13		
	Dam B surface (site 1& 2)	hardpan	12	4.3	**7.4+/-4**	1.6	-	0.12	**0.83+/-0.61**	
	Dam C surface	freshly deposited	5	3	**3.8+/-1**					
	Dam C 2-2.5m depth	uncemented				0.28		0.27		
	Dam C surface (site 1)	hardpan				31	-	5.2	**18.5+/-10**	
Elura	Dam 3	freshly deposited	33	5.9	**16+/-14.5**	0.83		0.45		**112+/-83.7 (a)**
										28.7+/-6.7 (b)
	Dam 1	Hardpan	2.9	0.52	**1.4+/-1.3**	7.5	-	1.2	**4+/-3.9**	**5.7+/-3.5 (a)**
										8.5+/-4.5 (b)
	Dam 2	Hardpan				92	-	0.28	**44+/-61**	
CSA	North Dam	freshly deposited	2.7	1.6	**2.3+/-0.6**	0.42		0.22		**4.0+/-1.1 (a)**
										2.1+/-0.4 (b)
	North Dam	hardpan	16	2.8	**8.9+/-6.9**	2.1	-	0.14	**0.92+/-1**	**25.2+/-9.7 (a)**
										13+/-2.2 (b)
	Coarse tailings	hardpan				120	-	110	**113+/-7**	
Brukunga	hole 4	uncemented				9.1		7		
	hole 4	cemented	40	24	**32+-/12**	1100	-	210	**720+/-460**	
	hole 4	grass surface	19	13	**16+/-3**					
Broken Hill	Site A/B	uncemented	110	29	**67+/-41**	8.3		7		
	Site D	freshly deposited	280	220	**250+/-34**	41		30		
	Alpine Dam- center	cemented	74	27	**50+/-23.6**					
	Alpine Dam- edge	cemented	170	64	**125+/-54.4**					
	Site C	cemented	160	45	**89+/-50**	490	-	68	**218+/-220**	
Woodcutters	General mix	uncemented				0.12		0.062		
	site 3 / site 4	hardpan				78	-	0.059	**33.4+/-47**	
Chesney	Upper Dam	uncemented	27	15	**19.6+/-6.2**	35		30		
	Upper Dam	hardpan	54	18	**33+/-19**	260	-	62	**155+/-70**	
	Lower Dam	uncemented	65	8.3	**33+/-28**					

Permeability measurements of freshly deposited tailings were taken as close as possible to the spigots and thus were taken on water saturated tailings with no desiccation crack morphology. Uncemented tailings results refer to tailings which have been exposed for a period of time, have not cemented and have in some cases desiccation crack morphologies.

Maximum and minimum results are presented for the triplicate field infiltrometer tests, together with averages and standard deviations (Table 7.1). The permeability results obtained on the uncemented tailings via oedometer tests are also presented. The maximum permeabilities correspond to the non-consolidated tailings (0 kPa), while the minimum permeabilities were achieved via a 19 kPa loading. The PVC permeability testing on hardpans took into account the varying thickness of the 2 or 3 hardpan

samples tested from each site. The maximum and minimum results presented were calculated from the minimum and maximum thickness of the samples. The average results presented in this case were calculated using the average thickness of the hardpan samples. The average and standard deviation results obtained from the triplicate field disk permeameter tests are also presented.

When comparing field infiltrometer tests with laboratory investigations, uncemented tailings oedometer tests produced permeability results consistently slower than those observed in the field. The hardpan testing showed variable results, with both field and laboratory tests producing lower permeabilities for different hardpans. A review of field infiltrometer results shows decreased permeability associated with hardpans at Elura and Broken Hill by up to an order of magnitude compared with fresh tailings. However uncemented tailings at Chesney, and fresh tailings from CSA and Renison Bell impoundments actually exhibited slower permeabilities than their associated hardpans. Infiltration measurements were also undertaken on the Renison Bell CFT (Cassiterite Flotation Tailings) surface. This surface exhibited faster infiltration rates than both the hardpans and fresh tailings (Hignett, 1997).

A comparison of permeability tests of hardpans in PVC with oedometer tests on fresh tailings showed that the fresh tailings always had lower permeabilities. In the case of the laboratory oedometer testing, samples were disturbed and re-packed. Under these conditions a number of errors may be involved including increased consolidation produced during re-packing, resulting in lower permeabilities. Additional problems with shaping the hardpans into cylinders and sealing them into the PVC tubing may have resulted in preferential flow paths. It is for these reasons that the validity of these results may be questionable.

Additional triplicate disc permeameter tests were carried out on the Elura and CSA hardpans and fresh tailings. These tests were carried out at 0.2 kPa and 0.6 kPa head settings. The 0.2 kPa setting excludes pores with diameters greater than 1.5mm diameter, whilst the 0.6 kPa excludes those greater than 0.5mm diameter. Using these methods, the hardpans at both locations exhibited permeabilities up to an order of magnitude lower than the freshly deposited tailings. A decrease in permeability was observed in measurements from the 0.2 kPa head to 0.6 kPa head within the CSA tailings and hardpans suggesting a substantial amount of water movement is in pores greater than 0.5mm diameter. The permeability results for the uncemented Elura tailings indicated a similar trend. A reduction in permeability was not observed for the 0.2 to 0.6 kPa testing of the Elura hardpan surface, which may have been due to the dissolution of the hardpan during testing. It should be noted that the permeabilities determined using the permeameter were higher than those measured using the infiltrometer (except for the CSA hardpan). The reason for this is uncertain, but is thought to be due to experimental technique and associated errors.

7.2.1 Discussion on Permeability

Studies of naturally developed hardpans in tailings (Boorman and Watson, 1976; Kennedy and Hawthorne, 1987; McSweeny and Madison, 1988 and Blowes et al. 1987 & 1991) have proposed a

decrease in permeability through the production of cements and the pore blocking associated with hardpan development. These authors have not presented data to substantiate these assertions. In a number of cases permeability testing has been carried out on the surface of dams where the hardpans have developed at depth within the tailings. The early review of hardpans at Heath Steel, Canada, reported surface permeabilities of the tailings (Boorman & Watson, 1976), while the more recent review reported permeabilities of the old and new dams which exhibited similar permeabilities but again did not present permeability data on the hardpan at depth (Blowes et al. 1988). When discussing hardpan permeability at the Sheridon and Farley impoundments, Kennedy and Hawthorn (1987) noted that the hardpan was an order of magnitude more impermeable than the other tailings but did not present any data. Additional investigations of the Sheridon and Farley impoundments, included measurement of permeability of the hardpan, which indicated the results were similar to those previously determined (McGregor and Kamineni, 1992). It was uncertain from this, whether the compared results were from cemented or uncemented tailings. A comprehensive review of previous permeability measurements in tailings dam is outlined in Chapter 1.

The results obtained during this study, along with those outlined in the literature, are not conclusive evidence that naturally formed hardpans have the ability to completely seal tailings surfaces. The permeability results presented in this section indicate that a number of the hardpans investigated have lower permeabilities than their respective fresh tailings, although this is not a universal trend. Variability is associated with a number of characteristics including:

- age of the hardpan and its degradation over time
- development of preferential flow paths during drying (desiccation cracks and shear planes)
- the highly heterogeneous nature of the tailings in general (grain size variation), and
- the methods of investigation employed.

7.3 Porosity Investigations

Movement of gas through hardpans is principally dictated by the air-filled porosity properties. Porosity investigations have been undertaken to permit gas diffusion modelling to ascertain the ability of hardpans to reduce oxygen infiltration into the underlying tailings. The ability of the hardpans to reduce gas diffusion is either by a decrease in total porosity or a persistent decrease in air-filled porosity. Investigations into transformations in pore size distribution during cementation were also undertaken. The effect these changes in pore size distribution have on water movement has been investigated through modelling the hydraulic conductivity of the tailings and hardpans over a range of water contents. These result have given further insight into the effect hardpans have on near-surface processes, especially evaporation and thus moisture saturation levels. The moisture saturation levels of the hardpans directly influence gas diffusion by restricting the air-filled porosity available for gas transport.

7.3.1 Total Porosity

The total porosity of both uncemented tailings and naturally developed hardpans or cemented layers at Chesney, CSA, Broken Hill, Woodcutters, Brukunga, Renison Bell and Elura were investigated. The range of porosity results are presented in Table 7.2. The methods utilised are outlined in Appendix 1A, method sections 1A.4.2 to 1A.4.5.

TABLE 7.2 POROSITY MEASUREMENTS FOR SELECTED HARDPANS AND FRESH TAILINGS

SITE	POROSITY OF HARDPAN/CEMENT (%)	POROSITY OF FRESH/UNCEMENTED TAILINGS (%)
Renison Bell -Dam A	36-39	
Renison Bell -Dam B	39-53	44
Renison Bell -Dam C	36-40	49
Elura - Dam 1	23-42	
Elura - Dam 2	37-50	
Elura - Dam 3		35-48
CSA - North Dam	31-40	45-46
Brukunga - Hole 4	47	36
Broken Hill - Site C	40-45	
Broken Hill - Site D		32-54
Woodcutters - Seepage Site	46-50	52-55
Chesney - Dam 1	43-46	45

A comparison of the results indicates that total porosity is highly variable at each site. The layered cements at Brukunga and Broken Hill and the hardpans at the Chesney and Elura sites have produced porosities which are similar or marginally higher than their uncemented counterparts. The CSA and Woodcutters hardpans have lower porosities than the fresh tailings, whilst the Renison Bell hardpans show variable results.

It would appear that the more coarse-grained tailings at Brukunga and Broken Hill have supported the development of cemented layers rather than surface hardpans. Weathering and oxidation by-products have concentrated along discrete non-continuous fine grained layers. This concentration and precipitation of secondary minerals has not resulted in a reduction of total porosity.

The coarse-grained tailings at Chesney have not produced cemented layers. However, due to solute inputs from seepage from the upper slopes at this site, cement has developed through-out the profile down to at least 1m depth. Even with this addition, the total porosity has not been substantially decreased. Conversely, the Woodcutters seepage hardpan has lower total porosity than the equivalent uncemented tailings. The low permeability of the fine-grained Woodcutters tailings may have reduced leaching of solutes from the surface, resulting in enhanced concentration and precipitation of secondary minerals at the surface and thus a reduction in porosity.

The total porosity investigations at the Renison Bell tailings dams suggest that a variation may occur with the ageing of the hardpans. The freshly developed hardpans at Dam C (less than 12 months old) have lower total porosities than the freshly deposited tailings. The hardpans developed at Dam B have total porosities similar to or greater than the underlying tailings, indicating a gradual degradation associated with hardpan exposure. However, total porosity of hardpans in Dam A, which is of equivalent age (16 years), did not produce similar results to substantiate this assumption. It should be noted that at this mine, rapid, continuous recycling of the hardpans has taken place through erosion, re-exposure and re-cementation processes. Thus a variety of total porosity values is to be expected.

The recycling of surface hardpans has also been observed at Elura and CSA. The results presented in Table 7.2 may simply reflect a snap shot in time and thus an indication of the age and state of degradation of the hardpan. Similar variations in total porosity were observed at the Elura dams with porosities ranging from 23-50%. The total porosities observed in the CSA hardpan is up to 15% lower than the fresh tailings however still varies between 31-40%.

7.3.2 Moisture Retention Characteristics and Pore Size Distribution

Samples of both fresh tailings and cements from Broken Hill, CSA, Elura, Woodcutters and Renison Bell were examined to determine the change in pore size distribution which occurs during the development of cements. To determine pore size distributions, moisture retention curves were constructed using the method outlined in Appendix 1A, method section 1A.4.6. The average curves for triplicate samples of both the fresh tailings and hardpans are presented in Figs 7.1 to 7.5. These results have been used to calculate the pore size distributions which are presented in Figs 7.6 to 7.10.

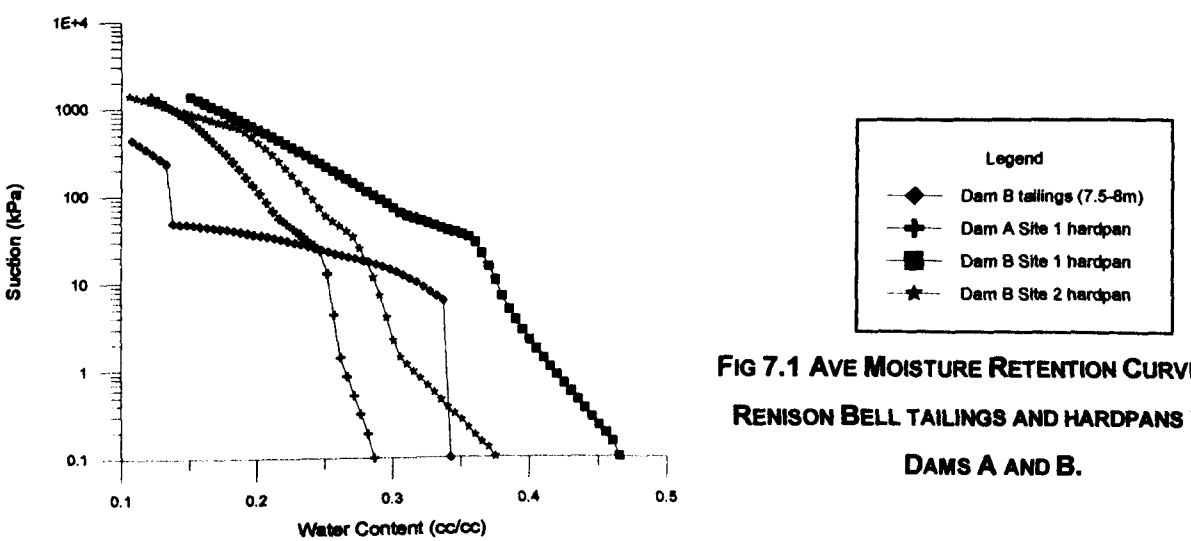

FIG 7.1 AVE MOISTURE RETENTION CURVES FOR RENISON BELL TAILINGS AND HARDPANS FROM DAMS A AND B.

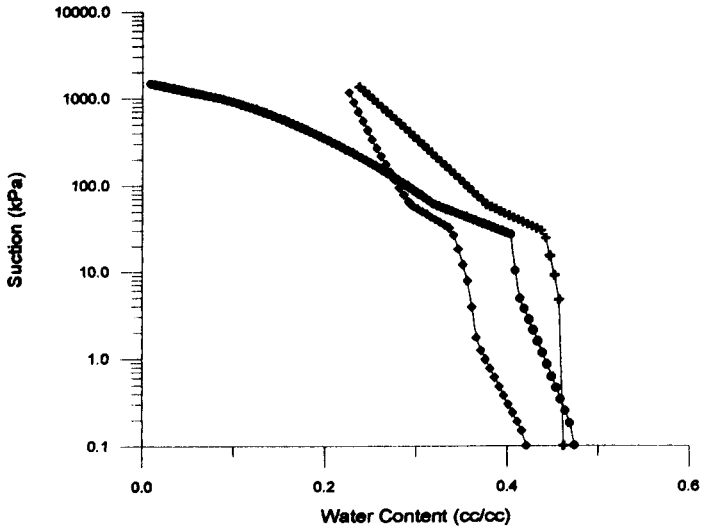

FIG 7.2 AVERAGE MOISTURE RETENTION CURVES FOR ELURA TAILINGS AND HARDPANS

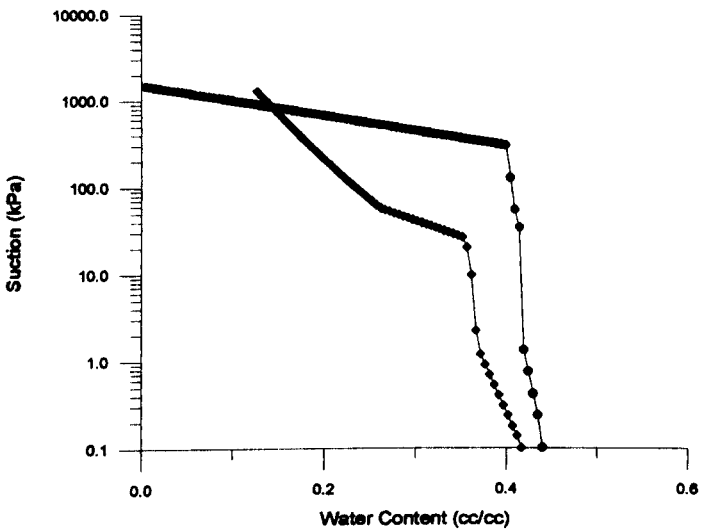

FIG 7.3 AVERAGE MOISTURE RETENTION CURVES FOR CSA TAILINGS AND HARDPANS

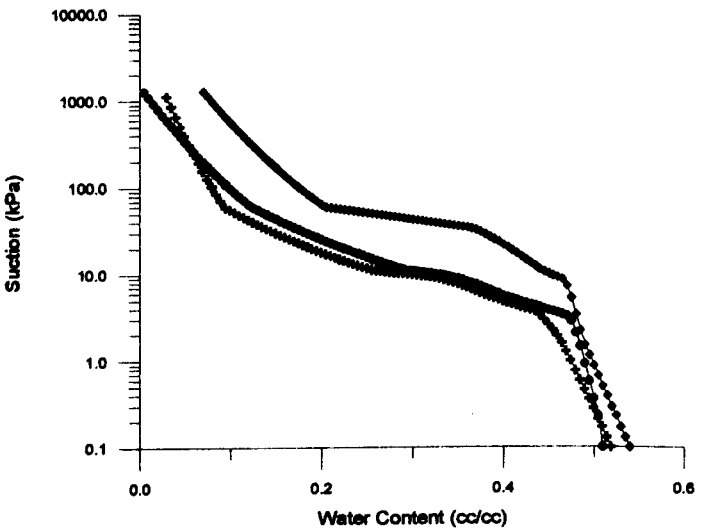

FIG 7.4 AVERAGE MOISTURE RETENTION CURVES FOR BROKEN HILL TAILINGS AND HARDPANS

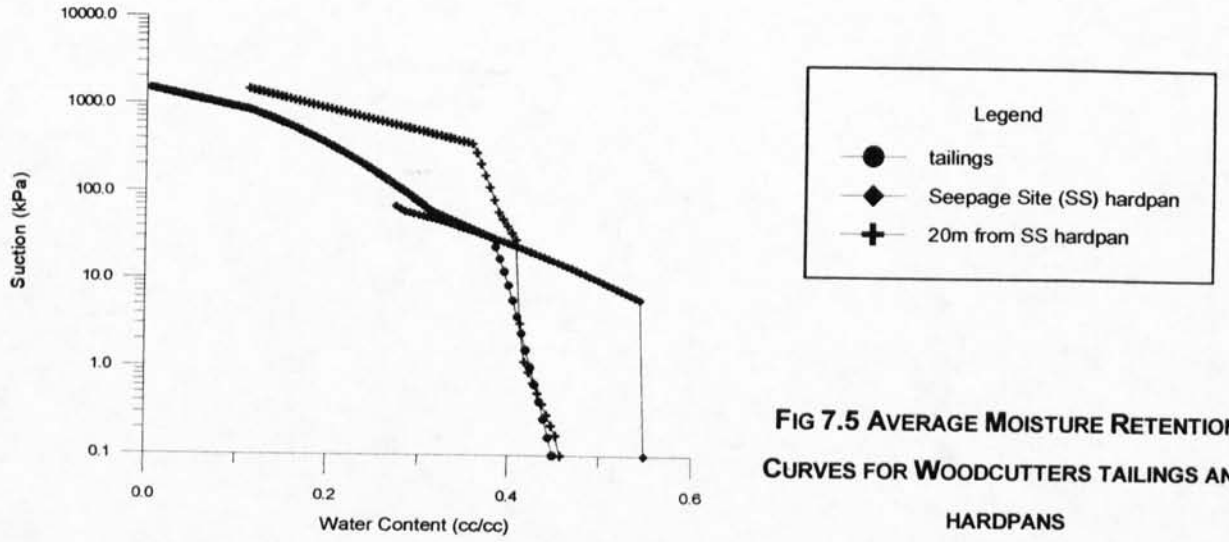

FIG 7.5 AVERAGE MOISTURE RETENTION CURVES FOR WOODCUTTERS TAILINGS AND HARDPANS

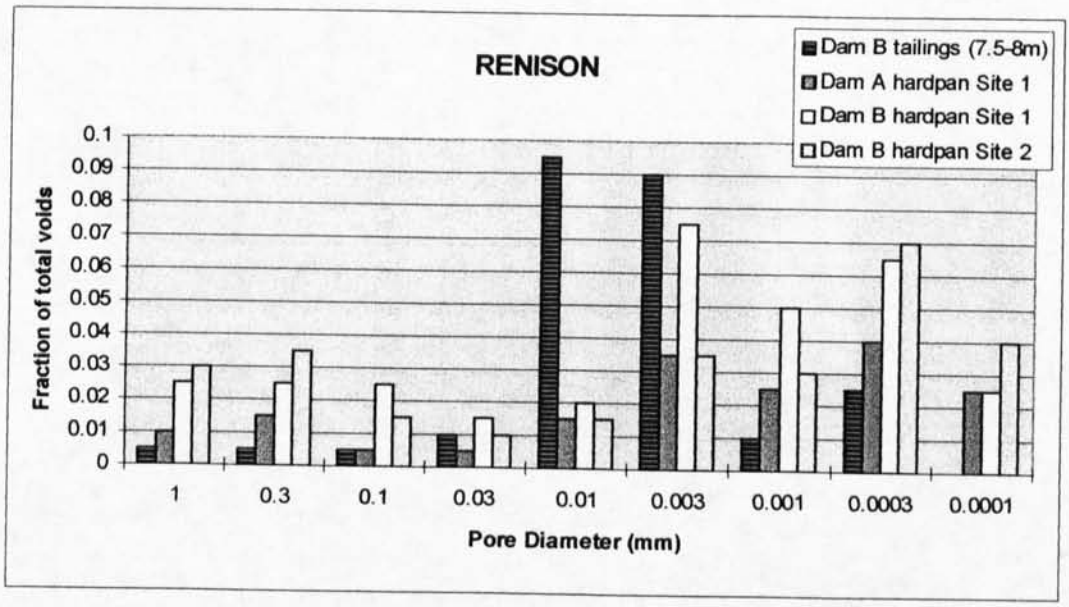

FIG 7.6 PORE SIZE DISTRIBUTION FOR RENISON BELL HARDPANS AND TAILINGS

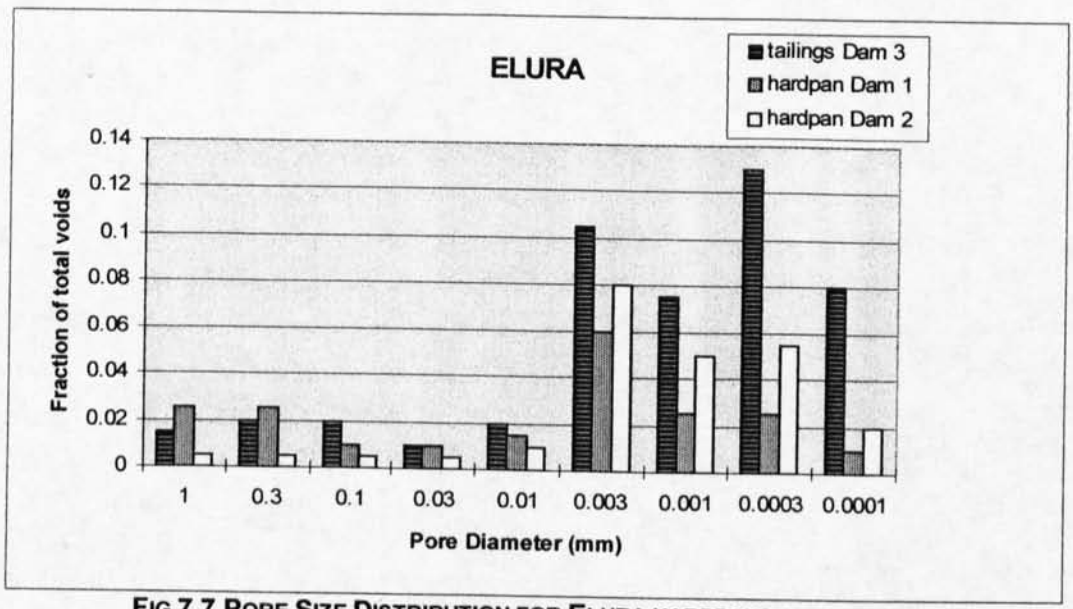

FIG 7.7 PORE SIZE DISTRIBUTION FOR ELURA HARDPANS AND TAILINGS

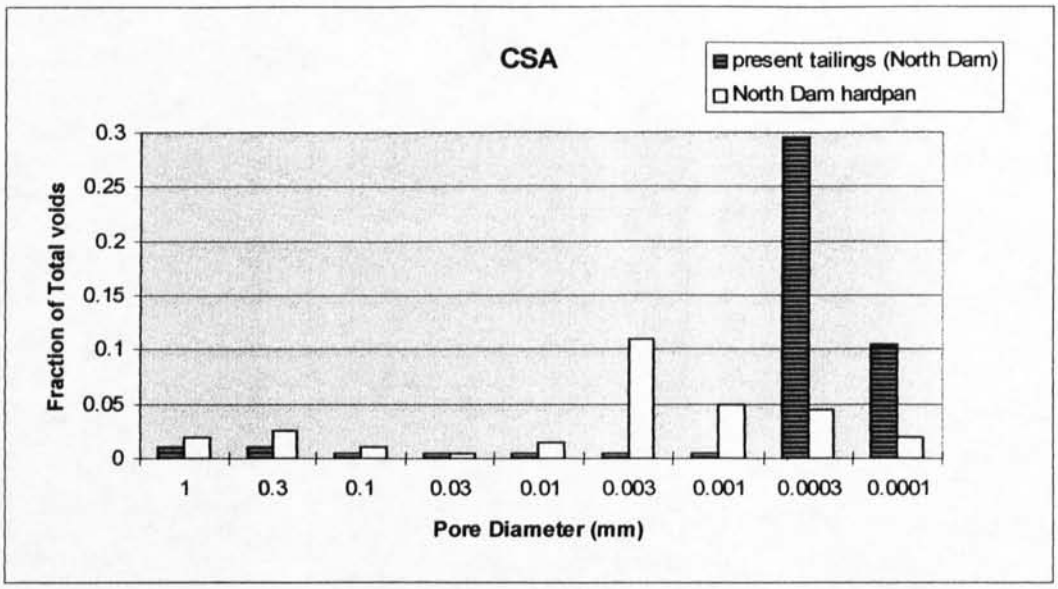

FIG 7.8 PORE SIZE DISTRIBUTION FOR CSA HARDPANS AND TAILINGS

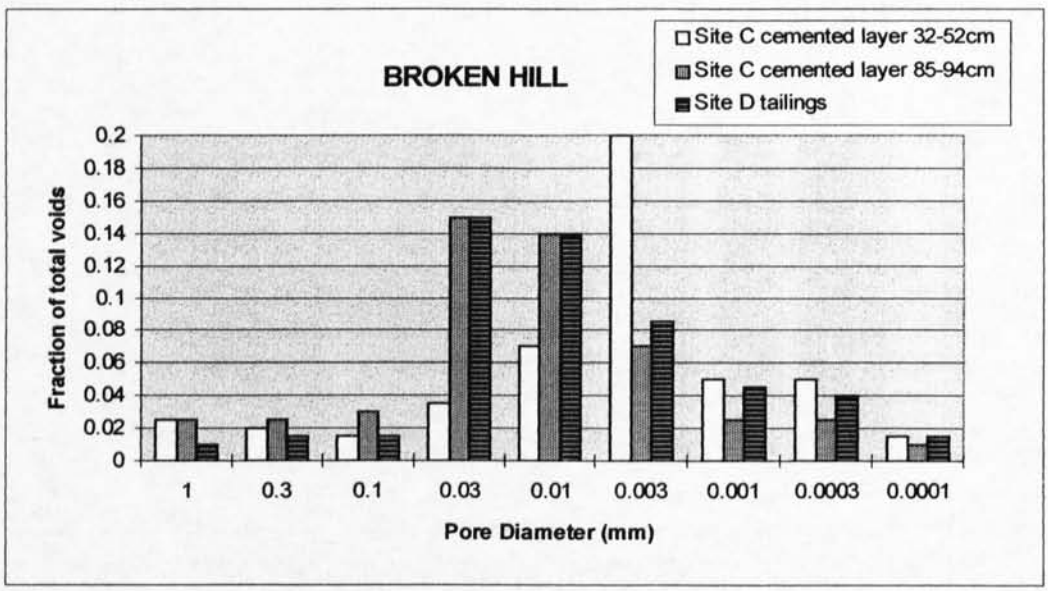

FIG 7.9 PORE SIZE DISTRIBUTION FOR BROKEN HILL HARDPANS AND TAILINGS

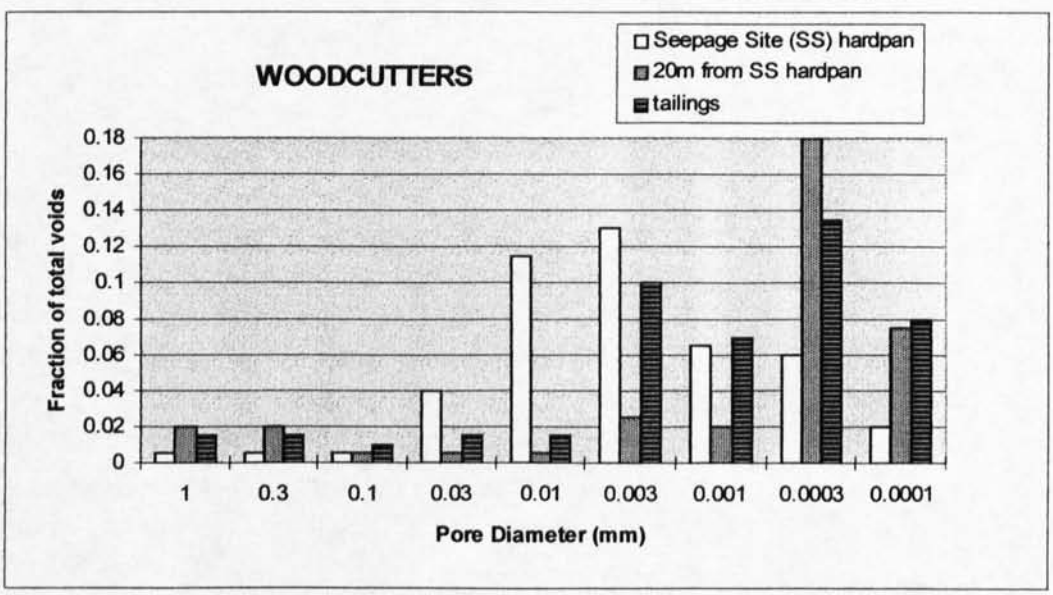

FIG 7.10 PORE SIZE DISTRIBUTION FOR WOODCUTTERS HARDPANS AND TAILINGS

7.3.2.1 Pore Size Distribution Results

Results indicate that a change in pore size distribution has taken place during the development of cements. In particular the CSA and Elura hardpans show trends that suggest the smallest pore sizes have been lost during hardpan development.

Although the Elura hardpans show reductions in the finest pore sizes, this has not been transformed into the development of larger pores. The quantities of small pores simply reduces over time with the greatest quantities in the new tailings from Dam 3 > new hardpan from Dam 2 > 8 year old hardpan from Dam 1. The greatest pore size fraction for these hardpans occur within the 0.003mm diameter range, while the largest pore fraction in fresh tailings occurs within the 0.0003mm diameter pore size (Fig 7.7).

The CSA tailings and hardpan trends are presented in Figure 7.8. At this site, a change in tailings particle size has occurred since the original deposition and hardpan development in the CSA North Dam. Thus the tailings trend does not necessarily represent the pore size distribution in the tailings prior to hardpan development. New deposition in the South and North Dams consists of tailings with the coarse sand removed for backfill with the result that the hardpan surface now has a slightly larger average pore diameter (0.0003-0.003 mm) than the fresh tailings (0.0001-0.0003mm).

The other tailings and hardpans investigated show less definite trends. The Woodcutters samples exhibit similar trends to the CSA and Elura, with the seepage site (SS) hardpan containing a greater component of the larger pore sizes compared with the tailings and the less cemented hardpan 20m away (Fig 7.10). The trends observed in the Broken Hill samples suggest that during cementation of the tailings, more fine pores have been formed (0.003mm pores), while there has been a loss of the 0.01-0.03mm size pores (Fig 7.9). The formation of smaller pores and loss of 0.01-0.03mm pores reflects the partial in-filling of larger pore spaces during cementation occurring in response to solute leaching from the surface and cement precipitation along textural boundaries.

Samples of the Brukunga cemented layers fell apart during the analysis and thus comparisons could not be made. This is evidence of the fragile nature of the cemented layers compared with the hardpan. Additionally no fresh tailings were available at the Chesney site because of the age of the deposit and thus no direct comparison could be made.

Results from a tailings sample from Renison Bell Dam B, along with 3 hardpan samples from Dams A and B are presented in Figure 7.6. Samples of tailings and hardpans from Dam C were also tested, however the results obtained were highly questionable due to large quantities of surface secondary salts produced during the 2 weeks of testing. These salts may have increased the osmotic suction associated with these samples, the result being the alteration of moisture retention properties resulting in artificially low levels of the smallest pore size investigated. It should be noted that many of the hardpan curves are

truncated (i.e. did not dry completely during testing). This is also thought to be due to elevated salt levels within the samples.

Results for the fresh tailings from Renison Dam B indicate the main fraction of pores occur within the 0.01-0.003mm range (data obtained from Jones, et. al. 1997). The hardpans developed within the Dams A and B have slightly lower pore size distribution trends, with increased pore content within the 0.0001-0.003 range. Thus at this site a the reduction in the 0.01-0.003mm pores has occurred and hardpans with generally smaller pore sizes have developed.

7.3.2.2 Relationship of Pore Size Distribution, Mineralogy and Grain size

The variations observed in the pore size distribution and the final hardpan and cemented layer morphology depends strongly on the initial grain size distribution of the tailings and the mineralogical contributions in each grain size.

Broken Hill and Brukunga tailings have a wide grain size distribution resulting in highly heterogeneous sedimentation within the tailings profile. Minor pyrrhotite and pyrite occurs within the silt fraction of the Broken Hill tailings while calcite occurs within the fine and coarse sand fractions. Oxidation of the silt size pyrite would result in acid generation and the loss of small pores at the surface. Acid attack on the coarse grained calcite would also result in the development of larger pores. Thus the pore structure at the surface of the tailings becomes larger over time. However, cementation within these dams does not take place directly at the surface but rather occurs at depth along particular layers. Weathering and oxidation by-products are leached down the profile and precipitation is induced by textural boundaries produced during tailings deposition. At these locations large pores overlying small pores are partially or totally infilled by cements. Figure 7.11 presents a schematic drawing of this process, (A) representing the initial pore size distribution, and (B) representing the infilling by cements and the final pore size distribution. The infilling by cements has resulted in the loss of the 0.01-0.03mm pore fraction, produced more fine pores (0.003mm) through partial infilling and has reduced the water permeability characteristics. EMG's 4.5 and 4.6 (Chapter 4) show similar cement development occurring in the Brukunga tailings.

The laterally extensive surface hardpans at CSA, Elura and Renison Bell have developed through very different processes of insitu formation. On exposure to oxygen and water, sulfide oxidation, acid generation and gangue mineral degradation occurs. The greater surface area of the smaller grains promotes their preferential consumption in these reactions. Much of the by-products developed remain at the tailings dam surface and coat the larger residual grains with secondary minerals. The limited rainfall and low tailings permeability at CSA and Elura sites ensure that very limited leaching of surface by-product occurs (Chapter 5).

The original CSA tailings consisted of a wide range of grain sizes in which quartz, clinochlore, muscovite and pyrite occurred in all fractions. Sphalerite and chalcopyrite were identified sporadically throughout

these fractions. Calcite was observed in both the silt and fine sand fractions. Once the tailings are exposed to oxygen and water the finest grained pyrite preferentially oxidises producing acid and decreasing the quantities of fine pores. The resultant acid would then preferentially attack the carbonates and result in the loss of the silt and fine sand sized calcite increasing the quantities of large pores. This has resulted in a shift in pore size distribution from small to larger pore structures. Figure 7.12 presents a schematic drawing of this process, where the fine pores are lost and larger pores created. Figure 7.12 (A) represents the initial pore size distribution, whilst (B) represents the infilling by cements and the final pore size distribution. This transformation may be responsible for the increased permeability observed in some hardpans compared with fresh tailings. This transformation can be seen in EMG 4.25 and 4.26 (Chapter 4) where multiple layers of secondary mineral coatings encapsulate the primary minerals.

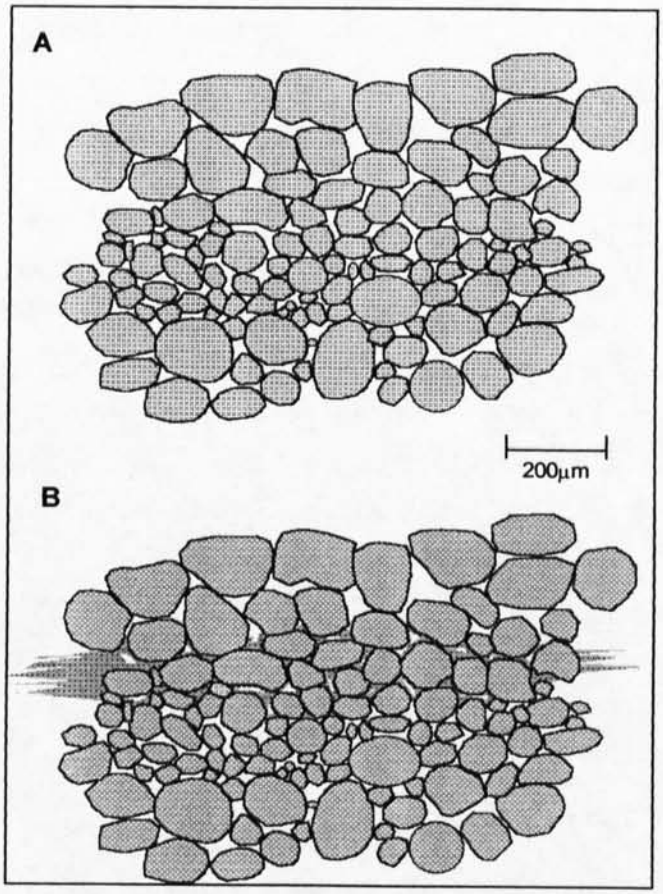

FIG 7.11 DEVELOPMENT OF CEMENTED LAYERS WITHIN BRUKUNGA AND BROKEN HILL TAILINGS, AND ITS EFFECT ON PORE SIZE DISTRIBUTION
A- INITIAL PORE SIZE DISTRIBUTION
B- PORE SIZE DISTRIBUTION DEVELOPED DURING CEMENTATION

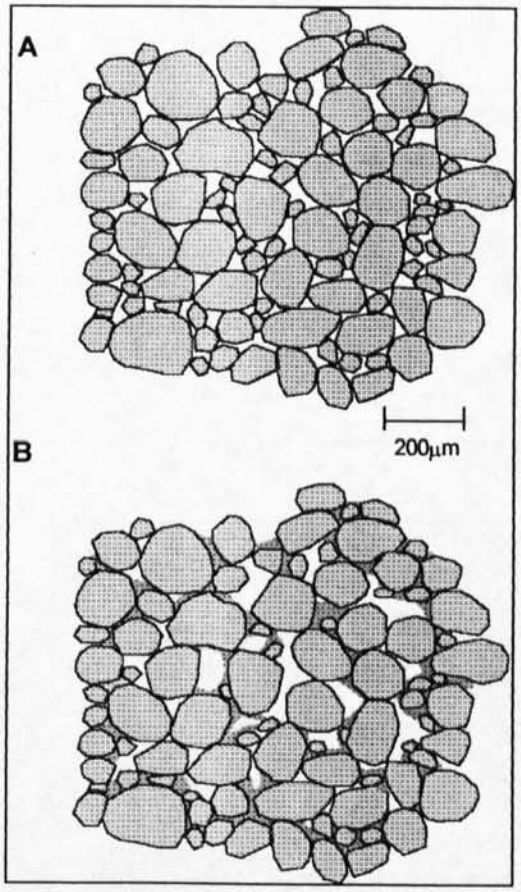

FIG 7.12 DEVELOPMENT OF SURFACE HARDPANS WITHIN CSA TAILINGS, AND ITS EFFECT ON PORE SIZE DISTRIBUTION
A- INITIAL PORE SIZE DISTRIBUTION
B- PORE SIZE DISTRIBUTION DEVELOPED DURING CEMENTATION

The Elura tailings are originally ground to less than 100μm, thus have no coarse sand fraction and generally small pore sizes. Hardpan development has resulted in the loss of the small pores. Sulfides and siderite occur in all grain sizes. The large surface area of the clay and silt sized grains would result in their preferential oxidation and dissolution. In this case pyrite oxidation supplies the acid to attack the

siderite, while the pyrrhotite simply oxidises. The loss of the smallest grains has not resulted in the development of larger pores due to the infilling of pores by secondary minerals with lower particle densities.

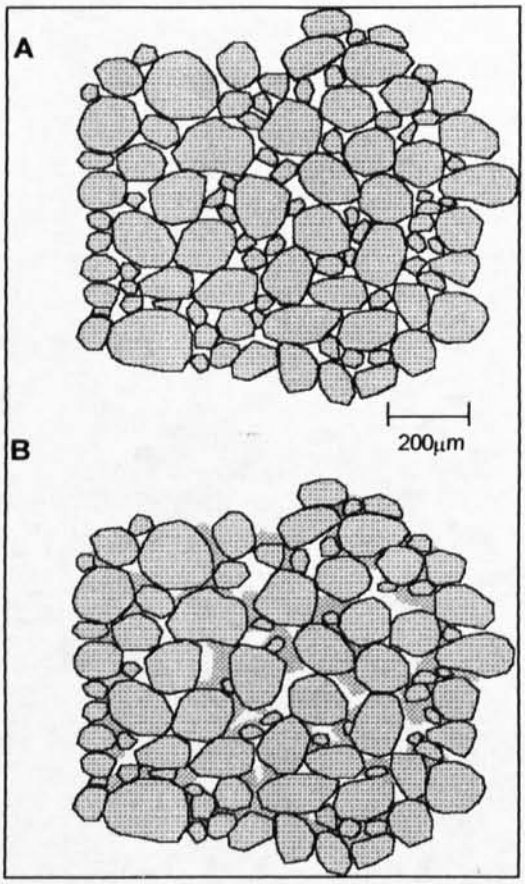

FIG 7.13 DEVELOPMENT OF SURFACE HARDPANS WITHIN ELURA TAILINGS, AND ITS EFFECT ON PORE SIZE DISTRIBUTION
A- INITIAL PORE SIZE DISTRIBUTION
B- PORE SIZE DISTRIBUTION DEVELOPED DURING CEMENTATION

The rainfall quantities and low tailings permeability characteristics ensure that there is very limited vertical solute transport within the Elura tailings (Chapter 5). If it is assumed therefore that the mass of the tailings remains the same, the loss of the porosity must occur in response to an increase in volume during secondary mineral precipitation. Only very minimal changes in the overall particle density (ρ_p) were observed during this transformation due to the small quantities of sulfide (ρ_p 4.7-5 g/cm^3) loss and Fe sulfate (ρ_p 2-3 g/cm^3) development. At this site, both sulfides and carbonates still remain in the hardpan due to the high reactivity of the pyrrhotite and the rapid encapsulation of both sulfides and gangue mineral which occurs. Figure 7.13 presents a schematic drawing of this process, where the fine pores are lost. Figure 7.13 (A) represents the initial pore size distribution, and (B) represents the infilling by secondary minerals with lower particle densities and thus greater volumes per unit mass and the final pore size distribution which results. This transformation may be responsible for the decreased permeability observed in some hardpans compared to fresh tailings.

The changes observed in pore size distribution at each site are different due to the original grain size distribution and the mineralogy of the various grain fractions. These transformations are complicated by the changes which take place as the hardpans degrade over time. As hardpans are exposed preferential removal of the more reactive and soluble minerals can result in the development of larger pores. EMG 4.12 (Chapter 4) shows the initial development of a surface hardpan at Elura. The cements coat much of the sulfide and gangue minerals. Over time the pores become larger as more of the fine primary grains react and soluble salts are dissolved or re-precipitated as more insoluble cements (EMG 4.17). These transformation are observed in all laterally extensive surface hardpans. Degradation over time of cemented layers was not observed.

7.4 Relative Hydraulic Conductivity Modelling

The effect these changes in pore size distribution have on water movement has been investigated through modelling the hydraulic conductivity of the tailings and hardpans over a range of water contents. A computer package - 'Advanced Moisture Retention Analysis' was used for this modelling (C. Hignett., pers. comm. 1998). The moisture retention data (Figs 7.1 to 7.5) from each of the representative samples were used to calculate the relative hydraulic conductivity of the materials, using the method of Jackson (1972). Results are presented in Figures 7.14 to 7.18.

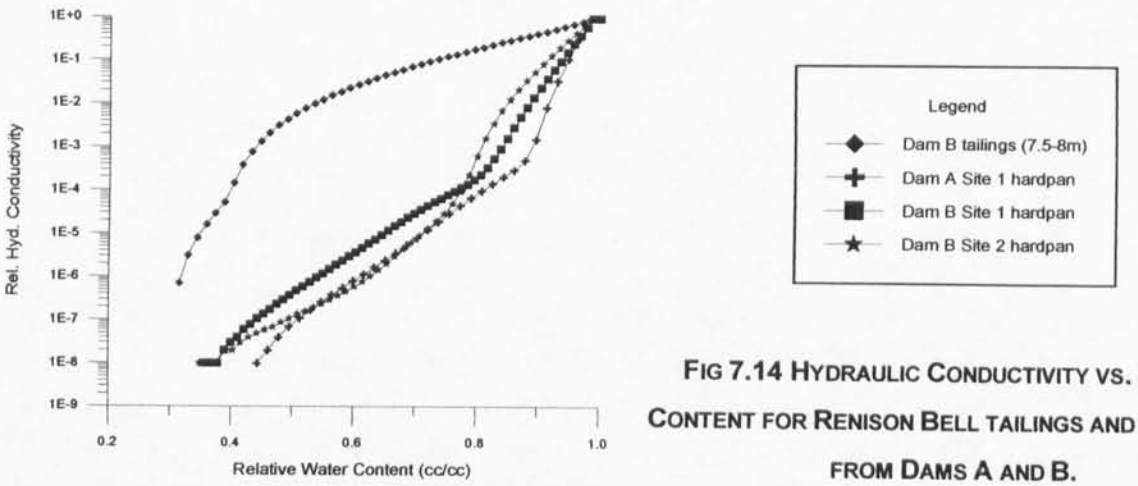

FIG 7.14 HYDRAULIC CONDUCTIVITY VS. WATER CONTENT FOR RENISON BELL TAILINGS AND HARDPANS FROM DAMS A AND B.

The Renison Bell tailings and hardpans have produced very different results, especially those of the older hardpans in Dams A and B. Here, for a reduction in relative water content from 1 to 0.9 cc/cc, the relative hydraulic conductivity of the hardpans is reduced by 3 to 4 orders of magnitude (Fig 7.14) whereas, the same change in water content of the tailings has only a very minor effect on the hydraulic conductivity. Thus, flow to the evaporating surface of the tailings would continue for a longer period at a rate close to that of the saturated hydraulic conductivity rate.

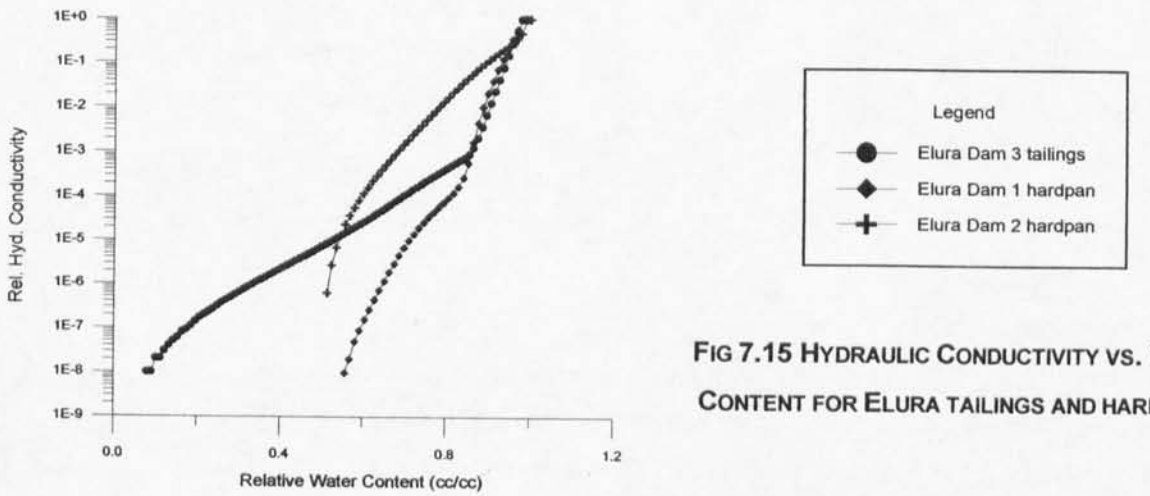

FIG 7.15 HYDRAULIC CONDUCTIVITY VS. WATER CONTENT FOR ELURA TAILINGS AND HARDPANS.

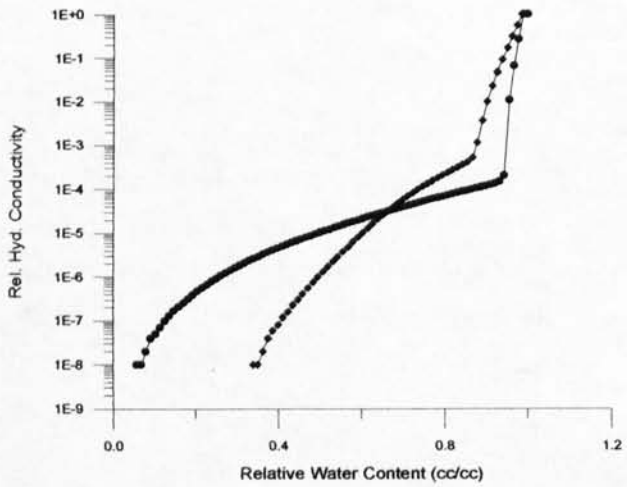

FIG 7.16 HYDRAULIC CONDUCTIVITY VS. WATER CONTENT FOR CSA TAILINGS AND HARDPANS.

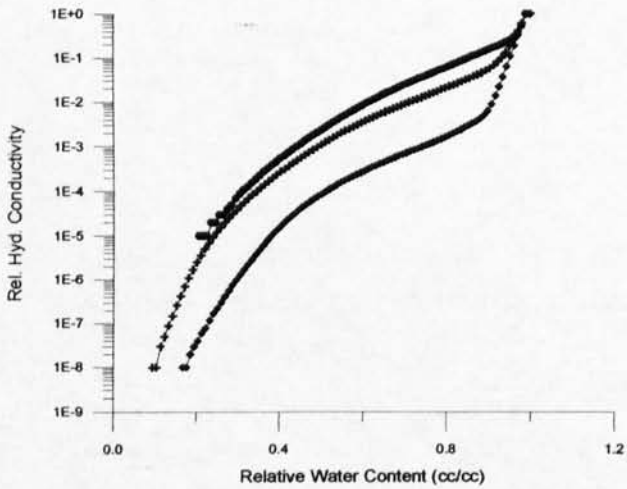

FIG 7.17 HYDRAULIC CONDUCTIVITY VS. WATER CONTENT FOR BROKEN HILL TAILINGS AND HARDPANS.

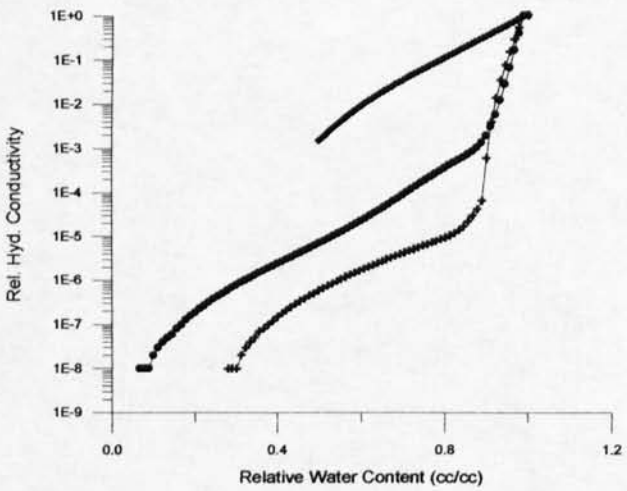

FIG 7.18 HYDRAULIC CONDUCTIVITY VS. WATER CONTENT FOR WOODCUTTERS TAILINGS AND HARDPANS.

Figures 7.15 (Elura), 7.16 (CSA) and 7.18 (Woodcutters) show, that for a relatively small reduction in water content below saturation (e.g. 1.0 to 0.9 cc/cc) the hydraulic conductivities of both tailings and hardpans are reduced by 3 to 4 orders of magnitude. Thus for both hardpans and fresh tailings alike, this

may be sufficient to effectively stop evaporation as soon as a relatively thin surface layer starts to dry. This trend is also present in the Broken Hill cemented layer at 32-35cm depth however the reduction in relative hydraulic conductivity is only 1 to 2 orders of magnitude (Fig 7.17). The 85-94cm depth cemented layer shows only a marginal reduction in relative hydraulic conductivity compared with the fresh tailings. Therefore the cements developed within all tailings (except Renison Bell) have not sufficiently altered the pore size distribution and thus have lesser effect on the surface hydraulic conductivity.

7.5 Extent of Evaporation

The relative hydraulic conductivities of the tailings and hardpans were further investigated with samples from the Elura and CSA sites. Chloride and deuterium concentrations were measured to determine the extent of infiltration into and evaporation from the hardpan surface (Barnes and Allison, 1983). A single profile was sampled in the CSA North dam through a 13 year old profile (Site 2, Fig 4.6) and two cores were removed from the Elura site for comparison, one aged (8 years - Site 10, Fig 4.5), the other fresh (1-2 months - Site 11, Fig 4.5).

In all cases Cl concentrations increase at the surface indicating evaporation is the dominant mechanism of water loss. These profiles also suggest that there is no active evaporation from the water table (1-1.5m depth), and that evaporation is only occurring at very shallow depths in the profile (<20cm) (Figs 7.19 to 7.21, Table 7.3). Comparisons of the Elura old and new tailings profiles were complicated by the recycling of mill water resulting in elevated Cl levels in the new tailings compared with the old. It is for this same reason that the Elura tailings have substantially higher Cl levels than the CSA tailings. Calculations using Cl concentrations suggest that it may only take months to attain the elevated surface Cl concentrations indicating present evaporation through the hardpan is very low. Present evaporation from the hardpan is thought to be of rainfall input only and not accessing residual process waters further down the profile.

Deuterium (δD‰) analyses suggest similar depths of evaporation, as shown by generally more positive signatures in the surface region developed through enrichment (Fig 7.19 & 7.20). The marked decrease (flip) of δD‰ at the surface is assumed to be caused by exchange with atmospheric water vapor. The position of the maximum δD‰ value indicates the depth in the profile to which liquid movement is taking place and thus is the depth to which evaporation is occurring (Barnes and Allison, 1983) (Figs 7.19 to 7.21, Table 7.3). The depth at which the Cl concentration begins to substantially increase corresponds with this flip in δD‰ signature. Thus both the Cl and deuterium results support the hypothesis that after a small reduction in water content below saturation, evaporation from both the tailings and hardpan surfaces is restricted and indicates that hardpan development has not significantly altered the surface evaporation processes at these sites. The development of salts on both these surfaces may also result in the reduction of evaporation (Emerson, et. al. 1994).

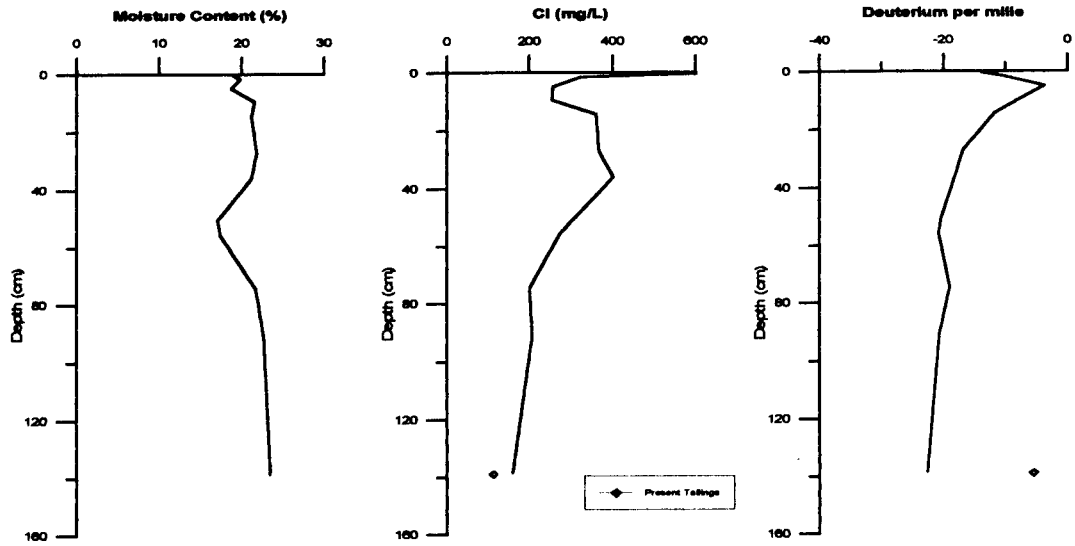

FIG 7.19 CL AND DEUTERIUM (δD‰) FOR CSA TAILINGS PROFILE WITH HARDPAN SURFACE (NORTH DAM - SITE 2)

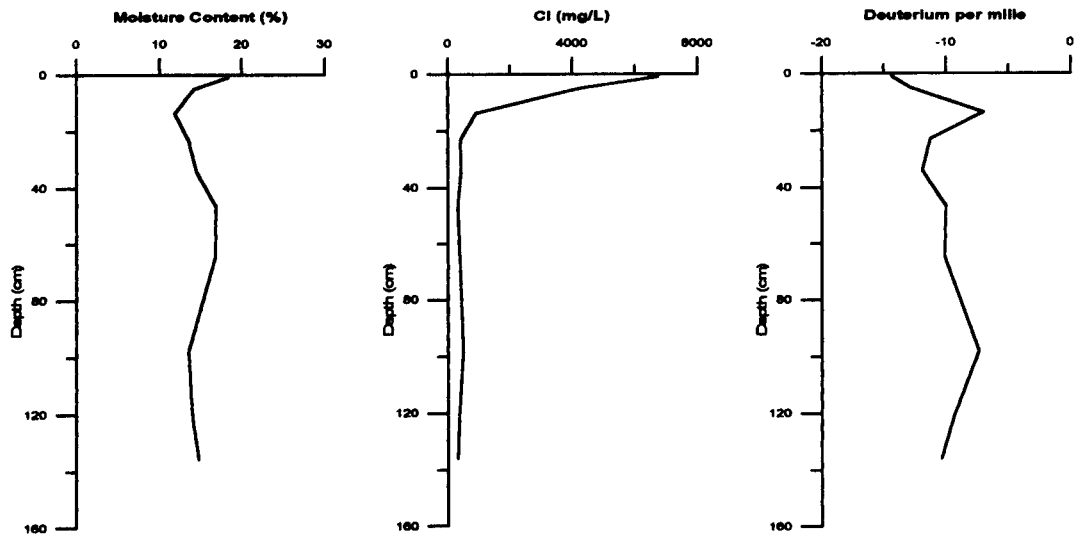

FIG 7.20 CL AND DEUTERIUM (δD‰) FOR ELURA TAILINGS PROFILE WITH HARDPAN SURFACE (SITE 10)

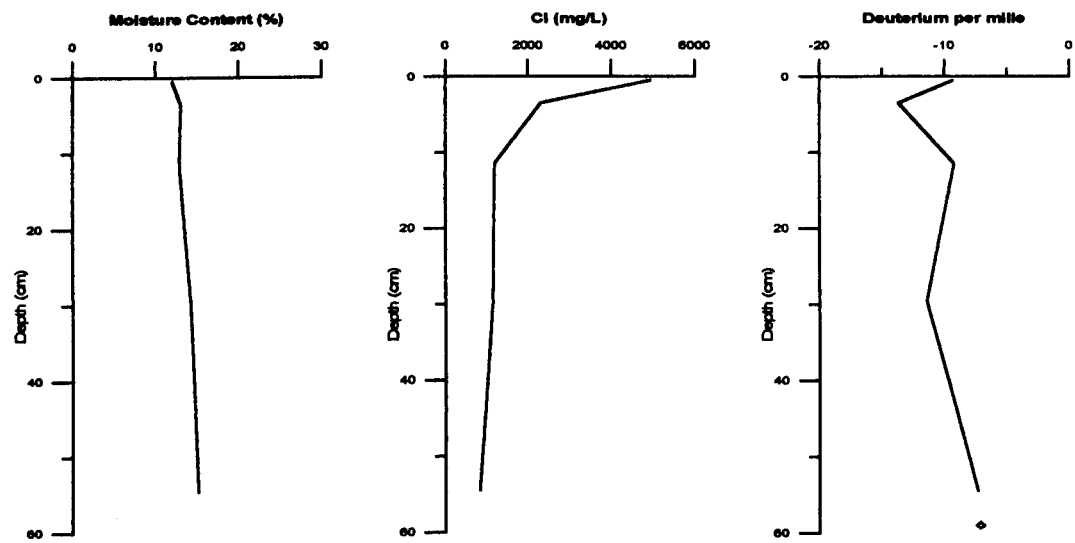

FIG 7.21 CL AND DEUTERIUM (δD‰) FOR ELURA TAILINGS PROFILE WITH FRESH TAILINGS (SITE 11)

TABLE 7.3 MOISTURE CONTENT, DEUTERIUM (δD‰) AND CL RESULTS FOR CSA AND ELURA PROFILES (sampled Jan 1997)

Name	depth (cm)	Moisture (%)	Cl (mg/L)	Deuterium per mille V-SMOW
CSA North Dam (hardpan surface)				
0–1	0.5	18.97	601.23	-13.8
1–3	1.5	19.87	323.06	-10.5
3–7	5.0	18.74	255.75	-3.7
7–12	9.5	21.58	254.50	-7.7
12–17	14.5	21.23	361.81	-11.8
25–29	27.0	21.86	367.38	-16.9
32–40	36.0	21.19	401.65	-18.2
48–53	50.5	17.08	307.24	-20.4
53–58	55.5	17.44	273.67	-20.8
70–79	74.5	21.73	200.22	-19
89–93	91.0	22.75	207.40	-20.7
135–142	138.5	23.54	159.72	-22.6
present tails		50.98	112.82	-5.5
Elura Site 10 (hardpan surface)				
0–2	1.0	18.34	6732.75	-14.4
2–8	5.0	14.10	4192.68	-12.8
10–17	13.5	11.86	888.71	-7
17–29	23.0	13.52	384.89	-11.3
29–39	34.0	14.40	414.61	-11.9
3–54	46.5	16.80	314.25	-10
54–75	64.5	16.76	370.28	-10.1
94–102	98.0	13.52	466.50	-7.4
115–127	121.0	13.99	352.46	-9.4
127–139	136.0	14.76	309.15	-10.4
Elura Site 11 (fresh tailings)				
0–1	0.5	12.02	4933.944	-9.3
2–5	3.5	13.03	2312.67	-13.7
8–15	11.5	12.91	1183.31	-9.2
24–35	29.5	14.23	1138.12	-11.4
42–67	54.5	15.23	816.83	-7.3
present water				-7.1

7.6 Gas Diffusion

7.6.1 Gas Diffusion Modelling

Gas diffusion modelling has been undertaken to investigate the ability of hardpans to reduce O_2 infiltration into the underlying tailings. The ability of the hardpans to reduce gas diffusion is either by a decrease in total porosity or a persistent decrease in air-filled porosity. Marshall, 1959, Penman, 1940 and Taylor, 1949, investigated the way in which diffusion of gases decreases with decreasing airfilled porosity (as caused by increasing water content). It was determined that once airfilled porosity dropped below 10%, diffusion was greatly restricted.

As previously mentioned the total porosity of the CSA hardpan is less than that of the tailings, whereas the Elura hardpan shows a slight increase in total porosity compared with the fresh tailings (Table 7.2). Determination of the air-filled porosity was achieved through sampling a single profile through the 13

year old hardpan at CSA and two profiles through the 8 year old hardpan at Elura. These were analysed for moisture content, bulk density and particle density to determine the total and air-filled porosity of the hardpans and tailings (Figs 7.22 to 7.24 and Table 7.4). The Elura profiles show greater air-filled porosity at the surface than at depth suggesting more rapid drying compared with the CSA profiles which have maintained lower levels of air-filled porosity at the surface.

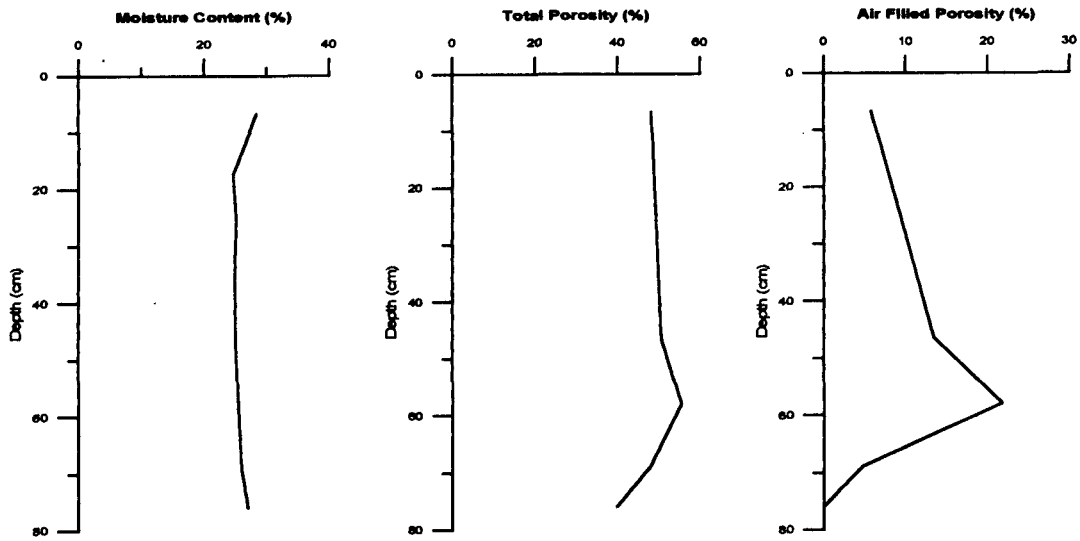

FIG 7.22 MOISTURE CONTENT, TOTAL POROSITY AND AIR FILLED POROSITY FOR CSA TAILINGS PROFILE WITH HARDPAN SURFACE (NORTH DAM - SITE 2)

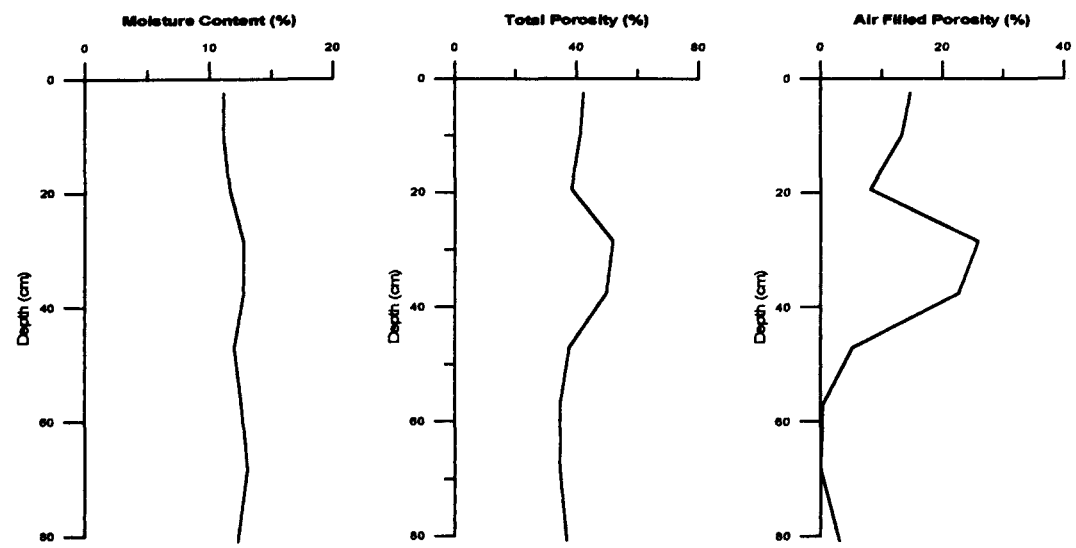

FIG 7.23 MOISTURE CONTENT, TOTAL POROSITY AND AIR FILLED POROSITY FOR ELURA TAILINGS PROFILE WITH HARDPAN SURFACE (SITE 10A)

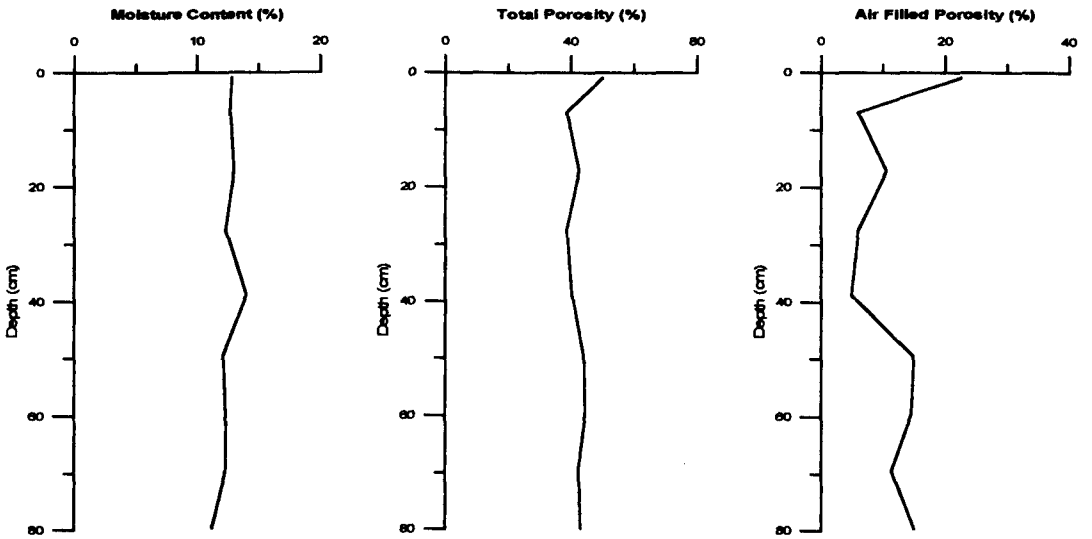

FIG 7.24 MOISTURE CONTENT, TOTAL POROSITY AND AIR FILLED POROSITY FOR ELURA TAILINGS PROFILE WITH HARDPAN SURFACE (SITE 10B)

TABLE 7.4 POROSITY AND ASSOCIATED MEASUREMENTS FOR CSA AND ELURA TAILINGS PROFILES (sampled July 1997)

Depth (cm)	Moisture Content (%)	Wet Bulk Density (g/cm^3)	Dry Bulk Density (g/cm^3)	Particle Density (g/cm^3)	Solid %	Void %	Water %	Void Ratio	Porosity (%)	Degree of Saturation (%)	Water filled Porosity (%)	Air filled porosity (%)
CSA North Dam Site 2 (hardpan surface)												
7	28.4	1.92	1.50	2.89	51.7	48.3	42.4	0.93	48.3	87.9	42.4	5.8
17	24.6											
25	25.2											
35	25.0											
46	25.1	1.85	1.48	3.00	49.4	50.6	37.2	1.02	50.6	73.5	37.2	13.4
58	25.4	1.67	1.33	2.99	44.5	55.5	33.8	1.25	55.5	60.9	33.8	21.7
69	26.0	2.09	1.66	3.19	52.1	47.9	43.2	0.92	47.9	90.2	43.2	4.7
Elura (site 10A - hardpan surface)												
3	11.2	2.75	2.47	4.28	57.7	42.3	27.6	0.73	42.3	65.2	27.6	14.7
10	11.2	2.79	2.51	4.28	58.7	41.3	28.0	0.70	41.3	67.8	28.0	13.3
20	11.7	2.89	2.58	4.19	61.7	38.3	30.2	0.62	38.3	78.8	30.2	8.1
29	12.8	2.31	2.05	4.27	48.0	52.0	26.2	1.08	52.0	50.3	26.2	25.9
38	12.8	2.41	2.13	4.25	50.2	49.8	27.2	0.99	49.8	54.7	27.2	22.6
47	12.1	3.01	2.69	4.33	62.4	37.6	32.4	0.60	37.6	86.2	32.4	5.2
57	12.6	3.04	2.70	4.30	65.5	34.5	34.1	0.53	34.5	98.8	34.1	0.4
68	13.1	3.07	2.71	4.13	65.7	34.3	35.5	0.52	34.3	103.5	35.5	0.0
81	12.4	3.07	2.73	4.32	63.2	36.8	33.7	0.58	36.8	91.7	33.7	3.1
Elura (site 10B - hardpan surface)												
1	12.8	2.41	2.14	4.27	50.0	50.0	27.4	1.00	50.0	54.9	27.4	22.5
7	12.7	2.89	2.56	4.17	61.4	38.6	32.6	0.63	38.6	84.5	32.6	6.0
17	13.1	2.77	2.45	4.26	57.4	42.6	32.0	0.74	42.6	75.1	32.0	10.6
28	12.4	2.96	2.64	4.30	61.3	38.7	32.7	0.63	38.7	84.5	32.7	6.0
39	14.1	2.87	2.52	4.22	59.6	40.4	35.4	0.68	40.4	87.6	35.4	5.0
50	12.2	2.68	2.39	4.28	55.9	44.1	29.1	0.79	44.1	66.1	29.1	14.9
60	12.4	2.72	2.42	4.37	55.4	44.6	29.9	0.80	44.6	67.2	29.9	14.6
70	12.3	2.82	2.51	4.36	57.6	42.4	31.0	0.74	42.4	73.2	31.0	11.4
80	11.3	2.76	2.48	4.36	56.9	43.1	28.0	0.76	43.1	64.9	28.0	15.1

Oxygen diffusion coefficients (D_{O2}) have been estimated using the Reardon & Moddle (1985) method, based on both total and air-filled porosity of the hardpan and total porosity of the tailings:

$$D_{O2} = 3.98x10\text{-}5[(\varepsilon\text{-}0.05)/0.95]^{1.7}\ T^{3/2}$$

where ε is the porosity and T is Temperature (Kelvin). Two comparisons have been made. Comparisons based on total porosity of the hardpans and tailings from samples collected in 1996 are presented in Table 7.5A. Table 7.5B compares diffusion results based on total and air-filled porosity of hardpans collected in 1997.

TABLE 7.5 OXYGEN DIFFUSION COEFFICIENTS, SULFIDE OXIDATION DEPTHS AND TOTAL TIMES FOR OXIDATION OF VADOSE ZONES FOR ELURA AND CSA TAILINGS IMPOUNDMENTS

A - Davis and Ritchie modelling comparisons for hardpans and tailings based on Reardon and Moddle diffusion calculations from total porosity measurements (sampled Aug 1996)

Total P H/P (%)	Total P T (%)	D O_2 H/P (m^2/s)	D O_2 T (m^2/s)	Sulfide (%)	Time of exposure (yr)	Depth to water table	t(d) yr H/P max	t(d) yr H/P min	t(d) yr T max	t(d) yr T min	X(t) m H/P min	X(t) m H/P max	X(t) m T min	X(t) m T max	Actual depth of ox (m)
CSA North Dam Site 1 hardpan (average total porosity) vs. freshly deposited tailing															
0.34	0.46	2.50E-06	4.33E-06	0.017	13	1.5	6.6	4.7	2.92	2.88	3	3.5	4.48	4.51	0.2-0.4
Elura Dam 1 Site 1 hardpan (average total porosity) vs. freshly deposited tailing															
0.40	0.37	3.33E-06	2.86E-06	0.3	8.5	1.5	120	80	140	80	0.57	0.7	0.5	0.7	0.03-0.07

B -Davis and Ritchie modelling comparisons for hardpans based on Reardon and Moddle diffusion calculations from air-filled and total porosity measurements (sampled July 1997)

Air filled P H/P (%)	Total P H/P (%)	D O_2 H/P air filled (m^2/s)	D O_2 H/P total (m^2/s)	Sulfide (%)	Time of exposure (yr)	Depth to water table	t(d) yr H/P air-filled max	t(d) yr H/P air-filled min	t(d) yr H/P total max	t(d) yr H/P total min	X(t) m H/P air-filled min	X(t) m H/P air-filled max	X(t) m H/P total min	X(t) m H/P total max	Actual depth of ox (m)
CSA North Dam Site 2 hardpan (single profile)															
0.06	0.48	5.72E-09	4.85E-06	0.017	13	1.5	2890	2070	3.4	2.4	0.14	0.17	4.14	4.90	0.2-0.4
Elura Dam 1 Site 10 hardpan (single profile)															
0.15	0.42	3.82E-07	3.76E-06	0.3	8.5	1.5	1020	680	100	70	0.19	0.24	0.61	0.74	0.03-0.07

where H/P - hardpan
T - tailings
P - porosity
t(d) - time to fully oxidise the vadose zone
X(t) - position of planar moving oxidation front

Table 7.5A shows that the D_{O2} based on the total porosity of the tailings at the CSA mine is faster than the D_{O2} for the hardpans. The reverse if true for the Elura samples as the hardpans removed from Dam 1 have slightly higher total porosities than the freshly deposited tailings. The results presented in Table 7.5B indicate that the D_{O2} of the Elura hardpans at the time of sampling was $3.82x10^{-7}$ m^2/s which increases to a maximum of $3.76x10^{-6}$ m^2/s for a completely dried surface. Similarly this would reduce to almost zero under saturation conditions immediately after a rainfall event. For the CSA hardpans, D_{O2} at the time of sampling was $5.72x10^{-9}$ m^2/s which increased to $4.85x10^{-6}$ m^2/s based on total porosity calculations. A direct comparison of D_{O2} of the fresh tailings and the hardpan based on air-filled porosities is unrealistic as the D_{O2} of the fresh tailings is dictated by the moisture content which is simply a function of the period of exposure to the atmosphere.

To assess which D_{O2} is realistic as an average yearly value, the Davis and Ritchie (1986) conceptual model of sulfide oxidation reactions was utilised. In this model sulfide oxidation occurs at the surface of a shrinking core of a sulfide mineral surrounded by an accumulating rim of Fe(III) hydroxide or oxide.

The rate of oxidation is controlled by oxygen diffusion from the tailings surface to the depth of oxidation coupled with diffusion through the oxide rim to the surface of a shrinking core of unreacted sulfide within the particle. This is a very simplistic model and does not take into account bacterial activity or grain size variations. Thus the results presented here should be used as a guide only.

This model allows the estimation of the time required to oxidise the vadose zone of the tailings (t(d)). Additionally it allows predictions of the movement of the oxidation front through the tailings impoundment over time (X(t)). The depth of the oxidation front was modelled using the air-filled porosity of the hardpan determined at the time of sampling (1997), the total porosity of the hardpan (1996 & 1997) and the total porosity of fresh tailings (1996). These results were then compared with the actual depth of oxidation observed in the field (Table 7.5A & B). In both cases the actual depth observed in the field correlated closely with the depth modelled on the air-filled porosity values, and not the total porosity values (Fig 7.25). For the Elura hardpan, the air-filled porosity calculations gave an oxidation depth of 19-24cm, compared with the field observations of 3-7cm depth. This suggests that the average D_{O_2} is less than the 3.82×10^{-7} m^2/s calculated from field sampling during autumn (1997). The oxidation depth at the CSA impoundment is 20-40cm. Modelled depths ranged from 14-17cm, suggesting the average D_{O_2} is slightly higher than the 5.72×10^{-9} m^2/s calculated from air-filled porosity determined at the time of sampling (Table 7.5B).

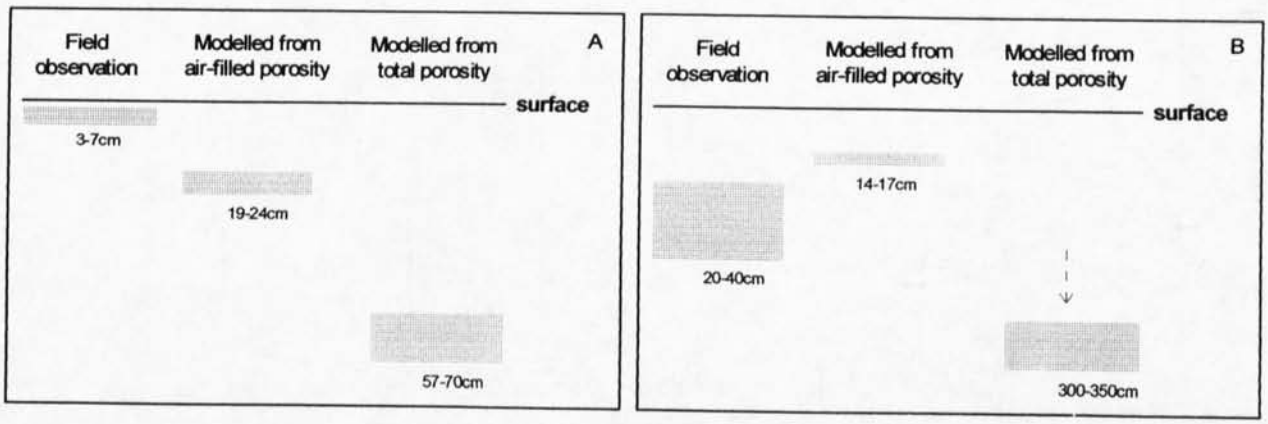

FIGURE 7.25 SCHEMATIC DRAWING OF DEPTHS TO THE OXIDATION FRONT OBSERVED IN THE FIELD, AND THE MODELLED DEPTHS USING THE DAVIS AND RITCHIE (1986) CONCEPTUAL MODEL BASED ON AIR-FILLED POROSITY AND TOTAL POROSITY, A REPRESENTS ELURA TAILINGS, B REPRESENTS CSA TAILINGS.

Using D_{O_2} determined using both total and air-filled porosities, the Davis and Ritchie conceptual model was utilised to estimate the time required to oxidise the vadose zone. The time to oxidise the vadose zone (1.5m depth at present) of the CSA tailings, based on the total porosity of the fresh tailings was estimated at approximately 2.9 years. Based on air-filled porosities of the hardpan, this time is extended to between 2070 and 2890 years. The Elura site shows a similar trend with 80 to 140 years based on tailings total porosity, which extends to between 680 and 1020 years when estimated using the air-filled porosity of the hardpans (Table 7.5A and B).

Thus calculations of gas movement at these sites suggest that the mature hardpans (8 & 13 years old) or the tailings directly below are in fact maintaining air-filled porosities much smaller than their total porosity. In response to this, D_{O2} is reduced and the rate of movement of the oxidation front is subsequently diminished. These results correlate well with investigations of the near-surface hydrology which indicate minimum water movement.

7.6.2 Variations in CO_2 Concentrations

In order to further verify the gas diffusion results, pore gas CO_2 concentrations were investigated using a similar methodology to that outlined by Blowes et al. (1991). Carbon dioxide is produced in the tailings during neutralisation reactions involving carbonate gangue minerals. The presence of elevated CO_2 concentrations within the tailings profile beneath the hardpan, is an indication of reduced upward gas diffusion. Pore gas samples were removed from beneath the mature hardpans at Elura (Dam 1 - Site 10) and CSA (North Dam - Site 2) utilising the method outlined in Appendix 1A, section 1A.5.1. Six to seven profiles were sampled at each site to ensure an average result was obtained. The results are presented in Figs 7.26 and 7.27 and Table 7.6.

TABLE 7.6 CO_2 CONCENTRATIONS (VOL %) IN CSA AND ELURA PROFILES

(sampled July 1997)

Depth (cm)	CSA gas 1	CSA gas 2	CSA gas 3	CSA gas 4	CSA gas 5	CSA gas 6	CSA gas 7
10	0.08	0.08	0.11	0.23	0.04	0.04	0.06
20	0.14	0.07	0.06	0.29	0.06	0.06	0.07
30	0.14		0.13	0.06	0.06	0.04	0.05
40	0.13		0.11	0.05	0.06		0.03
50	0.09		0.06	0.04	0.03		0.14
60	0.09		0.06	0.03	0.11		
70	0.14		0.06	0.03	0.13		
80	0.11		0.09	0.07	0.05		
90	0.08			0.05	0.03		

Depth (cm)	Elura gas 1	Elura gas 2	Elura gas 3	Elura gas 4	Elura gas 5	Elura gas 6
10	0.21	0.07	0.30	0.36	0.11	0.26
20	0.10	0.06	0.18	0.19	0.03	0.03
30	0.06	0.04	0.12	0.05	0.02	0.04
40	0.05	0.09	0.05	0.03	0.01	0.01
50	0.06	0.13	0.04	0.06	0.04	0.05
60	0.07	0.07	0.04	0.04	0.04	0.20
70	0.11	0.14	0.04	0.07	0.02	0.03
80	0.06	0.05	0.12	0.09	0.06	0.02
90	0.04		0.09		0.01	0.01

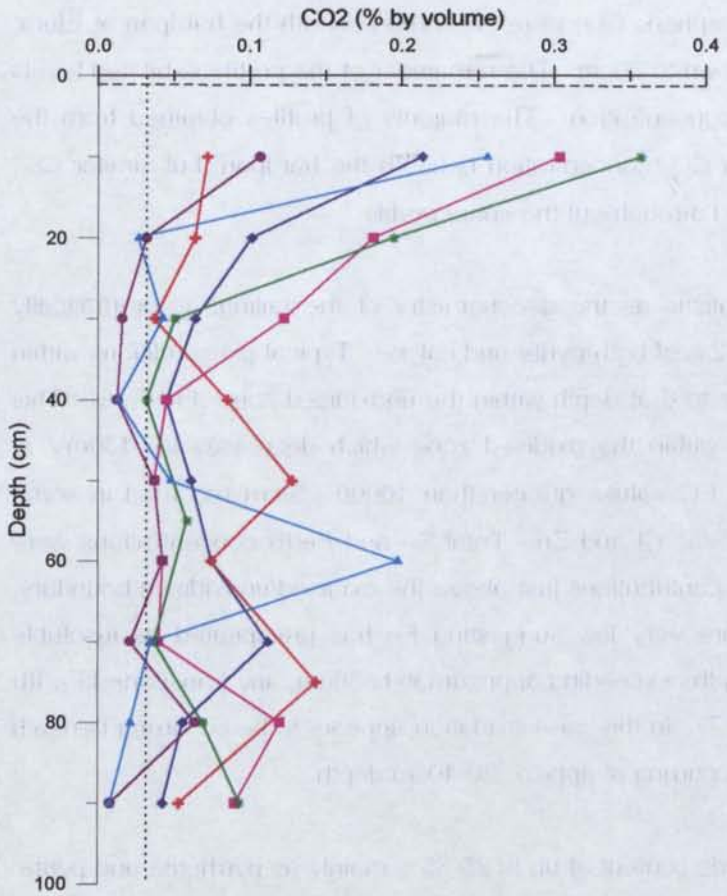

FIG 7.26 CO_2 PROFILES FROM ELURA DAM 1 - SITE 10

oxidation front

atmospheric CO_2 concentration

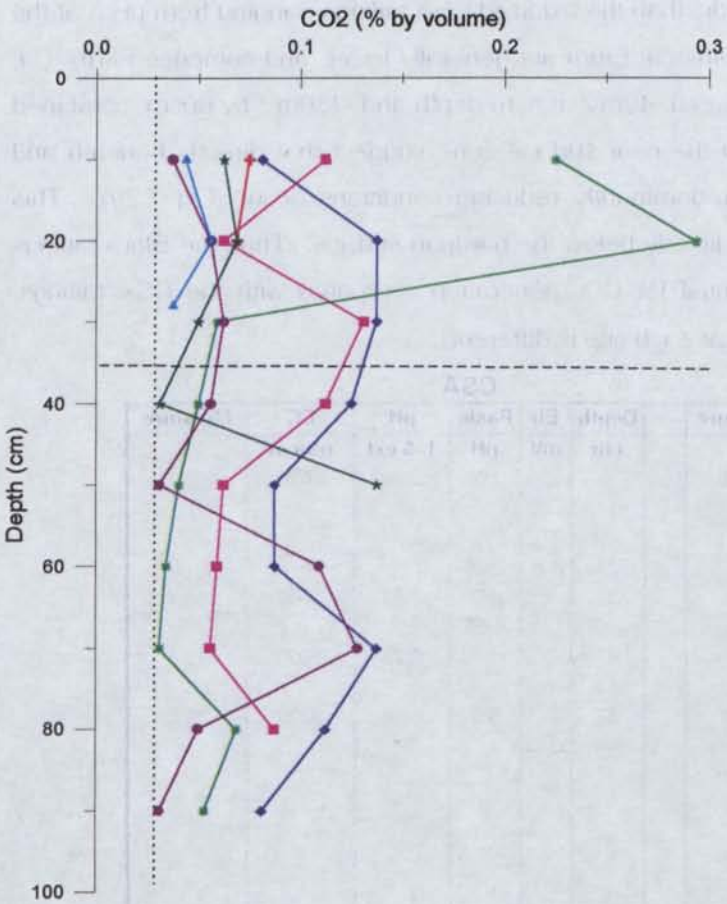

FIG 7.27 CO_2 PROFILES FROM CSA NORTH DAM - SITE 2

oxidation front

atmospheric CO_2 concentration

Concentrations of up to 10 times that of atmospheric CO_2 were observed beneath the hardpan at Elura, with elevated levels existing predominantly down to 30cm. The remainder of the profile exhibited levels marginally higher than that of atmospheric concentration. The majority of profiles obtained from the CSA site did not show this same increase in CO_2 concentration beneath the hardpan, but similar CO_2 levels as those at depth in Elura were detected through-out the entire profile.

A direct comparison of these sites is unrealistic as the geochemistry of the tailings is dramatically different. The CSA tailings contain less than 2% of both pyrite and calcite. Typical pH conditions within these old profiles range from 2 at the surface to 6 at depth within the unoxidised zone (Fig 7.28). This corresponds with Eh conditions of +400mV within the oxidised zone which decreases to -130mV at depth. Surface solute levels are high, with EC values greater than 10000 µS/cm recorded in some locations and consist mainly of Al, Ca, Mg, SO_4, Cl and Zn. Total Fe and Fe(II) concentrations were determined which indicated significant Fe (II) contributions just above the oxidised/unoxidised boundary. Iron (III) concentrations within the tailings are very low suggesting Fe has precipitated as insoluble cements within the oxidised zone, while at depths exceeding approximately 30cm, any transported Fe(III) has been reduced to Fe(II) (Fig 7.28, Table 7.7). In this case oxidation appears to be occurring beneath the surface hardpan with the oxidation front occurring at approx. 30-40cm depth.

The Elura tailings contain a much higher sulfide content of up to 25-35% mainly as pyrrhotite and pyrite. The siderite content is also high with levels up to 10%. In general the pH conditions within the oxidised zones of the Elura tailings are slightly less acidic than the oxidised CSA tailings, ranging from pH 3 at the surface to 5-6 at depth (Fig 7.29). The EC values at Elura are generally lower, and comprise Fe(II), Ca, Mg and SO_4 (Table 7.7). Eh conditions of between -40mV at 5cm depth and -130mV by 60cm, combined with significant levels of Fe(II) (900mg/kg) in the near surface zone suggest that directly beneath and potentially within the 3cm thick hardpan, predominantly reducing conditions occur (Fig 7.29). This suggests the oxidation front occurs within or directly below the hardpan surface. Thus the Elura tailings are more reactive and have a greater potential for CO_2 generation compared with the CSA tailings. Additionally the location of the oxidation front at each site is different.

Elura							CSA					
Depth	Eh	Paste	pH	EC	Moisture		Depth	Eh	Paste	pH	EC	Moisture
cm	mV	pH	1: 5 ext	uS/cm	%		cm	mV	pH	1: 5 ext	uS/cm	%
3			5.16	3550	10.2		9	324	3.03	2.98	5610	20
5	-43	4.1					14	289				
10	-71						19	372				
15	-71						25	401	2.95			
18			5.66	2210	10.1		33		2.75	3.53	3560	14.4
22	-79	4.5					40		4.65			
34		4.72					43	-81		5.28	1605	18.6
36			5.83	2400	11.3		53	-134				
50	-121	5.8	5.96	2580	10.6		57		5.6	6.04	2300	18.9
56	-130						63	-133				
61	-126	5.7										
65			6.03	2280	9.6							
71	-114											
74		5.84										
84		5.2										

TABLE 7.7 : TYPICAL EH, PH, AND EC IN ELURA AND CSA TAILINGS PROFILE (SAMPLED JULY 1997)

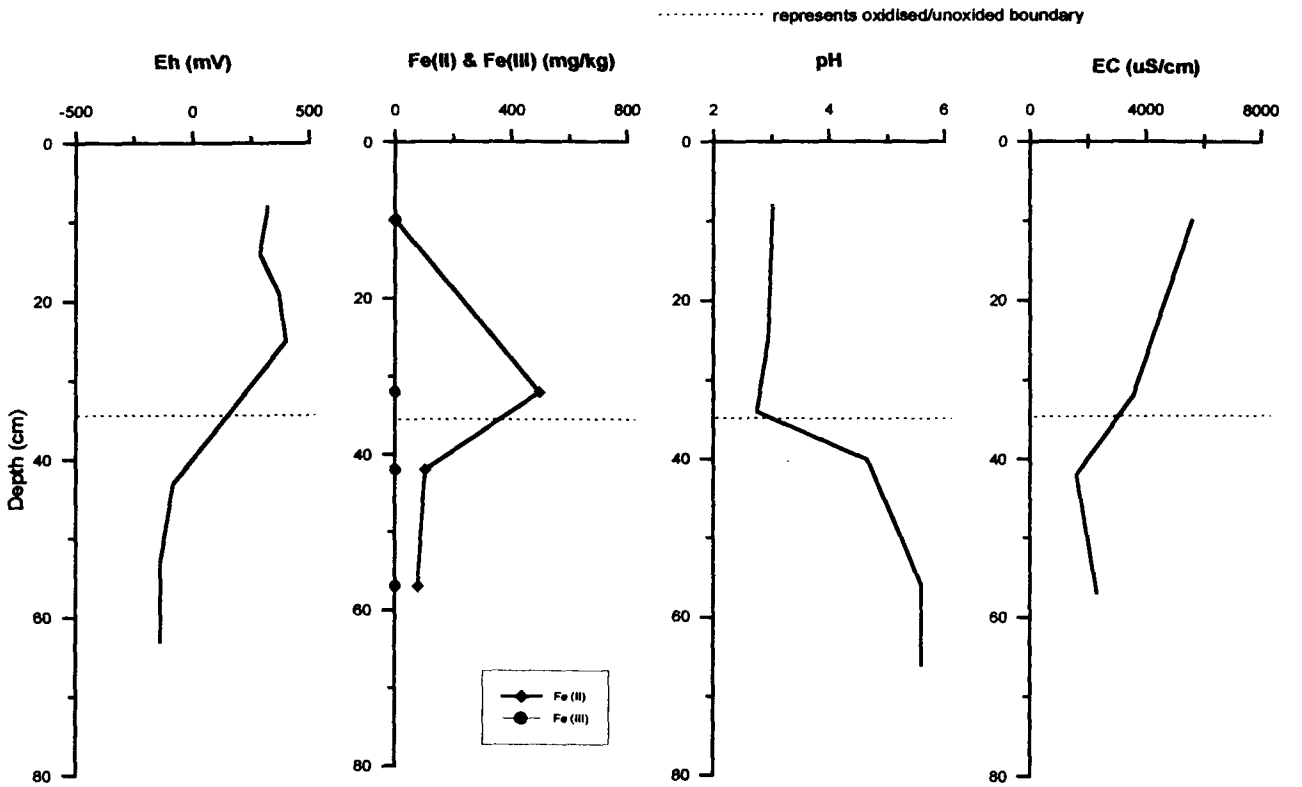

FIG 7.28 TYPICAL CSA GEOCHEMICAL PROFILES (NORTH DAM - SITE 2)

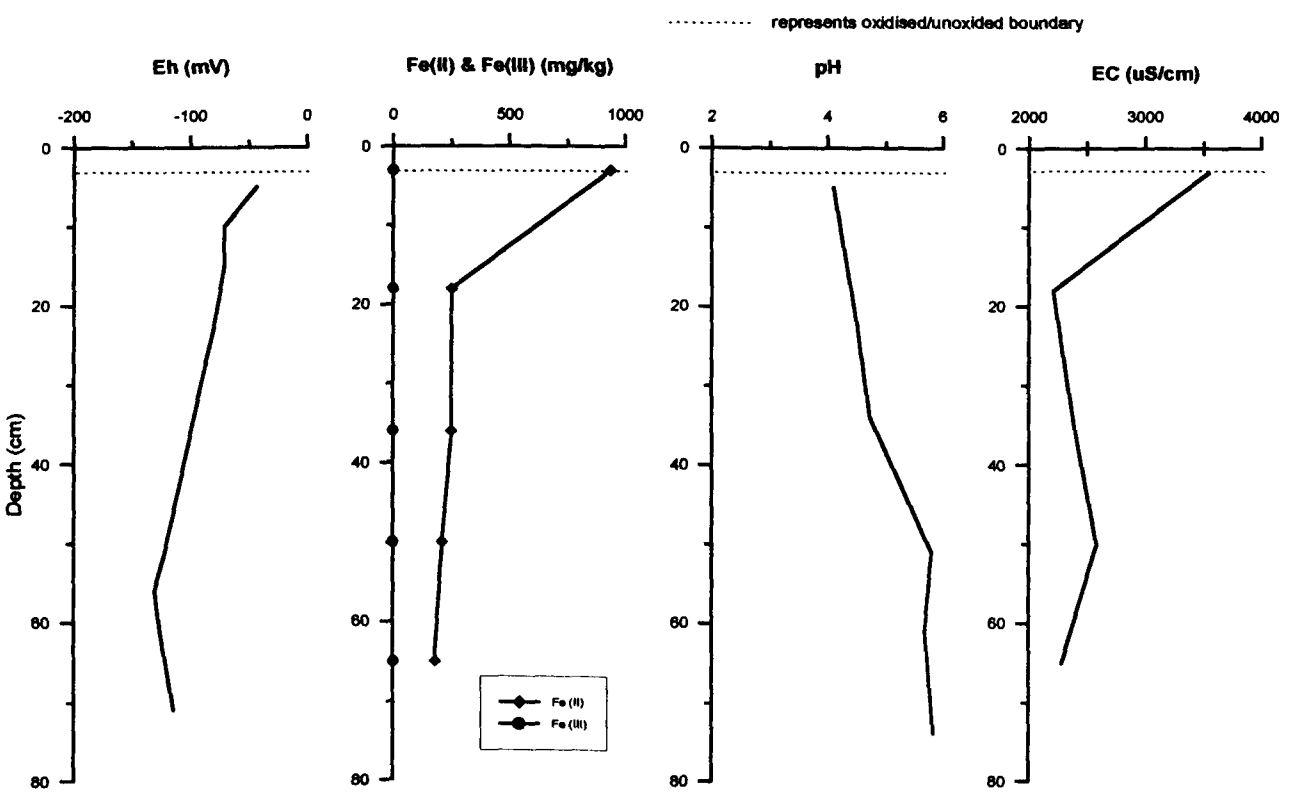

FIG 7.29 TYPICAL ELURA GEOCHEMICAL PROFILES (DAM 1 - SITE 10)

The elevated levels of CO_2 beneath the hardpan at the Elura site have developed through neutralisation reactions immediately below the hardpan. Similar reactions are probably taking place down to approximately 60cm depth where the pH of the pore water increases to 6 from 4 at the surface. Siderite exists within the hardpan and the tailings immediately below indicating these reactions may still occur.

Therefore, the CO_2 concentrations could be regarded as having developed through the reactions throughout the profile and could be simply a concentration gradient based on quantities of CO_2 sourced at the different depths.

Similar results were encountered during an investigation of the hardpans at Heath Steel tailings impoundment, where Blowes et al. (1991) described the development of cements at 27 to 42cm depth. Evidence of the effectiveness of this layer as a gas diffusion barrier was the development of concentrations of 60% CO_2 below the hardpan and less than 15% above.

The CO_2 build up beneath the Elura hardpan down to approximately 30cm depth could be similarly interpreted. CO_2 gas produced at the oxidation front would move along concentration gradients both up and out of the tailings and down into the tailings profile. The profiles suggest that upward escape has been inhibited by a reduced D_{CO2} of the surface and thus the downward movement of CO_2 would be promoted. This evidence could support the hypothesis that the hardpan surface is acting as a diffusion barrier.

The CO_2 concentrations at the CSA site are elevated throughout the profile with the source occurring between 30 and 40cm depth. Both upward and downward diffusion has occurred and elevated levels have developed through-out the profile. The fact that high concentrations have not built up below the hardpan may be a function of the lower reactivity of the tailings and the deeper location of the oxidation front. Obviously in the CSA case the surface hardpan is not acting as a competent seal as oxidation is still occurring within the tailings at depth, but is perhaps acting to reduce diffusivity as outlined in the modelling section. Similarly the hardpan at Elura may not be acting as a complete seal, but may be reducing the overall impact of the tailings on the surroundings.

7.6.3 Gas Diffusion Measurements

The gas diffusion modelling and CO_2 investigations give an indication of the potential of the hardpan to reduce gas diffusion. To ensure that this approach accurately estimates the influence of hardpans, and to further verify these results, direct gas diffusion measurements were carried out on selected CSA and Elura hardpan samples. These measurements were carried out at the Australian Nuclear Science and Technology Organisation (ANSTO) by Phil Layton. Details of the methods involved are presented in Appendix 1A, section 1A.5.3.

The hardpans were sealed into capped PVC cylinders which were subsequently purged with argon. A tracer gas (O_2) was then released into the top of the columns and a concentration vs. time curve was produced by sensors at the bottom. Two parameters were then used to model these curves: C_o, which is the concentration of O_2 in the bottom of each testing column and the tortuosity factor, a dimensionless constant which is a ratio of the gas diffusion coefficient of O_2 in air. The effective diffusion coefficient (D) is determined using the formula

D = RLMDA x DB

where RLMDA = the tortuosity factor

DB = diffusion coefficient of O_2 in air (813.6 cm^2/h)

Duplicate hardpan samples from both CSA and Elura sites were tested twice and average diffusion results were obtained (Table 7.8). The Reardon and Moddle (1985) method was again used to calculate the diffusion coefficients based on total porosity. These O_2 diffusion results are also presented in Table 7.8 for direct comparison. In both cases the diffusion coefficients calculated by the Reardon and Moddle method are higher than those determined from direct measurements (Table 7.8). The CSA diffusion coefficient measurements were similar, while the two Elura hardpan samples produced results almost an order of magnitude different.

The Davis and Ritchie (1986) conceptual model was employed to compare depths to the oxidation front (Table 7.9A & B). This modelling again over-estimated the depth to the oxidation front. Based on total porosity D_{O2} calculations the CSA oxidation front depth was modelled at 3.2-3.7m, using the measured effective diffusion coefficient this was reduced to 2.2-2.6m, however the actual field depth was 20-40cm (Table 7.9A and Fig 7.30B). The modelled depth of the Elura oxidation front was 38-46cm based on total porosity, 19-23cm based on the effective diffusion coefficient measured, compared with the actual 3-7cm depth (Fig 7.30A). Thus, when using the actual diffusion coefficients obtained by laboratory testing, the Davis and Ritchie model produced shallower depths to the oxidation front but these were still deeper than those observed in the field (Table 7.9B and Fig 7.30). These results again support the hypothesis that persistent elevated moisture levels within the hardpans or the tailings directly below, strongly influence that rate of oxidation of tailings.

TABLE 7.8 EFFECTIVE DIFFUSION COEFFICIENTS FOR SELECTED CSA AND ELURA HARDPANS

Sample	Porosity Range	Average Porosity	Tortuosity Range	Average Tortuosity	Effective Diffusion Coeff. (m/s^2) (D)	Modelled Diffusion Coeff. (m/s^2) (Reardon & Moddle, 1985)
CSA 1 - North Dam Site 1	33.4-35.5	34.6	0.06-0.055	0.0575	$1.3x10^{-6}$	
CSA 2 - North Dam Site 1	37.6-39.5	38.5	0.065-0.065	0.065	$1.47x10^{-6}$	
CSA North Dam Site 1 average					$1.39x10^{-6}$	$2.82x10^{-6}$
Elura 1 -Dam 1 Site 1	22.6-31.2	26.1	0.016-0.015	0.0155	$3.5x10^{-7}$	$1.43x10^{-6}$
Elura 2 - Dam 2 Site 8	44.2-50.1	46.6	0.016-0.016	0.016	$3.6x10^{-6}$	

TABLE 7.9 COMPARISON OF OXYGEN DIFFUSION COEFFICIENTS, SULFIDE OXIDATION DEPTHS AND TOTAL TIMES FOR OXIDATION OF VADOSE ZONES, FOR ELURA AND CSA HARDPANS

A - Davis and Ritchie modelling comparisons for hardpans based on Reardon and Moddle diffusion calculations from total porosity measurements (sampled Aug 1996)

Total P H/P (%)	D O_2 H/P (m^2/s)	Sulfide (%)	Time of exposure (yr)	Depth to water table	t(d) yr H/P max	t(d) yr H/P min	X(t) m H/P min	X(t) m H/P max	Actual depth of ox (m)
CSA North Dam Site 1 hardpan									
0.365	2.82E-06	0.017	13	1.5	5.9	4.2	3.2	3.7	0.2-0.4
Elura Dam 1 Site 1 hardpan									
0..261	1.43E-06	0.3	8.5	1.5	270	180	0.38	0.46	0.03-0.07

B - Davis and Ritchie modelling comparisons for hardpans based on measured diffusion rates (sampled Aug 1996)

	D O_2 H/P (m^2/s)	Sulfide (%)	Time of exposure (yr)	Depth to water table	t(d) yr H/P max	t(d) yr H/P min	X(t) m H/P min	X(t) m H/P max	Actual depth of ox (m)
CSA North Dam Site 1 hardpan									
	1.39E-06	0.017	13	1.5	11.9	8.5	2.2	2.6	0.2-0.4
Elura Dam 1 Site 1 hardpan									
	3.5E-07	0.3	8.5	1.5	1100	740	0.19	0.23	0.03-0.07

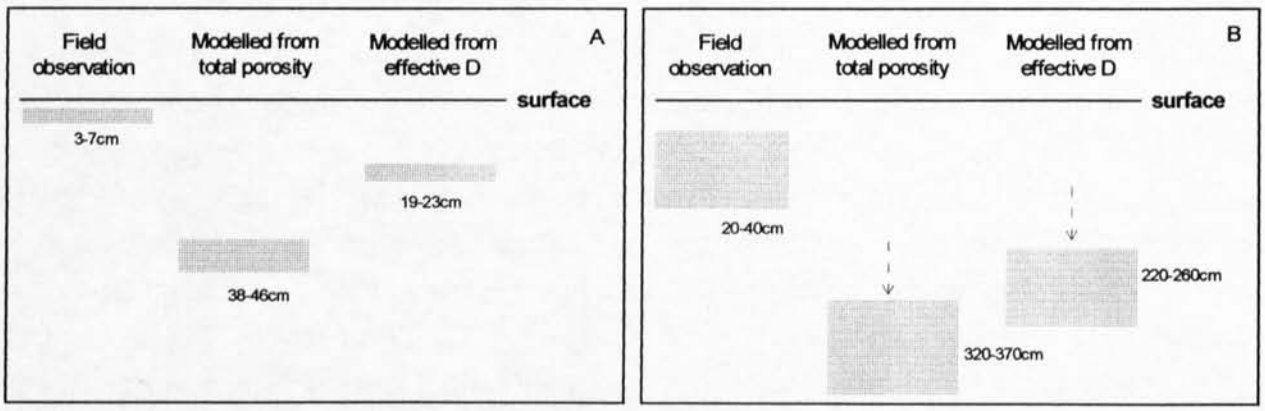

FIGURE 7.30 SCHEMATIC DRAWING OF DEPTHS TO THE OXIDATION FRONT OBSERVED IN THE FIELD, AND THE MODELLED DEPTHS USING THE DAVIS AND RITCHIE (1986) CONCEPTUAL MODEL BASED ON TOTAL POROSITY AND MEASURED EFFECTIVE DIFFUSION, A REPRESENTS ELURA TAILINGS, B REPRESENTS CSA TAILINGS.

7.7 The effectiveness of hardpan in the reduction of AMD and Contaminant Transport - An overview

While contaminant transport is dependent on water infiltration properties alone, the effectiveness of hardpans in inhibiting AMD generation is dependent on reducing both oxygen diffusion and water infiltration. Water infiltration rates through hardpans have been compared with fresh tailings. Permeability tests indicate that a number of the natural hardpans investigated have the ability to reduce water infiltration compared with their fresh tailings counterparts, however this is not a universal trend. Differences associated with the age and state of hardpan degradation, preferential flow paths and the heterogeneous nature of the tailings have produced highly variable results. This variability was also observed in porosity investigations and is attributed to similar properties.

Moisture retention characteristics of selected hardpans were used to assess the change in pore size distribution which occurs as cemented layers and hardpans develop. Results indicate that in many cases a reduction in the number of the smallest size pores occurs during hardpan formation, while larger pores are lost during cemented layer development. The effect this has on water movement at the tailings surface was modelled in order to observe moisture levels and thus air-filled porosities. The quantities of air-filled pores directly determined the gas diffusion characteristics and thus oxygen penetration. The change in pore size distribution of the Renison Bell hardpans caused major reductions in the relative hydraulic conductivity of the surface. A minor reduction in water content effectively stopped evaporation at the hardpan surface while the same reduction in water content of the uncemented tailings had only a very minor effect on the hydraulic conductivity and thus flow to the evaporating surface could continue for a longer period at a rate close to that of the saturated hydraulic conductivity.

This same effect was not observed for the CSA and Elura hardpans when compared with the fresh tailings. The results indicated that for both surfaces a minor reduction in moisture content from saturation levels caused a substantial reduction in their hydraulic conductivities. These results suggest that for both hardpan and fresh tailings alike, this reduction may be sufficient to effectively stop evaporation from the surface, sustaining elevated moisture saturation levels within the hardpans or within tailings directly below. Chloride and deuterium analysis confirmed that evaporation in these tailings impoundments is restricted to the surface and indicated that hardpan development has not significantly altered the surface evaporation processes at these sites. Surface salts produced at both locations would also help to inhibit evaporation.

The effect of porosity and moisture levels were further examined at the Elura and CSA sites by gas diffusion investigations which included modelling, sampling of CO_2 concentrations and laboratory testing. Calculations based on total porosity and direct measurements of gas diffusion coefficients produced very similar results of between 4.9×10^{-6} to 3.5×10^{-7} m^2/s, for the Elura and CSA hardpans. These diffusion coefficients were then used in modelling the movement of the oxidation front within the tailings dams. In all cases the diffusion coefficients produced a depth to the oxidation front far greater than those observed in the field.

Calculated and measured diffusion coefficients based on air-filled porosities produced modelled depths to the oxidation front significantly closer to those observed in the field. These results indicated that the hardpans or tailings directly underlying the hardpans are maintaining water-filled porosities great enough to substantially reduce oxygen infiltration and thus oxidation of the underlying tailings. These water-filled porosities are being maintained by the development of a surface cap through which evaporation is substantially reduced.

Carbon dioxide build up beneath these hardpan surfaces suggest that the upward escape has been inhibited by a reduced D_{CO_2} of the surface and thus downward movement has been promoted. This reduction in D_{CO_2} is also produced by continuously elevated moisture contents.

The investigations of permeability and porosity indicate that the surface hardpan can have highly variable properties which in turn effect infiltration rates and the geochemistry of the underlying tailings. This variability is a function of the dynamic nature of the hardpans which appear to have a cyclic existence of cementation, chemical or mechanical degradation, re-exposure of underlying tailings and re-cementation. Over time the physical properties of the hardpans change. The variation in permeability obviously has a strong influence on the availability of oxygenated water to the underlying tailings. The modification in porosity appears to have less of an effect as it is the persistent water-filled porosity that has dictated O_2 diffusion at the Elura and CSA sites.

Geochemical investigations indicate that the hardpans, especially at the CSA site are not completely sealing the tailings surface as oxidation is occurring at 20-40cm depth. The hardpans or directly underlying tailings are however reducing oxygen diffusion which controls the movement of the oxidation front and the time it takes to oxidise the vadose zone of the tailings. At present the water table is at approximately 1.5m depth in both of the older dams (Elura Dam 1 and CSA North Dam). Modelling based on these depths has been carried out using the simplistic Davis and Ritchie (1986) model. Because of the basic nature of this model the results obtained should only be used as a guide. The time to oxidise the vadose zone in the CSA tailings dam is modelled at 2.9 years based on total porosities of the uncemented tailings, while Elura it has been modelled at between 80-140 years. However, based on diffusion coefficients estimated from air-filled porosities of the hardpan surface, these times have been extended to 2100-2900 years for the CSA dams and 680-1020 years for the Elura dams. These results suggest that the yearly contaminant generation from the tailings will be lessened however sulfide oxidation and pollutant generation will continue for an extended period of time. It should be remember that the water table at 1.5m will continue to drop when deposition is completed. Eventually the tailings will become unsaturated, O_2 infiltration will not be inhibited and oxidation will take place, further extending the period of time to oxidise and produce contaminants.

Chapter 8 : Hardpans - Effectiveness in Environmental Management

8.1 Review of Aims

Hardpans have been observed forming in tailings dams, waste rock dumps and sulfide roaster waste in Canada, U.S.A and the U.K. It was initially thought that these hardpans had the ability to inhibit oxidation of underlying sulfidic waste materials through the reduction of oxygen and water penetration (Boorman and Watson, 1976). Over time this hypothesis has been questioned.

Many individual investigations have been carried out, which have identified the mineralogical and geochemical evolution of the hardpans at specific sites. Blowes et. al. (1991) made a comparison of hardpans at two sites and suggested that hardpans could be divided into two types based on mineralogy and location of development in the profile. Ritcey (1989) also discussed hardpans as inhibitors of AMD. He presented possible factors effecting hardpan development. These factors included mineralogy, metallurgical process, lime additions, bacteria, disposal technique and water table height as this determines the Eh-pH conditions and therefore the distance the hardpans form from the surface as well as the thickness.

The MEND program sponsored a project to characterise the mineralogy of hardpans at four Manitoba tailings sites and to assess if they could be used as an oxygen barrier. Petrographic studies and permeability tests were conducted and results indicated they were relatively impervious. It was recognised however that weathering and seasonal freeze and thaw tended to break down the hardpan, resulting in fractured, softened zones which possessed only moderate resistance to infiltration and continuous oxidation. As a result, serious doubts were raised about the use of hardpans to control acid generation and the project was terminated. Also, no suitable method of artificially creating a hardpan was determined (MEND, 1994 & 1995).

These conflicting reports and the little field evidence of factors controlling hardpan formation on a wider scale, led to this present study of hardpans at Australian mines. The aim of this research was two fold. Firstly it was to obtain an understanding of the physical and chemical characteristics of tailings residues which support the insitu formation of cemented layers and hardpans. Australia's variable climate allowed investigations into the role of the water table on hardpan development. The second aim was to investigate the promotion of hardpan formation to inhibit AMD and pollutant generation. To achieve this objective, the effectiveness of both the natural and artificial hardpans to reduce O_2 and H_2O infiltration needed to be assessed. Australia's arid to semi-arid climate allowed investigations of the ability of hardpans to reduce AMD generation without problems associated with thermal heaving, which has been noted in Canadian and American studies.

8.2 Natural development of hardpans and cemented layers in tailings dams

8.2.1 Development and classification of secondary mineral accumulations

Hardpans and cemented layers develop in tailings dams through the precipitation and accumulation of secondary minerals. Sulfide oxidation, acid generation and gangue mineral dissolution are typical geochemical reactions which occur at the tailings surface, generating solutes available for secondary mineral precipitation. As secondary mineral accumulation increases, cementing of the tailings can occur producing hardpans or cemented layers. Varying sulfide and gangue mineralogy and content, physical characteristics and climate control the nature and extent of hardpan and cemented layer formation. As a result of these variations, hardpan and cemented layer development differs in thickness, lateral extent, depth within the profile and composition.

Three main types of secondary mineral accumulations have been identified. Some secondary mineral accumulations result in hardpans and cemented layers which form uniformly over the entire dam either as a surface cement or at some depth. These have been termed ***laterally extensive hardpans/cemented layers.*** **Laterally extensive surface hardpans** have developed at CSA and Elura (NSW) and Renison Bell (Tas) tailings impoundments, while **laterally extensive cemented layers** have developed at depth within the tailings profiles at Broken Hill (NSW) and Brukunga (SA).

Other hardpans have developed only in locations of concentrated seepage, and have been termed ***laterally discontinuous hardpans.*** **Laterally discontinuous hardpans** have developed at the Chesney (NSW) and the Woodcutters (NT) impoundment and are restricted to seepage zones in low-lying areas. There is no widespread hardpan development in these dams.

8.2.2 Parameters Effecting Hardpan and Cemented Layer Development

The following section outlines the effect of sulfide and gangue mineralogy, climate, milling processes, water table and grain size distribution on laterally extensive hardpans and cemented layers. Laterally discontinuous hardpans developed in seepage zones are also discussed.

Tailings mineralogy and content which can vary greatly from mine to mine and also within a deposit can have a large impact on hardpan and cemented layer development. Field observations indicate tailings with high sulfide contents generally form hardpans more readily than when the sulfide content is low or absent. This is true for pyrrhotite-rich tailings dams (Elura and Renison) more so than pyrite-rich tailings (Woodlawn). This difference is directly related to mineral reactivity. Pyrrhotite being more reactive, oxidises quickly upon exposure producing secondary by-products which coat the mineral grains and bind the tailings together as a surface hardpan. Pyrite however takes longer to oxidise and in many cases the secondary minerals that develop are relocated vertically down preferential flow paths, cementing these regions through concentration of solutes rather than cementing the immediately exposed surface.

The variation in reactivity of these sulfides and their resultant hardpan formation becomes apparent in varying climatic conditions. In dams where sulfide content is high, consisting predominantly of pyrrhotite, hardpans appear to develop regardless of rainfall (Elura - low rainfall and Renison - high rainfall). However in pyritic tailings, climate and grain size can have a major impact. In tailings which have been finely ground during processing, saturation levels may be maintained high in the profile through the matrix and osmotic potentials. Under these conditions the quantity of tailings available for oxidation is reduced and because of the lower reactivity of the pyrite, fewer oxidation by-products are available for hardpan development. Finely ground pyritic tailings were sampled from the moderately high rainfall Woodlawn Mine in which hardpans had not developed after 8 years of exposure. These were subsequently treated in the laboratory under lower rainfall conditions (Chapter 6). The result was extensive cementing down preferential flow paths indicating the mineralogy favored cement development while the physical and climatic conditions at the mine did not.

In tailings which have low sulfide content, cement development is very differently. Only low sulfide content tailings in low rainfall areas have been investigated. It appears that grain size in this case does not determine whether or not secondary mineral accumulations will occur but rather dictates whether they are developed as surface hardpan or cemented layers at depth.

In tailings which have large variations in grain size, cement development can be dictated by textural differences resulting in varying unsaturated flow regimes. As tailings are deposited, mineral grains settle depending on size and specific gravity (beaching) resulting in layers of different permeability, which effects the rate and flow path of water through the profile. In tailings which have a large grain size distribution (e.g. Broken Hill and Brukunga), cements are precipitated in discrete layers through-out the profile and not at the surface. It appears that as water moves down through the tailings it collects weathering and oxidation by-products. Transportation via unsaturated water flow occurs within the fine material (Newman et al. 1997) which become the locus for concentration of solutes and secondary mineral precipitation. Concentration of solutes occurs when movement is reduced due to variations in permeability and during evaporation cycles. Concentration of solutes results in the precipitation of secondary salts and cements along the boundaries between coarse and fine tailings.

In low rainfall areas hardpans may also develop in tailings which are predominantly fine-grained and thus have less textural variations (e.g. CSA). In these cases cementing takes longer to mature and is restricted to the surface and along desiccation cracks. Under these conditions the hardpan morphologies are similar to those formed in high sulfide content tailings under dry conditions.

In both high and low sulfide content tailings the sulfide mineralogy not only plays a role in the rate of hardpan development and location of cementing within the profile but also dictates the composition of cementing minerals. In dams consisting predominantly of pyrite and pyrrhotite (e.g. Elura, CSA and

Renison), Fe sulfates (e.g. jarosite) and oxides (e.g. goethite) tend to occur, whereas in tailings with sphalerite as the predominant sulfide (Broken Hill- Alpine Country Dam), zinc secondary minerals such as hemimorphite dominate the system. The type of sulfide present can also influence the pH conditions and thus element mobility. Some sulfides oxidise producing acid (e.g. pyrite) while others do not (e.g. pyrrhotite) (Thornber and Taylor, 1992). These variations in elemental mobility also dictate the type of cement developed.

Variations in the gangue mineralogy can also influence the development of hardpans in different tailings environments. Under acidic conditions associated with sulfide oxidation, degradation of gangue minerals can be enhanced releasing solutes into the system. These reactions in turn can change the pH of the system and release solutes for precipitation of secondary salts and cements. Changes in pH determine the mobility of elements within the system and thus also dictate the type of cement produced. For example, Broken Hill tailings dominated by Mn-bearing gangue minerals with Fe and Zn sulfides has produced Mn and Fe oxide and hemimorphite cements, whereas tailings dominated by aluminosilicates and Fe sulfides may produce Fe oxide and siliceous cements (e.g. Brukunga and CSA).

Tailings produced from different parts of the ore deposit have also been investigated with regards to hardpan formation. Results indicate that minor changes in the mineralogy (e.g. carbonate/silicate ratio) of lodes can determine the form and nature of cement. During the life of the Broken Hill mine, mining has changed from more calcitic lodes to more siliceous lodes. This has changed the type of tailings produced and the cementing potential. The older calcitic tailings within Site A/B have very little cementing, while the more siliceous tailings of Site C, have goethite and gypsum rich cemented layers developed within the upper 2m.

Variations in ore processing techniques have been investigated at some of the older sites where multiple tailings dams exist. Changes in the extraction processes can be observed with final sulfide content and grain size varying dramatically. For example at Broken Hill, as sphalerite flotation processes have been refined, tailings cements in some locations have changed from hemimorphite and Mn oxides developed as by-products of the weathering of sphalerite containing Mn impurities, to minor Fe-based goethite cement from minor Fe-sulfide weathering.

At the Chesney Au-Cu Mine the first phase of mining processed the gossan to extract supergene gold. During this period, very coarse grains with high cementing potential were intermixed with fine slimes in a highly heterogeneous mixture, resulting in cemented layers. Subsequent mining of the sulfidic ore and advanced technologies resulted in generally finer tailings with low sulfide content and thus reduced the potential for cementing in succeeding dams.

Both Ritcey (1989) and Blowes et. al. (1991) discussed the importance of the water table in the formation of hardpans. Ritcey (1989) explained that the water table height determines the Eh-pH conditions within

the tailings profile and therefore dictates the distance from the surface the hardpans form as well as the thickness. In many locations around Australia evaporation far exceeds rainfall. When deposition into tailings dams located in these regions is completed, the water table drops continuously. The rate at which this occurs is dependent on the lateral and vertical permeability, and the matrix and osmotic suction potentials of the tailings, the decant system, the underlying material and evaporation intensity. The location of the hardpans and cemented layers is not dictated by the water table location, but rather by the permeability and thus leaching potential of the tailings. The thickness of the hardpans is strongly dependent on the reactivity of the tailings, which dictates the extent to which O_2 infiltration occurs before it is consumed in sulfide oxidation reactions i.e. movement of the oxidation front.

Within the Brukunga tailings, cemented layers have developed at 1-1.4m depth. Several hypotheses have been suggested for the location of their formation (Agnew, 1994). One suggestion is that formation was initiated during the period when seepage water from the toe of the dam was pumped back to the dam surface, maintaining an elevated water table within the valley fill structure. During this period minor fluctuations in the water table and additional solute input from the cycled seepage may have promoted cement development. During this study, no other cement development was observed at the water table.

In dams where hardpan development is restricted by mineralogy, grain size or climate, hardpan formation can be enhanced in low lying seepage zones. Waters laden with heavy metals and sulfate can develop in waste rock piles or tailings dam walls made of waste rock. When tailings are exposed to these waters they are not only exposed to increased solute loads available for secondary mineral formation but also are often exposed to increased levels of Fe^{3+} in acidic conditions. The ferric iron may then become available to enhance the sulfide oxidation under these conditions thus accelerating hardpan development.

8.2.3 The Morphology and Cycling of Hardpans and Cemented Layers

Laterally extensive hardpan surfaces are very dynamic, cycling through numerous stages of development and degradation. The type of morphological features and the rates of transformation depend principally on the reactivity of the tailings and how rapidly secondary mineral accumulation is achieved. Desiccation crack cements and pop-up features are commonly observed and form part of the cycle of hardpan generation and degradation. Similar features of weathering, along with seasonal frost degradation have been noted in the four Manitoba hardpans sites (MEND, 1994 & 1995). A flow chart combining the various hardpan and cemented layer features with the cycle of development and degradation is presented in Fig 8.1.

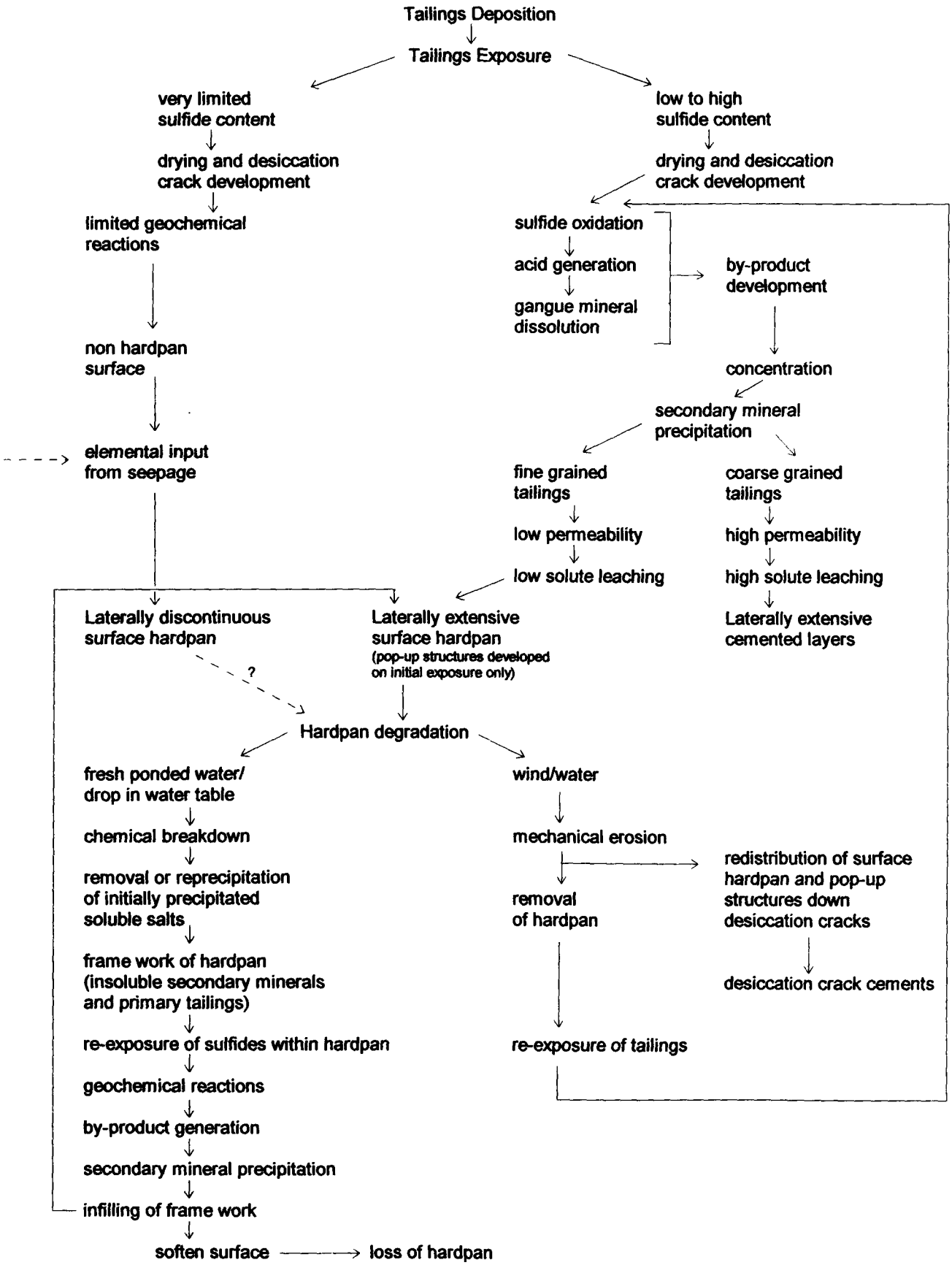

FIG 8.1 CYCLE OF HARDPAN DEVELOPMENT AND DEGRADATION

After tailings deposition is completed and the surface of the dam begins to dry out, desiccation cracks form. The desiccation cracks which may be in excess of 1m depth, will remain if the surface in not subject to rain or mill water (Fig 8.2A). Sulfide oxidation, acid generation and gangue mineral dissolution takes place not only at the surface of the tailings but also occurs down and along these cracks, the result being solute development and secondary mineral formation in both locations (Fig 8.2B & 8.3A). Accumulations of secondary minerals at these location may result in cementation of the tailings. In high sulfide content tailings both the surface and cracks develop cemented surfaces very quickly. In lower sulfide content tailings however, the reactions are subdued and cementing does not form as quickly.

The grain size of the tailings also plays a role at this stage. In coarse-grained tailings, vertical leaching of soluble secondary minerals is promoted due to the high permeability. As previously discussed, intermittently deposited slimes become the locus for secondary mineral precipitation, resulting in cemented layer development. In fine-grained tailings, laterally extensive surface hardpans develop more commonly. This is a function of tailings grain size, reactivity and the climate. In many locations in Australia rainfall is low and if infiltration is attenuated by the low permeability of the fine grain tailings, vertical leaching is restricted. As a result, secondary mineral accumulation occurs at the surface eventually resulting in cementation. In sulfide-rich tailings in particular, volume changes occur in response to these reactions, resulting in pop-up structures. As these cements rise (Fig 8.3B), the underlying tailings become exposed to oxygen and water and themselves oxidise and cement (Fig 8.3C).

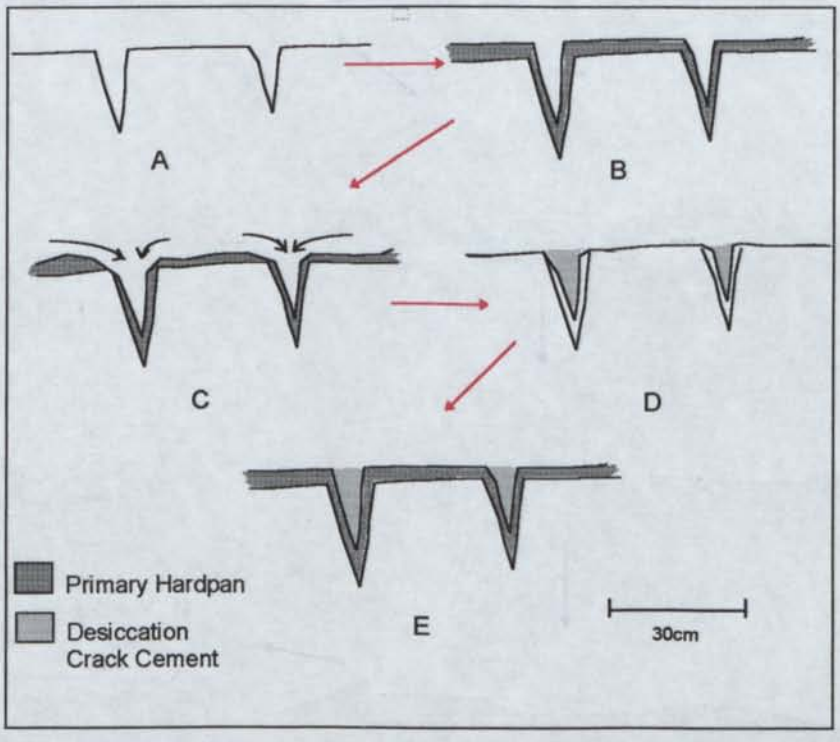

FIG 8.2 DESICCATION CRACKS ARE INFILLED WITH CEMENTS, PRODUCING SEALED CELLS.

A desiccation cracks developed in drying tailings dam
B oxidation of exposed tailings to develop original hardpan
C hardpan eroded by water in low lying areas
D desiccation cracks filled by eroded hardpan cements
E final surface morphology of hardpan with desiccation crack cements

Limitations to the number of visits prevented determining whether laterally discontinuous surface hardpans produced in tailings through additional element input from seepage exhibited these features.

Over time, all surface hardpans examined become degraded through either chemical or mechanical breakdown. This breakdown is often dependent on the final morphology of the dam. In areas which are topographically higher, rapid runoff of rainfall and increased wind action can result in the erosion of the surface hardpan and in particular pop-up structures (Fig 8.3D). Eventually the pop-up structures are completely eroded away, leaving different underlying structures dependent on the original pop-up morphology. Disc shapes can develop beneath triple point intersections of desiccation cracks, or within the central regions of large pans which have lifted as a result volume increases. Through default, areas which do not originally pop-up become strategically higher and as a result eventually become the focus of erosion and degradation (Fig 8.3E & F).

An additional feature of the surface hardpan erosion is the intermittent relocation of secondary minerals down into the desiccation cracks (Fig 8.2C), eventually completely infilling and cementing these regions (Fig 8.2D). Ultimately erosion results in the exposure of the underlying tailings which are then available to go through the same geochemical reaction resulting in a fresh hardpan surface (Fig 8.2E).

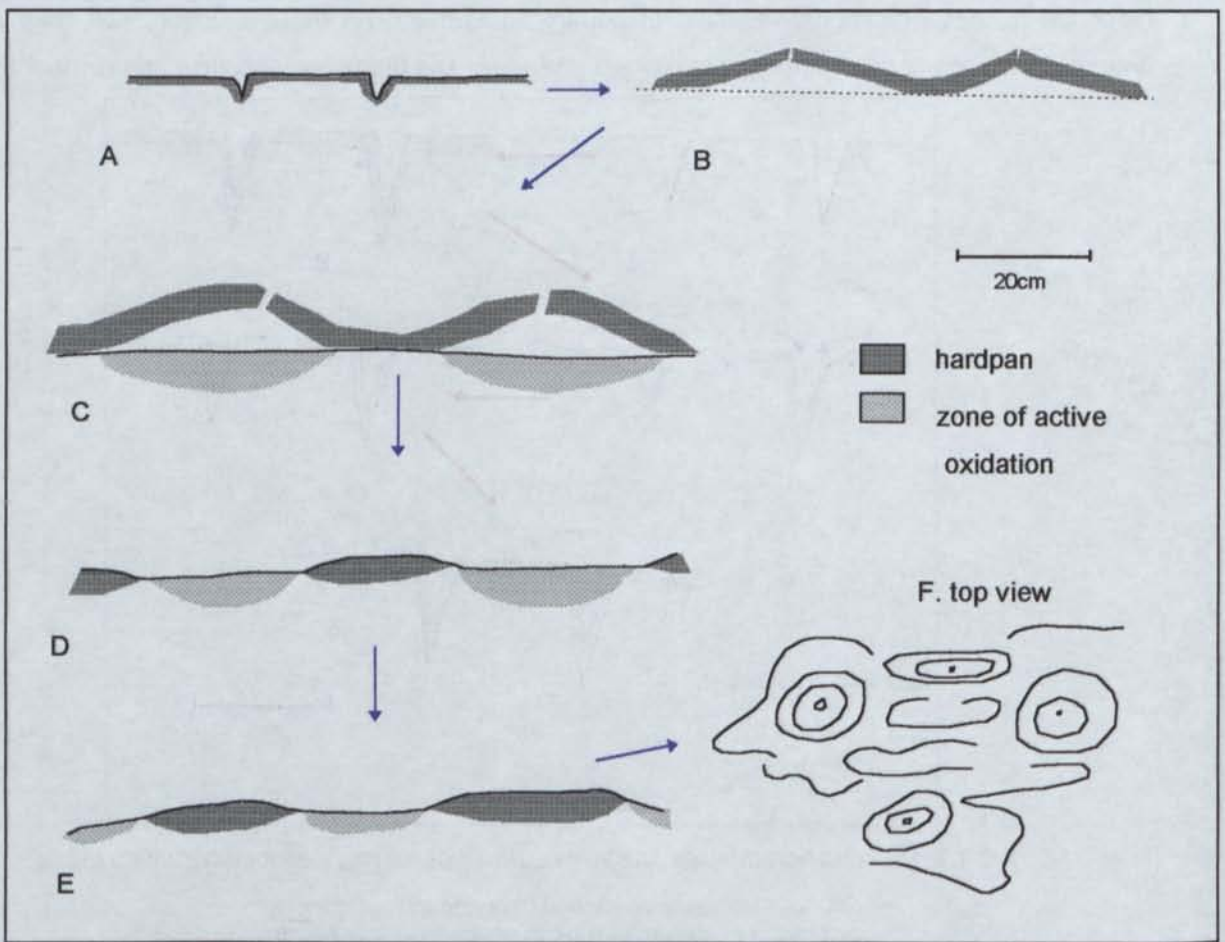

FIG 8.3 POP-UP STRUCTURES ALLOW OXIDATION OF UNDERLYING SULFIDIC TAILINGS RESULTING IN SECONDARY CEMENTS.

A desiccation cracks developed in drying tailings dam, subsequent oxidation of exposed tailings resulting in secondary mineral build up
B volume changes associated with secondary mineral precipitation resulting in pop-up structures
C oxidation and weathering of underlying tailings
D erosion of topographically higher pop-up structures
E inverted erosion resulting in disk shape structures
F final hardpan surface with combination disk-shaped morphology

In lower lying regions, water runoff may be less and if periodically inundated, may restrict wind and water erosion further. In these cases hardpans may remain intact for long periods. The chemistry of ponded water and hardpan mineralogy will determine the resistance of the hardpan to chemical attack (determined mainly by solute saturation levels). In fresh water ponds, developed as a result of rainfall and low permeable tailings, solute concentrations may be low and as a result secondary salt dissolution may be favoured. In the case of raised water levels in the dam due to complete saturation of the profile, solute concentrations may be high thus reducing dissolution potential.

Hardpans may also chemically breakdown in non ponded environments, simply through mineral instability due to a change in the physical conditions. For example, Fe^{2+} sulfates are often the first salts precipitated after the initial reactions of sulfide oxidation and acid generation. The Fe^{2+} sulfates remain, while the water table is high and O_2 consumption by sulfide oxidation at the surface restricts its conversion to Fe^{3+} sulfate. If the water table drops, O_2 diffusion is enhanced and oxidation of the Fe^{2+} sulfate may occur. As the surface ages the resultant Fe^{3+} sulfate may incorporate additional elements derived from gangue mineral dissolution enhanced by the acidic environment. Through cycles of rainfall infiltration, leaching, evaporation and concentration a wide variety of minerals may develop (Table 8.1), however in most cases as aging continues, Fe oxides and opaline siliceous material become the residual cements as other more soluble salts are leached from the surface.

Table 8.1 presents the secondary minerals which are common cementing agents within hardpans and cemented layers. This table outlines the types of soluble salts precipitated on the tailings surface, the less soluble minerals within the hardpans and cemented layers and the residual cements produced after an extended period of exposure.

TABLE 8.1 SECONDARY MINERALS ASSOCIATED WITH HARDPAN AND CEMENTED LAYERS DEVELOPED WITHIN TAILINGS.

Common Surface Salts	sulfur, rozenite, melanterite, halite, hexahydrite, halotrichite, pickeringite, kalinite, boussingaultite, wattevillite, beudantite
Common secondary minerals within hardpans and cemented layers	jarosite, natrojarosite, alunite, gypsum, melanterite, hemimorphite, Mn oxides, hydrobasaluminite, anglesite
Common residual cements within hardpans and cemented layers	goethite, lepidocrocite, ferrihydrite and siliceous material

If over time the soluble salts are completely removed and the highly porous framework of the hardpan maintained, re-exposure of the sulfide grains within the hardpan may produce additional secondary minerals through the same oxidation processes which originally took place. The resultant secondary minerals infill the open pore structure. This infilling may reinforce the surface hardpan, however field observations suggest that the surface may become soft, eventually resulting in the total loss of the initial hardpan (e.g. Elura).

8.3 Ability of Naturally Developed Hardpans and Cemented Layers to inhibit AMD, Contaminant Generation and Transport and Dusting

The parameters which determine whether hardpans and cemented layers are effective at reducing AMD generation, contaminant transport and dusting include cement permeability, porosity and stability. To inhibit AMD and contaminant generation, oxygen and water penetration into the tailings must be restricted. Oxygen penetration into the tailings is dependent on the gas diffusion rate which is primarily dictated by the air-filled porosity of the surface. Water penetration is dictated by the permeability which in turn determines the contaminant transport. Dust suppression simply requires a strong well cemented substrate which is erosion resistant.

All recent studies which have reported the presence of discrete, geochemically precipitated layers, propose a decrease in the movement of oxygen, water and dissolved metals through the tailings and a consequent moderation of the environmental impacts. In many of the studies it was recognised that hardpan development has the ability to decrease levels of heavy metals by incorporation into cements. The limited results presented in previous studies indicate that up to on order of magnitude reduction in permeability has been achieved through hardpan development. However in many of these cases similar permeability results for old tailings with hardpans at depth and new tailings were recorded. The only porosity measurements reported were from the Heath Steele site where the total porosity of the hardpan and tailings were similar, while the air-filled porosity of the hardpan was substantially reduced (Blowes et. al. 1991).

Permeability and porosity characteristics of naturally occurring hardpans and cemented layers investigated during with study were highly variable. In a number of cases a reduction in permeability and total porosity of the hardpan compared with fresh tailings was observed, however this was not a universal trend. Variability was attributed to age and state of hardpan degradation, preferential flow paths down desiccation cracks and shear planes produced during drying, and the heterogeneous nature of tailings i.e. grain size distribution resulting from deposition.

As total porosity was not universally reduced during cementation, moisture retention characteristics were used to investigate whether transformations in pore size distribution occurred. These results combined with SEM investigations indicated that the changes which occurred were site specific relating to the initial

grain size distribution and the mineralogy of the various fractions. Investigations of the CSA and Elura hardpan and tailings showed that during cementation a reduction in the number of the smallest pores occurred. The effect these changes had on water movement at the surface was examined by modelling the relative hydraulic conductivities and analysis of chloride and deuterium levels throughout the profiles. These investigations indicated that the variations in pore size distribution which occurs during hardpan development does did not significantly alter the evaporative process, thus has little direct effect on saturation levels.

The effect of porosity and moisture levels was further examined at the Elura and CSA sites by gas diffusion investigations which included modelling, sampling of CO_2 and laboratory testing. The Reardon & Moddle (1985) method was employed to calculated gas diffusion rates based on total and air-filled porosities. Direct measurements of diffusion rates were also undertaken. The simplistic Davis and Ritchie (1986) conceptual model was then utilised to model depths to the oxidation front based on these diffusion rates, which were compared with actual depths observed in the field. The results obtained indicated that the hardpans or tailings directly underlying the hardpans are maintaining water-filled porosities sufficient to substantially reduce oxygen infiltration and thus oxidation of the underlying tailings. Carbon dioxide concentrations within these profiles also indicated that upward diffusion of gas has been inhibited.

Similar tests were carried out at the Heath Steele site by Blowes et. al. (1991) and within the Malartic tailings by Tasse et. al. (1997). As with the CO_2 profiles investigated at Elura and CSA, CO_2 accumulations had taken place beneath the hardpan. Direct O_2 measurements were also taken. Within the Malartic tailings, O_2 concentrations terminated at the depth of the hardpan, whereas within the Heath Steele tailings, O_2 concentration terminated above the observed hardpan and thus the hardpan had no effect on O_2 infiltration at the time of sampling. Gas diffusion modelling of the Heath Steele hardpan indicated that diffusion was substantially inhibited. This was not due to a decrease in total porosity, rather a decrease in air-filled porosity similar to that observed in the CSA and Elura hardpans.

The geochemical investigations at the CSA and Elura sites indicate that the hardpans, especially at the CSA site, are not completely sealing the surface. The hardpans are however suppressing solute development through formation of cement coatings on both sulfide and gangue minerals, reducing oxidation and dissolution reactions and through the incorporation of potential contaminants into cements. The extent to which this occurs is influenced by the surface morphology and climatic conditions (wind/water), which effect the integrity and stability of the hardpans. It has been observed that the hardpan surfaces are dynamic, with a cyclic existence of cementation, chemical or mechanical degradation, re-exposure of underlying tailings and re-cementation. The effect this cycling has on acid and solute generation is dependent on the reactivity of the tailings and thus how long it takes for hardpan development to occur.

Thus naturally occurring laterally extensive surface hardpans have the ability to suppress oxygen infiltration through elevated moisture contents, thus inhibiting AMD and pollutant generation. They also have the ability to lessen solute generation through primary mineral coatings and incorporation of contaminants into cements. The long term stability of these surfaces still remains uncertain, and additional research is required to ascertain conditions necessary for the development of more stable cements such as silcretes and ferricretes.

8.4 Development of Artificially Enhanced Hardpans and their ability to inhibit AMD, contaminant generation and transport and dusting.

The variability observed within the naturally occurring hardpans, suggests that their use for restricting long term AMD, contaminant generation and transportation and dusting is questionable. It is for this reason that the use of additives to hasten hardpan formation and to increase long term integrity has been investigated. As with the naturally developed hardpans and cemented layers a successful artificially enhanced hardpan requires low permeability and porosity characteristics while maintaining a strong resistance to physical and chemical erosion.

Artificial enhancement of hardpans has been investigated in the past with limited success. Ahmed (1991, 1994 & 1995) studied hardpan development by electrochemical techniques and chemical additives, attempting to grow adherent and protective asphalt films on sulfides and through the production of goethite type structures. Chermak and Runnells (1995) produced hardpans in column tests through surface amendments of limestone and/or lime, with reductions in permeability by up to 3 orders of magnitude being recorded. Similar reductions in permeability were achieved using the self-healing/self-sealing cover system produced by McGregor et. al. 1997. Pore gas measurements were also carried out on the self-healing/self-sealing covered tailings and showed a marked decrease in O_2 concentration below the barrier and accumulations of pore gas CO_2 within the barrier. The calculated diffusivity of the pore gas O_2 was reported at 1/1000 that of the overlying tailings. This was achieved not through the reduction in total porosity, rather a reduction in air-filled porosity due to saturation conditions.

During this study both solid and liquid additives were incorporated with tailings and produced hardpans of varying quality. Liquid additives were successful as a method of artificial hardpan development but this technique was not pursued because of the perceived problems associated with dissolution of minerals along preferential flow paths and the associated potential instability of the dam structure.

In this study solid additives were utilised in large scale column tests, as discrete layers and surface mixtures with tailings. Solid additives of lime and flyash as a surface mixture with tailings was the most successful cementing additive type within all tailings trials. The flyash and lime layer trials were also

successful but to a lesser extent. Cementation in both cases resulted from the development of very fine-grained Al, Ca and Si cements throughout the additive zone. Variable elemental signatures were observed during SEM investigations inhibiting characterisation of the cements. It is assumed that these cements are predominantly calcsilicates at varying stages of formation. The phosphate and lime mix and lime mix trials produced cements, but in selected trials only.

Similar investigations of permeability, porosity, moisture content and CO_2 concentrations along with pore connectivity testing were carried out on the artificially developed hardpans. Based on permeability and total porosity characteristics alone, the calcsilicate cements within both the layer and surface mixtures of lime and flyash, did not have the ability to suppress AMD and contaminant generation. Permeability was reduced in 2 out of the 3 lime and flyash surface mixture trials. The flyash and lime layer trial did not significantly change the permeability characteristics, but did however produce very low air-filled porosity results indicating its potential to reduce oxygen diffusion.

The only additive which exhibited a universal reduction in permeability was the phosphate mix with tailings which also reduced total porosity in 2 out of the 3 trials. This reduction in permeability and porosity was due to packing rather than cement development. The lack of cementation allowed dewatering, consolidation and desiccation forces to take place resulting in repacking of the tailings. These forces were unable to take place within the flyash and lime trials as cementation took place rapidly, solidifying the tailings and additives into an open pore structure. Various flyash and lime trials did however show elevated CO_2 build up beneath the additive zone suggesting inhibition of gas movement, while elevated water contents within the underlying tailings and a reduction in pore connectivity suggests that modification of additive quantities may result in successful artificial hardpan development.

To obtain a reduction in permeability and porosity, an addition of phosphate rock could be used if a local, inexpensive source was available. There are many phosphate deposits around Australia, most are small or low grade with the exception of the deposits within the Georgina Basin. Many of these deposits have more than 100M tonne reserves (Costin and Williams, 1983). However in most cases around Australia an immediate source is not available and economic constraints inhibit transportation. As much of Australia has low rainfall, the use of flyash and lime as a surface mixture is equally viable. At these locations a surface application is required which has the ability to store rainfall, inhibiting vertical transportation of contaminants, while remaining resistant to both wind and water erosion.

8.6 Research Recommendations

The naturally formed tailings hardpans are unlikely to be stable to physical and/or chemical break down, as they do not form persistent indurated layers similar to naturally occurring ferricretes, calcretes and silcretes which are both resistant to erosion and have low porosity and permeability. The requirement is therefore to form such cements at a rate commensurate with environmental management. The use of flyash and lime may be an inexpensive source of Si, Al and Ca for these cements, however the ratios to obtain the characteristics required, while maintaining a cost effective method of decommissioning need to be addressed.

The trials carried out during this study have produced a platform for additional research to obtain reductions in permeability and porosity, while ensuring long term stability of the cements. Additional research using column testing should be carried out over a longer period to allow the geochemical reactions to evolve further, giving insight into the long term stability of the cements developed. Field studies, including large scale trials, would allow determination of long term stability and techniques for additive mixing and deposition to minimise variations in cement morphology.

Appendix 1A : Methods

Descriptions of field and laboratory sample collection, along with colour and texture determination have been previously outlined in Chapter 3.

1A.1 Physical Chemistry

Samples were initially prepared for pH, EC and ICP measurements using the standard 1:5 sample to water dilution, and agitated for 1hr (McDonald et al. 1984).

1A.1.1 pH

A Radiometer-Copenhagen:TTA80 instrument was used to achieve measurements of pH which were displayed on a PHM Ion meter. Method A was selected for acidic samples. The electrode was stabilized using previously used buffer solutions, then calibrated using new pH 7 and pH 4 buffers. pH values for each of the solutions were then obtained.

1A.1.2 Electrical Conductivity (EC)

A Radiometer-Copenhagen CDM 83 Conductivity Meter was used for EC measurements. The analysis equipment consists of 3 platinum electrodes which were initially stabilized using previously used KCl solution and then calibrated using new KCl solution. The cell constant was changed to achieve required calibration.

1A.1.3 Redox Potential

Redox Potential (Eh) was measured with an IONODE combined platinum/silver - silver chloride electrode connected to a HANNA HI 8521 instrument and was used in an argon filled glove box (oxygen excluded). All readings were adjusted to the standard Hydrogen electrode reference.

1A.2 Mineralogy

1A.2.1 X-ray Powder Diffraction

Finely ground powders of samples were lightly pressed into aluminum sample holders to achieve random orientation of the mineral particles for XRD analysis. Measurements were made using a Philips PW1800 microprocessor-controlled diffractometer with Co K alpha radiation, variable divergence slit, and a graphite monochromator. The diffraction patterns were acquired in steps of 0.05° 2θ with a 1 second count time per step. Data were logged to permanent files on an ABM PC/XT and subsequently analysed using a software package XPLOT developed by Raven and Self (1988).

1A.2.2 Microscopic examinations

Fragments of unground tailings and hardpans were inspected by reflected light in a Wild Makroscop M420 microscope. Selected small fragments were carbon-coated and examined in a Cambridge

Stereoscan 250 Scanning Electron Microscope (SEM) operating at 20 kV. The elemental composition of particles located in the SEM was determined with Link energy-dispersive X-ray (EDX) microanalyser attachment. Cemented tailings thin sections were also made. All tailings samples were impregnated with resin prior to slide making because of their friable nature. Initially the slides were observed under the reflected light microscope and specific regions identified for Microprobe analysis.

1A.2.3 Sulfate/Sulfide Determination by HCl - HNO_3 Extraction

Modified from Burns (1969)

Objective

To determine the sulfide and sulfate quantities within a sample, thus obtaining a better understanding of the oxidation condition and acid mine drainage potential of the material. A similar method has been used for many years in the U.S as a standard procedure.

Equipment

250ml conical flasks
Hot plate
No. 54 filter paper
funnels
100ml beakers
ICP tubes

Reagents

5N HCl
2N HNO_3
distilled water

Procedure

1. Pulverise samples using a tungsten mill until a uniform silt size is obtained. From subsequent SEM examination, most of the particles were below silt size (20μm) and all were less than the 75μm (200 mesh, Tyler) recommended by Coastech Manual (1991).
2. Select approximately 1g of sample for total sulfur analysis by LECO furnace method.
3. Weigh 2g of each sample into 250ml conical flasks and add 50ml 5N HCl (492ml conc HCl added to 508 ml water). Bring samples to the boil on hot plate at approximately 150°C and boil for 15 minutes.
4. Filter samples whilst hot through No. 54 filter paper. Retain approximately 10-12mls of sample for ICP analysis. Transfer the residue solids to filter papers using minimal water. Wash samples twice with 2ml 5N HCl each time. Then washed 6 times using distilled water. Allow samples to air-dry overnight. Retain approximately half of the solid for total sulfur analysis.
5. Transfer residue to 250ml conical flasks, add 50ml 2N HNO_3 (125ml conc HNO_3 added to 875ml distilled water). Bring samples to the boiled on the hot plate for 30 minutes and then filtered as in 4), retaining 10mls for ICP, then washed well. Air-dry residue and submit for total sulfur analysis.

1A.3 Chemistry

1A.3.1 Solute concentration determination - Inductively Coupled Plasma Atomic Emisson Spectrometry

As mentioned previously ICP analysis was undertaken in conjunction with pH and EC measurements using a standard 1:5 batch leaching of tailings with water. In the laboratory, sub-samples were removed for analysis to ensure contamination from pH and EC testing did not occur. Elemental analysis by inductively coupled plasma atomic emission spectrometry (ICPAES) against standards of an appropriate matrix was undertaken in the Analytical Chemistry Unit, CSIRO, Division of Land and Water, Urrbrae, S.A.

1A.3.2 X-Ray Fluorescence Major and Trace Elemental Analysis

The 'grab' weight method was employed in the preparation of the samples for major and trace element analysis. This involved accurately weighing approximately 1g of each of the finely ground oven dried (105°C) powders into glass vials with approximately 0.3g $NaNO_3$. The mixture was transferred to a Pt-Au crucible and preoxidised in an oven set to 750°C for 15 minutes. The preoxidised material was then fused into a homogeneous glass over an oxy-propane flame at a temperature of approximately 1050°C and the molten material was poured into a 32 mm diameter Pt-Au mould heated to a similar temperature. The melt was then cooled by air jets for approximately 30 seconds. The resulting glass disks were analysed on a Philips PW1480 XRF system using a control program developed by Philips. SO_3 errors are quoted for 1% and 30% as these were the ranges of S content encountered.

Error Determination for fusion Analysis

The errors quoted below for each component are the standard deviations based on standard rock compositions. Trace element errors are quoted for < 200 ppm and > 200 ppm.

Component	<200 ppm	>200 ppm	Component	<200 ppm	>200 ppm
SiO_2 (%)	-	0.24	Ni (ppm)	5.00	6.00
Al_2O_3 (%)	-	0.15	Rb (ppm)	4.00	5.00
Fe_2O_3 (%)	-	0.07	Ba (ppm)	14.00	40.0
MgO (%)	-	0.07	V (ppm)	4.00	7.00
CaO (%)	-	0.06	Cr (ppm)	7.00	10.0
Na_2O (%)	-	0.06	La (ppm)	18.00	21.0
K_2O (%)	-	0.03	Ce (ppm)	9.00	17.0
TiO_2 (%)	-	0.02	Pb (ppm)	6.00	6.00
P_2O_5 (%)	-	0.004	Y (ppm)	3.00	4.00
MnO (%)	-	0.005	Co (ppm)	3.00	3.00
Ga (ppm)	3.00	3.00	Cu (ppm)	11.0	11.0
U (ppm)	5.00	7.00	Sr (ppm)	3.00	7.00
Th (ppm)	5.00	7.00	Zr (ppm)	9.00	11.0
SO_3 (%)	0.003 (1%)	0.05 (30%)	Zn (ppm)	6.00	7.00

1A.3.3 Acid - Base Accounting

1A.3.3.1 Net Acid Generation - Performed by CRA-ATD

This method is used in the study of acid rock drainage to determine quantitative net acid generation (NAG) values. Method used CRA -ATD Method No. ATD-ES-CA-510.

Reagents

30% hydrogen peroxide
15% hydrogen peroxide
pH 4 & 7 buffer solutions
saturated (4M) potassium chloride

Apparatus

2L container
500ml conical beakers
data logger
magnetic stirrers
magnetic fleas
filter papers, millipore filters
glass funnel
250ml volumetric flasks
hotplate
pH meter and probe
temperature probes
watchglass

Procedure

1. Accurately weigh out approximately 2.5g of sample into conical beakers, add a magnetic flea to each beaker
2. Place in fume cupboard, setup magnetic stirrers, data logger, pH and temperature probes
3. Measure 250ml of 15% H_2O_2 into each of the individual beakers
4. Log temperature and pH values over and 24hr period, recording the final values.
5. Filter sample through filter paper, using a funnel, if filtrate still cloudy, filter solution again through a 5.0μm filter using the all glass millipore filtration unit
6. Quantitatively transfer filtrate to 500ml conical beakers, place on hot plate and boil the filtrate for 1 hr, ensuring the beaker is covered with a watch glass
7. Remove from hotplate and allow filtrate to cool. If filtrate cloudy, filter solution again through a 5.0μm filter. Transfer filtrate to 250ml volumetric flask and make up to the mark with milliQ water
8. Titrate acidity using ATD method ca-410.doc

Calculations

Determination of NAG Value

$$NAG = \frac{250*[H_2SO_4]}{\text{sample mass}} \quad \text{kg } H_2SO_4\text{/tonne}$$

NB. *acid concentration in g/l*
sample mass in grams

1A.3.3.2 H_2O_2 Modified "Acid Neutralising Capacity" - Performed by CRA-ATD

Method used CRA -ATD Method No. ATD-ES-CA-470.

The hydrogen peroxide (H_2O_2) Modified - Acid Neutralising Capacity (ANC) is a measure of the buffering capacity, or inherent neutralising capacity, of a soil material. The ANC is often due to presence of carbonate materials, however, it can also originate from any material that has the ability to reduce the acidity of soil leachate. The neutralisation capacity can be over estimated because some Fe^{2+} released may be incompletely oxidised to Fe^{3+} (due to the presence of materials such as siderite or pyrrhotite). The incomplete oxidation of Fe^{2+} may also cause the endpoint of the back titration to be unstable. This procedure was developed in an attempt to ensure greater oxidation of Fe^{2+} to Fe^{3+} via the use of H_2O_2.

Reagents

Certified Grade, 0.1M HCl, for standardisations of bases
0.1M NaOH, standardised
0.5M NaOH, standardised
0.1M HCl, standardised
0.5M HCl, standardised
25% HCl, for fizz tests
30 wt% H_2O_2

Apparatus

Aluminium foil
250ml Erlenmeyer flask
hot plate
2 Burettes, 50 or 100ml
pH meter and probe
millipore filtration apparatus and filter papers

Procedure

1. Use certified 0.1M HCl to standardise the 0.1M and 0.5M NaOH solutions, and then use the NaOH solutions to standardize the 0.1M and 0.5M HCl solutions respectively.

2. Perform the fizz test in fume hood. Place small amount of pulverised sample on a piece of aluminium foil, add 1-2 drops of 25% HCl to sample. The presence of carbonate materials is indicated by a bubbling or a audible fizz. A rating scale is given in Table 1. The Volume and Molarity of HCl for use in ANC determination is bases on Fizz Rate.

Table 1	Fizz Rating	HCl (mL)	HCl (Molarity)
	None	40	0.1
	Moderate	40	0.5
	Strong	80	0.5

3. Weight approx. 2.0g accurately (record exact mass) of pulverised sample into a 250mL Erlenmeyer Flask

4. Add the volume and molarity of HCl to flask as indicated by the fizz test, Table 1. Prepare blanks by adding the same volume and molarity into clean flasks. Blanks must be run for each volume and/or concentration of acid used.

5 Heat the mixtures, covered by watch glasses, on the hot plate in the fume hood at approx. 90°C, swirling the watch glass, on hot plate frequently. Reaction is complete when no further gas evolution is visible and particle settle evenly over the bottom of the flask.

6. Add milliQ water to make a total volume of approximately 125mL and boil contents for approx. 1 minute. Allow to cool to room temperature.

7. Add 5mL of 30wt% H_2O_2 and re-boil for 3-5 minutes, cool to room temperature.

8. If the solution has precipitate present - filter solution using a millipore apparatus and a 5μm filter paper.

9. Rinse burettes with required standardised NaOH solution that was indicated by the fizz test in Table 1. (same approx. molarity of NaOH in the burette as the HCl originally added to the sample).

10. Titrate the contents of the flask using standardised NaOH solution, until a constant reading of pH 7.0 remains for a least 30 seconds, using a calibrated pH meter. NB. If titration value is of 3mL or less is required to raise the pH to 7.0, it is unlikely that volume or concentration of acid was sufficient to neutralised all of the base present in the 2 gm sample - sample test should be repeated using HCl details assuming next higher 'fizz' rating, Table 1.

11. Titrate Blanks using NaOH solutions used in previous step.

Calculations

The ANC of the sample is given by

$$ANC = \frac{5.a.[x-(b/a).y]}{c}$$

where ANC = acid neutralising capacity in kg of $CaCO_3$ equivalent per tonne of material

a = molarity of HCl

b= molarity of NaOH

c= sample weight in gm

x = volume of HCl added in mls

y = volume of NaOH added to obtain pH 7.0 in mL

1A.3.4 Direct Extraction for Chloride Analysis

Chloride analysis was undertaken to obtain insight into the main mechanisms of water movement within the upper tailings (i.e. infiltration or evaporation).

Reagents

0.1M Barium Nitrate. Dissolve 104.5gm $Ba(NO_3)_2$ in deionised water and diluted to 4L

Apparatus

extraction containers, 125ml screw cap jars
solution dispenser
end-over-end shaking machine
10ml tube for auto analyser

Procedure

Weigh 10.0g of air drained <2mm sample into 125mL extraction jars. Add 50mL of 0.1M $Ba(NO_3)_2$ using an appropriate dispenser. Replace cap firmly to avoid leaking and shake end-over-end for 1 hour at 25°C. Allow to settle and transfer majority of liquid to centrifuge containers. Centrifuge samples at 2000 rpm for 20 minutes. Transfer clear liquid to 10ml auto analyser tubes, 2 per sample. Analyse using ICPAES.

1A.3.5 Isotope Analysis Extraction

Samples were distilled to obtain solutions for Deuterium analysis determined via gas chromatography.

Reagents

Kerosene
Wax Chips

Apparatus

Aiezotropic Distillation Apparatus
- heater
- gas collection system
- 500ml round bottom flasks

Procedure

Weigh approximately 5-10gm of wet sample into 500ml flasks. Add kerosene to approximately half fill the vessel.

Place the vessels into the distillation apparatus and boiled for approximately 1 hour or until all pore water is removed from the samples. Remove pore water from the condenser at regular intervals and place in small air tight jars.

Add wax chips to the samples to induce the removal of excess kerosene. Places jars in an oven at 20°C for approximately 1 hour. Once the wax is liquefied, remove the jars and place to cool on their sides. Remove sub-samples to be analysed in the gas chromatography unit.

1A.4 Geotechical Testing

1A.4.1 Particle Size Distribution

Method no. 11.1 from the CSIRO-ACU was used to perform this analysis. The procedure outlined below does not include the Pre-treatments for organic matter or highly calcareous materials as the samples tested did not require these treatments.

Reagents

Dispersant solution: weigh 200g sodium tripolyphosphate and 20g sodium carbonate into a beaker and add approx. 1.6L water, stir and then make up to 2L.

Apparatus

shaking bottles and machine
sedimentation cylinders
glass vials
sand vials
25mL pipette & pipetus (holder and pump)
glass siphon and U-tube
sand washing beakers
sand sieve

Procedure

Weigh 10g soil into a 250mL shaking bottle, add 10mL dispersant and half fill the bottle with water. Place bottles in an end-over-end shaker for 64hrs. After shaking, transfer the dispersed material into 500mL sedimentation cylinders in a 20°C constant temperature room. Make up to 500mL with water and allow to equilibrate.

Determination of Silt and Clay Particle (<20μm) fraction

Prepare the Pipetus by inserting a 25mL pipette and switch on. Prepare and pre-weigh a 30mL glass vial. Paddle the cylinder for 30 seconds vigorously at first to dislodge the soil pad at the bottom, then continuously up and down with the upward stroke reaching no higher than the 400mL mark. Insert the pipette carefully into the cylinder and hold it so the 104mm graduation is level with the surface of the

suspension. At time 5 mins draw up 25mL solution. Dispense the sample into the glass vial A. When all samples have been removed, clean the pipette, paddle the blank cylinder, sample 25mL and dispense into a Blank Vial. Place the vials into an oven at 105°C.

Determination of Clay Particles (<2μm)

Using the pipetus, place the pipette at the 75mm graduation mark level with the top of the soil suspension in the cylinder and take a 25mL sample 6 hours after paddling the cylinder for silt and clay. Dispense the sample into a glass vial Q and place in 105°C oven.

Determination of Coarse and Fine Sand (>20μm)

Pour or siphon off the remaining soil suspension from the 1st batch and use a wash bottle to transfer all the remaining residue to 600mL tall beakers. Place a 0-50°C thermometer into the beaker and fill with tap water. The settling time is temperature dependent so temperature measurements must be made eg. at 16°C the settling time is 5mins 20sec. After the required time has passed, siphon of the top 100mm of suspension. Repeat this timed washing until all the supernatant liquid is clear at the time when it should be siphoned off. With a smaller siphon, take off half of the remaining supernatant. Transfer the remainder of sample into the sieve and collection system. Place the retained contents into a pre-weighed polycarbonate Vial C and transfer the fine sand from the base into F vial. With the small siphon remove most of the supernatant in the vials and when all are complete, place in an oven at 80°C and leave until dry.

Calculations

After all sub-samples are oven dried, record their weights.
For 10g soil in 500mL sedimentation cylinder taking 25mL aliquot:

wt clay fraction = (wt of Q vial + fraction) - wt Q vial
% clay = (wt clay fraction - wt blank) x 200
wt silt + clay fraction = (wt of A vial + fraction) - wt A vial
% silt = (wt silt + clay fraction - wt clay fraction) x200
wt fine sand = (wt of F vial + fraction) - wt F vial
% fine sand = wt fine sand x 10
wt coarse sand = (wt of C vial + fraction) - wt C vial
% coarse sand = wt coarse sand x 10

1A.4.2 Gravimetric water content

Tailings were sub-sampled directly after exposure or extrusion. The sub-sample was weighed (W_w) and placed in an oven at 105°C for 24hr. The sample was then re-weighed after equilibrating in a desiccator for 24 hours (W_d). The water content expressed as a percentage of the oven dry weight was then calculated using the formulae:

$$w = ((W_w - W_d) / W_d) \times 100$$

1A.4.3 Particle Density

Australian Standards Method of testing soil for engineering purposes AS 1289.C5.1–1977

Apparatus

250mL density bottles

desiccator

drying oven

sieve

vacuum pump

Procedure

1. By riffling or quartering the material passing the 2.36mm sieve, obtain a sub-sample which will occupy about one-third of the density bottle.
2. Oven dry sub-sample at 105°C.
3. Pre-weigh the density bottles (m1), recording the weight of the bottle plus the stopper. After sample has cooled in a desiccator, weigh approx. 10g of sample into density bottles and record weight accurately (m2).
4. Add distilled water to fill the bottle to approx. two-third full and allow the soil particle to soak for about 24hr, under vacuum (lids removed).
5. Fill the bottle with distilled water, insert the stopper, dry the outside of the bottle, determine the mass of the bottle and contents (m3).
6. Empty the bottle and clean, fill the bottle with distilled water as necessary to maintain the water level, insert the stopper, dry the outside of the container and determine the mass (m4).

Calculations

Calculate the particle density ρ_s, g/cm^3

$$\rho_s = \frac{m_2-m_1}{(m_4-m_1)-(m_3-m_2)}\rho_w$$

m1 = mass of density bottle

m2 = mass of bottle and dry soil particles

m3 = mass of bottle, soil particles and water

m4 = mass of bottle when full of water

ρ_w = density of water at temperature of test

If the two particle density (ρ_s) results differ by more than 0.03, discard the results and repeat the tests.

1A.4.4 Bulk Density Determinations

The following procedure was used to determine the Wet and Dry Bulk densities of the tailings samples:

Undisturbed samples of know volume were removed from the sample cores or directly from laboratory column experiments. Sub-samples were also taken to determine the water content, immediately after extrusion or exposure. The Dry and Wet Bulk densities were then calculated using the following formulae:

Dry Bulk Density (γ_d)

$\gamma_d = 100 \times \rho_s / (100 + (w \times \rho_s)$

Wet Bulk Density (γ_w)

$\gamma_w = \gamma_d / (100 + w) / 100$

where

ρ_s = particle density

w = Gravimetric water content expressed as a percentage of oven dry weight

1A.4.5 Void Ratio and Porosity Determinations

The void ratio and porosity values were calculated using the following formulas:

Void Ratio (e)

$e = w \times \rho_s / 100$

Porosity (n)

$n = e / (1 + e)$

1A.4.6 Moisture Characteristics - Pore Size Distribution

Method outlined by Loveday, 1974. Experiment to determine the moisture characteristics of a sample, delineated by successive equilibrium of sample waters, and measurement of the moisture content retained at matric suction levels between 15-600 kPa.

Apparatus

plastic or steel cores (approx. 2.5-3cm diameter, 1.5-2cm high)
thin cloth large enough to cover core bases tied with rubber bands
ceramic suction plates with hanging water column control of suction

Procedure

1. Prepare cores by attaching a thin cloth to base of cores with a rubber band. Weigh core, rubber band and wet cloth. Separately, saturate sample and transfer required quantity into core, almost filling to surface, weigh sample filled core.

2. Set suction of the draining plates to the lowest value to be used in the determination of the moisture characteristic curve. Place cores on the suction plates ensuring complete contact.
3. Allow sample to reach equilibrium for a number a days depending on level of suction.
4. Carefully transfer core to a balance and record weight
5. Replace sample on suction plate, change suction to required intensity.
6. Repeat steps 3, 4 & 5, until all suction levels are completed. Oven dry samples at 105°C for 24hrs and re-weigh.

The procedure for clods of sample is the same, however when wetting up the clod, the sample must be evacuated using a vacuum for up to 1 day or until all gas has been expelled. Additionally a water saturated fine grained silica powder is usually used to coat the suction plate to sustain contact between sample and suction plate.

Calculations

Determine gravimetric moisture content for each suction level

gravimetric moisture content (%) =

$$\frac{\text{(wet sample wt + core wt) - (dry sample wt + core wt)}}{\text{(dry sample wt + core wt) - (core wt)}} * 100$$

Determine volumetric moisture content for each suction level

volumetric moisture content (%) =

gravimetric moisture content (%) x particle density

Determination of pore size drained at specific suctions:

pore size = 0.3 / suction (kPa)

The differences in moisture content between successive suctions, indicates the amount of water drained from the specific pore sizes, and thus gives a direct indication of the quantity of that pore size within the sample.

1A.4.7 Permeability Tests

1A.4.7.1 Falling Head Infiltration Tests

Field Testing

Single ringed infiltrometer tests were carried out in triplicate. For this test a 500mm diameter steel ring was used. When tests were carried out on fresh tailings this ring was pressed 100mm into the surface, however when testing hardpan surfaces, the ring was sealed to the surface using bentonite clay. Once in place a cloth was placed over the surface to minimise disturbance, as the ring quickly filled with water. The rate of water infiltration was measured by means of a straight edge ruler set at a 1:10 slope to magnify the change in water depth. Initially measurements were taken at 15 second intervals and depending on the rate, these time intervals were extended. Results were calculated as a simple average of the rates of infiltration measured over each time interval.

Permeability (m/s) = change in water depth (m) / time (s)

Laboratory Testing

Infiltration tests were carried out on each of the columns. Water was added to the top of the tailings filled column and the water infiltration rate was measured by means of a ruler set against the edge of the column. The measurements and calculations were the same as presented above.

1A.4.7.2 Field Permeameter Tests

Reagents

acid washed sand

RO water

Apparatus

disk permeameter

stainless steel ring

Procedure

Select a flat area and using the ring establish a round, flat ring of sand. Remove the ring ensuring the sand bed is not disturbed.

Check the water supply potential of the permeameter and record the value. Assemble the Permeameter ensuring that the base plate has been immersed in water for at least 12 hours. Fill the permeameter with water removing any excess water from the apparatus. The water level in the large supple tube L_o should be recorded as the zero reading.

Place the permeameter on the sand bed, start timing as soon as the sand is wetted through. Record the level of water in the tube at regular short intervals. Continue making measurements until ten constant measurements are obtained. Calculate Permeability via

P = Area of tube / Area of Disk x q

$= (\pi r_t^2 / \pi r_d^2) \times q$

where q = volume flow rate (mm^3h^{-1})

r_d = radius of supply disc (mm)

r_t = radius of supply tube (mm)

1A.4.7.3 Laboratory Oedometer Tests

Oedometer tests allow permeability to be calculated from the direct measurements of water outflow rates under a range of hydraulic heads. Modified oedometer cells in loading frames allowed saturated samples to be tested at varying vertical stresses.

Sample Preparation

Bulk samples were sub-sampled and prepared to approximately plastic limit by mixing with deionised water.

Preparation of Apparatus

Oedometer cells (Fig 3A.1) were installed with 20μm porous steel base plates. The plates were saturated by soaking in deionised water under vacuum. A 76mm inside diameter ring (64mm high) was installed above the base-plate. The bottom outside edge was sealed with silicone sealant to provide a water tight sample chamber. Plastic tubing was connected to both outlet ports, with a tube on one side being connected to a sample collection container. As required, the outlet ports were closed by clamping the plastic tubing.

Procedure

1. A quantity of sample was weighed and added to the sample chamber. The quantity added was determined by estimating the amount required to yield a sample thickness of approximately 20mm when consolidated.
2. The cell was assembled, placed in the load frame and deionised water was introduced through a port in the cell lid to saturate the sample. The outlet ports were unclamped to allow free drainage of the sample. Outflow was determined by weighing the pre-weighed sample collection containers at regulated periods depending on flow rate. Sample collections and weighing continued until a constant flow rate was achieved.
3. The cell was then loaded with 250gm to achieve a vertical stress of 5.3 kPa. Sample consolidation was monitored using a dial gangue micrometer. After approximately twenty minutes, (or when it was apparent that consolidation had leveled off) water was added through the port in the cell lid as required. Outflow was again determined.
4. The cell was loaded with additional weights of 1lb and 2lb to achieve loads of 9.7 and 19.4 kPa respectively. Consolidation rates and outflow rates were measured at each loading.

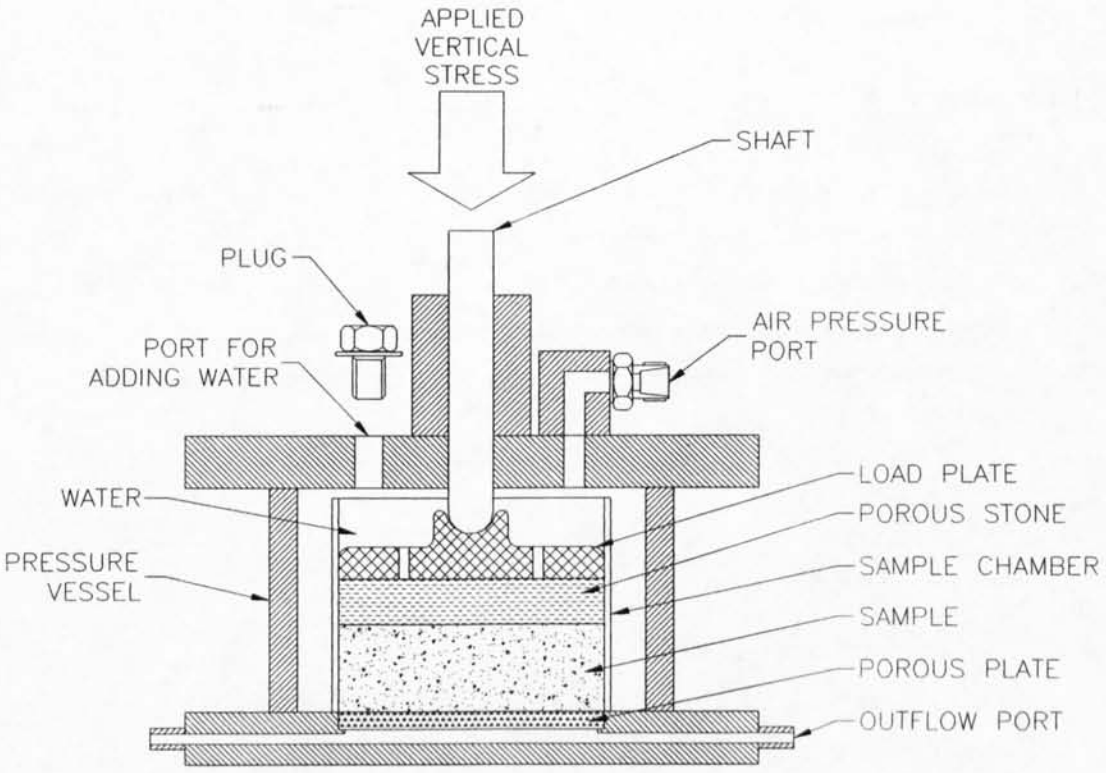

FIG 1A.1 SCHEMATIC DRAWING OF OEDOMETER CELL

1A.4.7.4 Laboratory Constant Head Infiltration Tests

Constant Head infiltration tests were carried out on selected hardpan samples to determine their permeability.

Apparatus Preparation

PVC columns approximately 25cm high were made from varying diameter piping depending on sample size. Drainage holes were drilled into PVC caps of the required diameter and 10cm tubing was attached to these base caps. The columns were placed onto a frame to allow free drainage and collection in pre-weighed beakers.

Sample Preparation

Hardpan samples were cut using a disk grinder to the required cylindrical shape for each column. Silicone sealant was then used to seal the shaped hardpan into the base of the PVC column. The sealant was allowed to dry for 2 days.

Procedure

A mark 2cm from the top of each column was made as a water level mark. Water was added to this level and maintained through out the entire experiment. Outflow was collected at regular intervals depending on flow rate, in pre-weighed beakers and weighed. Collection and weighing was undertaken until a constant flow rate was attained.

1A.5 Gas Analysis

1A.5.1 Gas Sampling

Gas samples were removed using a hollow stainless steel rod with a porous filter directly above the driving tip (Fig 3A.2). A removable driving head was attached to the top of the rod when hammering was required to force the rod through the profile. An exterior needle and syringe system was coupled to an interior tube which was connected to the porous panel, allowing gas samples to be collected at the required depths. Gas samples were then placed in evacuated glass vials through caps which incorporated septums.

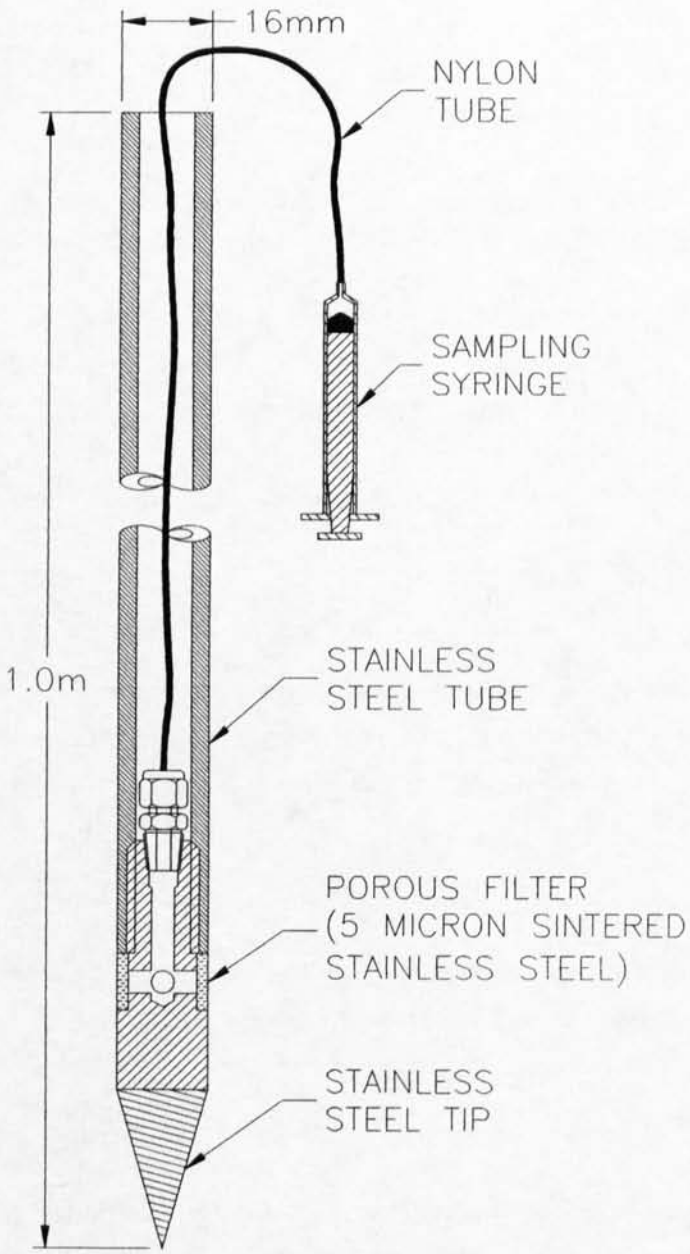

FIG 1A.2 SCHEMATIC DRAWING OF GAS SAMPLING ROD

1A.5.2 CO_2 Concentration Determination

Sub-samples of gas were removed using a syringe through the septum of glass vials. This gas was then expelled into a gas chromatography unit previously calibrated using a selection of CO_2 concentrations similar to those of the sample gas. The amount of gas added was directly related to the concentration of CO_2 within the sample. The analysis was repeated if concentrations higher than the calibration levels were encountered. This was achieved through the addition of reduced gas quantities. Peak heights were recorded and back calculations from control samples were used to determine CO_2 concentrations.

1A.5.3 Diffusion Measurements (performed by ANSTO)

Gas diffusion measurements were carried out on selected hardpans to obtain further insight into gas movement within the tailings profile.

These measurements were carried out by members of the ANSTO staff in particular Phil Layton a vacation student employed over the summer of 1997-1998. A booklet outlining the methods employed was constructed and is available from ANSTO - *Procedures in measuring Gas Diffusion rates through Porous Media: an example, Phil Layton, February, 1988.* The following is a brief outline of the procedures detailed in the manual.

Apparatus

Preparation of the testing column

1. The apparatus used for testing gas diffusion rates should ideally be a cylinder and have an airtight seal at both ends.
2. The sample must be mounted into the cylinder so that the sample acts as a barrier between two compartments of air that are of similar volume (Fig 3A.3). Therefore any movement of gas from top to bottom or vice versa needs to pass through the sample. Depending on the apparatus, the sample may need to be fastened to the column using an appropriate resin or glue.
3. Four ports must be constructed, two on each side of the apparatus. The top two ports are used for sampling and sample recycling. The sample is taken from one port to the gas chromatograph for analysis, and then recycled back into the apparatus so that a vacuum is not created, which would pull the tracer gas through the sample. The bottom ports are a tracer gas injection port and a pressure relief port.

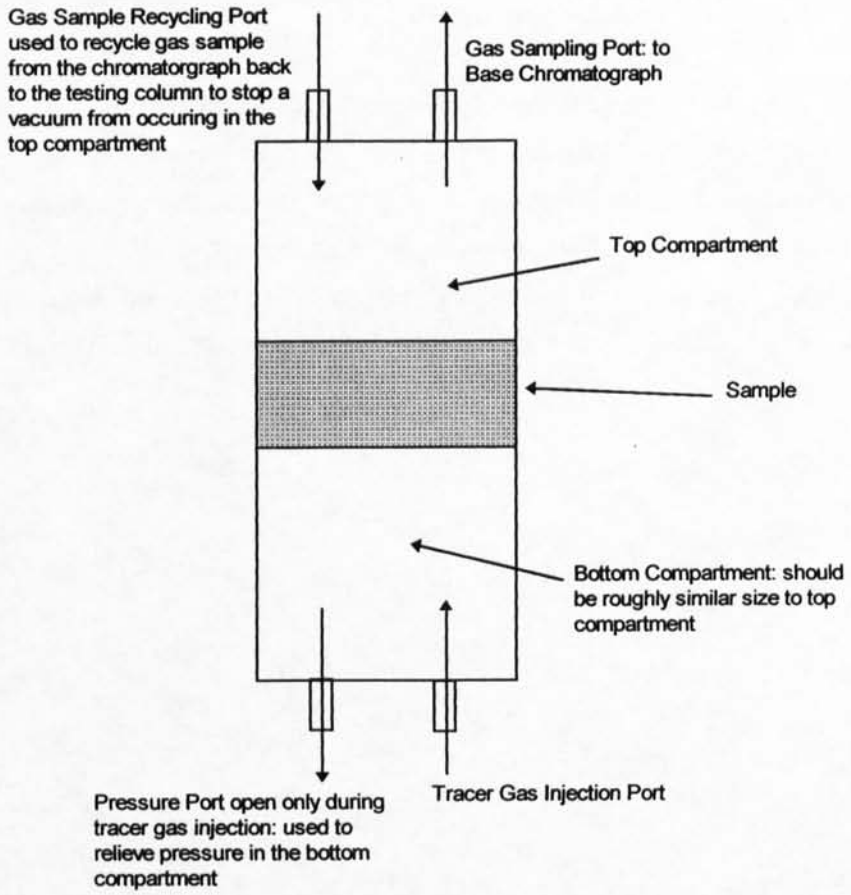

FIG 1A.3 COLUMN SETUP FOR DIFFUSION MEASUREMENTS

The Gas Chromatograph

1. A MTI P200 Portable Gas Chromatograph was used to measure gas concentrations. The carrier gas used was Argon.
2. The chromatograph was equipped with two columns; column A was used for oxygen and methane, while column B was used for carbon dioxide.

The Computer Program

1. The chromatograph was connected to a computer through the serial port on the back of the chromatograph.
2. The program used for analysis was called EZChrom 200, compatible for this particular chromatograph.

Procedures

Injection of the tracer gas

1. The three tracer gases used were oxygen, carbon dioxide and methane.
2. The tracer gas was injected into the bottom compartment of the testing apparatus for a period of 30 to 60 seconds, depending on the volume of the bottom compartment. The pressure relief port was

kept open during the injection. After injecting the tracer gas, the pressure relief port was closed, the injection wire was clamped, and the chromatograph program started.

3. The apparatus and column was flushed between tests.

Chromatograph Results

1. For all tests, a concentration/time curve was generated using the percentage composition values for each sample, and the time at which each sample was taken.
2. Once concentration/ time curves were generated, the curves were then modelled.

Modelling

The PDE2D program

1. The program used for modelling was called PDE2D. The program solves partial differential equations in space.
2. After generating concentration/time curves for the samples, the diffusion coefficient was determined. A modelled concentration/ time curve was created that was the line of best fit for the experimental concentration/ time curve. This is done by manipulating the RLMDA (the tortuosity factor) and UOO (full name not given) for the tracer gas in the bottom compartment.

The effective diffusion coefficient (D) was determined using the formula:

$$D = RLMDA \times DB$$

where RLMDA = the tortuosity factor

DB = diffusion coefficient of O_2 in air (813.6 cm^2/h)

Appendix 2A Tailings Dam Geochemistry

2A.1 Kanmantoo Trough, S.A

2A.1.1 Brukunga Pyrite Mine

The upper 1m of tailings at Holes 4, 5 and 7 at the Brukunga Mine were analysed for solute concentrations. The pH of these upper tailings ranged from 3.5-4.5, with a minimal increase in pH with depth (Fig 2A.1). The EC ranged from 0-1.5 mS/cm and generally decreased with depth (Fig 2A.1). The solutes at this site consist mainly of Ca and S with lesser Al, Fe, K, Mg, Na and Zn (Table 2A.1). The Ca and S trend mimic the EC profile suggesting the most abundant soluble salt producing these concentrations is gypsum. Gypsum was observed throughout the upper profile, where it consolidated and produced cementing properties.

A general increase in concentration with depth was observed for Al, Co, Cu, Fe, Mn, Cd, Ni and Zn concentrations at all sampling locations (Figs 2A.2, 2A.3 and 2A.6). The Ca, K, Na, Mg and S profiles are variable (Figs 2A.2, 2A.4 and 2A.5). Variations of this kind are attributed to preferential elemental incorporation into cemented layers existing throughout the upper tailings. Ferrihydrite, jarosite and alunite were all identified as cementing agents at this site. These secondary minerals have the ability to scavenge elements, incorporating them within their structures or through adsorption processes. An extensive review of the geochemistry of the Brukunga site is presented in Agnew, 1994.

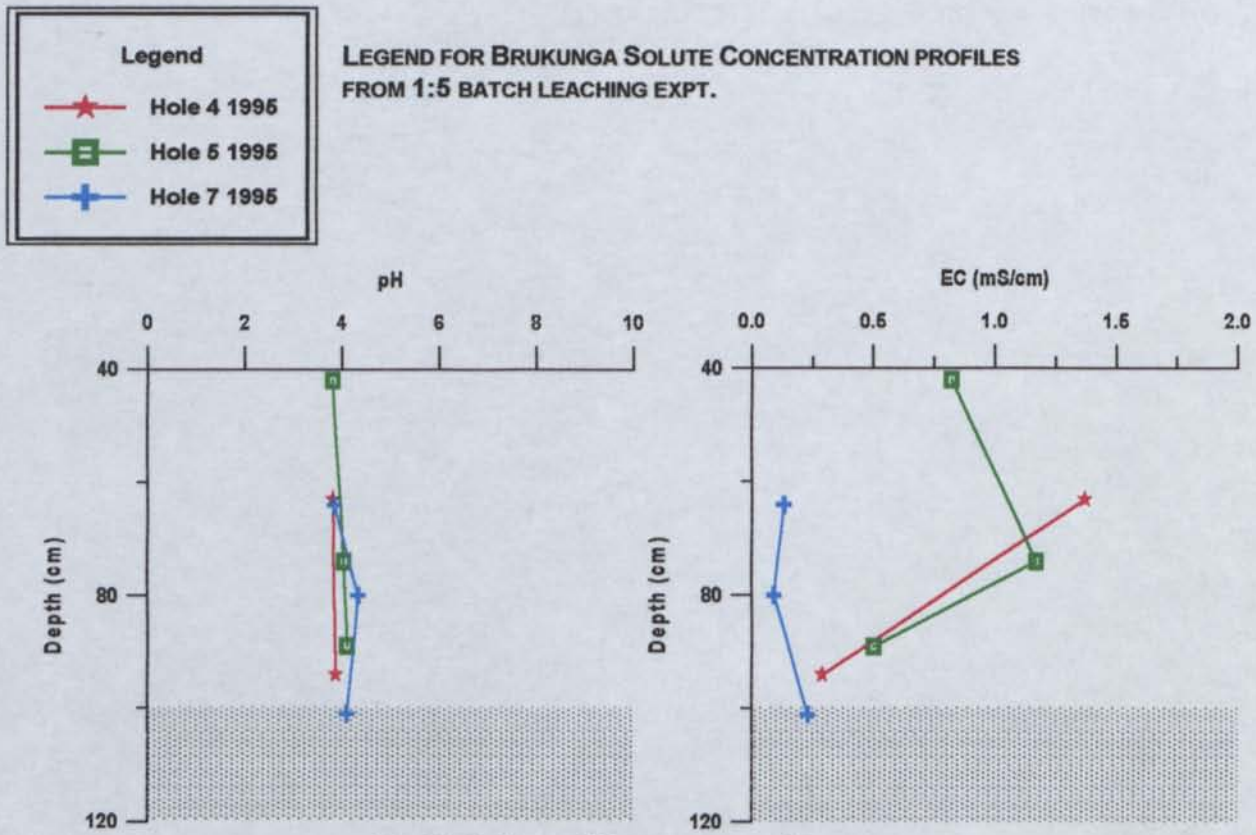

LEGEND FOR BRUKUNGA SOLUTE CONCENTRATION PROFILES FROM 1:5 BATCH LEACHING EXPT.

FIG 2A.1 pH AND EC PROFILES FOR BRUKUNGA

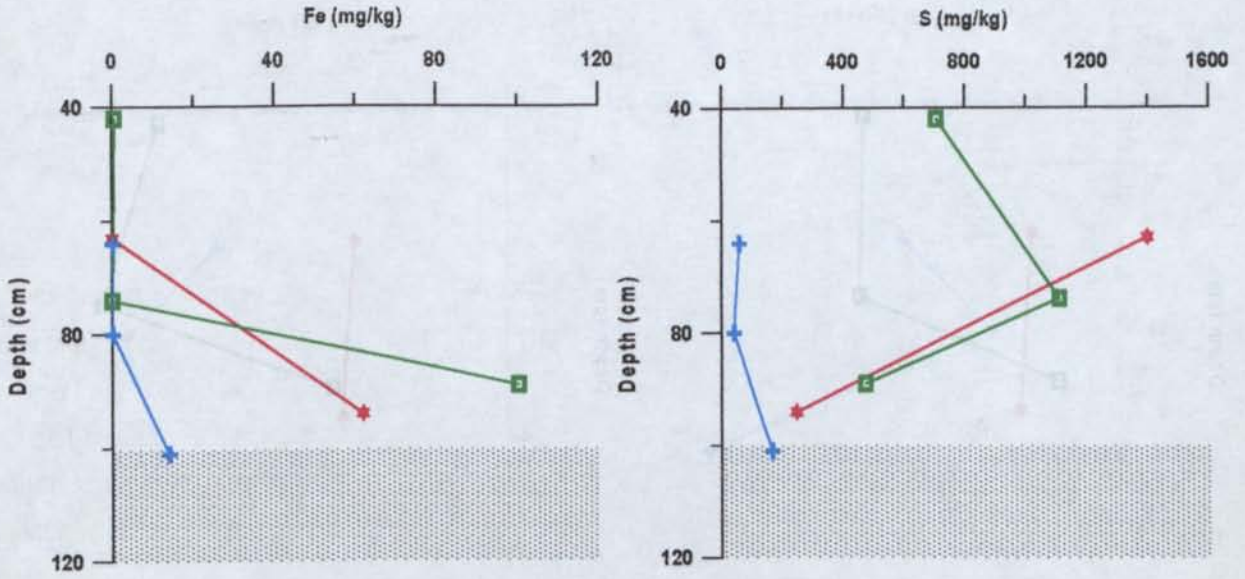

FIG 2A.2 FE AND S PROFILES FOR BRUKUNGA

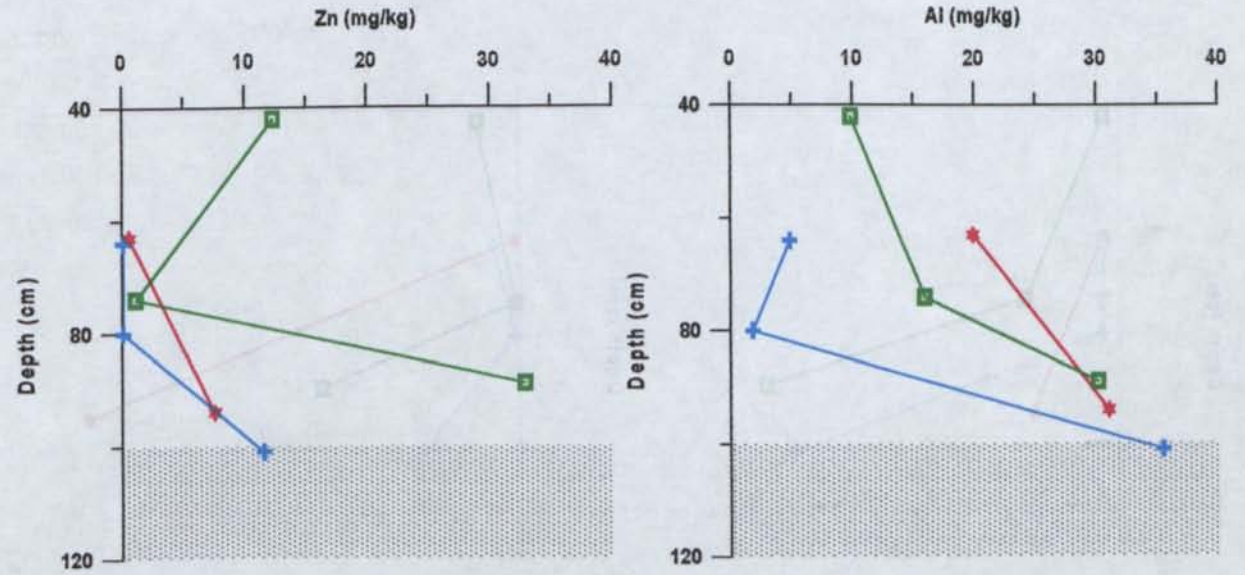

FIG 2A.3 ZN AND AL PROFILES FOR BRUKUNGA

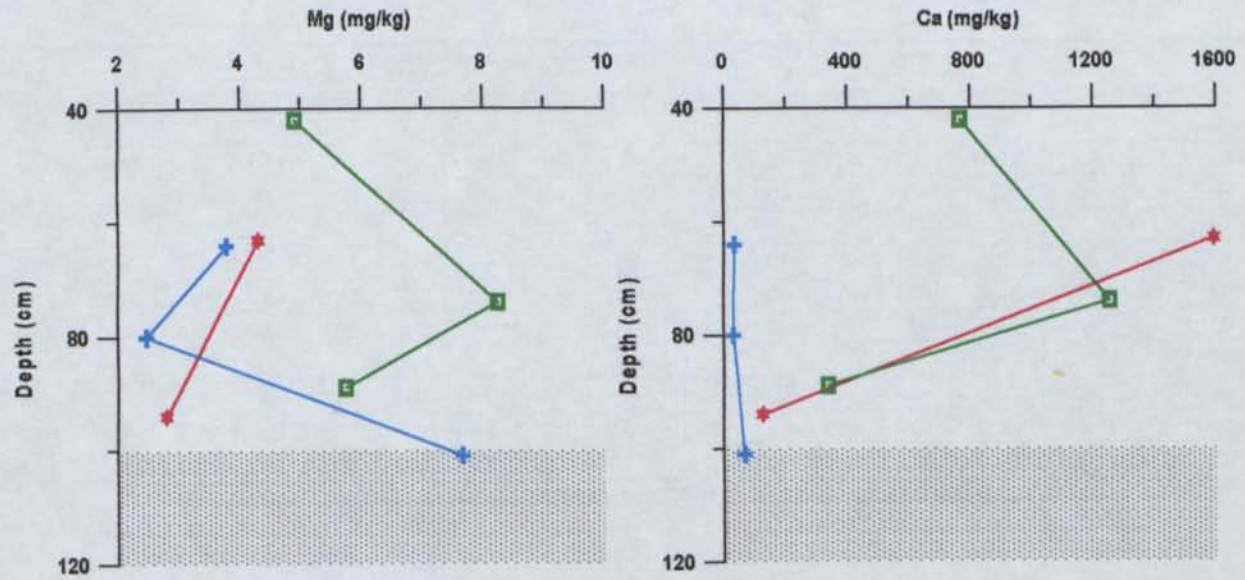

FIG 2A.4 MG AND CA PROFILES FOR BRUKUNGA

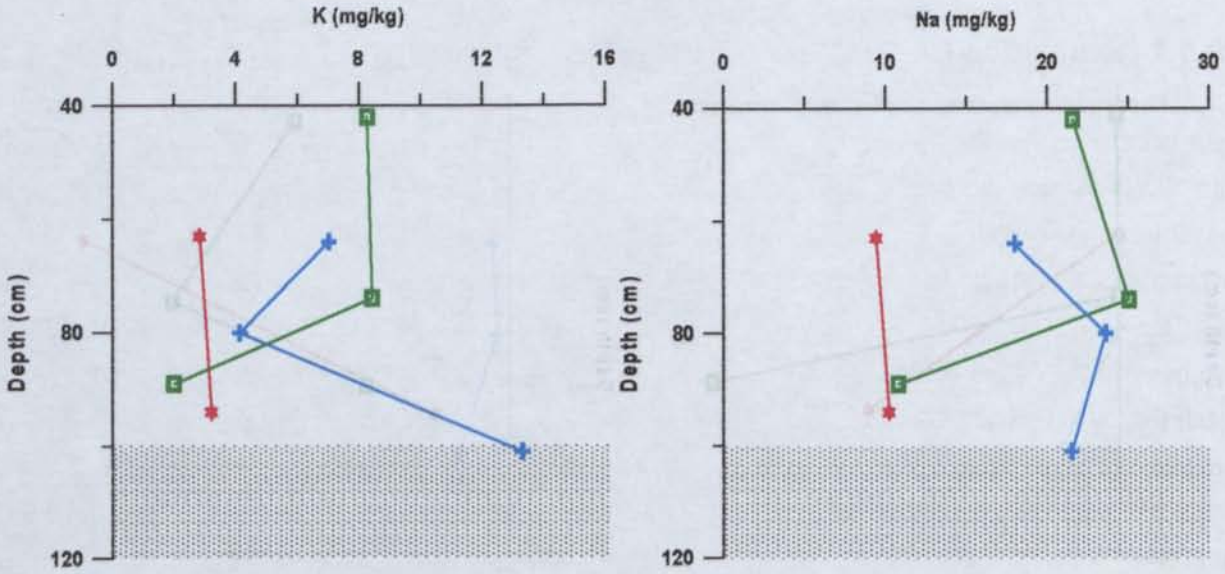

FIG 2A.5 K AND NA PROFILES FOR BRUKUNGA

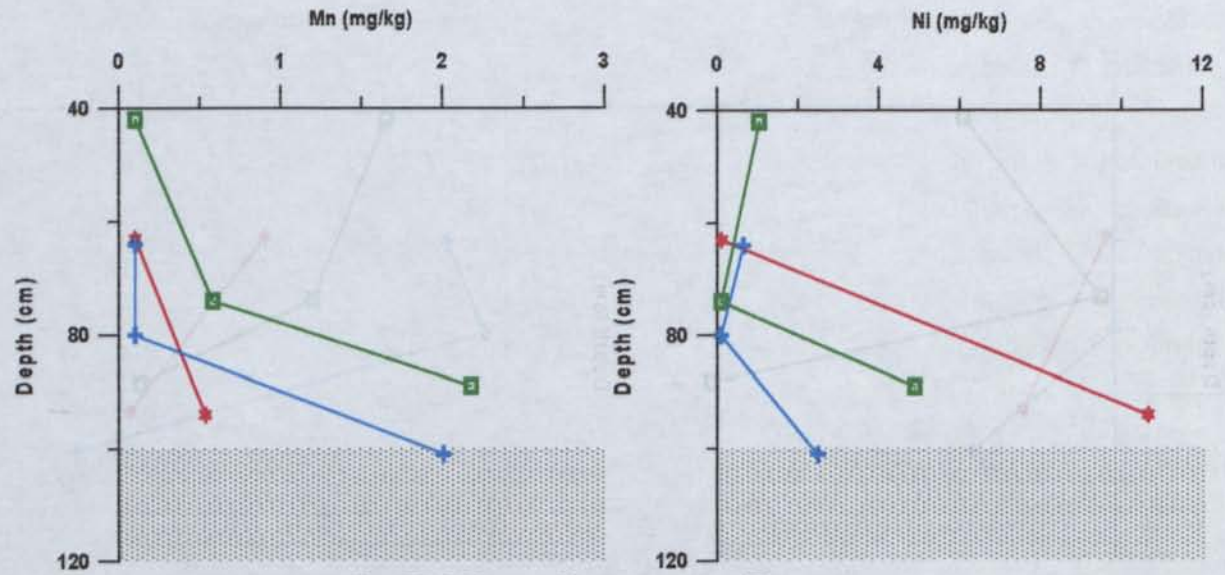

FIG 2A.6 MN AND NI PROFILES FOR BRUKUNGA

	Al	B	Ca	Cd	Co	Cr	Cu	Fe	K	Mg	Mn	Na	Ni	Pb	S	Zn
	mg/kg	mg/kg	mg/kg	mg/kg	mg/kg	mg/kg	mg/kg	mg/kg	mg/kg	mg/kg	mg/kg	mg/kg	mg/kg	mg/kg	mg/kg	mg/kg
Hole 4																
64	19.9	<0.1	1594	<0.1	<0.1	<0.1	<0.1	<0.1	2.8	4.3	<0.1	9.4	<0.1	<0.1	1400	0.62
94	31.1	<0.1	128	0.98	2.9	<0.1	0.12	62.0	3.2	2.8	0.54	10.2	10.65	<0.1	248	7.6
Hole 5																
42	9.9	<0.1	769	<0.1	<0.1	<0.1	<0.1	0.59	8.3	4.9	<0.1	21.5	1.03	<0.1	707	12.3
74	15.9	<0.1	1256	<0.1	<0.1	<0.1	<0.1	<0.1	8.4	8.3	0.58	25.0	<0.1	<0.1	1110	1.12
89	30.2	<0.1	340	<0.1	0.5	<0.1	<0.1	100.4	2.0	5.7	2.18	10.8	4.88	<0.1	474	32.9
Hole 7																
64	4.9	<0.1	33.8	<0.1	<0.1	<0.1	<0.1	<0.1	7.0	3.8	<0.1	18.0	0.64	<0.1	57.7	<0.1
80	1.8	<0.1	31.8	<0.1	<0.1	<0.1	<0.1	<0.1	4.1	2.5	<0.1	23.6	<0.1	<0.1	40.1	<0.1
101	35.6	<0.1	67.2	1.4	0.6	<0.1	9.2	14.1	13.3	7.7	2.01	21.5	2.49	<0.1	167	11.6

TABLE 2A.1 BRUKUNGA SOLUTE CONCENTRATIONS (1:5 BATCH LEACHING)

2A.1.2 Kanmantoo Cu Mine

Four sites were investigated at the Kanmantoo Dam with only 3 being cored for geochemical analysis, Site 1 located near the central front piezometer, Site 3 in the center of the dam and Site 4 adjacent to the artificial dam wall. This sampling strategy ensured that the different grain size fractions were investigated, the coarse tailings at the front of the dam to the fine tailings at the back.

The general pH values in the dam ranged from 3 to 5, however no trend appeared to be developing with depth (Fig 2A.7). The EC of the pore waters ranged from 0-2.5 mS/cm, each profile showing a general increase in EC with depth (Fig 2A.7). The highest values were observed within the center of the dam at Site 3 and consisted mainly of Al, Ca, Cu, Mg, Mn, and S with lesser amounts of Co, Fe, K, Na, Ni and Zn (Table 2A.2). All sites exhibited an increase in concentration with depth for S, Ni, Mg, K, Co, Fe and Cu (Figs 8 to 11). However the maximum concentrations of Al, Ca and Mn occurred at approximately 120-130cm depth. There was no significant textural similarity in any of the profiles at this depth with Site 1 consisting of coarse to medium sand, Site 3 medium to fine sand while Site 4 contained fine sand at this depth. The Zn profiles developed through the dam varied dramatically; Site 1 exhibited increased concentrations in the upper tailings and a general decrease with depth, while Sites 2 and 3 showed increasing concentrations with depth (Fig 2A.9). As very little cementing or secondary mineralogy was identified within these tailings it is suggested that the trends of increasing concentrations with depth are attributed to leaching mechanisms rather than the incorporation of elemental concentrations as insoluble cements in the upper tailings.

LEGEND FOR KANMANTOO SOLUTE CONCENTRATION PROFILES FROM 1:5 BATCH LEACHING EXPT.

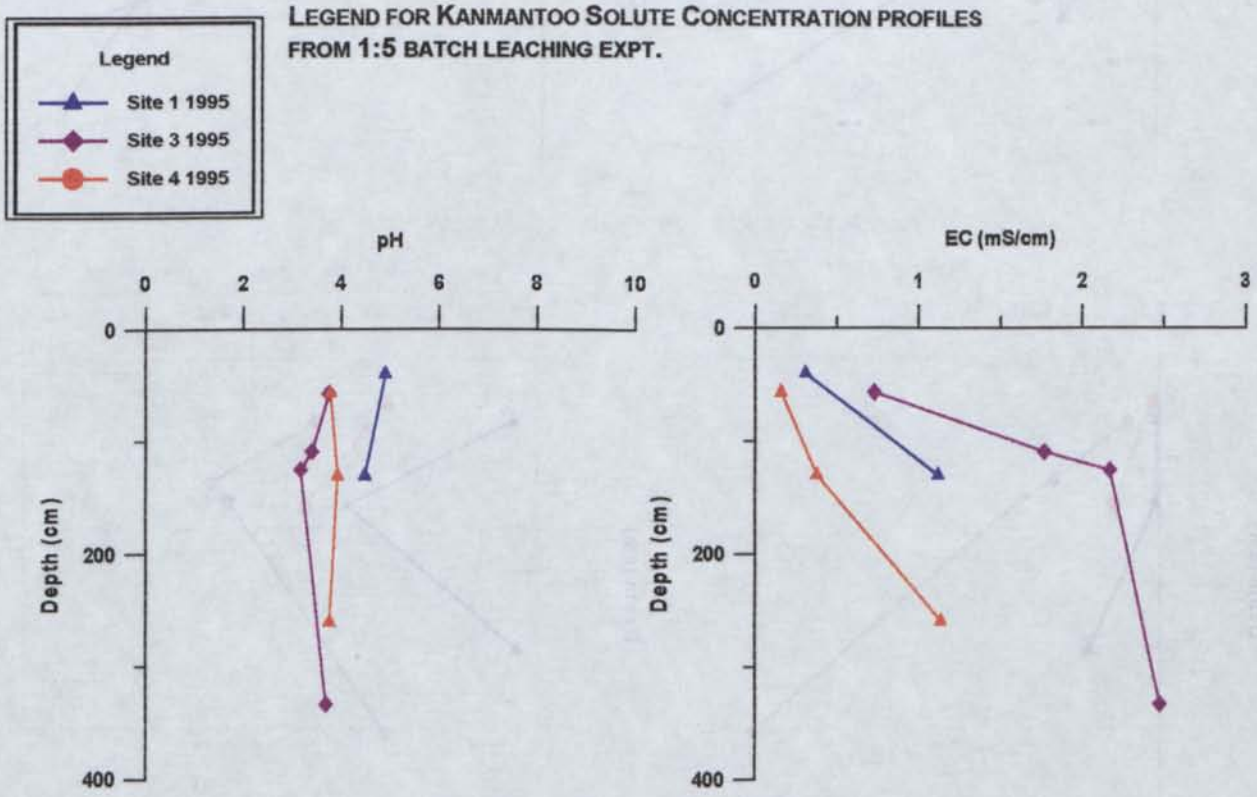

FIG 2A.7 PH AND EC PROFILES FOR KANMANTOO

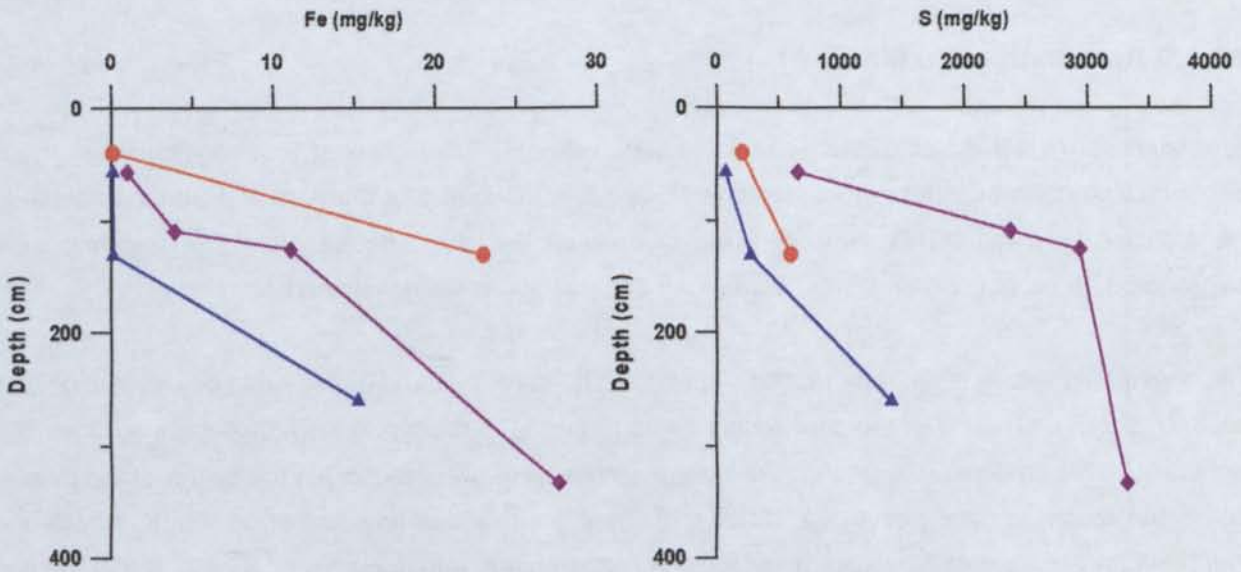

FIG 2A.8 FE AND S PROFILES FOR KANMANTOO

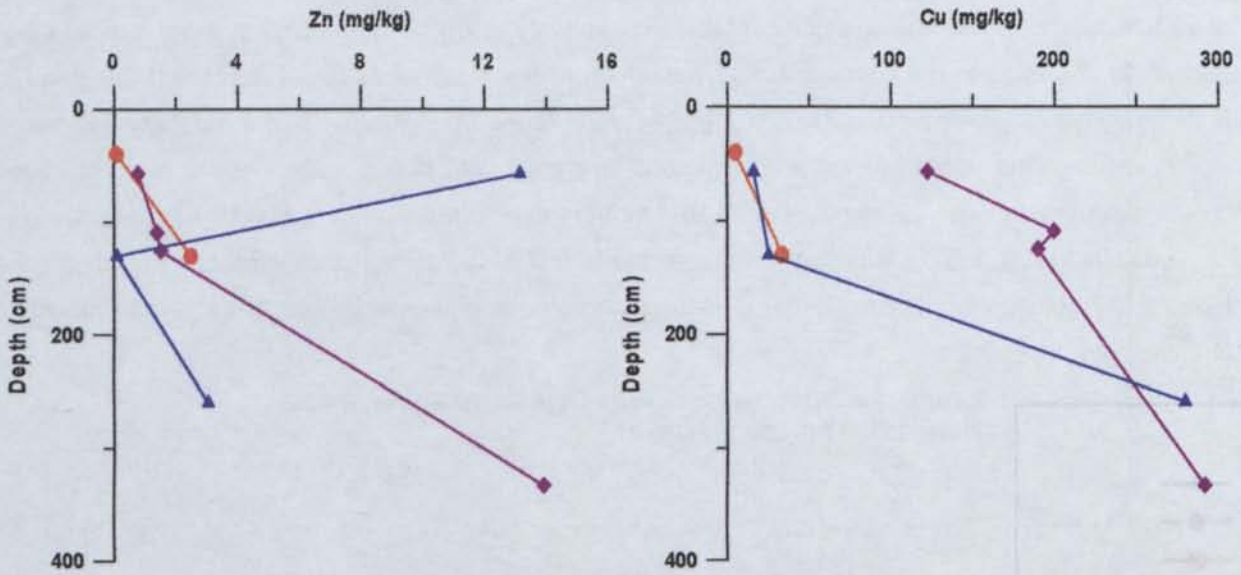

FIG 2A.9 ZN AND CU PROFILES FOR KANMANTOO

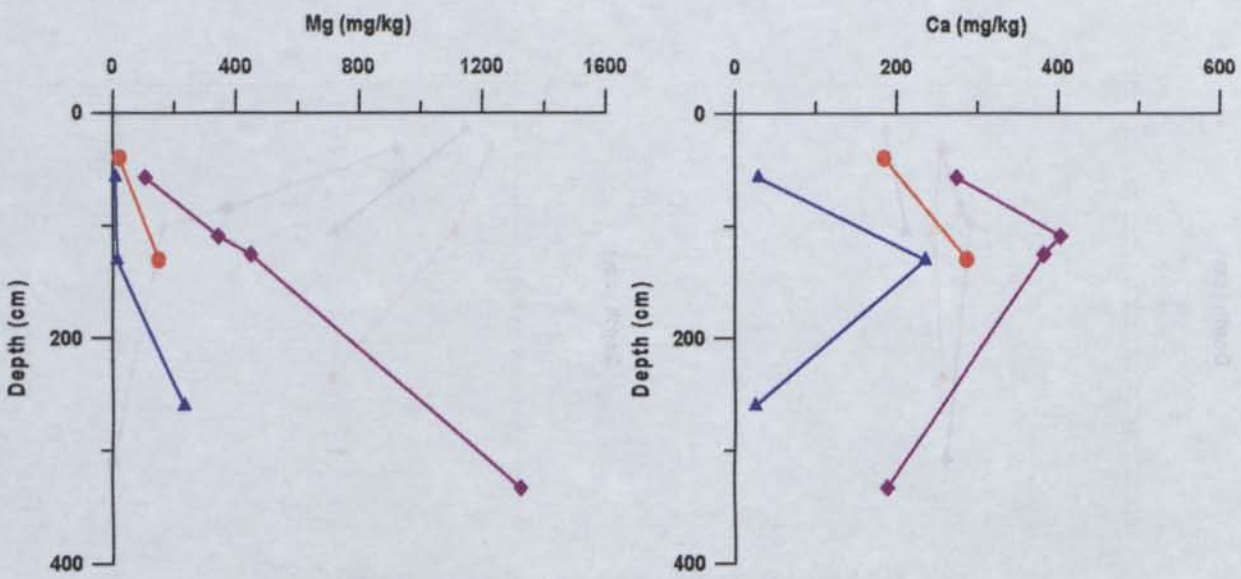

FIG 2A.10 MG AND CA PROFILES FOR KANMANTOO

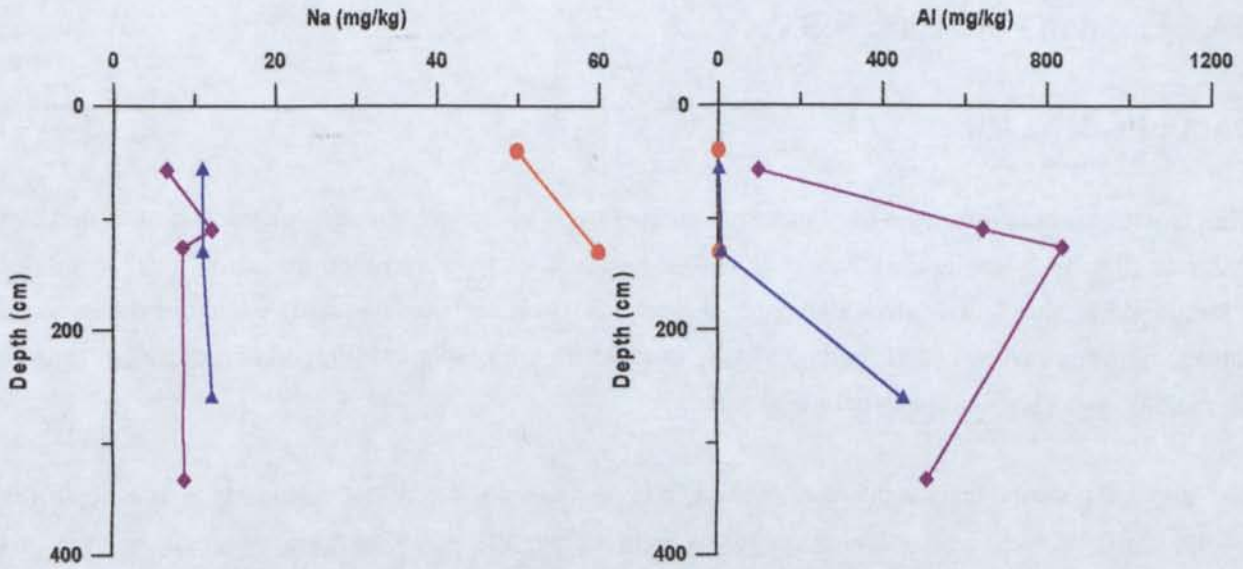

FIG 2A.11 NA AND AL PROFILES FOR KANMANTOO

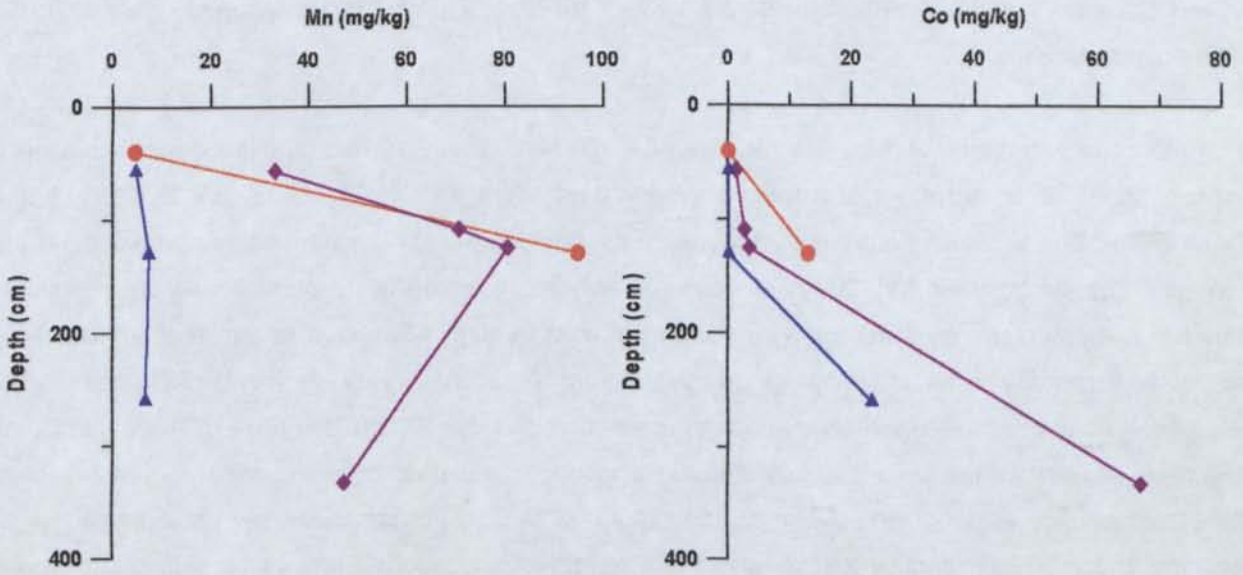

FIG 2A.12 MN AND CO PROFILES FOR KANMANTOO

	Al	Ca	Co	Cu	Fe	K	Mg	Mn	Na	Ni	S	Zn
	mg/kg	mg/kg	mg/kg	mg/kg	mg/kg	mg/kg	mg/kg	mg/kg	mg/kg	mg/kg	mg/kg	mg/kg
Site 1												
57	3.0	29.0	<0.1	16.3	<0.1	3.0	9.6	4.8	11	<0.1	71.0	13.2
130	6.8	235	<0.1	25.2	<0.1	1.8	13.8	7.4	11	<0.1	270	<0.1
260	451.8	24.7	23.3	280	15.3	7.6	232	6.79	12.2	7.94	1414	3.05
Site 3												
57	99	275	1.32	123	1.00	1.29	106	33.3	6.61	<0.1	659	0.8
109	643	403	2.64	200	3.9	<0.1	342	70.7	12.2	0.76	2376	1.39
125	837	382	3.44	190	11.1	0.81	448	80.6	8.51	0.98	2939	1.52
333	509	189	67.1	292	27.6	25.5	1325	47.3	8.79	24.7	3320	13.9
Site 4												
40	1.1	185	<0.1	5.2	<0.1	19.9	22.7	4.71	49.89	<0.1	206	<0.1
130	3.5	287	13	33.5	23	105	150	95	60	3.5	600	2.5

TABLE 2A.2 KANMANTOO SOLUTE CONCENTRATIONS (1:5 BATCH LEACHING)

2A.2 Lachlan Fold Belt, N.S.W

2A.2.1 Peak Au Mine

The geochemistry of tailings in the Peak impoundment was investigated through sampling at 4 sites over a 2 year period. A single core was removed from Site 1 in 1995 and then the same location was re-cored in 1996. Site 1 is located adjacent to the central spigot and thus had had continuous deposition of tailings between sampling. Three additionally sites, in an area thought to have been exposed for up to 12 months, were also sampled in 1996.

The general pH conditions within the Peak tailings ranged from 4-8 at the surface to 6-8 at depth (Fig 2A.13). Surface EC values were up to 7mS/cm during the 1995 sampling of fresh tailings, and decreased with depth to 1mS/cm (Fig 2A.13). The 12 month old 1996 cores however portrayed much lower EC values ranging from approximately 0.5 to 3 mS/cm. This EC modification is reflected in the solute concentrations.

In 1995, concentrations of Mg, Mn, K, Na, Ca, B and S all showed similar trends, exhibiting concentrations at the surface and a rapid decrease over 10cm (Fig 2A.14, 2A.17, 2A.18 & 2A.19 and Table 2A.3). The accumulations were attributed to the development of gypsum, halite and blodite at the surface. The increases in Mn, B and K observed may have been due to precipitation of amorphous minerals not detectable by XRD analysis or concentrated through adsorption or substitution processes with other secondary minerals precipitating in this region. Additionally very low levels of Cu and P were also observed at the surface with little or none present at depth (Fig 2A.15). Nickel, Al, Fe, Pb and Co all displayed similar profiles, with concentrations at 3cm depth and then decreases to very low levels or complete absence at depth (Fig 2A.14, 2A.15, 2A.16 & 2A.20). These trends are attributed to slight leaching effects. Unfortunately XRD analysis did not detect any discrete phases responsible for these concentrations. Zinc and Cd were different again in that they were concentrated at the surface and at 10cm depth, however they still showed the general decrease in concentration at depth (Fig 2A.15).

As Site 1 has had continual deposition since the initial sampling, a direct comparison is not applicable. However it would appear the Sites 2, 3 and 4, after exposure of up to 1 year, have much lower solute concentrations. Site 2 has slightly elevated surface concentrations of Fe, Ca, Ni, Si, Pb and Zn existing under pH conditions of approximately 4. Generally these levels are lower than those observed in 1995, but are slightly higher than the 1996 pore waters for Sites 1, 3 and 4. The decrease in surface concentrations can be attributed to a number of different conditions including leaching and precipitation of insoluble cements (see section 5.3.4).

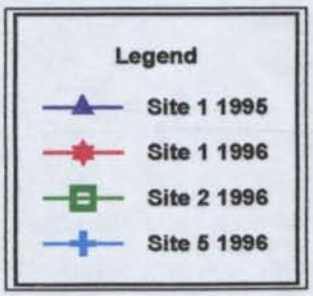

LEGEND FOR PEAK SOLUTE CONCENTRATION PROFILES FROM 1:5 BATCH LEACHING EXPT.

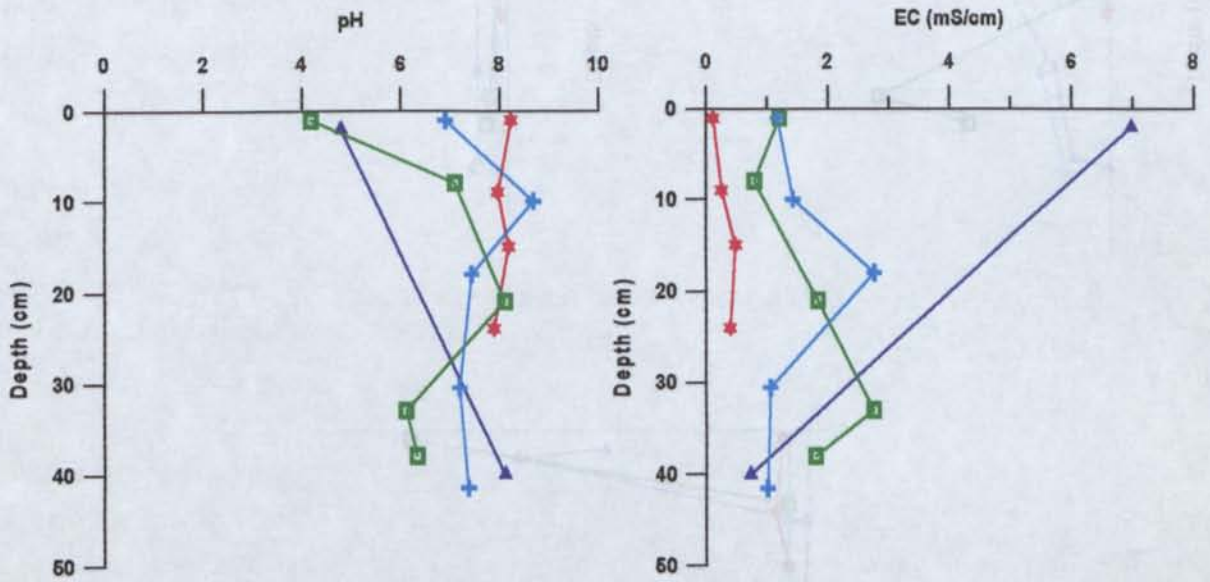

FIG 2A.13 pH AND EC PROFILES FOR PEAK

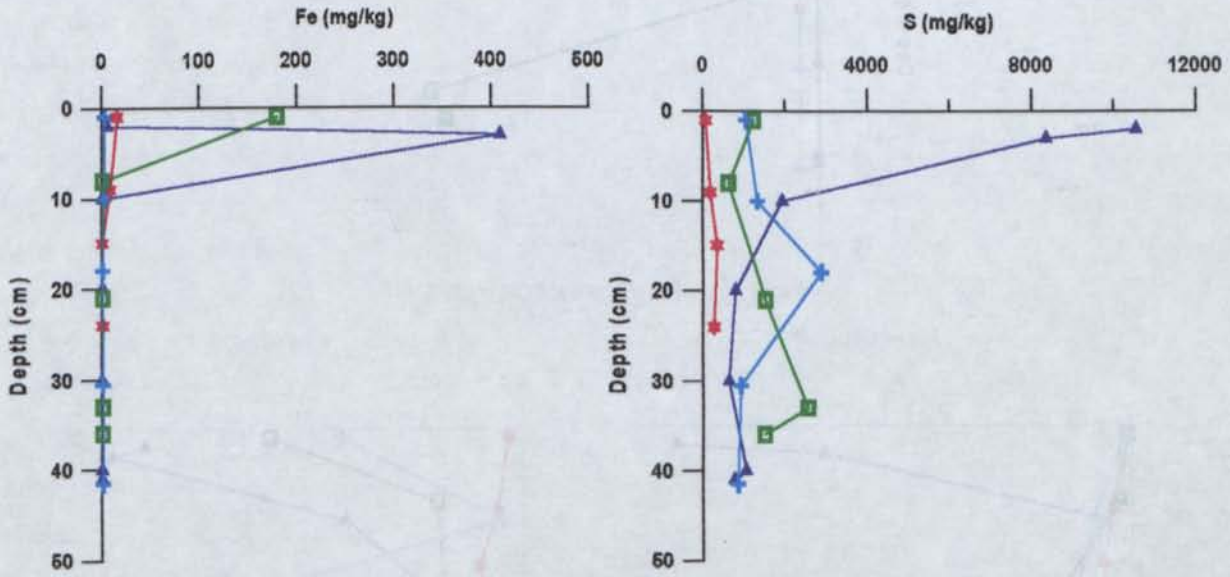

FIG 2A.14 FE AND S PROFILES FOR PEAK

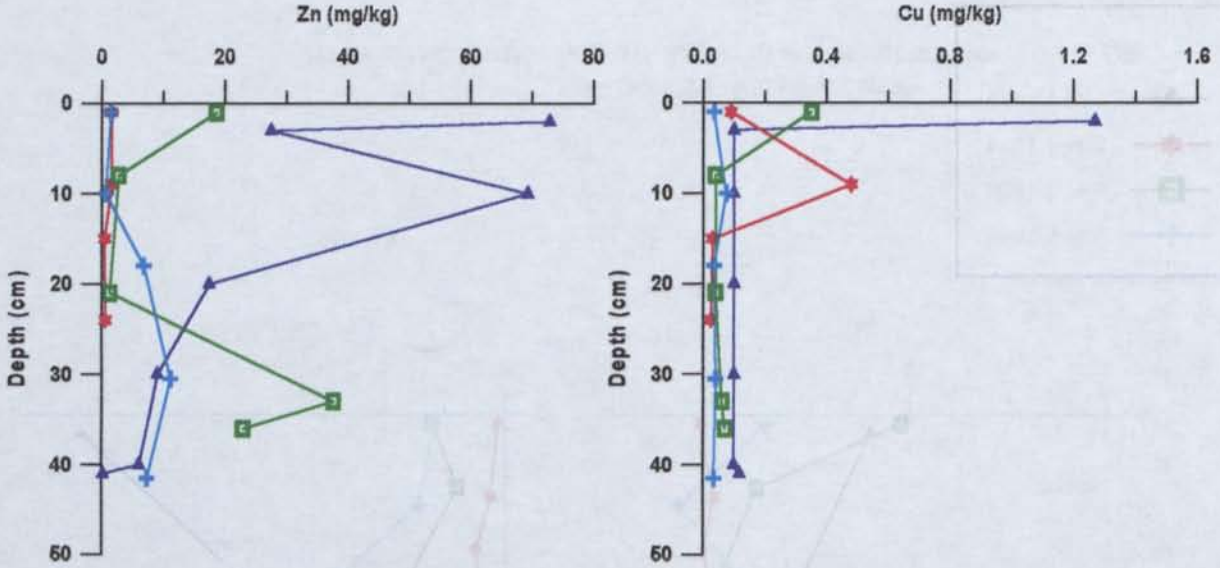

FIG 2A.15 ZN AND CU PROFILES FOR PEAK

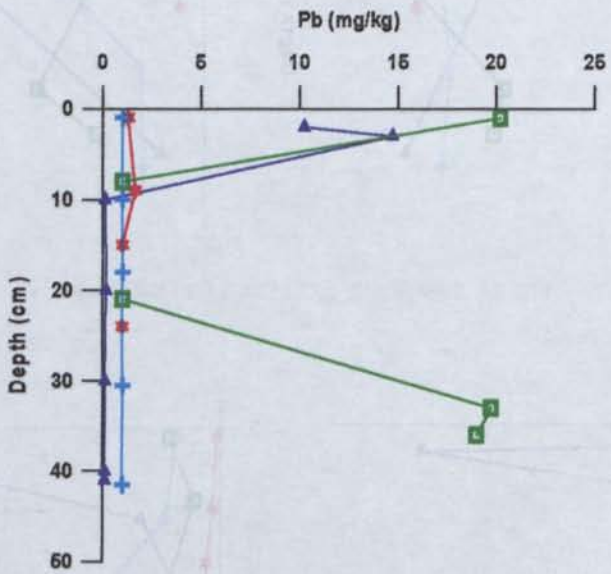

FIG 2A.16 PB PROFILE FOR PEAK

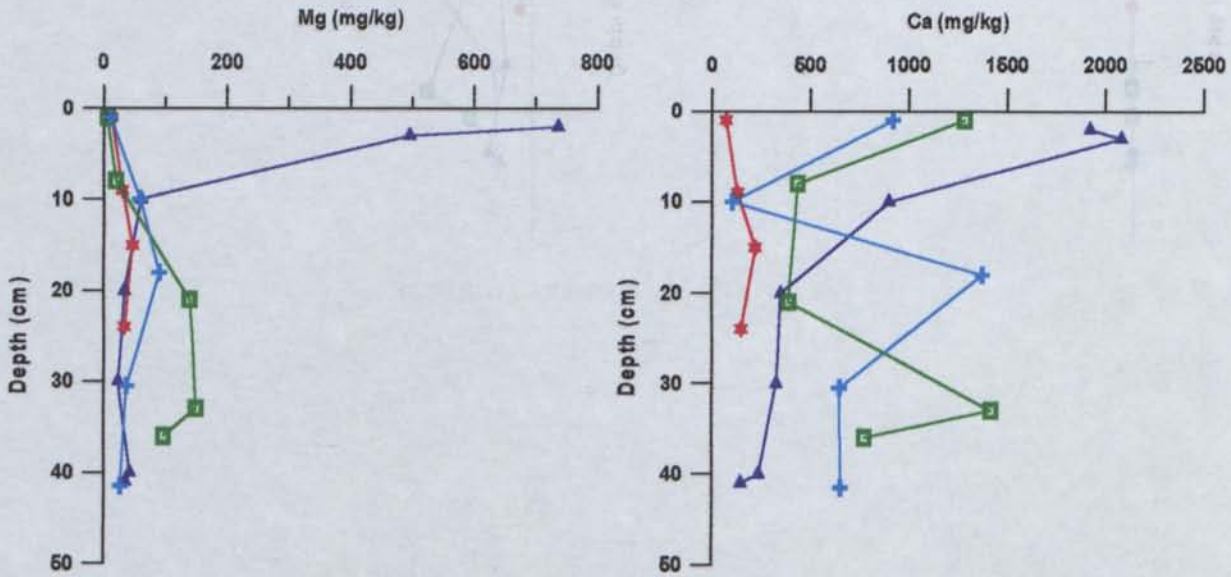

FIG 2A.17 MG AND CA PROFILES FOR PEAK

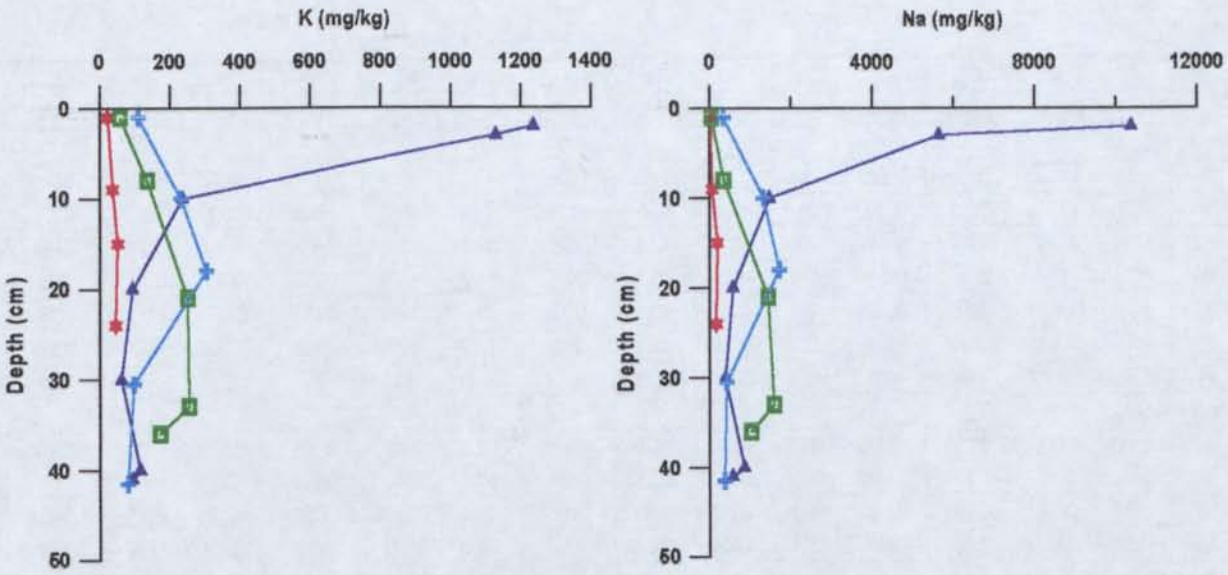

FIG 2A.18 K AND NA PROFILES FOR PEAK

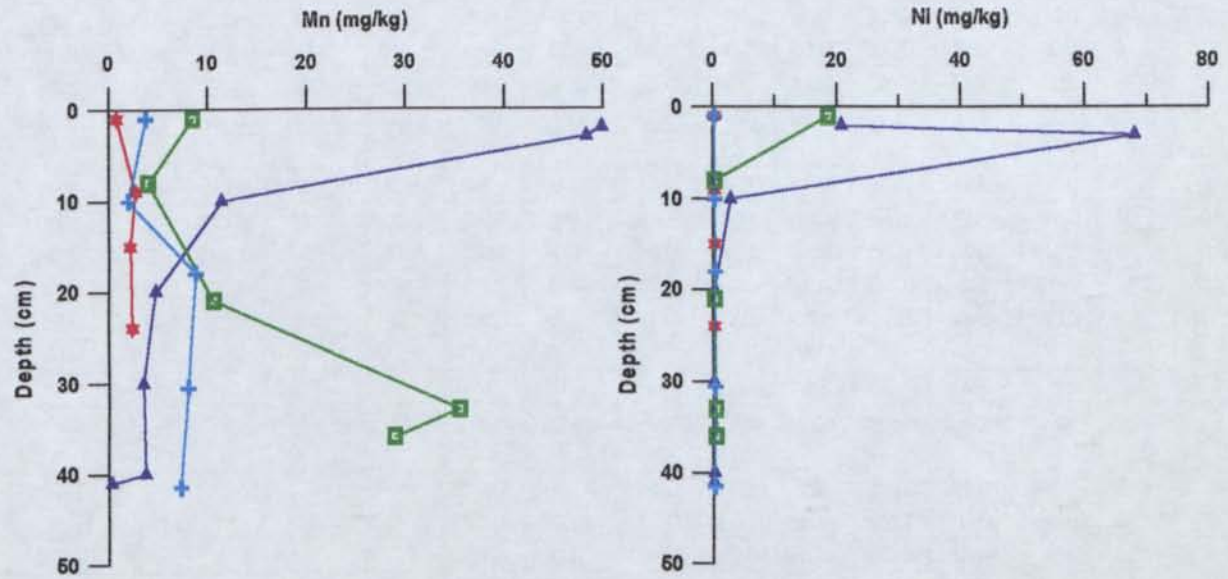

FIG 2A.19 MN AND NI PROFILES FOR PEAK

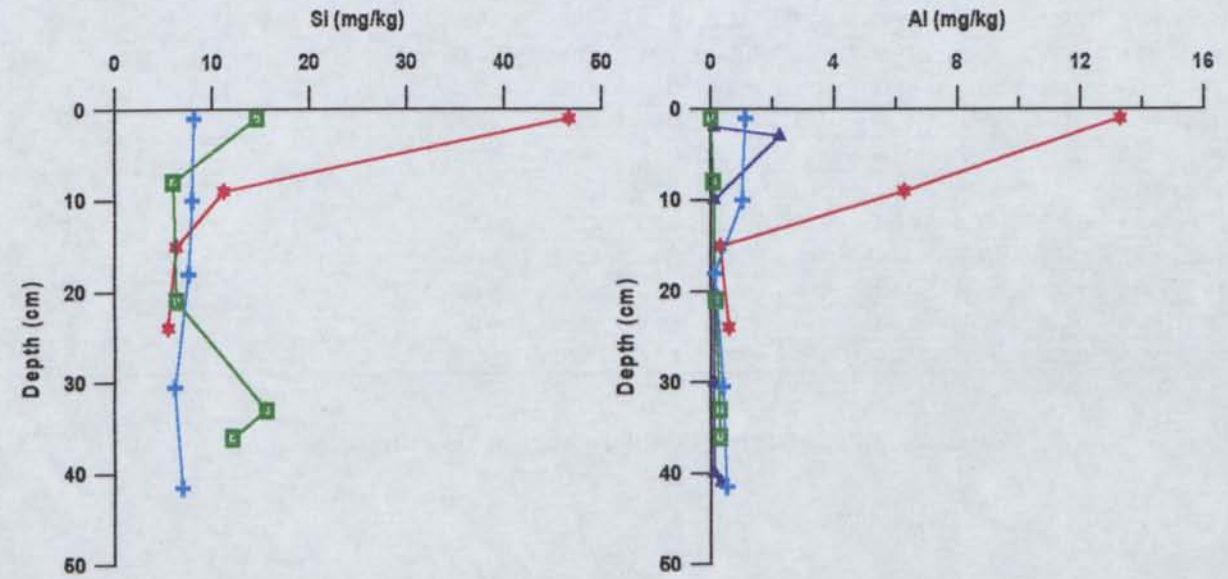

FIG 2A.20 SI AND AL PROFILES FOR PEAK

	Al	B	Ca	Cd	Co	Cu	Fe	K	Mg	Mn	Na	Ni	Pb	S	Zn
	mg/kg	mg/kg	mg/kg	mg/kg	mg/kg	mg/kg	mg/kg	mg/kg	mg/kg	mg/kg	mg/kg	mg/kg	mg/kg	mg/kg	mg/kg
Site 1 (1995)															
2	<0.1	1.226	1922	0.88	1.998	1.27	5.38	1235	737	49.9	10374	20.7	10.24	10547	72.8
3	2.24	1.073	2081	0.44	2.354	<0.1	409	1129	496	48.3	5638	68.0	14.7	8357	27.5
10	<0.1	0.33	898	0.73	0.16	<0.1	<0.1	236	59.9	11.4	1464	2.87	0.13	1934	69.2
20	<0.1	0.14	350	0.21	<0.1	<0.1	<0.1	92.1	34.2	4.73	569	0.27	0.17	796	17.4
30	<0.1	0.125	327	0.10	<0.1	<0.1	<0.1	60.9	23.9	3.46	380	0.155	<0.1	638	9.02
40	<0.1	0.135	236	<0.1	<0.1	<0.1	<0.1	115	42.7	3.75	855	0.205	<0.1	1055	6.08
41	0.322	0.177	144	<0.1	<0.1	0.12	0.21	92.7	35.0	0.31	563	0.1	<0.1	778	0.15
Site 1 (1996)															
1	13.3	0.055	71.7	<0.05	<0.05	0.09	15.6	21.8	12.8	0.80	8.14	<0.25	1.29	65.01	1.54
9	6.28	0.16	129	<0.05	<0.05	0.48	8.21	36.8	30.6	2.73	58.3	<0.25	1.65	181	1.53
15	0.31	0.18	219	<0.05	<0.05	0.03	0.39	50.6	46.6	2.17	184	<0.25	<0.1	348	0.43
24	0.58	0.105	148	<0.05	<0.05	0.025	0.68	45.4	33.5	2.38	160	<0.25	<0.1	274	0.54
Site 2 (1996)															
1	0	0	1282	0	0.755	0.35	180	57.8	5.89	8.49	43.4	18.6	20.2	1225	18.6
8	0.08	0.06	434	0.05	0.05	0.04	0.25	136	19.8	3.99	340	<0.25	<0.1	624	2.69
21	0.16	0.09	389	0.085	0.05	0.04	0.25	250	140	10.60	1431	<0.25	<0.1	1517	1.25
33	0.29	0.11	1417	0.55	0.41	0.06	0.86	254	150	35.5	1582	0.42	19.7	2555	37.6
36	0.29	0.075	774	0.48	0.385	0.07	0.37	171	96.9	28.9	1021	0.49	19.0	1503	22.9
Site 5 (1996)															
1	1.12	0.16	919	0.05	0.095	0.035	2.21	109	10.41	3.74	332	<0.25	<0.1	1047	1.48
10	1.02	0.19	103	0.05	0.225	0.075	2.265	231	59.0	2.00	1317	<0.25	<0.1	1330	0.65
18	0.13	0.18	1373	0.16	0.265	0.035	0.25	304	90.3	8.78	1704	0.335	<0.1	2874	6.79
30.5	0.40	0.07	648	0.115	0.085	0.04	0.76	96.2	37.4	8	413	<0.25	<0.1	914	11.2
41.5	0.51	0.05	652	0.11	0.05	0.035	1.005	79.6	26.8	7.3	359	<0.25	<0.1	855	7.36
	As	Ba	Be	Li	Sb	Si	Sr	Ti	V						
	mg/kg	mg/kg	mg/kg	mg/kg	mg/kg	mg/kg	mg/kg	mg/kg	mg/kg						
Site 1 (1996)															
1	<0.5	0.19	<0.01	0.045	<0.5	46.7	0.16	0.235	<0.025						
9	<0.5	0.085	<0.01	0.065	<0.5	11.2	0.27	<0.025	<0.025						
15	<0.5	0.06	<0.01	0.09	<0.5	6.28	0.43	<0.025	<0.025						
24	<0.5	0.07	<0.01	0.095	<0.5	5.46	0.52	<0.025	<0.025						
Site 2 (1996)															
1	<0.5	0.025	<0.01	0.025	<0.5	14.57	0.21	<0.025	<0.025						
8	<0.5	0.31	<0.01	0.05	<0.5	5.94	0.44	<0.025	<0.025						
21	<0.5	0.185	<0.01	0.17	<0.5	6.34	0.56	<0.025	<0.025						
33	<0.5	0.025	<0.01	0.19	<0.5	15.6	0.86	<0.025	<0.025						
36	<0.5	0.065	<0.01	0.145	<0.5	12.0	0.21	<0.025	<0.025						
Site 5 (1996)															
1	<0.5	0.285	<0.01	0.065	<0.5	8.13	2.70	<0.025	<0.025						
10	<0.5	0.16	<0.01	0.115	<0.5	7.90	0.46	<0.025	<0.025						
18	<0.5	0.29	<0.01	0.135	<0.5	7.55	2.18	<0.025	<0.025						
30.5	<0.5	0.225	<0.01	0.085	<0.5	6.15	1.23	<0.025	<0.025						
41.5	<0.5	0.195	<0.01	0.06	<0.5	6.92	1.14	<0.025	<0.025						

TABLE 2A.3 PEAK SOLUTE CONCENTRATIONS (1:5 BATCH LEACHING)

2A.2.2 Woodlawn Cu-Pb-Zn Mine

Two cores were removed from the NW corner of the Woodlawn South Tailings Dam. At each of the locations, different geochemical profiles appear to be developing which may be an effect of the sampling depth ranges and the frequency of profile analysis (i.e. even though the core sampled from the Site 1 was only 10cm compared with the 48cm sample removed from the Site 2 a similar number of analyses were carried out on each core). This difference in frequency of analysis gives an indication of the highly variable nature of the tailings and that any results obtained can only give a general understanding of the processes taking place.

Concentration profiles of Zn, S, Mn, Na, Co, Al, Cd, Cu and Mg at Site 1 show a very similar pattern, with a general decreasing concentration with depth and accumulations at the surface and 6cm depth (Fig 2A.21 to 2A.26 and Table 2A.4). Samples removed from the surface and 6cm depth were both oxidised. The surface sample represents the present sulfide oxidation region, while the 6cm sample probably represents a palaeosurface. It would appear that many of the soluble salts developed directly from oxidation by-products are being retained at these depths. The increased elemental levels of S, Na and Mg can be directly attributed to the precipitation of natrojarosite and hexahydrite occurring at these depths. While Ca levels along with a portion of S concentrations can be attributed to gypsum precipitation. Discrete secondary phases which can be attributed to the concentrations of Zn, Mn, Co, Al, Cd and Cu were not detected by XRD. Their detection may have been limited by the low concentrations of secondary minerals available for analysis. Additionally these elements may be concentrated, not in discrete phases but through adsorption or substitution processes with the other secondary minerals.

The Pb profile (Fig 2A.23) which has developed is very different to any other observed in that it is concentrated, not at the surface or the paleaosurfaces but in the unoxidised layers between. In this case Pb is not being incorporated into the secondary mineralogy but must be forming a discrete phase unobserved by XRD due to the low quantities available for detection.

The geochemical profiles observed at Site 2 give more of an indication of the overall leaching that has taken place on a larger scale. These profiles also give an insight into the effect textures may be playing on profile development. The profiles for Mn, Zn, Ni and Ca at the Site 2 are presented in Figs 2A.22, 2A.24 & 2A.26. Generally these profiles show concentrations at depth, a result of vertical leaching. Many of the oxidation by-products are removed from the surface but at varying rates. Mn and Zn show a systematic increase in concentration with depth however Ni and Ca are depleted near the surface but are at constant concentrations in the remainder of the profile.

Iron, P, S, Mg, Cu, Pb, Al and Co profiles show depletion at the surface which is followed by concentrations at approximately 15-30cm depth. This may be attributed to the very fine sand-silt sized tailings present at this depth range. It is suggested that the low permeability of this layer may sufficiently slow down leaching so that concentrations of elements can build up producing a saturated solution,

allowing precipitation of salt to occur. Additionally the profiles presented here are a function of leaching/mobility of the different elements. It appears B, K and Na are more mobile in this system as they are essentially absent in the shallow region and concentrated only at depth. Sodium is slightly different as it is a main constituent of the natrojarosite precipitating in the surface regions and thus is also accumulated there. However excess Na is obviously readily leached from the surface and concentrated at depth.

The EC results corroborate the leaching mechanism suggested for this site. Results show an increase in conductivity and thus solute concentration at depth (1.8 to 3.7 mS/cm at depth) with levels up to 5.1 mS/cm observed in the surface crust. pH shows a similar trend, also increasing with depth. pH 2.8 conditions exist at the surface which increases to 4.6 at depth. These profiles suggests that oxidation and acid production is occurring very strongly at the surface and that the soluble products are being leached downwards.

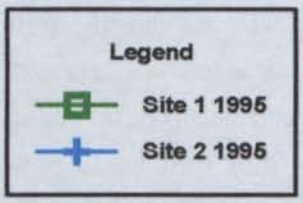

KEY FOR WOODLAWN SOLUTE CONCENTRATION PROFILES FROM 1:5 BATCH LEACHING EXPT.

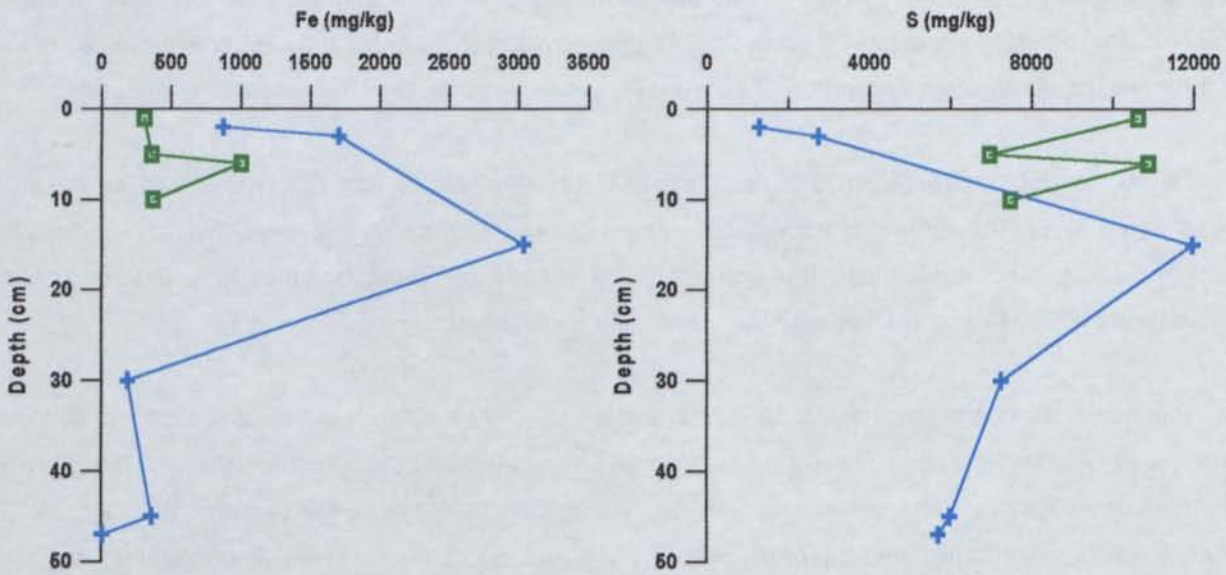

FIG 2A.21 FE AND S PROFILES FOR WOODLAWN

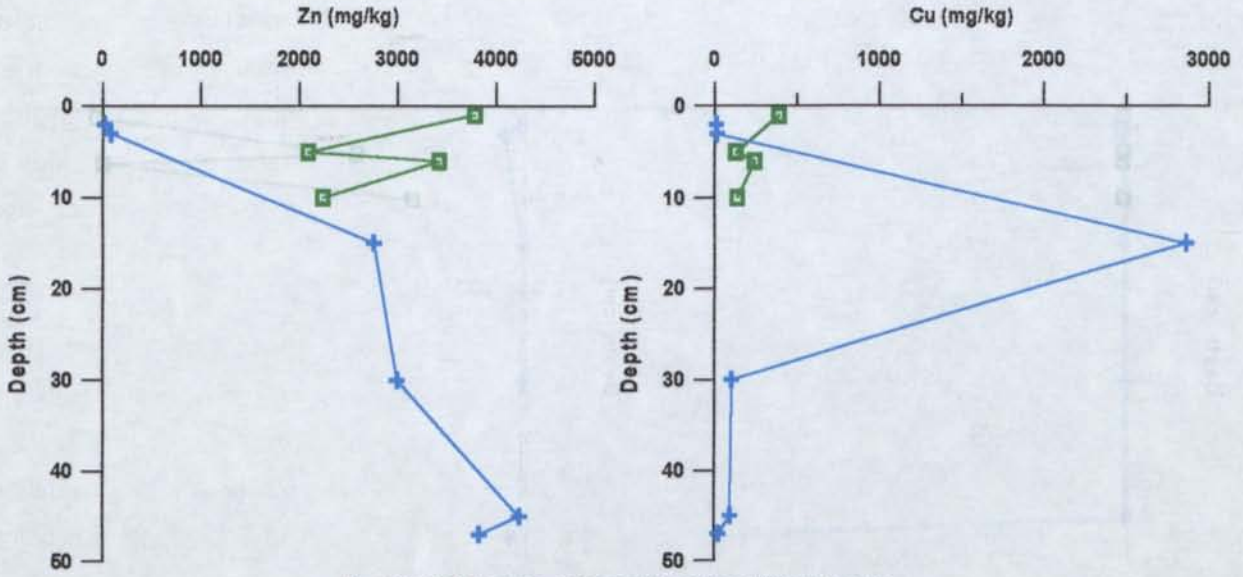

FIG 2A.22 ZN AND CU PROFILES FOR WOODLAWN

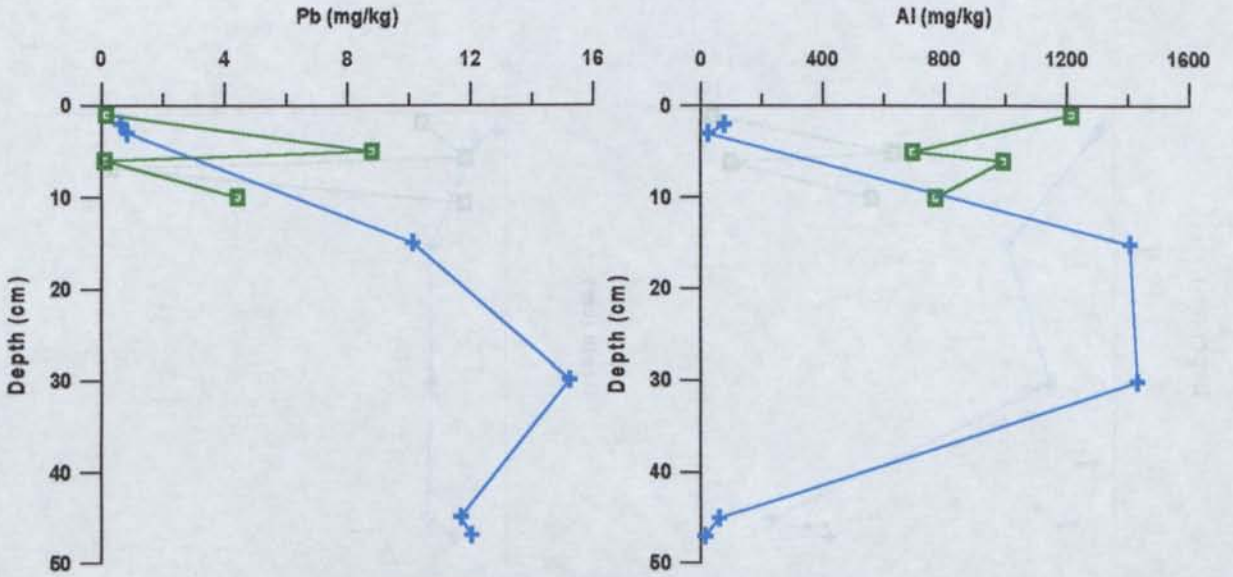

FIG 2A.23 PB AND AL PROFILES FOR WOODLAWN

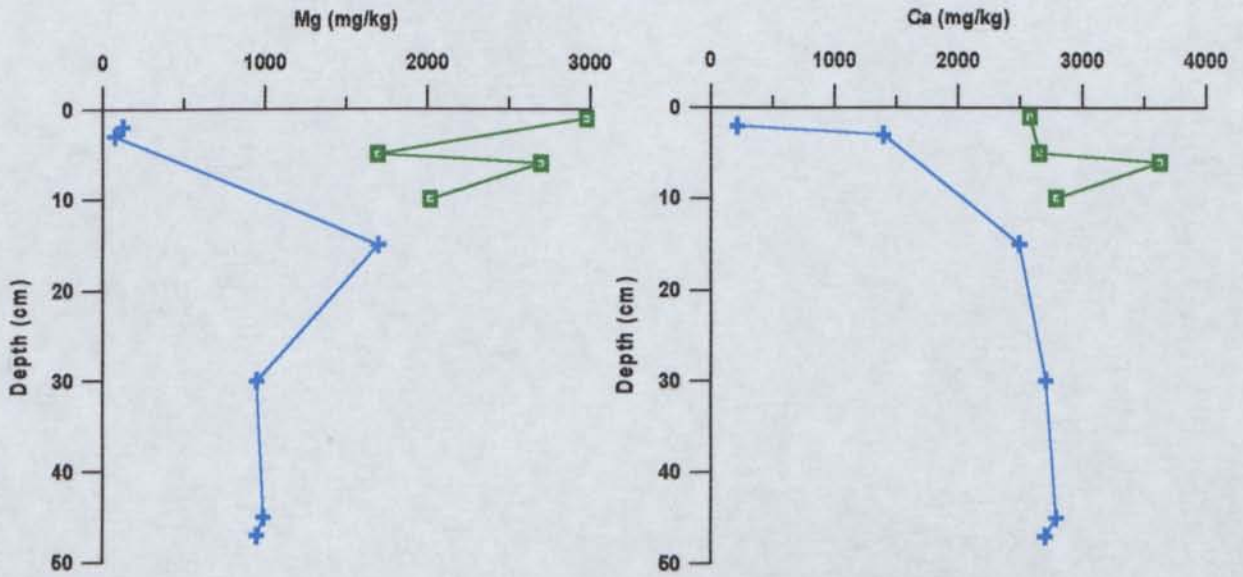

FIG 2A.24 MG AND CA PROFILES FOR WOODLAWN

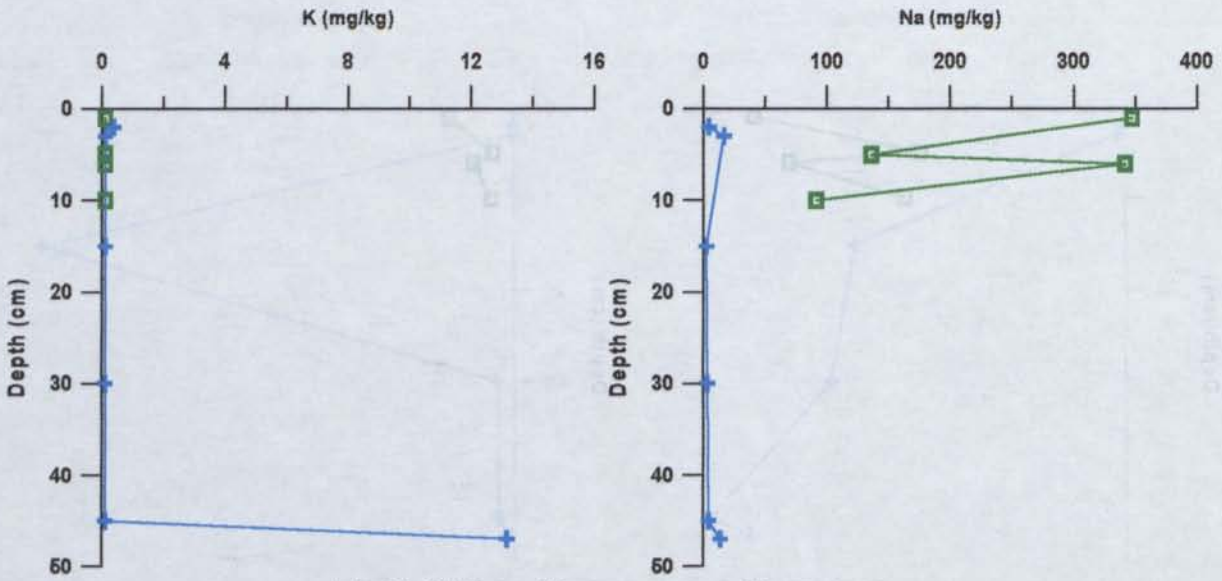

FIG 2A.25 K AND NA PROFILES FOR WOODLAWN

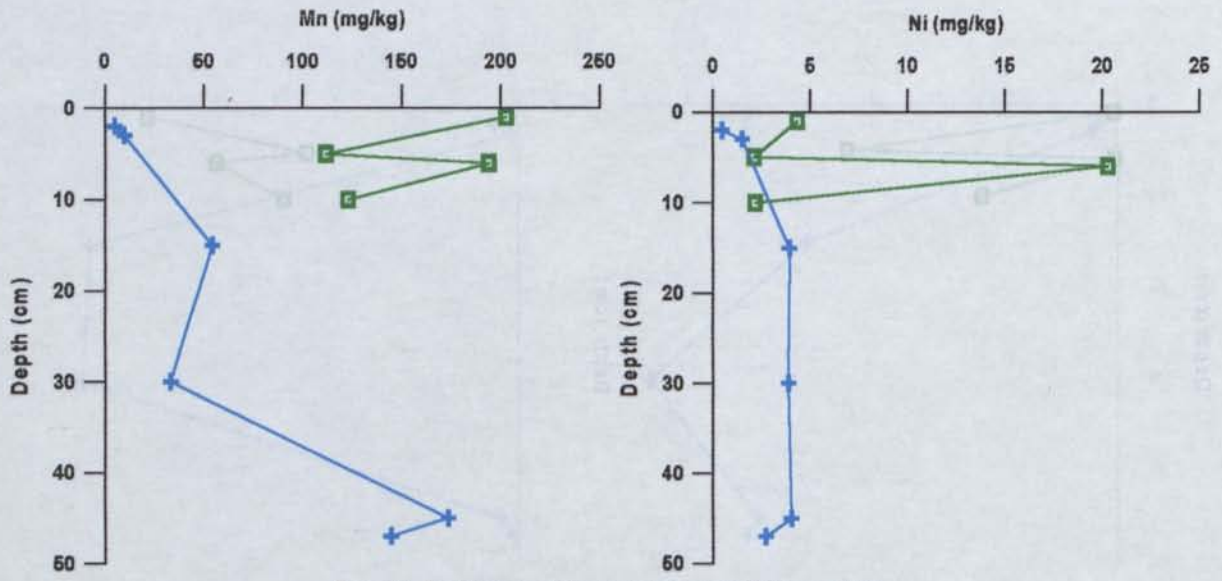

FIG 2A.26 MN AND NI PROFILES FOR WOODLAWN

	Al	Ca	Cd	Co	Cr	Cu	Fe	K
	mg/kg	mg/kg	mg/kg	mg/kg	mg/kg	mg/kg	mg/kg	mg/kg
Site 1								
2	75.5	212	0.13	0.19	<0.1	6.87	871	0.37
3	23.3	1395	0.55	0.1	<0.1	10.8	1702	<0.1
15	1405	2494	18.5	4.33	0.24	2860	3030	<0.1
30	1428	2708	43.1	2.68	0.45	100	186	<0.1
45	59.1	2789	5.04	2.28	<0.1	93.4	356	<0.1
47	13.1	2701	1.97	1.28	<0.1	21.1	1.81	13.2
Site 2								
1	1214	2576	19.1	2.40	1.407	387	304	<0.1
5	694	2654	10.7	1.43	0.635	128	358	<0.1
6	990	3625	23.1	5.10	6.275	242	1002	<0.1
10	768	2790	10.8	1.57	0.592	137	367	<0.1
	Mg	Mn	Na	Ni	P	Pb	S	Zn
	mg/kg	mg/kg	mg/kg	mg/kg	mg/kg	mg/kg	mg/kg	mg/kg
Site 1								
2	122	4.83	4.23	0.45	<0.1	0.62	1278	17.9
3	73.2	9.73	16.4	1.49	2.345	0.83	2729	78.8
15	1696	54.2	2.16	3.91	3.187	10.13	11954	2757
30	945	33.0	3.17	3.85	<0.1	15.24	7237	2990
45	985	173	4.15	4.01	<0.1	11.70	5973	4235
47	945	144	13.5	2.70	<0.1	12.04	5688	3826
Site 2								
1	2978	203	347	4.32	0.594	0.15	10610	3780
5	1693	112	136	2.09	<0.1	8.79	6955	2086
6	2695	194	342	20.3	17.435	<0.1	10868	3421
10	2014	123	91.2	2.15	<0.1	4.42	7473	2239

TABLE 2A.4 WOODLAWN SOLUTE CONCENTRATIONS (1:5 BATCH LEACHING)

2A.2.2.1 Discussion

As mentioned in Chapter 4, the fact that 7 years of exposure has produced less than 1cm of surface crust and that a 2 day old vertical profile produces just as much secondary mineral formation indicates that climate and grain size are playing a large role at this site. It is suggested that much of the oxidation by-products forming at the surface are in fact being relocated vertically before they are able to precipitate out as salts. This has been verified through analysis of solutes. A combination of climatic conditions and the physical nature of the tailings appears to be restricting hardpan formation in this case, even thought large quantities of oxidation by-products are available.

2A.3 Pine Creek Inlier, N.T

2A.3.1 Ranger U Mine

The geochemical examination of the Ranger Uranium tailings was restricted by water coverage, restraining sampling to only one section of the dam. Thus investigations into the geochemistry of this site is very limited. However, it was observed that the elements which play a major role within this system include S, Mn, Mg, and Ca with lesser contributions from K, Na and Zn and minor supplements from Ni, Cu, Fe and B (Table 2A.5, Figs 2A.28 to 2A.32).

Concentration through evaporation and precipitation has resulted in elevated levels of most elements near the surface. Quantities of Mg, S, Na and Ca have resulted in the precipitation of gypsum, boussingaulitite, wattevillite and hexahydrite. Elevated levels of the other elements can be attributed to the development of discrete mineral phases either too amorphous (as in the case of many Mn salts) or in quantities too low for detection by XRD. Additionally, elemental concentrations may occur through absorption or co-precipition reactions associated with the secondary minerals already discussed.

Calcium appears to be the only element which in fact increases concentration with depth, resulting in the precipitation of gypsum throughout the profile. It would appear that the S profile is dictated more by boussingaulitite, wattevillite and hexahydrite precipitation at the surface while at depth its presence can be attributed to gypsum.

There appears to be little variation in pH down the profile with all samples above pH 7 (Fig 2A.27). The electrical conductivity profile shows a strong increase to 11 mS/cm at the surface down to 3 at depth, indicating the general decrease of soluble salt content with depth (Fig 2A.27).

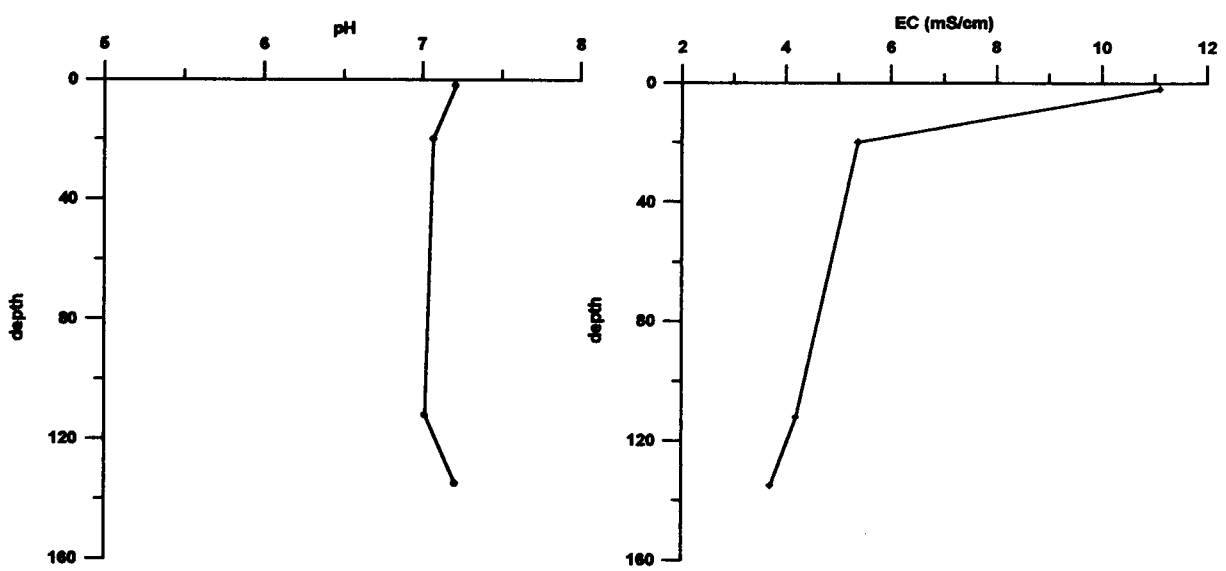

FIG 2A.27 pH AND EC PROFILES FOR RANGER

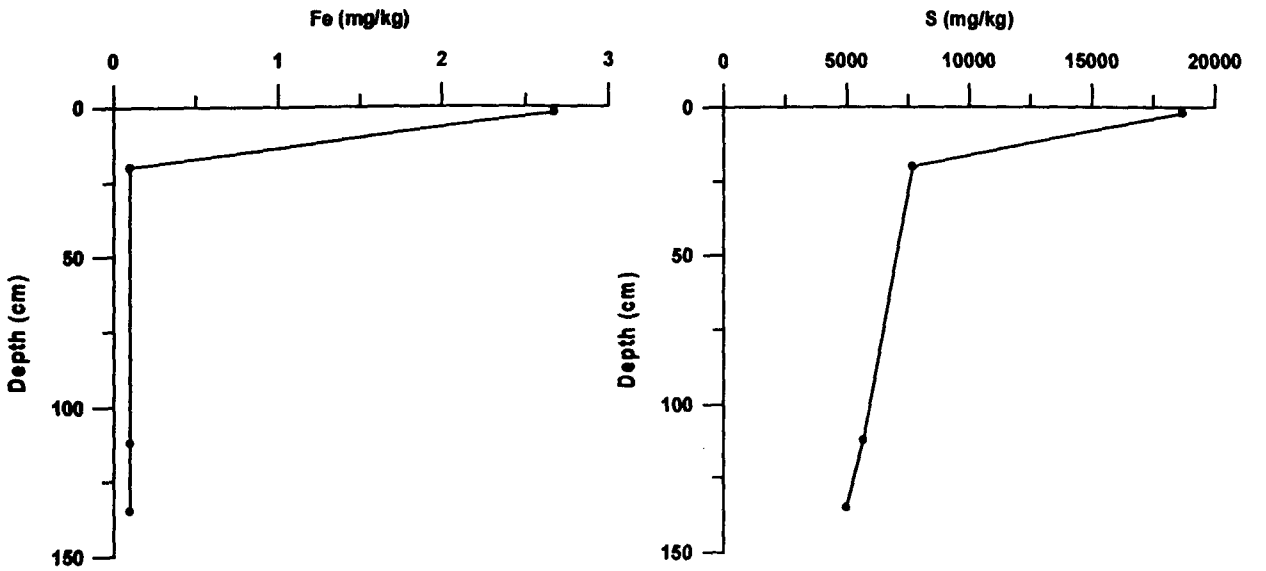

FIG 2A.28 FE AND S PROFILES FOR RANGER

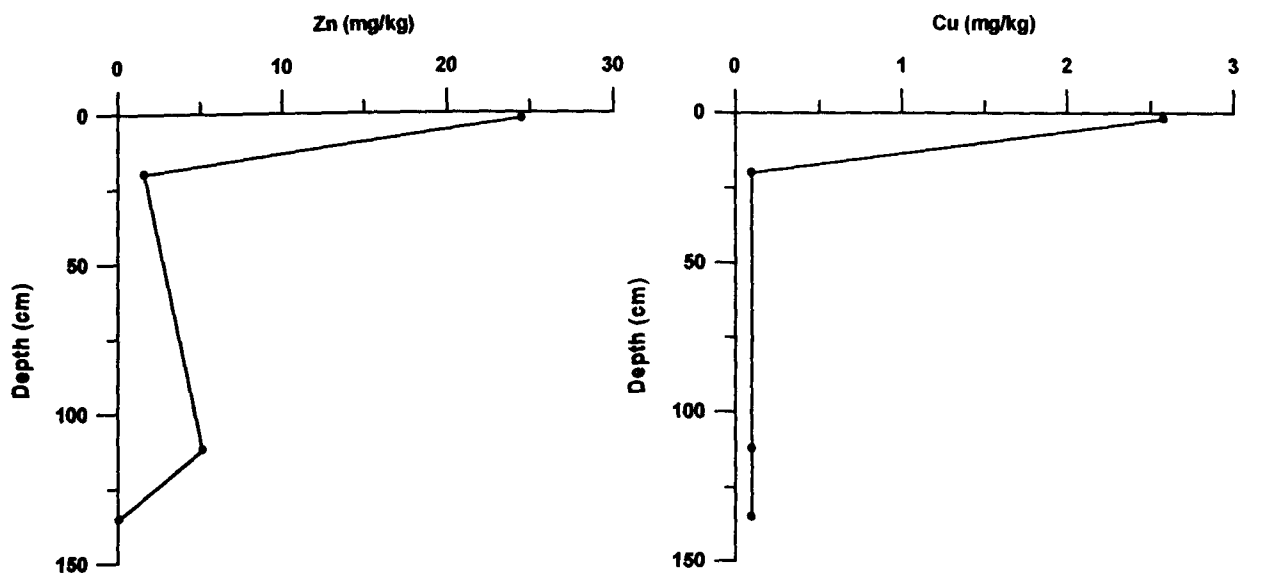

FIG 2A.29 ZN AND CU PROFILES FOR RANGER

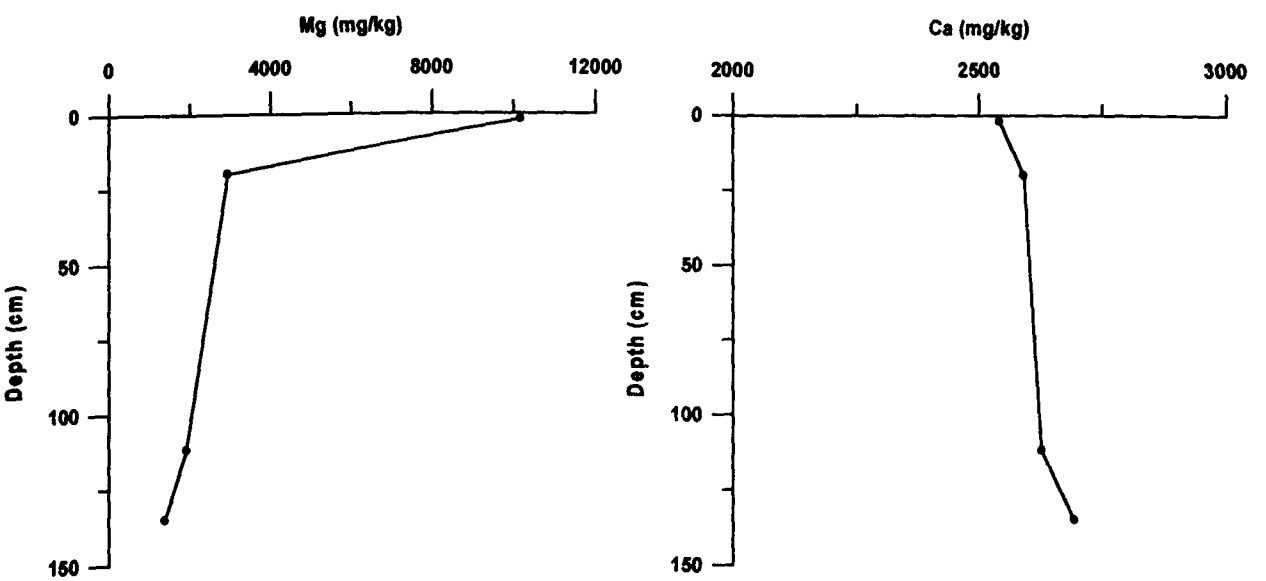

FIG 2A.30 MG AND CA PROFILES FOR RANGER

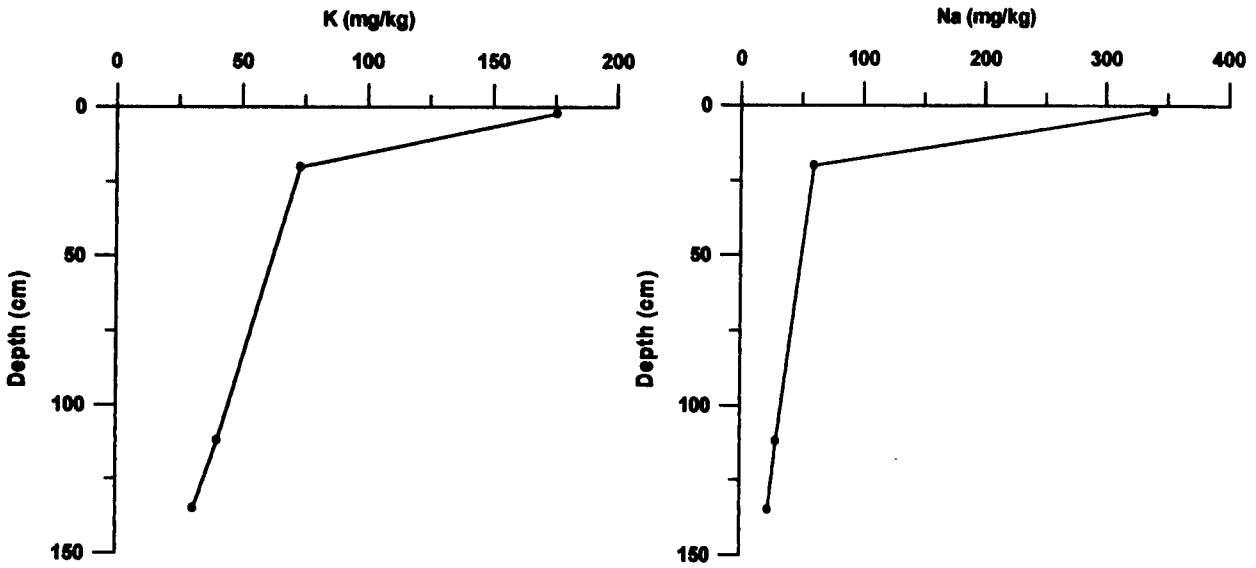

FIG 2A.31 K AND NA PROFILES FOR RANGER

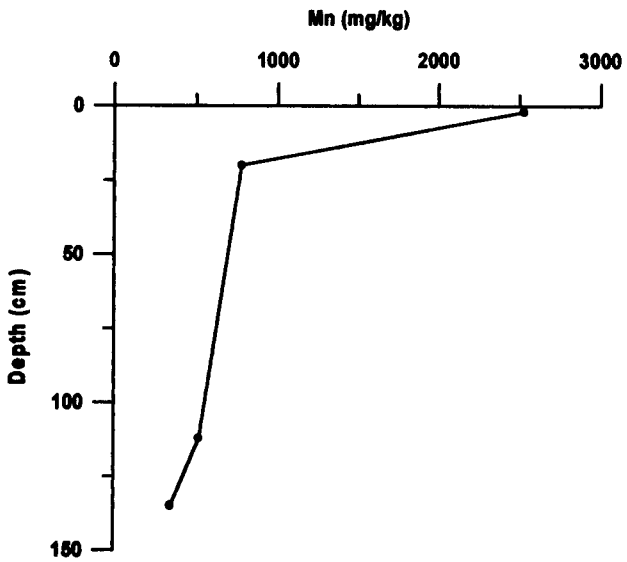

FIG 2A.32 MN PROFILE FOR RANGER

	Al	B	Ca	Cu	Fe	K	Mg	Mn	Na	Ni	S	Zn
	mg/kg	mg/kg	mg/kg	mg/kg	mg/kg	mg/kg	mg/kg	mg/kg	mg/kg	mg/kg	mg/kg	mg/kg
coarse tailings	<0.1	1.115	2638	<0.1	1.05	52.6	2122	475	39.9	0.5	6361	67.2
2cm depth	<0.1	2.99	2543	2.58	2.68	176	10175	2528	339	1.04	18692	24.6
20 cm depth	<0.1	1.205	2591	<0.1	<0.1	73.0	2946	777	59.2	<0.1	7666	1.61
112 cm depth	<0.1	1.095	2628	<0.1	<0.1	40.4	1911	521	29.1	0.54	5680	5.16

TABLE 2A.5 RANGER SOLUTE CONCENTRATIONS (1:5 BATCH LEACHING)

2A.3.2 Pine Creek Au Mine

Sub samples from Sites 1 and 2 described in Chapter 4, were analysed for solute concentrations. Additionally chemistry of the water from Site 1 at the location of seepage from TD3 and Site 2 from ponded water were analysed. The main solutes are Ca, Na, S and K (Table 2A.6). The major concentrations of these elements are associated with the slightly oxidised sulfide tailings at the seepage zone (Site 1) occurring as jarosite and gypsum and where Na is probably substituting for K in the jarosite structure.

The red and orange oxide tailings investigated appear to contain lower solute concentrations, however levels of Ca and S are such that gypsum is readily precipitated. The highest Mg content of 64 mg/kg present within the orange oxide tailings has resulted in the development of hexahydrite, while the red oxide tailings contain very minor increases in Fe levels.

A comparison of the seepage water from the sulfide tailings at depth within TD3 (Site 1) and the ponded water in TD1 (Site 2) indicates the large difference in the mineralogy and thus pollutant generation. The sulfide water contains elevated Ca, Cu, Fe, K, Mg, Mn, Na, S and Zn compared with the ponded water which contained solutes derived only from the oxide tailings (Table 2A.6).

	Al	Ca	Co	Cu	Fe	K	Mg	Mn	Na	Ni	P	S	Zn
	mg/kg	mg/kg	mg/kg	mg/kg	mg/kg	mg/kg	mg/kg	mg/kg	mg/kg	mg/kg	mg/kg	mg/kg	mg/kg
Site 1													
oxidised sulfide tailings	<0.1	525	2.415	<0.1	<0.1	83.5	20.7	0.36	402	<0.1	<0.1	755	<0.1
slightly oxidised sulfide tailings	<0.1	1457	0.525	<0.1	<0.1	257	22.5	<0.1	1052	<0.1	<0.1	2118	<0.1
Site 2													
Orange oxide tailings	<0.1	389	<0.1	<0.1	0.70	90	64.2	0.07	634	<0.1	<0.1	798	<0.1
Red oxide tailings	<0.1	233	1.135	<0.1	7.84	44.0	1.5	<0.1	301	<0.1	<0.1	376	<0.1
	Al	Ca	Co	Cu	Fe	K	Mg	Mn	Na	Ni	P	S	Zn
	mg/L	mg/L	mg/L	mg/L	mg/L	mg/L	mg/L	mg/L	mg/L	mg/L	mg/L	mg/L	mg/L
Site 1 seepage water	0.22	576	1.16	6.77	18.9	132	169	27.0	954	0.97	0.99	1566	8.50
Site 2 ponded water	<0.1	292	<0.1	<0.1	<0.1	25.3	31.0	2.44	85	<0.1	0.22	346	0.72

TABLE 2A.6 PINE CREEK SOLUTE CONCENTRATIONS (1:5 BATCH LEACHING)

2A.3.2.1 Discussion

As core samples could not be removed from these dams a good understanding of the geochemistry developing down the profile could not be achieved. It is obvious however that compared with the sulfide tailings, the oxide capping has a very low reactivity. This is shown by the lack of soluble secondary mineralogy, cement development, and low solute concentrations. A comparison of tailings and waters from both the sulfidic and oxide zones indicate that the oxide tailings have little potential for hardpan development. However, the oxide cover has been effective in reducing the oxidation and pollutant generation of the underlying reactive sulfidic tailings.

Appendix 3A : Laboratory Simulation Individual Results

3A.1 Review of Preliminary Experiments - Brukunga Tailings

3A.1.1 Natural Hardpan Enhancement (E1) vs Biological and Chemical Hardpan Enhancement (E2) - Brukunga Trials

As mentioned in Chapter 6, two Brukunga tailings samples were used in these experiments, to observe the differences in cementing ability of slightly oxidised tailings which were air dried in the lab prior to packing (B1) and fresh unoxidised tailings (B2). The cements developed within the Brukunga Experiment 1 - natural enhancement (E1) and Experiment 2 - biological and chemical enhancement (E2) varied depending on the original mineralogy of the tailings. The acid producing potential of B2 was determined as being greater than that for B1 (Method sections 1A.3.3.1 & 1A.3.3.2 Appendix 1A), however the cementing ability was more a function of the oxidation state of the tailings prior to packing. The NAP of B1 was determined as 15.9 kg/ton and the NAG was 18.8 kg/ton. B2 was higher in both tests with NAP at 27.8 kg/ton and NAG at 33.9 kg/ton.

In general, the B1 (dried sample) trial produced cements throughout both E1 and E2. In both cases the upper 0.5-1cm remained uncemented however below this, cements of jarosite and gypsum were widespread throughout the tailings and were concentrated down preferential flow paths in the lower tailings. In both B1 experiments all tailings were oxidised to a certain extent and had taken on an orange appearance. The B2 (fresh sample) trial showed more development of an oxidation front compared with B1, especially in E1 where oxidation had only taken place down to the textural boundary at 5cm depth. Below this, unoxidised tailings remained and cements were restricted to minor preferential flow paths. Cementing in both B1 and B2 was promoted by the liquid additives, however was enhanced in the B1 compared with B2, which had been air dried prior to packing and thus was already slightly oxidised.

Several samples were removed for 1:5 tailings / water extracts to determine solute concentrations (Table 3A.2 & 3A.3). Some samples targeted cemented and oxidised tailings of preferential flow paths while other removed the available unoxidised tailings for comparison. Within the B1 trial, pH conditions ranged from 3-4, with pH 4 observed only in the base of E1 (Table 3A.1). Both E1 and E2 showed similar EC profiles, up to 14-15mS/cm at the surface and decreases with depth. In general, solute profiles for both E1 and E2 reflected the EC results, with surface accumulations and reductions with depth (Table 3A.1). E2 had larger concentrations of Al, Cr, Cu, Fe, K, Na, P, Pb and S, while E1 produced the greatest concentrations of Zn, Ni, Co, Cd, Mg and Mn, but such differences were not large. The B2 trial showed similar EC trends, with surface solute accumulations and rapid decrease with depth. EC levels up to 18mS/cm occurred in E2 compared with 13mS/cm for E1. The pH ranged from 3 to 4 for E1 and was approximately 3 throughout E2. All of the solute profiles showed increased surface concentrations and marked decreases with depth, except Na which increased with depth. In general E2 exhibited greater concentrations of all elements, except Pb and B. Thus in the B2 trial it appears that oxidation and byproduct development has been promoted via E2.

A comparison of E2 for B1 and B2 showed that B2 had generally larger concentrations of solute elemental loads than B1. This maybe due to the fact that the B2 tailings were unoxidised when packed and were therefore more reactive (ie. no coatings). The increase in B2 may actually reflect cementation within the trials, ie. B1 had lower solute concentrations due to the greater levels of secondary mineral precipitation with low solubility eg. jarosite and gypsum.

A

depth (cm)	pH	EC (mS/cm)
E1 including all oxidised tailings		
0.5	3.20	14.10
1	3.17	5.53
2.5	3.10	2.21
5.5	3.14	1.75
11.5	3.04	2.31
19.5	3.05	2.02
30.5	3.08	1.63
E1 including both ox and unox tailings		
0.5	3.20	14.10
1	3.17	5.53
2.5	3.10	2.21
5.5	3.14	1.75
11.5	3.04	2.31
19.5	3.23	1.42
30.5	3.84	0.58
E2		
0.5	3.09	15.40
1	3.19	5.28
1.5	3.08	2.66
3.5	3.10	2.28
5.5	3.22	2.26
15.5	3.13	2.28
25.5	3.12	1.98

B

depth (cm)	pH	EC (mS/cm)
E1 no cements included		
0.5	3.1	13.1
1.5	3.2	7.83
3.5	3.3	2.06
5.5	3.4	2.26
11	3.6	1.99
21	3.5	1.95
26	3.5	1.63
36	3.8	1.14
E1 including cements		
0.5	3.1	13.1
1.5	3.2	7.83
3.5	3.3	2.06
5.5	3.4	2.26
11	3.6	1.99
21	3.0	2.61
26	3.0	2.47
36	3.8	1.14
E2		
0.5	3.1	18.0
1.5	3.2	7.76
4	3.2	2.89
8	3.1	2.84
15	3.1	2.84
23	3.1	2.50
30	3.3	1.93

TABLE 3A.1 pH AND EC RESULTS FOR BRUKUNGA (B1) - A AND BRUKUNGA (B2) - B NATURAL (E1) AND CHEMICAL AND BIOLOGICAL (E2) HARDPAN ENHANCED TRIALS

depth	Al	B	Ca	Cd	Co	Cr	Cu	Fe	K	Mg	Mn	Mo	Na	Ni	P	Pb	S	Zn
cm	mg/kg	mg/kg	mg/kg	mg/kg	mg/kg	mg/kg	mg/kg	mg/kg	mg/kg	mg/kg	mg/kg	mg/kg	mg/kg	mg/kg	mg/kg	mg/kg	mg/kg	mg/kg
E1 including all oxidised tailings																		
0.1	19200	<0.5	2810	25.4	46.4	1.4	89.2	1680	4.9	2190	4190	<0.2	24.4	271	12	4.5	46350	7870
0.5	4450	<0.5	2070	6.2	10.1	0.5	29.3	443	0.7	454	920	<0.2	4.4	61.5	2	1.1	12450	2020
2.5	735	<0.5	1400	1.1	1.5	<0.2	6.0	19.9	2.0	54.9	101	<0.2	6.7	8.8	<2	<0.2	2720	335
5.5	795	<0.5	720	1.3	1.6	0.3	6.1	7.4	<0.5	53.4	107	0.2	8.1	8.8	<2	1.2	2250	340
11.5	1240	<0.5	990	2.0	2.1	0.4	8.4	29.5	<0.5	65.9	146	<0.2	6.2	13.9	<2	0.9	3400	500
19.5	850	<0.5	990	1.5	1.7	<0.2	5.2	42.4	1.8	65.2	142	<0.2	7.8	12.1	<2	0.2	2730	443
30.5	420	<0.5	850	1.1	1.1	<0.2	2.0	22.2	<0.5	71.1	150	<0.2	12.1	10.6	<2	<0.2	1830	330
E1 including both oxidised and unoxidised tailings																		
0.1	19200	<0.5	2810	25.4	46.4	1.4	89.2	1680	4.9	2190	4190	<0.2	24.4	271	12	4.5	46350	7870
0.5	4450	<0.5	2070	6.2	10.1	0.5	29.3	443	0.7	454	920	<0.2	4.4	61.5	2	1.1	12450	2020
2.5	735	<0.5	1400	1.1	1.5	<0.2	6.0	19.9	2.0	54.9	101	<0.2	6.7	8.8	<2	<0.2	2720	335
5.5	795	<0.5	720	1.3	1.6	0.3	6.1	7.4	<0.5	53.4	107	0.2	8.1	8.8	<2	1.2	2250	340
11.5	1240	<0.5	990	2.0	2.1	0.4	8.4	29.5	<0.5	65.9	146	<0.2	6.2	13.9	<2	0.9	3400	500
19.5	510	<0.5	270	1.8	1.8	<0.2	4.2	112	<0.5	83.3	181	<0.2	6.0	16.4	<2	0.5	1690	471
30.5	126	<0.5	120	0.8	0.9	<0.2	1.6	50.7	1.1	44.4	94.1	<0.2	12.8	8.5	<2	<0.2	570	206
E2																		
0.1	21650	<0.5	2820	21.3	39.0	2.3	134	3510	98.9	2130	2970	<0.2	83.6	187	32	7.2	49950	6980
0.5	4450	<0.5	2690	4.9	7.3	0.6	25.7	325	3.9	320	575	<0.2	13.9	37.4	4	1.1	11750	1610
1.5	1480	<0.5	1180	2.1	2.7	0.2	10.5	38.8	4.3	107	193	<0.2	12.2	13.3	<2	0.4	4110	620
3.5	1040	<0.5	1270	1.6	1.9	0.2	7.5	6.4	<0.5	69.3	125	<0.2	5.2	10.1	<2	0.7	3220	426
5.5	1100	<0.5	1510	1.6	1.9	0.3	7.2	2.0	<0.5	58.3	118	<0.2	8.0	10.5	<2	0.6	3470	424
15.5	1210	<0.5	1290	1.7	2.0	0.3	8.6	10.2	<0.5	60.8	130	<0.2	11.3	12.2	<2	1.4	3570	450
25.5	940	<0.5	910	1.7	1.9	<0.2	7.9	30.8	<0.5	61.8	132	<0.2	5.0	12.3	<2	1.3	2790	404

TABLE 3A.2 ICP-AES RESULTS FOR BRUKUNGA (B1) NATURAL (E1) AND CHEMICAL AND BIOLOGICAL (E2) HARDPAN ENHANCED TRIALS

depth	Al	B	Ca	Cd	Co	Cr	Cu	Fe	K	Mg	Mn	Mo	Na	Ni	P	Pb	S	Zn
cm	mg/kg	mg/kg	mg/kg	mg/kg	mg/kg	mg/kg	mg/kg	mg/kg	mg/kg	mg/kg	mg/kg	mg/kg	mg/kg	mg/kg	mg/kg	mg/kg	mg/kg	mg/kg
E1 - no cements included																		
surf	20302	<5	2604	13.9	14.9	<1	49.3	3178	<1	538.1	538	<1	<1	211	27.5	<5	42148	4203
1-2cm	9078	<1	1796	5.6	5.4	<1	20.3	424	<1	222.8	250	<1	2.2	113	17.7	<1	20626	2035
3-4cm	1206	<1	772	0.9	0.9	<1	3.1	52.9	<1	35.2	37.0	<1	5.1	45.0	<1	<1	3128	313
5-6cm	1519	<1	684	1.4	1.4	<1	3.4	221	<1	34.6	41.5	<1	5.9	30.5	<1	<1	3595	395
10-12cm	1421	<1	418	1.8	1.7	<1	1.8	228	<1	22.7	35.3	<1	6.4	20.1	<1	<1	3220	360
20-22cm	1418	<1	409	1.5	1.4	<1	7.1	168	<1	16.2	31.5	<1	7.7	18.8	<1	<1	3165	321
25-27cm	1106	<1	387	1.1	1.1	<1	3.3	162	<1	14.5	25.2	<1	8.0	16.2	<1	<1	2463	248
35-37cm	917	<1	717	0.9	0.8	<1	<1	176	<1	13.8	17.2	<1	7.7	14.6	<1	<1	2708	301
E1 - including cements																		
surf	20302	<5	2604	13.9	14.9	<1	49.3	3178	<1	538.1	538	<1	<1	211	27.5	<5	42148	4203
1-2cm	9078	<1	1796	5.6	5.4	<1	20.3	424	<1	222.8	250	<1	2.2	113	17.7	<1	20626	2035
3-4cm	1206	<1	772	0.9	0.9	<1	3.1	52.9	<1	35.2	37.0	<1	5.1	45.0	<1	<1	3128	313
5-6cm	1519	<1	684	1.4	1.4	<1	3.4	221	<1	34.6	41.5	<1	5.9	30.5	<1	<1	3595	395
10-12cm	1421	<1	418	1.8	1.7	<1	1.8	228	<1	22.7	35.3	<1	6.4	20.1	<1	<1	3220	360
20-22cm	1776	<1	787	1.2	1.1	<1	8.3	123	<1	21.7	35.9	<1	9.0	14.3	<1	<1	4033	323
25-27cm	1494	<1	677	1.1	1.1	<1	6.6	180	<1	21.0	33.9	<1	10.3	14.7	<1	<1	3653	290
35-37cm	917	<1	717	0.9	0.8	<1	<1	176	<1	13.8	17.2	<1	7.7	14.6	<1	<1	2708	301
E2																		
surf	22236	<5	2725	23.4	47.9	1.9	135.9	5345	<1	2733	3582	<1	0.9	230	47.1	<5	56863	6630
1-2cm	8798	<1	2137	6.1	6.4	<1	26.3	269	<1	220.5	232	<1	1.8	105	18.0	<1	20287	1779
3-5cm	2350	<1	934	1.6	1.6	<1	7.8	22.3	<1	54.7	53.9	<1	5.0	26.1	<1	<1	5172	453
7-9cm	2215	<1	793	1.5	1.5	<1	9.6	38.0	<1	37.6	48.9	<1	4.1	20.6	<1	<1	4774	395
14-16cm	2056	<1	715	1.6	1.4	<1	13.1	248	<1	21.9	43.8	<1	3.9	23.7	<1	<1	4625	398
22-24cm	1752	<1	435	1.6	1.6	<1	10.7	318	<1	17.0	37.4	<1	7.5	24.5	<1	<1	4026	373
29-31cm	1255	<1	337	1.6	1.6	<1	3.5	208	<1	15.3	32.9	<1	8.8	31.4	<1	<1	2940	369

TABLE 3A.3 ICP-AES RESULTS FOR BRUKUNGA (B2) NATURAL (E1) AND CHEMICAL AND BIOLOGICAL (E2) HARDPAN ENHANCED TRIALS

3A.1.2 Leaching Characteristics of the Brukunga Tailings

Brukunga 1 (air dried sample prior to packing) :B1

The leachate from this sample was continuously acidic, with initial values of pH = 3.6 which decreased to 2.7 during the experiment (Table 3A.4). The initial EC was 5.75mS/cm which continued to increase to 12.5mS/cm by day 99 and then decreased to a final 6.9mS/cm (Table 3A.4). The major contributors to this were Al, Ca, Fe, Mg, Mn, S and Zn with lesser input from Cu, Na and Ni (Table 3A.5). The solute concentrations exhibited very variable trends, with different solutes peaking in concentration at different times. Ultimately most elements decreased with time. Calcium, Co, Mg, Mn and Na peaked when the slurry was first mixed whilst Fe, Ni and P peaked in the second leach, and Al, Cd, Cr, Cu, Pb, S and Zn did not peak until the fifth leach.

Calcite levels are very low in the Brukunga tailings. The fact that Ca levels are initially high suggests soluble secondary Ca minerals (e.g. gypsum) must have been present prior to packing. Similar Fe trends were observed and cognate mechamisms of release are suggested. In this highly reactive system in which all the tailings were oxidised to some extent by the end on the experiment, the Fe and reduction in concentration of other solutes must be due to the development of secondary minerals throughout the profile.

date	day	pH	EC		date	day	pH	EC
			mS/cm					mS/cm
Indivdual leaching results					average for each leaching week			
23/08/95	1	3.56	5.75		23/08/95	1	3.56	5.75
22/09/95	32	3.09	8.7		25/09/95	32	3.09	8.70
16/10/95	55	2.83	11.63		18/10/95	57	2.95	10.35
18/10/95	57	2.95	10.1		8/11/95	78	2.79	9.84
20/10/95	59	3.06	9.33		29/11/95	99	2.62	12.47
6/11/95	76	2.72	11.52		20/12/95	120	2.77	10.32
8/11/95	78	2.76	10.3		10/01/96	141	2.66	9.23
9/11/95	79	2.89	7.71		1/02/96	163	2.72	6.93
27/11/95	97	2.59	14.5					
1/12/95	101	2.65	10.44					
20/12/95	120	2.77	10.32					
10/01/96	141	2.67	10.09					
12/01/96	143	2.64	8.36					
31/01/96	162	2.7	7.87					
2/02/96	164	2.73	5.99					

TABLE 3A.4 pH AND EC RESULTS FOR BRUKUNGA (B1) LEACHING CHARACTERISATION EXPERIMENT

	Al	B	Ca	Cd	Co	Cr	Cu	Fe	K	Mg	Mn	Mo	Na	Ni	P	Pb	S	Zn
day	mg/L	mg/L	mg/L	mg/L	mg/L	mg/L	mg/L	mg/L	mg/L	mg/L	mg/L	mg/L	mg/L	mg/L	mg/L	mg/L	mg/L	mg/L
1	238	<0.1	487	0.6	2.7	0.1	1.4	1052	1.9	180	231	0.1	24.6	14.9	<0.1	0.1	1954	144
2	226	<0.1	425	0.5	2.7	0.1	0.5	1156	2.8	160	242	0.1	19.2	15.3	<0.1	0.1	2050	145
32	382	0.2	865	1.3	4.8	<0.1	2.4	1574	0.5	311	366	0.2	40.2	21.4	2.3	<0.1	2948	234
55	1256	<0.1	582	1.5	4.3	<0.1	6.2	1937	<0.1	199	334	<0.1	11.9	30.2	3.0	<0.1	4716	395
57	953	<0.1	589	1.3	3.8	<0.1	4.5	1702	1.7	185	306	<0.1	12.8	25.8	2.8	0.3	4002	334
59	899	<0.1	623	1.3	4.0	<0.1	5.6	1481	0.3	200	300	<0.1	10.0	27.1	2.2	0.2	3594	310
76	2180	<0.1	534	2.0	3.7	<0.1	13.9	990	<0.1	182	344	<0.1	8.7	27.0	0.5	0.7	5620	480
78	1560	<0.1	518	1.6	3.0	<0.1	8.7	1180	<0.1	154	296	<0.1	9.3	21.8	0.5	0.4	4670	371
79	1260	<0.1	561	1.4	2.7	<0.1	6.0	1360	<0.1	144	258	<0.1	9.6	19.6	0.5	0.4	4030	326
80	1120	<0.1	455	1.1	2.0	<0.1	4.5	646	<0.1	111	227	<0.1	6.4	14.1	0.5	0.3	3330	299
97	2360	<0.1	551	3.0	2.9	0.2	16.4	493	0.1	113	261	<0.1	8.6	19.0	0.5	0.5	2280	839
101	1590	<0.1	681	2.7	2.7	<0.1	15.3	626	<0.1	97.2	205	<0.1	12.0	16.7	1.0	0.5	4480	696
118	3870	<0.1	761	5.3	4.4	0.4	30.3	300	<0.1	142	342	<0.1	35.8	27.4	1.0	1.0	8940	1520
120	2050	<0.1	686	3.5	2.8	0.2	18.5	371	<0.1	85.9	210	<0.1	21.7	16.4	1.0	0.7	5510	953
122	1240	<0.1	667	2.4	1.6	<0.1	10.5	301	<0.1	47.8	142	<0.1	18.4	9.2	1.0	0.4	3560	662
139	2230	<0.1	749	3.9	2.7	0.3	18.9	180	<0.1	65.3	191	<0.1	42.2	12.9	1.0	0.9	6060	1170
141	1570	<0.1	656	2.8	1.8	<0.1	12.6	371	<0.1	43.5	144	<0.1	32.0	8.6	1.0	0.5	4220	797
143	1220	<0.1	695	2.4	1.5	<0.1	9.7	266	<0.1	35.5	117	<0.1	33.7	6.9	1.0	0.5	3490	685
162	1130	<0.1	537	1.5	1.0	<0.1	6.7	261	<0.1	22.7	66.5	<0.1	28.8	4.1	0.4	0.6	2890	456
164	647	<0.1	536	0.9	0.6	<0.1	3.9	166	<0.1	14.1	39.0	<0.1	22.5	2.4	0.4	0.5	1850	265
average for each leaching week																		
1	232	<0.1	456	0.6	2.7	0.1	0.9	1104	2.4	170.1	236.7	0.1	21.9	15.1	<0.1	0.1	2002	145
32	382	0.232	865	1.3	4.8	<0.1	2.4	1574	0.5	310.7	366.0	0.2	40.2	21.4	2.3	<0.1	2948	234
57	1036	<0.1	598	1.4	4.1	<0.1	5.4	1707	0.7	194.8	313.5	<0.1	11.6	27.7	2.7	0.2	4104	346
78	1530	<0.1	517	1.5	2.8	<0.1	8.3	1044	<0.1	147.9	281.2	<0.1	8.5	20.6	0.5	0.4	4412	369
99	1985	<0.1	616	2.8	2.8	0.1	15.8	560	0.1	105.2	233.1	<0.1	10.3	17.8	0.8	0.5	3380	768
120	2367	<0.1	705	3.7	3.0	0.2	19.8	324	<0.1	91.9	231.7	<0.1	25.3	17.7	1.0	0.7	6003	1045
141	1673	<0.1	700	3.0	2.0	0.2	13.7	272	<0.1	48.1	150.6	<0.1	36.0	9.5	1.0	0.6	4590	884
163	889	<0.1	537	1.2	0.8	<0.1	5.3	214	<0.1	18.4	52.7	<0.1	25.6	3.2	0.4	0.5	2370	360
D.W	0.2	0.3		0.002		0.05	1.5	0.3			0.5	0.05		0.02		0.01	500	3
F.A	0.005			0.002		0.01	0.005	1						0.15		0.01		0.05
LS	5	5	1000	0.01	1	1	0.5					0.01		1		<0.1	1000	20

TABLE 3A.5 SOLUTE LEACHING RESULTS FOR BRUKUNGA (B1) - LEACHING CHARACTERISATION EXPERIMENT

Brukunga 2 (fresh tailings when packed): B2

The pH of B2 started slightly higher than B1 (3.8) but dropped to lower levels (2.5) during the experiment (Table 3A.6). The initial leach showed high EC levels of 6.1mS/cm, which increased to a maximum of 17mS/cm and a subsequent decrease over time (Table 3A.6). The major contributors were Al, Ca, Fe, S and Zn and to a lesser extent Cu, Mg, Mn, Na and Ni (Table 3A.7). The majority of elements peaked

during the first (day 45) or second (day 66) leach cycles. Copper lagged behind, peaking during day 87 but was only a minor contributor to the system.

Most elements peaked and then decreased over time with Al, Ca, Cd, Mg, Mn, Pb, S and Zn showing a secondary concentration at day 87, the reason for which is uncertain. The overall decrease in concentration through time is suggested to be due to the development of preferential flow path cements which have directed the flow resulting in a limited leaching ability. It should be noted that the entire tailings were oxidised but cements were only developed in particular regions. Additionally Ca and Na appeared to be continually increasing in concentration throughout the life of the experiment.

Date	Days	pH	EC (mS/cm)		Date	Days	pH	EC (mS/cm)
individual leaching results					**average of weekly leachate**			
4/12/96	1	3.82	6.10		4/12/96	1	3.82	6.10
8/01/96	35	2.99	24.80		10/01/96	37	3.14	17.13
10/01/96	37	3.17	13.30		31/01/96	58	2.90	12.93
12/01/96	39	3.25	13.30		21/02/96	79	2.57	14.27
29/01/96	56	2.83	13.60		13/03/96	100	2.58	11.59
31/01/96	58	2.82	13.70		2/04/96	120	2.69	8.15
2/02/96	60	3.06	11.50					
19/02/96	77	2.44	17.60					
21/02/96	79	2.60	13.40					
23/02/96	81	2.68	11.60					
11/03/96	98	2.44	15.90					
13/03/96	100	2.64	10.26					
15/03/96	102	2.67	8.60					
1/04/96	119	2.66	9.64					
3/04/96	121	2.72	6.66					

TABLE 3A.6 pH AND EC RESULTS FOR BRUKUNGA (B2) - LEACHING CHARACTERISATION EXPERIMENT

Sampling	Al	B	Ca	Cd	Co	Cr	Cu	Fe	K	Mg	Mn	Mo	Na	Ni	P	Pb	S	Zn
Days	mg/L	mg/L	mg/L	mg/L	mg/L	mg/L	mg/L	mg/L	mg/L	mg/L	mg/L	mg/L	mg/L	mg/L	mg/L	mg/L	mg/L	mg/L
1	727	<0.1	366	0.6	0.8	<0.1	0.1	730	1.2	55.1	16.8	<0.1	31.9	18.9	0.5	0.7	2500	156
35	6620	<0.1	569	5.0	6.3	<0.1	5.7	3110	0.1	82.9	124	<0.1	22.5	91.7	2.0	1.9	14600	1410
37	2840	<0.1	517	2.8	3.5	<0.1	2.4	2070	0.1	59.1	74.3	<0.1	12.0	47.5	1.0	0.9	7250	675
39	2470	<0.1	586	2.6	3.1	<0.1	3.4	2240	0.1	57.3	72.7	<0.1	13.5	43.2	1.0	0.7	6700	633
56	3480	<0.1	444	2.0	1.9	<0.1	20.8	1170	0.4	35.6	62.3	<0.1	13.7	35.7	6	0.8	7760	604
58	2650	<0.1	448	2.1	1.8	<0.1	9.0	1530	2.9	35.8	53.2	<0.1	14.1	26.1	5	0.9	6630	572
60	2350	<0.1	428	2.0	1.5	<0.1	5.2	1750	2.9	32.5	48.6	<0.1	12.8	22.6	3	0.6	6010	532
77	5136	<0.1	573	3.2	2.0	<0.1	29.1	995	1.4	49.4	89.6	<0.1	8.4	23.6	5	<1	10590	947
79	3583	<0.1	549	2.5	1.4	<0.1	17.9	585	<1	40.9	67.9	<0.1	10.4	16.8	2	<1	7375	730
81	2235	<0.1	529	1.9	1.1	<0.1	10.0	474	<1	24.5	50.7	<0.1	11.5	11.9	<1	<1	5045	534
98	3395	<0.1	573	2.4	1.3	<0.1	15.0	562	<1	29.1	68.7	<0.1	11.5	11.8	1	<1	7224	733
100	2661	<0.1	571	1.9	1.1	<0.1	11.5	359	<1	24.0	54.5	<0.1	12.7	9.5	<1	<1	5590	551
102	1558	<0.1	519	1.1	0.7	<0.1	6.8	214	<1	15.8	32.9	<0.1	12.9	6.0	<1	<1	3502	322
119	2497	<0.1	634	1.4	1.0	<0.1	10.8	207	<1	20.3	42.8	<0.1	21.4	6.8	<1	<1	5465	402
121	1268	<0.1	502	0.7	0.5	<0.1	5.5	274	<1	10.7	20.9	<0.1	17.1	3.7	<1	<1	2986	188
average of weekly leachate																		
1	727	<0.1	366	0.6	0.8	<0.1	0.1	730	1.2	55.1	16.8	<0.1	31.9	18.95	0.50	0.67	2500	156
37	3977	<0.1	557	3.5	4.3	<0.1	3.8	2473	0.1	66.4	90.4	<0.1	16.0	60.81	1.33	1.19	9517	906
58	2827	<0.1	440	2.0	1.7	<0.1	11.7	1483	2.1	34.7	54.7	<0.1	13.5	28.14	4.89	0.76	6800	569
79	3651	<0.1	550	2.5	1.5	<0.1	19.0	685	1.121	38.3	69.4	<0.1	10.1	17.45	2.72	<1	7670	737
100	2538	<0.1	554	1.8	1.0	<0.1	11.1	378	<1	23.0	52.1	<0.1	12.4	9.10	1.13	<1	5439	535
120	1882	<0.1	568	1.0	0.8	<0.1	8.1	240	<1	15.5	31.9	<0.1	19.3	5.26	1	<1	4226	295
D.W	0.2	0.3		0.002		0.05	1.5	0.3			0.5	0.05		0.02		0.01	500	3
F.A	0.005			0.002		0.01	0.005	1						0.15		0.01		0.05
L.S	5	5	1000	0.01	1	1	0.5					0.01		1		0.1	1000	20

TABLE 3A.7 SOLUTE LEACHING RESULTS FOR BRUKUNGA (B2) - LEACHING CHARACTERISATION EXPERIMENT

Comparison of B1 and B2

There appears to be a very distinct separation between the two Brukunga experiments based on the solute concentrations. In B1, much of the acid generation and thus neutralisation reaction with gangue minerals must have already started, as release from gangue minerals is more pronounced (Al, Mg etc). Whereas for B2, major releases were due to direct sulfide oxidation and release (Fe & S). A comparison of the EC trend for both experiments indicates that B2 released greater solute loads with maximum EC levels of 17mS/cm compared to B1 which peaked at 12.5mS/cm. In B2 the EC maximum occurs during the first leach at 37 days whilst in B1 the maximum EC occurs at 99 days during the 4th leaching cycle. This may indicate that either B2 is more reactive as fresh tailings become exposed or that the B1 release takes longer because of the secondary mineral coatings developed prior to packing and the lag period is associated with destabilisation of these coatings. Subsequent releases are associated with this and further sulfide oxidation. It should be noted that the B2 maximum of 17mS/cm within the initial leach may simply reflect solute loads within the tailings prior to sampling.

Similar solute load decreases for both B1 and B2 suggests secondary mineral coatings play a major role in this system as sealing mechanisms to both sulfides and gangue minerals alike. It would appear that the preferential flow cements in B2 may well be having more of an effect, as the trends of the main contributors are essentially the same ie. all decrease in a similar time frame. Whereas the major contributors in B1 peak at different stages in the experiment. This may be a function of preferential coating of particular particles, differences in element mobility and/or variations in solubility of the secondary mineral coatings developed prior to packing.

Results obtained in the study can be compared with the ANZECC's Australian Water Quality Guidelines (1992) for the protection of aquatic ecosystems and livestock watering, along with NHMRC/AWRC guidelines (1987) for drinking water (Table 6A.7). The comparison indicated the solute levels released from both B1 and B2 were unacceptably high for drinking water, fresh aquatic life and livestock watering.

3A.2 Review of Preliminary Experiments - Broken Hill Tailings

3A.2.1 Natural Hardpan Enhancement (E1) vs Biological and Chemical Hardpan Enhancement (E2) - Broken Hill Trials

The basic trend observed throughout both E1 and E2 is the general increase of solute loads at the surface compared with depth (Table 3A.9). This simply reflects the concentration of soluble salts through evaporation at the surface. This general trend can be seen in the EC trends (Table 3A.8). This concentration has resulted in the precipitation of gypsum with minor melanterite and jarosite in E2. Large variations exist between pH profiles, with E1 remaining approximately 7 throughout the profile, whilst within E2 the surface pH has dropped to 4.7 which increased to approximately 7 at depth (Table 3A.8).

As E2 is the addition of Fe/SO_4 at pH 3, these results suggest Broken Hill tailings have a low neutralising potential. NAP and NAG results of less then 2.5 kg/ton confirm this assumption. Additionally increased surface concentration of Al, Cd, Co and Mn in E2 reflect the degradation of gangue minerals associated with the addition of acid. Increased surface levels of Zn, Ni and Pb however suggest that oxidation of minor sulfide must also be enhanced under these conditions. Increased surface levels of Ca, K, Mg and Na in E1 may reflect the fact that jarosite is the dominate secondary mineral in E2 and thus may have preferentially incorporated these elements into its structure. The effect of E1 on Broken Hill tailings was to concentrate the already present soluble salts at the surface of the column. E2 however produced distinct cementing of jarosite and gypsum and promoted the release of Zn via the oxidation of remaining sphalerite.

depth (cm)	pH	EC (mS/cm)
E1		
0.5	7.36	6.71
1	7.69	3.37
6.5	6.98	1.27
15.5	6.97	0.83
24.5	7.20	0.66
31.5	7.24	0.67
E2		
0.5	4.69	6.07
1	4.57	3.51
2.5	4.93	2.70
5.5	6.60	1.53
15.5	6.63	1.02
25.5	7.10	0.64

TABLE 3A.8 pH AND EC RESULTS FOR BROKEN HILL NATURAL (E1) AND CHEMICAL AND BIOLOGICAL (E2) HARDPAN ENHANCED TRIALS

depth	Al	B	Ca	Cd	Co	Cr	Cu	Fe	K	Mg	Mn	Mo	Na	Ni	P	Pb	S	Zn
cm	mg/kg	mg/kg	mg/kg	mg/kg	mg/kg	mg/kg	mg/kg	mg/kg	mg/kg	mg/kg	mg/kg	mg/kg	mg/kg	mg/kg	mg/kg	mg/kg	mg/kg	mg/kg
E1																		
0.1	<0.5	0.9	3640	0.3	<0.2	<0.2	<0.2	<0.5	424	451	0.8	<0.2	4850	<0.2	<2	0.7	4080	11.2
0.5	<0.5	<0.5	470	<0.2	<0.2	<0.2	<0.2	<0.5	312	146	0.7	<0.2	2940	<0.2	<2	<0.2	530	1.2
6.5	<0.5	<0.5	1290	0.3	0.2	<0.2	<0.2	<0.5	38.1	19.2	51.6	<0.2	243	<0.2	<2	0.4	1040	35.4
15.5	<0.5	<0.5	610	0.2	0.3	<0.2	<0.2	<0.5	28.9	16.1	62.3	<0.2	217	<0.2	<2	<0.2	525	28.0
24.5	<0.5	<0.5	400	<0.2	<0.2	<0.2	<0.2	<0.5	29.1	15.3	60.7	<0.2	221	0.2	<2	<0.2	347	7.7
31.5	<0.5	<0.5	370	<0.2	<0.2	<0.2	<0.2	<0.5	78.0	16.0	59.4	<0.2	216	0.2	<2	<0.2	332	4.9
E2																		
1	65	0.7	2960	4.8	24.4	<0.2	<0.2	2550	26.6	308	6080	<0.2	1230	6.0	2	4.6	9260	1220
1.5	9.7	<0.5	2360	2.7	8.5	<0.2	<0.2	47.6	65.4	110	1920	<0.2	1010	2.0	<2	8.6	3510	373
2.5	4.0	<0.5	2990	1.2	3.4	<0.2	<0.2	6.9	37.7	48.1	765	<0.2	409	1.2	<2	10.8	2980	164
5.5	0.7	<0.5	1010	1.1	2.2	<0.2	<0.2	<0.5	30.9	43.4	550	<0.2	377	1.3	<2	1.9	1240	133
15.5	<0.5	<0.5	710	0.7	0.8	<0.2	<0.2	<0.5	32.4	25.4	163	<0.2	284	0.9	<2	0.5	715	87.7
25.5	<0.5	<0.5	380	<0.2	0.3	<0.2	<0.2	<0.5	29.5	14.6	69.3	<0.2	203	0.4	<2	0.3	347	15.5

TABLE 3A.9 ICP-AES RESULTS FOR BROKEN HILL NATURAL (E1) AND CHEMICAL AND BIOLOGICAL (E2) HARDPAN ENHANCED TRIALS

3A.2.2 Leaching Characteristics of the Broken Hill Tailings

The leaching results observed for Broken Hill are essentially an overall removal of all solutes from the tailings over time. The major components of the leachate are Ca, K, Mn, S and Na (Table 3A.10). All of these show an initial increase and eventual decrease in concentration. It is understood that mine water

is recycled along with town water for reprocessing and thus has a residue high TDS. Obviously much of this leachate load is residual but Ca and Na levels are enhanced by additives from processing.

Similar trends are observed throughout the suite of elements investigated however Fe, Zn, Cu and Pb show a slight lag in leaching response. This probably reflects oxidation of the minor sulfide still present within the tailings and thus the subsequent elemental release associated with this. Minimal acid has been produced (Table 6A.11).

A comparison with water quality guidelines (Table 3A.10), indicates that the leachate was unacceptable for fresh aquatic life or drinking water. It was also unsuitable for livestock consumption due to elevated levels of Cd, Pb, S and Zn.

	Al	B	Ca	Cd	Co	Cr	Cu	Fe	K	Mg	Mn	Na	Ni	P	Pb	S	Zn
day	mg/L	mg/L	mg/L	mg/L	mg/L	mg/L	mg/L	mg/L	mg/L	mg/L	mg/L	mg/L	mg/L	mg/L	mg/L	mg/L	mg/L
1	0.1	0.2	625	0.3	<0.182	0.1	0.1	<0.1	121.7	62.7	172.0	1180.6	0.1	<0.1	0.1	690	30.5
32	<0.1	0.4	730	0.9	0.4	<0.1	<0.153	<0.1	173.9	80.6	241.9	1299.7	0.2	0.8	1.1	1006	53.8
35	<0.1	0.5	775	1.3	0.5	<0.1	<0.1	<0.1	206.5	96.4	284.4	1617.0	0.2	0.8	1.6	1076	74.4
55	0.2	0.4	703	1.1	0.4	<0.1	<0.1	0.8	144.5	84.6	217.9	1141.6	0.1	1.4	0.9	931	55.7
57	<0.1	0.4	667	0.3	0.2	<0.1	<0.1	<0.1	41.2	18.6	76.4	174.8	0.1	0.5	0.1	656	40.6
59	0.2	0.2	620	0.6	0.2	<0.1	0.3	1.4	13.4	11.7	37.4	41.5	0.1	0.5	0.3	623	110.0
76	0.2	<0.101	534	0.1	0.1	<0.1	<0.1	0.3	7.6	1.4	20.6	3.9	0.1	0.5	0.3	447	19.4
78	<0.1	<0.1	528	0.1	<0.1	<0.1	<0.1	<0.1	12.5	0.4	10.4	4.3	0.1	0.5	<0.1	416	16.6
79	1.4	<0.1	582	0.1	<0.1	<0.1	0.1	6.5	13.2	0.9	15.7	3.5	0.1	0.5	1.7	440	19.3
80	0.1	<0.1	437	<0.1	<0.1	<0.1	<0.1	0.6	9.1	0.4	6.5	1.4	<0.1	<0.1	0.4	323	16.4
97	<0.1	<0.1	453	<0.1	<0.1	<0.1	<0.1	<0.1	15.1	1.0	8.9	2.1	<0.1	<0.1	0.1	307	9.4
99	<0.1	<0.1	229	<0.1	<0.1	<0.1	<0.1	<0.1	8.6	0.3	4.5	1.6	<0.1	<0.1	<0.1	179	8.1
101	<0.1	<0.1	133	<0.1	<0.1	<0.1	<0.1	<0.1	7.7	0.2	3.4	0.9	<0.1	0.2	<0.1	96	6.6
118	<0.1	<0.1	321	<0.1	<0.1	<0.1	<0.1	<0.1	13.8	1.1	5.5	1.5	<0.1	0.2	<0.1	250	8.7
120	<0.1	<0.1	104	<0.1	<0.1	<0.1	<0.1	<0.1	7.2	0.4	2.6	0.9	<0.1	0.2	<0.1	78	5.3
122	<0.1	<0.1	86	<0.1	<0.1	<0.1	<0.1	<0.1	7.1	0.3	2.2	1.0	<0.1	0.2	<0.1	60	3.5
139	<0.1	<0.1	341	<0.1	<0.1	<0.1	<0.1	<0.1	17.4	1.4	2.2	1.8	<0.1	0.2	<0.1	276	4.2
141	<0.1	<0.1	106	<0.1	<0.1	<0.1	<0.1	<0.1	7.8	0.6	1.0	1.0	<0.1	0.2	<0.1	83	3.2
143	<0.1	<0.1	80	<0.1	<0.1	<0.1	<0.1	<0.1	6.4	0.4	0.8	1.0	<0.1	0.2	<0.1	58	2.1
160	<0.1	<0.1	237	<0.1	<0.1	<0.1	<0.1	<0.1	10.9	1.1	1.2	1.3	<0.1	<0.1	<0.1	181	5.4
162	<0.1	<0.1	82	<0.1	<0.1	<0.1	<0.1	<0.1	6.3	0.3	0.5	0.7	<0.1	<0.1	<0.1	51	1.6
164	<0.1	<0.1	61	<0.1	<0.1	<0.1	<0.1	<0.1	5.2	0.2	0.4	1.0	<0.1	<0.1	<0.1	35	1.4
average for each leaching week																	
1	0.1	0.2	625	0.3	0.2	0.1	0.1	<0.1	121.7	62.7	172.0	1180.6	0.1	<0.1	0.1	690	30.5
33	<0.1	0.5	752	1.1	0.5	<0.1	0.1	<0.1	190.2	88.5	263.2	1458.4	0.2	0.8	1.3	1041	64.1
57	0.2	0.3	663	0.7	0.2	<0.1	0.2	0.8	66.4	38.3	110.6	452.6	0.1	0.8	0.4	736	68.8
78	0.5	0.1	520	0.1	0.1	<0.1	0.1	1.9	10.6	0.8	13.3	3.3	0.1	0.4	0.6	407	17.9
99	<0.1	<0.1	271	<0.1	<0.1	<0.1	<0.1	<0.1	10.5	0.5	5.6	1.5	<0.1	0.1	<0.1	194	8.1
120	<0.1	<0.1	170	<0.1	<0.1	<0.1	<0.1	<0.1	9.4	0.6	3.4	1.1	<0.1	0.2	<0.1	129	5.8
141	<0.1	<0.1	176	<0.1	<0.1	<0.1	<0.1	<0.1	10.6	0.8	1.4	1.3	<0.1	0.2	<0.1	139	3.2
162	<0.1	<0.1	127	<0.1	<0.1	<0.1	<0.1	<0.1	7.5	0.5	0.7	1.0	<0.1	<0.1	<0.1	89	2.8
D.A	0.2	0.3		0.002		0.05	1.5	0.3			0.5		0.02		0.01	500	3
F.A	0.005			0.002		0.01	0.005	1					0.15		0.01		0.05
L.S	5	5	1000	0.01	1	1	0.5						1		0.1	1000	20

TABLE 3A.10 SOLUTE LEACHING RESULTS FOR BROKEN HILL - LEACHING CHARACTERISATION EXPERIMENT

date	day	pH	EC (mS/cm)		date	day	pH	EC (mS/cm)
individual leaching results					average for each leaching week			
23/08/95	1	7.57	8.48		23/08/95	1	7.57	8.48
22/09/95	32	6.89			24/09/95	33	6.82	10.51
26/09/95	35	6.75	10.51		18/10/95	57	6.42	4.78
16/10/95	55	6.52	8.57		8/11/95	78	7.25	1.93
18/10/95	57	6.60	3.36		29/11/95	99	6.88	1.14
20/10/95	59	6.15	2.41		20/12/95	120	6.99	0.78
6/11/95	76	7.27	2.14		10/01/96	141	6.86	0.82
8/11/95	78	7.32	2.09					
10/11/95	80	7.15	1.57					
27/11/95	97	6.98	1.75					
29/11/95	99	6.77	1.03					
1/12/95	101	6.89	0.63					
18/12/95	118	6.83	1.26					
20/12/95	120	6.98	0.60					
22/12/95	122	7.17	0.47					
8/01/96	139	6.72	1.38					
10/01/96	141	6.92	0.59					
12/01/96	143	6.94	0.48					
29/01/96	160	7.32	1.08					
31/01/96	162	7.13	0.43					
2/02/96	164	7.28	0.33					

TABLE 3A.11 pH AND EC RESULTS FOR BROKEN HILL - LEACHING CHARACTERISATION EXPERIMENT

3A.3 Review of Preliminary Experiments - Elura Tailings

3A.3.1 Natural Hardpan Enhancement (E1) vs Biological and Chemical Hardpan Enhancement (E2) - Elura Trials

As with the majority of tailings trials, the basic trend observed through both E1 and E2 is the general increase of solute loads at the surface compared with depth reflecting solute concentrations through evaporation (Table 3A.13). This concentration has resulted in the precipitation of gypsum, hexahydrite, bianchite and boyleite (Ca, Mg, Fe and Pb sulfates) in E1, whilst E2 has produced gypsum, hexahydrite, rozenite, boyleite, mirabilite and szomolnokite.

NAP values for Elura tailings were determined as 301 kg/ton while its NAG was less than 2.5 kg/ton. These results along with solute concentrations, pH and EC profiles for 1:5 water extracts of both E1 and E2 columns indicate that Elura has highly reactive tailings. These result reflect the strongly oxidising conditions and large elemental loads produced with or without enhancement. For example even though E2 received Fe/SO_4 additions throughout the experiment, levels of surface soluble S were approximately the same for both E1 and E2 (Table 3A.13). However, Cu, Zn, and Fe levels in E2 were much higher than E1 indicating enhanced oxidising conditions were occurring in E2. This increased oxidation is not reflected to any great extent in the pH profiles (Table 3A.12).

Increased concentrations of the majority of elements also exist within the surface zones of E2. This is not so for the Pb profiles. In both E1 and E2, Pb surface levels were lower than at 3-8cm depth. This is potentially due to Pb incorporation into insoluble cements at the surface and therefore resulting in their non-availablity for this type of soluble salt analysis. Cements developed during these trials were not enhanced greatly within E2 compared with E1 during the time frame of this experiment, partly due to the

strong cementing potential already present within the tailings. ICP results do however suggest solute loads are definitely increased in E2 compared with E1, and which may eventually become incorporated within the cements, unless leached from the surface.

depth (cm)	pH	EC (mS/cm)
E1		
0.5	4.44	22.50
1	4.40	11.12
3.5	5.31	3.69
7.5	6.36	2.67
18.5	6.33	2.32
27.5	6.47	2.41
35.5	6.40	2.17
E2		
0.5	3.97	22.20
1	4.12	11.35
3.5	5.75	3.76
12.5	5.98	2.75
20.5	6.01	2.61
27.5	6.09	2.48

TABLE 3A.12 pH AND EC RESULTS FOR ELURA NATURAL (E1) AND CHEMICAL AND BIOLOGICAL (E2) HARDPAN

depth	Al	B	Ca	Cd	Co	Cr	Cu	Fe	K	Mg	Mn	Mo	Na	Ni	P	Pb	S	Zn
cm	mg/kg	mg/kg	mg/kg	mg/kg	mg/kg	mg/kg	mg/kg	mg/kg	mg/kg	mg/kg	mg/kg	mg/kg	mg/kg	mg/kg	mg/kg	mg/kg	mg/kg	mg/kg
E1																		
1	2.2	2.1	2600	11.1	<0.2	0.6	0.7	660	<0.5	28500	10400	<0.2	3940	2.3	22	3.6	50250	5060
1.5	<0.5	0.6	2520	5.0	<0.2	<0.2	1.3	295	18.2	10800	3760	<0.2	1430	11.4	8	13.1	20000	1910
3.5	<0.5	<0.5	3040	2.6	<0.2	<0.2	0.7	5.8	22.8	1360	442	<0.2	316	16.6	<2	14.1	4920	485
7.5	<0.5	<0.5	2930	2.6	0.4	0.3	0.3	<0.5	3.2	550	53.3	<0.2	121	1.1	<2	12.8	3820	270
18.5	<0.5	<0.5	2550	2.0	0.2	0.2	<0.2	<0.5	6.9	560	56.9	<0.2	127	1.1	<2	4.6	3520	275
2.5	<0.5	<0.5	2660	2.2	<0.2	<0.2	<0.2	<0.5	3.7	415	44.1	<0.2	84.2	0.8	<2	11.0	3500	296
35.5	<0.5	<0.5	2570	2.0	<0.2	<0.2	<0.2	<0.5	2.4	305	41.7	<0.2	62.4	1.3	<2	11.4	3200	271
E2																		
1	71.5	2.1	2600	31.5	1.4	0.3	29.8	2070	<0.5	26300	11600	<0.2	2040	5.6	23	7.5	50100	9550
1.5	10.2	0.6	2580	11.9	0.6	<0.2	58.2	472	<0.5	10400	4070	<0.2	880	56.5	9	13.7	21950	6120
3.5	<0.5	<0.5	2940	2.8	<0.2	<0.2	0.4	<0.5	19.7	1280	790	<0.2	207	17.4	<2	9.3	5040	1270
12.5	<0.5	<0.5	2940	3.1	0.3	<0.2	<0.2	<0.5	1.9	690	87.7	<0.2	91.5	2.2	<2	11.1	4440	394
20.5	<0.5	<0.5	2840	2.8	0.3	0.2	0.3	<0.5	0.6	600	74.7	0.2	80.6	2.5	<2	10.7	4070	387
27.5	<0.5	<0.5	2880	2.6	0.3	0.2	<0.2	<0.5	1.9	471	41.8	<0.2	72.9	2.1	<2	13.0	4020	327

TABLE 3A.13 ICP-AES RESULTS FOR ELURA NATURAL (E1) AND CHEMICAL AND BIOLOGICAL (E2) HARDPAN ENHANCED TRIALS

3A.3.2 Leaching Characteristics of the Elura Tailings

The solute concentrations developed from the Elura tailings leaching experiment are verification of the ability of secondary minerals to dictate contaminant loads. The EC trend gives a generalised view of the overall mechanisms taking place within the tailings (Table 3A.15). The initial stages show distinct eluviation in which soluble salts produced prior to sampling were released. The following decrease represents the period prior to oxidation by-product build-up. This subsequent continual low reflects the initial release of oxidation by-products and then the coating of sulfide and gangue minerals with insoluble cements resulting in a general solute load decrease. These mechanisms are also observed in the pH profile where the initial values of 7.5 decreased to pH 4 as a result of sulfide oxidation and was sustained at this level throughout the remainder of the experiment.

The main components of the leachate are Ca, Mg, Mn, Na, S and Zn with much of the Na and Ca attributed to milling additives, while Mg and Mn release occurs through degradation of gangue minerals in the acidic environment (Table 3A.14). High levels of Zn and Cd during the initial stages of the trial indicates sphalerite oxidation is dominating the sulfide oxidation reactions along with pyrrhotite. Sphalerite and pyrrhotite oxidation does not add acid to the system unlike pyrite oxidation. The decrease in pH and Fe released in the final stages indicate that pyrite oxidation is to some extent still occurring.

Overall these tailings show large potential for solute release however secondary mineral coatings along preferential flow paths are at least reducing this load. A comparison with water quality guidelines (Table 3A.14), indicates that this leachate was not suitable to support fresh aquatic life or drinking water supplies. Nor was it acceptable for livestock consumption as levels of Cd, Pb, S and Zn are much greater than recommended levels.

	Al	B	Ca	Cd	Co	Cr	Cu	Fe	K	Mg	Mn	Na	Ni	P	Pb	S	Zn
day	mg/L	mg/L	mg/L	mg/L	mg/L	mg/L	mg/L	mg/L	mg/L	mg/L	mg/L	mg/L	mg/L	mg/L	mg/L	mg/L	mg/L
1	0.1	0.2	748.1	0.1	0.1	0.1	0.1	<0.1	60.9	359	2.4	836.9	0.1	2.2	1.3	1301	6.6
2	<0.1	<0.1	31.5	<0.1	<0.1	<0.1	<0.1	<0.1	1.0	11	1.7	15.3	<0.1	0.1	4.4	65	23.0
35	<0.1	0.2	29.5	0.1	<0.1	<0.1	0.2	<0.1	1.3	21	4.6	17.3	<0.1	<0.1	3.6	100	53.9
55	<0.1	0.1	70.5	0.5	<0.1	<0.1	0.3	3.2	2.5	289	37.3	54.4	0.3	0.5	3.0	745	511.0
57	<0.1	0.3	177.0	3.5	0.3	<0.1	0.1	97.0	6.1	831	242.2	220.6	1.0	1.6	2.3	2515	2276.0
59	<0.1	0.1	180.1	2.9	0.2	<0.1	0.4	66.1	4.8	713	224.8	206.3	0.8	1.0	2.5	2252	1869.0
76	<0.1	<0.1	63.3	0.4	<0.1	<0.1	0.2	27.7	0.8	281	62.0	37.1	0.3	0.5	2.0	698	415.8
78	<0.1	0.1	131.2	1.5	<0.1	<0.1	0.1	108.6	0.8	769	233.7	130.9	0.5	0.5	2.9	1830	845.6
80	0.1	<0.1	74.1	0.7	<0.1	<0.1	0.2	88.8	2.2	553	132.8	70.1	0.3	0.5	2.2	1270	720.7
97	<0.1	<0.1	69.4	0.4	<0.1	<0.1	0.3	80.9	1.6	603	132.5	43.2	0.3	0.5	1.2	1470	628.9
99	<0.1	<0.1	70.1	0.3	<0.1	<0.1	0.1	55.6	1.1	427	108.1	47.9	0.2	0.5	0.9	899	325.4
101	<0.1	<0.1	42.8	0.2	<0.1	<0.1	0.1	27.8	1.1	257	88.3	40.9	<0.1	0.2	0.9	663	232.9
118	<0.1	<0.1	28.8	0.1	<0.1	<0.1	0.3	10.7	<0.1	310	86.8	13.6	<0.1	0.2	0.5	746	271.7
120	<0.1	<0.1	40.1	0.1	<0.1	<0.1	0.2	14.8	0.4	187	49.6	20.2	<0.1	0.2	0.7	387	99.8
122	<0.1	<0.1	22.8	<0.1	<0.1	<0.1	0.1	18.2	0.4	198	56.5	18.9	<0.1	0.2	0.4	454	110.1
139	<0.1	<0.1	53.0	<0.1	<0.1	<0.1	0.2	24.6	<0.1	333	90.0	11.5	<0.1	0.2	0.3	762	167.8
141	<0.1	<0.1	25.7	<0.1	<0.1	<0.1	0.2	19.1	0.1	224	54.7	12.0	<0.1	0.2	0.2	396	69.4
143	<0.1	<0.1	16.7	<0.1	<0.1	<0.1	<0.1	21.2	<0.1	169	47.4	10.9	<0.1	0.2	0.2	372	58.8
160	<0.1	<0.1	47.7	<0.1	<0.1	<0.1	0.3	67.6	<0.1	583	114.7	14.9	<0.1	0.2	0.3	859	130.7
162	<0.1	<0.1	33.1	<0.1	<0.1	<0.1	0.2	39.8	<0.1	297	57.2	20.6	<0.1	0.2	0.4	444	51.6
164	<0.1	<0.1	23.8	<0.1	<0.1	<0.1	0.1	23.1	0.3	158	<0.1	19.0	<0.1	0.2	0.3	299	33.3
average for each leaching week																	
1	0.1	0.2	748.1	0.1	0.1	0.1	0.1	<0.1	60.9	359	2.4	836.9	0.1	2.2	1.3	1301	6.6
33	<0.1	0.1	30.5	0.1	<0.1	<0.1	0.1	<0.1	1.2	16	3.2	16.3	<0.1	0.1	4.0	83	38.4
57	<0.1	0.2	145.9	2.3	0.2	<0.1	0.3	55.5	4.5	611	168.1	160.4	0.7	1.0	2.6	1837	1552.0
78	0.1	0.1	89.5	0.9	<0.1	<0.1	0.2	75.0	1.3	534	142.8	79.3	0.4	0.5	2.3	1266	660.7
99	<0.1	<0.1	60.8	0.3	<0.1	<0.1	0.2	54.7	1.3	429	109.6	44.0	0.2	0.4	1.0	1011	395.7
120	<0.1	<0.1	30.6	0.1	<0.1	<0.1	0.2	14.6	0.3	232	64.3	17.5	<0.1	0.2	0.5	529	160.5
141	<0.1	<0.1	31.8	<0.1	<0.1	<0.1	0.1	21.6	0.1	242	64.0	11.5	<0.1	0.2	0.3	510	98.7
162	<0.1	<0.1	34.9	<0.1	<0.1	<0.1	0.2	43.5	0.2	346	57.3	18.2	<0.1	0.2	0.3	534	71.9
D.W	0.2	0.3		0.002		0.05	1.5	0.3			0.5		0.02		0.01	500	3
F.A	0.005			0.002		0.01	0.005	1					0.15		0.01		0.05
LS	5	5	1000	0.01	1	1	0.5						1		<0.1	1000	20

TABLE 3A.14 SOLUTE LEACHING RESULTS FOR ELURA - LEACHING CHARACTERISATION EXPERIMENT

date	day	pH	EC (mS/cm)		date	day	pH	EC (mS/cm)
individual leaching results					average of weekly leachate			
23/08/95	1	7.01	7.38		23/08/95	1	7.01	7.38
22/09/95	2	5.98	0.38		24/09/95	33	5.68	0.46
26/09/95	35	5.38	0.54		18/10/95	57	4.72	6.04
16/10/95	55	4.88	2.87		8/11/95	78	4.51	4.93
18/10/95	57	4.57	7.65		29/11/95	99	4.37	4.00
20/10/95	59	4.7	7.59		20/12/95	120	4.40	2.27
6/11/95	76	4.6	2.96		10/01/96	141	4.51	2.26
8/11/95	78	4.42	6.79		31/01/96	162	4.18	2.41
27/11/95	97	4.22	5.45					
29/11/95	99	4.42	3.64					
1/12/95	101	4.46	2.9					
18/12/95	118	4.42	2.89					
20/12/95	120	4.64	1.75					
22/12/95	122	4.15	2.17					
6/01/96	139	4.63	3.12					
10/01/96	141	4.55	1.82					
12/01/96	143	4.36	1.83					
29/01/96	160	4.22	3.64					
31/01/96	162	4.16	2.13					
2/02/96	164	4.15	1.47					

TABLE 3A.15 pH AND EC RESULTS FOR ELURA - LEACHING CHARACTERISATION EXPERIMENT

3A.4 Review of Preliminary Experiments - CSA Tailings

3A.4.1 Natural Hardpan Enhancement (E1) vs Biological and Chemical Hardpan Enhancement (E2) - CSA Trials

Again the basic trend observed throughout both E1 and E2 is the general increase of soluble elemental loads at the surface compared with depth (Table 3A.17). Concentration has resulted in the precipitation of gypsum, hexahydrite and goethite in E1 while gypsum, hexahydrite and jarosite developed in E2.

In the CSA tailings it was noted that EC surface values were almost twice as high in E2 as in E1. pH profiles developed are also very different with E2 showing a pH of less than 4 throughout the profile, while E1 varies between 4 and 6. The decrease to approximately pH 4 between 5-15cm depth within E1 corresponds to the position of cements developed along minor textural variations within the column (Table 3A.16). The CSA tailings NAP was determined as 8.8 kg/ton while the NAG was determined as 7.09 kg/ton.

In general, E2 shows increased surface levels of the majority of elements resulting from enhanced degradation of gangue minerals associated with acid additions and generation. Increased levels of Zn, Cu, Fe, Ni and S can, to some extent, be attributed to oxidation of sphalerite, chalcopyrite and pyrite, where Ni is often present as an impurity in pyrite. Obviously some levels of Fe and S must be attributed to the Fe/SO_4 additions during the experiment. Enhanced levels of K, Ca and Na at the surface of E1 compared with E2 may simply reflect the development of insoluble/less soluble secondary minerals in E2 which reduce comparatively the released concentration of these elements. The low pH in E1 between 5-15cm occurs directly below a textural boundary within the column. This corresponds to increased Ca and Pb levels and minor increases in Fe, Al, Ca, Cu, Ni and Zn. These increased levels reflect an

enhanced zone of oxidation and by-product precipitation developing beneath a fine tailings layer. Perhaps reduced permeability above this area impeded flow sufficiently so that concentration and thus precipitation could occur.

depth (cm)	pH	EC (mS/cm)
E1		
0.5	6.38	6.13
1.5	6.98	2.87
5.5	4.17	1.95
11.5	4.09	1.77
21.5	7.46	1.04
31.5	7.58	1.06
E2		
1.5	3.61	12.74
3.5	3.61	4.40
5.5	3.91	1.99
13.5	4.21	1.67
21.5	4.02	1.98
29.5	4.08	2.22

TABLE 3A.16 pH AND EC RESULTS FOR CSA NATURAL (E1) AND CHEMICAL AND BIOLOGICAL (E2) HARDPAN

depth	Al	B	Ca	Cd	Co	Cr	Cu	Fe	K	Mg	Mn	Mo	Na	Ni	P	Pb	S	Zn
cm	mg/kg	mg/kg	mg/kg	mg/kg	mg/kg	mg/kg	mg/kg	mg/kg	mg/kg	mg/kg	mg/kg	mg/kg	mg/kg	mg/kg	mg/kg	mg/kg	mg/kg	mg/kg
E1																		
0.1	<0.5	<0.5	2700	<0.2	<0.2	<0.2	<0.2	<0.5	217	3890	55.3	<0.2	1500	<0.2	2	<0.2	8420	1.4
1.5	<0.5	<0.5	1570	<0.2	<0.2	<0.2	<0.2	<0.5	157	774	24.3	<0.2	970	<0.2	<2	<0.2	2820	0.4
5.5	20.9	<0.5	2270	<0.2	2.6	<0.2	17.9	34.5	55.2	203	35.3	<0.2	149	1.1	<2	0.6	2170	15.0
11.5	28.5	<0.5	2150	<0.2	2.6	<0.2	13.9	43.7	21.5	201	23.7	<0.2	54.7	1.3	<2	1.0	2030	12.4
21.5	<0.5	<0.5	1210	0.2	<0.2	<0.2	<0.2	<0.5	9.1	86.8	1.6	<0.2	16.3	0.5	<2	<0.2	1060	<0.2
31.5	<0.5	<0.5	1250	<0.2	<0.2	<0.2	<0.2	<0.5	5.6	80.2	4.2	<0.2	12.1	0.5	<2	<0.2	1070	<0.2
E2																		
1.5	1750	<0.5	2880	0.8	85.8	<0.2	321	610	<0.5	13700	1730	<0.2	1190	16.1	5	0.7	25400	755
3.5	230	<0.5	2880	0.3	18.2	<0.2	104	104	5.4	1810	334	<0.2	610	3.8	<2	0.2	5440	167
5.5	28.8	<0.5	2390	<0.2	3.4	<0.2	19.8	52.2	17.0	198	44.9	<0.2	83.8	1.5	<2	0.5	2220	24.9
13.5	11.9	<0.5	2050	0.3	3.6	<0.2	14.1	29.5	16.7	161	39.3	<0.2	27.4	1.2	<2	0.4	1860	23.2
21.5	33.8	<0.5	2500	<0.2	4.8	<0.2	24.0	55.9	15.6	234	60.4	<0.2	32.3	1.6	<2	0.7	2400	31.4
29.5	31.4	<0.5	2630	<0.2	6.8	<0.2	30.7	50.0	27.7	409	100	<0.2	61.8	2.7	<2	0.4	2800	44.1

TABLE 3A.17 ICP-AES RESULTS FOR CSA NATURAL (E1) AND CHEMICAL AND BIOLOGICAL (E2) HARDPAN ENHANCED TRIALS

3A.4.2 Leaching Characteristics of the CSA Tailings

Within this leaching trial a variety of mechanisms were taking place throughout life of the experiment. These processes can be readily observed through the EC profile (Table 3A.19). Results show an initial flushing of the secondary salts developed prior to sampling. This is followed by reduced concentrations, suggesting reactions during this leaching week were limited and oxidation by-products were not developed. Subsequent leaches show a large release predominantly of Mg, Na, K, Ca and S and then a gradual decline over time (Table 3A.18).

Sodium and Ca levels can be attributed to milling additives resulting in soluble sulfate salts which subsequently are dissolved. Calcium levels continued to increase throughout the experiment suggesting gypsum (precipitated prior to sampling) and calcite dissolution was taking place. In the final stages of the trial, Fe and Zn concentrations showed very minor increases suggesting oxidation of sulfides was starting. This would result in enhanced calcite dissolution via neutralising reactions during this period.

Throughout the experiment pH remained between 7 and 8, which combined with the Ca profile, indicates that calcite and gypsum dissolution is the predominant mechanism occurring (Table 3A.19). It is suggested that if the experiment was allowed to continue, the entire contaminant potential would be observed and the effect secondary minerals precipitation would have on these loads could be investigated more adequately.

A comparison with water quality guidelines (Table 3A.18), reveals that the leachate was obviously not acceptable for drinking water or fresh aquatic life. However at the initial stages, seepage was almost acceptable for livestock consumption with levels of Cd, Mo and S marginally above recommended values. It should be remembered however that the leachate developed during this experiment only reflects the very initial stages of reactions and thus by no means indicates long term quality.

	Al	B	Ca	Cd	Co	Cr	Cu	Fe	K	Mg	Mn	Mo	Na	Ni	P	Pb	S	Zn
day	mg/L	mg/L	mg/L	mg/L	mg/L	mg/L	mg/L	mg/L	mg/L	mg/L	mg/L	mg/L	mg/L	mg/L	mg/L	mg/L	mg/L	mg/L
1	0.1	0.1	560	0.1	0.1	0.1	0.1	<0.1	78.1	253	4.9	0.1	372	0.1	<0.1	0.1	1033	0.1
2	0.1	0.2	506	0.1	0.1	0.1	0.1	<0.1	70.3	240	3.0	0.1	327	0.1	<0.1	0.1	1040	0.1
32	<0.1	<0.1	35	<0.1	<0.1	<0.1	<0.1	<0.1	0.7	2.4	<0.1	<0.1	3	<0.1	<0.1	<0.1	28	<0.1
35	2.0	0.3	661	<0.1	<0.1	<0.1	<0.1	3.6	24.4	161	4.5	<0.1	121	0.2	0.6	<0.1	760	0.9
55	1.0	0.3	640	<0.1	<0.1	<0.1	0.3	1.8	40.8	320	6.1	<0.1	311	0.1	0.7	<0.1	1031	0.8
57	0.5	0.2	664	<0.1	<0.1	<0.1	<0.1	0.5	31.5	256	5.1	<0.1	216	<0.1	0.6	<0.1	940	1.9
59	0.3	0.1	625	<0.1	<0.1	<0.1	<0.1	0.8	44.1	325	5.7	<0.1	311	<0.1	0.7	<0.1	1044	1.7
76	<0.1	<0.1	162	<0.1	<0.1	<0.1	<0.1	<0.1	8.5	35.9	0.9	<0.1	27	<0.1	<0.1	<0.1	187	0.3
78	<0.1	<0.1	629	<0.1	<0.1	<0.1	<0.1	<0.1	40.7	255	5.3	<0.1	248	0.1	0.5	<0.1	916	0.2
79	<0.1	<0.1	613	<0.1	<0.1	<0.1	<0.1	<0.1	38.9	258	5.1	<0.1	214	<0.1	0.5	<0.1	901	0.1
80	0.3	<0.1	442	<0.1	<0.1	<0.1	<0.1	1.1	18.8	112	2.3	<0.1	87	<0.1	<0.1	<0.1	435	0.1
97	<0.1	<0.1	638	<0.1	<0.1	<0.1	<0.1	<0.1	21.9	131	3.3	<0.1	76	<0.1	0.5	<0.1	701	0.4
99	<0.1	<0.1	634	<0.1	<0.1	<0.1	<0.1	<0.1	22.8	149	3.5	<0.1	99	0.1	0.5	<0.1	729	1.0
101	<0.1	<0.1	565	<0.1	<0.1	<0.1	<0.1	<0.1	21.7	154	3.0	<0.1	75	<0.1	0.2	<0.1	747	0.1
118	<0.1	<0.1	555	<0.1	<0.1	<0.1	<0.1	<0.1	15.2	113	2.9	<0.1	28	<0.1	0.2	<0.1	675	<0.1
120	<0.1	<0.1	553	<0.1	<0.1	<0.1	<0.1	<0.1	15.0	109	2.6	<0.1	27	<0.1	0.2	<0.1	693	0.4
122	<0.1	<0.1	511	<0.1	<0.1	<0.1	<0.1	<0.1	13.5	98.3	2.4	<0.1	21	<0.1	0.2	<0.1	640	<0.1
139	<0.1	<0.1	625	<0.1	<0.1	<0.1	<0.1	<0.1	12.5	84.7	2.8	<0.1	12	<0.1	0.2	<0.1	625	<0.1
141	<0.1	<0.1	656	<0.1	<0.1	<0.1	<0.1	<0.1	12.9	81.3	2.8	<0.1	12	<0.1	0.2	<0.1	624	<0.1
143	<0.1	<0.1	616	<0.1	<0.1	<0.1	<0.1	<0.1	12.8	71.7	2.5	<0.1	10	<0.1	0.2	<0.1	619	<0.1
160	4.5	<0.1	655	<0.1	<0.1	<0.1	<0.1	3.6	9.6	76.7	3.4	<0.1	5	0.1	0.2	<0.1	618	0.8
162	<0.1	<0.1	623	<0.1	<0.1	<0.1	<0.1	<0.1	8.3	61.9	2.9	<0.1	4	<0.1	0.2	<0.1	619	<0.1
164	<0.1	<0.1	584	<0.1	<0.1	<0.1	<0.1	<0.1	8.3	59.6	2.9	<0.1	4	<0.1	0.2	<0.1	608	<0.1
average for each leaching week																		
1	0.1	0.2	533	0.1	0.1	0.1	0.1	<0.1	74.2	246	3.9	0.1	350	0.1	<0.1	0.1	1036	0.1
33	1.1	0.2	348	<0.1	<0.1	<0.1	<0.1	1.9	12.6	81.7	2.3	<0.1	62	0.1	0.3	<0.1	394	0.5
57	0.6	0.2	643	<0.1	<0.1	<0.1	0.2	1.0	38.8	300	5.6	<0.1	279	0.1	0.7	<0.1	1005	1.4
78	0.2	<0.1	461	<0.1	<0.1	<0.1	<0.1	0.3	26.7	165	3.4	<0.1	144	0.1	0.3	<0.1	610	0.2
99	<0.1	<0.1	613	<0.1	<0.1	<0.1	<0.1	<0.1	22.1	145	3.3	<0.1	83	0.1	0.4	<0.1	726	0.5
120	<0.1	<0.1	540	<0.1	<0.1	<0.1	<0.1	<0.1	14.6	107	2.6	<0.1	26	<0.1	0.2	<0.1	669	0.2
141	<0.1	<0.1	632	<0.1	<0.1	<0.1	<0.1	<0.1	12.7	79.3	2.7	<0.1	11	<0.1	0.2	<0.1	623	<0.1
162	1.6	<0.1	621	<0.1	<0.1	<0.1	<0.1	1.3	8.8	66.0	3.1	<0.1	5	0.1	0.2	<0.1	615	0.3
D.W	0.2	0.3		0.002		0.05	1.5	0.3			0.5	0.05		0.02		0.01	500	3
F.A	0.005			0.002		0.01	0.005	1						0.15		0.01		0.05
L.S	5	5	1000	0.01	1	1	0.5					0.01		1		<0.1	1000	20

TABLE 3A.18 SOLUTE LEACHING RESULTS FOR CSA - LEACHING CHARACTERISATION EXPERIMENT

date	day	pH	EC (mS/cm)		date	day	pH	EC (mS/cm)
individual leaching results					average for each leaching week			
23/08/95	1	7.97	4.9		23/08/95	1	7.97	4.90
23/09/95	32	7.58	0.2		24/09/95	33	7.43	1.61
26/09/95	35	7.28	3.41		18/10/95	57	7.51	4.61
16/10/95	55	7.36	4.12		8/11/95	78	7.60	2.68
18/10/95	57	7.66	4.75		29/11/95	99	7.70	3.33
20/10/95	59	7.5	4.95		20/12/95	120	7.47	2.69
6/11/95	76	7.33	1.14		10/01/96	141	7.32	2.78
8/11/95	78	7.79	4.44		31/01/96	162	7.52	2.54
10/11/95	80	7.69	2.46					
27/11/95	97	7.43	3					
29/11/95	99	7.66	3.46					
1/12/95	101	8.01	3.52					
18/12/95	118	7.35	2.51					
20/12/95	120	7.49	2.94					
22/12/95	122	7.57	2.61					
8/01/96	139	6.87	2.74					
10/01/96	141	7.5	2.82					
12/01/96	143	7.6	2.79					
29/01/96	160	7.47	2.46					
31/01/96	162	7.42	2.53					
2/02/96	164	7.67	2.63					

TABLE 3A.19 pH AND EC RESULTS FOR CSA - LEACHING CHARACTERISATION EXPERIMENT

3A.5 Review of Preliminary Experiments - Peak Tailings

3A.5.1 Natural Hardpan Enhancement (E1) vs Biological and Chemical Hardpan Enhancement (E2) - Peak Trials

The Peak E1 and E2 columns developed pH profiles between 4 - 5 with E2 slightly more acidic (Table 3A.20). A pH of 5 and below (especially in E1) suggests that the tailings have limited neutralising potential or high acid generating potential. The NAP was determined as 22.7 kg/ton, while the NAG was 7.6 kg/ton. As shown in Table 3A.21, E2 contained higher surface concentrations of many of the solutes e.g. Al, B, Ca, Cd, Co, Cu Fe, Mg, Mn, Ni, P, S and Zn, with Fe and Zn being double that in E1. For Fe such increases can be partly attributed to the Fe/SO_4 additives during the experiment. However increased levels of Zn are testimony to the enhanced oxidising conditions present within the column. Surface concentrations of Na were greater in E1 than E2 resulting in the precipitation of thenardite, blodite and halite. Soluble K levels were also greater in E1 however this may only be comparatively higher as much of the K released in E2 would have been incorporated in the less soluble jarosite cements precipitated in the surface zone. A similar situation may have developed with Pb, which may have been incorporated in other secondary minerals in E2. Levels of Pb are very minor and thus no discrete minerals were identified.

depth (cm)	pH	EC (mS/cm)
E1		
0.5	4.82	24.70
1	4.83	9.25
2.5	5.32	3.60
6.5	4.92	1.34
20.5	4.80	1.08
29.5	4.70	0.96
E2		
0.5	4.20	26.50
0.5	4.06	8.18
3.5	4.40	2.65
7.5	4.98	1.36
15.5	5.03	1.33
25.5	4.76	1.25

TABLE 3A.20 pH AND EC RESULTS FOR PEAK NATURAL (E1) AND CHEMICAL AND BIOLOGICAL (E2) HARDPAN

depth	Al	B	Ca	Cd	Co	Cr	Cu	Fe	K	Mg	Mn	Mo	Na	Ni	P	Pb	S	Zn
cm	mg/kg	mg/kg	mg/kg	mg/kg	mg/kg	mg/kg	mg/kg	mg/kg	mg/kg	mg/kg	mg/kg	mg/kg	mg/kg	mg/kg	mg/kg	mg/kg	mg/kg	mg/kg
E1																		
0.1	2.1	0.9	2430	12.9	22.9	<0.2	<0.2	175	2150	4210	740	<0.2	31400	13.3	7	13.2	34650	1410
0.5	<0.5	0.6	2070	9.3	9.4	<0.2	<0.2	51.7	1420	970	165	<0.2	8050	7.1	3	15.6	10300	1030
2.5	<0.5	<0.5	480	2.2	2.6	<0.2	<0.2	4.3	520	220	35.9	<0.2	2580	2.7	<2	14.9	2920	378
6.5	<0.5	<0.5	470	0.9	1.7	<0.2	<0.2	11.6	156	131	19.2	<0.2	670	3.1	<2	10.4	1160	179
20.5	<0.5	<0.5	490	0.8	1.5	0.3	0.2	13.5	89.0	109	16.6	<0.2	429	2.3	<2	11.6	980	167
29.5	<0.5	<0.5	500	0.8	1.3	0.2	0.2	19.6	75.7	89.2	12.9	<0.2	307	2.5	<2	11.4	870	159
E2																		
0.1	50.5	1.5	2590	26.3	66.4	<0.2	0.4	13500	<0.5	6980	1210	<0.2	30200	47.3	16	0.4	45800	6360
0.5	8.3	0.5	2030	7.3	10.7	<0.2	<0.2	1580	11.2	1320	232	<0.2	6290	9.9	2	11.0	10300	1410
3.5	<0.5	<0.5	505	1.7	2.2	<0.2	<0.2	133	45.6	206	32.0	<0.2	1910	3.6	<2	10.6	2170	223
7.5	<0.5	<0.5	520	0.7	1.2	<0.2	<0.2	9.0	61.6	100	15.0	<0.2	580	2.5	<2	16.9	1150	160
15.5	<0.5	<0.5	595	1.1	1.8	<0.2	<0.2	5.2	101	149	23.0	<0.2	540	4.4	<2	10.7	1240	212
25.5	<0.5	<0.5	430	1.2	2.0	<0.2	<0.2	24.9	100	161	24.1	<0.2	520	2.8	<2	9.5	1170	273

TABLE 3A.21 ICP-AES RESULTS FOR PEAK NATURAL (E1) AND CHEMICAL AND BIOLOGICAL (E2) HARDPAN ENHANCED TRIALS

3A.5.2 Leaching Characteristics of the Peak Tailings

The leachate concentrations for Peak vary dramatically. The overall release of solutes can be seen in the EC profile (Table 3A.22) where initially high levels of solutes developed prior to sampling were first flushed out. This was then followed by a continual release of 2-3 mS/cm. During this period, the gradual decline in some solutes were off-set by the gradual increase in others.

The main solutes developed during this leaching were K, Mg, Ca, Na, S and Zn (Table 3A.23). Some of these elements along with Al, B, P and Cu, peaked within the first and second leachate cycles and therefore reflect the initial flush of residual solute loads. Manganese, Mg, and Fe show similar flushing effects during the final stages. Cadmium, Co, Ni, Pb and Zn profiles were completely opposite as they all began at low concentrations and continue to increase throughout the life of the experiment. This evidence combined with the gradual decrease in pH suggests that oxidation of sulfides is just starting and thus the true leaching potential of these tailings has not been fully realised during the experiment due to the time constraints.

The major contributors of Ca and Na can to some extent be attributed to additives in the milling process. Calcium levels can also be attributed to the dissolution of gypsum and calcite, where calcite is being utilised in neutralising reactions.

As mentioned previously higher levels of Zn and Pb in the final stages suggest that oxidation of sulfides is increasing. The oxidation of sphalerite does not produce acid itself however the slight increase in Fe release in the final stages suggest that the pyrite present is starting to oxidise and this has resulted in more acidic conditions. This combined with the continual decrease in Ca release suggests the neutralising capacity is being exhausted and the acid generating reactions are beginning to dominate.

A longer period of leaching treatment would have not only shown the contaminant potential of the tailings but also the effect of secondary mineral precipitation on their release. A comparison with water quality guidelines (Table 3A.23), indicates that this water was definitely not acceptable for aquatic life or drinking water. Many of the contaminant levels were acceptable for livestock consumption however Cd, Co, Mn, Pb, S and Zn levels remain in most cases far too high.

date	day	pH	EC (mS/cm)		date	day	pH	EC (mS/cm)
individual leaching results					average of weekly leachates			
16/10/95	55	6.67	18.7		18/10/95	57	6.60	17.56
18/10/95	57	6.63	21.8		8/11/95	78	6.77	4.09
20/10/95	59	6.5	12.18		29/11/95	99	5.91	2.99
6/11/95	76	6.78	5.09		20/12/95	120	5.68	2.78
8/11/95	78	7.02	4.15		10/01/96	141	4.88	2.85
9/11/95	79	6.52	3.03		31/01/96	162	4.92	2.45
27/11/95	97	6.11	3.25					
29/11/95	99	5.77	3					
1/12/95	101	5.85	2.71					
18/12/95	118	6.13	2.93					
20/12/95	120	5.53	2.81					
22/12/95	122	5.39	2.61					
8/01/96	139	5.06	3.41					
10/01/96	141	5.21	2.78					
12/01/96	143	4.36	2.35					
29/01/96	160	5.11	3.42					
31/01/96	162	4.97	2.42					
2/02/96	164	4.68	1.51					

TABLE 3A.22 pH AND EC RESULTS FOR PEAK - LEACHING CHARACTERISATION EXPERIMENT

	Al	B	Ca	Cd	Co	Cr	Cu	Fe	K	Mg	Mn	Mo	Na	Ni	P	Pb	S	Zn
day	mg/L	mg/L	mg/L	mg/L	mg/L	mg/L	mg/L	mg/L	mg/L	mg/L	mg/L	mg/L	mg/L	mg/L	mg/L	mg/L	mg/L	mg/L
1	0.5	0.3	645	0.5	0.4	0.1	0.2	0.2	617.9	205.7	25.6	0.1	3421	0.1	0.6	0.8	3643	25.6
55	2.7	0.5	650	0.7	0.3	<0.1	0.1	3.4	672.4	250.5	37.4	<0.1	4021	0.3	2.5	0.6	4179	34.0
57	<0.1	0.5	609	1.1	0.5	<0.1	0.2	1.0	801.3	408.2	63.4	<0.1	5105	0.3	3.1	0.6	5262	26.4
59	1.7	0.4	589	0.7	0.4	<0.1	<0.1	2.8	409.0	217.6	44.4	<0.1	2352	0.3	<0.1	<0.1	2785	21.9
76	<0.1	0.3	519	0.6	0.3	<0.1	<0.1	0.3	175.5	71.0	29.8	<0.1	576	0.1	0.5	1.1	1100	36.7
78	<0.1	0.3	583	0.7	0.4	<0.1	<0.1	<0.1	138.6	41.5	22.6	<0.1	315	0.2	0.5	1.5	872	41.5
79	<0.1	0.3	632	0.7	0.4	<0.1	0.1	0.9	134.8	36.5	21.2	<0.1	286	0.2	0.5	2.5	885	44.3
80	<0.1	0.2	597	0.7	0.4	<0.1	<0.1	0.2	85.3	23.4	15.0	<0.1	142.3	0.2	0.5	2.3	708	60.0
97	<0.1	0.3	594	1.1	0.8	<0.1	<0.1	<0.1	94.7	42.1	19.3	<0.1	59.6	0.3	0.5	2.3	729	116.9
99	<0.1	0.2	588	1.0	0.8	<0.1	<0.1	<0.1	58.3	37.7	13.1	<0.1	30.9	0.3	0.5	2.1	659	122.5
101	<0.1	0.2	489	0.8	0.5	<0.1	<0.1	<0.1	41.1	24.1	7.4	<0.1	13.0	0.2	0.2	3.1	616	133.4
118	<0.1	0.2	481	1.1	1.1	<0.1	<0.1	<0.1	44.6	55.0	11.8	<0.1	9.2	0.5	0.2	2.4	667	251.2
120	<0.1	0.1	477	0.9	0.8	<0.1	<0.1	<0.1	32.2	43.2	7.0	<0.1	5.7	0.4	0.2	2.8	606	225.4
122	<0.1	0.1	490	1.0	1.0	<0.1	<0.1	<0.1	34.8	55.9	9.3	<0.1	7.1	0.5	0.2	2.7	687	255.9
139	1.7	0.2	399	1.4	1.6	<0.1	0.1	1.6	42.2	114.6	15.7	<0.1	6.9	1.0	0.2	2.9	800	385.4
141	<0.1	0.2	340	1.0	1.1	<0.1	0.1	0.1	30.0	79.0	10.0	<0.1	4.2	0.7	0.2	2.9	627	285.4
143	<0.1	0.2	376	0.8	0.8	<0.1	0.1	<0.1	26.7	48.1	6.5	<0.1	2.8	0.6	0.2	3.0	532	224.9
160	<0.1	0.2	401	1.5	2.1	<0.1	0.2	1.7	38.1	126.6	14.8	<0.1	4.5	1.6	0.3	4.1	737	475.1
162	<0.1	0.1	288	0.7	1.0	<0.1	<0.1	1.0	22.5	64.3	6.9	<0.1	2.5	0.8	0.2	3.1	449	231.1
164	0.1	<0.1	192	0.3	0.4	<0.1	<0.1	1.3	15.1	29.1	3.0	<0.1	1.5	0.4	0.2	3.9	312	129.8
average of weekly leachates																		
1	0.5	0.3	645	0.5	0.4	0.1	0.2	0.2	617.9	205.7	25.6	0.1	3421	0.1	0.6	0.8	3643	25.6
57	1.5	0.5	616	0.8	0.4	<0.1	0.1	2.4	627.6	292.1	46.4	<0.1	3826	0.3	1.9	0.4	4075	27.4
78	<0.1	0.3	583	0.7	0.4	<0.1	0.1	0.4	133.5	43.1	22.2	<0.1	330	0.2	0.5	1.9	891	45.6
99	<0.1	0.2	557	1.0	0.7	<0.1	<0.1	<0.1	64.7	34.6	13.3	<0.1	35	0.3	0.4	2.5	668	124.3
120	<0.1	0.1	483	1.0	1.0	<0.1	<0.1	<0.1	37.2	51.4	9.4	<0.1	7	0.5	0.2	2.6	653	244.1
141	0.6	0.2	372	1.1	1.2	<0.1	0.1	0.6	33.0	80.6	10.7	<0.1	5	0.8	0.2	2.9	653	298.5
162	0.1	0.2	294	0.8	1.2	<0.1	0.1	1.3	25.3	73.3	8.3	<0.1	3	1.0	0.2	3.7	499	278.7
D.W	0.2	0.3		0.002		0.05	1.5	0.3			0.5	0.05		0.02		0.01	500	3
F.A	0.005			0.002		0.01	0.005	1						0.15		0.01		0.05
L.S	5	5	1000	0.01	1	1	0.5					0.01		1		<0.1	1000	20

TABLE 3A.23 SOLUTE LEACHING RESULTS FOR PEAK - LEACHING CHARACTERISATION EXPERIMENT

3A.6 Review of Preliminary Experiments - Woodlawn Tailings

3A.6.1 Natural Hardpan Enhancement (E1) vs Biological and Chemical Hardpan Enhancement (E2) - Woodlawn Trials

The cements developed in both E1 and E2 occur predominantly down preferential flow paths. Sulfide oxidation and gangue mineral degradation reactions have been concentrated along these paths, resulting in lower pH and higher EC values. Two sets of samples were removed down the profile in both E1 and E2. One included cemented, oxidised and unoxidised tailings depending on what was available at each depth and the other targeted tailings from the preferential flow paths and contained cements and oxidised tailings. In E1, non cemented samples could be obtained from all depths, whereas E2 had produced cement throughout the basal region.

The E1 pH conditions ranged from 3-6 depending on whether or not preferential flow paths were sampled (Table 3A.24). E2 produced more acidic surface pH conditions than E1. The EC profiles ranged from 2-8mS/cm. Elevated EC levels were observed at the surface, with decreases at depth. E2 produced slightly higher EC results with surface concentrations up to 10mS/cm reducing to 2mS/cm with depth. Solute concentrations at the surface in E1 were dictated by Ca, Mg, Na, S and Zn and to a lesser extent Cd, K and Mn (Table 3A.25). Most of these profiles exhibited elevated surface concentrations which decreased with depth. These concentrations have resulted in precipitation of zinc blodite, hexahydrite and basaluminite. Low levels of Ca were observed at the surface, probably due to the precipitation of gypsum in the upper tailings. The surface solute concentrations of E2 were dictated by the same suite of elements however Al, Cu, Fe, Mg, Mn, S and Zn were in greater quantities, while K was reduced. These concentrations have resulted in the precipitation of gypsum, zinc blodite, hexahydrite and loweite. The reduction in K concentration at the surface was probably due to the precipitation of the less soluble jarosite within the column.

depth (cm)	pH	EC (mS/cm)	depth (cm)	pH	EC (mS/cm)
E1 - including cements			**E2 - including only basal cements**		
1	5.01	7.93	0.5	3.95	9.73
3	5.46	3.97	2.5	4.79	5.00
8	5.02	2.92	5.5	3.40	5.68
13	6.20	2.60	6.5	3.15	5.94
18	5.02	2.71	9	3.58	5.76
24	5.47	2.85	13	3.26	5.85
30	3.20	3.30	15	3.42	5.81
34	5.79	3.00	20	3.11	4.57
			28	2.97	3.56
E1 - no cements			**E2 - including all cements**		
1	5.01	7.93	0.5	3.95	9.73
3	5.46	3.97	2.5	4.79	5.00
9	6.03	2.91	5.5	3.40	5.68
13	6.27	2.58	6.5	3.15	5.94
18	6.26	2.67	7.5	2.97	6.10
24	6.33	2.58	9.5	3.35	4.36
30	6.18	2.55	14.5	4.54	3.67
34	6.16	2.92	20	3.11	4.57
			28	2.97	3.56

TABLE 3A.24 PH AND EC RESULTS FOR WOODLAWN NATURAL (E1) AND CHEMICAL AND BIOLOGICAL (E2) HARDPAN

depth	Al	B	Ca	Cd	Co	Cr	Cu	Fe	K	Mg	Mn	Mo	Na	Ni	P	Pb	S	Zn
cm	mg/kg	mg/kg	mg/kg	mg/kg	mg/kg	mg/kg	mg/kg	mg/kg	mg/kg	mg/kg	mg/kg	mg/kg	mg/kg	mg/kg	mg/kg	mg/kg	mg/kg	mg/kg
E1 - including cements																		
1	4.3	0.6	2140	48.0	2.0	0.1	24.4	0.7	153	1610	300	0.2	2820	4.0	10	11.2	10700	8590
3	<0.1	0.3	2750	22.9	1.0	0.1	5.5	<0.1	47.8	326	83.1	0.2	941	1.8	3	10.1	4980	3520
8	1.4	0.2	3010	12.6	0.5	0.1	11.0	<0.1	24.5	226	44.8	0.1	324	1.3	3	11.0	3590	1250
13	<0.1	0.3	2850	8.1	0.7	0.1	<0.1	<0.1	21.1	200	49.6	0.1	291	1.1	2	9.3	3290	570
18	2.3	0.3	3030	23.0	0.5	0.1	7.4	<0.1	13.9	92.1	22.5	0.2	136	1.3	2	11.7	3370	1410
24	<0.1	0.3	2920	16.0	0.7	0.1	1.6	<0.1	19.4	208	57.3	0.2	251	1.4	3	9.7	3590	1430
30	<0.1	0.3	2920	14.8	0.9	0.1	0.8	<0.1	21.8	298	83.6	0.2	339	1.8	3	11.4	4010	1760
32	<0.1	0.3	2890	11.9	0.7	0.1	<0.1	<0.1	23.2	276	72.2	0.2	342	1.5	3	11.1	3810	1480
E1 - no cements																		
1	4.3	0.6	2140	48.0	2.0	0.1	24.4	0.7	153	1610	300	0.2	2820	4.0	10	11.2	10700	8590
3	<0.1	0.3	2750	22.9	1.0	0.1	5.5	<0.1	47.8	326	83.1	0.2	941	1.8	3	10.1	4980	3520
9	<0.1	0.3	2950	15.2	0.7	0.1	<0.1	<0.1	23.2	224	52.9	0.1	333	1.4	3	11.1	3660	1260
11	<0.1	0.3	2850	11.4	0.9	0.1	0.2	<0.1	21.8	191	51.6	0.1	270	1.3	3	10.3	3510	760
18	<0.1	0.3	2800	9.6	0.8	0.2	0.1	<0.1	29.3	247	68.4	0.2	316	1.0	3	11.7	3700	720
24	<0.1	0.4	2880	9.0	0.7	0.1	<0.1	<0.1	25.1	192	55.6	0.2	210	1.2	2	12.8	3520	700
30	<0.1	0.4	2900	13.3	1.0	0.1	0.5	<0.1	20.8	151	55.2	0.1	171	1.5	3	12.8	3590	990
32	<0.1	0.4	2870	13.7	0.8	0.1	<0.1	<0.1	27.4	268	70.2	0.1	318	1.7	3	12.9	3880	1370
E2 - including only basal cements																		
0.5	48.9	0.5	2270	69.0	2.5	0.3	126	79.9	8.2	2720	477	0.1	3520	6.0	14	13.0	15600	13500
2.5	3.9	0.5	2400	22.3	0.7	0.2	17.0	0.7	18.1	686	144	0.1	1290	2.0	5	10.9	6460	4580
5.5	<0.1	0.5	2780	13.8	0.7	0.2	3.4	<0.1	18.8	286	83.1	0.2	504	1.5	4	10.6	4510	2550
6.5	<0.1	0.4	2830	21.2	0.6	0.1	<0.1	<0.1	18.6	261	66.9	0.2	392	1.5	3	12.8	4120	1850
9	<0.1	0.5	2600	23.1	0.8	0.1	2.5	<0.1	20.2	463	114	0.1	424	2.0	4	13.5	4880	2970
13	<0.1	0.5	2470	17.0	0.9	0.1	1.7	<0.1	23.4	368	93.7	0.1	277	1.9	3	12.0	4030	2240
15	<0.1	0.5	2640	16.1	1.0	0.1	2.1	<0.1	19.7	455	119	0.2	355	2.3	3	12.0	4620	2580
20	15.5	0.5	2530	13.4	0.7	0.2	58.3	2.1	25.6	222	61.4	0.2	126	1.8	3	14.0	3870	2460
28	56.3	0.4	2410	10.4	0.5	0.1	306	10.8	18.4	187	41.7	0.1	128	1.3	3	13.7	3650	2140
E2 - including all cements																		
0.5	48.9	0.5	2270	69.0	2.5	0.3	126	79.9	8.2	2720	477	0.1	3520	6.0	14	13.0	15600	13500
2.5	3.9	0.5	2400	22.3	0.7	0.2	17.0	0.7	18.1	686	144	0.1	1290	2.0	5	10.9	6460	4580
5.5	<0.1	0.5	2780	13.8	0.7	0.2	3.4	<0.1	18.8	286	83.1	0.2	504	1.5	4	10.6	4510	2550
6.5	<0.1	0.4	2830	21.2	0.6	0.1	<0.1	<0.1	18.6	261	66.9	0.2	392	1.5	3	12.8	4120	1850
7.5	<0.1	0.5	2590	27.2	0.7	<0.1	<0.1	<0.1	24.4	205	52.1	0.1	264	1.6	3	13.4	3560	1650
9.5	24.7	0.5	2480	13.5	0.7	0.2	101	4.3	22.7	305	73.1	0.1	199	1.7	3	12.6	4080	2610
14.5	263	0.2	2340	37.2	1.1	0.3	445	51.7	20.9	475	61.3	0.1	81.3	2.0	4	12.5	6600	6350
20	15.5	0.5	2530	13.4	0.7	0.2	58.3	2.1	25.6	222	61.4	0.2	126	1.8	3	14.0	3870	2460
28	56.3	0.4	2410	10.4	0.5	0.1	306	10.8	18.4	187	41.7	0.1	128	1.3	3	13.7	3650	2140

TABLE 3A.25 ICP-AES RESULTS FOR WOODLAWN NATURAL (E1) AND CHEMICAL AND BIOLOGICAL (E2) HARDPAN ENHANCED TRIALS

3A.6.2 Leaching Characteristics of the Woodlawn Tailings

ICP-AES results indicate that the major solutes are Na, S, Zn, Fe and Mg (Table 3A.27). Sulfur, Zn and Fe presumably have resulted from the oxidation of sulfides particularly pyrite and sphalerite near the surface, while Mg has resulted from neutralisation reactions involving dolomite and Mg-bearing chlorites. Sodium levels are attributed to additives of sodium xanthates (SIBX) and sodium bisulfide (SBS) during mill processing. The pH profile, dropping from 8-3, indicates that the acid generation associated with the sulfide oxidation is outweighing the input of neutralisation from the dolomite available at this site (NAP 209 kg/ton, NAG 56.23 kg/ton).

All solutes analysed show variations in concentration over time. The tailings obtained from Woodlawn initially contained readily soluble Na, Ca, K, Mg and S as shown by an initial decrease in the profiles which were rapidly flushed from the column. The tailings themselves were not oxidised (as they were obtained from depth) but must have contained transported oxidation and neutralisation reaction by-products from the surface region, along with Na from the mill processing. This flushing is reflected in the EC results (Table 3A.26).

During the life of the experiment the majority of elements increased to peak concentrations and have then subsided. This is reflected in the overall EC trend of the leachate (Table 3A.26). The only element which did not behave this way was Cu which has continued to increase. This may have been a function of the lower reactivity of chalcopyrite (Jambor, 1994). It is suggested that over time chalcopyrite has been less effected by oxidation and only after 75 days was Cu substantially released. Thus the Cu profile appears to be lagging behind the majority of elements.

It was noted that as the experiment continued the flow rate through the tailings (ie. leachate quantity obtained) decreased with time. It is suggested in this case that the reduction in observed permeability, was due to the precipitation of secondary minerals near the surface, cementing the tailings and effectively plugging the profile. As in the pyrrhotitic tailings of Elura, the decreased solute concentrations may be a function of elemental capture associated with secondary mineral precipitation. It could be argued however that the decrease in solute concentration is directly related to the amount of water moving through the profile. Thus the decreased permeability has resulted in reduced water movement through the profile and thus reduced potential for transport of soluble salts to be collected as leachate. It should be remembered that the results presented here show the amount of elemental release in milligrams only ie. the volume of leachate has been accounted for. Thus a decrease in permeability may show an increase in soluble concentration per volume, however the total amount transported is in fact decreased.

The main indication that the latter perhaps is not the case for the Woodlawn site is the continued increase in Cu concentration, while the majority of other solute concentrations are decreasing. It would be expected that if elemental concentrations were decreasing because of reduced water flow, Cu would also decrease even if chalcopyrite was continuing to oxidise. Therefore it could be suggested that the secondary minerals developing may be coating the sulfides and thus reducing oxidation and acid generation and thus neutralisation reactions resulting in a general decrease in leachate concentrations. However the fact that the Cu is still increasing indicates that sulfides (especially chalcopyrite) must still be exposed to oxygen and water. Thus hardpan-type cementing has probably effected the solute loads released from these tailings but not to the extent as those observed in the highly pyrrhotitic Elura tailings. Adsorption and co-precipitation reactions may have played a larger role in pollutant capture in the Woodlawn case. A comparison of leachate characteristics was made with water quality guidelines (Table 3A.27). With regards to drinking water and the protection of fresh aquatic systems, the majority of concentrations released were either too high throughout the experiment or increased above the recommended limits within 2 or 3 leaching cycles. Levels of B, Ca and Cr levels were considered

reasonable for livestock watering however the remaining elements were either continuously above acceptable limits or increased to unacceptable levels within initial leaching cycles.

date	days	pH	EC (mS/cm)		date	days	pH	EC (mS/cm)
individual leaching results					average of weekly leachate			
23/08/95	1	8.48	11.03		23/08/95	1	8.48	11.03
22/09/95	32	5.53	0.43		24/09/95	33	5.13	0.59
26/09/95	35	4.73	0.75		18/10/95	57	4.66	15.27
16/10/95	55	5.6	6.23		8/11/95	78	3.83	28.90
18/10/95	57	4.22	24.3		29/11/95	99	3.59	27.93
20/10/95	59	4.15			20/12/95	120	3.51	29.20
6/11/95	76	3.82	28.4		10/01/96	141	3.18	25.87
8/11/95	78	3.7	30.6		31/01/96	162	3.27	23.10
10/11/95	80	3.96	27.7					
27/11/95	97	3.59	25.8					
29/11/95	99	3.61	28.4					
1/12/95	101	3.56	29.6					
20/12/95	120	3.51	29.2					
8/01/96	139	3.05	29.4					
10/01/96	141	3.28	24.8					
12/01/96	143	3.21	23.4					
29/01/96	160	3.65						
31/01/96	162	3.07	26.2					
2/02/96	164	3.09	20					

TABLE 3A.26 pH AND EC RESULTS FOR WOODLAWN - LEACHING CHARACTERISATION EXPERIMENT

	Al	B	Ca	Cd	Co	Cr	Cu	Fe	K	Mg	Mn	Mo	Na	Ni	P	Pb	S	Zn
days	mg/L	mg/L	mg/L	mg/L	mg/L	mg/L	mg/L	mg/L	mg/L	mg/L	mg/L	mg/L	mg/L	mg/L	mg/L	mg/L	mg/L	mg/L
1.0	0.1	<0.1	522.7	0.1	0.1	0.1	0	<0.1	115.8	744.7	5.1	0.1	2004.4	0	<0.1	0.05	2715	0.4
32.0	<0.1	<0.1	89.6	<0.1	<0.1	<0.1	1	<0.1	0.8	3.0	0.5	<0.1	5.1	<0.1	<0.1	5.413	73.7	19.5
35.0	0.1	0.3	120.8	0.3	<0.1	<0.1	1	<0.1	1.6	9	1.7	<0.1	13.3	<0.1	0	3.769	145.6	51.8
55.0	0.1	0.2	250.5	5.3	1	<0.1	1	<0.1	6.5	489	62.3	<0.1	220.9	2	1	2.206	1985	1994
57.0	32.0	0.4	529.3	77.8	5	<0.1	10	230	52.4	1063	413.9	<0.1	906.2	9	17	2.062	11847	19159
59.0	30.1	0.2	568.7	85	5	<0.1	6	300	58.6	1161	442.7	<0.1	1062.8	9	17	3.541	12996	19874
76.0	57	0.2	518.3	97.0	5	<0.1	179	222	48.4	1000	350.7	<0.1	1150	8	1	3.683	12850	20080
78.0	55.8	0.3	516.0	100.1	5	<0.1	18	478	41.9	1040	359.3	<0.1	1270	8	1	3.764	14160	21020
80.0	39.4	0.2	450.4	86	4	<0.1	1	585	49.8	962	329.6	<0.1	1410	7	1	3.386	14010	20380
97.0	72.6	0.2	459.1	85.2	3	<0.1	170	385	20.3	788	246.4	<0.1	1140	5	1	2.322	12980	19230
99.0	91	0.1	535.3	97.2	4	<0.1	78	585	19.0	895	289.0	<0.1	1370	6	1	2.375	12270	18080
101	72	<0.1	629.1	115	4	<0.1	7	947	8.4	994	327.9	<0.1	1650	6	2	2.571	12650	18900
118	163	<0.1	700.5	155	4	<0.1	741	359	<0.1	979	319.2	<0.1	1230	6	2	0.499	16300	26750
120	168	<0.1	750.5	169.6	4	<0.1	618	574	<0.1	1020	342.8	<0.1	1330	6	2	2.167	17700	29750
122	133	<0.1	644.8	119	3	<0.1	86	836	<0.1	740	240.9	<0.1	932.9	4	2	2.202	12450	20100
139	268	<0.1	653.2	148	2	0.1	800	886	<0.1	684	207.9	<0.1	546.0	3	2	3.859	15200	24800
141	217.2	<0.1	565.3	126.1	2	<0.1	392	933	1.6	566	163.1	<0.1	414.0	3	2	3.637	12750	20550
143	155.1	<0.1	575.8	88	2	<0.1	44	1189.6	0.8	480.0	134.4	<0.1	345.1	2	2	1.029	10400	16400
160	157.0	<0.1	368.3	52	1	0.2	807	482.0	<0.1	264	65.7	<0.1	95.2	1	3	3.378	7160	10400
162	167.5	<0.1	416.0	67	1	<0.1	573	658.7	<0.1	303	80.6	<0.1	140.6	1	1	2.195	8460	12300
164	170.413	<0.1	527.2	69.1	1.2	<0.1	311.7	933	<0.1	332.387	85.833	<0.1	157	1.41	1.14	2.03	8830	13000
average of weekly leachate																		
1	0.1	<0.1	522.7	0.1	0.1	0.1	0.1	<0.1	115.8	744.7	5.1	0.1	2004.4	0.1	<0.1	0.1	2715	0
33	0.1	0.2	95.2	0.2	<0.1	<0.1	1.1	<0.1	1.2	6.1	1.1	<0.1	9.2	<0.1	0	4.6	110	36
57	20.7	0.3	449.5	56.1	3.8	<0.1	5.8	176.6	39.2	910.8	308.3	<0.1	730.0	6.4	11.5	2.6	8943	13676
78	50.7	0.2	494.9	94.4	4.4	<0.1	66.1	428.3	46.7	1007.5	346.6	<0.1	1276.7	7.4	1.0	3.6	13673	20493
99	78.8	0.1	541.2	99.2	3.4	<0.1	84.7	638.8	15.9	892.1	287.7	<0.1	1386.7	5.7	1.3	2.4	12633	18737
120	154.8	<0.1	698.6	148.0	3.4	<0.1	481.6	589.4	<0.1	913.0	301.0	<0.1	1164.3	5.3	2.0	1.6	15483	25533
141	213.5	<0.1	598.1	120.5	2.2	0.1	412.3	1002.9	0.8	576.4	168.5	<0.1	435.0	2.8	2.0	2.8	12783	20583
162	164.97	<0.1	437.2	62.6	1.1	0.1	563.8	691.4	<0.1	299.7	77.4	<0.1	130.8	1.2	1.8	2.5	8150	11900
D.W	0.200	0.3		0.002		0.05	1.5	0.3			0.5	0.05		0.02		0.01	500	3
F.A	0.005			0.002		0.01	0.005	1						0.15		0.005		0.05
L.S	5	5	1000	0.01	1	1	0.5					0.01		1		<0.1	1000	20

TABLE 3A.27 SOLUTE LEACHING RESULTS FOR WOODLAWN - LEACHING CHARACTERISATION EXPERIMENT

3A.7 Review of Preliminary Experiments - Ranger Tailings

3A.7.1 Natural Hardpan Enhancement (E1) vs Biological and Chemical Hardpan Enhancement (E2) - Ranger Trials

The sulfide content of the Ranger ore is very low and thus the tailings have little or no potential to produce acidic conditions (NAP 12.7 kg/ton, NAG <2.5 kg/ton). This is reflected in the pH profile for E1 which exhibits levels between 6.4-7.1 (Table 3A.28). The addition of acid on a weekly basis has resulted in slightly more acidic conditions developing at the surface of E2. The development of pH 6.4 at the surface of E2 suggests the tailings have a fairly high potential for acid neutralisation.

The cementing potential of E1 and E2 did not vary dramatically, with basically no cements developed in either case. Upon exposure and drying, soluble salt precipitation occurred. The soluble salt profiles of E1 and E2 were not very different, with minor increases in surface concentration in E2 compared with E1 (Table 3A.29). The majority of these surface elemental increases can be attributed to the breakdown of gangue minerals due to additions of pH 3 solution throughout the trial. Compared with many of the other tailings trials, the E2 chemical and biological additions made only minimal changes to both the physical and chemical nature of the tailings compared to E1 due to the absence of sulfide.

depth (cm)	pH	EC (mS/cm)
E1		
0.5	6.4	32.4
1.5	6.7	14.5
4	7.0	6.98
7	7.0	5.45
14	7.1	4.23
24	7.1	4.08
31	7.1	4.14
E2		
0.5	5.1	41.4
1.5	6.5	9.21
5	6.9	5.01
12	7.1	4.03
19	7.0	3.62
27	6.5	6.56

TABLE 3A.28 pH AND EC RESULTS FOR RANGER NATURAL (E1) AND CHEMICAL AND BIOLOGICAL (E2) HARDPAN

depth	Al	B	Ca	Cd	Co	Cr	Cu	Fe	K	Mg	Mn	Mo	Na	Ni	P	Pb	S	Zn
cm	mg/kg	mg/kg	mg/kg	mg/kg	mg/kg	mg/kg	mg/kg	mg/kg	mg/kg	mg/kg	mg/kg	mg/kg	mg/kg	mg/kg	mg/kg	mg/kg	mg/kg	mg/kg
E1																		
surf	6	2.2	2582	<1	<1	0.7	<1	12.7	561.5	42667	9852	<1	182	1.3	19.9	<5	73480	6.5
1-2cm	4	3.7	2311	<1	<1	<1	<1	2.8	198.7	13780	4321	<1	206	1.6	<1	<5	26390	1.2
3-5cm	<1	2.3	2381	<1	<1	<1	<1	<1	112.5	4317	1148	<1	101	<1	<1	<1	9221	<1
6-8cm	<1	1.8	2505	<1	<1	<1	<1	<1	76.3	2849	737	<1	52.0	<1	<1	<1	6903	<1
13-15cm	<1	1.5	2619	<1	<1	<1	<1	<1	54.9	1666	453	<1	28.3	<1	<1	<1	4990	<1
23-25cm	<1	1.4	2623	<1	<1	<1	<1	<1	51.8	1495	402	<1	23.6	<1	<1	<1	4659	<1
30-32cm	<1	1.4	2653	<1	<1	<1	<1	<1	54.5	1560	395	<1	25.2	<1	<1	<1	4814	<1
E2																		
surf	<5	3.0	2754	<1	1.8	0.9	<1	241	659.7	68875	17580	<1	411	2.0	49.7	<5	113700	1.0
1-2cm	<5	2.8	2352	<1	<1	<1	<1	1.5	152.4	6483	1920	<1	132	<1	<1	<5	12976	<1
4-6cm	<1	1.6	2520	<1	<1	<1	<1	<1	75.9	2189	691	<1	43.8	<1	<1	<1	5927	<1
11-13cm	1.4	1.5	2647	<1	<1	<1	<1	<1	58.2	1362	541	<1	23.3	<1	<1	<1	4651	<1
18-20cm	<1	1.4	2674	<1	<1	<1	<1	<1	40.4	1057	524	<1	16.8	<1	<1	<1	4092	<1
26-28cm	<1	1.3	2762	<1	<1	<1	<1	<1	33.5	1048	490	<1	15.0	<1	<1	<1	4130	<1

TABLE 3A.29 ICP-AES RESULTS FOR RANGER NATURAL (E1) AND CHEMICAL AND BIOLOGICAL (E2) HARDPAN ENHANCED TRIALS

3A.7.2 Leaching Characteristics of the Ranger Tailings

The leaching experiment carried out on the Ranger tailings showed trends of general elutriation of the total salts over time. These levels were not replenished during the drying/rest periods each week through sulfide oxidation, acid generation and neutralising reactions observed in other tailings. The tailings have very low sulfide content and thus acid producing potential, and therefore the EC (Table 3A.30) and solute trends (Table 3A.31) show a general decrease over time through exhaustion of soluble components.

Initially concentrated levels of Na, S, Zn, Fe, Mg, Mn, Al and Ca were released during the first leaching cycle, which reflects the soluble salts already present in the tailings prior to sampling. Concentrated levels of Mg and S were readily observed within the dam as salt crusts of magnesium sulfates at the surface. Insitu degradation of Mg-chlorites, along with sulfuric acid added during the milling process, would have contributed to these concentrations.

The subsequent low in the leaching profile indicates either the time lag before potentially less soluble salts were released, or the period in which additional soluble salts are being produced which are then available for leaching. By the third leaching cycle much of the Na, K, S, Mg and Mn has been mobilised shown by increased levels in solution. These concentrations decreased from that point. Calcium levels however appear to remain at constant levels throughout the final stages of the trial and may reflect the direct dissolution of large quantities of gypsum present in the tailings.

The results obtained were compared with water quality guidelines (Table 3A.31), which indicated that the leachate was unacceptable for fresh aquatic life, drinking water and for livestock consumption due to increased levels of S and Mn in particular.

date	days	pH	EC (mS/cm)		date	days	pH	EC (mS/cm)
individual leaching results					**average of weekly leachate**			
4/12/96	1	7.38	27.3		4/12/96	1	7.38	27.30
8/01/96	35	6.74	12.88		10/01/96	37	6.50	6.61
10/01/96	37	6.4	3.95		31/01/96	58	7.24	18.93
12/01/96	39	6.37	3.01		21/02/96	79	6.98	13.41
29/01/96	56	7.05	23.6		13/03/96	100	7.13	7.93
31/01/96	58	7.15	15.2		2/04/96	120	7.15	6.55
2/02/96	60	7.53	18					
19/02/96	77	6.09	19.1					
21/02/96	79	7.46	12.8					
23/02/96	81	7.38	8.32					
11/03/96	98	6.62	7.1					
13/03/96	100	7.45	9.27					
15/03/96	102	7.31	7.41					
1/04/96	119	7.12	6.41					
3/04/96	121	7.17	6.69					

TABLE 3A.30 pH AND EC RESULTS FOR RANGER - LEACHING CHARACTERISATION EXPERIMENT

	Al	B	Ca	Cd	Co	Cr	Cu	Fe	K	Mg	Mn	Na	Ni	P	Pb	S	Zn
days	mg/L	mg/L	mg/L	mg/L	mg/L	mg/L	mg/L	mg/L	mg/L	mg/L	mg/L	mg/L	mg/L	mg/L	mg/L	mg/L	mg/L
1	5.4	1.4	534	<0.1	0.1	0.2	<0.1	4.5	124	6430	1580	95.5	0.3	<2	<0.1	11000	6.5
35	<0.1	0.3	511	<0.1	<0.1	<0.1	<0.1	<0.1	30.0	2180	422	8.8	0.1	<1	<0.1	3860	1.5
37	<0.1	0.1	128	<0.1	<0.1	<0.1	<0.1	<0.1	5.5	584	97.3	3.6	<0.1	<0.2	<0.1	987	<0.1
39	<0.1	0.1	73.7	<0.1	<0.1	<0.1	<0.1	<0.1	5.8	361	72.3	4.0	<0.1	<0.2	<0.1	641	<0.1
56	<0.1	1.0	480	<0.1	<0.1	0.1	<0.1	<0.1	75.4	5260	1380	53.4	0.2	<0.5	0.2	9470	<0.1
58	<0.1	1.1	483	<0.1	<0.1	<0.1	<0.1	<0.1	58.9	2710	798	51.6	0.2	<0.5	0.1	5130	<0.1
60	<0.1	1.1	458	<0.1	<0.1	<0.1	<0.1	<0.1	60.4	2650	842	49.1	0.2	<0.5	<0.1	5190	<0.1
77	<0.1	0.7	582	<0.1	<0.1	<0.1	<0.1	<0.1	73.1	4955	1401	59.7	<0.1	0.3	0.2	8393	<0.1
79	<0.1	0.5	515	<0.1	<0.1	<0.1	<0.1	<0.1	39.8	1303	414	28.7	<0.1	<0.1	<0.1	2641	<0.1
81	<0.1	0.8	578	<0.1	<0.1	<0.1	<0.1	<0.1	57.2	1717	539	36.8	<0.1	<0.1	<0.1	3422	<0.1
98	<0.1	0.6	454	<0.1	<0.1	<0.1	<0.1	<0.1	40.3	1792	502	31.2	<0.1	<0.1	<0.1	3287	<0.1
100	<0.1	0.7	531	<0.1	<0.1	<0.1	<0.1	<0.1	45.5	1361	415	27.3	<0.1	<0.1	<0.1	2721	<0.1
102	<0.1	0.6	533	<0.1	<0.1	<0.1	<0.1	<0.1	37.7	1054	333	22.4	<0.1	<0.1	<0.1	2247	<0.1
119	<0.1	0.4	509	<0.1	<0.1	<0.1	<0.1	<0.1	27.1	807	234	16.8	<0.1	<0.1	<0.1	1783	<0.1
121	<0.1	0.4	525	<0.1	<0.1	<0.1	<0.1	<0.1	30.3	798	242	15.8	<0.1	<0.1	<0.1	1785	<0.1
average of weekly leachate																	
1	5.4	1.4	534	0.1	0.1	0.2	0.1	4.5	124.3	6430	1580	95.5	0.3	2.0	0.1	11000	6.5
37	<0.1	0.2	238	0.1	0.1	0.1	0.1	0.1	13.8	1041	197	5.5	0.1	0.5	0.1	1829	0.6
58	<0.1	1.1	474	0.1	0.1	0.1	0.1	0.1	64.9	3540	1006	51.4	0.2	0.5	0.1	6597	0.1
79	<0.1	0.7	558	0.1	0.1	0.1	0.1	0.1	56.7	2659	785	41.8	0.1	0.2	0.1	4819	0.1
100	<0.1	0.6	506	0.1	0.1	0.1	0.1	0.1	41.2	1402	417	27.0	0.1	0.1	0.1	2752	0.1
120	<0.1	0.4	517	0.1	0.1	0.1	0.1	0.1	28.7	802	238	16.3	0.1	0.1	0.1	1784	0.1
D.W	0.2	0.3		0.002		0.05	1.5	0.3			0.5		0.02		0.01	500	3
F.A	0.005			0.002		0.01	0.005	1					0.15		0.01		0.05
L.S	5	5	1000	0.01	1	1	0.5						1		0.1	1000	20

TABLE 3A.31 SOLUTE LEACHING RESULTS FOR RANGER - LEACHING CHARACTERISATION EXPERIMENT

3A.8 Review of Preliminary Experiments - Woodcutters Tailings

3A.8.1 Natural Hardpan Enhancement (E1) vs Biological and Chemical Hardpan Enhancement (E2) - Woodcutters Trials

In general the Woodcutters E2 appeared to have developed more pronounced solute levels during the life of the experiment, however the E1 and E2 cements did not vary greatly. Solute 1:5 extract profiles indicated that up to twice as much soluble Zn was produced throughout the E2 experiment however the surface concentrations of E1 were much greater. At depth, similar profiles were observed for Ni, Ca and S (Table 3A.33). The elevated surface Zn values in E1 compared with elevated values at depth in E2 suggest that Zn has been leached down the profile under the influence of the pH 3 solution used in E2.

E2 had slightly higher EC values throughout the profile and a very minor reduction in pH compared with E1 (Table 3A.34). E1 exhibited a decrease in pH at 4-5cm depth corresponding closely to a textural variation within the profile, but this was not strongly reflected within any of the solute profiles. The slight increase in Ni, Zn, Ca, Cu, Mg, Mn, Cd and Co down the profiles of E2, suggests that oxidation and/or gangue mineral degradation has been enhanced through the chemical and biological additives. However the minimal variations in pH and EC suggest that perhaps the dissolution of dolomite is dictating the system and that the majority of pH 3 solution was being neutralised on contact (as shown in the pH

profile of approx. 6). Additional evidence of this is the elevated concentrations of Mg and Ca at the surface. The NAP of the Woodlawn tailings was determined as 253.6 kg/ton and the NAG as 120.1 kg/ton.

depth (cm)	pH	EC (mS/cm)
E1		
0.5	6.2	26.6
1.5	6.4	7.90
4.5	5.0	3.50
13	6.4	2.46
24	6.6	2.13
33	6.5	2.24
E2		
0.5	5.8	28.3
1.5	6.2	9.30
5	6.2	4.73
11	5.7	4.16
20	5.6	3.38
28	4.7	2.89

TABLE 3A.32 pH AND EC RESULTS FOR WOODCUTTERS NATURAL (E1) AND CHEMICAL AND BIOLOGICAL (E2) HARDPAN

depth	Al	B	Ca	Cd	Co	Cr	Cu	Fe	K	Mg	Mn	Mo	Na	Ni	P	Pb	S	Zn
cm	mg/kg	mg/kg	mg/kg	mg/kg	mg/kg	mg/kg	mg/kg	mg/kg	mg/kg	mg/kg	mg/kg	mg/kg	mg/kg	mg/kg	mg/kg	mg/kg	mg/kg	mg/kg
E1																		
surf	<5	1.3	2531	10.9	9.1	<1	<1	<1	273.1	43839	561	<1	708	17.0	<1	12.5	61532	4400
1-2cm	<1	1.6	2403	5.6	2.2	<1	<1	<1	104.8	7263	103	<1	329	3.7	<1	9.9	12450	1102
4-5cm	<1	1.4	2588	3.3	0.9	<1	<1	<1	58.8	1390	30.3	<1	134	5.8	<1	10.4	4389	714
12-14cm	<1	1.5	2005	4.9	1.1	<1	<1	<1	28.9	769.1	21.6	<1	53.7	3.2	<1	15.5	2872	596
23-25cm	<1	1.5	1835	1.8	0.7	<1	<1	<1	31.2	693.1	24.0	<1	46.1	1.0	<1	7.6	2435	133
32-34cm	<1	1.4	1802	3.4	0.9	<1	<1	<1	31.6	753.6	22.8	<1	45.7	1.3	<1	9.0	2573	267
E2																		
surf	<5	1.3	2516	8.3	8.9	<1	<1	26.5	496.2	46463	597.6	<1	1153	16.7	<1	11.8	64532	2613
1-2cm	<5	1.7	2346	7.3	5.8	<1	<1	<1	113.2	8891	162.5	<1	284	10.0	<1	9.5	14673	1602
4-6cm	<1	1.4	2541	6.1	2.1	<1	<1	<1	55.3	2813	60.6	<1	108	6.9	<1	8.0	6460	1251
10-12cm	<1	1.3	2624	4.9	1.8	<1	1.0	<1	40.2	1925	41.2	<1	62.0	7.1	<1	11.6	5420	1500
19-21cm	<1	1.3	2481	3.9	1.1	<1	1.4	<1	26.8	1194	31.2	<1	49.4	4.6	<1	11.2	4267	1341
27-29cm	<1	1.4	2261	3.1	0.7	<1	1.5	<1	28.2	855	25.9	<1	46.4	4.6	<1	13.3	3512	940

TABLE 3A.33 ICP-AES RESULTS FOR WOODCUTTERS NATURAL (E1) AND CHEMICAL AND BIOLOGICAL (E2) HARDPAN ENHANCED TRIALS

3A.8.2 Leaching Characteristics of the Woodcutters Tailings

Both pH and EC profiles suggest that this system is in the very preliminary stages of oxidation and release. Leachate pH was initially 8 and subsequently dropped to 6 - 6.5 after the second leaching cycle and remained at that level (Table 3A.34). Initial EC values of 9.4 mS/cm originated from the solutes associated with the initially collected tailings. The level increased slowly to 10.8 mS/cm and remained at approximately that level throughout the remainder of the experiment (Table 3A.34). These continuous EC values are supported by the slow decrease or increase in different elements with time.

In general Al, B, Ca, Fe, K, Na, P and Pb concentrations decreased with time while Cd, Co, Mg, Mn, Ni, S and Zn showed increases (Table 3A.35). The Ca profile exhibited an initial flush out, followed by a

constant release of approximately 440 mg/kg, which decreased in the final stages. Calcite and gypsum dissolution may be potentially responsible for this release. This dissolution may be enhanced by acid generation associated with sulfide oxidation. Iron curves indicate Fe produced through this oxidation is not being released. This lack of release is potentially due to adsorption of Fe or precipitation as insoluble secondary minerals, however only limited signs of this were present. Magnesium release increased with time suggesting that dolomite dissolution is becoming the more dominant carbonate mineral available for dissolution reactions, as calcite may be beginning to be exhausted. It is understood that dolomite is the dominant carbonate mineral available, however calcite is more reactive and would thus be preferentially utilised.

Increased Zn release over time suggests that oxidation of sphalerite is occurring preferentially to pyrite because of its greater reactivity, but in this case oxidation does not produce acid. Thus oxygen consumption within the column would be preferentially used by Zn releasing reactions. Once Zn sources are reduced/degraded, pyrite may preferentially begin to oxidise producing a more acidic environment.

It should be noted that a number of solute concentrations decrease in the final stages of the E3 trial. This decrease in S, Ni, Pb, P, Al, B, Ca, Cd, Co, Fe, K, Mn and Mg may be attributed to incorporation in secondary minerals within the profile. As mentioned previously, secondary mineral development was not observed optically or by XRD.

The results obtained were compared with water quality guidelines (Table 3A.35), which indicate that the leachate was unacceptable for fresh aquatic life, drinking water and livestock consumption due to very high levels of Zn, S, Pb, Ni, Mn, Cd and minor increases in Al, B, Co, Cr, Mg and Fe.

The Woodcutters ore body has a large sulfide and carbonate content and thus has strongly reactive tailings. It is for this reason that the short term nature of this experiment has not fully explored the potential seepage characteristics of the dam. During the trial, only the most reactive minerals have been utilised. The large number of reactions still available outweigh those which have taken place. Significant Fe sulfide oxidation has yet to happen and thus acid generation has not extensively developed. Therefore the release associated with Fe sulfide oxidation and with acid degradation of gangue minerals has yet to occur. Longer term leaching experiments are therefore required.

date	day	pH	EC (mS/cm)		date	day	pH	EC (mS/cm)
individual leaching results					average of weekly leachates			
4/12/96	1	7.88	9.38		4/12/96	1	7.88	9.38
8/01/96	35	6.23	2.16		10/01/96	37	6.28	8.26
10/01/96	37	6.36	8.61		31/01/96	58	6.57	9.32
12/01/96	39	6.24	14		21/02/96	79	6.58	10.26
29/01/96	56	6.72	7.36		13/03/96	100	6.10	10.00
31/01/96	58	6.61	11.88		2/04/96	120	6.50	10.06
2/02/96	60	6.39	8.71					
19/02/96	77	6.58	10.12					
21/02/96	79	6.64	11.13					
23/02/96	81	6.53	9.52					
11/03/96	98	5.32	10.41					
13/03/96	100	6.48	10.77					
15/03/96	102	6.51	8.81					
1/04/96	119	6.46	10.6					
3/04/96	121	6.53	9.52					

TABLE 3A.34 pH AND EC RESULTS FOR WOODCUTTERS - LEACHING CHARACTERISATION EXPERIMENT

	Al	B	Ca	Cd	Co	Cr	Cu	Fe	K	Mg	Mn	Na	Ni	P	Pb	S	Zn
day	mg/L	mg/L	mg/L	mg/L	mg/L	mg/L	mg/L	mg/L	mg/L	mg/L	mg/L	mg/L	mg/L	mg/L	mg/L	mg/L	mg/L
1	0.3	1.8	704	<0.1	<0.1	<0.1	<0.1	7.0	160.2	1720	9.8	450.9	0.3	<1	1.2	2970	31.1
35	0.2	0.1	264	0.4	0.1	<0.1	0.2	7.8	5.8	360	5.5	12.5	0.2	<0.2	3.6	563	44.7
37	0.3	0.3	300	1.1	0.5	<0.1	0.2	14.3	48.3	1750	30.6	158.1	0.7	<1	3.4	3560	176.6
39	<0.1	0.6	558	2.7	1.2	<0.1	<0.1	1.7	82.3	2830	56.5	261.8	1.8	<1	4.1	7190	460.9
56	<0.1	0.3	484	2.4	0.8	<0.1	<0.1	<0.1	24.1	1150	24.1	56.0	1.0	<0.4	1.9	2270	295.1
58	0.2	0.4	463	2.6	1.2	<0.1	<0.1	<0.1	46.2	2320	45.8	125.8	1.4	1.0	2.4	5440	399.8
60	<0.1	0.3	364	1.9	0.8	<0.1	<0.1	<0.1	29.9	1440	28.9	76.4	1.1	<0.5	1.6	3410	317.3
77	<0.1	0.2	472	2.5	1.1	<0.1	<0.1	0.3	26.2	1819	36.9	66.7	1.4	0.2	2.8	3666	422.2
79	<0.1	0.2	420	2.1	1.2	<0.1	<0.1	0.2	29.7	2578	46.0	72.9	1.3	0.3	2.7	4887	425.9
81	<0.1	0.1	410	1.8	0.9	<0.1	<0.1	0.5	23.1	2140	37.0	55.1	1.1	<0.1	2.3	4000	359.6
98	<0.1	0.1	450	2.4	1.0	<0.1	<0.1	0.6	17.3	1879	33.6	41.9	1.2	0.2	2.4	3459	376.3
100	<0.1	0.1	408	1.9	1.0	<0.1	<0.1	0.2	18.6	2558	37.6	39.7	1.2	0.2	1.9	4425	414.2
102	<0.1	0.1	375	1.6	0.8	<0.1	<0.1	0.1	13.9	1903	27.8	28.1	0.9	0.2	1.6	3365	304.9
119	<0.1	0.1	389	2.0	0.9	<0.1	<0.1	0.1	12.5	1866	26.6	26.2	1.0	<0.1	1.5	3285	372.9
121	<0.1	0.1	349	1.8	1.0	<0.1	<0.1	<0.1	12.7	2185	32.6	23.4	1.2	<0.1	1.5	3691	447.6
average of weekly leachates																	
1	0.3	1.8	704	0.1	0.1	0.1	0.1	7.0	160.2	1720	9.8	450.9	0.3	1.0	1.2	2970	31.1
37	0.2	0.3	374	1.4	0.6	0.1	0.1	7.9	45.5	1647	30.9	144.1	0.9	0.7	3.7	3771	227.4
58	0.1	0.3	437	2.3	0.9	0.1	0.1	0.1	33.4	1637	32.9	86.1	1.2	0.6	2.0	3707	337.4
79	0.1	0.2	434	2.2	1.1	0.1	0.1	0.3	26.3	2179	40.0	64.9	1.3	0.2	2.6	4184	402.5
100	0.1	0.1	411	1.9	0.9	0.1	0.1	0.3	16.6	2113	33.0	36.6	1.1	0.2	2.0	3750	365.1
120	0.1	0.1	369	1.9	0.9	0.1	0.1	0.1	12.6	2026	29.6	24.8	1.1	0.1	1.5	3488	410.3
D.W	0.2	0.3		0.002		0.05	1.5	0.3			0.5		0.02		0.01	500	3
F.A	0.005			0.002		0.01	0.005	1					0.15		0.01		0.05
L.S	5	5	1000	0.01	1	1	0.5						1		0.1	1000	20

TABLE 3A.35 SOLUTE LEACHING RESULTS FOR WOODCUTTERS - LEACHING CHARACTERISATION EXPERIMENT

3A.9 Review of Preliminary Experiments - Pine Creek Tailings

3A.9.1 Natural Hardpan Enhancement (E1) vs Biological and Chemical Hardpan Enhancement (E2) - Pine Creek Trials

The Pine Creek oxide tailings are similar to the Ranger tailings as they both contain very minor sulfide and thus have little or no potential to produce acidic conditions (NAP <2.5 kg/ton, NAG <2.5 kg/ton). This is reflected in the pH profile for E1 which exhibits values between 7.6-8.3 (Table 3A.36). The addition of acid on a weekly basis has resulted in more acidic conditions developing at the surface of E2. The development of pH 4.6 at the surface of E2 suggests the tailings have a low potential for acid neutralisation.

The cementing potential of E1 and E2 did not vary dramatically, with basically no real cements developed in either case. Upon exposure and drying, soluble salt precipitation however did develop. The solute profiles were also not very different, with minor surface concentration increases in E2 compared with E1 (Table 3A.37). In the majority of profiles increased levels can be attributed to the breakdown of gangue minerals due to additions of pH 3 solution throughout the trial (Table 3A.36). Increased surface levels of Zn in E2 suggest that oxidation of residual sphalerite has taken place, promoted by the chemical and/or biological additives. As with the Ranger tailings, the E2 chemical and biological additions made only minimal changes to both the physical and chemical nature of the tailings compared with E1.

depth (cm)	pH	EC (mS/cm)
E1		
0.5	7.7	13.5
1.5	7.6	8.58
5.5	8.3	1.30
11	8.2	0.12
17.5	8.2	0.10
28	8.2	0.09
E2		
0.5	4.6	15.4
1.5	5.6	9.65
5.5	7.3	1.15
11	7.6	1.35
20	7.7	1.50
27	6.7	1.54

TABLE 3A.36 PH AND EC RESULTS FOR PINE CREEK NATURAL (E1) AND CHEMICAL AND BIOLOGICAL (E2) HARDPAN

depth	Al	B	Ca	Cd	Co	Cr	Cu	Fe	K	Mg	Mn	Mo	Na	Ni	P	Pb	S	Zn
cm	mg/kg	mg/kg	mg/kg	mg/kg	mg/kg	mg/kg	mg/kg	mg/kg	mg/kg	mg/kg	mg/kg	mg/kg	mg/kg	mg/kg	mg/kg	mg/kg	mg/kg	mg/kg
E1																		
surf	<5	1.2	3881	<1	16.8	<1	<1	8.5	773.2	1049	<1	<1	13684	<1	<1	<5	12144	3.8
1-2cm	<5	1.0	2747	<1	16.8	<1	<1	3.1	452.6	744.3	<1	<1	7145	<1	<1	<5	5252	<1
5-6cm	<1	1.3	435	<1	0.9	<1	<1	2.0	137.0	99.4	<1	<1	744	<1	<1	<1	876	<1
10-12cm	<1	1.0	621	<1	<1	<1	<1	<1	113.3	77.1	<1	<1	464	<1	<1	<1	883	<1
16-19cm	<1	1.0	589	<1	<1	<1	<1	<1	108.7	75.3	<1	<1	348	<1	<1	<1	786	<1
27-29cm	<1	0.9	457	<1	<1	<1	<1	<1	74.6	50.1	<1	<1	288	<1	<1	<1	661	<1
E2																		
surf	19	<1	2888	<1	10.3	<1	4.8	10.5	213.6	4082	505	<1	14642	4.3	<1	<5	16758	149
1-2cm	<5	1.3	2607	<1	4.7	<1	<1	<1	155.6	2099	183	<1	7928	5.6	<1	<5	8378	52.7
5-6cm	<1	1.1	278	<1	1.0	<1	<1	<1	108.6	79.1	<1	<1	700	<1	<1	<1	819	<1
10-12cm	<1	1.1	749	<1	<1	<1	<1	<1	124.4	117.7	<1	<1	538	<1	<1	<1	1119	<1
19-22cm	<1	1.2	947	<1	<1	<1	<1	<1	132.4	178.4	<1	<1	514	<1	<1	<1	1262	<1
26-28cm	<1	1.1	982	<1	<1	<1	<1	<1	98.1	205.9	5.9	<1	425	<1	<1	<1	1317	<1

TABLE 3A.37 ICP-AES RESULTS FOR PINE CREEK NATURAL (E1) AND CHEMICAL AND BIOLOGICAL (E2) HARDPAN ENHANCED TRIALS

3A.9.2 Leaching Characteristics of the Pine Creek Tailings

The leaching trends observed for Pine Creek are not easily interpreted. In general initially high levels of Na, S, Mg, K and Ca, along with minor concentration of P, Zn, Fe, Mn, Al and Co are released during the first leaching cycle (Table 3A.39). This release reflects the leaching of soluble salts developed in the tailings prior to sampling. This is followed by a subsequent low as shown in the EC profile (Table 3A.38). The following leaching cycles vary between lower pH values with higher EC releases and higher pH values with lower EC results (Table 3A.38). This may reflect a lag period between the oxidation reactions, acid generation and gangue minerals degradation associated with the very minor sulfide content (< 0.1% S), or more likely, lag periods associated with the dissolution of variably mobile secondary minerals.

In the final stages however levels of Na, S, Fe, Mg, Ca and Co appear to be increasing. As the oxide tailings have a very low sulfide content, it must be assumed that this release is not related to acid generation and resulting gangue mineral degradation in any great quantity. It may represent however the gradual dissolution of gypsum and potentially Fe bearing minerals over time. Additionally, general weathering degradation of aluminosilicates would contribute to the Mg, K and Ca values. The results obtained here were compared with water quality guidelines (Table 3A.39), which indicate that the leachate is unacceptable for fresh aquatic life, drinking water and for livestock consumption due to increased levels S.

date	day	pH	EC(mS/cm)		date	day	pH	EC(mS/cm)
individual leaching results					**average of weekly leachate**			
4/12/96	1	8.2	8.79		4/12/96	1	8.20	8.79
8/01/96	35	6.87	2.31		10/01/96	37	7.60	1.36
10/01/96	37	8.15	0.72		31/01/96	58	6.97	3.38
12/01/96	39	7.78	1.05		21/02/96	79	8.17	1.37
29/01/96	56	4.3	2.64		13/03/96	100	5.34	3.45
31/01/96	58	8.37	1.37		2/04/96	120	7.80	4.38
2/02/96	60	8.25	6.13					
19/02/96	77	8.56	2.07					
21/02/96	79	7.55	0.85					
23/02/96	81	8.4	1.18					
11/03/96	98	4.57	2.42					
13/03/96	100	6.11	4.47					
1/04/96	119	7.65	3.5					

TABLE 3A.38 pH AND EC RESULTS FOR PINE CREEK - LEACHING CHARACTERISATION EXPERIMENT

	Al	B	Ca	Cd	Co	Cr	Cu	Fe	K	Mg	Mn	Mo	Na	Ni	P	Pb	S	Zn
day	mg/L	mg/L	mg/L	mg/L	mg/L	mg/L	mg/L	mg/L	mg/L	mg/L	mg/L	mg/L	mg/L	mg/L	mg/L	mg/L	mg/L	mg/L
1	7.7	<0.1	686	<0.1	1.2	<0.1	0.2	13.7	178.0	207.7	1.2	<0.1	2080	0.2	<1	0.3	1700	1.6
35	<0.1	<0.1	211	<0.1	0.2	<0.1	<0.1	0.2	15.0	19.2	<0.1	<0.1	397	<0.1	<0.2	<0.1	404	<0.1
37	<0.1	<0.1	126	<0.1	<0.1	<0.1	<0.1	<0.1	5.1	6.8	<0.1	<0.1	92	<0.1	<0.2	<0.1	179	<0.1
39	<0.1	<0.1	67.5	<0.1	<0.1	<0.1	<0.1	<0.1	10.0	9.6	<0.1	<0.1	130	<0.1	<0.2	<0.1	160	<0.1
56	0.2	<0.1	60.5	<0.1	0.2	<0.1	<0.1	<0.1	11.9	21.7	<0.1	<0.1	456	<0.1	<0.2	<0.1	401	<0.1
58	<0.1	<0.1	41.6	<0.1	<0.1	<0.1	<0.1	<0.1	12.7	11.8	<0.1	<0.1	225	<0.1	<0.1	<0.1	190	<0.1
60	0.5	0.2	527	<0.1	0.3	<0.1	<0.1	0.9	85.3	94.4	<0.1	<0.1	865	0.1	<0.4	<0.1	1250	<0.1
77	<0.1	<0.1	76.6	<0.1	0.2	<0.1	<0.1	<0.1	16.5	32.1	<0.1	<0.1	368	<0.1	0.1	<0.1	313	<0.1
79	<0.1	<0.1	54.4	<0.1	0.1	<0.1	<0.1	<0.1	14.4	12.6	<0.1	<0.1	117	<0.1	<0.1	<0.1	115	<0.1
81	<0.1	<0.1	195	<0.1	0.3	<0.1	<0.1	<0.1	29.9	26.9	<0.1	<0.1	201	<0.1	0.0	<0.1	298	<0.1
98	<0.1	<0.1	94.0	<0.1	0.4	<0.1	<0.1	0.1	32.3	33.7	<0.1	<0.1	460	<0.1	0.1	<0.1	376	<0.1
100	<0.1	<0.1	554	<0.1	0.9	<0.1	<0.1	3.9	98.8	83.1	<0.1	<0.1	662	<0.1	0.2	<0.1	942	<0.1
119	<0.1	<0.1	464	<0.1	0.5	<0.1	<0.1	2.8	66.5	54.3	<0.1	<0.1	385	<0.1	0.2	<0.1	613	<0.1
121	<0.1	<0.1	674	<0.1	1.1	<0.1	<0.1	5.7	109.6	105.4	<0.1	<0.1	799	<0.1	0.1	<0.1	1019	<0.1
average of weekly leachate																		
1	7.7	<0.1	686	<0.1	1.2	<0.1	0.2	13.7	178.0	207.7	1.2	<0.1	2080	0.2	<1	0.3	1700	1.6
37	0.1	0.1	135	0.1	0.1	0.1	0.1	0.1	10.1	11.9	0.1	0.1	206	0.1	0.2	0.1	248	0.1
58	0.3	0.1	210	0.1	0.2	0.1	0.1	0.4	36.6	42.6	0.1	0.1	515	0.1	0.2	0.1	614	0.1
79	0.1	0.1	109	0.1	0.2	0.1	0.1	0.1	20.3	23.8	0.1	0.1	229	0.1	0.1	0.1	242	0.1
100	0.1	0.1	324	0.1	0.6	0.1	0.1	2.0	65.6	58.4	0.1	0.1	561	0.1	0.1	0.1	659	0.1
120	0.1	0.1	569	0.1	0.8	0.1	0.1	4.2	88.1	79.9	0.1	0.1	592	0.1	0.1	0.1	816	0.1
D.W	0.2	0.3		0.002		0.05	1.5	0.3			0.5	0.05		0.02		0.01	500	3
F.A	0.005			0.002		0.01	0.005	1						0.15		0.01		0.05
L.S	5	5	1000	0.01	1	1	0.5					0.01		1		0.1	1000	20

TABLE 3A.39 SOLUTE LEACHING RESULTS FOR PINE CREEK - LEACHING CHARACTERISATION EXPERIMENT

3A.10 Additional Information Tables referred to in Chapter 6

	Total Al available (mg)	Total Al leached (mg)	Total Al leached (%)	Average rate of Al release	Initial rate of Al release	Final rate of Al release
Brukunga 2	176960	2479.80	1.4013	$1x10^{-3}x$	$1x10^{-3}x$	$9x10^{-4}x$
Brukunga 1	159360	965.00	0.6055	$4x10^{-4}x$	$3x10^{-4}x$	$3x10^{-4}x$
Elura	21209	0.10	0.0005	$2x10^{-7}x$	$2x10^{-7}x$	$2x10^{-7}x$
Woodlawn	60822	52.55	0.0864	$4x10^{-5}x$	$2x10^{-5}x$	$7x10^{-5}x$
Woodcutters	50560	0.13	0.0003	$1x10^{-7}x$	$2x10^{-7}x$	$1x10^{-7}x$
Broken Hill	51986	0.15	0.0003	$1x10^{-7}x$	$2x10^{-7}x$	$1x10^{-7}x$
Ranger	107100	0.38	0.0004	$5x10^{-6}x$	$5x10^{-6}x$	$5x10^{-6}x$
Pine Creek	138600	0.26	0.0002	$3x10^{-6}x$	$4x10^{-6}x$	$2x10^{-6}x$
CSA	82500	0.47	0.0006	$2x10^{-7}x$	$3x10^{-7}x$	$3x10^{-7}x$
Peak	64074	0.37	0.0006	$2x10^{-7}x$	$3x10^{-7}x$	$2x10^{-7}x$
	Total Ca available (mg)	**Total Ca leached (mg)**	**Total Ca leached (%)**	**Average rate of Ca release**	**Initial rate of Ca release**	**Final rate of Ca release**
Brukunga 2	21728	451.84	2.0795	$1.4x10^{-3}x$	$1.2x10^{-3}x$	$1.7x10^{-3}x$
Brukunga 1	19776	439.19	2.2208	$1.1x10^{-3}x$	$1.1x10^{-3}x$	$1.1x10^{-3}x$
Elura	7181	94.92	1.3218	$4x10^{-4}x$	$2x10^{-4}x$	$2x10^{-4}x$
Woodlawn	5450	257.21	4.7194	$2.5x10^{-3}x$	$2x10^{-3}x$	$2.8x10^{-3}x$
Woodcutters	38560	383.54	0.9947	$7x10^{-4}x$	$6x10^{-4}x$	$7x10^{-4}x$
Broken Hill	39738	390.40	0.9825	$4x10^{-4}x$	$7x10^{-4}x$	$2x10^{-4}x$
Ranger	14450	362.01	2.5053	$1.6x10^{-3}x$	$1.2x10^{-3}x$	$2x10^{-3}x$
Pine Creek	3267	85.15	2.6062	$1.4x10^{-3}x$	$1.4x10^{-3}x$	$1.5x10^{-3}x$
CSA	3548	610.60	17.2120	$5x10^{-4}x$	$7.6x10^{-3}x$	$8.6x10^{-3}x$
Peak	1416	433.55	30.6179	$1.9x10^{-2}x$	$2x10^{-2}x$	$1.6x10^{-2}x$
	Total Cu available (mg)	**Total Cu leached (mg)**	**Total Cu leached (%)**	**Average rate of Cu release**	**Initial rate of Cu release**	**Final rate of Cu release**
Brukunga 2	112	8.93	7.9773	$6.7x10^{-3}x$	$4.7x10^{-3}x$	$6.7x10^{-3}x$
Brukunga 1	96	6.53	6.7973	$4.2x10^{-3}x$	$2.5x10^{-3}x$	$4.8x10^{-3}x$
Elura	3173	0.18	0.0057	$3x10^{-6}x$	$3x10^{-6}x$	$3x10^{-6}x$
Woodlawn	5014	125.90	2.5109	$1.2x10^{-3}x$	$2x10^{-4}x$	$2.4x10^{-3}x$
Woodcutters	480	0.10	0.0204	$1x10^{-5}x$	$1x10^{-5}x$	$1x10^{-5}x$
Broken Hill	94	0.12	0.1246	$6x10^{-5}x$	$7x10^{-5}x$	$5x10^{-5}x$
Ranger	170	0.08	0.0460	$3x10^{-5}x$	$3x10^{-5}x$	$3x10^{-5}x$
Pine Creek	198	0.05	0.0250	$2x10^{-5}x$	$2x10^{-5}x$	$1x10^{-5}x$
CSA	743	0.12	0.0156	$7x10^{-5}x$	$8x10^{-5}x$	$6x10^{-5}x$
Peak	2213	0.10	0.0047	$2x10^{-5}x$	$2x10^{-5}x$	$2x10^{-5}x$
	Total Fe available (mg)	**Total Fe leached (mg)**	**Total Fe leached (%)**	**Average rate of Fe release**	**Initial rate of Fe release**	**Final rate of Fe release**
Brukunga 2	53984	872.02	1.6153	$1x10^{-3}x$	$1.7x10^{-3}x$	$5x10^{-4}x$
Brukunga 1	33216	612.70	1.8446	$9x10^{-4}x$	$1.6x10^{-3}x$	$3x10^{-4}x$
Elura	592850	37.27	0.0063	$3x10^{-5}x$	$5x10^{-5}x$	$2x10^{-5}x$
Woodlawn	209280	265.63	0.1269	$7x10^{-5}x$	$3x10^{-5}x$	$9x10^{-5}x$
Woodcutters	382400	1.83	0.0005	$2x10^{-7}x$	$4x10^{-7}x$	$5x10^{-8}x$
Broken Hill	51425	0.39	0.0008	$4x10^{-7}x$	$6x10^{-7}x$	$1x10^{-7}x$
Ranger	51255	0.33	0.0006	$1x10^{-7}x$	$9x10^{-8}x$	$1x10^{-7}x$
Pine Creek	73656	0.59	0.0008	$2x10^{-7}x$	$8x10^{-8}x$	$4x10^{-7}x$
CSA	103950	0.62	0.0006	$2x10^{-7}x$	$4x10^{-7}x$	$2x10^{-7}x$
Peak	53897	0.67	0.0012	$4x10^{-7}x$	$6x10^{-7}x$	$5x10^{-7}x$
	Total K available (mg)	**Total K leached (mg)**	**Total K leached (%)**	**Average rate of K release**	**Initial rate of K release**	**Final rate of K release**
Brukunga 2	29792	0.93	0.0031	$2x10^{-6}x$	$2x10^{-6}x$	$2x10^{-6}x$
Brukunga 1	28128	0.32	0.0011	$3x10^{-7}x$	$7x10^{-7}x$	$1x10^{-7}x$
Elura	5010	4.11	0.0820	$1x10^{-5}x$	$2x10^{-5}x$	$2x10^{-5}x$
Woodlawn	7303	10.41	0.1426	$6x10^{-5}x$	$1x10^{-4}x$	$3x10^{-5}x$
Woodcutters	10720	31.92	0.2978	$2x10^{-4}x$	$2x10^{-4}x$	$1x10^{-4}x$
Broken Hill	5797	40.60	0.7003	$2x10^{-4}x$	$6x10^{-4}x$	$8x10^{-5}x$
Ranger	6715	36.40	0.5421	$3x10^{-4}x$	$3x10^{-4}x$	$3x10^{-4}x$
Pine Creek	32274	15.32	0.0475	$2x10^{-5}x$	$2x10^{-5}x$	$3x10^{-5}x$
CSA	3795	27.77	0.7317	$3x10^{-4}x$	$4x10^{-4}x$	$2x10^{-4}x$
Peak	14160	153.47	1.0838	$3x10^{-4}x$	$8x10^{-4}x$	$1x10^{-4}x$

TABLE 3A.40 ELEMENT AVAILABILITY, RELEASE AND RATE OF RELEASE (mg/day) - EXPT 3 : LEACHING CHARACTERISATION

	Total Mg available (mg)	Total Mg leached (mg)	Total Mg leached (%)	Average rate of Mg release	Initial rate of Mg release	Final rate of Mg release
Brukunga 2	36960	31.62	0.0856	$5x10^{-5}x$	$6x10^{-5}x$	$4x10^{-5}x$
Brukunga 1	33120	90.78	0.2741	$1x10^{-4}x$	$2x10^{-4}x$	$6x10^{-5}x$
Elura	15531	358.56	2.3086	$1.2x10^{-3}x$	$1.5x10^{-3}x$	$9x10^{-4}x$
Woodlawn	67362	356.42	0.5291	$3x10^{-4}x$	$3x10^{-4}x$	$2x10^{-4}x$
Woodcutters	107520	1724.19	1.6036	$1.1x10^{-3}x$	$9x10^{-4}x$	$1.3x10^{-3}x$
Broken Hill	7948	17.32	0.2179	$5x10^{-5}x$	$2x10^{-4}x$	$4x10^{-5}x$
Ranger	85850	1666.27	1.9409	$1.2x10^{-3}x$	$1.5x10^{-3}x$	$8x10^{-4}x$
Pine Creek	12474	17.49	0.1402	$8x10^{-5}x$	$7x10^{-5}x$	$7x10^{-5}x$
CSA	41003	165.70	0.4041	$2x10^{-4}x$	$2x10^{-4}x$	$1x10^{-4}x$
Peak	23807	87.53	0.3677	$1x10^{-4}x$	$2x10^{-4}x$	$1x10^{-4}x$
	Total Na available (mg)	**Total Na leached (mg)**	**Total Na leached (%)**	**Average rate of Na release**	**Initial rate of Na release**	**Final rate of Na release**
Brukunga 2	15344	12.84	0.0837	$5x10^{-5}x$	$4x10^{-5}x$	$6x10^{-5}x$
Brukunga 1	14784	14.10	0.0954	$4x10^{-5}x$	$3x10^{-5}x$	$6x10^{-5}x$
Elura	1837	88.79	4.8334	$1.4x10^{-3}x$	$2.6x10^{-3}x$	$5x10^{-4}x$
Woodlawn	2071	421.78	20.3659	$1.3x10^{-2}x$	$1.1x10^{-2}x$	$8.9x10^{-3}x$
Woodcutters	2560	86.19	3.3669	$1.8x10^{-3}x$	$2.6x10^{-3}x$	$1x10^{-3}x$
Broken Hill	1029	260.39	25.3170	$5.6x10^{-3}x$	$2.7x10^{-2}x$	$6x10^{-3}x$
Ranger	850	25.37	2.9848	$1.9x10^{-3}x$	$1.9x10^{-3}x$	$1.7x10^{-3}x$
Pine Creek	1584	199.13	12.5714	$7.8x10^{-3}x$	$8.6x10^{-3}x$	$5.7x10^{-3}x$
CSA	825	128.10	15.5279	$6.9x10^{-3}x$	$1.2x10^{-2}x$	$1.5x10^{-3}x$
Peak	1593	717.08	45.0147	$1.5x10^{-2}x$	$4.8x10^{-2}x$	$3x10^{-4}x$
	Total Pb available (mg)	**Total Pb leached (mg)**	**Total Pb leached (%)**	**Average rate of Pb release**	**Initial rate of Pb release**	**Final rate of Pb release**
Brukunga 2	112	0.85	0.7567	$5x10^{-5}x$	$4x10^{-5}x$	$6x10^{-5}x$
Brukunga 1	96	0.30	0.3087	$2x10^{-4}x$	$1x10^{-4}x$	$2x10^{-4}x$
Elura	22378	1.44	0.0065	$3x10^{-6}x$	$5x10^{-6}x$	$9x10^{-7}x$
Woodlawn	13625	1.42	0.0104	$5x10^{-6}x$	$8x10^{-6}x$	$5x10^{-6}x$
Woodcutters	37120	2.07	0.0056	$4x10^{-6}x$	$4x10^{-6}x$	$3x10^{-6}x$
Broken Hill	1215	0.33	0.0272	$1x10^{-5}x$	$5x10^{-5}x$	$4x10^{-5}x$
Ranger	595	0.09	0.0144	$9x10^{-6}x$	$1x10^{-5}x$	$9x10^{-6}x$
Pine Creek	198	0.05	0.0271	$2x10^{-6}x$	$2x10^{-5}x$	$1x10^{-5}x$
CSA	83	0.17	0.2032	$7x10^{-6}x$	$6x10^{-5}x$	$8x10^{-5}x$
Peak	1239	1.99	0.1603	$8x10^{-6}x$	$5x10^{-5}x$	$1x10^{-4}x$
	Total S available (mg)	**Total S leached (mg)**	**Total S leached (%)**	**Average rate of S release**	**Initial rate of S release**	**Final rate of S release**
Brukunga 2	50400	5622.12	11.1550	$8.3x10^{-3}x$	$8.2x10^{-3}x$	$7.5x10^{-3}x$
Brukunga 1	26112	2742.80	10.5040	$6x10^{-3}x$	$6x10^{-3}x$	$5.7x10^{-3}x$
Elura	581160	877.55	0.1510	$8x10^{-5}x$	$1x10^{-4}x$	$5x10^{-5}x$
Woodlawn	275443	5386.76	1.9557	$1.1x10^{-3}x$	$9x10^{-4}x$	$1.1x10^{-3}x$
Woodcutters	496800	3373.27	0.6790	$5x10^{-4}x$	$5x10^{-4}x$	$5x10^{-4}x$
Broken Hill	9163	384.94	4.2010	$1.6x10^{-3}x$	$3.6x10^{-3}x$	$8x10^{-4}x$
Ranger	31110	3103.53	9.9760	$6.4x10^{-3}x$	$7.7x10^{-3}x$	$4.9x10^{-3}x$
Pine Creek	5346	201.00	3.7598	$2.3x10^{-3}x$	$2.6x10^{-3}x$	$1.8x10^{-3}x$
CSA	19635	778.72	3.9660	$1.8x10^{-3}x$	$1.9x10^{-3}x$	$1.6x10^{-3}x$
Peak	24603	1178.39	4.7896	$1.8x10^{-3}x$	$3.1x10^{-3}x$	$1.2x10^{-3}x$
	Total Zn available (mg)	**Total Zn leached (mg)**	**Total Zn leached (%)**	**Average rate of Zn release**	**Initial rate of Zn release**	**Final rate of Zn release**
Brukunga 2	1904	512.33	26.9083	$2.3x10^{-2}x$	$2x10^{-2}x$	$2.2x10^{-2}x$
Brukunga 1	576	371.60	64.5132	$5.5x10^{-2}x$	$2.5x10^{-2}x$	$8.2x10^{-2}x$
Elura	32064	420.09	1.3102	$7x10^{-4}x$	$1.4x10^{-3}x$	$2x10^{-4}x$
Woodlawn	26051	8207.14	31.5041	$2.1x10^{-2}x$	$1.5x10^{-2}x$	$2.5x10^{-2}x$
Woodcutters	27520	295.20	1.0727	$8x10^{-4}x$	$6x10^{-4}x$	$9x10^{-4}x$
Broken Hill	1964	23.26	1.1844	$4x10^{-4}x$	$1.2x10^{-3}x$	$1x10^{-4}x$
Ranger	85	0.52	0.6170	$8x10^{-5}x$	$1x10^{-4}x$	$7x10^{-5}x$
Pine Creek	594	0.09	0.0152	$6x10^{-6}x$	$7x10^{-6}x$	$4x10^{-6}x$
CSA	248	0.45	0.1825	$9x10^{-5}x$	$1x10^{-4}x$	$4x10^{-5}x$
Peak	2213	140.03	6.3292	$3.5x10^{-3}x$	$1x10^{-3}x$	$5.8x10^{-3}x$

TABLE 3A.40 CONT ELEMENT AVAILABILITY, RELEASE AND RATE OF RELEASE (mg/day)- EXPT 3 : LEACHING CHARACTERISATION

	SiO_2	Al_2O_3	Fe_2O_3	MnO	MgO	CaO	K_2O	TiO_2	P_2O_5	SO_3
Error	0.005	0.005	0.002	0.001	0.006	0.001	0.001	0.001	0.001	0.01
	%	%	%	%	%	%	%	%	%	%
Sample										
KP Limestone A	4.74	0.65	0.8	0.032	0.8	50.1	0.25	0.003	0.02	0.03
KP Limestone B	2.68	0.65	0.63	0.022	0.9	51.5	0.16	<0.001	0.018	0.02
KP Limestone C	3.31	0.58	1	0.028	0.8	51.2	0.17	<0.001	0.028	0.01
KP Limestone D	14.72	0.87	1.1	0.034	0.9	44.7	0.42	0.026	0.034	0.03
KP Limestone E	5.59	0.83	0.94	0.027	1.8	48.4	0.24	0.018	0.027	0.03
	Ba	Ce	Co	Cr	Cu	Ga	La	Ni	Pb	Rb
Error	15	9	3	7	11	3	18	4	10	3
	ppm	ppm	ppm	ppm	ppm	ppm	ppm	ppm	ppm	ppm
Sample										
KP Limestone A	56	<18.	26	<14.	66	16	<36.	28	14	< 7.
KP Limestone B	<29.	<18.	20	<14.	75	16	<36.	17	18	< 7.
KP Limestone C	<29.	<18.	25	<14.	58	19	<36.	17	15	< 7.
KP Limestone D	61	<18.	25	<14.	68	19	<36.	20	13	10
KP Limestone E	<29.	<18.	24	<14.	63	16	<36.	22	15	7
	Sr	Th	U	V	Y	Zn	Zr			
Error	3	6	5	4	3	10	9			
	ppm	ppm	ppm	ppm	ppm	ppm	ppm			
Sample										
KP Limestone A	14	54	<10.	< 9.	7	10	134			
KP Limestone B	< 7.	42	12	16	13	15	126			
KP Limestone C	< 7.	39	<10.	< 9.	11	<10.	130			
KP Limestone D	59	26	13	20	14	14	190			
KP Limestone E	78	25	<10.	21	12	<10.	157			

TABLE 3A.41 LIMESTONE XRF DATA FOR SOLID ADDITIVE HARDPAN ENHANCEMENT

	SiO_2	Al_2O_3	Fe_2O_3	MnO	MgO	CaO	K_2O	TiO_2	P_2O_5	SO_3
Error	0.005	0.005	0.002	0.001	0.006	0.001	0.001	0.001	0.001	0.01
	%	%	%	%	%	%	%	%	%	%
Sample										
RP Blend	3.42	1.03	0.85	0.034	0.6	48.3	0.075	0.065	34.4	0.81
Nauru	0.016	0.12	0.14	0.013	0.4	53.1	0.005	<0.001	39.5	0.19
Florida	4.25	1.19	1.35	0.043	0.5	47.3	0.11	0.13	32.8	1.14
Christmas Island B	1	8.31	4.38	0.158	0.4	39.1	0.026	0.53	35.6	1.98
	Ba	Ce	Co	Cr	Cu	Ga	La	Ni	Pb	Rb
Error	15	9	3	7	11	3	18	4	10	3
	ppm	ppm	ppm	ppm	ppm	ppm	ppm	ppm	ppm	ppm
Sample										
RP Blend	55	48	32	51	92	20	<36.	27	59	16
Nauru	<29.	<18.	36	51	99	22	<36.	20	64	10
Florida	70	81	30	47	92	22	<36.	39	61	16
Christmas Island B	250	59	39	153	191	31	<36.	42	86	25
	Sr	Th	U	V	Y	Zn	Zr			
Error	3	6	5	4	3	10	9			
	ppm	ppm	ppm	ppm	ppm	ppm	ppm			
Sample										
RP Blend	594	21	127	41	95	382	193			
Nauru	242	20	98	< 9.	24	1317	133			
Florida	816	25	138	60	150	101	297			
Christmas Island B	1884	54	81	17	71	553	282			

TABLE 3A.42 PHOSPHATE XRF DATA FOR SOLID ADDITIVE HARDPAN ENHANCEMENT

	pH of extraction	Al	B	Ba	Be	Ca	Cd	Co	Cr	Cu	Fe	K	Li	
Sample	water	mg/L	mg/L	mg/L	mg/L	mg/L	mg/L	mg/L	mg/L	mg/L	mg/L	mg/L	mg/L	
Nauru	6.5	<0.005	0.013	<0.005	<0.002	94	<0.01	<0.01	<0.005	0.021	<0.05	32	<0.005	
	5.5	<0.005	0.010	<0.005	<0.002	82	<0.01	<0.01	<0.005	0.019	<0.05	29	<0.005	
	3.5	0.006	0.010	<0.005	<0.002	84	<0.01	<0.01	<0.005	0.016	<0.05	30	<0.005	
	2	0.060	0.026	0.008	<0.002	665	0.02	0.03	0.012	0.225	<0.05	38	<0.005	
Florida	6.5	0.031	<0.005	<0.005	<0.002	22	<0.01	<0.01	<0.005	<0.005	<0.05	1.1	<0.005	
	5.5	0.030	<0.005	<0.005	<0.002	22	<0.01	<0.01	<0.005	<0.005	<0.05	1.1	<0.005	
	3.5	0.044	<0.005	<0.005	<0.002	24	<0.01	<0.01	<0.005	<0.005	<0.05	1.2	<0.005	
	2	0.630	0.038	0.016	<0.002	525	0.01	0.05	0.010	0.011	<0.05	2.7	<0.005	
Christmas	6.5	0.313	0.069	0.011	<0.002	490	0.01	0.14	<0.005	0.243	0.07	19	0.006	
	5.5	0.257	0.075	0.013	<0.002	425	<0.01	0.11	<0.005	0.169	<0.05	18	0.005	
	3.5	0.146	0.083	0.015	<0.002	480	0.01	0.11	<0.005	0.165	0.07	17	0.007	
	2	1.63	0.112	0.017	<0.002	885	0.05	0.26	0.013	1.54	0.12	26	0.013	
Blend	6.5	0.023	0.036	<0.005	<0.002	61	<0.01	<0.01	<0.005	<0.005	<0.05	5.0	<0.005	
	5.5	0.020	0.037	<0.005	<0.002	62	<0.01	<0.01	<0.005	<0.005	<0.05	4.8	<0.005	
	3.5	0.028	0.036	<0.005	<0.002	63	<0.01	<0.01	<0.005	<0.005	<0.05	4.9	<0.005	
	2	0.217	0.071	0.010	<0.002	525	<0.01	0.03	0.005	0.015	<0.05	7.0	<0.005	
	pH of extraction	Mg	Mn	Mo	Na	Ni	P	Pb	S	Si	Sr	Ti	V	Zn
Sample	water	mg/L	mg/L	mg/L	mg/L	mg/L	mg/L	mg/L	mg/L	mg/L	mg/L	mg/L	mg/L	mg/L
Nauru	6.5	18	0.064	<0.01	4.9	0.02	3.2	<0.20	124	0.56	0.169	<0.005	<0.005	0.23
	5.5	17	0.051	<0.01	4.3	0.01	2.8	<0.20	109	0.49	0.149	<0.005	<0.005	0.22
	3.5	17	0.052	<0.01	4.2	<0.01	3.3	<0.20	112	0.49	0.153	<0.005	<0.005	0.14
	2	43	0.933	<0.01	7.1	0.04	214	<0.20	514	0.69	0.756	<0.005	<0.005	4.7
Florida	6.5	7.3	0.018	0.04	6.2	0.02	0.95	<0.20	28	1.7	0.041	<0.005	0.131	<0.05
	5.5	7.3	0.018	0.05	6.3	0.02	0.89	<0.20	28	1.7	0.041	<0.005	0.133	<0.05
	3.5	7.7	0.021	0.04	6.4	0.02	1.0	<0.20	30	1.8	0.045	<0.005	0.129	<0.05
	2	35	0.902	<0.01	15	0.28	136	<0.20	411	4.6	1.01	<0.005	0.014	<0.05
Christmas	6.5	36	8.6	<0.01	14	0.29	35	<0.20	454	13	0.571	<0.005	<0.005	1.2
	5.5	35	7.1	<0.01	13	0.24	24	<0.20	398	16	0.492	<0.005	<0.005	0.67
	3.5	35	6.8	<0.01	13	0.24	27	<0.20	444	11	0.559	<0.005	<0.005	0.81
	2	47	21	<0.01	16	0.52	253	<0.20	701	14	0.925	0.010	<0.005	10.2
Blend	6.5	23	0.007	0.04	8.7	0.02	1.8	<0.20	51	17	0.096	<0.005	0.085	<0.05
	5.5	23	0.019	0.04	8.7	0.02	1.8	<0.20	52	17	0.097	<0.005	0.086	<0.05
	3.5	23	0.006	0.04	8.7	0.04	1.9	<0.20	54	17	0.100	<0.005	0.085	<0.05
	2	55	0.749	<0.01	15	0.15	135	<0.20	429	23	0.689	<0.005	0.018	<0.05

TABLE 3A.43 SOLUTE RESULTS FOR VARIOUS pH WATER 1:5 EXTRACTIONS FOR SELECTED PHOSPHATE SAMPLES

	SiO_2	Al_2O_3	Fe_2O_3	MnO	MgO	CaO	K_2O	TiO_2	P_2O_5	SO_3
Error	0.005	0.005	0.002	0.001	0.006	0.001	0.001	0.001	0.001	0.01
Sample	%	%	%	%	%	%	%	%	%	%
NPS Bottom Ash	58.7	22	6.16	0.101	2.1	5.09	0.9	2	0.77	0.06
NPS Zone 2-3 (S)	51.9	29.1	3.87	0.055	1.9	4.47	0.87	2.56	1.11	0.25
NPS Unit 1 Zone 1	55	24.8	4.28	0.05	2.1	5.01	0.87	2.44	0.79	1.03
NPS Unit 1 Zone 2	52.1	27.7	3.87	0.046	2.3	5.26	0.89	2.48	0.89	0.73
	Ba	Ce	Co	Cr	Cu	Ga	La	Ni	Pb	Rb
Error	15	9	3	7	11	3	18	4	10	3
Sample	ppm	ppm	ppm	ppm	ppm	ppm	ppm	ppm	ppm	ppm
NPS Bottom Ash	736	99	24	97	171	29	52	93	73	40
NPS Zone 2-3 (S)	618	131	17	121	153	54	67	47	86	49
NPS Unit 1 Zone 1	594	123	21	113	153	36	79	40	66	36
NPS Unit 1 Zone 2	538	124	19	124	161	49	69	42	76	39
	Sr	Th	U	V	Y	Zn	Zr			
Error	3	6	5	4	3	10	9			
Sample	ppm	ppm	ppm	ppm	ppm	ppm	ppm			
NPS Bottom Ash	380	23	16	68	69	2810	683			
NPS Zone 2-3 (S)	277	25	<10.	59	70	83	619			
NPS Unit 1 Zone 1	246	31	<10.	72	77	77	712			
NPS Unit 1 Zone 2	229	24	<10.	62	74	92	649			

TABLE 3A.44 FLYASH XRF DATA FOR SOLID ADDITIVE HARDPAN ENHANCEMENT

	pH of extraction	Al	B	Ba	Be	Ca	Cd	Co	Cr	Cu	Fe	K	Li	
Sample	water	mg/L	mg/L	mg/L	mg/L	mg/L	mg/L	mg/L	mg/L	mg/L	mg/L	mg/L	mg/L	
Bot Ash	6.5	0.034	0.363	0.071	<0.002	34	<0.01	<0.01	<0.005	<0.005	<0.05	6.2	0.037	
	5.5	0.030	0.429	0.071	<0.002	34	<0.01	<0.01	<0.005	<0.005	<0.05	6.6	0.043	
	3.5	0.079	0.396	0.063	<0.002	38	<0.01	<0.01	<0.005	<0.005	<0.05	6.7	0.043	
	2	17	1.47	0.050	0.007	280	<0.01	0.02	0.019	0.102	0.17	11	0.118	
U1-Z1 Ash	6.5	8.8	3.60	0.325	<0.002	500	<0.01	<0.01	0.304	<0.005	<0.05	5.4	0.259	
	5.5	6.6	3.55	0.149	<0.002	480	<0.01	<0.01	0.303	<0.005	<0.05	5.4	0.250	
	3.5	8.1	3.51	0.318	<0.002	485	<0.01	<0.01	0.296	<0.005	<0.05	5.5	0.257	
	2	0.081	4.50	0.021	<0.002	685	<0.01	<0.01	0.006	<0.005	<0.05	7.6	0.430	
U1-Z2 Ash	6.5	6.7	4.01	0.192	<0.002	405	<0.01	<0.01	0.383	<0.005	<0.05	5.0	0.247	
	5.5	5.1	3.95	0.133	<0.002	410	<0.01	<0.01	0.382	<0.005	<0.05	5.3	0.250	
	3.5	7.2	3.97	0.186	<0.002	405	<0.01	<0.01	0.373	<0.005	<0.05	5.5	0.248	
	2	0.049	5.0	0.020	<0.002	610	<0.01	<0.01	0.238	<0.005	<0.05	7.2	0.441	
Z2-3 Ash	6.5	4.32	2.98	0.050	<0.002	185	<0.01	<0.01	0.140	<0.005	<0.05	1.6	0.131	
	5.5	1.65	2.89	0.051	<0.002	185	<0.01	<0.01	0.137	<0.005	<0.05	1.6	0.128	
	3.5	3.57	2.92	0.048	<0.002	180	<0.01	<0.01	0.137	<0.005	<0.05	1.7	0.130	
	2	0.035	5.5	0.019	<0.002	510	<0.01	0.01	0.175	<0.005	<0.05	4.4	0.307	
	pH of extraction	Mg	Mn	Mo	Na	Ni	P	Pb	S	Si	Sr	Ti	V	Zn
Sample	water	mg/L	mg/L	mg/L	mg/L	mg/L	mg/L	mg/L	mg/L	mg/L	mg/L	mg/L	mg/L	mg/L
Bot Ash	6.5	16	<0.002	<0.01	153	<0.01	0.16	<0.20	30	1.5	0.236	<0.005	0.037	<0.05
	5.5	17	<0.002	<0.01	171	0.02	0.18	<0.20	33	1.5	0.238	<0.005	0.037	<0.05
	3.5	18	<0.002	<0.01	168	0.02	0.26	<0.20	36	1.5	0.256	<0.005	0.037	<0.05
	2	103	1.06	<0.01	163	0.05	2.2	<0.20	393	87	2.29	<0.005	0.170	0.46
U1-Z1 Ash	6.5	2.2	<0.002	0.28	350	<0.01	<0.05	<0.20	584	0.57	3.13	<0.005	0.166	<0.05
	5.5	1.7	<0.002	0.28	332	<0.01	<0.05	<0.20	557	0.23	3.02	<0.005	0.154	<0.05
	3.5	2.5	<0.002	0.28	338	<0.01	<0.05	<0.20	567	0.58	3.02	<0.005	0.164	<0.05
	2	103	0.779	0.17	339	0.12	24	<0.20	904	74	3.78	<0.005	0.780	<0.05
U1-Z2 Ash	6.5	3.8	<0.002	0.39	342	0.01	<0.05	<0.20	496	0.37	2.17	<0.005	0.139	<0.05
	5.5	4.3	<0.002	0.39	351	<0.01	<0.05	<0.20	511	0.33	2.19	<0.005	0.131	<0.05
	3.5	6.1	<0.002	0.38	341	<0.01	<0.05	<0.20	507	0.67	2.09	<0.005	0.127	<0.05
	2	90	0.255	0.29	353	0.07	16	<0.20	849	68	2.30	<0.005	0.991	<0.05
Z2-3 Ash	6.5	7.6	<0.002	0.49	136	0.02	<0.05	<0.20	196	0.35	1.09	<0.005	0.258	<0.05
	5.5	7.2	<0.002	0.48	133	0.01	<0.05	<0.20	191	0.37	1.06	<0.005	0.240	<0.05
	3.5	7.4	<0.002	0.49	134	0.02	<0.05	<0.20	189	0.43	1.02	<0.005	0.284	<0.05
	2	52	0.296	0.45	158	0.06	41	<0.20	540	82	1.72	<0.005	1.31	<0.05

TABLE 3A.45 SOLUTE RESULTS FOR VARIOUS pH WATER 1:5 EXTRACTIONS FOR SELECTED FLYASH SAMPLES

Test No.	Applied Vertical Stress (kPa)	Average Sample Height (mm)	Average Dry Bulk Density (t/m³)	Average Permeability (m/s)	Porosity %	Test No.	Applied Vertical Stress (kPa)	Average Sample Height (mm)	Average Dry Bulk Density (t/m³)	Average Permeability (m/s)	Porosity %
CSA Control						Lime and Flyash					
1	0.0	18.39	1.25	4.22E-08	0.56	1	0.0	18.14	1.08	1.61E-08	0.59
2	5.3	17.37	1.33	3.51E-08	0.54	2	5.3	17.83	1.10	1.11E-08	0.59
3	9.7	17.21	1.34	3.11E-08	0.53	3	9.7	17.53	1.11	1.09E-08	0.57
4	19.4	16.92	1.36	3.05E-08	0.53	4	19.4	17.52	1.11	1.09E-08	0.57
5	38.7	16.62	1.39	2.68E-08	0.52						
6	77.4	16.23	1.42	2.33E-08	0.51	Flyash					
7	154.8	16.07	1.43	2.15E-08	0.50	1	0.0	20.02	1.47	1.07E-08	0.35
						2	5.3	19.56	1.51	7.43E-09	0.33
Elura Control						3	9.7	19.53	1.51	7.41E-09	0.33
1	0.0	19.69	2.30	8.33E-08	0.46	4	19.4	19.47	1.52	7.13E-09	0.33
2	5.3	18.75	2.42	7.25E-08	0.43						
3	9.7	18.53	2.45	6.52E-08	0.42	Lime					
4	19.4	18.25	2.49	5.67E-08	0.41	1	0.0	18.85	0.95	2.40E-08	0.60
5	38.7	18.06	2.51	5.39E-08	0.41	2	5.3	17.82	1.00	2.16E-08	0.58
6	77.4	17.79	2.55	5.07E-08	0.40	3	9.7	17.56	1.02	2.11E-08	0.57
7	154.8	17.50	2.59	4.48E-08	0.39	4	19.4	17.39	1.03	2.15E-08	0.59
Peak Control						Phosphate and Lime					
1	0.0	20.12	1.50	5.91E-08	0.46	1	0.0	21.55	1.38	1.21E-08	0.51
2	5.3	19.63	1.54	5.29E-08	0.45	2	5.3	20.57	1.44	1.29E-08	0.49
3	9.7	19.49	1.55	5.34E-08	0.44	3	9.7	20.53	1.44	1.22E-08	0.49
4	19.4	19.39	1.56	4.69E-08	0.44	4	19.4	20.47	1.45	1.21E-08	0.49
5	38.7	19.10	1.59	4.53E-08	0.43						
6	77.4	18.77	1.61	3.57E-08	0.42						
7	154.8	18.47	1.64	2.89E-08	0.41						
Phosphate						Phosphate and Limestone					
1	0.0	17.85	1.69	1.00E-08	0.44	1	0.0	22.31	1.52	6.47E-07	0.48
2	5.3	16.78	1.79	7.39E-09	0.41	2	5.3	22.19	1.53	1.41E-07	0.48
3	9.7	16.68	1.81	6.74E-09	0.40	3	9.7	22.05	1.53	1.19E-07	0.47
4	19.4	16.61	1.82	5.92E-09	0.40	4	19.4	21.99	1.54	1.14E-07	0.47
Limestone											
1	0.0	18.43	1.31	4.21E-08	0.50						
2	5.3	18.41	1.32	8.59E-08	0.50						
3	9.7	18.38	1.32	1.31E-08	0.50						
4	19.4	18.33	1.32	1.25E-08	0.50						

TABLE 3A.46 BULK DENSITY, PERMEABILITY AND POROSITY RESULTS FROM OEDOMETER TESTING OF PURE TAILINGS AND ADDITIVES.

Test No.	Applied Vertical Stress (kPa)	Average Sample Height (mm)	Average Dry Bulk Density (t/m³)	Average Permeability (m/s)	Porosity %	Test No.	Applied Vertical Stress (kPa)	Average Sample Height (mm)	Average Dry Bulk Density (t/m³)	Average Permeability (m/s)	Porosity %
CSA Flyash and Lime Mix						**CSA Flyash Mix**					
1	0.0	21.42	1.09	6.36E-08	0.60	1	0.0	19.29	1.33	4.06E-08	0.44
2	5.3	19.59	1.20	5.08E-08	0.57	2	5.3	18.69	1.37	3.20E-08	0.43
3	9.7	19.56	1.20	4.77E-08	0.57	3	9.7	18.50	1.39	2.95E-08	0.42
4	19.4	19.52	1.20	4.70E-08	0.56	4	19.4	18.47	1.39	2.71E-08	0.42
Elura Flyash and Lime Mix						**Elura Flyash Mix**					
1	0.0	23.56	1.63	1.63E-07	0.56	1	0.0	18.57	2.10	4.23E-08	0.40
2	5.3	23.04	1.66	1.78E-07	0.55	2	5.3	18.50	2.11	4.43E-08	0.40
3	9.7	22.92	1.67	1.82E-07	0.55	3	9.7	18.45	2.12	4.47E-08	0.40
4	19.4	22.67	1.69	1.60E-07	0.54	4	19.4	18.38	2.12	4.47E-08	0.39
Peak Flyash and Lime Mix						**Peak Flyash Mix**					
1	0.0	21.32	1.36	6.76E-08	0.50	1	0.0	20.35	1.55	3.86E-08	0.40
2	5.3	21.20	1.37	6.13E-08	0.50	2	5.3	20.27	1.56	3.44E-08	0.40
3	9.7	21.16	1.37	5.52E-08	0.50	3	9.7	20.18	1.57	3.39E-08	0.40
4	19.4	21.12	1.38	5.36E-08	0.50	4	19.4	20.12	1.57	3.76E-08	0.39
CSA Lime Mix						**CSA Phosphate and Lime Mix**					
1	0.0	22.40	0.92	8.39E-08	0.66	1	0.0	18.73	1.25	4.92E-08	0.56
2	5.3	21.35	0.97	7.92E-08	0.65	2	5.3	18.41	1.27	4.48E-08	0.56
3	9.7	21.21	0.97	7.44E-08	0.65	3	9.7	18.38	1.27	4.58E-08	0.56
4	19.4	21.02	0.98	7.23E-08	0.64	4	19.4	18.23	1.28	4.55E-08	0.56
Elura Lime Mix						**Elura Phosphate and Lime Mix**					
1	0.0	20.33	1.65	4.08E-08	0.57	1	0.0	20.93	1.84	6.77E-08	0.51
2	5.3	19.44	1.73	3.42E-08	0.55	2	5.3	20.65	1.87	3.88E-08	0.50
3	9.7	19.38	1.73	2.67E-08	0.55	3	9.7	20.64	1.87	3.66E-08	0.50
4	19.4	19.35	1.73	2.38E-08	0.55	4	19.4	20.62	1.87	3.29E-08	0.50
Peak Lime Mix						**Peak Phosphate and Lime Mix**					
1	0.0	20.43	1.19	5.03E-08	0.57	1	0.0	21.80	1.36	6.65E-08	0.52
2	5.3	19.41	1.25	4.43E-08	0.55	2	5.3	20.75	1.43	4.35E-08	0.50
3	9.7	19.35	1.25	4.19E-08	0.55	3	9.7	20.70	1.43	4.32E-08	0.50
4	19.4	19.21	1.26	4.29E-08	0.55	4	19.4	20.48	1.45	4.47E-08	0.49
CSA Phosphate Mix						**CSA Limestone Mix**					
1	0.0	22.90	1.50	2.88E-08	0.49	1	0.0	20.07	1.63	4.72E-08	0.42
2	5.3	20.55	1.68	1.93E-08	0.43	2	5.3	20.07	1.63	5.41E-08	0.42
3	9.7	20.20	1.70	1.75E-08	0.42	3	9.7	20.06	1.63	5.40E-08	0.42
4	19.4	20.00	1.72	1.66E-08	0.42	4	19.4	20.03	1.64	4.41E-08	0.42
Elura Phosphate Mix						**Elura Limestone Mix**					
1	0.0	20.94	2.03	4.63E-08	0.46	1	0.0	24.07	1.80	1.63E-07	0.51
2	5.3	20.00	2.12	4.13E-08	0.44	2	5.3	23.37	1.85	1.75E-07	0.51
3	9.7	19.51	2.18	3.08E-08	0.43	3	9.7	23.03	1.88	1.84E-07	0.50
4	19.4	19.32	2.20	2.86E-08	0.42	4	19.4	22.53	1.92	1.60E-07	0.49
Peak Phosphate Mix						**Peak Limestone Mix**					
1	0.0	21.73	1.70	2.27E-08	0.41	1	0.0	20.53	1.59	4.63E-08	0.42
2	5.3	20.64	1.79	1.50E-08	0.38	2	5.3	20.39	1.60	3.98E-08	0.42
3	9.7	20.28	1.83	1.23E-08	0.37	3	9.7	20.33	1.61	3.88E-08	0.42
4	19.4	20.05	1.85	9.28E-09	0.36	4	19.4	20.89	1.56	4.93E-08	0.44

TABLE 3A.47 BULK DENSITY, PERMEABILITY AND POROSITY RESULTS FROM OEDOMETER TESTING OF TAILINGS AND ADDITIVE MIXTURES

Depth	Al	B	Ca	Cd	Cr	Cu	Fe	Fe(II)	K	Mg	Mn	Na	Ni	P	Pb	S	Si	Zn
(cm)	mg/kg	mg/kg	mg/kg	mg/kg	mg/kg	mg/kg	mg/kg	mg/kg	mg/kg	mg/kg	mg/kg	mg/kg	mg/kg	mg/kg	mg/kg	mg/kg	mg/kg	mg/kg
CSA Control																		
2	0.05	0.19	1397	<0.1	<0.05	0.06	79	80	154	620	41	847	<0.5	<0.5	<0.2	2512	20	1.1
22	0.17	0.09	609	<0.1	<0.05	<0.05	52	52	58	595	134	619	<0.5	<0.5	<0.2	1694	6.7	212
35	0.23	<0.05	685	<0.1	<0.05	<0.05	0.83	<0.8	43	177	0.99	175	<0.5	<0.5	<0.2	866	6.4	<0.5
Elura control 1																		
2	n.d.	<0.05	3130	1.5	0.23	<0.05	2191	185	322	17425	5365	13617	0.6	<0.5	24	38139	9.4	8764
13	0.06	0.10	3545	<0.1	<0.05	<0.05	333	317	56	1033	247	1284	<0.5	0.9	<0.2	5327	6.1	218
31	0.49	<0.05	4320	<0.1	<0.05	<0.05	294	362	47	850	100	945	<0.5	1.2	<0.2	5343	7.9	15
58	1.1	0.10	5139	<0.1	<0.05	<0.05	146	146	49	729	16	879	<0.5	1.4	<0.2	5788	12	1.1
75	0.10	0.13	3660	<0.1	<0.05	<0.05	52	52	37	516	6.8	775	<0.5	1.3	<0.2	3909	9.6	<0.5
Elura control 2																		
2	n.d.	<0.05	2528	<0.1	<0.05	<0.05	1280	1273	43	1150	159	1069	<0.5	0.8	<0.2	6388	8.0	199
22	0.07	0.06	2252	6.3	0.06	<0.05	353	347	97	3340	1091	3055	1.0	<0.5	45	15080	6.9	4668
40	0.17	0.11	2503	<0.1	<0.05	<0.05	23	22	52	1512	412	1154	<0.5	<0.5	2.1	7079	5.8	396
54	0.10	0.13	1987	<0.1	<0.05	<0.05	86	87	44	1348	265	998	<0.5	0.9	1.8	6135	6.8	656
Peak Control																		
3	1.4	0.36	415	<0.1	<0.05	<0.05	3.3	<0.8	735	762	57	4213	<0.5	2.9	<0.2	4585	14	6.4
20	0.26	<0.05	289	<0.1	<0.05	<0.05	0.44	0.42	125	115	4.1	497	<0.5	0.4	<0.2	762	7.1	0.24
37	0.38	<0.05	438	<0.1	<0.05	<0.05	7.1	7.7	169	270	23	518	<0.5	0.4	<0.2	1200	11	1.6
53.5	0.27	<0.05	533	<0.1	<0.05	<0.05	54	55	81	248	38	164	<0.5	<0.5	1.0	1095	14	13
65.5	0.27	<0.05	572	<0.1	<0.05	<0.05	0.71	<0.8	57	107	3.3	152	<0.5	<0.5	<0.2	694	9.7	0.54

TABLE 3A.48 ICP-AES RESULTS OF 1:5 EXTRACTS FROM THE SOLID ADDITIVE HARDPAN ENHANCEMENT EXPERIMENT - CONTROL TRIALS

Depth	Al	B	Ca	Cd	Cr	Cu	Fe	Fe(II)	K	Mg	Mn	Na	Ni	P	Pb	S	Si	Zn
(cm)	mg/kg	mg/kg	mg/kg	mg/kg	mg/kg	mg/kg	mg/kg	mg/kg	mg/kg	mg/kg	mg/kg	mg/kg	mg/kg	mg/kg	mg/kg	mg/kg	mg/kg	mg/kg
CSA flyash lime layer																		
2	0.17	0.68	1137	<0.1	<0.05	0.65	0.35	<0.8	3318	295	1.6	8276	<0.5	<0.5	<0.2	8484	6.5	<0.5
6	41	1.3	144	<0.1	<0.05	0.84	7.1	5.9	840	24	9.1	2468	<0.5	0.8	<0.2	2212	70	31
7	0.40	0.28	520	<0.1	<0.05	0.10	1.0	<0.8	1316	56	0.79	3107	<0.5	0.5	<0.2	3162	13	0.67
20	2.2	0.17	347	<0.1	<0.05	<0.05	0.27	<0.8	210	1.6	0.01	621	<0.5	<0.5	<0.2	814	5.2	<0.5
40	0.30	0.18	571	<0.1	<0.05	<0.05	5.3	5.8	150	79	14	527	<0.5	<0.5	<0.2	960	5.6	33
70	0.14	<0.05	417	<0.1	<0.05	<0.05	0.47	<0.8	47	91	0.23	192	<0.5	<0.5	<0.2	579	11	<0.5
Elura flyash lime layer																		
3	n.d.	<0.05	3906	0.50	0.11	<0.05	1089	1085	2327	6836	2021	13987	<0.5	<0.5	2.5	30693	8.9	2646
19	11	<0.05	42139	<0.1	<0.05	5.1	4.4	<0.8	1938	34	6.5	7736	<0.5	<0.5	50	8072	31	17
30	0.25	0.15	2118	<0.1	<0.05	<0.05	4.3	<0.8	110	952	108	1120	<0.5	1.1	<0.2	5386	4.3	30
61	0.13	<0.05	4672	<0.1	<0.05	<0.05	338	339	69	648	175	782	<0.5	1.0	<0.2	5628	6.8	201
81	0.12	<0.05	3739	<0.1	<0.05	<0.05	435	426	71	753	184	751	<0.5	0.9	<0.2	4825	7.6	180
Peak flyash lime layer																		
1	0.35	0.52	1954	0.90	<0.05	46	9.3	9.5	11232	338	63	34139	<0.5	2.6	70	34459	59	126
2	0.36	0.17	1250	<0.1	<0.05	0.71	8.7	8.6	2698	60	6.8	5162	<0.5	4.8	<0.2	6703	48	5.4
10	11	0.74	408	<0.1	<0.05	3.8	23	<0.8	2388	167	7.5	6780	<0.5	4.3	<0.2	7770	72	9.1
24	80	0.93	65	<0.1	<0.05	0.14	3.3	<0.8	843	0.22	0.02	2160	<0.5	0.6	<0.2	5392	33	<0.5
27	1.6	0.77	550	<0.1	<0.05	1.5	1.0	<0.8	716	28	0.25	2056	<0.5	1.1	<0.2	2931	18	<0.5
54	0.65	<0.05	458	<0.1	<0.05	<0.05	4.1	<0.8	189	126	3.2	750	<0.5	0.7	<0.2	1753	17	0.65
75	0.73	<0.05	344	<0.1	<0.05	<0.05	1.4	<0.8	153	87	1.1	584	<0.5	0.6	<0.2	1374	15	0.51

TABLE 3A.49 ICP-AES RESULTS OF 1:5 EXTRACTS FROM THE SOLID ADDITIVE HARDPAN ENHANCEMENT EXPERIMENT - FLYASH AND LIME LAYER TRIALS

Depth	Al	B	Ca	Cd	Cr	Cu	Fe	Fe(II)	K	Mg	Mn	Na	Ni	P	Pb	S	Si	Zn
(cm)	mg/kg	mg/kg	mg/kg	mg/kg	mg/kg	mg/kg	mg/kg	mg/kg	mg/kg	mg/kg	mg/kg	mg/kg	mg/kg	mg/kg	mg/kg	mg/kg	mg/kg	mg/kg
CSA flyash lime mix																		
2	213	103	2493	<0.1	<0.05	7.7	22	<0.8	10090	217	6.0	61113	<0.5	49	<0.2	50570	380	<0.5
25	132	1.6	708	<0.1	<0.05	<0.05	11	9.1	769	28	4.2	1728	<0.5	<0.5	<0.2	721	30	5.9
30	3.8	0.21	138	<0.1	<0.05	<0.05	1.7	<0.8	307	1.2	0.06	794	<0.5	<0.5	<0.2	1021	14	<0.5
48	0.48	<0.05	312	<0.1	<0.05	<0.05	1.3	<0.8	114	38	0.19	368	<0.5	<0.5	<0.2	562	8.9	<0.5
77	27	0.09	199	<0.1	<0.05	0.26	85	21	91	24	1.1	331	<0.5	0.7	<0.2	397	64	<0.5
Elura flyash lime mix																		
2	5.7	3.7	4961	0.16	<0.05	0.59	3.7	<0.8	913	284	19	5927	<0.5	3.3	<0.2	10764	11	10
24	0.65	1.4	7585	8.8	<0.05	<0.05	294	298	213	1582	640	1193	<0.5	<0.5	26	11037	56	2252
28	0.13	0.14	2234	<0.1	<0.05	<0.05	334	<0.8	92	650	212	895	<0.5	<0.5	<0.2	3491	6.3	74
46	0.05	<0.05	4676	<0.1	<0.05	<0.05	1.1	<0.8	101	460	17	1208	<0.5	1.5	<0.2	4979	1.8	<0.5
65	0.09	0.08	4057	<0.1	<0.05	<0.05	35	36	81	520	8.5	1270	<0.5	2.8	<0.2	4492	7.4	5.8
81	0.14	<0.05	2773	<0.1	<0.05	<0.05	3.4	2.7	43	281	0.76	732	<0.5	1.5	<0.2	2732	4.4	0.32
Peak flyash lime mix																		
1	160	3.9	540	<0.1	<0.05	4.3	10	3.9	1616	25	0.19	5191	<0.5	1.9	<0.2	43359	52	<0.5
25	131	0.45	719	<0.1	<0.05	0.42	6.0	<0.8	416	2.2	0.48	1188	<0.5	0.9	<0.2	11509	10	1.8
27	0.36	0.11	356	<0.1	<0.05	0.23	1.7	<0.8	277	16	0.19	950	<0.5	0.4	<0.2	1689	9.1	<0.5
75	4.1	0.11	63	<0.1	<0.05	<0.05	9.0	1.7	170	24	1.4	839	<0.5	0.7	2.6	1678	23	0.79

TABLE 3A.50 ICP-AES RESULTS OF 1:5 EXTRACTS FROM THE SOLID ADDITIVE HARDPAN ENHANCEMENT EXPERIMENT - FLYASH AND LIME MIX TRIALS

Depth	Al	B	Ca	Cd	Cr	Cu	Fe	Fe(II)	K	Mg	Mn	Na	Ni	P	Pb	S	Si	Zn
(cm)	mg/kg	mg/kg	mg/kg	mg/kg	mg/kg	mg/kg	mg/kg	mg/kg	mg/kg	mg/kg	mg/kg	mg/kg	mg/kg	mg/kg	mg/kg	mg/kg	mg/kg	mg/kg
CSA lime mix																		
3	0.10	<0.05	3919	<0.1	<0.05	0.08	0.37	<0.8	137	5.9	0.02	194	<0.5	0.6	<0.2	262	1.8	0.25
20	0.11	<0.05	4711	<0.1	<0.05	<0.05	0.38	<0.8	65	0.11	0.02	93	<0.5	0.5	1.3	279	1.8	<0.5
27	0.45	<0.05	491	<0.1	<0.05	0.05	1.1	<0.8	92	33	0.38	178	<0.5	<0.5	<0.2	592	7.6	<0.5
48	2.0	<0.05	417	<0.1	<0.05	<0.05	5.3	0.58	59	38	0.18	170	<0.5	<0.5	<0.2	382	9.4	<0.5
71	1.2	<0.05	249	<0.1	<0.05	<0.05	2.6	<0.8	39	17	0.25	128	<0.5	<0.5	<0.2	313	11	0.38
Elura lime mix																		
3	0.37	<0.05	12427	<0.1	<0.05	0.31	7.4	6.8	704	1384	33	6236	<0.5	12	<0.2	43179	7.0	6.6
23	2.3	<0.05	9329	<0.1	<0.05	<0.05	66	62	235	453	112	2065	<0.5	<0.5	3.2	90962	2.6	158
28	0.16	<0.05	2693	<0.1	<0.05	<0.05	0.45	4.9	60	638	53	1204	<0.5	1.4	1.8	3470	3.9	18
84	0.10	<0.05	2568	<0.1	<0.05	<0.05	110	111	44	469	12	898	<0.5	2.3	<0.2	3872	12	2.7
Peak lime mix																		
2	11	<0.05	9565	<0.1	<0.05	2.4	124	<0.8	4905	110	36	10329	<0.5	13	14	47911	38	52
11	0.26	<0.05	4723	<0.1	<0.05	0.05	0.90	<0.8	242	0.21	0.03	385	<0.5	0.5	27	1638	2.8	2.8
25	0.10	<0.05	5993	<0.1	<0.05	0.12	0.80	<0.8	146	20	0.06	359	<0.5	0.6	84	4477	2.6	3.3
29	1.7	<0.05	307	<0.1	<0.05	<0.05	0.62	<0.8	160	0.46	0.16	447	<0.5	0.5	<0.2	3403	10	0.92
52	3.7	<0.05	143	<0.1	<0.05	<0.05	3.2	2.9	146	2.3	0.07	454	<0.5	0.5	1.8	2580	25	0.50
70	3.4	<0.05	107	<0.1	<0.05	<0.05	5.1	<0.8	125	5.0	0.18	350	<0.5	<0.5	<0.2	1920	28	0.52

TABLE 3A.51 ICP-AES RESULTS OF 1:5 EXTRACTS FROM THE SOLID ADDITIVE HARDPAN ENHANCEMENT EXPERIMENT - LIME MIX TRIALS

Depth	Al	B	Ca	Cd	Cr	Cu	Fe	Fe(II)	K	Mg	Mn	Na	Ni	P	Pb	S	Si	Zn
(cm)	mg/kg	mg/kg	mg/kg	mg/kg	mg/kg	mg/kg	mg/kg	mg/kg	mg/kg	mg/kg	mg/kg	mg/kg	mg/kg	mg/kg	mg/kg	mg/kg	mg/kg	mg/kg
CSA phosphate lime mix																		
3	0.36	<0.05	3467	<0.1	<0.05	<0.05	0.82	0.44	54	0.23	0.06	88	<0.5	1.0	<0.2	253	2.5	1.5
25	1.5	<0.05	3449	<0.1	<0.05	<0.05	0.72	<0.8	52	0.18	0.03	100	<0.5	0.5	<0.2	621	3.0	0.29
34	0.56	<0.05	545	<0.1	<0.05	<0.05	3.5	<0.8	61	15	1.6	134	<0.5	<0.5	<0.2	591	11	0.68
56	2.8	<0.05	295	<0.1	<0.05	<0.05	7.2	<0.8	60	31	1.2	203	<0.5	<0.5	<0.2	411	15	<0.5
74	0.53	<0.05	272	<0.1	<0.05	<0.05	1.4	<0.8	43	12	0.57	136	<0.5	0.5	<0.2	320	12	<0.5
Elura phosphate lime mix																		
1	0.86	47	21918	14	<0.05	33	84	83	23649	4734	181	184279	<0.5	243	65	313527	115	1179
3	0.17	<0.05	11385	0.79	<0.05	0.34	1.3	<0.8	495	2791	48	5991	<0.5	15	<0.2	29379	4.4	81
23	0.34	<0.05	7708	0.66	<0.05	0.18	1.4	0.77	596	4186	212	2303	<0.5	0.8	5.6	35722	5.4	111
35	n.d.	<0.05	3861	<0.1	<0.05	<0.05	1459	1458	65	1491	499	1218	<0.5	<0.5	<0.2	7372	7.9	701
58	0.08	<0.05	3545	<0.1	<0.05	<0.05	44	43	59	565	21	1038	<0.5	2.0	<0.2	4059	5.9	4.8
80	0.15	<0.05	3664	<0.1	<0.05	<0.05	1.7	0.40	53	476	1.6	1061	<0.5	2.6	<0.2	3910	7.3	0.61
Peak phosphate lime mix																		
1	120	<0.05	14535	<0.1	<0.05	95	91	49	7773	188	12	17808	<0.5	22	<0.2	56663	427	17
2	0.22	<0.05	3941	<0.1	<0.05	0.05	1.0	<0.8	318	1.6	0.14	634	<0.5	1.0	13	1826	2.6	1.4
26	0.12	<0.05	4261	<0.1	<0.05	<0.05	7.3	6.7	173	10	2.5	450	<0.5	0.6	12	5983	3.0	3.7
26	0.25	<0.05	4902	<0.1	<0.05	<0.05	0.87	<0.8	137	0.79	0.04	364	<0.5	0.5	21	5949	2.2	1.4
31	4.4	<0.05	540	<0.1	<0.05	0.52	0.86	<0.8	186	0.60	0.05	519	<0.5	0.4	<0.2	1455	7.3	0.39
47	1.3	<0.05	237	<0.1	<0.05	<0.05	6.1	6.7	148	37	0.55	487	<0.5	0.5	<0.2	1160	19	<0.5
66	1.0	0.12	187	<0.1	<0.05	<0.05	2.1	<0.8	188	13	0.44	792	<0.5	1.0	<0.2	2058	23	2.1

TABLE 3A.52 ICP-AES RESULTS OF 1:5 EXTRACTS FROM THE SOLID ADDITIVE HARDPAN ENHANCEMENT EXPERIMENT - PHOSPHATE AND LIME MIX TRIALS

Depth	Al	B	Ca	Cd	Cr	Cu	Fe	Fe(II)	K	Mg	Mn	Na	Ni	P	Pb	S	Si	Zn
(cm)	mg/kg	mg/kg	mg/kg	mg/kg	mg/kg	mg/kg	mg/kg	mg/kg	mg/kg	mg/kg	mg/kg	mg/kg	mg/kg	mg/kg	mg/kg	mg/kg	mg/kg	mg/kg
CSA phosphate mix																		
2	<0.01	<0.05	1714	<0.1	<0.05	<0.05	9.7	9	144	1432	4.3	860	<0.5	<0.5	<0.2	3626	16.8	<0.5
17	<0.01	<0.05	590	<0.1	<0.05	<0.05	<0.05	<0.4	28	250	2.7	122	<0.5	<0.5	<0.2	859	3.6	<0.5
23	0.20	<0.05	308	<0.1	<0.05	<0.05	46	43	28	286	30	124	<0.5	<0.5	<0.2	704	4.2	<0.5
46	<0.01	<0.05	321	<0.1	<0.05	<0.05	<0.05	<0.4	18	94	1.0	86	<0.5	<0.5	<0.2	409	2.0	<0.5
65	0.22	<0.05	584	<0.1	<0.05	<0.05	<0.05	<0.4	19	178	3.8	81	<0.5	<0.5	<0.2	753	3.2	<0.5
Elura phosphate mix																		
2	<0.01	<0.05	4809	<0.1	<0.05	<0.05	642	638	41	15477	1875	10673	<0.5	3.4	<0.2	27459	8.4	5190
22	<0.01	<0.05	6629	<0.1	<0.05	<0.05	737	732	61	2078	164	2001	<0.5	6.2	<0.2	8492	5.1	94
27	0.29	<0.05	5576	<0.1	<0.05	<0.05	275	274	72	1947	274	1857	<0.5	3.3	<0.2	7461	1.8	38
55	0.31	<0.05	7281	<0.1	<0.05	<0.05	290	308	81	1587	39	1911	<0.5	3.6	<0.2	8084	0.8	<0.5
79	1.41	<0.05	6557	<0.1	<0.05	<0.05	179	178	83	1370	15	1687	<0.5	4.2	<0.2	7593	3.1	<0.5
Peak phosphate mix																		
2	0.82	<0.05	529	<0.1	<0.05	1.27	<0.05	<0.4	691	1209	2.6	5284	<0.5	8.3	<0.2	6221	16.3	<0.5
20	0.34	<0.05	1355	<0.1	<0.05	<0.05	<0.05	<0.4	295	316	3.3	1368	<0.5	2.4	<0.2	2468	13.2	<0.5
29	0.17	<0.05	1186	<0.1	<0.05	<0.05	<0.05	<0.4	247	222	4.7	1074	<0.5	<0.5	<0.2	2036	19.3	<0.5
48	1.46	<0.05	794	<0.1	<0.05	<0.05	<0.05	<0.4	178	165	5.3	651	<0.5	<0.5	<0.2	1488	12.3	<0.5
65	0.52	<0.05	733	<0.1	<0.05	<0.05	<0.05	<0.4	134	144	3.6	349	<0.5	<0.5	<0.2	1097	3.7	<0.5

TABLE 3A.53 ICP-AES RESULTS OF 1:5 EXTRACTS FROM THE SOLID ADDITIVE HARDPAN ENHANCEMENT EXPERIMENT - PHOSPHATE MIX TRIALS

Depth (cm)	pH	Eh modified (mv)	Depth (cm)	pH	Eh modified (mv)	Depth (cm)	pH	Eh modified (mv)
CSA Control			**Elura Control**			**Peak Control**		
			2	5.1	-101			
1	6.3	10	16	5.5	-126	3	7	-127
15	7.3	-190	32	5.1	-156	20	7.21	-192
28	7.25	-205	48	5.55	-176	37	6.82	-107
35	7.3	-185	64	6.3	-266	54	6.55	-77
			77	6.6	-286	65	6.63	-92
			Elura Control 2					
			2	5.15	15			
			12	5.96	-80			
			27	5.04	-80			
			42	5.35	-75			
			47	5.5	-110			
			54	5.5	-130			
			65	5.1	-120			
CSA Flyash Lime Layer			**Elura Flyash Lime Layer**			**Peak Flyash Lime Layer**		
2	7.4	-67	3	10.55	-66	1	7.44	
7	7.55	-187	19	5.1	-306	12	10.29	
20		-237	30	5.5	-131	24	10.72	-267
40		-297	51	5.35	-101	27	7.89	-127
70		-287	67	5.25	-106	41	7.68	
			81	5.25	-106	54	7.4	-187
						63	7.46	
						75	7.83	-157
CSA Flyash Layer			**Elura Flyash Layer**			**Peak Flyash Layer**		
4	7.2	-188	2	4.75	-71	3	6.82	-33
17	7.9	2	11	4.7	-26	12	7.05	-77
28	7.6	-88	17	6.1	-32	17	7.41	-7
50	7.55	-233	25	5.25	-116	23	6.7	-97
68	7.5	-173	49	5.5	-126	36	6.09	
			64	5.5	-156	50	7.13	-157
			80	5.8	-226	66	7.02	-97
CSA Lime Layer			**Elura Lime Layer**			**Peak Lime Layer**		
2	4.81	236	2	5.68	-167	2	7.49	-207
13	10.3	-104	9	8.2	-177	11		-172
20	11.86		17	11.82	-337	14	11.33	
27	10.9	-214	30	6.67	-197	20	12.07	-257
38	7.5	-234	43	5.54		27	10.5	-267
40	6.1		59	5.48	-157	37	7.4	
55	4.2		70	5.44		50	7.58	-182
63	8.11		81	5.48	-167	58	7.13	
68	7.24	-199				70	7.36	-227
CSA Phosphate Lime Layer			**Elura Phosphate Lime Layer**			**Peak Phosphate Lime Layer**		
3	8.25	-1	3	11.7	-141	2	7.63	-87
17	12.4		9	6	-216	10	10.5	-102
32	7.1		16	6.8	-326	17	11.56	-237
25	10.88	-206	26	6.35	-176	26	9.02	-147
50	7.8	-66	41	5.5	-136	40	6.8	
70	7.8	-211	52	5.4	-146	53	6.62	-137
			70	5.65	-156	70	6.34	-197
			81	5.65	-206			
CSA Phosphate Limestone Layer			**Elura Phosphate Limestone Layer**			**Peak Phosphate Limestone Layer**		
6	7.01	-86	2	5	-75	2	7.07	-177
16	7.58		14	5.75	-135	9	7.45	-187
25	7.03	-176	23	7.2		17	8.06	
47	7.06	-181	28	5.5	-140	25	7.18	-257
66	7.5	-106	40	5.5		35	7.27	
			54	5.8	-240	45	7.15	-197
			69	6.55	-255	55	7.15	
			80	6.7	-255	63	7.72	-167

TABLE 3A.54 PH AND EH RESULTS FROM THE SOLID ADDITIVE HARDPAN ENHANCEMENT EXPERIMENT

Depth (cm)	pH	Eh modified (mv)	Depth (cm)	pH	Eh modified (mv)	Depth (cm)	pH	Eh modified (mv)
CSA Phosphate Layer			Elura Phosphate Layer			Peak Phosphate Layer		
2	4.44	161	1	5	-100	2	6.82	-20
15	4.7	136	14	5.27	-115	15	6.9	-147
22	6.72		21	6.59	35	28	7.05	-187
31	6.77	-204	29	5.43	-130	43	7.13	
39	6.95		45		-140	53	7.49	-217
46	7.09	-224	55	5.68	-175	60	7.49	
55	6.7		69	6.17	-210	70	7.45	-177
65	7.34	-184	81	6.11	-215			
73	5.56							
CSA Limestone Layer			Elura Limestone Layer			Peak Limestone Layer		
2	7.35	-19	1	5.5	-74	2	7.02	36
12	7.18	-64	11	6.4	-134	10	7.24	56
20	8.41		20	7.8	-24	20	8.8	
26	7.05	-189	26	5.6	-109	25	7.3	-39
41	7.49	-214	36	4.95		35	7.41	
53	7.33	-219	51	5.15	-109	45	7.24	-179
65	7.24	-179	64	5.4	-169	55	7.39	
			77	5.92	-164	65	7.7	-199
CSA Limestone Mix			Elura Limestone Mix			Peak Limestone Mix		
2	7.4	57	2	6.8	-200	2	7.25	-80
19	7.15	-228	13	6.55	-220	16	7.06	-145
27	6.95	-53	28	5.32	-180	21		-90
43	7	-218	35	5.32	-120	24	6.9	-105
62	7.2	-268	42	5.22	-100	34	6.65	-59
			60	5.36	-120	40	6.65	
			79	5.7	-130	49	7	-185
						62	7.3	-190
CSA Phosphate Lime Mix			Elura Phosphate Lime Mix			Peak Phosphate Lime Mix		
3	11.65	-518	2	6.75		2	11.71	-367
25	11.25	-563	23	6.6		15	11.72	
34	8.85	-238	35	5.5	-160	24	11.63	-417
56	8.1	-233	59	6.1	-180	32	11.34	-237
74	8.3	-168	70	6.35	-200	47	8.41	-257
			81	6.7	-190	56	8.44	
						66	8.61	-287
CSA Flyash Lime Mix			Elura Flyash Lime Mix			Peak Flyash Lime Mix		
2	9.55		2	6.85		13	11.6	
25	11.55		24	6		27	10.86	-114
30	9.55	-238	28	5.7	-155	41	8.98	
48	7.7	-183	46	5.75	-215	50	8.22	-224
63	7.35	-168	58	6.6	-225	60	8.44	
77	8.2	-138	71	6.55	-335	75	8.98	-244
			81	6.6	-335			
CSA Phosphate Mix			Elura Phosphate Mix			Peak Phosphate Mix		
2	7.1	-236	2	5.35	-80	2	7.71	-224
17	6.7	-151	13	5.95	-110	20	7.45	-214
23	6.9	-106	22	5.8	-155	29	7.52	-214
46	7.5	-176	27	5.35	-115	48	7.29	-194
65	7.4	-136	40	5.4	-135	65	7.35	-134
			55	5.75	-165			
			67	6.1	-200			
			79	6.15	-195			
CSA Lime Mix			Elura Lime Mix			Peak Lime Mix		
3	12.25	-91	3	8.7		2	11.73	
20	12	-301	23	9.4		11	11.55	-347
27	8.35	-316	28	6.7	-170	25	11.8	-287
48	8	-236	31	5.7	-195	29	10.38	-187
71	8.1	-206	42	5.75	-165	39	9.58	
			54	5.53	-165	52	9.41	-227
			69	5.35	-140	68	9.07	-237
			84	5.54	-125			
CSA Flyash Mix			Elura Flyash Mix			Peak Flyash Mix		
3	8.1	-34	2	6.65	-255	2	7.76	-137
20	7.05	-8	11		-165	12	8.48	
26	5.45	-103	13		-35	22	7.73	-197
40	5.6	-158	17	6.35	-205	31	7	-127
55	6.2	-198	25	6.3	-65	45	6.94	-237
69	7.4	-208	29	5.4	-110	56	6.96	
			43	5.4	-135	70	7.09	-137
			58	5.5	-145			
			72	5.65	-145			
			84	5.9	-155			

TABLE 3A.54 CONT. pH AND Eh RESULTS FROM THE SOLID ADDITIVE HARDPAN ENHANCEMENT EXPERIMENT

Bibliography

Agnew, M.K., 1994. Weathering Products and Geochemistry of Waste residues at the Brukunga Pyrite Mine, Adelaide Hills, S.A., in relation to Environmental Impacts. Unpublished. B.Sc (Hons) University of Adelaide.

Ahmed, S.M., 1991. Electrochemical and surface chemical methods for the prevention of the atmospheric oxidation of sulfide tailings in Proc. Second International Conf. Abatement of Acid Drainage, Montreal. pp 305-319.

Ahmed, S.M., 1994. Surface chemical methods of forming hardpan in pyrrhotite tailings and prevention of the Acid Mine Drainage in International Land Reclamation and Third International Conference on the Abatement of Acidic Drainage, Pittsburg, Pa. pp 57-66.

Ahmed, S.M., 1995. Chemistry of Pyrrhotite Harpdan Formation in Sudbury '95, Conference on Mining and the Environment, Sudbury, Ontario. pp 171-180.

Alpers, C. and Blowes, D., 1994. Environmental Geochemistry of Sulfide Oxidation, ACS symposium series **550**. American Chemical Society Washington D.C. 681 pp.

Alpers, C., Blowes, D. and Nordstrom, D., 1994. Secondary mineral and acid mine water chemistry in J. Jambor, and D. Blowes, (Eds) Short course Handbook on environmental geochemistry of sulfide mine-wastes, Mineralogical Ass. of Canada, Waterloo, Ontario. pp 247-270.

American Geological Institute, (1997) Glossary of Geology, 4th Ed. J.A. Jackson (Ed). Alexandria, Va. 769 pp.

Andrew, E.C., 1911. Report on the Cobar copper and gold field:Part I. N.S.W. Dept of Mine Geol. Surv. Mineral Resources **17**, pp 121-128.

ANZECC/NHMRC., 1992. Australia and New Zealand guidelines for the assessment of contaminated sites. 57pp.

Barnes, C. and Allison, G., 1983. The distribution of Deuterium and ^{18}O in Dry soils 1. Theory. Journal of Hydrology. **60**, 141-156.

Bigham, J., Schwertmann, U. and Carlson, L., 1992. Mineralogy of precipitates formed by the biogeochemical oxidation of Fe(II) in mine drainage, in H. Skinner, and R. Fitzpatrick, (Eds) Biomineralisation - Processes of iron and manganese Catena Verlag, Germany. pp 219-232.

Bigham, J., Schwermann, U., Carlson, L. and Murad, E., 1990. A poorly crystallized oxyhydroxysulfate of iron formed by bacterial oxidation of Fe(II) in acid mine water, Geochimica et Cosmochimica Acta **54**, 2743-2758.

Blesing, N., Lackley, J. and Spry, A., 1974. Rehabilitation of Brukunga Mine : Nairne Pyrites Ltd, Amdel Report **1015**. 51 pp.

Blight, G.E., Rea, C.E, Caldwell, J.A. and Davidson, K.W., 1981. Environmental Protection of Abandoned Tailings Dams in Proc. of 10th Inter. Conf. on Soil Mechanics and Foundation Engineering, Stockholm. pp 303-308.

Blowes, D., Cherry, J. and Reardon, E., 1987. The hydrogeochemisty of four inactive tailings impoundments: Perspectives on tailings pore-water evolution in Proc., National symposium on Mining, Hydrology, Sedimentology and Reclamation, University of Kentucky, Lexington, Kentucky. pp 253-261.

Blowes, D., Cherry, J. and Reardon, E., 1988. Field observations on the rate of Geochemical Evolution of tailings ore waters at the Heath Steele mine, New Brunswick in International Groundwater Symposium of the International Assoc. of Hydrogeologists, Canadian National Chapt, Atlanta Region, Halifax, Nova Scotia. pp 5-17.

Blowes, D. and Jambor, J., 1990. The porewater geochemistry and the mineralogy of the vadose zone of sulfide tailings, Waite Amulet, Quebec, Canada, Applied Geochemistry **5**, 327-346.

Blowes, D., Jambor, J., Appleyard, E., Reardon, E. and Cherry, J., 1992. Temporal Observations of the geochemistry and mineralogy of a sulfide rich mine-tailings impoundment, Heath Steele Mines, New Brunswick, Explo. Mining Geol, **1**, pp 251-264.

Blowes, D. and Ptacek, C., 1992. Geochemical remediation of groundwater by permeable reactive walls: Removal of chromate by reaction with iron bearing solid in Proc. Subsurface Restoration Conf. 3rd Inter. Conf. Groundwater Qual. Research, Dallas, Texas. pp 214-216.

Blowes, D. and Ptacek, C., 1994. Acid neutralisation mechanisms in inactive mine tailings. in J. Jambor, and D. Blowes, (Eds) Short course Handbook on environmental geochemistry of sulfide mine-wastes, Mineralogical Ass. of Canada, Waterloo, Ontario. pp 271-291.

Blowes, D., Ptacek, C., Frind, E., Johnson, R., Robertson, W. and Molson, J., 1994a. Acid-neutralisation reactions in inactive mine tailings impoundments and their effect on the transport of dissolved metals in International Land Reclamation and Mine Drainage Conference and the 3rd International Conference on Abatement of Acidic Drainage, Pittsburgh. pp 429-438.

Blowes, D., Ptacek, C. and Jambor, J., 1994b. Remediation and prevention of low quality drainage from tailings impoundments. in J. Jambor, and D. Blowes, (Eds) Short course Handbook on environmental geochemistry of sulfide mine-wastes, Mineralogical Ass. of Canada, Waterloo, Ontario. pp 365-379.

Blowes, D., Reardon, E., Jambor, J. and Cherry, J., 1991. The formation and potential importance of cemented layers in inactive sulfide mine tailings, Geochimica et Cosmochimica Acta **55**, 965-978.

Boorman, R.S. and Watson, D., 1976. Chemical processes in abandoned sulfide tailings dumps and environmental implication for Northeastern New Brunswick, Environmental Control. CIM Bulletin, **69**, 86-96.

Both, R., 1990. Kanmantoo Trough-Geology and mineral deposits, in F. Hughes (Ed) Geology of the mineral deposits of Australia and Papua New Guinea **2**, 1195-1203. The Australian Institute of Mining and Metallurgy, Melbourne, Vic.

Bowders, J.J. and Chiado, E.D., 1990. Engineering Evaluation of Waste Phosphate Clay for Producing Low Permeability Barriers in Mining and Reclamation Conf. and Exhibition, Charleston, West Virginia. pp 11-15.

Bowders, J.J., Gabr, M.A., Boury, E.M. and Baker, R.C., 1994. Engineering Evaluation of Amended Flyash for Hydraulic Barriers in International Land Reclamation and Third International conference on the Abatement of Acidic Drainage, Pittsburg, Pa. pp 226-231.

Bureau of Meterology, (Online, accessed, 6/1/98) http://www.bom.gov.au/climate/averages/

Burns, M., 1969. The determination of pyritic sulfur in Australian coals, CSIRO Division of Mineral Chemistry, Investigation Report **82**. 7 pp.

Carlson, L. and Schwertmann, U., 1981. Natural ferrihydrites in surface deposits from Finland and their association with silica, Geochimica et Cosmochimica Acta **45**, 421-429.

Carne, F.E., 1908. The Copper mining industry and the distribution of Cu ores. N.S.W. Dept of Mines Geol. Surv. Mineral Resource **6**, 2nd Edition. 198-199.

Chen, T.T. and Petruk, W., 1980. Mineralogy and Characteristics that affect recoveries of metals and trace metals from the ore at Heath Steele Mine, New Brunswick. Canadian Inst. Mining Metall. Bull. **73**, 167-179.

Chermak, J.A. and Runnells, D.D., 1995. Self-sealing hardpan barriers to minimise infiltration of water into sulfide-bearing overburden, ore and tailings piles in Tailings and Mine Waste '95. Proceedings of the 2nd International Conf. on tailings and mine waste, Fort Collins, Colorado, U.S.A. Balkema, Rotterdam. pp 265-273.

Coastech Manual, 1991. Acid rock drainage prediction manual, Prepared for CANMET, Dept of Energy, Mines and Resources, Canada. SSC File **0095Q.23440-9-9149**. 70 pp.

Costin, A.B. and Williams, C.H., 1983. Phosphorus in Australia. Centre for Resource and Environmental Studies, The Australian National University. Monograph 8. Canberra Publishing and Printing Co. 284 pp.

Davis, G.B. and Ritchie, A.I.M., 1986. A model of oxidation in pyritic mine waste : Part 1 equations and approximate solution. Applied. Math. Modelling. **10**, 314-322.

Davis, L.W., 1990. Synclinorial Zone and the Hill end Synclinorial Zone. in F.E. Hughes (Ed) Geology of the mineral deposits of Australia and Papua New Guinea, **2**, 1375-1384. The Australasian Institute of Mining and Metallurgy, Melbourne, Vic.

Day, S.J., 1994. Evaluation of Acid generating rock and acid consuming rock mixing to prevent acid rock drainage in International Land Reclamation and Mine Drainage Conference and the Third Internation Conference on the Abatement of Acidic Drainage, Pittsburg, Pa. pp 77-86.

de Roo, J.A., 1987. Structurally controlled ore genesis at Elura and Mt Carbine, Australia, Ph.D Thesis (unpub) James Cook University of North Qld.

Doepker, R., 1991. Column leach Study IV : Factors affecting the dissolution of metals from sulfidic metal mine tailings in Proc. International conf. on Abatement of Acidic Drainage, MEND, NEDEM, Montreal, pp 115-138.

Doherty, L., 1978. Rehabilitation of Brukunga Pyrite mine, SADME Mining Resource File **B-S-1**. 17 pp.

Elberling, B., Nicholson, R.V. and David, D.J., 1993. Field Evaluation of Sulfide Oxidation Rates. Hydrology **24**, 323-338.

Emerson, W., Peter, P., McClure, S. and Weissman, D., 1994. Neutralized tailings and sulphates: settlement, drying and consolidation. Geotechniques **44**, 503-512.

Environmental Geochemistry International (EGI) Pty Ltd, 1993. Rehabilitation Planning for the Brukunga Minesite and Tailings Dam, SADME Report. 41 pp.

Evangelou, V.P., 1994. Potential Microencapsulation of pyrite by artificial inducement of $FePO_4$ Coatings in International Land Reclamation and Third International conference on the Abatemnt of Acidic Drainage, Pittsburg, Pa. pp 96-103.

Fanning, D. and Fanning, M., 1989. Soil - Morphology, Genesis and Classification, John Wiley and sons, Inc. 395 pp.

Fordham, A., 1993. Porewater Quality of uranium tailings during laboratory aging and its relation to solid phase. Aust. J. Soil. Res., **31**, 365-390.

George, R., 1969. Sulfide-silicate reactions during metamorphism of the Nairne pyrite deposit, Proc. Australas. Inst. Min. Metall., **230**, 1-7.

Gilligan, L.B. and Suppel, D.W., 1978. Mineral deposits in the Cobar Supergroup and their structural setting. Geol. Surv. N.S.W Q. Notes **33**, 15-22.

Glen, R.A., 1987 Copper and gold rich deposits in deformed turbidites at Cobar, Australia : their structural control and hydrothermal origin. Econ Geol **82**, 124-140.

Glen, R.A. and Pogson, D.J., 1985. Summary of geology and controls of mineralisation in Cobar region in Cobar field Conference, Cobar. 91 pp.

Grote, W.N., Gutierrez, N., Lim, C., Low, K., Madgwick, J., Peddie, F. and Ibrahim-Rajoka, M., 1981. Effect of interrupted irrigation on copper release and bacterial activity during leaching of chalcopyrite ore. Proc. Australas. Inst. Min. Metall. **278**, 39-42.

Hignett, C.T., 1997. Hydrological properties of the surface layers of the tailings dams at the Renison Bell Mine. CSIRO-Minesite Rehabilitation Research Program Report. 23 pp.

Hillel, D., 1971. Soil and water - Physical principles and processes. Academic Press New York. 288 pp.

Hinman, M.C and Scott, A.K., 1990. The Peak Gold deposit, Cobar. in F.E. Hughes (Ed) Geology of the mineral deposits of Australia and Papua New Guinea, **2**, 1345-1352. The Australasian Institute of Mining and Metallurgy, Melbourne, Vic.

Huang, X. and Evangelou, V.P., 1994. Suppression of pyrite oxidation rate by phosphate addtiion. in C.N. Alpers and D.W. Blowes (Eds) Environmental geochemistry of sulfide oxidation. Am. Chem. Soc. Symp. Series 550, pp 562-573.

Jackson, R.D., 1972. On the calculation of hydraulic conductivity. Soil Sc. Soc. America Proc., **36**. 380-382.

Jambor, J., 1994. Mineralogy of sulfide rich tailings and their oxidation products. in J. Jambor and D. Blowes (Eds) Short course Handbook on environmental geochemistry of sulfide mine-wastes, Mineralogical Ass. of Canada, Waterloo, Ontario. pp 59-102

Jambor, J. and Blowes, D., 1990. Major-element variations in the reactive sulfide-rich tailings at the Waite Amulet Minesite, Noranda Area, Quebec, Canada in W. Petruk, R. Hagni, S. Pignolet and D. Hausen (Eds), Process Mineralogy IX, pp 511-523.

Jambor, J. and Blowes, D., (Eds) 1994. Short course Handbook on environmental geochemistry of sulfide mine-wastes, Mineralogical Ass. of Canada, Waterloo, Ontario. 438 pp.

Jones, D.R., Ellerbroek, D., Eames, J.C., Smith, M., Agnew, M., Wright, M. and Nefiodovas, A., 1997. Closeout Options for tailings dams at Renison Bell. CSIRO Minesite Rehabilitation Research Program Report no. CET/IR544R. 191 pp.

Kendall, C.J., 1990. Ranger Uranium deposits. in F.E. Hughes (Ed) Geology of the mineral deposits of Australia and Papua New Guinea, **1**, 799-806. The Australasian Institute of Mining and Metallurgy, Melbourne, Vic.

Kennedy, L.P and Hawthorne, F.C., 1987. A mineralogical study of mine tailings from Farley and Sherridon, Northern Manitoba. Phase I Report. Manitoba Dept of Energy and Mines. 35 pp.

Lapakko, K. and Antonson, D., 1990. Treatment of Waste Rock Drainage with limestone beds in AMD Designing for closure - GAC/MAC Joint annual meeting, Vancouver, B.C. Canada. pp 273-283.

Learmonth, N and Learmonth, A. 1971. Regional Landscapes of Australia, Form, Function and Change. Heinemann Educational Books Ltd. 493 pp.

Loveday, J., 1974. Water Retention and Moisture Characteristics in Methods for analysis of irrigated solid. Commonwealth Bureau of Soils. Technical Communication No. **54**. pp 43-62.

Mabutt, J.A., 1980. Weathering history and landform development in C.R.M. Butt and R.E. Smith (Eds) Conceptual Models in Exploration geochemistry, Australia. Journal of Geochemical Exploration. **12**, 96-116.

Mackenzie, D.H. and Davis, R.H., 1990. Broken Hill Lead-Siver-Zinc deposit at ZC mine. in F.E. Hughes (Ed) Geology of the mineral deposits of Australia and Papua New Guinea, **2**, 1079-1088. The Australasian Institute of Mining and Metallurgy, Melbourne, Vic.

Madgwick, J.C. and Ralph, B.J., 1980. Laboratory Studies on Mineral leaching in P. Trudinger, M. Watter and B. Ralph (Eds) Biogeochemistry of Ancient and Modern Environments. Australian Academy of Science, Canberra. pp 589-600.

Malhotra, V.M., 1992. Advances in concrete technology. Canadian Centre for Mineral and Energy technology. pp 247-279.

Marshall, B. and Sangamosthwar, S.R., 1982. Commonality and differences in ores of the Cobar Super-group, N.S.W. Symp. on Geology and Mineralisation in Lachlan Fold Belt. Geol. Soc. Aust. Abstract. **6**, 15-16.

Marshall, T.J., 1959. Relations between water and soil. Commonwealth Agricultural Bureaux Farnham Royal, Bucks, England. 91 pp.

McDonald, R., Isbell, R., Speignt, J., Walker, J. and Hopkins, M., 1984. Australian soil and land survey field handbood, Inkata Press, Melbourne. 160 pp.

McFarlane, M.J., 1976. Laterite and Landscape. Academic Press, London. 151 pp.

McGregor, R.G. and Kamineni, D.C., 1992. The saturated hydraulic conductivity of hardpan samples from the Sherridon Mine Site, Manitoba. Whiteshell Nuclear Research Establishment, Atomic Energy of Canada Report, Pinawa, Manitoba. 25 pp.

McGregor, R.G., Stegemann, J.A. and van der Sloot, H.A., 1997. Preliminary Results of a Field study of a Self-Sealing/Self-Healing Cover System in Fourth International Conference on Acid Rock Drainage, Vancouver, B.C, Canada. **4**, 1435-1450.

McSweeny, K. and Madison, F.W., 1988. Formation of a cemented subsurface horizon in sulfidic mine waste. J. Environ. Qual., **17**, 256-262.

Meek, F.A., 1991. Evaluation of acid prevention techniques used in surface mining. in AIME Conference, Denver, Co. pp 41-48.

Mele, S., 1995. Resource evaluation of the Chesney tailings. Peak Gold Mine Report (unpub). 6 pp.

MEND: Mine Environment Neutral Drainage Program, 1994. Annual Report. CANMET Canada Centre for Mineral and Energy Technology.

MEND: Mine Environment Neutral Drainage Program, 1995. Annual Report. CANMET Canada Centre for Mineral and Energy Technology.

Merrington, G. and Alloway B.J., 1993. Environmental significance of heterogeneous metal distribution in historical Pb-Zn mine tailings heaps. Trans. Instn Min. Metall (Section A: Min. Industry), **102**, A71-A74.

Milnes, A.R., 1992. Calcrete in I. Martin and W. Chesworth (Eds) Weathering, Soils and Paleosols in Developments in Earth Surface Processes **2**, Elsevier. 309-347.

Milnes, A.R. and Thiry, M., 1992. Silcrete in I. Martin and W. Chesworth (Eds) Weathering, Soils and Paleosols. in Developments in Earth Surface Processes **2**, Elsevier. 349-377.

Milnes, A.R., Wright, M.J. and Thiry, M., 1991. Silica Accumulations in Saprolites and Soils in South Australia in W.D. Nettleton, (Ed) Occurrence, Characteristics, and Genesis of Carbonate, Gypsum and Silica Accumulations in Soil. Soil Science Society of America Special Publication **26**, 121-149.

Morin, K., 1988. Physical and chemical hydrogeology of uranium tailings in Canada and the United States of America in Proceedings Internat. Groundwater Symp., Internat. Assoc, Hydrogeologists, Halifax, Nova Scotia. pp 175-187.

Morin, K. and Cherry, J., 1988. Migration of acid groundwater seepage from uranium tailings impoundments, 3. Simulation of the conceptual model with application to seepage area A. J. Contam. Hydrology **2**, 323-342.

Morin, K., Cherry, J., Dave, N., Lim, T., and Vivyurka, A., 1988a. Migration of acidic groundwater seepage from uranium-tailings impoundments, 1. Field study and conceptual hydrogeochemical model, J. Contam. Hydrology **2**, 271-303.

Morin, K., Cherry, J., Dave, N., Lim, T., and Vivyurka, A., 1988b. Migration of acidic groundwater seepage from uranium-tailings impoundments, 2. Behaviour of radionuclides in water, J. Contam. Hydrology **2**, 304-321.

Morland, R., 1990. Renison Bell tin deposit. in F.E. Hughes (Ed) Geology of the mineral deposits of Australia and Papua New Guinea, **2**, 1249-1252. The Australasian Institute of Mining and Metallurgy, Melbourne, Vic.

Needham, R.S. and de Ross, G.J., 1990. Pine Creek - regional geology and mineralisation. in F.E. Hughes (Ed) Geology of the mineral deposits of Australia and Papua New Guinea, **1**, 727-738. The Australasian Institute of Mining and Metallurgy, Melbourne, Vic.

Needham, R.S., Crick, I.H. and Stuart-Smith, P.G., 1980. Regional geology of the Pine Creek Geosyncline. in J. Ferguson and A.B. Goleby (Eds) Uranium in the Pine Creek Syncline. Inter. Atomic energy Agency, Vienna. pp 1-22.

Newman, L., Herasymuite, G., Barbour, S., Fredlund, D. and Smith, T., 1997. The hydrology of waste rock dumps and a mechanism for unsaturated preferential flow in 4th International Conf. on ARD, Vancouver. pp 551-566.

NHMRC/AWRC, 1987. Guidelines for drinking water quality in Australia. National Health and Medical Research Council and Australian Water Resources Council. Australian Government Publishing Service, Canberra.

Nicholson, P.M. and Eupene, G.S., 1990. Gold deposits of the Pine Creek Inlier in F.E. Hughes (Ed) Geology of the mineral deposits of Australia and Papua New Guinea, **1**, 739-742. The Australasian Institute of Mining and Metallurgy, Melbourne, Vic.

Nordstrom, D., 1982. Aqueous pyrite oxidation and the consequent formation of secondary iron minerals in J. Kittrick, D. Fanning and L. Hossner (Eds) 1987. Acid sulfate weathering, Soil Sci. Soc. of Am., Wisconsin, pp 37-62.

Nordstrom, D., Jenne, E.A. and Ball, J.W., 1979. Redox equilibria of Fe in acid mine waters. in E.A Jenne, (Ed) Chemical modeling in aqueous systems. ACS Symposium Series 93, American Chemical Society, Washington D.C. pp 50-59.

Parks, G.A., 1967. Aqueous surface chemistry of oxides and complex oxide minerals. Advances in chemistry Series **67**, 121-160.

Penman, H.L., 1940. Gas and vapour movements in the soil. 1. The diffusion of vapours through porous solids. Journal of Agricultural Science **30**, 437-462.

Plimer, I.R., 1984. The mineralogical history of the Broken Hill Lode, N.S.W. Australian Journal of Earth Sciences **31**, pp 379-402.

Plumb, T., 1980. Atlas of Australian resources : third series - **2** Population. Canberra: Divisions of National Mapping. 23 pp.

Ptacek C.J and Blowes, D.W., 1994. Influence of siderite on the pore water chemistry of inactive mine tailings impoundments in C.N. Alpers and D.W. Blowes (Eds) Environmental geochemistry of sulfide oxidation. ACG Symposium Series 550. American Chemical Society, Washington, D.C. pp 172-189.

Rao, S.R., Gehr, R., Riendeau, M., Lu, D. and Finch, J.A., 1991. Potential of Acid Mine Drainage as a Coagulant in Proc. 2nd International Conference on Abatement of Acid Drainage, Montreal. pp 71-87.

Raven, M. and Self, P.G., 1988. XPLOT User Manual - Manipulation of Powder X-ray diffraction data. CSIRO, Div. of Soils, Technical Memorandum 30/1988.

Rayment, G. and Higgenson, F., 1992. Australian laboratory handbook of soil and water chemical methods, Inkata Press, Sydney, Aust. 330 pp.

Rayner, E.O., 1969. The Copper ores of the Cobar Region, N.S.W. Memoirs of the Geological Survey of N.S.W. Dept of Mines, Geology **10**, 131.

Reardon, E. J. and Moddle, P.M., 1985. Gas Diffusion Coefficient measurements on Uranium Mill Tailings : Implications to Cover Layer design. Uranium. **2**, 111-131.

Ritcey, G.M., 1989. Tailings Management - Problems and solutions in the mining industry. Elsevier Science Pub. 970 pp.

Robertson, A.M., 1987. in Proc. 11th Annual British Columbia Mine Reclamation Symp., April, 1987, Campbell River, British Columbia.

Robertson, J.G,., 1974. The environmental features and petrogenesis of the mineral zone of Cobar, N.S.W. Ph.D Thesis (unpub) The University of New England.

Robertson, W.D., 1994. The physical hydrology of mill tailings impoundments in J. Jambor and D. Blowes (Eds) Short course Handbook on environmental geochemistry of sulfide mine-wastes, Mineralogical Ass. of Canada, Waterloo, Ontario. pp 1-17.

Rose, W.A. and Daub, G.A., 1994. Simulated Weathering of pyritic shale with added limestone and lime in International Land Reclamation and Third International conference on the Abatement of Acidic Drainage, Pittsburg, Pa. pp 334-340.

Sangster, D.F., 1979. Evidence of an exhalative origin for deposits of Cobar district, N.S.W. BMR J. Aust. Geol. Geophys., **4**, 15-24.

Schmidt, B.L., 1990. Elura Zinc-Lead-Silver deposit Cobar. in F.E. Hughes (Ed) Geology of the mineral deposits of Australia and Papua New Guinea, **2**, 1329-1336. The Australasian Institute of Mining and Metallurgy, Melbourne, Vic.

Scott, A.K. and Phillips, K.G., 1990. CSA Copper-Lead-Zinc deposit, Cobar. in F.E. Hughes (Ed) Geology of the mineral deposits of Australia and Papua New Guinea, **2**, 1337-1343. The Australasian Institute of Mining and Metallurgy, Melbourne, Vic.

Scott, K., 1987. Solid solution in, and classification of, gossan-derived members of the alunite-jarosite family, north west Qld, Aust., American Mineralogist, **73**, 178-187.

Seccombe, P., Spry, P., Both, R., Jones, M. and Schiller, J., 1985. Base metal mineralisation in the Kanmantoo Group, SA: a regional sulfur isotope study, Economic Geology, **80**, 1824-1841.

Sprigg, R.C. and Campana, B., 1953. The age and facies of the Kanmantoo Group. Aust. J. Sci. **16**, 12-14.

St-Arnaud, L.C., Yanful, E.K., Prairie, R. and Dave, N. K., 1989. Evolution of acidic pore water at the Waite Amulet tailings site, Noranda, Quebec in Proc. of the International Symposium on Tailings and Effluent Management, Halifax, CIM, **14**, 93-102

Suppel, D.W. and Scheibner, E., 1990. Lachlan Fold belt in New South Wales - regional geology and mineral deposits. in F.E. Hughes (Ed) Geology of the mineral deposits of Australia and Papua New Guinea, **2**, 1321-1328. The Australasian Institute of Mining and Metallurgy, Melbourne, Vic.

SADME, 1972. Operations at Kanmantoo by Kanmantoo Mines Ltd. SADME Mining Resource file **K-2-6**. 11 pp.

SADME, 1985. Kanmantoo Mine closure and site rehabilitation. SADME report Env. **5534/DME 423/82**. 12 pp.

SADME, 1989. Brukunga mine rehabilitation conceptual plan - April, JN Report **5059A**. 30 pp.

Tasse, N., Germain, D., Dufour, C. and Tremblay, R., 1997. Hardpan formation in the Canadian Malartic Mine tailings: Implications for the Reclamation of the abandoned impoundments in 4th Internation Conf. Acid Rock Drainage, Vancouver, B.C. Canada. **4**, 1797-1812.

Taylor, S.A., 1949. Oxygen diffusion in porous media as a measure of soil aeration. Soil Sci. Soc. Amer. Proc. **14**, 55-61.

Thornber, M.R. and Taylor, G.F., 1992. The mechanism of sulfide oxidation and gossan formation. in C.R.M Butt and H. Zeeger (Eds) Regolith Exploration Geochemistry in Tropical and Subtropical Terrains. Elsevier, Amsterdam. pp 119-138.

Thornber, M. R. and Wildman. J.E., 1984. Supergene Alteration of Sulfides, VI. The binding of Cu, Ni, Zn, Co and Pb with Gossan (iron bearing) minerals. Chemical Geology, **44**, 399-434.

Van der Heyden, A. and Edgecombe, D.R., 1985. Silver-Lead-Zinc deposit at South Mine, Broken Hill. in F.E. Hughes (Ed) Geology of the mineral deposits of Australia and Papua New Guinea, **2**, 1073-1078. The Australasian Institute of Mining and Metallurgy, Melbourne, Vic.

Whitney, G., Esposito, K. and Sweeney, K., 1995. Mineral Reactions in a Colorado Mine Dump: Implications for remediation in arid and semi arid environments in National Meeting of the American Society for Surface Mining and Reclamation, Gillette, Wyoming. pp 577-586.

Yanful, E. and St Arnaud, L., 1991. The Waite Amulet hydrogeochemical evolution in Proc. 2nd Int. Conf. on the Abatement of acidic drainage, Montreal, MEND CANMET, pp 91-114.

Zachara, J.M. and Streile, G. P., 1991. Use of batch and column methodologies to assess utility waste leaching and subsurface chemical attentuation. Electric Power Research Institute, California, Interim report (project 2485-8). 56 pp.